STEREOSELECTIVE SYNTHESIS OF DIAZAHETEROCYCLES BY DECARBOXYLATIVE ASYMMETRIC ALLYLIC ALKYLATION

Thesis by

Alexander W. Sun

In Partial Fulfillment of the Requirements

for the Degree of

Doctor of Philosophy

CALIFORNIA INSTITUTE OF TECHNOLOGY

Pasadena, California

2019

(Defended April 19, 2019)

Alexander W. Sun
ORCID: 0000-0001-6639-4469

To mom & dad,

for their unconditional love & support

ACKNOWLEDGEMENTS

Caltech is a special place. I've been incredibly fortunate to pursue my graduate studies here. Where else can one meet so many talented people from so many disciplines—chemistry, biology, engineering, physics, computer science, math—all just a short walk away? It's been a pleasure to meet and learn from these true Techers.

At Caltech, I met my amazing advisor, Professor Brian M. Stoltz; you may have heard Brian is a compassionate mentor, an affable person, and a brilliant chemist. This is all true. Thank you Brian, for all the time, effort, and support you've put into mentoring me over the past five years. It has been an honor to work in your research group.

Additionally, thank you to the Caltech faculty and staff who have influenced my career path: thank you Professor Peter Dervan for chairing my committee and for allowing me to spend a summer in your research group. Thank you Professor Mark Davis and Professor Bob Grubbs for serving on my committee. Thank you Dr. Scott Virgil, Professor Sarah Reisman, Professor Greg Fu, and Professor Alison Ondrus, for your support and guidance throughout my graduate studies. Furthermore, I am very grateful for Dr. David VanderVelde and all his NMR assistance. Thank you Joe Drew, Agnes Tong, Alison Ross, and the entire CCE staff for maintaining the division.

At Caltech, I met the many members of the Stoltz group; there are dozens (by my count, at least 110 Stoltz members) that I've interacted with over the years. Postdocs, visiting scholars, graduate students, undergraduates, even high schoolers. They are a truly talented group of chemists in which I've had great fortune to learn

from. Thank you all for being great labmates. Specifically, I'd like to acknowledge the following individuals in which I've collaborated with on projects or mentored as undergraduates/high schoolers: Dr. Marchello Cavitt, Stephan N. Hess, Dr. Brendan O' Boyle, Dr. Gerit Pototschnig, Zachary P. Sercel, Ryan Dempsey, Yuanzhe Xie, and Angus Wu. The members of the Reisman, Fu, and Peters groups, who occupy the rest of the second and third floors of Schlinger (and the members of the Grubbs lab) have also been great people interact with and learn from.

Apart from Caltech, I have many others to thank: My parents, for their love, support, and sacrifice without which I could not have progressed to where I am today. My undergraduate research advisors Professor David R. Tyler and Professor Amos B. Smith—their support and guidance have shaped the research path I've taken so far. Professor Neil K. Garg, for allowing me to work in his lab over a summer. Yoyo Luo, for her love and support throughout graduate school. The many students, faculty, and administrators of the UCLA-Caltech Medical Scientist Training Program, and especially the entering class of 2012—thank you for your support and friendship.

Much of the chemistry in this thesis chemistry would not have happened in the absence of the individuals mentioned above, as well as many others—thank you.

ABSTRACT

The Stoltz group has developed transition-metal catalyzed methods to synthesize quaternary and tetrasubstituted stereocenters over the past fourteen years. Using iridium, palladium, copper, and nickel, the group has synthesized a myriad cyclic and acylic quaternary motifs of incredible synthetic and medicinal utility. This thesis presents several projects that further expand the scope of Pd-catalyzed decarboxylative allylic alkylation and examine its applications to the synthesis of medicinally important small molecules. The synthesis of chiral *gem*-disubstituted five-, six-, and seven-membered diazaheterocycles is presented. Their utility as building blocks for complex medicinal compounds is highlighted. Then, we explore the utility of gem-disubstituted heterocycles in the context of medicinal chemistry.

PUBLISHED CONTENT AND CONTRIBUTIONS

1. Sun, A. Discussion Addendum for: Preparation of (S)-Tert-ButylPHOX and (S)-2-Allyl-2-Methylcyclohexanone. *Org. Synth.* **2018**, *95*, 439–454. DOI: 10.15227/orgsyn.095.0439.

   A.W.S. led the writing of this review manuscript.

2. Sun, A. W.;‡ Hess, S. N.;‡ Stoltz, B. M. Enantioselective Synthesis of Gem-Disubstituted N-Boc Diazaheterocycles via Decarboxylative Asymmetric Allylic Alkylation. *Chem. Sci.* **2019**, *10*, 788–792. DOI: 10.1039/C8SC03967D.

   A.W.S. led project design, experimental work, data acquisition and analysis, and manuscript preparation.

   .

TABLE OF CONTENTS

Dedication iii
Acknowledgements iv
Abstract vii
Published Content and Contributions vii
Table of Contents viii
List of Figures xii
List of Schemes xxiii
List of Tables xxv
List of Abbreviations xxvii

CHAPTER 1 ***1***
Enantioselective Synthesis of gem-Disubstituted N-Boc Diazaheterocycles via Decarboxylative Asymmetric Allylic Alkylation

1.1 Introduction 1
1.2 Piperazinone and Tetrahydropyrimidinones 4
1.3 Conclusions 15
1.4 Experimental Section 16
1.4.1 Materials and Methods 16
1.4.1.1 Preparation of Known Compounds 18
1.4.2 Experimental Procedures and Spectroscopic Data 18
1.4.2.1 Procedures for the Synthesis of Piperazinone Allylic Alkylation Substrates 18
1.4.2.2 Procedures for the Synthesis of Tetrahydropyrimidinone Allylic Alkylation Substrates 32
1.4.2.3 General Procedure Allylic Alkylation Optimization Screen 44
1.4.2.4 General Procedure for Pd-Catalyzed Decarboxylative Allylic Alkylation Reactions 45
1.4.2.5 Experimental Procedures and Spectroscopic data for the Pd-Catalyzed Decarboxylative Asymmetric Allylic Alkylation of Piperazinone Substrates 46
1.4.2.6 Experimental Procedures and Spectroscopic Data for the Pd-Catalyzed Decarboxylative Asymmetric Allylic Alkylation of Tetrahydropyrimidinone Substrates 56

1.4.2.7 Experimental Procedure for the Gram Scale Decarboxylative Asymmetric Allylic Alkylation of Benzyl Tetrahydropyrimidinone 1.5e 65
1.4.2.8 Experimental Procedures for the Transformations of Decarboxylative Allylic Alkylation Products 66
1.4.2.9 Determination of Enantiomeric Excess 77
1.5 References and Notes 80

APPENDIX 1 ***89***
Spectra Relevant to Chapter 1

APPENDIX 2 ***203***
Decarboxylative Asymmetric Allylic Alkylation of gem-Disubstituted Diazepanes

A2.1 Introduction 203
A2.2 Conclusions 208
A2.3 Experimental Section 209
A2.3.1 Materials and Methods 209
A2.3.2 Experimental Procedures and Spectroscopic Data 210
A2.3.3 Procedures for the Synthesis of Oxodiazepane Allylic Alkylation Substrates 211
A2.3.4 General Procedure for Allylic Alkylation Optimization Screen 220
A2.3.5 General Procedure for Pd-Catalyzed Decarboxylative Allylic Alkylation Reactions 220
A2.3.6 Experimental Procedures and Spectroscopic data for the Pd-Catalyzed Decarboxylative Asymmetric Allylic Alkylation of Oxodiazepane Substrates 221
A2.4 References and Notes 225

APPENDIX 3 ***227***
Spectra Relevant to Appendix 2

APPENDIX 4 ***254***
Stereoselective Synthesis of α,α-Disubstituted Amino Acids via Decarboxylative Alkylation of Imidazolinones

A4.1 Introduction 254
A4.2 Synthesis of Cyclic Amino Acid Scaffolds 258
A4.3 Decarboxylative Asymmetric Allylic Alkylation of Imidazolinones 260

A4.4 Conclusions....262
A4.5 Experimental Section....263
A4.5.1 Materials and Methods....263
A4.5.2 Experimental Procedures and Spectroscopic Data....264
A4.5.2.1 Procedures for the Synthesis of Imidazolinone Allylic Alkylation Substrates....264
A4.5.2.2 General Procedure for Allylic Alkylation Optimization Screen....271
A4.5.2.3 General Procedure for Pd-Catalyzed Decarboxylative Allylic Alkylation Reactions....272
A4.5.2.4 Experimental Procedures and Spectroscopic data for the Pd-Catalyzed Decarboxylative Asymmetric Allylic Alkylation of Imidazolinone Substrates....272
A4.6 References and Notes....274

APPENDIX 5 ***279***
Spectra Relevant to Appendix 4

CHAPTER 2 ***296***
gem-Disubstituted Morpholine Analogues of Linezolid

2.1 Introduction and Background....296
2.2 Results....298
2.3 Conclusions....307
2.4 Experimental Section....308
2.4.1 Materials and Methods....308
2.4.2 Experimental Procedures and Spectroscopic Data....310
2.4.2.1 Determination of Absolute Configuration of **2.19a** and **2.19b**....310
2.4.2.2 Experimental Procedures for Biological Assays....315
2.4.2.3 Procedures and Spectroscopic Data for the Synthesis of Linezolid Analogues....317
2.4.2.4 Preparation of linezolid analogues via Cu-Catalyzed Ullman Coupling....323
2.5 References and Notes....340

APPENDIX 6 ***346***
Spectra Relevant to Chapter 2

APPENDIX 7 ***384***
Decarboxylative Asymmetric Allylic Alkylation of Tertiary Alcohols

A7.1 Introduction and Background 384
A7.2 Conclusions 391
A7.3 Experimental Section 391
A7.3.1 Materials and Methods 391
A7.3.2 Experimental Procedures and Spectroscopic Data 393
A7.3.2.1 Experimental Procedures and Spectroscopic Data for the Synthesis of Tertiary Alcohol Allylic Alkylation Substrates and Corresponding Decarboxylative Alkylation Products 393
A7.4 References and Notes 413

Comprehensive Bibliography 790
Index 819
About the Author 822

APPENDIX 8 ***417***
Spectra Relevant to Chapter 7

LIST OF FIGURES

CHAPTER 1

Enantioselective Synthesis of gem-Disubstituted N-Boc Diazaheterocycles via Decarboxylative Asymmetric Allylic Alkylation

Figure 1.1 Representative piperazine and piperazine-2-one pharmaceuticals and natural products 4

Figure 1.2 Advantages of chiral gem-disubstituted piperazines 5

APPENDIX 1

Spectra Relevant to Chapter 1

Figure A1.1 ^{1}H NMR (400 MHz, $CDCl_3$) of compound **1.2** 63

Figure A1.2 Infrared spectrum (Thin Film, NaCl) of compound **1.2** 64

Figure A1.3 ^{13}C NMR (101 MHz, $CDCl_3$) of compound **1.2** 64

Figure A1.4 ^{1}H NMR (400 MHz, $CDCl_3$) of compound **1.3b** 65

Figure A1.5 Infrared spectrum (Thin Film, NaCl) of compound **1.3b** 66

Figure A1.6 ^{13}C NMR (101 MHz, $CDCl_3$) of compound **1.3b** 66

Figure A1.7 ^{1}H NMR (400 MHz, $CDCl_3$) of compound **1.3c** 67

Figure A1.8 Infrared spectrum (Thin Film, NaCl) of compound **1.3c** 68

Figure A1.9 ^{13}C NMR (101 MHz, $CDCl_3$) of compound **1.3c** 68

Figure A1.10 ^{1}H NMR (400 MHz, $CDCl_3$) of compound **1.3d** 69

Figure A1.11 Infrared spectrum (Thin Film, NaCl) of compound **1.3d** 70

Figure A1.12 ^{13}C NMR (101 MHz, $CDCl_3$) of compound **1.3d** 70

Figure A1.13 ^{1}H NMR (400 MHz, $CDCl_3$) of compound **1.3e** 71

Figure A1.14 Infrared spectrum (Thin Film, NaCl) of compound **1.3e** 72

Figure A1.15 ^{13}C NMR (101 MHz, $CDCl_3$) of compound **1.3e** 72

Figure A1.16 ^{1}H NMR (400 MHz, $CDCl_3$) of compound **1.3f** 73

Figure A1.17 Infrared spectrum (Thin Film, NaCl) of compound **1.3f** 74

Figure A1.18 ^{13}C NMR (101 MHz, $CDCl_3$) of compound **1.3f** 74

Figure A1.19 ^{1}H NMR (400 MHz, $CDCl_3$) of compound **1.3h** 75

Figure A1.20 Infrared spectrum (Thin Film, NaCl) of compound **1.3h** 76

Figure A1.21 ^{13}C NMR (101 MHz, $CDCl_3$) of compound **1.3h** 76

Figure A1.22 ^{1}H NMR (400 MHz, $CDCl_3$) of compound **1.3i** 77

Figure A1.23 Infrared spectrum (Thin Film, NaCl) of compound **1.3i** 78

Figure A1.24 ^{13}C NMR (101 MHz, $CDCl_3$) of compound **1.3i** 78

Figure A1.25 ^{1}H NMR (400 MHz, $CDCl_3$) of compound **1.3j** 79

Figure A1.26 Infrared spectrum (Thin Film, NaCl) of compound **1.3j** 80

Figure A1.27 ^{13}C NMR (101 MHz, $CDCl_3$) of compound **1.3j** 80

Figure A1.28 ^{1}H NMR (400 MHz, $CDCl_3$) of compound **1.3k** 81
Figure A1.29 Infrared spectrum (Thin Film, NaCl) of compound **1.3k** 82
Figure A1.30 ^{13}C NMR (101 MHz, $CDCl_3$) of compound **1.3k** 82
Figure A1.31 ^{1}H NMR (400 MHz, $CDCl_3$) of compound **1.3l** 83
Figure A1.32 Infrared spectrum (Thin Film, NaCl) of compound **1.3l** 84
Figure A1.33 ^{13}C NMR (101 MHz, $CDCl_3$) of compound **1.3l** 84
Figure A1.34 ^{1}H NMR (400 MHz, $CDCl_3$) of compound **1.3m** 85
Figure A1.35 Infrared spectrum (Thin Film, NaCl) of compound **1.3m** 86
Figure A1.36 ^{13}C NMR (101 MHz, $CDCl_3$) of compound **1.3m** 86
Figure A1.37 ^{1}H NMR (400 MHz, $CDCl_3$) of compound **1.4a** 87
Figure A1.38 Infrared spectrum (Thin Film, NaCl) of compound **1.4a** 88
Figure A1.39 ^{13}C NMR (101 MHz, $CDCl_3$) of compound **1.4a** 88
Figure A1.40 ^{1}H NMR (400 MHz, $CDCl_3$) of compound **1.4b** 89
Figure A1.41 Infrared spectrum (Thin Film, NaCl) of compound **1.4b** 90
Figure A1.42 ^{13}C NMR (101 MHz, $CDCl_3$) of compound **1.4b** 90
Figure A1.43 ^{1}H NMR (400 MHz, $CDCl_3$) of compound **1.4c** 91
Figure A1.44 Infrared spectrum (Thin Film, NaCl) of compound **1.4c** 92
Figure A1.45 ^{13}C NMR (101 MHz, $CDCl_3$) of compound **1.4c** 92
Figure A1.46 ^{1}H NMR (400 MHz, $CDCl_3$) of compound **1.4d** 93
Figure A1.47 Infrared spectrum (Thin Film, NaCl) of compound **1.4d** 94
Figure A1.48 ^{13}C NMR (101 MHz, $CDCl_3$) of compound **1.4d** 94
Figure A1.49 ^{1}H NMR (400 MHz, $CDCl_3$) of compound **1.4e** 95
Figure A1.50 Infrared spectrum (Thin Film, NaCl) of compound **1.4e** 96
Figure A1.51 ^{13}C NMR (101 MHz, $CDCl_3$) of compound **1.4e** 96
Figure A1.52 ^{1}H NMR (400 MHz, $CDCl_3$) of compound **1.4f** 97
Figure A1.53 Infrared spectrum (Thin Film, NaCl) of compound **1.4f** 98
Figure A1.54 ^{13}C NMR (101 MHz, $CDCl_3$) of compound **1.4f** 98
Figure A1.55 ^{1}H NMR (400 MHz, $CDCl_3$) of compound **1.4h** 99
Figure A1.56 Infrared spectrum (Thin Film, NaCl) of compound **1.4h** 100
Figure A1.57 ^{13}C NMR (101 MHz, $CDCl_3$) of compound **1.4h** 100
Figure A1.58 ^{1}H NMR (400 MHz, $CDCl_3$) of compound **1.4i** 101
Figure A1.59 Infrared spectrum (Thin Film, NaCl) of compound **1.4i** 102
Figure A1.60 ^{13}C NMR (101 MHz, $CDCl_3$) of compound **1.4i** 102
Figure A1.61 ^{1}H NMR (400 MHz, $CDCl_3$) of compound **1.4j** 103
Figure A1.62 Infrared spectrum (Thin Film, NaCl) of compound **1.4j** 104
Figure A1.63 ^{13}C NMR (101 MHz, $CDCl_3$) of compound **1.4j** 104
Figure A1.64 ^{1}H NMR (400 MHz, $CDCl_3$) of compound **1.4k** 105
Figure A1.65 Infrared spectrum (Thin Film, NaCl) of compound **1.4k** 106

Figure A1.66 ^{13}C NMR (101 MHz, $CDCl_3$) of compound **1.4k** 106
Figure A1.67 ^{1}H NMR (400 MHz, $CDCl_3$) of compound **1.4l** 107
Figure A1.68 Infrared spectrum (Thin Film, NaCl) of compound **1.4l** 108
Figure A1.69 ^{13}C NMR (101 MHz, $CDCl_3$) of compound **1.4l** 108
Figure A1.70 ^{1}H NMR (400 MHz, $CDCl_3$) of compound **1.4m** 109
Figure A1.71 Infrared spectrum (Thin Film, NaCl) of compound **1.4m** 110
Figure A1.72 ^{13}C NMR (101 MHz, $CDCl_3$) of compound **1.4m** 110
Figure A1.73 ^{1}H NMR (400 MHz, $CDCl_3$) of compound **1.5a** 111
Figure A1.74 Infrared spectrum (Thin Film, NaCl) of compound **1.5a** 112
Figure A1.75 ^{13}C NMR (101 MHz, $CDCl_3$) of compound **1.5a** 112
Figure A1.73 ^{1}H NMR (400 MHz, $CDCl_3$) of compound **1.5b** 111
Figure A1.74 Infrared spectrum (Thin Film, NaCl) of compound **1.5b** 112
Figure A1.75 ^{13}C NMR (101 MHz, $CDCl_3$) of compound **1.5b** 112
Figure A1.76 NOESY (400 MHz, $CDCl_3$) of compound **1.5c** 113
Figure A1.77 ^{1}H NMR (400 MHz, $CDCl_3$) of compound **1.5c** 114
Figure A1.78 Infrared spectrum (Thin Film, NaCl) of compound **1.5c** 115
Figure A1.79 ^{13}C NMR (101 MHz, $CDCl_3$) of compound **66** 115
Figure A1.80 ^{1}H NMR (400 MHz, $CDCl_3$) of compound **1.5d** 81
Figure A1.81 Infrared spectrum (Thin Film, NaCl) of compound **1.5d** 82
Figure A1.82 ^{13}C NMR (101 MHz, $CDCl_3$) of compound **1.5e** 82
Figure A1.83 ^{1}H NMR (400 MHz, $CDCl_3$) of compound **1.5e** 83
Figure A1.84 Infrared spectrum (Thin Film, NaCl) of compound **1.5e** 84
Figure A1.85 ^{13}C NMR (101 MHz, $CDCl_3$) of compound **1.5f** 84
Figure A1.86 ^{1}H NMR (400 MHz, $CDCl_3$) of compound **1.5f** 85
Figure A1.87 Infrared spectrum (Thin Film, NaCl) of compound **1.5f** 86
Figure A1.88 ^{13}C NMR (101 MHz, $CDCl_3$) of compound **1.5g** 86
Figure A1.89 ^{1}H NMR (400 MHz, $CDCl_3$) of compound **1.5g** 87
Figure A1.90 Infrared spectrum (Thin Film, NaCl) of compound **1.5g** 88
Figure A1.91 ^{13}C NMR (101 MHz, $CDCl_3$) of compound **1.5h** 88
Figure A1.92 ^{1}H NMR (400 MHz, $CDCl_3$) of compound **1.5h** 89
Figure A1.93 Infrared spectrum (Thin Film, NaCl) of compound **1.5h** 90
Figure A1.94 ^{13}C NMR (101 MHz, $CDCl_3$) of compound **1.5i** 90
Figure A1.95 ^{1}H NMR (400 MHz, $CDCl_3$) of compound **1.5i** 91
Figure A1.96 Infrared spectrum (Thin Film, NaCl) of compound **1.5i** 92
Figure A1.97 ^{13}C NMR (101 MHz, $CDCl_3$) of compound **1.6a** 92
Figure A1.98 ^{1}H NMR (400 MHz, $CDCl_3$) of compound **1.6a** 93
Figure A1.99 Infrared spectrum (Thin Film, NaCl) of compound **1.6a** 94
Figure A1.100 ^{13}C NMR (101 MHz, $CDCl_3$) of compound **1.6b** 94

Figure A1.101 ^{1}H NMR (400 MHz, $CDCl_3$) of compound **1.6b** 95
Figure A1.102 Infrared spectrum (Thin Film, NaCl) of compound **1.6b** 96
Figure A1.103 ^{13}C NMR (101 MHz, $CDCl_3$) of compound **1.6c** 96
Figure A1.104 ^{1}H NMR (400 MHz, $CDCl_3$) of compound **1.6c** 97
Figure A1.105 Infrared spectrum (Thin Film, NaCl) of compound **1.6c** 98
Figure A1.106 ^{13}C NMR (101 MHz, $CDCl_3$) of compound **1.6d** 98
Figure A1.107 ^{1}H NMR (400 MHz, $CDCl_3$) of compound **1.6d** 99
Figure A1.108 Infrared spectrum (Thin Film, NaCl) of compound **1.6d** 100
Figure A1.109 ^{13}C NMR (101 MHz, $CDCl_3$) of compound **1.6e** 100
Figure A1.110 ^{1}H NMR (400 MHz, $CDCl_3$) of compound **1.6e** 101
Figure A1.111 Infrared spectrum (Thin Film, NaCl) of compound **1.6e** 102
Figure A1.112 ^{13}C NMR (101 MHz, $CDCl_3$) of compound **1.6f** 102
Figure A1.113 ^{1}H NMR (400 MHz, $CDCl_3$) of compound **1.6f** 103
Figure A1.114 Infrared spectrum (Thin Film, NaCl) of compound **1.6f** 104
Figure A1.115 ^{13}C NMR (101 MHz, $CDCl_3$) of compound **1.6f** 104
Figure A1.116 ^{1}H NMR (400 MHz, $CDCl_3$) of compound **1.6f** 105
Figure A1.117 Infrared spectrum (Thin Film, NaCl) of compound **1.6f** 106
Figure A1.118 ^{13}C NMR (101 MHz, $CDCl_3$) of compound **1.6g** 106
Figure A1.119 ^{1}H NMR (400 MHz, $CDCl_3$) of compound **1.6g** 107
Figure A1.120 Infrared spectrum (Thin Film, NaCl) of compound **1.6g** 108
Figure A1.121 ^{13}C NMR (101 MHz, $CDCl_3$) of compound **1.6h** 108
Figure A1.122 ^{1}H NMR (400 MHz, $CDCl_3$) of compound **1.6h** 109
Figure A1.123 Infrared spectrum (Thin Film, NaCl) of compound **1.6h** 110
Figure A1.124 ^{13}C NMR (101 MHz, $CDCl_3$) of compound **1.6i** 110
Figure A1.125 ^{1}H NMR (400 MHz, $CDCl_3$) of compound **1.6i** 111
Figure A1.126 Infrared spectrum (Thin Film, NaCl) of compound **1.6i** 112
Figure A1.127 ^{13}C NMR (101 MHz, $CDCl_3$) of compound **1.8** 112
Figure A1.128 ^{1}H NMR (400 MHz, $CDCl_3$) of compound **1.8** 111
Figure A1.129 Infrared spectrum (Thin Film, NaCl) of compound **1.8** 112
Figure A1.130 ^{13}C NMR (101 MHz, $CDCl_3$) of compound **1.9** 112
Figure A1.131 NOESY (400 MHz, $CDCl_3$) of compound **1.9** 113
Figure A1.132 ^{1}H NMR (400 MHz, $CDCl_3$) of compound **1.9** 114
Figure A1.133 Infrared spectrum (Thin Film, NaCl) of compound **1.10** 115
Figure A1.134 ^{13}C NMR (101 MHz, $CDCl_3$) of compound **1.10** 115
Figure A1.135 ^{1}H NMR (400 MHz, $CDCl_3$) of compound **1.10** 81
Figure A1.136 Infrared spectrum (Thin Film, NaCl) of compound **1.11** 82
Figure A1.137 ^{13}C NMR (101 MHz, $CDCl_3$) of compound **1.11** 82
Figure A1.138 ^{1}H NMR (400 MHz, $CDCl_3$) of compound **1.11** 83

Figure A1.139 Infrared spectrum (Thin Film, NaCl) of compound **1.12** 84
Figure A1.140 ^{13}C NMR (101 MHz, $CDCl_3$) of compound **1.12** 84
Figure A1.141 ^{1}H NMR (400 MHz, $CDCl_3$) of compound **1.12** 85
Figure A1.142 Infrared spectrum (Thin Film, NaCl) of compound **1.13** 86
Figure A1.143 ^{13}C NMR (101 MHz, $CDCl_3$) of compound **1.13** 86
Figure A1.144 ^{1}H NMR (400 MHz, $CDCl_3$) of compound **1.13** 87
Figure A1.145 Infrared spectrum (Thin Film, NaCl) of compound **1.14** 88
Figure A1.146 ^{13}C NMR (101 MHz, $CDCl_3$) of compound **1.14** 88
Figure A1.147 ^{1}H NMR (400 MHz, $CDCl_3$) of compound **1.14** 89
Figure A1.148 Infrared spectrum (Thin Film, NaCl) of compound **1.15** 90
Figure A1.149 ^{13}C NMR (101 MHz, $CDCl_3$) of compound **1.15** 90
Figure A1.150 ^{1}H NMR (400 MHz, $CDCl_3$) of compound **1.15** 91
Figure A1.151 Infrared spectrum (Thin Film, NaCl) of compound **1.15** 92
Figure A1.152 ^{13}C NMR (101 MHz, $CDCl_3$) of compound **1.16** 92
Figure A1.153 ^{1}H NMR (400 MHz, $CDCl_3$) of compound **1.16** 93
Figure A1.154 Infrared spectrum (Thin Film, NaCl) of compound **1.16** 94
Figure A1.155 ^{13}C NMR (101 MHz, $CDCl_3$) of compound **SI-3** 94
Figure A1.156 Infrared spectrum (Thin Film, NaCl) of compound **SI-3** 84
Figure A1.157 ^{13}C NMR (101 MHz, $CDCl_3$) of compound **SI-3** 84
Figure A1.158 ^{1}H NMR (400 MHz, $CDCl_3$) of compound **SI-4** 85
Figure A1.159 Infrared spectrum (Thin Film, NaCl) of compound **SI-4** 86
Figure A1.160 ^{13}C NMR (101 MHz, $CDCl_3$) of compound **SI-4** 86
Figure A1.161 ^{1}H NMR (400 MHz, $CDCl_3$) of compound **SI-5** 87
Figure A1.162 Infrared spectrum (Thin Film, NaCl) of compound **SI-5** 88
Figure A1.163 ^{13}C NMR (101 MHz, $CDCl_3$) of compound **SI-5** 88
Figure A1.164 ^{1}H NMR (400 MHz, $CDCl_3$) of compound **SI-6** 89
Figure A1.165 Infrared spectrum (Thin Film, NaCl) of compound **SI-6** 90
Figure A1.166 ^{13}C NMR (101 MHz, $CDCl_3$) of compound **SI-6** 90

APPENDIX 2

Decarboxylative Asymmetric Allylic Alkylation of gem-Disubstituted Diazepanes

Figure A2.1 Diazepines and diazepanes are medicinally important heterocycles 117
Figure A2.2 gem-Disubstituted diazepanes can augment biological properties of small molecules 125

APPENDIX 3

Spectra Relevant to Appendix 2

Figure A3.1 ^{1}H NMR (400 MHz, $CDCl_3$) of compound **A2S1** 169

Figure A3.2 Infrared spectrum (Thin Film, NaCl) of compound **A2S1** 170

Figure A3.3 ^{13}C NMR (101 MHz, $CDCl_3$) of compound **A2S1** 170

Figure A3.4 ^{1}H NMR (400 MHz, $CDCl_3$) of compound **A2S3** 171

Figure A3.5 Infrared spectrum (Thin Film, NaCl) of compound **A2S3** 172

Figure A3.6 ^{13}C NMR (101 MHz, $CDCl_3$) of compound **A2S3** 172

Figure A3.7 ^{1}H NMR (400 MHz, $CDCl_3$) of compound **A2S4** 173

Figure A3.8 Infrared spectrum (Thin Film, NaCl) of compound **A2S4** 174

Figure A3.9 ^{13}C NMR (101 MHz, $CDCl_3$) of compound **A2S4** 174

Figure A3.10 ^{1}H NMR (400 MHz, $CDCl_3$) of compound **A2.4f** 175

Figure A3.11 Infrared spectrum (Thin Film, NaCl) of compound **A2.4f** 176

Figure A3.12 ^{13}C NMR (101 MHz, $CDCl_3$) of compound **A2.4f** 176

Figure A3.13 ^{1}H NMR (400 MHz, $CDCl_3$) of compound **A2.4g** 177

Figure A3.14 Infrared spectrum (Thin Film, NaCl) of compound **A2.4g** 178

Figure A3.15 ^{13}C NMR (101 MHz, $CDCl_3$) of compound **A2.4g** 178

Figure A3.16 ^{1}H NMR (400 MHz, $CDCl_3$) of compound **A2.4h** 179

Figure A3.17 Infrared spectrum (Thin Film, NaCl) of compound **A2.4h** 180

Figure A3.18 ^{13}C NMR (101 MHz, $CDCl_3$) of compound **A2.4h** 180

Figure A3.19 ^{1}H NMR (400 MHz, $CDCl_3$) of compound **A2.4i** 181

Figure A3.20 Infrared spectrum (Thin Film, NaCl) of compound **A2.4i** 182

Figure A3.21 ^{13}C NMR (101 MHz, $CDCl_3$) of compound **A2.4i** 182

Figure A3.22 ^{1}H NMR (400 MHz, $CDCl_3$) of compound **A2.4j** 183

Figure A3.23 Infrared spectrum (Thin Film, NaCl) of compound **A2.4j** 184

Figure A3.24 ^{13}C NMR (101 MHz, $CDCl_3$) of compound **A2.4j** 184

Figure A3.25 ^{1}H NMR (400 MHz, $CDCl_3$) of compound **A2.4l** 185

Figure A3.26 Infrared spectrum (Thin Film, NaCl) of compound **A2.4l** 186

Figure A3.27 ^{13}C NMR (101 MHz, $CDCl_3$) of compound **A2.4l** 186

Figure A3.28 ^{1}H NMR (400 MHz, $CDCl_3$) of compound **A2.5f** 187

Figure A3.29 Infrared spectrum (Thin Film, NaCl) of compound **A2.5f** 188

Figure A3.30 ^{13}C NMR (101 MHz, $CDCl_3$) of compound **A2.5f** 188

Figure A3.31 ^{1}H NMR (400 MHz, $CDCl_3$) of compound **A2.5g** 189

Figure A3.32 Infrared spectrum (Thin Film, NaCl) of compound **A2.5g** 190

Figure A3.33 ^{13}C NMR (101 MHz, $CDCl_3$) of compound **A2.5g** 190

Figure A3.34 ^{1}H NMR (400 MHz, $CDCl_3$) of compound **A2.5h** 191

Figure A3.35 Infrared spectrum (Thin Film, NaCl) of compound **A2.5h** 192

Figure A3.36 ^{13}C NMR (101 MHz, $CDCl_3$) of compound **A2.5h** 192

Figure A3.37 ^{1}H NMR (400 MHz, $CDCl_3$) of compound **A2.5l**.....193
Figure A3.38 Infrared spectrum (Thin Film, NaCl) of compound **A2.5l** 194
Figure A3.39 ^{13}C NMR (101 MHz, $CDCl_3$) of compound **A2.5l**.....194

APPENDIX 4

Stereoselective Synthesis of α,α-Disubstituted Amino Acids via Decarboxylative Alkylation of Imidazolinones

Figure A4.1 Biological important of disubstituted amino acids 250

APPENDIX 5

Spectra Relevant to Appendix 4

Figure A5.1 ^{1}H NMR (400 MHz, $CDCl_3$) of compound **A4.8**.....370
Figure A5.2 Infrared spectrum (Thin Film, NaCl) of compound **A4.8** 371
Figure A5.3 ^{13}C NMR (101 MHz, $CDCl_3$) of compound **A4.8**.....371
Figure A5.4 ^{1}H NMR (400 MHz, $CDCl_3$) of compound **A4.9**.....372
Figure A5.5 Infrared spectrum (Thin Film, NaCl) of compound **A4.9** 373
Figure A5.6 ^{13}C NMR (101 MHz, $CDCl_3$) of compound **A4.9**.....373
Figure A5.7 ^{1}H NMR (400 MHz, $CDCl_3$) of compound **A4.11b** 374
Figure A5.8 Infrared spectrum (Thin Film, NaCl) of compound **A4.11b** 375
Figure A5.9 ^{13}C NMR (101 MHz, $CDCl_3$) of compound **A4.11b**.....375
Figure A5.10 ^{1}H NMR (400 MHz, $CDCl_3$) of compound **A4.11d**.....376
Figure A5.11 Infrared spectrum (Thin Film, NaCl) of compound **A4.11d** 377
Figure A5.12 ^{13}C NMR (101 MHz, $CDCl_3$) of compound **A4.11c**d.....377
Figure A5.13 ^{1}H NMR (400 MHz, $CDCl_3$) of compound **A4.11c** 378
Figure A5.14 Infrared spectrum (Thin Film, NaCl) of compound **A4.11c** 379
Figure A5.15 ^{13}C NMR (101 MHz, $CDCl_3$) of compound **A4.11c**.....379
Figure A5.16 ^{1}H NMR (400 MHz, $CDCl_3$) of compound **A4.11e** 380
Figure A5.17 Infrared spectrum (Thin Film, NaCl) of compound **A4.11e** 381
Figure A5.18 ^{13}C NMR (101 MHz, $CDCl_3$) of compound **A4.11e**.....381
Figure A5.19 ^{1}H NMR (400 MHz, $CDCl_3$) of compound **A4.10**.....382
Figure A5.20 Infrared spectrum (Thin Film, NaCl) of compound **A4.10** 383
Figure A5.21 ^{13}C NMR (101 MHz, $CDCl_3$) of compound **A4.10**.....383
Figure A5.22 ^{1}H NMR (400 MHz, $CDCl_3$) of compound **A4.12b** 384
Figure A5.23 Infrared spectrum (Thin Film, NaCl) of compound **A4.12b** 385
Figure A5.24 ^{13}C NMR (101 MHz, $CDCl_3$) of compound **A4.12b**.....385

APPENDIX 6

Spectra Relevant to Chapter 2

Figure A6.1 ^{1}H NMR (400 MHz, $CDCl_3$) of compound **2.5** 370

Figure A6.2 Infrared spectrum (Thin Film, NaCl) of compound **2.5** 371

Figure A6.3 ^{13}C NMR (101 MHz, $CDCl_3$) of compound **2.5** 371

Figure A6.4 ^{1}H NMR (400 MHz, $CDCl_3$) of compound **2.10** 372

Figure A6.5 Infrared spectrum (Thin Film, NaCl) of compound **2.10** 373

Figure A6.6 ^{13}C NMR (101 MHz, $CDCl_3$) of compound **2.10** 373

Figure A6.7 ^{1}H NMR (400 MHz, $CDCl_3$) of compound **2.12** 374

Figure A6.8 Infrared spectrum (Thin Film, NaCl) of compound **2.12** 375

Figure A6.9 ^{13}C NMR (101 MHz, $CDCl_3$) of compound **2.12** 375

Figure A6.10 ^{1}H NMR (400 MHz, $CDCl_3$) of compound **2.13** 376

Figure A6.11 Infrared spectrum (Thin Film, NaCl) of compound **2.13** 377

Figure A6.12 ^{13}C NMR (101 MHz, $CDCl_3$) of compound **2.13** 377

Figure A6.13 ^{1}H NMR (400 MHz, $CDCl_3$) of compound **2.14** 378

Figure A6.14 Infrared spectrum (Thin Film, NaCl) of compound **2.14** 379

Figure A6.15 ^{13}C NMR (101 MHz, $CDCl_3$) of compound **2.14** 379

Figure A6.16 ^{1}H NMR (400 MHz, $CDCl_3$) of compound **2.17** 380

Figure A6.17 Infrared spectrum (Thin Film, NaCl) of compound **2.17** 381

Figure A6.18 ^{13}C NMR (101 MHz, $CDCl_3$) of compound **2.17** 381

Figure A6.19 ^{1}H NMR (400 MHz, $CDCl_3$) of compound **2.18** 382

Figure A6.20 Infrared spectrum (Thin Film, NaCl) of compound **2.18** 383

Figure A6.21 ^{13}C NMR (101 MHz, $CDCl_3$) of compound **2.18** 383

Figure A6.22 ^{1}H NMR (400 MHz, $CDCl_3$) of compound **2.19a** 384

Figure A6.23 Infrared spectrum (Thin Film, NaCl) of compound **2.19a** 385

Figure A6.24 ^{13}C NMR (101 MHz, $CDCl_3$) of compound **2.19a** 385

Figure A6.25 ^{1}H NMR (400 MHz, $CDCl_3$) of compound **2.19b** 386

Figure A6.26 Infrared spectrum (Thin Film, NaCl) of compound **2.19b** 387

Figure A6.27 ^{13}C NMR (101 MHz, $CDCl_3$) of compound **2.19b** 387

Figure A6.28 ^{1}H NMR (400 MHz, $CDCl_3$) of compound **2.21** 388

Figure A6.29 Infrared spectrum (Thin Film, NaCl) of compound **2.21** 389

Figure A6.30 ^{13}C NMR (101 MHz, $CDCl_3$) of compound **2.21** 389

Figure A6.31 ^{1}H NMR (400 MHz, $CDCl_3$) of compound **2.22** 390

Figure A6.32 Infrared spectrum (Thin Film, NaCl) of compound **2.22** 391

Figure A6.33 ^{13}C NMR (101 MHz, $CDCl_3$) of compound **2.22** 391

Figure A6.34 ^{1}H NMR (400 MHz, $CDCl_3$) of compound **2.23** 392

Figure A6.35 Infrared spectrum (Thin Film, NaCl) of compound **2.23** 393

Figure A6.36 ^{13}C NMR (101 MHz, $CDCl_3$) of compound **2.23** 393

Figure A6.37 ^{1}H NMR (400 MHz, $CDCl_3$) of compound **2.24** 394
Figure A6.38 Infrared spectrum (Thin Film, NaCl) of compound **2.24** 395
Figure A6.39 ^{13}C NMR (101 MHz, $CDCl_3$) of compound **2.24** 395
Figure A6.40 ^{1}H NMR (400 MHz, $CDCl_3$) of compound **2.25** 396
Figure A6.41 Infrared spectrum (Thin Film, NaCl) of compound **2.25** 397
Figure A6.42 ^{13}C NMR (101 MHz, $CDCl_3$) of compound **2.25** 397
Figure A6.43 ^{1}H NMR (400 MHz, $CDCl_3$) of compound **2.26** 398
Figure A6.44 Infrared spectrum (Thin Film, NaCl) of compound **2.26** 399
Figure A6.45 ^{13}C NMR (101 MHz, $CDCl_3$) of compound **2.26** 399
Figure A6.46 ^{1}H NMR (400 MHz, $CDCl_3$) of compound **2.27** 400
Figure A6.47 Infrared spectrum (Thin Film, NaCl) of compound **2.27** 401
Figure A6.48 ^{13}C NMR (101 MHz, $CDCl_3$) of compound **2.27** 401
Figure A6.49 ^{1}H NMR (400 MHz, $CDCl_3$) of compound **2.27** 402
Figure A6.50 Infrared spectrum (Thin Film, NaCl) of compound **SI3a** 403
Figure A6.51 ^{13}C NMR (101 MHz, $CDCl_3$) of compound **SI3a** 403
Figure A6.52 ^{1}H NMR (400 MHz, $CDCl_3$) of compound **SI4** 404
Figure A6.53 Infrared spectrum (Thin Film, NaCl) of compound **SI4** 405
Figure A6.54 ^{13}C NMR (101 MHz, $CDCl_3$) of compound **SI4** 405

CHAPTER 2
gem-Disubstituted Morpholine Analogues of Linezolid

Figure 2.1 N-Heterocycles are valuable components of small molecule drugs. 141
Figure 2.2 Substitution patterns of common saturated heterocycles found in small molecule drugs. 141
Figure 2.3 Biological properties altered by hypothetical gem-disubstitution of the antibiotic linezolid.. 141
Figure 2.4 Summary of oxazolidinone antibiotics 141
Figure 2.5 gem-Disubstituted linezolid analogues synthesized via Ullmann coupling. .. 141
Figure 2.6 Diastereomers of analogue **2.19**. 141

APPENDIX 8
Spectra Relevant to Appendix 7

Figure A8.1 ^{1}H NMR (500 MHz, $CDCl_3$) of compound **A7.1** 530
Figure A8.2 Infrared spectrum (Thin Film, NaCl) of compound **A7.1** 531
Figure A8.3 ^{13}C NMR (125 MHz, $CDCl_3$) of compound **A7.1** 531
Figure A8.4 ^{1}H NMR (500 MHz, $CDCl_3$) of compound **A7.2** 532
Figure A8.5 Infrared spectrum (Thin Film, NaCl) of compound **A7.2** 533

Figure A8.6 ^{13}C NMR (125 MHz, $CDCl_3$) of compound **A7.2** 533
Figure A8.7 ^{1}H NMR (500 MHz, $CDCl_3$) of compound **A7.3** 534
Figure A8.8 Infrared spectrum (Thin Film, NaCl) of compound **A7.3** 535
Figure A8.9 ^{13}C NMR (125 MHz, $CDCl_3$) of compound **A7.3** 535
Figure A8.10 ^{1}H NMR (500 MHz, $CDCl_3$) of compound **A7.5** 536
Figure A8.11 Infrared spectrum (Thin Film, NaCl) of compound **A7.5** 537
Figure A8.12 ^{13}C NMR (125 MHz, $CDCl_3$) of compound **A7.5** 537
Figure A8.13 ^{1}H NMR (500 MHz, $CDCl_3$) of compound **A7.6a** 538
Figure A8.14 Infrared spectrum (Thin Film, NaCl) of compound **A7.6a** 539
Figure A8.15 ^{13}C NMR (125 MHz, $CDCl_3$) of compound **A7.6a** 539
Figure A8.16 ^{1}H NMR (500 MHz, $CDCl_3$) of compound **A7.6b** 540
Figure A8.17 Infrared spectrum (Thin Film, NaCl) of compound **A7.6b** 541
Figure A8.18 ^{13}C NMR (125 MHz, $CDCl_3$) of compound **A7.6b** 541
Figure A8.19 ^{1}H NMR (500 MHz, $CDCl_3$) of compound **A7.6c** 542
Figure A8.20 Infrared spectrum (Thin Film, NaCl) of compound **A7.6c** 543
Figure A8.21 ^{13}C NMR (125 MHz, $CDCl_3$) of compound **A7.6c** 543
Figure A8.22 ^{1}H NMR (500 MHz, $CDCl_3$) of compound **A7.6d** 544
Figure A8.23 Infrared spectrum (Thin Film, NaCl) of compound **A7.6d** 545
Figure A8.24 ^{13}C NMR (125 MHz, $CDCl_3$) of compound **A7.6d** 545
Figure A8.25 ^{1}H NMR (500 MHz, $CDCl_3$) of compound **A7.6d** 546
Figure A8.26 Infrared spectrum (Thin Film, NaCl) of compound **A7.6d** 547
Figure A8.27 ^{13}C NMR (125 MHz, $CDCl_3$) of compound **A7.6d** 547
Figure A8.28 ^{1}H NMR (500 MHz, $CDCl_3$) of compound **A7.6e** 548
Figure A8.29 Infrared spectrum (Thin Film, NaCl) of compound **A7.6e** 549
Figure A8.30 ^{13}C NMR (125 MHz, $CDCl_3$) of compound **A7.6e** 549
Figure A8.31 ^{1}H NMR (500 MHz, $CDCl_3$) of compound **A7.7a** 550
Figure A8.32 Infrared spectrum (Thin Film, NaCl) of compound **A7.7a** 551
Figure A8.33 ^{13}C NMR (125 MHz, $CDCl_3$) of compound **A7.7a** 551
Figure A8.34 ^{1}H NMR (500 MHz, $CDCl_3$) of compound **A7.7b** 552
Figure A8.35 Infrared spectrum (Thin Film, NaCl) of compound **A7.7b** 553
Figure A8.36 ^{13}C NMR (125 MHz, $CDCl_3$) of compound **A7.7b** 553
Figure A8.37 ^{1}H NMR (500 MHz, $CDCl_3$) of compound **A7.7c** 554
Figure A8.38 Infrared spectrum (Thin Film, NaCl) of compound **A7.7c** 555
Figure A8.39 ^{13}C NMR (125 MHz, $CDCl_3$) of compound **A7.7c** 555
Figure A8.40 ^{1}H NMR (500 MHz, $CDCl_3$) of compound **A7.7d** 556
Figure A8.41 Infrared spectrum (Thin Film, NaCl) of compound **A7.7d** 557
Figure A8.42 ^{13}C NMR (125 MHz, $CDCl_3$) of compound **A7.7d** 557
Figure A8.43 ^{1}H NMR (500 MHz, $CDCl_3$) of compound **A7.7e** 558

Figure A8.44 Infrared spectrum (Thin Film, NaCl) of compound **A7.7e** 559
Figure A8.45 ^{13}C NMR (125 MHz, $CDCl_3$) of compound **A7.7e** 559
Figure A8.46 ^{19}F vs ^{13}C HSQC (376 MHz, $CDCl_3$) of compound **A7.8**.....560
Figure A8.47 ^{1}H NMR (500 MHz, $CDCl_3$) of compound **A7.8**.....561
Figure A8.48 Infrared spectrum (Thin Film, NaCl) of compound **A7.8** 562
Figure A8.49 ^{13}C NMR (125 MHz, $CDCl_3$) of compound **A7.9**.....562
Figure A8.50 ^{1}H NMR (500 MHz, $CDCl_3$) of compound **A7.9**.....563
Figure A8.51 Infrared spectrum (Thin Film, NaCl) of compound **A7.9** 564
Figure A8.52 ^{13}C NMR (125 MHz, $CDCl_3$) of compound **A7.11**.....564
Figure A8.53 ^{1}H NMR (500 MHz, $CDCl_3$) of compound **A7.11**.....565
Figure A8.54 Infrared spectrum (Thin Film, NaCl) of compound **A7.11** 566

LIST OF SCHEMES

CHAPTER 1

Enantioselective Synthesis of gem-Disubstituted N-Boc Diazaheterocycles via Decarboxylative Asymmetric Allylic Alkylation

Scheme 1.1 Key Developments in Decarboxylative Allylic Alkylation Reactions 8

Scheme 1.2 Existing approaches for gem-disubstituted piperazines and piperazinones 9

Scheme 1.3 Comparison of routes to piperazin-2-one decarboxylative alkylation substrates. 10

Scheme 1.4 Synthetic approaches toward $\beta^{2,2}$-amino acids using the allylic alkylation reaction 11

Scheme 1.5 Product derivatization 12

CHAPTER 2

gem-Disubstituted Morpholine Analogues of Linezolid

Scheme 2.1 Synthesis of gem-disubstituted linezolid analogues via Cu-catalyzed Ullmann coupling 146

Scheme 2.2 Synthesis of gem-disubstituted morpholines by benzoyl cleavage and reduction of morpholinone decarboxylative alkylation products 146

Scheme 2.3 Additional analogues synthesized by derivatization 146

APPENDIX 2

Decarboxylative Asymmetric Allylic Alkylation of gem-Disubstituted Diazepanes

Scheme A2.1 Synthetic route toward diazepane DAAA substrates 472

Scheme A2.2 *Attempted synthesis of other medicinally relevant DAAA substrates* 475

APPENDIX 4

Stereoselective Synthesis of α,α-Disubstituted Amino Acids via Decarboxylative Alkylation of Imidazolinones

Scheme A4.1 Synthetic methods for disubstituted amino acids 472

Scheme A4.2 Transition metal catalyzed asymmetric allylic alkylation methods 475

Scheme A4.3 Previous attempts toward the decarboxylative alkylation of cyclic amino acid scaffolds 476

Scheme A4.4 Routes toward a cyclic amino acid imidazolinone scaffold.....476

Scheme A4.5 Synthesis of the imidazolinone DAAA substrate.....476

APPENDIX 7
Decarboxylative Asymmetric Allylic Alkylation of Tertiary Alcohols

Scheme A7.1 Approaches toward tertiary α-hydroxy carbonyl compounds 472
Scheme A7.2 Unexpected formation of a tertiary alcohol 475
Scheme A7.3 Mechanistic rationale for formation of isomeric tetralone products.....476
Scheme A7.4 Decarboxylative alkylation of a primary alcohol 476

LIST OF TABLES

CHAPTER 1

Enantioselective Synthesis of gem-Disubstituted N-Boc Diazaheterocycles via Decarboxylative Asymmetric Allylic Alkylation

Table 1.1 Chiral α-disubstituted carbocycles/lactams accessible by decarboxylative allylic alkylation 20

Table 1.2 Optimization of the reaction conditions 23

Table 1.3 Substrate scope exploration 25

Table 1.4 Pd-catalyzed decarboxylative alkylation of tetrahydropyrimidin-2-ones. Scope of α-substituents 36

APPENDIX 2

Decarboxylative Asymmetric Allylic Alkylation of gem-Disubstituted Diazepanes

Table A2.1 Optimization studies on the DAAA of benzyl substrate **A2.4a** 117

Table A2.2 Oxodiazepane substrate scope exploration 118

APPENDIX 4

Stereoselective Synthesis of α,α-Disubstituted Amino Acids via Decarboxylative Alkylation of Imidazolinones

Table A4.1 Initial screening results on carbamate **A4.11a** 143

Table A4.2 Initial screening results on methyl substrate **A4.11b** 144

Table A4.3 Initial Substrate Scope 145

CHAPTER 2

gem-Disubstituted Morpholine Analogues of Linezolid

Table 3.1 Optimization of reaction parameters 204

Table 3.2 Electrophile isomers 205

Table 3.3 Aryl substituent substrate scope 207

Table 3.4 Non-aryl substituent substrate scope 208

Table 3.5 Substrate scope limitations 209

Table 3.6 Determination of enantiomeric excess 242

APPENDIX 7

Decarboxylative Asymmetric Allylic Alkylation of Tertiary Alcohols

Table A7.1 Attempts to optimize reaction conditions for model substrate **A7.3** 432

Table A7.2 Investigation into reaction outcomes for isomeric tetralone **A7.5** 433

Table A7.3 Decarboxylative alkylation of α-hydroxyl dicarbonyl compounds 434

LIST OF ABBREVIATIONS

$[\alpha]_D$	specific rotation at wavelength of sodium D line
°C	degrees Celsius
Ac	acetyl
AcOH	acetic acid
APCI	atmospheric pressure chemical ionization
app	apparent
aq	aqueous
Ar	aryl
atm	atmosphere
Bn	benzyl
Boc	*tert*-butyloxycarbonyl
bp	boiling point
br	broad
Bu	butyl
Bz	benzoyl
c	concentration for specific rotation measurements (g/100 mL)
ca.	about (Latin circa)
calc'd	calculated
cat	catalytic
CDI	1,1'-carbonyldiimidazole
cm^{-1}	wavenumber(s)
CSA	camphorsulfonic acid
Cy	cyclohexyl
d	doublet
D	deuterium
dba	dibenzylideneacetone

DBU	1,8-diazabicyclo[5.4.0]undec-7-ene
DAAA	decarboxylative asymmetric allylic alkylation
DCE	1,2-dichloroethane
DDQ	2,3-dichloro-5,6-dicyano-*p*-benzoquinone
DIPEA	*N,N*-diisopropylethylamine
DMAP	4-dimethylaminopyridine
dmdba	bis(3,5-dimethoxybenzylidene)acetone
DME	1,2-dimethoxyethane
DMF	*N,N*-dimethylformamide
DMSO	dimethyl sulfoxide
dr	diastereomeric ratio
e.g.	for example (Latin exempli gratia)
EDC	*N*-(3-dimethylaminopropyl)-*N′*-ethylcarbodiimide
EDCI	1-ethyl-3-(3-dimethylaminopropyl)carbodiimide
ee	enantiomeric excess
EI+	electron impact
equiv	equivalent(s)
ESI	electrospray ionization
Et	ethyl
EtOAc	ethyl acetate
EWG	electron withdrawing group
FAB	fast atom bombardment
g	gram(s)
GC	gas chromatography
gCOSY	gradient-selected correlation spectroscopy
h	hour(s)
HMBC	heteronuclear multiple bond correlation
HMDS	1,1,1,3,3,3-hexamethyldisilazane
HMPA	hexamethylphosphoramide

HPLC	high-performance liquid chromatography
HRMS	high-resolution mass spectroscopy
HSQC	heteronuclear single quantum correlation
Hz	hertz
$h\nu$	light
i-Pr	isopropyl
i.e.	that is (Latin id est)
IBX	2-iodoxybenzoic acid
IPA	isopropanol, 2-propanol
IR	infrared (spectroscopy)
J	coupling constant
K	Kelvin(s) (absolute temperature)
kcal	kilocalorie
KHMDS	potassium hexamethyldisilazide
L	liter; ligand
L*	chiral ligand
LDA	lithium diisopropylamide
LG	leaving group
lit.	literature value
m	multiplet; milli
m	meta
M	metal; molar; molecular ion
m/z	mass to charge ratio
Me	methyl
mg	milligram(s)
MHz	megahertz
min	minute(s)
MM	mixed method
mol	mole(s)

mp	melting point
Ms	methanesulfonyl (mesyl)
MS	molecular sieves
n	nano
N	normal
n-Bu	butyl
NBS	*N*-bromosuccinimide
NMO	*N*-methylmorpholine *N*-oxide
NMR	nuclear magnetic resonance
Ns	2-nitrobenzenesulfonyl
Nu	nucleophile
o	ortho
p	para
Pd/C	palladium on carbon
Ph	phenyl
pH	hydrogen ion concentration in aqueous solution
PHOX	phosphinooxazoline ligand
p*Ka*	p*K* for association of an acid
pmdba	bis(4-methoxybenzylidene)acetone
ppm	parts per million
PPTS	pyridinium *p*-toluenesulfonate
Pr	propyl
Py	pyridine
q	quartet
R	generic for any atom or functional group
Ref.	reference
R_f	retention factor
s	singlet or strong or selectivity factor
sat.	saturated

SFC	supercritical fluid chromatography
t	triplet
t-Bu	*tert*-butyl
TBAF	tetrabutylammonium fluoride
TBAI	tetrabutylammonium iodide
TBAT	tetrabutylammonium difluorotriphenylsilicate
TBD	1,3,4-triazabicyclo[4.4.0]dec-5-ene
TBHP	*tert*-butyl hydroperoxide
TBME	*tert*-butyl methyl ether
Tf	trifluoromethanesulfonyl (triflyl)
TFA	trifluoroacetic acid
TFAA	trifluoroacetic anhydride
TFE	2,2,2-trifluoroethanol
THF	tetrahydrofuran
TLC	thin-layer chromatography
TMEDA	*N,N,N',N'*-tetramethylethylenediamine
TOF	time-of-flight
Tol	tolyl
t_R	retention time
Ts	*p*-toluenesulfonyl (tosyl)
UV	ultraviolet
v/v	volume to volume
w	weak
w/v	weight to volume
X	anionic ligand or halide
λ	wavelength
μ	micro

CHAPTER 1

Enantioselective Synthesis of gem-Disubstituted N-Boc Diazaheterocycles via Decarboxylative Asymmetric Allylic Alkylation[†]

1.1 INTRODUCTION AND BACKGROUND

The catalytic decarboxylative allylic alkylation, originally reported by Tsuji and Saegusa in 1980,[1,2] is a powerful transformation to effect C–C bond formation between an enolate precursor and an allyl group (Scheme 1.1A). However, an enantioselective version of the reaction was not developed until 2004 by the Tunge and Stoltz groups, who reported enantioselective alkylations of acyclic esters and cyclic allyl enol carbonates using DACH-Trost ligand and (*S*)-*t*-BuPHOX, respectively (Scheme 1.1B & C).[3,4] In 2005, Trost reported a similar carbocyclic system, though using the ANDEN phenyl trost ligand to achieve high stereoselectivity.[5,6] In an important advance, the Stoltz group in 2005 reported the DAAA of *β*-keto allyl esters, which significantly expanded the substrate scope of this

transformation; such bench stable ketoesters can be alkylated under mild basic conditions to afford a variety of decarboxylative alkylation substrates that would normally be difficult to access by other means (Scheme 1.1D).[7]

Scheme. 1.1 *Key Developments in Decarboxylative Allylic Alkylation Reactions*

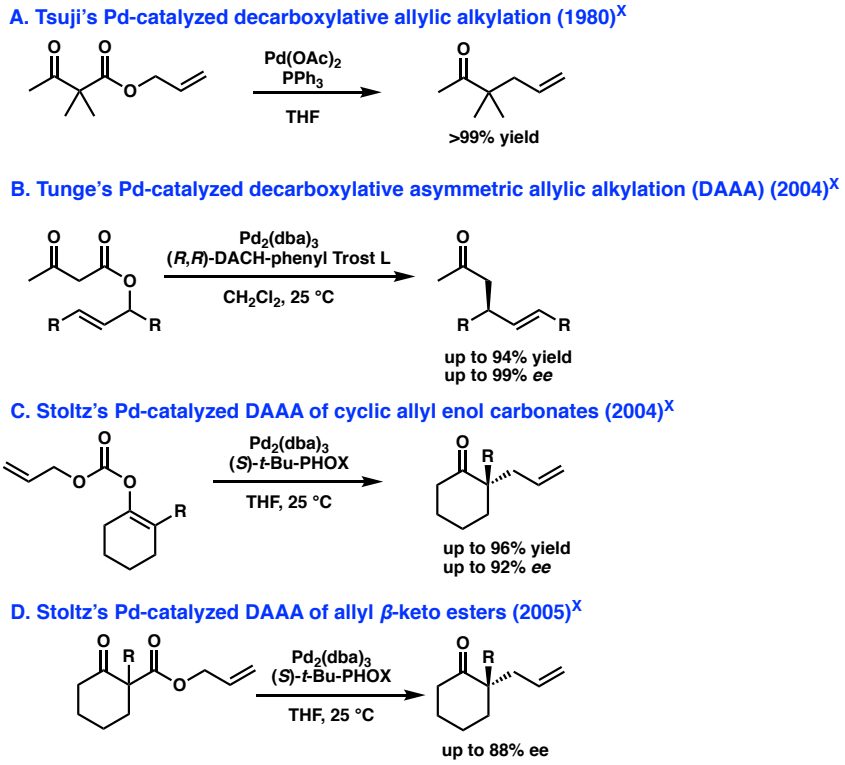

Since these fundamental developments in asymmetric decarboxylative alkylation, numerous groups have further contributed to the expansion of this methodology to encompass a variety of acyclic and cyclic substrates.[8,9] Summarized below in Table 1.1 are some of the many *gem*-disubstituted cyclic products that our laboratory has synthesized utilizing the DAAA reaction, highlighting the incredible versatility of this mild reaction.[4,7,10–16]

Table. 1.1 *Chiral α-disubstituted carbocycles/lactams accessible by decarboxylative allylic alkylation*

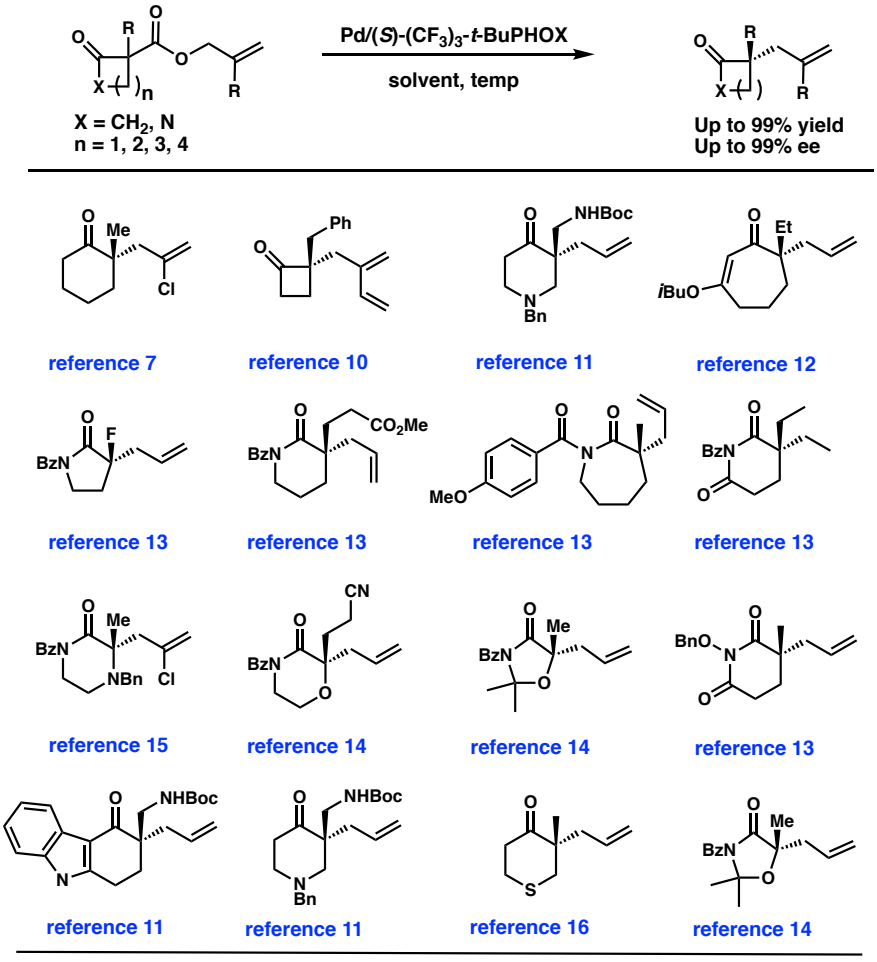

Despite the incredibly broad substrate scope of this reaction, there is still room for innovation, including novel medicinally relevant cyclic scaffolds, and the next frontier: acyclic scaffolds.[17] In this chapter, we describe the extension of the DAAA reaction toward Boc-protected six-membered diazaheterocycles, including piperazinones and tetrahydropyrimidinones. Then, in the accompanying two appendices, we describe the DAAA of five and seven-membered diazaheterocycles.

1.2 PIPERAZINONE and TETRAHYDROPYRIMIDINONE DAAA

Nitrogen containing heterocycles are ubiquitous components of biologically active small molecules.[18] For instance, piperazine, a representative diazaheterocycle, is the third most prevalent heterocycle in small molecule pharmaceuticals[18] and can be found in bioactive molecules such as the antiviral natural product Herquline A,[19] blockbuster psychiatric drug aripiprazole,[20] and the HIV integrase inhibitor dolutegravir[21,22] (as the oxidized counterpart, piperazin-2-one) (Fig. 1.1).

Fig. 1.1 *Representative piperazine and piperazine-2-one pharmaceuticals and natural products.*

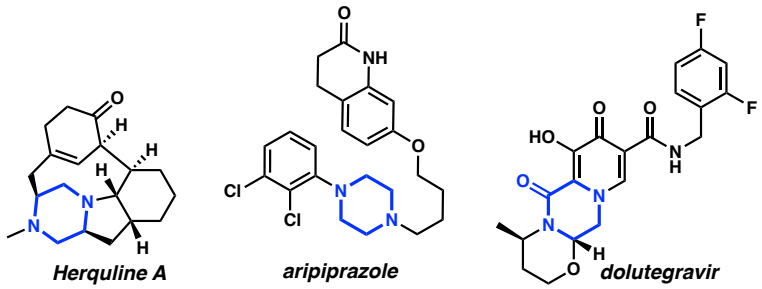

In the field of medicinal chemistry and fragment-based drug discovery, an emerging paradigm to enhance drug-like properties of small molecules involves reducing molecular flatness by incorporating chiral centers.[23–27] This method of increasing molecular complexity can enhance binding affinity and specificity for a target, as receptor-ligand binding is often defined by three dimensional contacts.[24] Furthermore, depending on the chemical composition of the chiral center, other properties such as metabolism, aqueous solubility, and cell-penetration may be optimized.[23] The prevalence of piperazine in bioactive molecules makes it an excellent scaffold upon which to introduce chirality and increase molecular complexity. Chiral *gem*-disubstitution on any

of four carbon atoms in the piperazine ring could dramatically alter physicochemical properties (Fig. 1.2). Despite this potential, there are no *gem*-disubstituted piperazines among the current 98 FDA approved piperazine-containing non-natural product derived drugs.[28] **Error! Reference source not found.** In contrast, a significant number contain mono-substituted piperazines, which can be prepared through a variety of strategies,[29–39] including cyclization of chiral precursors, enantioselective hydrogenation of pyrazines,[32,33] palladium-catalyzed cyclizations,[34–36] or asymmetric lithiation.[37,38]

Fig. 1.2 *Advantages of chiral gem-disubstituted piperazines*

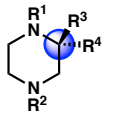

Increased molecular complexity[5c]
Augmented properties: specificity, metabolism, solublity, permeability
Absent in all 98 FDA-approved piperazine containing drugs[6]

gem-Disubstituted piperazine

The dearth of piperazine *gem*-disubstitution in the pharmacopoeia highlights the significant challenge of installing fully substituted chiral centers into diazaheterocycles. The state of the art is perhaps best exemplified by the Bode laboratory's extensive development of tin (SnAP) and silicon (SLAP) coupling reagents to generate spiro-substituted piperazines (Scheme 1.2A).[40–42] However, this method is not yet enantioselective and involves potentially toxic tin reagents. Other non-enantioselective methods to synthesize *gem*-disubstituted piperazines include [4+2] cycloadditions of 1,2 diamines with propargyl alcohols developed by Rawal (Scheme 1.2B),[34] and the ring expansion of oxetane spirocycles by Carreira (Scheme 1.2C).[43]

To our knowledge, the only method enabling the highly enantioselective synthesis of *gem*-disubstituted piperazines was published by our group in 2015.[15] **Error! Reference source not found.** We leveraged the

Scheme. 1.2 *Existing approaches for gem-disubstituted piperazines and piperazinones*

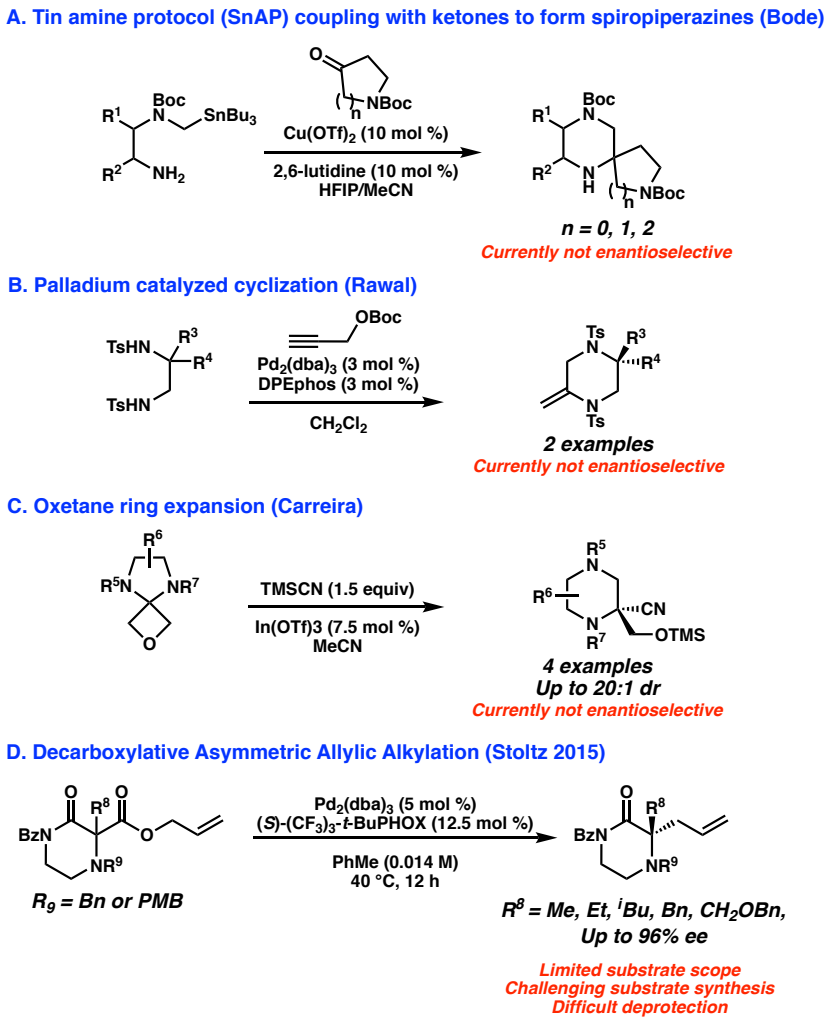

palladium-catalyzed decarboxylative asymmetric allylic alkylation reaction to synthesize chiral α,α-disubstituted N4-benzylated piperazin-2-ones (Scheme 1.2D). These piperazin-2-ones could then be reduced into desirable chiral *gem*-disubstituted piperazines. However, we encountered two issues during the course of our attempts to utilize this method to synthesize disubstituted piperazines for medicinal chemistry purposes: first, the optimal nucleophilic benzyl-protected N4 significantly complicated substrate

synthesis via nucleophilic side reactions, leading to low yields of products. As a result, we failed to synthesize many desired substrates via standard enolate functionalization of the dicarbonyl precursor. Instead, we resorted to a low-yielding 5-step convergent sequence beginning from an amino acid (Scheme 1.3A). As a result, our substrate scope displayed limited functional group diversity. Second, noting that heterocycles such as piperidines, pyrollidines, and piperazines are prevalent in compounds of medicinal interest, we initiated a medicinal chemistry program to explore their utility in the context of cancer and infectious disease therapeutics. With a robust method of DAAA to generate chiral gem-disubstituted versions of medicinally relevant heterocycles, we initially sought to utilize our piperazinones[15] in a collaboration with the Kurosu group at UTennessee to design novel *C. dificile* inhibitors. During this collaboration we worked with a N4-PMB-protected piperazin-2-one, in which we failed to remove the recalcitrant PMB group using a variety of common cleavage conditions that were orthogonal to the sensitive allyl functionality.

Scheme 1.3. *Comparison of routes to piperazin-2-one decarboxylative alkylation substrates.*

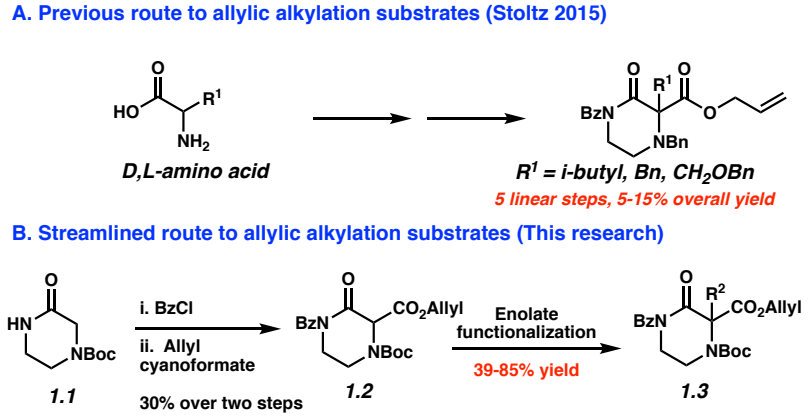

The substrate-dependent drawbacks of our approach leave room for an improved method to synthesize chiral disubstituted piperazines. In an effort to expand upon our group's longstanding interest in transition-metal catalyzed allylic alkylation, we sought to identify an alternative protecting group that could overcome the aforementioned limitations by enabling both facile substrate synthesis and protecting group cleavage. After extensive explorations directed toward this goal, we were pleased to discover that replacing the N4-benzyl protecting group with a simple Boc (tert-butoxycarbonyl) protecting group addressed the issue of difficult substrate synthesis. Presumably, the electron-withdrawing Boc group attenuates the nucleophilicity of N4, enabling divergent access to a wider array of substrates **1.3** via enolate functionalization of dicarbonyl compound **1.2**, which could be synthesized in only two steps from Boc-piperazinone **1.1** (Scheme 1.3B)

With a streamlined approach toward a wide range of decarboxylative alkylation substrates, we began optimizing the reaction conditions: with model substrate **1.3m**, conditions based on our previous report[15] using 10 mol % (*S*)-$(CF_3)_3$-*t*-BuPHOX ligand and 4 mol % $Pd_2(pmdba)_3$ in 0.014 M toluene gave the product 3m in only 76% ee (Table 1.2, entry 1). Other commonly used allylic alkylation ligands such as (*S*)-*t*-BuPHOX (**L2**) and (*S*,*S*)-ANDEN-Ph Trost (**L3**) were tested, both giving suboptimal enantioselectivities (entries 2–3). We then examined the effect of solvent on the enantioselectivity (entries 4–6), ultimately finding that 2:1 hexanes-toluene provided high yield and *ee*.

Table 1.2 *Optimization of the reaction conditions*[a]

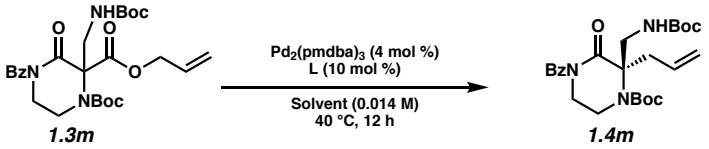

Entry	Ligand	Solvent	Yield (%)[b]	ee (%)[c]
1	**L2**	Tol	75	76
2	**L2**	Tol	70	1
3	**L3**	Tol	83	52
4	**L1**	THF	—	13
5	**L1**	MTBE	—	80
6	**L1**	2:1 Hex/Tol	93	93

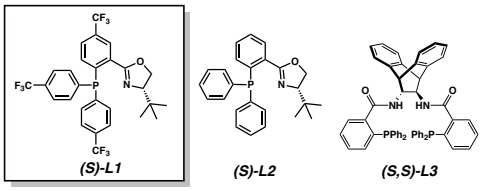

[a] Screens performed on a 0.04 mmol scale. [b] All reported yields are for isolated products. [c] The *ee* values were determined by chiral SFC analysis. Bz = benzoyl, Boc = tert-butoxycarbonyl, pmdba = bis(4-methoxybenzylidene)acetone

Employing these satisfactory reaction conditions, we then explored the substrate scope of the decarboxylative alkylation of various N4-Boc protected piperazinones (Table 1.3). We first tested the α-monosubstituted piperazinone **1.3a**, finding that typical conditions in a 0.033 M solution of toluene afforded the product **1.4a** in high yield and enantioselectivity. Another monosubstituted piperazinone **1.4b** with a N1-anisoyl protecting group, was also obtained in high yield and ee. Furthermore, replacement of the N4-Boc protecting group with Cbz (**1.3c**), and 2-chloro substitution of the allyl group (**1.3d**) similarly provided good results.

Next, we examined α,α-disubstituted substrates, finding that for the simple cases of methyl substitution (**1.3e**, **1.3f**), performing the reaction at 0.033 M concentration in toluene gave high yields and *ee*, with no improvement with the use of 2:1 hexanes-toluene at 0.014 M concentration. The exception was N4-benzoyl protected substrate **1.3g**, which in our previous work gave 52% *ee* in toluene; under our optimized conditions in 2:1 hexanes-toluene, the substrate gave an improved albeit modest *ee* of 70%. Larger substituents such as α-benzylated compound **1.3h** or benzyloxymethyl ether **1.3i** required the use of 2:1 hexanes-toluene to achieve high enantioselectivity. This unique mixed-solvent requirement was observed in all substituents other than methyl. A wide range of functional groups was tolerated: notably, the nitrile, ketone, and methylcarbamate substrates, which could not be accessed in our previously described efforts, gave high *ee* and yields (**1.3j**-**m**).

Table 1.3. *Substrate scope exploration.*

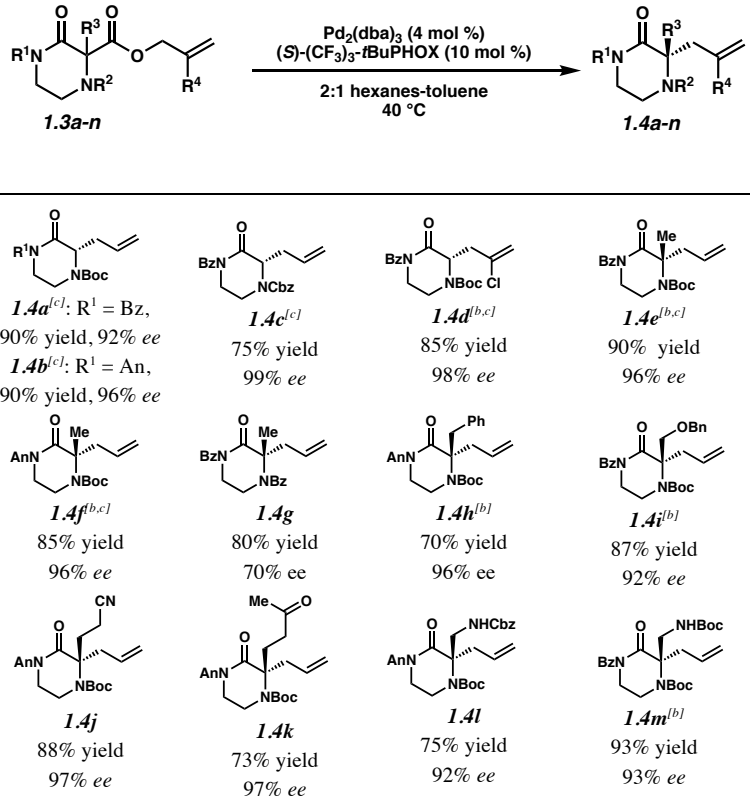

[a] Conditions: piperazin-2-one **3** (1.0 equiv), $Pd_2(dba)_3$ (4 mol %), (*S*)-$(CF_3)_3$-*t*BuPHOX (10 mol %), in 2:1 hexanes/toluene (0.014 M) at 40 °C for 12-24 h. [b] $Pd_2(pmdba)_3$ (4 mol %) instead of $Pd_2(dba)_3$. [c] Toluene (0.033 M) instead of 2:1 hexanes/toluene. All reported yields are for isolated products. The *ee* values were determined by chiral SFC analysis. An = 4-methoxybenzoyl, dba = dibenzylideneacetone.

With the *N*-Boc piperazin-2-one substrates providing excellent results, we wondered whether an isomeric substrate class, the *N*-Boc tetrahydropyrimidin-2-ones (**1.5**), would perform similarly as well (Scheme 1.4c). The resulting α,α-disubstituted tetrahydropyrimidin-2-one products (**1.6**) are especially interesting as they may be hydrolyzed to afford valuable $\beta^{2,2}$-amino acids (**1.7**), which are used in peptidomimetic therapeutics and in the design of unnatural peptides and proteins with unique secondary and tertiary structures.[44–46] In fact, there is strong precedent for an allylic alkylation

approach toward $\beta^{2,2}$-amino acids. In 2018 the Shibasaki group described the decarboxylative allylic alkylation of an *N,O* heterocycle to set the quaternary stereocenter, followed by N−O bond heterolysis to generate $\beta^{2,2}$-amino acids (Scheme 1.4a).[47] Later in 2018, Cossy and co-workers described a similar approach involving intermolecular allylic alkylation (Scheme 1.4b).[48] Notably, the substrate scope for these two examples is limited to mostly α-benzylic and α-aryl compounds. If decarboxylative alkylation could be achieved with the versatile tetrahydropyrimidin-2-one scaffold, a broader range of chiral $\beta^{2,2}$-amino acids might be accessible (Scheme 1.4c). Additionally, tetrahydropyrimidinones may be reductively transformed into hexahydropyrimidines, which are found in bioactive molecules such as the antibiotic hexetidine and the macrocyclic natural product verbamethine.[49,50]

Scheme 1.4. *Synthetic approaches toward $\beta^{2,2}$-amino acids using the allylic alkylation reaction*

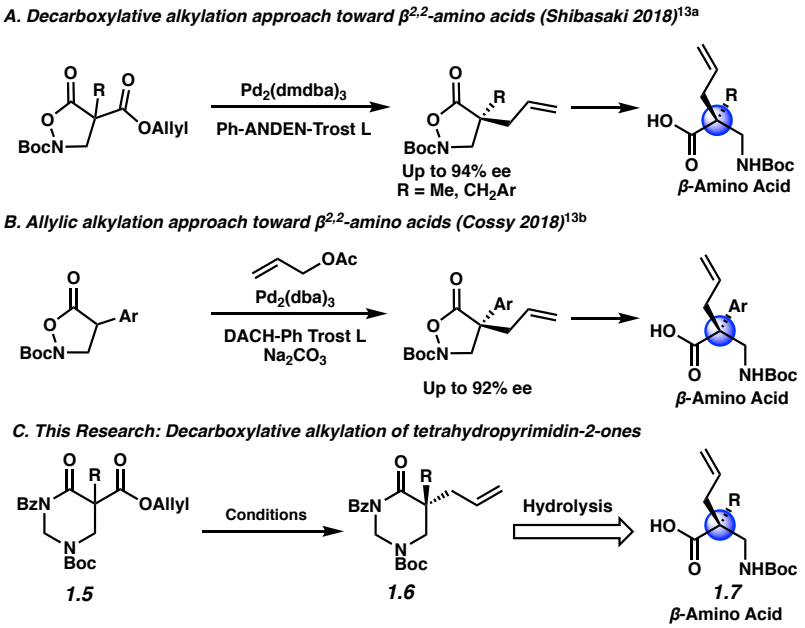

Beginning our investigations with methyl substrate 1.**5a** (Table 1.4), we were pleased to find that our optimized conditions in 2:1 hexanes-toluene furnished the desired decarboxylative alkylation product **1.6a** in high yield and ee. The reaction proved amenable to a variety of α-substituents, including ethyl (**1.6b**), methyl ester (**1.6c**), 2-chloroallyl (**1.6d**), and benzyl (**1.6e**). Furthermore, the reaction is scalable, with the benzyl substrate **1.5e** giving good results in a 1 gram reaction. In contrast, the nitrile and benzyloxymethyl ether products **1.6f** and **1.6g** were isolated with reduced enantioselectivities. Pleasingly, the fluorine and propargyl substrates **1.5h** and **1.5i** performed well, and may serve as a precursor to a novel fluorinated $\beta^{2,2}$-amino acid, or for biorthogonal click reactions, respectively.

Table 1.4. *Pd-catalyzed decarboxylative alkylation of tetrahydropyrimidin-2-ones. Scope of* **α***-substituents*[a]

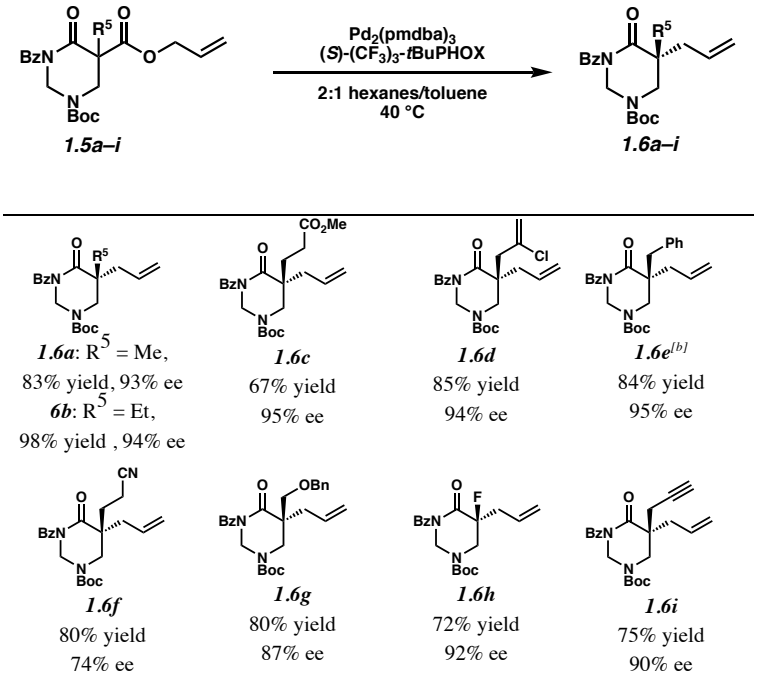

[a] Conditions: tetrahydropyrimidin-2-one **5** (1.0 equiv), $Pd_2(pmdba)_3$ (4 mol %), (*S*)-$(CF_3)_3$-*t*BuPHOX (10 mol %), in 2:1 hexanes/toluene (0.014 M) at 40 °C for 12-24 h. All reported yields are for isolated products. [b] Reaction performed with 1 gram of substrate **5e**. The *ee* values were determined by chiral SFC analysis.

Having demonstrated excellent results for the decarboxylative alkylation of piperazin-2-ones and tetrahydropyrimidin-2-ones, we began exploring their synthetic utility. In contrast to the relative difficulty of removing the N4-benzyl type protecting groups in our previous work, both Boc groups of **1.4m** were easily removed by treatment with excess TFA to give aminopiperazinone **1.8** (Scheme 1.5a). With LiOH, the benzoyl group could be orthogonally removed to provide the free amide **1.9** (Scheme 1.5b). The amide **1.9** could then be reduced with $LiAlH_4$ to the corresponding chiral aminopiperazine **1.10**. To further illustrate the synthetic versatility realized by Boc-deprotection of N4, we hydrogenated the allyl olefin of methyl piperazinone **1.4e** before

cleaving the Boc group to obtain **1.11**. We then applied Gaunt's[51] method of C–H carbonylation on the aliphatic amine of **1.11** to forge the fused β-lactam **1.12**, which

bears resemblance to the core of various *β*-lactam antibiotics and *β*-lactamase inhibitors (Scheme 1.5c). Lastly, we transformed four tetrahydropyrimidinone substrates, **1.6c-e** and **1.6h**, into their corresponding acyclic forms (Scheme 1.5d & e). Using a two-step protocol involving TFA-mediated Boc cleavage followed by saponification with LiOH, we successfully obtained the crude $\beta^{2,2}$-amino acid (Scheme 1.5d); to facilitate silica gel chromatographic isolation, we chose to mask the free amine and carboxylic acid with Boc and benzyl groups, respectively, resulting in protected $\beta^{2,2}$-amino acid **1.13**. We note that in this four step sequence, we only performed one chromatographic separation to isolate the protected β-amino acid. In contrast, novel unprotected $\beta^{2,2}$-amino acids **1.14**–**16** bearing pendant carboxylic acid, chloroallyl, and fluorine atom functional groups could be obtained directly by purification with reverse phase preparatory HPLC following the two-step deprotection sequence (Scheme 1.5e).

Scheme 1.5. *Product derivatization*

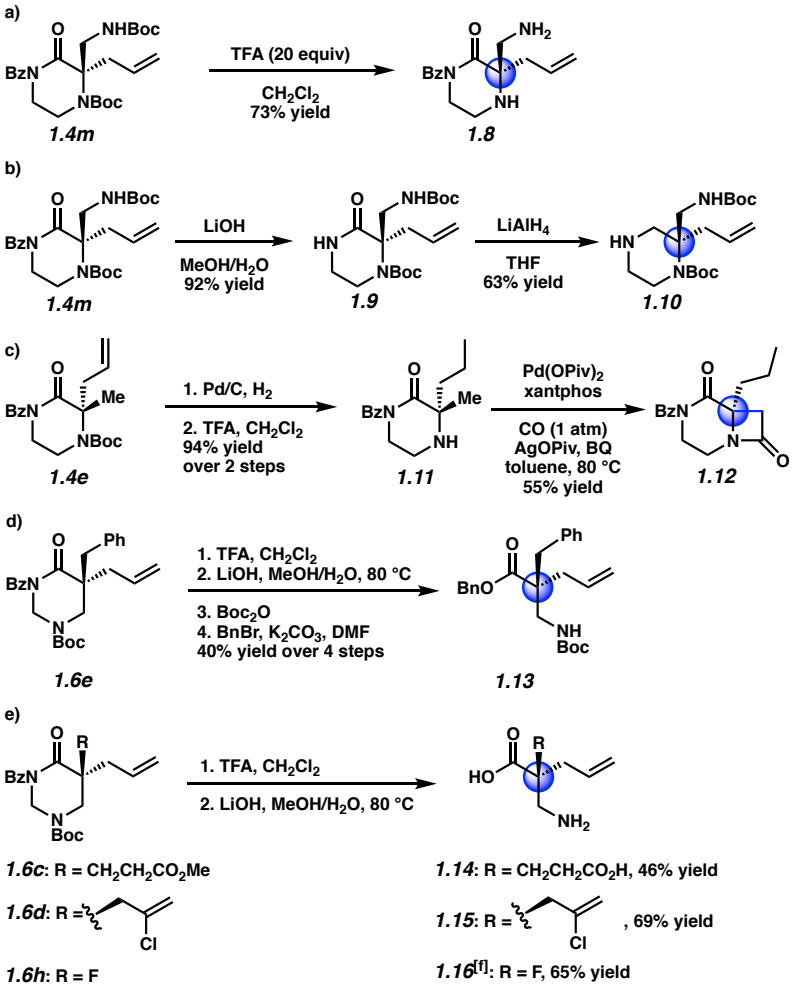

[a] Boc cleavage to the free amine. [b] Benzoyl cleavage and reduction to the piperazine. [c] Boc cleavage, allyl hydrogenation, and C–H carbonylation of the free amine. [d,e] hydrolysis and subsequent protection of the $\beta^{2,2}$-amino acid. [f] KOH, 1:1 $MeOH/H_2O$, rt; then, HCl, MeOH, rt. BQ = benzoquinone. Piv = pivalate.

1.3 CONCLUSIONS

In summary, we have developed a decarboxylative asymmetric allylic alkylation reaction to synthesize unprecedented chiral α,α-disubstituted piperazin-2-ones and tetrahydropyrimidin-2-ones. This work represents a significant improvement upon existing technology, featuring ease of substrate synthesis, facile N4-Boc deprotection, and broader substrate scope. The resulting piperazinones can be transformed into

valuable chiral *gem*-disubstituted piperazines that are anticipated to provide stereodefined access to new chemical space in drug discovery. Similarly, the tetrahydropyrimidinone scaffold could be hydrolyzed to provide access to corresponding protected and free $\beta^{2,2}$-amino acids. We anticipate this decarboxylative allylic alkylation protocol will find utility in the field of medicinal chemistry as well as in natural products synthesis.

1.4 EXPERIMENTAL SECTION

1.4.1 MATERIALS AND METHODS

Unless otherwise stated, reactions were performed in flame-dried glassware under an argon or nitrogen atmosphere using dry, deoxygenated solvents. Solvents were dried by passage through an activated alumina column under argon. *tert*-Butyl 3-oxopiperazine-1-carboxylate **1.1** was obtained from Combi-Blocks. Commercially obtained reagents were used as received. Chemicals were purchased from Sigma Aldrich/Strem/Alfa Aesar/Combi-Blocks and used as received.

Reaction temperatures were controlled by an IKAmag temperature modulator. Glove box manipulations were performed under a nitrogen atmosphere. Thin-layer chromatography (TLC) was performed using E. Merck silica gel 60 F254 precoated plates (0.25 mm) and visualized by UV fluorescence quenching, iodine on silica, ninhydrin, or $KMnO_4$ staining. Silia*Flash* P60 Academic Silica gel (particle size 0.040–0.063 mm) was used for flash chromatography.

Analytical SFC was performed with a Mettler SFC supercritical CO_2 analytical chromatography system utilizing a Chiralpak IC column (4.6 mm x 25 cm) obtained from Daicel Chemical Industries, Ltd. with visualization at 254 nm. Reverse Phase Preparatory

HPLC was performed with a Teledyne ISCO ACCQPrep HP125 preparative liquid chromatography system equipped with a RediSep Prep C18 5 μm column (20 x 250 mm). ^{1}H NMR spectra were recorded on a Varian Inova 600 MHz or 500 MHz spectrometer or a Bruker Avance HD 400 MHz spectrometer and are reported relative to residual $CHCl_3$ (δ 7.26 ppm) or CH_3OH (δ 3.31 ppm). ^{13}C NMR spectra were recorded on a Varian Inova 500 MHz spectrometer or a Bruker Avance HD 400 MHz spectrometer and are reported relative to residual $CDCl_3$ (δ 77.16 ppm) or CD_3OD (δ 49.00 ppm). Data for ^{1}H NMR are reported as follows: s = singlet, d = doublet, t = triplet, q = quartet, p = pentet, sept = septuplet, m = multiplet, br s = broad singlet. Data for ^{13}C NMR are reported in terms of chemical shifts (δ ppm). Some reported spectra include minor solvent impurities of water (δ 1.56 or 4.87 ppm), ethyl acetate (δ 4.12, 2.05, 1.26 ppm), methylene chloride (δ 5.30 ppm), acetone (δ 2.17 ppm), grease (δ 1.26, 0.86 ppm), and/or silicon grease (δ 0.07 ppm), which do not impact product assignments.

IR spectra were obtained using a Perkin Elmer Paragon 1000 spectrometer using thin films deposited on NaCl plates and reported in frequency of absorption (cm^{-1}). High resolution mass spectra (HRMS) were obtained from an Agilent 6200 Series TOF with an Agilent G1978A Multimode source in electrospray ionization (ESI+), atmospheric pressure chemical ionization (APCI+), or mixed ionization mode (MM: ESI-APCI+). Optical rotations were measured with a Jasco P-2000 polarimeter operating on the sodium D-line (589 nm), using a 100 mm pathlength cell and are reported as: $[\alpha]_D^T$ (concentration in g/100 mL, solvent). Stereochemistry is assigned by analogy to previous results.[4,7,10,13,52,53]

1.4.1.1 Preparation of Known Compounds

Allyl cyanoformate was prepared according to the method of Weber.[54] Phosphinooxazoline (PHOX) ligands **(*S*)-L1**, **(*S*)-L2**, and achiral GlyPhox were prepared by methods described in our previous work.[4,55] Di-benzoylated allylic alkylation substrate **1.3g** was prepared according to the method of Korch.[15] Tris(4,4'-methoxydibenzylideneacetone)dipalladium(0) [$Pd_2(pmdba)_3$] was prepared according to the method of Ibers[56] or Fairlamb.[57] AgOPiv was prepared using Grubbs' procedure.[58] *tert*-Butyl ((phenylsulfonyl)methyl)carbamate and benzyl ((phenylsulfonyl)methyl)carbamate were prepared according to the method of Zwierzak or Dikshit.[59,60] Benzyl 3-oxopiperazine-1-carboxylate was prepared according to the method of Batey.[61] 2-chloroallyl chloroformate was prepared according to the method of Stoltz.[62]

1.4.2 EXPERIMENTAL PROCEDURES AND SPECTROSCOPIC DATA

1.4.2.1 Procedures for the Synthesis of Piperazinone Allylic Alkylation Substrates

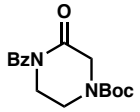

tert-butyl 4-benzoyl-3-oxopiperazine-1-carboxylate. To a solution of *tert*-butyl 3-oxopiperazine-1-carboxylate **1.1** (5.0 g, 24.9 mmol, 1 equiv) in THF (250 mL) at −78 °C was added dropwise *n*BuLi (11.4 mL, 2.4M solution in hexane, 27.5 mmol, 1.1 equiv) over 20 minutes. The resulting yellow solution was stirred for 10 min at −78 °C. Benzoyl chloride (3.48 mL, 30.0 mmol, 1.2 equiv) was then added dropwise at −78 °C, giving an

orange solution. The reaction was stirred for 2.5 h at −78 °C, quenched by addition of saturated aqueous NH_4Cl (100 mL), and diluted with ethyl acetate (100 mL). The layers were separated and the aqueous layer was extracted with ethyl acetate (3 × 100 mL). The combined organic layers were dried over anhydrous Na_2SO_4, decanted, and concentrated under reduced pressure onto silica gel. The silica-loaded crude reaction mixture was purified by silica gel flash column chromatography (10% →15% →20% EtOAc/hexanes) to give protected ketopiperazine as a white solid (3.2 g, 42.1% yield). Product identity was confirmed by comparison to previously reported characterization data.[63]

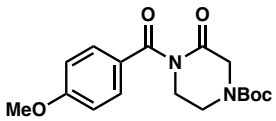

tert-butyl 4-(4-methoxybenzoyl)-3-oxopiperazine-1-carboxylate. To a solution of *tert*-Butyl 3-oxopiperazine-1-carboxylate (5.0 g, 24.9 mmol, 1 equiv) in THF (250 mL) at −78 °C was added dropwise *n*BuLi (11.4 mL, 2.4M solution in hexane, 27.5 mmol, 1.1 equiv) over 20 minutes. The resulting yellow solution was stirred for 10 min at −78 °C. Anisoyl chloride (4.1 mL, 30.0 mmol, 1.2 equiv) was then added dropwise at −78 °C, giving a bright orange solution. The reaction was stirred for 2 h at −78 °C, quenched by addition of saturated aqueous NH_4Cl (100 mL), and diluted with ethyl acetate (100 mL). The layers were separated and the aqueous layer was extracted with ethyl acetate (3 × 100 mL). The combined organic layers were dried over anhydrous Na_2SO_4, decanted, and concentrated under reduced pressure onto silica gel. The silica-loaded crude reaction mixture was filtered through a plug of silica (1% →2% MeOH/CH_2Cl_2) to give crude

anisoyl protected ketopiperazine as a white foam, which was directly used without further purification in subsequent acylation reactions with allyl cyanoformate.

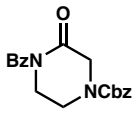

benzyl 4-benzoyl-3-oxopiperazine-1-carboxylate. To a solution of benzyl 3-oxopiperazine-1-carboxylate[61] (1.0 g, 4.3 mmol, 1.0 equiv) in THF (42 mL) at −78 °C was added dropwise *n*BuLi (1.96 mL, 2.4M solution in hexane, 4.7 mmol, 1.1 equiv) over 20 minutes. The solution was stirred for 10 min at −78 °C. Benzoyl chloride (0.595 mL, 5.1 mmol, 1.2 equiv) was then added dropwise at −78 °C, giving a light yellow solution. The reaction was stirred for 1 h at −78 °C, quenched by addition of saturated aqueous NH_4Cl (50 mL), and diluted with ethyl acetate (50 mL). The layers were separated and the aqueous layer was extracted with ethyl acetate (3 × 50 mL). The combined organic layers were dried over anhydrous Na_2SO_4, decanted, and concentrated under reduced pressure onto silica gel. The silica-loaded crude reaction mixture was purified by silica gel flash column chromatography (33% EtOAc/hexanes) to give Bz-Cbz-protected ketopiperazine **SI-3** as a white solid (1.0 g, 70.0% yield); **^{1}H NMR (500 MHz, $CDCl_3$)** δ 7.61 – 7.56 (m, 2H), 7.54 – 7.49 (m, 1H), 7.44 – 7.31 (m, 7H), 5.21 (s, 2H), 4.30 (s, 2H), 3.95 (dd, *J* = 6.8, 4.4 Hz, 2H), 3.83 (dd, *J* = 6.9, 4.3 Hz, 2H); **^{13}C NMR (126 MHz, $CDCl_3$)** δ (a mixture of two rotamers) 172.8, 168.0, 167.6, 154.5, 136.0, 135.0, 132.3, 128.7, 128.5, 128.4, 128.3, 128.3, 68.0, 48.5, 43.3, 41.7, 41.4; **IR (Neat Film, NaCl)** 3386, 3063, 3033, 2954, 2894, 1706, 1600, 1584, 1498, 1449, 1422, 1394, 1367, 1302, 1231, 1177, 1162, 1123, 1060, 1028, 1010, 944, 857, 796, 765, 731,

699, 639, 612 cm^{-1}; **HRMS (MM: ESI-APCI)** *m/z* calc'd for $C_{19}H_{19}N_2O_4$ $[M+H]^+$: 339.1339, found 339.1338.

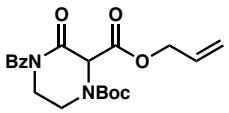

2-allyl 1-(tert-butyl) 4-benzoyl-3-oxopiperazine-1,2-dicarboxylate (1.2). To a solution of Bz-protected oxopiperazine (1.5 g, 4.9 mmol, 1.0 equiv) in THF (40 mL) at −78 °C was added LiHMDS (907 mg, 5.42 mmol, 1.10 equiv.) in THF (10mL) dropwise. The resulting orange reaction mixture was stirred for 15 min at −78 °C. Then, allyl cyanoformate (590 μL, 5.2 mmol, 1.05 equiv) was added dropwise at −78 °C, giving a yellow solution. After stirring for 1.5 h at −78 °C, the reaction was quenched with saturated aqueous NH_4Cl (20 mL) and diluted with ethyl acetate (50 mL). The aqueous phase was extracted with ethyl acetate (3 x 100 mL). The combined organic layers were dried over anhydrous Na_2SO_4, decanted, and concentrated under reduced pressure onto silica. The silica-loaded crude mixture was purified by silica gel flash chromatography (10% → 20% EtOAc/hexanes) to give the allyl ester **1.2** as a white solid (1.3 g, 68% yield): **^{1}H NMR (500 MHz, $CDCl_3$)** δ (a mixture of two rotamers) 7.59 (d, *J* = 7.7 Hz, 2H), 7.52 (t, *J* = 7.6 Hz, 1H), 7.40 (t, *J* = 7.6 Hz, 2H), 5.92 (m, 1H), 5.44 – 5.07 (m, 3H), 4.84 – 4.57 (m, 2H), 4.28 – 3.61 (m, 4H), 1.43 (br s, 9H); **^{13}C NMR (126 MHz, $CDCl_3$)** δ (a mixture of two rotamers) 172.7, 166.9, 164.4, 154.1, 153.5, 134.6, 132.6, 131.0, 128.6, 128.4, 119.9, 119.4, 82.2, 82.0, z67.1, 62.7, 61.7, 43.2, 42.6, 41.5, 40.2, 29.4, 28.3; **IR (Neat Film, NaCl)** 2978 1746 1695 1600 1450 1393 1367 1310 1277 1231 1177 1158

1127 1088 1059 1009 958 861 794 770 728 694 623 cm^{-1}; **HRMS (MM: ESI-APCI)** *m/z* calc'd for $C_{16}H_{17}N_2O_6$ $[(M-tBu)+H]^+$: 333.1081, found 333.1075.

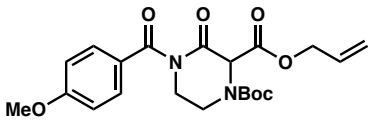

2-allyl 1-(tert-butyl) 4-(4-methoxybenzoyl)-3-oxopiperazine-1,2-dicarboxylate (1.3b). Following the procedure described for the preparation of **1.2**, anisoyl protected oxopiperazine (1.0 g, 3.0 mmol, 1.0 equiv) was treated with LiHMDS (550 mg, 3.3 mmol, 1.1 equiv) and acylated with allyl cyanoformate (336 μL, 3.1 mmol, 1.05 equiv) to give, after purification by silica gel flash chromatography (Dry load SiO_2, 18% EtOAc/hexanes), allyl ester **1.3b** as a white solid (566 mg, 45% yield): **^{1}H NMR (400 MHz, $CDCl_3$)** δ (a mixture of two rotamers) 7.61 (d, *J* = 8.6 Hz, 2H), 6.86 (d, *J* = 8.8 Hz, 2H), 5.91 (ddt, *J* = 16.4, 10.8, 5.8 Hz, 1H), 5.46–5.12 (m, 3H), 4.70 (s, 2H), 4.13–3.65 (m, 4H), 3.81 (s, 3H), 1.46 (m, 9H); **^{13}C NMR (101 MHz, $CDCl_3$)** δ (a mixture of two rotamers) 171.9, 171.8, 167.0, 164.4, 164.2, 163.4, 154.0, 153.4, 131.4, 131.0, 126.3, 119.6, 119.2, 113.6, 82.0, 81.8, 66.9, 62.5, 61.6, 55.5, 43.3, 42.8, 41.5, 40.1, 28.2; **IR (Neat Film, NaCl)** 3384, 3060, 2978, 2843, 2568, 2049, 1732, 1605, 1580, 1513, 1456, 1372, 1258, 1088, 1059, 959, 844, 769, 736, 706, 634 cm^{-1}; **HRMS (MM: ESI-APCI)** *m/z* calc'd for $C_{21}H_{27}N_2O_7$ $[M+H]^+$: 419.1813, found 419.1815.

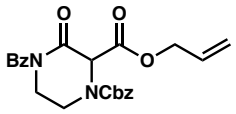

2-allyl 1-benzyl 4-benzoyl-3-oxopiperazine-1,2-dicarboxylate (1.3c). Following the procedure described for the preparation of **2**, Cbz protected oxopiperazine (1.0 g, 3.0 mmol, 1.0 equiv) was treated with LiHMDS (544 mg, 3.3 mmol, 1.1 equiv) and acylated with allyl cyanoformate (331 μL, 3.1 mmol, 1.05 equiv) to give, after purification by silica gel flash chromatography (dry load SiO_2, 20 → 25% EtOAc/hexanes), allyl ester **1.3a** as a white solid (720 mg, 58% yield): **^{1}H NMR (500 MHz, $CDCl_3$)** δ (a mixture of two rotamers) 7.65 – 7.56 (m, 2H), 7.56 – 7.46 (m, 1H), 7.46 – 7.28 (m, 7H), 5.87 (dtd, *J* = 47.5, 10.7, 5.4 Hz, 1H), 5.55 – 5.04 (m, 5H), 4.84 – 4.48 (m, 2H), 4.24 – 3.99 (m, 2H), 3.99 – 3.66 (m, 2H); **^{13}C NMR (126 MHz, $CDCl_3$)** δ (a mixture of two rotamers) 172.4, 172.3, 166.5, 164.0, 163.8, 154.8, 154.2, 135.7, 135.6, 134.4, 132.5, 130.9, 130.8, 128.7, 128.6, 128.5, 128.5, 128.4, 128.3, 128.2, 128.1, 119.6, 119.5, 68.3, 68.2, 67.2, 67.1, 62.1, 61.9, 42.8, 42.3, 41.3, 40.8; **IR (Neat Film, NaCl)** 3386, 3064, 3033, 2955, 2897, 1746, 1713, 1694, 1651, 1600, 1584, 1498, 1450, 1417, 1368, 1304, 1278, 1229, 1195, 1178, 1160, 1124, 1088, 1061, 1014, 985, 951, 860, 794, 768, 729, 696, 675, 623 cm^{-1}; **HRMS (MM: ESI-APCI)** *m/z* calc'd for $C_{23}H_{23}N_2O_6$ $[M+H]^+$: 423.1551, found 423.1547.

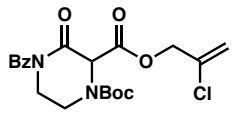

1-(tert-butyl) 2-(2-chloroallyl) 4-benzoyl-3-oxopiperazine-1,2-dicarboxylate (1.3d). Following the procedure described for the preparation of **1.2**, benzoyl protected oxopiperazine (440 mg, 1.5 mmol, 1.0 equiv) was treated with LiHMDS (267 mg, 1.6

mmol, 1.1 equiv) and acylated with 2-chloroallyl chloroformate[62] (235 mg, 1.5 mmol, 1.05 equiv) to give, after purification by silica gel flash chromatography (Dry load SiO_2, 15% EtOAc/hexanes), 2-chloroallyl ester **1.3d** as an off-white solid (431 mg, 70% yield): **^{1}H NMR (500 MHz, $CDCl_3$)**: δ (a mixture of two rotamers) 7.59–7.54 (m, 2H), 7.50–7.44 (m, 1H), 7.43–7.37 (m, 2H), 6.67 (m, 1H), 5.42–5.33 (m, 2H), 4.54 (m, 2H), 3.95–3.89 (m, 2H), 3.72 (t, J = 5.2 Hz, 2H), 1.51 (s, 9H); **^{13}C NMR (101 MHz, $CDCl_3$)**: δ (a mixture of two rotamers) 167.5, 167.3, 152.4, 152.2, 151.1, 151.0, 135.1, 134.9, 134.3, 131.3, 131.2, 128.5, 128.4, 128.0, 127.9, 126.7, 115.9, 115.7, 107.9, 107.6, 82.3, 82.2, 69.9, 69.8, 44.2, 43.1, 42.3, 41.7, 28.3; **IR (Neat Film, NaCl)** 3396, 3129, 3062, 2979, 2936, 2253, 1770, 1691, 1372, 1242, 1050, 987, 950, 922, 859, 839, 764, 731, 707, 647 cm^{-1}; **HRMS (MM: ESI-APCI)** *m/z* calculated for $C_{20}H_{24}ClN_2O_6$ $[M+H]^+$: 423.1317, found 423.1316.

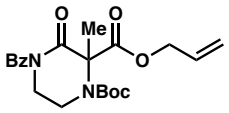

2-allyl 1-(tert-butyl) 4-(4-methoxybenzoyl)-2-methyl-3-oxopiperazine-1,2-dicarboxylate (1.3e). Sodium hydride (60% in mineral oil, 25 mg, 0.62 mmol, 1.2 equiv) was added to a solution of allyl ester **2** (200 mg, 0.52 mmol, 1.0 equiv) in THF (5 mL) at 0 °C. After stirring for 30 min at 0 °C, MeI (160 μL, 2.57 mmol, 5.0 equiv) was added. The reaction mixture was allowed to warm to room temperature and stirred for 16 h. The reaction was quenched with aqueous NH_4Cl (10 mL) and extracted with EtOAc (3 x 5 mL). The combined organic phases were dried over anhydrous Na_2SO_4, decanted, and concentrated under reduced pressure onto silica gel. The silica-loaded residue was

purified by silica gel flash chromatography (20% EtOAc/hexanes) to give methylated allyl ester **3e** as a colorless oil (180 mg, 85% yield): **^{1}H NMR (400 MHz, $CDCl_3$)**: δ 7.59 – 7.46 (m, 3H), 7.46 – 7.32 (m, 2H), 5.92 (ddt, *J* = 17.2, 10.4, 5.8 Hz, 1H), 5.41 – 5.19 (m, 2H), 4.66 (d, *J* = 5.8 Hz, 2H), 4.24 – 4.09 (m, 1H), 4.05 – 3.90 (m, 2H), 3.81 – 3.64 (m, 1H), 1.84 (s, 3H), 1.46 (s, 9H); **^{13}C NMR (101 MHz, $CDCl_3$)**: δ (a mixture of two rotamers) 172.5, 169.2, 168.0, 153.2, 134.8, 132.4, 131.5, 128.4, 128.0, 119.1, 82.7, 68.7, 66.9, 43.7, 40.9, 28.3, 21.5; **IR (Neat Film, NaCl)** 3384, 3064, 2980, 2939, 2876, 1962, 1766, 1694, 1600, 1584, 1451, 1394, 1368, 1306, 1270, 1232, 1206, 1164, 1096, 1060, 1032, 1016, 993, 968, 936, 854, 795, 770, 727, 696, 675, 633, 618 cm^{-1}; **HRMS (MM: ESI-APCI)** *m/z* calculated for C16H19N2O4 $[(M-Boc)+H]^+$: 303.1341, found 303.1339.

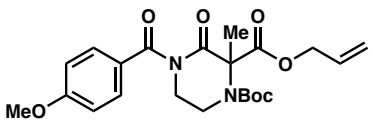

2-allyl 1-(tert-butyl) 4-(4-methoxybenzoyl)-2-methyl-3-oxopiperazine-1,2-dicarboxylate (1.3f). Following the procedure described for the preparation of **1.3e**, anisoyl protected oxopiperazine **1.3b** (120 mg, 0.29 mmol, 1.0 equiv) was treated with NaH (60% in mineral oil, 13 mg, 0.32 mmol, 1.1 equiv) and methylated with MeI (90 μL, 1.43 mmol, 5.0 equiv) to give, after purification by silica gel flash chromatography (dry load SiO_2, 15% → 20% → 25% → 30% EtOAc/hexanes), methylated allyl ester **1.3f** as a colorless oil (110 mg, 89% yield): **^{1}H NMR (400 MHz, $CDCl_3$)** δ 7.56 (d, *J* = 8.8 Hz, 2H), 6.85 (d, *J* = 8.9 Hz, 2H), 5.92 (ddt, *J* = 17.2, 10.4, 5.8 Hz, 1H), 5.40 – 5.17 (m, 2H), 4.66 (d, *J* = 5.8 Hz, 2H), 4.15 – 4.02 (m, 1H), 4.02 – 3.87 (m, 2H), 3.83 (s, 3H), 3.80 – 3.67 (m, 1H), 1.84 (s, 3H), 1.46 (s, 9H); **^{13}C NMR (101 MHz, $CDCl_3$)** δ 171.8, 169.0,

168.1, 163.4, 153.2, 131.5, 131.0, 126.6, 119.0, 113.7, 82.6, 68.5, 66.8, 55.5, 43.8, 41.0, 28.3, 21.6; **IR (Neat Film, NaCl)** 3081, 2978, 2938, 2842, 1766, 1702, 1604, 1579, 1512, 1460, 1394, 1368, 1308, 1287, 1259, 1235, 1208, 1169, 1114, 1095, 1060, 1021, 1004, 969, 933, 845, 789, 770, 733, 706, 648, 634 cm^{-1}; **HRMS (MM: ESI-APCI)** *m/z* calculated for $C_{18}H_{21}N_2O_7$ $[(M-tBu)+H]^+$: 377.1343, found 377.1339.

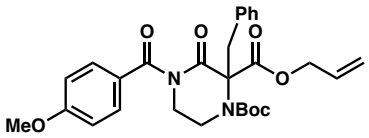

2-allyl 1-(tert-butyl) 2-benzyl-4-(4-methoxybenzoyl)-3-oxopiperazine-1,2-dicarboxylate (**1.3h)**. Following the procedure described for the preparation of **1.3e**, anisoyl-protected allyl ester **1.3b** (200 mg, 0.48 mmol, 1.0 equiv) was treated with potassium hydride (23 mg, 0.57 mmol, 1.2 equiv) and alkylated with benzyl bromide (170 μL, 1.43 mmol, 3.0 equiv) to give, after purification by silica gel flash chromatography (Dry load SiO_2, 20% → 25% EtOAc/hexanes), the benzyl ester **1.3h** as a colorless oil (100 mg, 41% yield) (Note: attempts using sodium hydride as a base failed to give conversion of starting material. Instead, potassium hydride resulted in conversion to the desired product.): **^{1}H NMR (400 MHz, $CDCl_3$)** δ (a mixture of two rotamers) 7.52 (m, 2H), 7.42 – 7.23 (m, 3H), 7.11 (m, 2H), 6.92 – 6.75 (m, 2H), 5.97 (ddt, *J* = 17.2, 10.4, 5.8 Hz, 1H), 5.50 – 5.17 (m, 2H), 4.87 – 4.57 (m, 2H), 3.86 (s, 3H), 3.79 – 3.56 (m, 4H), 2.95 (ddd, *J* = 13.3, 7.4, 3.0 Hz, 1H), 2.86 (br s, 1H), 1.55 (s, 9H); **^{13}C NMR (101 MHz, $CDCl_3$)** δ (a mixture of two rotamers) 172.1, 168.0, 167.4, 166.9, 163.4, 153.6, 153.4, 136.0, 135.3, 131.8, 131.3, 130.7, 128.8, 128.7, 128.4, 128.2, 127.8, 127.7, 127.5, 126.6, 119.4, 118.9, 113.7, 82.9, 81.8, 72.7, 67.0, 66.5, 55.6, 44.5, 43.0, 42.2, 41.4, 40.8,

40.0, 38.8, 28.5; **IR (Neat Film, NaCl)** 2978, 1764, 1698, 1604, 1512, 1496, 1455, 1394, 1366, 1307, 1282, 1256, 1196, 1155, 1078, 1020, 1000, 921, 844, 768 733, 704 cm^{-1}; **HRMS (MM: ESI-APCI)** *m/z* calculated for C28H33N2O7 $[M+H]^+$: 509.2282, found 509.2285.

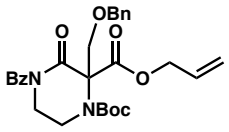

2-allyl 1-(tert-butyl) 4-benzoyl-2-((benzyloxy)methyl)-3-oxopiperazine-1,2-dicarboxylate (1.3i). Following the procedure described for the preparation of **1.3e**, allyl ester **1.2** (150 mg, 0.39 mmol, 1.00 equiv) was treated with sodium hydride (17 mg, 0.42 mmol, 1.1 equiv) and alkylated with benzyl chloromethyl ether (107 μL, 0.77 mmol, 2.0 equiv) to give, after purification by silica gel flash chromatography (Dry load SiO_2, 10% → 15% EtOAc/hexanes), benzyloxy methyl ether **1.3i** as a colorless oil (50 mg, 55% yield BRSM): **^{1}H NMR (500 MHz, $CDCl_3$)** δ (a mixture of two rotamers) 7.64 – 7.55 (m, 2H), 7.51 – 7.44 (m, 1H), 7.41 – 7.27 (m, 7H), 5.88 (ddt, J = 17.3, 10.4, 5.8 Hz, 1H), 5.40 – 5.17 (m, 2H), 4.74 – 4.47 (m, 4H), 4.38 (m, 1H), 4.17 (m, 1H), 4.08 – 3.84 (m, 4H), 1.42 (m, 9H); **^{13}C NMR (126 MHz, $CDCl_3$)** δ (a mixture of two rotamers) 173.0, 167.4, 167.2, 166.5, 153.6, 153.1, 141.0, 137.9, 137.5, 134.8, 132.4, 131.6, 131.1, 128.7, 128.7, 128.6, 128.4, 128.3, 128.0, 127.7, 127.6, 127.1, 119.5, 118.9, 82.7, 81.9, 73.9, 73.3, 72.6, 71.2, 71.1, 66.8, 65.4, 43.6, 43.4, 42.5, 41.7, 28.4, 28.3; **IR (Neat Film, NaCl)** 3528, 3064, 3031, 2978, 2934, 1762, 1694, 1600, 1496, 1453, 1394, 1366, 1314, 1270, 1231, 1205, 1161, 1094, 1055, 1014, 972, 941, 854, 795, 770, 730, 696, 674, 624 cm^{-1}; **HRMS (MM: ESI-APCI)** *m/z* calculated for C24H25N2O7 $[(M-t\text{Bu})+H]^+$: 453.1656, found 453.1649.

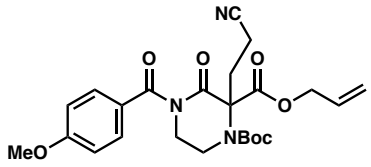

2-allyl 1-(tert-butyl) 2-(2-cyanoethyl)-4-(4-methoxybenzoyl)-3-oxopiperazine-1,2-dicarboxylate (1.3j). DBU (7.1 μL, 0.048 mmol, 0.10 equiv) was added to a solution of allyl ester **1.3b** (200 mg, 0.478 mmol, 1.0 equiv) and acrylonitrile (94 μL, 1.43 mmol, 3.0 equiv) in DMF (2.4 mL) at room temperature. After stirring for 2 h at 70 °C and 24 h at 55 °C, additional DBU (14 μL, 0.1 mmol, 0.2 equiv) was added and the orange solution was maintained at 70 °C for 4 h. Then, additional DBU (21 μL, 0.143 mmol, 0.30 equiv) was added and the mixture was stirred at 70 °C for 3 h. After allowing the reaction mixture to cool to room temperature, the reaction was quenched with saturated aqueous NH_4Cl (2 mL) and diluted with EtOAc (6 mL). The aqueous phase was extracted with EtOAc (3 x 5 mL). The combined organic layers were dried over anhydrous Na_2SO_4, decanted, and concentrated under reduced pressure onto silica gel. The silica-loaded residue was purified by flash chromatography (20% EtOAc/hexanes) to give the *α*-cyanoethylated allyl ester **1.3j** as a pale yellow oil (77.6 mg, 34% yield): **^{1}H NMR (400 MHz, $CDCl_3$)** δ 7.54 (s, 2H), 6.85 (d, *J* = 8.9 Hz, 2H), 5.92 (ddt, *J* = 17.2, 10.4 Hz, 5.9 Hz, 1H), 5.36 (dd, *J* = 17.2, 1.4 Hz, 1H), 5.29 (d, J = 10.5 Hz, 1H), 4.69 (d, *J* = 5.8 Hz, 2H), 4.25 (s, 1H), 4.06 (ddd, *J* = 13.1, 5.7, 3.1 Hz, 1H), 3.96 (ddd, *J* = 13.1, 8.6, 3.4 Hz, 1H), 3.83 (s, 3H), 3.64 – 3.49 (m, 1H), 2.77 (s, 2H), 2.49 (m, 1H), 2.44 – 2.31 (m, 1H), 1.47 (s, 9H); **^{13}C NMR (101 MHz, $CDCl_3$)** δ 171.7, 167.24, 166.3, 163.5, 153.4, 131.1, 126.2, 119.6, 119.1, 113.8, 82.9, 70.5, 67.3, 55.5, 43.9, 42.3, 29.8, 28.2, 12.8; **IR (Neat Film, NaCl)** 2978, 2249, 1760, 1694, 1604, 1579, 1512, 1462, 1394, 1368, 1311, 1258,

1160, 1018, 933, 846, 769, 737, 704 cm^{-1}; **HRMS (MM: ESI-APCI):** *m/z* calc'd for $C_{24}H_{30}N_3O_7$ $[M+H]^+$: 472.2078, found 472.2078.

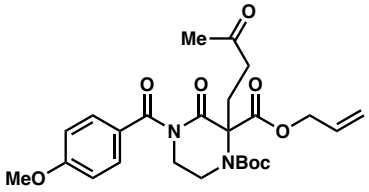

2-allyl 1-(tert-butyl) 4-(4-methoxybenzoyl)-3-oxo-2-(3-oxobutyl)piperazine-1,2-dicarboxylate (1.3k). To a solution of allyl ester **1.3b** (200 mg, 0.5 mmol, 1.0 equiv) and methyl vinyl ketone (80 μL, 0.96 mmol, 2.0 equiv) in acetone (2 mL) at room temperature was added DBU (7.1 μL, 0.05 mmol, 0.1 equiv). After stirring for 24 h at 55 °C, additional DBU (7.1 μL, 0.05 mmol, 0.1 equiv) was added and the orange solution was maintained at 55 °C for an additional 24 h. The reaction mixture was allowed to cool to ambient temperature and concentrated under reduced pressure onto silica gel. The silica-loaded crude reaction mixture was purified by silica gel flash column chromatography (33% EtOAc/hexanes) to afford the ketone **1.3k** as a pale yellow oil (90 mg, 39% yield): **^{1}H NMR (400 MHz, $CDCl_3$)** δ 7.56 (d, *J* = 8.8 Hz, 2H), 6.84 (d, *J* = 8.9 Hz, 2H), 5.92 (ddt, *J* = 17.2, 10.4, 5.8 Hz, 1H), 5.35 (dd, *J* = 17.2, 1.5 Hz, 1H), 5.26 (d, *J* = 10.4 Hz, 1H), 4.71 – 4.60 (m, 2H), 4.11 – 3.93 (m, 3H), 3.82 (s, 3H), 3.71 – 3.59 (m, 1H), 2.72 (q, *J* = 9.3, 8.1 Hz, 1H), 2.60 (dt, *J* = 9.6, 6.2 Hz, 3H), 2.10 (s, 3H), 1.45 (s, 9H); **^{13}C NMR (101 MHz, $CDCl_3$)** δ 207.8, 172.0, 167.9, 167.4, 163.4, 153.5, 131.5, 131.1, 126.6, 119.2, 113.7, 82.4, 70.6, 66.9, 55.5, 43.5, 42.1, 38.8, 29.8, 28.7, 28.3; **IR (Neat Film, NaCl):** 2977, 2934, 1761, 1704, 1604, 1512, 1456, 1394, 1367, 1312, 1257, 1199, 1168, 1090, 1018, 845, 768 cm^{-1}; **HRMS (MM: ESI-APCI)**: *m/z* calc'd for $C_{25}H_{33}N_2O_8$ $[M+H]^+$: 489.2231, found: 489.2228.

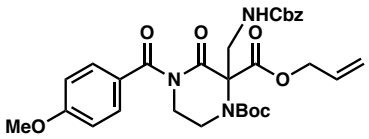

2-allyl 1-(tert-butyl) 2-((((benzyloxy)carbonyl)amino)methyl)-4-(4-methoxybenzoyl)-3-oxopiperazine-1,2-dicarboxylate (**1.3l)**. Following the procedure described for the preparation of **1.3m**, anisoyl-protected allyl ester **1.3b** (400 mg, 0.96 mmol, 1.0 equiv) was treated with Cs_2CO_3 (779 mg, 02.39 mmol, 2.5 equiv) and alkylated with benzyl ((phenylsulfonyl)methyl)carbamate[59,60] (350 mg, 1.15 mmol, 2.5 equiv) to give, after purification by silica gel flash chromatography (Dry load SiO_2, 10% → 15% → 20% EtOAc/hexanes), the aminomethyl allyl ester **1.3l** as a white foam (300 mg, 54% yield): **^{1}H NMR (400 MHz, $CDCl_3$)** δ (a mixture of two rotamers) 7.69 – 7.50 (m, 2H), 7.41 – 7.25 (m, 5H), 6.95 – 6.72 (m, 2H), 5.92 (ddt, *J* = 17.3, 10.4, 5.9 Hz, 1H), 5.49 – 4.96 (m, 5H), 4.85 – 4.53 (m, 2H), 4.27 – 3.87 (m, 5H), 3.83 (d, *J* = 14.6 Hz, 3H), 3.60 (d, *J* = 22.7 Hz, 1H), 1.47 (s, 9H); **^{13}C NMR (101 MHz, $CDCl_3$)** δ (a mixture of two rotamers) 171.7, 167.3, 166.5, 163.4, 156.8, 153.7, 152.7, 136.4, 134.21, 132.5, 131.5, 131.2, 129.4, 129.3, 128.9, 128.6, 128.3, 126.5, 119.8, 119.3, 113.7, 83.1, 82.1, 71.4, 70.6, 68.3, 67.8, 67.0, 55.5, 45.0, 44.2, 43.7, 42.9, 41.9, 28.3; **IR (Neat Film, NaCl)** 3366, 2977, 1704, 1604, 1513, 1456, 1394, 1367, 1313, 1257, 1232, 1169, 1091, 1018, 1002, 845, 767, 698 cm^{-1}; **HRMS (MM: ESI-APCI):** *m/z* calc'd for C30H36N3O9 $[M+H]^+$: 582.2446, found 582.2438.

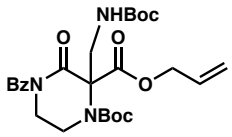

2-allyl 1-(tert-butyl) 4-benzoyl-2-(((tert-butoxycarbonyl)amino)methyl)-3-oxopiperazine-1,2-dicarboxylate (1.3m). To a suspension of allyl ester **1.2** (200 mg, 0.5 mmol, 1.0 equiv) and *tert*-butyl ((phenylsulfonyl)methyl)carbamate[59,60] (168 mg, 0.6 mmol, 1.2 equiv), in dichloromethane (2.5 mL) at room temperature was added Cs_2CO_3 (419 mg, 1.3 mmol, 2.5 equiv). After stirring for 3 h, saturated aqueous NH_4Cl (1 mL) was added and the biphasic mixture was vigorously stirred for 20 min. The aqueous phase was extracted with dichloromethane (3 x 3 mL). The combined organic phases were dried over anhydrous Na_2SO_4, decanted, and concentrated under reduced pressure onto silica gel. The silica-loaded crude reaction mixture was purified by silica gel flash column chromatography (15% EtOAc/hexanes) to give methylcarbamate allyl ester **1.3m** as a white foam (202 mg, 76% yield): **^{1}H NMR (400 MHz, $CDCl_3$)** δ (a mixture of two rotamers) 7.55 (d, *J* = 7.5 Hz, 2H), 7.49 (t, *J* = 7.5 Hz, 1H), 7.36 (t, *J* = 7.7 Hz, 2H), 5.91 (ddt, *J* = 16.5, 10.4, 5.8 Hz, 1H), 5.34 – 5.27 (m, 2H), 4.96 (m, 1H), 4.66 (br s, 2H), 4.19 – 3.85 (m, 5H), 3.79 – 3.64 (m, 1H), 1.48 (s, 9H), 1.40 (s, 9H); **^{13}C NMR (101 MHz, $CDCl_3$)** δ (a mixture of two rotamers) 172.4, 167.3, 166.8, 156.1, 153.6, 152.9, 134.9, 132.4, 131.7, 131.1, 128.3, 128.3, 119.6, 119.0, 83.1, 82.1, 79.9, 71.4, 70.6, 67.0, 44.3, 43.8, 43.2, 42.2, 41.6, 28.4, 28.3; **IR (Neat Film, NaCl)** 3386, 2978, 1760, 1698, 1601, 1505, 1451, 1394, 1367, 1314, 1232, 1203, 1164, 1092, 1067, 1012, 915, 854, 766, 730, 696 cm^{-1}; **HRMS (MM: ESI-APCI):** *m/z* calc'd for $C_{26}H_{36}N_3O_8$ $[M+H]^+$: 518.2497, found 518.2496.

1.4.2.2 Procedures for the Synthesis of Tetrahydropyrimidinone Allylic Alkylation Substrates

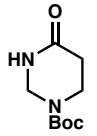

***tert*-Butyl 4-oxotetrahydropyrimidine-1(2*H*)-carboxylate**. A solution of 3-aminopropanamide hydrochloride (5 g, 40.1 mmol, 1.0 equiv), potassium hydroxide (3.38 g, 60.2 mmol, 1.5 equiv), and formaldehyde (37% in water, 5.97 mL, 80.3 mmol, 2.0 equiv) in ethanol (13 mL) was stirred at reflux for 4 h. The suspension was then maintained at 55 °C while triethylamine (5.5 mL, 40.1 mmol, 1 equiv) and di-*tert*-butyl dicarbonate (9.2 g, 42.1 mmol, 1.05 equiv) were added successively. The reaction was stirred for 2 h at 55 °C and then allowed to cool to ambient temperature. The precipitate was filtered off, the filtrate was concentrated under reduced pressure, and was then purified by silica gel flash chromatography (1 → 3% MeOH/CH_2Cl_2) to afford Boc-protected tetrahydropyrimidinone as a white solid (4.09 g, 51% yield over two steps): **^{1}H NMR (500 MHz, $CDCl_3$)** δ 8.14 – 7.60 (m, 1H), 4.77 – 4.61 (m, 2H), 3.58 (t, *J* = 6.5 Hz, 2H), 2.41 (t, *J* = 6.5 Hz, 2H), 1.41 (s, 9H); **^{13}C NMR (126 MHz, $CDCl_3$)** δ (a mixture of two rotamers) 171.5, 153.8, 153.4, 81.1, 54.8, 54.0, 40.4, 39.4, 31.4, 28.3; **IR (Neat Film, NaCl)** 3193, 2970, 1710, 1643, 1488, 1404, 1366, 1326, 1276, 1245, 1210, 1159, 1136, 1020, 949, 776 cm^{-1}; **HRMS (MM: ESI-APCI):** *m/z* calc'd for C9H17N2O3 $[M+H]^+$: 201.1234, found 201.1231.

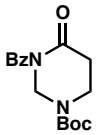

***tert*-Butyl 3-benzoyl-4-oxotetrahydropyrimidine-1(2*H*)-carboxylate.** To a solution of tetrahydropyrimidinone (2.07 g, 10.4 mmol, 1.0 equiv) in THF (100 mL) at −78 °C was added *n*-butyllithium (2.2 M in hexanes, 4.94 mL, 10.9 mmol, 1.05 equiv) dropwise over 10 min. After stirring the solution at −78 °C for 20 min, benzoyl chloride (1.43 mL, 12.4 mmol, 1.2 equiv) was added dropwise at −78 °C. The reaction solution was stirred at −78 °C for 40 min, allowed to warm up to room temperature, and was then quenched with saturated aqueous NH_4Cl (50 mL). The mixture was diluted with EtOAc (100 mL) and the aqueous phase was extracted with EtOAc (3 x 80 mL). The combined organic phases were dried over anhydrous Na_2SO_4, filtered and concentrated under reduced pressure onto silica gel. The silica-loaded residue was purified by silica gel flash chromatography (30% EtOAc/hexanes) to give Bz-protected tetrahydropyrimidinone as a white solid (2.72 g, 86% yield): **^{1}H NMR (400 MHz, Chloroform-*d*)** δ 7.55 (dt, *J* = 8.3, 1.4 Hz, 2H), 7.50 (t, *J* = 7.4 Hz, 1H), 7.39 (t, *J* = 7.6 Hz, 2H), 5.28 (s, 2H), 3.74 (t, *J* = 6.6 Hz, 2H), 2.68 (t, *J* = 6.6 Hz, 2H), 1.49 (s, 9H); **^{13}C NMR (101 MHz, $CDCl_3$)** δ 172.3, 170.7, 153.8, 135.0, 132.2, 128.4, 128.2, 81.7, 57.0, 40.4, 33.4, 28.3; **IR (Neat Film, NaCl)** 2978, 1698, 1480, 1450, 1408, 1367, 1304, 1266, 1239, 1141, 1015, 936, 863, 797, 700, 618 cm^{-1}; **HRMS (MM: ESI-APCI):** *m/z* calc'd for C16H21N2O4 $[M+H]^+$: 305.1496, found 305.1500.

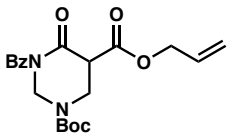

5-Allyl 1-(*tert*-butyl) 3-benzoyl-4-oxotetrahydropyrimidine-1,5(2*H*)-dicarboxylate. To a solution of diisopropylamine (224 μL, 1.59 mmol, 1.2 equiv) in THF (3 mL) at −78 °C was added *n*-butyllithium (2.2 M in hexanes, 664 μL, 1.46 mmol, 1.1 equiv). The solution was maintained at −78 °C for 15 min and then cannulated over 10 min into a solution of Bz-protected tetrahydropyrimidine (404 mg, 1.33 mmol, 1.0 equiv) in THF (10 mL) at −78 °C. After stirring the solution at −78 °C for 25 min, allyl cyanoformate (156 μL, 1.46 mmol, 1.1 equiv) was added dropwise at −78 °C. The reaction mixture was maintained at −78 °C for 50 min and was then quenched with saturated aqueous NH_4Cl (10 mL). The reaction mixture was diluted with EtOAc (10mL) and allowed to warm to room temperature. The aqueous phase was extracted with EtOAc (3 x 15 mL) and the combined organic phases were dried over anhydrous Na_2SO_4, decanted, and concentrated under reduced pressure onto silica gel. The silica-loaded residue was purified by silica gel flash chromatography (18 → 20 → 30% EtOAc/hexanes) to give re-isolated starting material (154 mg, 38% yield) and allyl ester as a white crystalline solid (310 mg, 60% yield, 97% yield based on recovered starting material): **^{1}H NMR (400 MHz, $CDCl_3$)** δ 7.70 (d, *J* = 7.2 Hz, 2H), 7.51 (t, *J* = 7.4 Hz, 1H), 7.40 (t, *J* = 7.6 Hz, 2H), 5.95 (ddt, *J* = 17.2, 10.4, 5.9 Hz, 1H), 5.37 (dq, *J* = 17.2, 1.5 Hz, 1H), 5.36 (m, 1H), 5.30 (dd, *J* = 10.4, 1.3 Hz, 1H), 5.17 (d, *J* = 12.6 Hz, 1H), 4.69 (d, *J* = 6.0 Hz, 2H), 4.27 (ddd, *J* = 13.7, 5.4, 1.2 Hz, 1H), 3.85 (dd, *J* = 13.7, 6.2 Hz, 1H), 3.63 (t, *J* = 5.7 Hz, 1H), 1.49 (s, 9H); **^{13}C NMR (101 MHz, $CDCl_3$)** δ 172.9, 167.8, 167.0, 153.4, 134.6, 132.5, 131.3, 128.7, 128.3, 119.7, 82.3, 67.0, 58.5, 50.1, 43.9, 28.3; **IR (Neat Film, NaCl)** 3406, 3064, 2978, 2935,

1714, 1601, 1480, 1450, 1416, 1369, 1287, 1148, 1072, 1017, 934 , 859, 796, 768, 736, 703, 626 cm^{-1}; **HRMS (MM: ESI-APCI):** *m/z* calc'd for C20H25N2O6 $[M+H]^+$: 389.1707, found 389.1708.

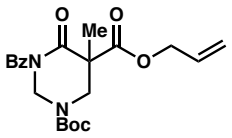

1-(*tert*-butyl) 3-benzoyl-5-methyl-4-oxotetrahydropyrimidine-1,5(2*H*)-dicarboxylate (1.5a). To a solution of allyl ester (100 mg, 0.26 mmol, 1.0 equiv) in acetonitrile (2.6 mL) at 0 °C was added cesium carbonate (168 mg, 0.52 mmol, 2.0 equiv). After stirring the suspension for 30 min at 0 °C, methyl iodide (48 μL, 0.77 mmol, 3.0 equiv) was added. The reaction mixture was stirred for 3 h at 0 °C and diluted with saturated aqueous NH_4Cl (2 mL) and EtOAc (2 mL). The aqueous phase was extracted with EtOAc (4 x 3 mL) and the combined organic phases were dried over anhydrous Na_2SO_4, decanted, and concentrated under reduced pressure onto silica gel. The residue was purified by silica gel flash chromatography (15% EtOAc/hexanes) to give methylated allyl ester **1.5a** as a colorless oil (100 mg, 95% yield): **^{1}H NMR (500 MHz, $CDCl_3$)** δ (a mixture of two rotamers) 7.71 (d, *J* = 15.3 Hz, 2H), 7.51 (t, *J* = 7.4 Hz, 1H), 7.39 (t, *J* = 6.8 Hz, 2H), 5.96 (ddt, *J* = 16.6, 10.4, 6.0 Hz, 1H), 5.48 – 5.17 (m, 4H), 4.71 (d, *J* = 6.1 Hz, 2H), 4.43 (m, 1H), 3.38 (m, 1H), 1.49 (s, 9H), 1.47 (s, 3H); **^{13}C NMR (101 MHz, $CDCl_3$)** δ (a mixture of two rotamers) 173.2, 170.9, 170.7, 153.2, 135.0, 132.3, 131.3, 128.4, 128.2, 119.7, 82.1, 67.1, 58.9, 58.1, 52.8, 50.6, 50.3, 28.3, 19.3; **IR (Neat Film, NaCl)** 3406, 3065, 2980, 2939, 1714, 1602, 1450, 1423, 1369, 1288, 1251, 1162, 1134, 1104, 1028, 984, 938, 902, 857, 804, 765, 732, 697, 657, 635 cm^{-1}; **HRMS (MM: ESI-APCI):** *m/z* calc'd for $C_{21}H_{27}N_2O_6$ $[M+H]^+$: 403.1864, found 403.1868.

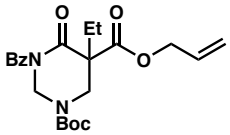

5-allyl 1-(tert-butyl) 3-benzoyl-5-ethyl-4-oxotetrahydropyrimidine-1,5(2H)-dicarboxylate (1.5b). Following the procedure described for the preparation of **1.5a**, allyl ester (200 mg, 0.52 mmol, 1.0 equiv) was treated with cesium carbonate (336 mg, 1.03 mmol, 2.0 equiv) and alkylated with ethyl iodide (124 μL, 1.54 mmol, 3.0 equiv) to give, after purification by silica gel flash chromatography (dry load SiO_2, 15% EtOAc/hexanes), ethylated allyl ester **1.5b** as a colorless oil (182 mg, 85% yield): **^{1}H NMR (400 MHz, $CDCl_3$)** δ (a mixture of two rotamers) 7.70 (d, *J* = 8.0 Hz, 2H), 7.50 (t, *J* = 7.4 Hz, 1H), 7.38 (t, *J* = 7.7 Hz, 2H), 5.95 (ddt, *J* = 16.6, 10.4, 6.0 Hz, 1H), 5.38 (dd, *J* = 17.2, 1.5 Hz, 1H), 5.31 (d, *J* = 10.3 Hz, 2H), 5.20 (d, *J* = 12.5 Hz, 1H), 4.70 (t, *J* = 5.5 Hz, 2H), 4.47 – 4.26 (m, 1H), 3.49 (d, *J* = 13.5 Hz, 1H), 1.96 (q, *J* = 7.5 Hz, 2H), 1.49 (s, 9H), 0.96 (t, *J* = 7.4 Hz, 3H); **^{13}C NMR (101 MHz, $CDCl_3$)** δ (a mixture of two rotamers) 172.9, 170.4, 170.1, 169.8, 153.2, 135.0, 132.3, 131.2, 128.4, 128.2, 119.8, 81.9, 66.9, 57.9, 57.4, 56.7, 47.8, 47.4, 28.3, 26.4, 9.1; **IR (Neat Film, NaCl)** 2976, 1703, 1450, 1422, 1367, 1288, 1247, 1156, 1134, 1015, 942, 894, 802, 766, 718, 696 cm^{-1}; **HRMS (MM: ESI-APCI):** *m/z* calc'd for $C_{22}H_{29}N_2O_6$ $[M+H]^+$: 417.2020, found 417.2019.

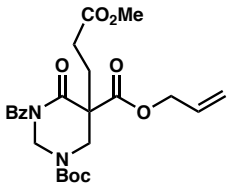

5-allyl 1-(tert-butyl) 3-benzoyl-5-(3-methoxy-3-oxopropyl)-4-oxotetrahydropyrimidine-1,5(2H)-dicarboxylate (1.5c). To a suspension of allyl ester (100 mg, 0.26 mmol, 1.0 equiv) and potassium carbonate (178 mg, 1.29 mmol, 5.0 equiv) in acetone (1.0 mL) at room temperature was added methyl acrylate (47 μL, 0.52 mmol, 2.0 equiv). The reaction mixture was stirred for 3.5 h at 55 °C, allowed to cool to room temperature, and filtered through a cotton plug. The filter cake was washed with acetone (3 x 1 mL) and the combined organic phases were concentrated by under reduced pressure onto silica gel. The silica-loaded residue was purified by silica gel flash chromatography (19% EtOAc/hexanes) to give pyrimidinone **1.5c** as a colorless oil (101 mg, 83% yield): **^{1}H NMR (400 MHz, $CDCl_3$)** δ (a mixture of two rotamers) 7.70 (br s, 2H), 7.50 (t, *J* = 7.4 Hz, 1H), 7.38 (t, *J* = 7.7 Hz, 2H), 5.95 (ddt, *J* = 16.6, 10.3, 6.0 Hz, 1H), 5.38 (dd, *J* = 17.1, 1.6 Hz, 1H), 5.32 (d, *J* = 10.4 Hz, 1H), 5.25 (m, 2H), 4.70 (d, *J* = 6.0 Hz, 2H), 4.41 (m, 1H), 3.62 (s, 3H), 3.47 (m, 1H), 2.58 (ddd, *J* = 16.0, 9.5, 6.4 Hz, 1H), 2.46 – 2.33 (m, 1H), 2.21 (ddd, *J* = 10.0, 6.3, 3.2 Hz, 2H), 1.48 (s, 9H); **^{13}C NMR (101 MHz, $CDCl_3$)** δ (a mixture of two rotamers) 173.0, 172.9, 169.7, 153.1, 134.9, 132.4, 131.1, 128.4, 128.3, 120.1, 82.2, 67.2, 58.3, 57.6, 55.6, 51.9, 48.7, 48.2, 29.7, 28.3; **IR (Neat Film, NaCl)** 2978, 1704, 1423, 1368, 1248, 1153, 987, 803, 722, 696 cm^{-1}; **HRMS (MM: ESI-APCI):** *m/z* calc'd for $C_{24}H_{31}N_2O_8$ $[M+H]^+$: 475.2075, found 475.2074.

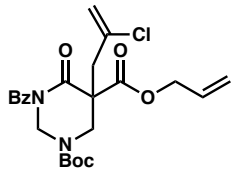

5-allyl 1-(tert-butyl) 3-benzoyl-5-(2-chloroallyl)-4-oxotetrahydropyrimidine-1,5(2H)-dicarboxylate (1.5d). To a suspension of allyl ester (200 mg, 0.51 mmol, 1.0 equiv) and tetrabutylammonium iodide (17 mg, 0.05 mmol, 0.1 equiv), in THF (5.1 mL) at 0 °C was added NaH (60% in mineral oil, 25 mg, 0.62 mmol, 1.2 equiv). After stirring for 30 min at 0 °C, 2,3-dichloro-1-propene (95 μL, 1.02 mmol, 2 equiv) was added and the reaction mixture heated at 40 °C for 16 h. The reaction was quenched with aqueous NH_4Cl (10 mL) and extracted with EtOAc (3 x 5 mL). The combined organic phases were dried over anhydrous Na_2SO_4, decanted, and concentrated under reduced pressure onto silica gel. The silica-loaded residue was purified by silica gel flash chromatography (10% → 15% EtOAc/hexanes) to give 2-chloro-allyl allyl ester **1.5d** as a colorless oil (140 mg, 59% yield): **^{1}H NMR (400 MHz, $CDCl_3$)** δ 7.75 (d, *J* = 8.6 Hz, 2H), 7.51 (s, 1H), 7.39 (t, *J* = 7.5 Hz, 2H), 6.07 – 5.90 (m, 1H), 5.71 – 5.48 (m, 1H), 5.33 (m, 4H), 5.03 (d, *J* = 12.5 Hz, 1H), 4.85 – 4.43 (m, 3H), 3.58 (mz, 1H), 3.32 (d, *J* = 15.1 Hz, 1H), 3.03 (d, *J* = 15f.1 Hz, 1H), 1.48 (s, 9H); **^{13}C NMR (101 MHz, $CDCl_3$)** δ (a mixture of two rotamers) 173.3, 169.9, 168.7, 153.4, 136.3, 134.9, 132.4, 131.2, 128.7, 128.2, 120.1, 118.8, 82.1, 67.7, 58.5, 57.8, 55.1, 47.7, 47.2, 41.0, 28.3; **IR (Neat Film, NaCl)** 2978, 1703, 1632, 1478, 1450, 1423, 1368, 1289, 1246, 1137, 902, 803, 721, 695, 633 cm^{-1}; **HRMS (MM: ESI-APCI):** *m/z* calc'd for C23H28ClN2O6 $[M+H]^+$: 463.1630, found 463.1641.

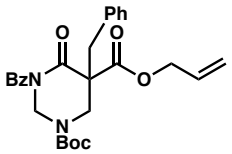

5-Allyl 1-(*tert*-butyl) 3-benzoyl-5-benzyl-4-oxotetrahydropyrimidine-1,5(2*H*)-dicarboxylate (1.5e). To a solution of allyl ester (100 mg, 0.26 mmol, 1.0 equiv) in THF (2.6 mL) at room temperature was added sodium hydride (11 mg, 0.28 mmol, 1.1 equiv). After stirring for 15 min, benzyl bromide (37 μL, 0.31 mmol, 1.2 equiv) was added. The reaction mixture was maintained at room temperature for 22 h and at 55 °C for 24 h. The reaction was quenched with aqueous NH_4Cl (2 mL) and diluted with EtOAc (2mL). The aqueous phase was extracted with EtOAc (3 x 3mL) and the combined organic phases were dried over anhydrous Na_2SO_4, decanted, and concentrated under reduced pressure onto silica gel. The silica-loaded residue was purified by silica gel flash chromatography (15% EtOAc/hexanes) to give benzylated allyl ester **1.5e** as a colorless oil (94 mg, 76% yield): **^{1}H NMR (400 MHz, $CDCl_3$)** δ 7.71 (d, *J* = 7.6 Hz, 2H), 7.52 (t, *J* = 7.5 Hz, 1H), 7.39 (t, *J* = 7.5 Hz, 2H), 7.29 – 7.19 (m, 3H), 7.14 (dd, *J* = 7.4, 2.2 Hz, 2H), 5.95 (ddt, *J* = 16.6, 10.4, 6.0 Hz, 1H), 5.44 – 5.19 (m, 3H), 4.73 (m, 3H), 4.56 – 4.37 (m, 1H), 3.50 (d, *J* = 14.0 Hz, 1H), 3.33 (d, *J* = 13.9 Hz, 1H), 3.14 (d, *J* = 14.0 Hz, 1H), 1.45 (s, 9H); **^{13}C NMR (101 MHz, $CDCl_3$)** δ (a mixture of two rotamers) 173.1, 170.4, 169.3, 153.2, 135.0, 134.9, 132.4, 131.3, 130.9, 128.7, 128.7, 128.2, 127.5, 119.9, 81.9, 67.3, 58.0, 57.5, 57.3, 47.8, 47.2, 38.1, 28.3; **IR (Neat Film, NaCl)** 3063, 2978, 2935, 1704, 1602, 1479, 1451, 1418, 1368, 1287, 1251, 1152, 1093, 1002, 927, 902, 857, 804, 764, 727, 697, 635 cm^{-1}; **HRMS (MM: ESI-APCI):** *m/z* calc'd for $C_{27}H_{31}N_2O_6$ $[M+H]^+$: 479.2177, found 479.2180.

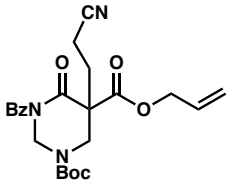

5-allyl 1-(tert-butyl) 3-benzoyl-5-(2-cyanoethyl)-4-oxotetrahydropyrimidine-1,5(2H)-dicarboxylate (1.5f). To a solution of allyl ester (100 mg, 0.26 mmol, 1.0 equiv) and acrylonitrile (34 μL, 0.52 mmol, 2.0 equiv) in acetonitrile (1.3 mL) at room temperature was added DBU (1.9 μL, 0.013 mmol, 0.05 equiv). After 22 h at room temperature, the reaction mixture was heated to 70 °C for 32 h, allowed to cool to room temperature, and treated with additional DBU (1.9 μL, 0.013 mmol, 0.05 equiv). After 2 h at 70 °C, the reaction mixture was allowed to cool to room temperature, directly concentrated onto silica gel, and purified by silica gel flash chromatography (22% EtOAc/hexanes) to give cyanoethylated pyrimidinone **1.5f** as a colorless oil (71.5 mg, 63% yield): **^{1}H NMR (400 MHz, $CDCl_3$)** δ 7.72 (d, *J* = 7.7 Hz, 2H), 7.53 (t, *J* = 7.4 Hz, 1H), 7.41 (t, *J* = 7.6 Hz, 2H), 5.97 (ddt, *J* = 16.7, 10.3, 6.1 Hz, 1H), 5.41 (dd, *J* = 17.4, 1.5 Hz, 1H), 5.36 (d, *J* = 10.5 Hz, 1H), 5.28 (m, 2H), 4.74 (m, 2H), 4.41 (d, *J* = 13.8 Hz, 1H), 3.49 (d, *J* = 13.8 Hz, 1H), 2.72 (dt, *J* = 16.2, 7.9 Hz, 1H), 2.50 (dt, *J* = 16.6, 7.8 Hz, 1H), 2.20 (t, *J* = 7.9 Hz, 2H), 1.49 (s, 9H); **^{13}C NMR (101 MHz, $CDCl_3$)** δ (a mixture of two rotamers) 173.0, 169.4, 169.0, 153.1, 134.6, 132.7, 130.8, 128.4, 128.4, 120.6, 118.9, 82.6, 67.6, 67.6, 58.8, 57.9, 55.1, 49.0, 48.4, 29.2, 28.4, 13.6; **IR (Neat Film, NaCl)** 2979, 2250, 1698, 1450, 1423, 1369, 1286, 1250, 1155, 1030, 939, 857, 803, 718, 696, 635 cm^{-1}; **HRMS (MM: ESI-APCI):** *m/z* calc'd for $C_{23}H_{31}N_4O_6$ $[M+NH_4]^+$: 459.2238, found 459.2243.

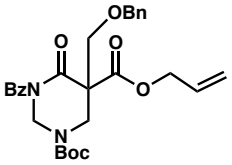

5-allyl 1-(tert-butyl) 3-benzoyl-5-((benzyloxy)methyl)-4-oxotetrahydropyrimidine-1,5(2H)-dicarboxylate (1.5g). Following the procedure described for the preparation of **1.5a**, allyl ester (200 mg, 0.52 mmol, 1.0 equiv) was treated with sodium hydride (29 mg, 0.72 mmol, 1.4 equiv) and alkylated with benzyl chloromethyl ether (127 μL, 0.93 mmol, 1.8 equiv) to give, after two rounds of purification by silica gel flash chromatography (dry load SiO_2, 16 → 25% EtOAc/hexanes), BOM-alkylated allyl ester **1.5g** as a colorless oil (57 mg, 22% yield): **^{1}H NMR (400 MHz, $CDCl_3$)** δ 7.73 (t, *J* = 8.3 Hz, 2H), 7.50 (t, *J* = 7.9 Hz, 1H), 7.41 – 7.24 (m, 7H), 5.94 (ddt, *J* = 16.5, 10.3, 6.0 Hz, 1H), 5.63 (d, *J* = 12.2 Hz, 1H), 5.43 – 5.25 (m, 2H), 4.95 (d, *J* = 12.4 Hz, 1H), 4.74 (dd, *J* = 13.0, 5.9 Hz, 1H), 4.70 – 4.36 (m, 4H), 4.07 (d, *J* = 9.2 Hz, 1H), 3.96 – 3.80 (m, 1H), 3.74 (d, *J* = 9.3 Hz, 1H), 1.48 (s, 9H); **^{13}C NMR (101 MHz, $CDCl_3$)** δ (a mixture of two rotamers) 173.2, 169.0, 168.7, 168.3, 153.6, 153.3, 137.5, 134.9, 132.2, 131.3, 131.0, 128.6, 128.1, 128.0, 127.7, 119.9, 119.7, 81.9, 73.9, 70.0, 67.1, 58.7, 57.9, 57.0, 47.0, 46.7, 28.3; **IR (Neat Film, NaCl)** 2978, 2360, 1704, 1453, 1418, 1368, 1290, 1248, 1153, 1128, 1072, 1003, 904, 857, 803, 735, 697, 633 cm^{-1}; **HRMS (MM: ESI-APCI):** *m/z* calc'd for $C_{28}H_{33}N_2O_7$ $[M+H]^+$: 509.2282, found 509.2279.

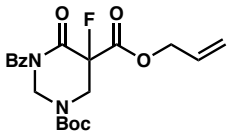

5-allyl 1-(tert-butyl) 3-benzoyl-5-fluoro-4-oxotetrahydropyrimidine-1,5(2H)-dicarboxylate (1.5h). To a solution of allyl ester (100 mg, 0.257 mmol, 1.0 equiv) in THF (2.6 mL) at room temperature was added sodium hydride (11 mg, 0.28 mmol, 1.1 equiv). After stirring for 15 min, Selectfluor (109 mg, 0.31 mmol, 1.2 equiv) was added and the reaction mixture was stirred for 1.5 h at room temperature. The reaction was quenched with aqueous NH_4Cl (2 mL) and diluted with EtOAc (2 mL). The aqueous phase was extracted with EtOAc (3 x 3 mL) and the combined organic phases were dried over anhydrous Na_2SO_4, filtered and concentrated by reduced pressure onto silica gel. The residue was purified by silica gel flash chromatography (4:1 hexanes/EtOAc) to give fluorinated allyl ester **1.5h** as a colorless oil (92 mg, 0.226 mmol, 88%); **^{1}H NMR (400 MHz, $CDCl_3$)** δ (a mixture of two rotamers) 7.67 (s, 2H), 7.52 (t, J = 7.5 Hz, 1H), 7.39 (t, J = 7.6 Hz, 2H), 5.95 (ddt, J = 16.6, 10.3, 6.0 Hz, 1H), 5.63 – 5.07 (m, 4H), 4.88 – 4.77 (m, 1H), 4.75 (s, 1H), 4.43 (m, 1H), 3.99 (m, 1H), 1.49 (s, 9H); **^{13}C NMR (101 MHz, $CDCl_3$)** δ (a mixture of two rotamers) 172.4, 165.3, 164.4, 153.1, 133.8, 132.9, 130.5, 128.6, 128.5, 120.4, 89.3 (d, J_{CF} = 192.9 Hz, appears as four peaks due to the presence of two rotamers and coupling with fluorine), 82.8, 67.8, 59.0, 58.4, 49.2, (d, J_{CF} = 28.3 Hz), 48.4 (d, J_{CF} = 27.3 Hz), 28.2; **IR (Neat Film, NaCl)** 2979, 2360, 1770, 1715, 1601, 1478, 1450, 1418, 1369, 1287, 1252, 1157, 1134, 1072, 1018, 907, 857, 829, 803, 764, 730, 695, 658, 633 cm^{-1}; **HRMS (MM: ESI-APCI):** *m/z* calc'd for $C_{20}H_{27}FN_3O_6$ $[M+NH_4]^+$: 424.1878, found 424.1877.

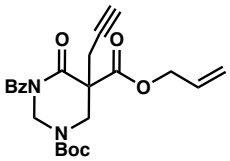

5-allyl 1-(tert-butyl) 3-benzoyl-4-oxo-5-(prop-2-yn-1-yl)tetrahydropyrimidine-1,5(2H)-dicarboxylate 1.5i. To a solution of allyl ester (200 mg, 0.51 mmol, 1.0 equiv) in THF (5 mL) at 0 °C was quickly added sodium hydride (23 mg, 0.57 mmol, 1.1 equiv). After stirring at 0 °C for 30 minutes, propargyl bromide (111 μL, 1.03 mmol, 2 equiv) was added and the reaction mixture was heated to 50 °C. After three hours, more propargyl bromide (111 μL, 1.03 mmol, 2 equiv) was added and the reaction was allowed to continue for 16 h at 50 °C. The reaction was quenched with aqueous NH_4Cl (10 mL) and extracted with EtOAc (3 x 5 mL). The combined organic phases were dried over anhydrous Na_2SO_4, decanted, and concentrated under reduced pressure. The crude residue was purified by silica gel flash chromatography (50% CH_2Cl_2/hexanes → 70% CH_2Cl_2/hexanes → 20% EtOAc/hexanes) to afford the propargylated allyl ester **1.5i** as a colorless oil (160 mg, 73% yield): **^{1}H NMR (400 MHz, $CDCl_3$)** δ 7.74 (s, 2H), 7.50 (d, *J* = 7.4 Hz, 1H), 7.38 (t, *J* = 7.5 Hz, 2H), 5.96 (dd, *J* = 17.0, 10.6 Hz, 1H), 5.64 (dd, *J* = 12.4, 2.1 Hz, 1H), 5.39 (d, *J* = 17.2 Hz, 1H), 5.33 (d, *J* = 10.4 Hz, 1H), 5.16 – 4.88 (m, 1H), 4.82 – 4.32 (m, 3H), 4.01 – 3.63 (m, 1H), 3.03 (d, *J* = 18.2 Hz, 1H), 2.71 (dd, *J* = 17.0, 2.7 Hz, 1H), 2.09 (t, *J* = 2.6 Hz, 1H), 1.49 (s, 9H); **^{13}C NMR (101 MHz, $CDCl_3$)** δ (a mixture of two rotamers) 173.3, 169.6, 168.6, 153.5, 134.9, 132.4, 131.2, 130.9, 128.6, 128.2, 120.0, 82.2, 78.8, 72.6, 67.5, 58.9, 58.2, 55.2, 48.2, 28.3, 23.0; **IR (Neat Film, NaCl)** 3280, 2978, 1704, 1600, 1479, 1450, 1422, 1368, 1287, 1245, 1155, 1140, 1073, 1016, 929, 904, 856, 803, 765, 733 695, 656 cm^{-1}; **HRMS (MM: ESI-APCI):** *m/z* calc'd for C23H27N2O6 $[M+H]^+$: 427.1864, found 427.1859.

1.4.2.3 General Procedure for Allylic Alkylation Optimization Screen

Optimization of Reaction Parameters

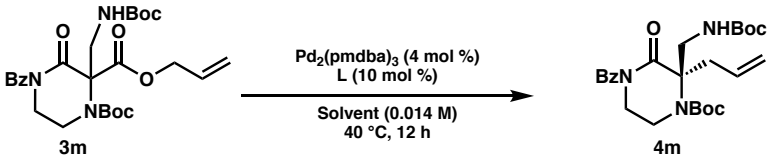

Entry	L	Solvent	Yield (%)[b]	ee (%)[c]
1	L1	Tol	75	76
2	L2	Tol	70	1
3	L3	Tol	83	52
4	L1	THF	–	13
5	L1	MTBE	–	80
6	L1	2:1 Hex/Tol	93	93

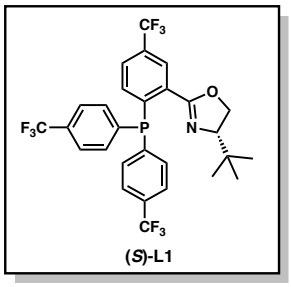

(*S*)-L1

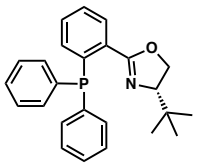

(*S*)-L2

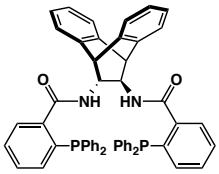

(*S,S*)-L3

[a] Screens performed on a 0.04 mmol scale. All reported yields are for isolated products. The ee values were determined by chiral SFC analysis. Bz = benzoyl, Boc = tert-butoxycarbonyl, pmdba = bis(4-methoxybenzylidene)acetone

In a nitrogen-filled glovebox, an oven-dried 1 dram vial was charged with $Pd_2(pmdba)_3$ (1.7 mg, 0.0015 mmol, 4 mol %), ligand (10 mol %), solvent (1 mL), and a magnetic stir bar. The vial was stirred at ambient glovebox temperature (27 °C) for 30 min and then substrate **1.3m** (20 mg, 0.04 mmol, 1.0 equiv) was added as a solution in solvent (1.8 mL, total concentration 0.014 M). The vial was sealed with a teflon cap and heated to 40 °C. When complete consumption of the starting material was observed by

thin layer chromatography, the reaction mixture was removed from the glovebox and concentrated under reduced pressure. The residue was purified by silica gel flash chromatography to afford the oxopiperazine **1.4m**.

1.4.2.4 General Procedure for Pd-Catalyzed Decarboxylative Allylic Alkylation Reactions

Please note The absolute configuration for all other products has been inferred by analogy.[4,7,10,13,52,53] For respective SFC conditions, please refer to the section **Determination of Enantiomeric Excess**.

In a nitrogen-filled glovebox, an oven-dried 1 dram vial or 20 mL scintillation vial was charged with $Pd_2(pmdba)_3$ or $Pd_2(dba)_3$ (4 mol %), (*S*)-$(CF_3)_3$-*t*Bu-PHOX (10 mol %), hexane/toluene (2:1), and a magnetic stir bar. The vial was stirred at ambient glovebox temperature (27 °C) for 30 min and then the substrate (1.0 equiv) was added as a solution in hexane/toluene (2:1, total concentration 0.014 M or 0.033 M). The vial was sealed with a teflon cap and heated to 40 °C. When complete consumption of the starting material was observed by thin layer chromatography, the reaction mixture was removed from the glovebox and concentrated under reduced pressure. The residue was purified by silica gel flash chromatography to afford the desired oxopiperazine.

1.4.2.5 Experimental Procedures and Spectroscopic data for the Pd-Catalyzed Decarboxylative Asymmetric Allylic Alkylation of Piperazinone Substrates

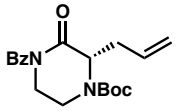

***tert*-butyl (*S*)-2-allyl-4-benzoyl-3-oxopiperazine-1-carboxylate (1.4a)**. Following the general procedure, allyl ester **3a** (25 mg, 0.064 mmol, 1.0 equiv) in toluene (1.45 mL) was added to a solution of $Pd_2(dba)_3$ (2.3 mg, 0.0026 mmol, 4 mol %) and (*S*)-$(CF_3)_3$-*t*Bu-PHOX (3.8 mg, 0.0064 mmol, 10 mol %) in toluene (0.5 mL). Purification by flash chromatography (20% EtOAc/hexanes) gave monosubstituted oxopiperazine **1.4a** as a yellow oil (21 mg, 90% yield, 92% ee). **^{1}H NMR (400 MHz, $CDCl_3$)** δ (a mixture of two rotamers) 7.64 – 7.46 (m, 3H), 7.41 (m, 2H), 5.83 (ddt, *J* = 17.2, 10.0, 7.3 Hz, 1H), 5.22 – 5.07 (m, 2H), 4.70 (m, 1H), 4.45 – 3.99 (m, 1H), 3.99 – 3.70 (m, 2H), 3.42 (m, 1H), 2.90 – 2.52 (m, 2H), 1.50 (s, 9H); **^{13}C NMR (101 MHz, $CDCl_3$)** δ (a mixture of two rotamers) 173.6, 170.6, 153.8, 135.3, 133.2, 132.2, 128.3, 128.3, 119.0, 81.3, 58.4, 44.5, 38.1, 37.2, 28.5. **IR (Neat Film, NaCl)** 2977, 2930, 1692, 1600, 1450, 1413, 1392, 1366, 1300, 1231, 1159, 1130, 1008, 973, 920, 856, 795, 762, 729, 696, 656 cm^{-1}; **HRMS (MM: ESI-APCI):** *m/z* calc'd for C19H25N2O4 $[M+H]^+$: 345.1809, found 345.1810; **$[\alpha]_D^{23.0}$** +49.5 (c 1.00, $CHCl_3$); **SFC conditions**: 15% IPA, 2.5 mL/min, Chiralpak AD–H column, λ = 210 nm, t_R (min): major = 3.741, minor = 2.682.

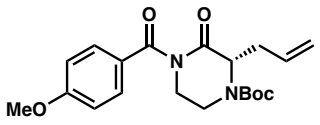

***tert*-butyl (*S*)-2-allyl-4-(4-methoxybenzoyl)-3-oxopiperazine-1-carboxylate (1.4b)**. Following the general procedure, anisoyl-protected allyl ester **1.3b** (15 mg, 0.036 mmol,

1.0 equiv) in toluene (0.6 mL) was added to a solution of $Pd_2(dba)_3$ (1.7 mg, 0.0014 mmol, 4 mol %) and (*S*)-$(CF_3)_3$-*t*Bu-PHOX (2.8 mg, 0.0036 mmol, 10 mol %) in toluene (0.5 mL). Purification by flash chromatography (20% EtOAc/hexanes) gave monosubstituted oxopiperazine **1.4b** as a light yellow oil (12 mg, 92% yield, 96% ee): **^{1}H NMR (400 MHz, $CDCl_3$)** δ (a mixture of two rotamers) 7.60 (d, *J* = 8.9 Hz, 2H), 6.89 (d, *J* = 8.9 Hz, 2H), 5.85 (ddt, *J* = 17.1, 10.0, 7.3 Hz, 1H), 5.24 – 5.04 (m, 2H), 4.69 (m, 1H), 4.19 (m, 1H), 3.85 (m, 5H), 3.42 (m, 1H), 2.89 – 2.56 (m, 2H), 1.49 (s, 9H); **^{13}C NMR (101 MHz, $CDCl_3$)** δ 173.0, 170.6, 163.3, 153.9, 133.4, 131.2, 127.1, 118.9, 113.7, 81.3, 58.4, 55.6, 44.6, 38.3, 37.4, 28.5; **IR (Neat Film, NaCl)** 2976, 1694, 1605, 1512, 1462, 1416, 1366, 1315, 1257, 1234, 1170, 1130, 1003, 973, 842, 770 cm^{-1}; **HRMS (MM: ESI-APCI):** *m/z* calc'd for C20H27N2O5 $[M+H]^+$: 375.1914, found 375.1931; **$[\alpha]_D^{23.0}$** +41.7 (c 1.00, $CHCl_3$); **SFC conditions**: 15% IPA, 2.5 mL/min, Chiralpak AD–H column, λ = 210 nm, t_R (min): major = 4.708, minor = 3.998.

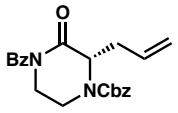

benzyl (*S*)-2-allyl-4-benzoyl-3-oxopiperazine-1-carboxylate (1.4c). Following the general procedure, Cbz-protected allyl ester **1.3c** (20 mg, 0.047 mmol, 1.0 equiv) in toluene (0.9 mL) was added to a solution of $Pd_2(dba)_3$ (2.2 mg, 0.0019 mmol, 4 mol %) and (*S*)-$(CF_3)_3$-*t*Bu-PHOX (3.5 mg, 0.0047 mmol, 10 mol %) in toluene (0.5 mL). Purification by flash chromatography (20% EtOAc/hexanes) gave monosubstituted

oxopiperazine **1.4c** as a colorless oil (15 mg, 83% yield, 99% ee): **^{1}H NMR (500 MHz, $CDCl_3$)** δ (a mixture of two rotamers) 7.62 – 7.46 (m, 3H), 7.44 – 7.29 (m, 7H), 5.79 (m, 1H), 5.16 (m, 4H), 4.83 (m, 1H), 4.26 (m, 1H), 3.97 (m, 1H), 3.87 (m, 1H), 3.49 (m, 1H), 2.89 – 2.53 (m, 2H**); ^{13}C NMR (126 MHz, $CDCl_3$)** δ (a mixture of two rotamers) 173.5, 170.2, 154.7, 136.0, 135.2, 132.9, 132.3, 128.8, 128.6, 128.6, 128.4, 128.3, 119.3, 68.0, 58.4, 44.3, 39.6, 38.9, 37.2, 36.9; **IR (Neat Film, NaCl)** 3065, 2951, 1702, 1600, 1449, 1427, 1395, 1362, 1302, 1228, 1163, 1127, 1015, 975, 922, 796, 761,730, 697, 656 cm^{-1}; **HRMS (MM: ESI-APCI):** *m/z* calc'd for C22H23N2O4 $[M+H]^+$: 379.1652, found 379.1659; **$[\alpha]_D^{23.0}$** +66.0 (c 1.0, $CHCl_3$); **SFC conditions**: 30% IPA, 2.5 mL/min, Chiralpak IC column, λ = 210 nm, t_R (min): major = 4.873, minor = 6.748.

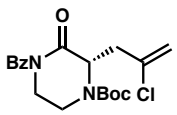

***tert*-butyl (*S*)-4-benzoyl-2-(2-chloroallyl)-3-oxopiperazine-1-carboxylate (1.4d)**. Following the general procedure, 2-chloroallyl ester **1.3d** (20 mg, 0.047 mmol, 1.0 equiv.) in hexanes/toluene (2:1, 1.9 mL) was added to a solution of $Pd_2(pmdba)_3$ (2.1 mg, 0.0019 mmol, 4 mol %) and (*S*)-$(CF_3)_3$-*t*Bu-PHOX (2.8 mg, 0.0047 mmol, 10 mol %) in hexanes/toluene (2:1, 1.5 mL). Purification by silica gel flash chromatography (15% EtOAc/hexanes) gave oxopiperazine **1.4d** as a light yellow oil (15 mg, 85% yield, 98% ee). **^{1}H NMR (400 MHz, $CDCl_3$)** δ (A mixture of two rotamers) 7.56 (d, *J* = 7.8 Hz, 2H), 7.51 (t, *J* = 7.4 Hz, 1H), 7.41 (t, *J* = 7.5 Hz, 2H), 5.30 (s, 1H), 5.24 (s, 1H), 5.06 – 4.88 (m, 1H), 4.40 – 4.06 (m, 1H), 3.94 (m, 1H), 3.84 (m, 1H), 3.55 – 3.29 (m, 1H), 2.95 (dd, *J* = 13.1, 7.4 Hz, 2H), 1.51 (s, 9H); **^{13}C NMR (101 MHz, $CDCl_3$)** δ 173.5, 169.8, 153.7,

137.5, 135.3, 132.3, 128.4, 128.3, 116.8, 81.9, 57.0, 44.6, 41.8, 37.7, 28.4. **IR (Neat Film, NaCl)** 2977, 2359, 1694, 1635, 1456, 1418, 1394, 1367, 1284, 1232, 1200, 1158, 1007, 971, 892, 856, 796, 730, 696 cm^{-1}; **HRMS (MM: ESI-APCI):** *m/z* calc'd for $C_{19}H_{24}ClN_2O_4$ $[M+H]^+$: 379.1419, found 379.1416; $\mathbf{[\alpha]_D^{23.1}}$ +33.8 (c 1.00, $CHCl_3$); **SFC conditions**: 15% IPA, 2.5 mL/min, Chiralpak AD–H column, λ = 254 nm, t_R (min): major = 4.482, minor = 3.224.

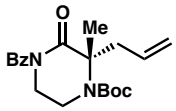

***tert*-butyl (*S*)-2-allyl-4-benzoyl-2-methyl-3-oxopiperazine-1-carboxylate (1.4e).** Following the general procedure, methylated allyl ester **1.3e** (23 mg, 0.057 mmol, 1.0 equiv) in toluene (1.2 mL) was added to a solution of $Pd_2(pmdba)_3$ (2.7 mg, 0.0023 mmol, 4 mol %) and (*S*)-$(CF_3)_3$-*t*Bu-PHOX (3.7 mg, 0.0057 mmol, 10 mol %) in toluene (0.5 mL). Purification by flash chromatography (15% EtOAc/hexanes) gave di-substituted oxopiperazine **1.4e** as a light yellow oil (17 mg, 85% yield, 96% ee). **^{1}H NMR (500 MHz, $CDCl_3$)** δ 7.57 – 7.46 (m, 3H), 7.40 (t, J = 7.6 Hz, 2H), 5.81 – 5.67 (m, 1H), 5.17 – 5.13 (m, 1H), 5.12 (d, *J* = 1.1 Hz, 1H), 4.16 – 4.02 (m, 1H), 4.03 – 3.91 (m, 1H), 3.79 (ddd, *J* = 12.9, 9.0, 3.0 Hz, 1H), 3.53 (ddd, *J* = 14.1, 9.0, 2.8 Hz, 1H), 3.11 (m, 1H), 2.84 – 2.70 (m, 1H), 1.77 (s, 3H), 1.53 (s, 9H); **^{13}C NMR (126 MHz, $CDCl_3$)** δ 174.3, 172.8, 135.8, 133.1, 131.8, 128.3, 127.6, 119.5, 81.2, 67.3, 44.2, 42.7, 41.0, 28.6, 25.5; **IR (Neat Film, NaCl)** 3076, 2977, 2934, 1692, 1641, 16001,102, 1450, 1392, 1366, 1301, 1230, 1166, 1106, 1047, 1016, 955, 922, 852, 790, 757, 727, 695 cm^{-1}; **HRMS (MM: ESI-APCI):** *m/z* calc'd for C20H27N2O4 $[M+H]^+$: 359.1965, found

359.1966; **$[\alpha]_D^{22.8}$** +6.5 (c 2.0, $CHCl_3$); **SFC conditions**: 7% IPA, 2.5 mL/min, Chiralpak AD-H column, λ = 210 nm, t_R (min): major = 7.208, minor = 4.714.

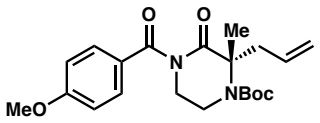

***tert*-butyl (*S*)-2-allyl-4-(4-methoxybenzoyl)-2-methyl-3-oxopiperazine-1-carboxylate (1.4f)**. Following the general procedure, anisoyl-protected allyl ester **1.3f** (25 mg, 0.058 mmol, 1.0 equiv) in toluene (1.3 mL) was added to a solution of $Pd_2(pmdba)_3$ (2.5 mg, 0.0023 mmol, 4 mol %) and (*S*)-$(CF_3)_3$-*t*Bu-PHOX (3.4 mg, 0.0058 mmol, 10 mol %) in toluene (0.5 mL). Purification by flash chromatography (20% EtOAc/hexanes) gave di-substituted oxopiperazine **1.4f** as a light pink oil (19 mg, 86% yield, 96% ee). **^{1}H NMR (400 MHz, $CDCl_3$)** δ 7.70 – 7.53 (m, 2H), 6.99 – 6.82 (m, 2H), 5.86 – 5.67 (m, 1H), 5.23 – 5.04 (m, 2H), 4.01 (dddd, *J* = 33.5, 13.9, 5.8, 2.8 Hz, 2H), 3.85 (s, 3H), 3.74 (ddd, *J* = 12.7, 9.0, 2.8 Hz, 1H), 3.52 (ddd, *J* = 13.9, 9.0, 2.7 Hz, 1H), 3.20 (s, 1H), 2.80 (ddt, *J* = 14.0, 7.1, 1.2 Hz, 1H), 1.77 (s, 3H), 1.52 (s, 9H); **^{13}C NMR (101 MHz, $CDCl_3$)** δ 174.1, 172.4, 163.0, 153.9, 133.2, 130.6, 127.5, 119.4, 113.6, 81.2, 67.1, 55.5, 44.2, 42.8, 41.1, 28.6, 25.6; **IR (Neat Film, NaCl)** 3076, 2977, 2934, 1692, 1641, 16001,102, 1450, 1392, 1366, 1301, 1230, 1166, 1106, 1047, 1016, 955, 922, 852, 790, 757, 727, 695 cm^{-1}; **HRMS (MM: ESI-APCI):** *m/z* calc'd for C21H29N2O5 $[M+H]^+$: 389.2071, found 389.2083; **$[\alpha]_D^{22.0}$** +75.6 (c 2.9, $CHCl_3$); **SFC conditions**: 10% IPA, 2.5 mL/min, Chiralpak AD-H column, λ = 210 nm, t_R (min): major = 5.370, minor = 4.278.

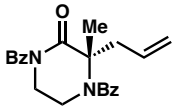

***tert*-butyl (*S*)-2-allyl-4-(4-methoxybenzoyl)-2-methyl-3-oxopiperazine-1-carboxylate (1.4g)**. Following the general procedure, di-Bz-protected allyl ester **1.3g** (10 mg, 0.025 mmol, 1.0 equiv) in toluene (1.3 mL) was added to a solution of $Pd_2(dba)_3$ (0.9 mg, 0.00098 mmol, 4 mol %) and (*S*)-$(CF_3)_3$-*t*Bu-PHOX (1.5 mg, 0.0025 mmol, 10 mol %) in toluene (0.5 mL). Purification by flash chromatography (20% EtOAc/hexanes) gave di-substituted oxopiperazine **1.4f** as a colorless oil (8 mg, 89% yield, 70% ee). Product identity matched previously reported characterization data.[4] **SFC conditions**: 10% MeOH, 2.5 mL/min, Chiralpak OJ-H column, λ = 254 nm, t_R (min): major = 5.574, minor = 6.659.

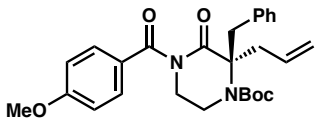

***tert*-butyl (*R*)-2-allyl-2-benzyl-4-(4-methoxybenzoyl)-3-oxopiperazine-1-carboxylate (1.4h).** Following the general procedure, benzylated allyl ester **1.3h** (10 mg, 0.02 mmol, 1.0 equiv) in hexanes/toluene (2:1, 0.9 mL) was added to a solution of $Pd_2(pmdba)_3$ (0.86 mg, 0.00078 mmol, 4 mol %) and (*S*)-$(CF_3)_3$-*t*Bu-PHOX (1.2 mg, 0.002 mmol, 10 mol %) in hexanes/toluene (2:1, 0.5 mL). Purification by flash chromatography (5% → 10% → 15% EtOAc/hexanes) gave di-substituted oxopiperazine **1.4h** as a colorless oil (7 mg, 77% yield, 96% ee): **^{1}H NMR (400 MHz, $CDCl_3$)** δ (A mixture of two rotamers) 7.57 (t, *J* = 8.5 Hz, 2H), 7.29 (d, *J* = 5.7 Hz, 3H), 7.22 – 7.07 (m, 2H), 6.91 (d, *J* = 8.3 Hz, 2H), 5.82 (ddt, *J* = 17.0, 9.6, 7.1 Hz, 1H), 5.29 – 5.13 (m, 2H), 3.88 (m, 4H), 3.74 – 3.45 (m, 2H), 3.31 (m, 1H), 3.16 (d, *J* = 12.0 Hz, 2H), 2.98 – 2.57 (m, 2H), 1.57 (s, 9H); **^{13}C**

NMR (101 MHz, $CDCl_3$) δ (A mixture of two rotamers) 172.7, 172.3, 172.0, 163.2, 154.7, 153.4, 137.1, 136.4, 133.1, 132.6, 131.3, 130.4, 128.7, 128.5, 127.5, 127.2, 119.9, 119.7, 113.5, 82.2, 80.6, 71.7, 55.6, 43.6, 43.3, 42.9, 42.6, 41.8, 29.8, 28.9, 28.6; **IR (Neat Film, NaCl)** 2975, 1691, 1604, 1512, 1454, 1365,1309, 1282, 1258, 1167, 1104, 1077, 1021, 993, 925, 839, 768, 740, 704cm^{-1}; **HRMS (MM: ESI-APCI):** *m/z* calc'd for C27H33N2O5 $[M+H]^+$: 465.2384, found 465.2390; **$[\alpha]_D^{23.4}$** +31.0 (c 0.47, $CHCl_3$); **SFC conditions**: 15% IPA, 2.5 mL/min, Chiralpak AD-H column, λ = 254 nm, t_R (min): major = 7.471, minor = 5.802.

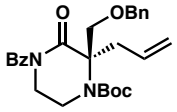

***tert*-butyl (*R*)-2-allyl-4-benzoyl-2-((benzyloxy)methyl)-3-oxopiperazine-1-carboxylate (1.4i).** (Following the general procedure, benzyloxy methyl ether allyl ester **1.3i** (25 mg, 0.049 mmol, 1.0 equiv) in hexanes/toluene (2:1, 3.0 mL) was added to a solution of $Pd_2(pmdba)_3$ (2.2 mg, 0.0020 mmol, 4 mol %) and (*S*)-$(CF_3)_3$-*t*Bu-PHOX (2.9 mg, 0.0049 mmol, 10 mol %) in hexanes/toluene (2:1, 0.5 mL). Purification by flash chromatography (15% EtOAc/hexanes) gave di-substituted oxopiperazine **1.4i** as a colorless oil (20 mg, 87% yield, 92% ee): **^{1}H NMR (500 MHz, $CDCl_3$)** δ (A mixture of two rotamers) 7.61 (dd, *J* = 8.2, 1.4 Hz, 2H), 7.51 – 7.43 (m, 1H), 7.38 – 7.26 (m, 7H), 5.72 (ddt, *J* = 17.6, 10.3, 7.4 Hz, 1H), 5.21 – 5.09 (m, 2H), 4.57 (t, *J* = 13.3 Hz, 3H), 4.32 – 3.63 (m, 5H), 3.25 – 2.93 (m, 1H), 2.60 (br s, 1H), 1.50 (s, 9H); **^{13}C NMR (126 MHz, $CDCl_3$)** δ 173.3, 172.5, 153.4, 135.6, 132.1, 131.9, 128.6, 128.3, 128.2, 127.9, 127.5, 120.0, 75.1, 74.2, 73.7, 70.6, 43.5, 38.5, 37.0, 28.6; **IR (Neat Film, NaCl)** 3064, 2976,

2931, 1692, 1601, 1474, 1452, 1392, 1365, 1317, 1286, 1251, 1232, 1164, 1102, 1062, 1016, 969, 924, 857, 730, 696, 671 cm^{-1}; **HRMS (MM: ESI-APCI):** *m/z* calc'd for C27H33N2O5 $[M+H]^+$: 465.2384, found 465.2388; **$[\alpha]_D^{23.8}$** –13.9 (c 0.33, $CHCl_3$); **SFC conditions**: 7% IPA, 2.5 mL/min, Chiralpak OJ-H column, λ = 254 nm, t_R (min): major = 3.737, minor = 4.398.

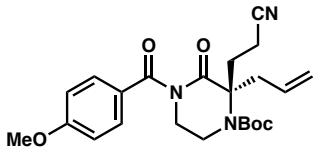

***tert*-butyl (*S*)-2-allyl-2-(2-cyanoethyl)-4-(4-methoxybenzoyl)-3-oxopiperazine-1-carboxylate (1.4j)**. Following the general procedure, *α*-cyanoethylated allyl ester **1.3j** (25 mg, 0.053 mmol, 1.0 equiv) in hexanes/toluene (2:1, 2.8 mL) was added to a solution of $Pd_2(dba)_3$ (1.9 mg, 0.0021 mmol, 4 mol %) and (*S*)-$(CF_3)_3$-*t*Bu-PHOX (3.1 mg, 0.0053 mmol, 10 mol %) in hexanes/toluene (2:1, 1.0 mL). Purification by silica gel flash chromatography (dry load SiO_2, 3:1 hexanes/EtOAc) gave oxopiperazine **1.4j** as a colorless oil (20 mg, 88% yield, 97% ee): **^{1}H NMR (400 MHz, $CDCl_3$)** δ 7.63 (d, *J* = 8.8 Hz, 2H), 6.92 (d, *J* = 8.9 Hz, 2H), 5.79 (ddt, *J* = 16.6, 10.4, 7.5 Hz, 1H), 5.24 (d, *J* = 1.7 Hz, 1H), 5.20 (dd, *J* = 9.9, 1.9 Hz, 1H), 3.98 – 3.87 (m, 2H), 3.86 (s, 3H), 3.84 – 3.71 (m, 2H), 3.27 (m, 1H), 2.82 (m, 1H), 2.69 (dd, *J* = 13.8, 7.4 Hz, 1H), 2.47 (dt, *J* = 14.1, 7.4 Hz, 1H), 2.32 (t, *J* = 7.2 Hz, 2H), 1.53 (s, 9H); **^{13}C NMR (101 MHz, $CDCl_3$)** δ 172.4, 171.5, 163.4, 153.6, 132.0, 131.2, 127.0, 120.6, 119.1, 113.7, 82.0, 69.0, 55.6, 43.8, 43.2, 42.0, 32.3, 28.5, 13.1; **IR (Neat Film, NaCl)** 2976, 2933, 2359, 2247, 1694, 1605, 1579, 1512, 1456, 1366, 1281, 1258 1168, 1113, 1020, 974, 928, 843, 768, 614 cm^{-1}; **HRMS (MM: ESI-APCI):** *m/z* calc'd for $C_{23}H_{30}N_3O_5$ $[M+H]^+$: 428.2180, found 428.2182;

$[\alpha]_D^{23.2}$ –4.3 (c 1.0, $CHCl_3$); **SFC conditions**: 15% IPA, 2.5 mL/min, Chiralpak OD-H column, λ = 210 nm, t_R (min): major = 6.049, minor = 5.143.

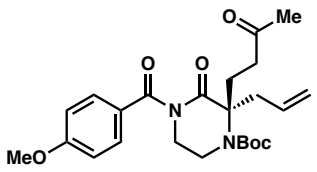

***tert*-butyl (*S*)-2-allyl-4-(4-methoxybenzoyl)-3-oxo-2-(3-oxobutyl)piperazine-1-carboxylate (1.4k).** Following the general procedure, ketone **1.3k** (25 mg, 0.051 mmol, 1.0 equiv) in hexanes/toluene (2:1, 2.2 mL) was added to a solution of $Pd_2(dba)_3$ (1.9 mg, .002 mmol, 4 mol %) and (*S*)-$(CF_3)_3$-*t*Bu-PHOX (3.0 mg, 0.0051 mmol, 10 mol %) in hexanes/toluene (2:1, 1.5 mL). Purification by silica gel flash chromatography (dry load SiO_2, 30% EtOAc/hexanes) gave ketone **1.4k** as a pale yellow oil (17 mg, 73% yield, 97% ee); **^{1}H NMR (400 MHz, $CDCl_3$)** δ 7.59 (d, *J* = 8.9 Hz, 2H), 6.89 (d, *J* = 8.9 Hz, 2H), 5.79 (ddt, *J* = 14.6, 9.4, 7.5 Hz, 1H), 5.18 (dd, *J* = 13.8, 1.9 Hz, 2H), 3.92 – 3.81 (m, 6H), 3.80 – 3.66 (m, 1H), 3.22 (s, 1H), 2.74 (dd, *J* = 13.8, 7.3 Hz, 1H), 2.72, (m, 1H), 2.50 – 2.27 (m, 3H), 2.13 (s, 3H), 1.51 (s, 9H); **^{13}C NMR (101 MHz, $CDCl_3$)** δ 207.5, 172.6, 172.4, 163.2, 132.8, 131.0, 127.3, 120.0, 113.6, 81.6, 69.5, 55.6, 43.9, 43.2, 39.1, 32.3, 30.0, 28.6, 24.8; **IR (Neat Film, NaCl)** 2975, 1694, 1605, 1512, 1456, 1392, 1366, 1282, 1258, 1168, 1113, 1062, 1019, 974, 923, 841, 768 cm^{-1}; **HRMS (MM: ESI-APCI):** *m/z* calc'd for $C_{24}H_{33}N_2O_6$ $[M+H]^+$: 445.2333, found 445.2335; **$[\alpha]_D^{23.2}$** +25.1 (c 0.97, $CHCl_3$); **SFC conditions**: 7% IPA, 2.5 mL/min, Chiralpak OD-H column, λ = 235 nm, t_R (min): major = 9.712, minor = 10.434.

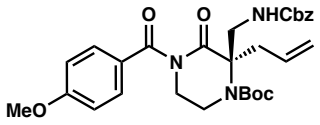

***tert*-butyl (*R*)-2-allyl-2-((((benzyloxy)carbonyl)amino)methyl)-4-(4-methoxybenzoyl)-3-oxopiperazine-1-carboxylate (1.4l)**. Following the general procedure, aminomethyl allyl ester **3l** (100 mg, 0.17 mmol, 1.0 equiv) in hexanes/toluene (2:1, 10 mL) was added to a solution of $Pd_2(dba)_3$ (6.3 mg, 0.0069 mmol, 4 mol %) and (*S*)-$(CF_3)_3$-*t*Bu-PHOX (10 mg, 0.017 mmol, 10 mol %) in hexanes/toluene (2:1, 2 mL). Purification by silica gel flash chromatography (15% → 20% → 30% EtOAc/hexanes) gave di-substituted oxopiperazine **1.4l** as a yellow oil (60 mg, 65% yield, 92% ee); **^{1}H NMR (400 MHz, $CDCl_3$)** δ (a mixture of two rotamers) 7.64 (t, *J* = 8.9 Hz, 2H), 7.44 – 7.23 (m, 5H), 6.89 (d, *J* = 8.5 Hz, 2H), 5.79 (dq, *J* = 16.8, 7.8 Hz, 1H), 5.32 – 4.93 (m, 5H), 4.31 – 3.97 (m, 1H), 3.95 – 3.64 (m, 7H), 3.64 – 3.45 (m, 1H), 3.45 – 2.87 (m, 1H), 2.64 (dd, *J* = 14.0, 7.3 Hz, 1H), 1.48 (s, 9H); **^{13}C NMR (101 MHz, $CDCl_3$)** δ 172.6, 172.3, 163.1, 156.4, 153.7, 136.6, 132.2, 131.1, 128.6, 128.4, 128.3, 127.3, 120.1, 113.6, 70.2, 67.0, 55.6, 46.9, 43.8, 43.2, 39.6, 28.6; **IR (Neat Film, NaCl)** 3357, 2975, 2361, 1694, 1605, 1512, 1456, 1366, 1317, 1283, 1255, 1169, 1094, 1061, 1020, 923, 841, 768, 699 cm^{-1}; **HRMS (MM: ESI-APCI):** *m/z* calc'd for C29H36N3O7 $[M+H]^+$: 538.2548, found 538.2543; **$[\alpha]_D^{22.8}$** +3.74 (c 2.0, $CHCl_3$); **SFC conditions:** 15% IPA, 2.5 mL/min, Chiralpak OD-H column, λ = 280 nm, t_R (min): major = 8.425, minor = 7.817.

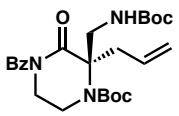

***tert*-Butyl (*R*)-2-allyl-4-benzoyl-2-(((tert-butoxycarbonyl)amino)methyl)-3-oxopiperazine-1-carboxylate (1.4m)**. Following the general procedure, allyl ester **1.3m** (100 mg, 0.19 mmol, 1.0 equiv) in hexanes/toluene (2:1, 8.0 mL) was added to a solution of $Pd_2(pmdba)_3$ (8.5 mg, 0.0077 mmol, 4 mol %) and (*S*)-$(CF_3)_3$-*t*Bu-PHOX (11.4 mg, 0.019 mmol, 10 mol %) in hexanes/toluene (2:1, 4.0 mL). Purification by flash chromatography (15% EtOAc/hexanes) gave di-substituted oxopiperazine **1.4m** as a pale yellow foam (85 mg, 93% yield, 93% ee): **^{1}H NMR (400 MHz, $CDCl_3$)** δ (a mixture of two rotamers) 7.61 (d, *J* = 7.6 Hz, 2H), 7.51 (tt, *J* = 7.5, 2.1 Hz, 1H), 7.41 (t, *J* = 7.5 Hz, 2H), 5.91 – 5.66 (m, 1H), 5.19 (d, *J* = 15.6 Hz, 2H), 4.73 (s, 1H), 4.09 – 3.72 (m, 5H), 3.67 (dd, *J* = 14.0, 7.0 Hz, 1H), 3.43 – 2.97 (m, 1H), 2.72 – 2.51 (m, 1H), 1.54 (s, 9H), 1.43 (s, 9H); **^{13}C NMR (101 MHz, $CDCl_3$)** 172.9, 172.8, 155.7, 153.6, 135.8, 132.3, 131.9, 128.2, 128.0, 120.1, 81.2, 79.7, 70.5, 46.5, 43.7, 43.2, 39.4, 28.6, 28.5; **IR (Neat Film, NaCl):** = 3374, 2977, 1694, 1504, 1454, 1392, 1366, 1317, 1286, 1231, 1165, 1094, 1060, 1014, 921, 855, 765, 729, 696 cm^{-1}; **HRMS (MM: ESI-APCI)**: m/z calc'd for $C_{25}H_{36}N_3O_6$ $[M+H]^+$: 474.2599, found: 474.2602; **$[\alpha]_D^{23.2}$** +2.7 (c 1.00, CH_3Cl); **SFC conditions**: 10% IPA, 2.5 mL/min, Chiralpak OD-H column, λ = 254 nm, t_R (min): major = 4.429, minor = 3.910.

1.4.2.6 Experimental Procedures and Spectroscopic Data for the Pd-Catalyzed Decarboxylative Asymmetric Allylic Alkylation of Tetrahydropyrimidinone Substrates

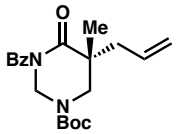

***tert*-butyl (*R*)-5-allyl-3-benzoyl-5-methyl-4-oxotetrahydropyrimidine-1(2H)-carboxylate (1.6a).** Following the general procedure, methylated pyrimidinone **1.5a** (15 mg, 0.037 mmol, 1.0 equiv) in hexanes/toluene (2:1, 1.0 mL) was added to a solution of $Pd_2(pmdba)_3$ (1.6 mg, 0.0015 mmol, 4 mol %) and (*S*)-$(CF_3)_3$-*t*Bu-PHOX (2.2 mg, 0.0037 mmol, 10 mol %) in hexanes/toluene (2:1, 1.7 mL). Purification by silica gel flash chromatography (13% EtOAc/hexanes) gave *α*-methyl pyrimidinone **1.6a** as a colorless oil (11 mg, 83% yield, 93% ee): **^{1}H NMR (500 MHz, $CDCl_3$)** δ 7.57 – 7.46 (m, 3H), 7.40 (t, *J* = 7.6 Hz, 2H), 5.78 (dq, *J* = 16.9, 8.0 Hz, 1H), 5.31 (d, *J* = 8.4 Hz, 1H), 5.25 – 5.09 (m, 3H), 3.69 (d, *J* = 13.8 Hz, 1H), 3.55 (m, 1H), 2.52 (m, 1H), 2.31 (dd, *J* = 13.9, 8.0 Hz, 1H), 1.51 (s, 9H), 1.26 (s, 3H); **^{13}C NMR (101 MHz, $CDCl_3$)** δ (a mixture of two rotamers) 176.8, 176.5, 173.9, 153.7, 135.6, 132.5, 132.1, 128.3, 127.9, 120.0, 81.8, 59.4, 59.0, 50.6, 49.7, 45.2, 41.0, 28.4, 22.4; **IR (Neat Film, NaCl)** 2976, 2932, 1698, 1426, 1367, 1286, 1246, 1136, 1027, 924, 858, 802, 750, 719, 695, 635 cm^{-1}; **HRMS (MM: ESI-APCI):** *m/z* calc'd for $C_{20}H_{27}N_2O_4$ $[M+H]^+$: 359.1965, found 359.1963; **$[\alpha]_D^{23.2}$** – 25.7 (c 1.0, $CHCl_3$); **SFC conditions**: 7% IPA, 2.5 mL/min, Chiralpak OJ-H column, λ = 254 nm, t_R (min): major = 3.209, minor = 2.569.

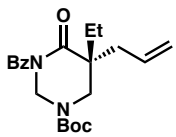

***tert*-butyl (*R*)-5-allyl-3-benzoyl-5-ethyl-4-oxotetrahydropyrimidine-1(2H)-carboxylate (1.6b).** Following the general procedure, ethylated allyl ester **1.5b** (15 mg, 0.036 mmol, 1.0 equiv) in hexanes/toluene (2:1, 1.0 mL) was added to a solution of $Pd_2(pmdba)_3$ (1.6 mg, 0.0014 mmol, 4 mol %) and (*S*)-$(CF_3)_3$-*t*Bu-PHOX (2.1 mg, 0.0036 mmol, 10 mol %) in hexanes/toluene (2:1, 1.6 mL). Purification by silica gel flash chromatography (13% EtOAc/hexanes) gave α-ethyl tetrahydropyrimidinone **1.6b** as a colorless oil (13 mg, 98% yield, 94% ee); **^{1}H NMR (400 MHz, $CDCl_3$)** δ 7.57 – 7.45 (m, 3H), 7.39 (t, *J* = 7.5 Hz, 2H), 5.87 – 5.62 (m, 1H), 5.48 – 5.24 (m, 1H), 5.20 – 5.03 (m, 3H), 3.75 (dd, *J* = 14.0, 1.4 Hz, 1H), 3.65 – 3.52 (m, 1H), 2.50 (dd, *J* = 14.2, 6.7 Hz, 1H), 2.27 (d, *J* = 16.1 Hz, 1H), 1.79 (dq, *J* = 14.9, 7.5 Hz, 1H), 1.68 (dq, *J* = 14.6, 7.4 Hz, 1H), 1.51 (s, 9H), 0.95 (t, *J* = 7.5 Hz, 3H); **^{13}C NMR (101 MHz, $CDCl_3$)** δ (a mixture of two rotamers) 175.8, 174.1, 153.7, 135.8, 132.9, 132.0, 128.3, 128.0, 119.7, 81.7, 59.2, 58.8, 48.6, 48.0, 47.6, 39.1, 38.6, 28.7, 28.4, 8.4; **IR (Neat Film, NaCl)** 2976, 2927, 1698, 1426, 1367, 1286, 1263, 1246, 1136, 1017, 923, 859, 801, 738, 695, 635 cm^{-1}; **HRMS (MM: ESI-APCI):** *m/z* calc'd for $C_{21}H_{29}N_2O_4$ $[M+H]^+$: 373.2122, found: 373.2122; **$[\alpha]_D^{22.2}$** –21.0 (c 1.0, $CHCl_3$); **SFC conditions**: 7% IPA, 2.5 mL/min, Chiralpak OJ-H column, λ = 254 nm, t_R (min): major = 3.956, minor = 2.585.

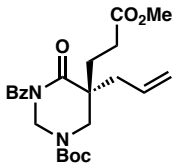

***tert*-butyl (*R*)-5-allyl-3-benzoyl-5-(3-methoxy-3-oxopropyl)-4-oxotetrahydropyrimidine-1(2H)-carboxylate (1.6c)**. Following the general procedure,

methyl ester pyrimidinone **1.5c** (15 mg, 0.032 mmol, 1.0 equiv) in hexanes/toluene (2:1, 1.0 mL) was added to a solution of $Pd_2(pmdba)_3$ (1.2 mg, 0.0013 mmol, 4 mol %) and (*S*)-$(CF_3)_3$-*t*Bu-PHOX (1.9 mg, 0.0032 mmol, 10 mol %) in hexanes/toluene (2:1, 1.3 mL). Purification by silica gel flash chromatography (15% EtOAc/hexanes) gave methyl ester **1.6c** as a colorless oil (9.1 mg, 67% yield, 95% ee): **^{1}H NMR (400 MHz, $CDCl_3$)** δ 7.50 (dd, *J* = 13.1, 7.2 Hz, 3H), 7.38 (t, *J* = 7.5 Hz, 2H), 5.73 (dq, *J* = 16.6, 7.4 Hz, 1H), 5.47 – 5.22 (m, 1H), 5.22 – 5.04 (m, 3H), 3.66 (m, 5H), 2.49 (dt, *J* = 12.9, 6.4 Hz, 1H), 2.37 (m, 2H), 2.31 – 2.19 (m, 1H), 2.14 – 1.91 (m, 2H), 1.51 (s, 9H); **^{13}C NMR (101 MHz, $CDCl_3$)** δ (a mixture of two rotamers) 175.2, 174.9, 173.9, 173.3, 153.5, 135.6, 132.1, 132.0, 128.4, 127.9, 120.3, 82.0, 59.2, 58.8, 51.1, 48.7, 47.7, 39.1, 38.8, 30.3, 28.9, 28.3; **IR (Neat Film, NaCl)** 2978, 1738, 1698, 1428, 1368, 1286, 1247, 1147, 925, 856, 802, 764, 696 cm^{-1}; **HRMS (MM: ESI-APCI):** *m/z* calc'd for $C_{23}H_{31}N_2O_6$ $[M+H]^+$: 431.2177, found 431.2173; **$[\alpha]_D^{23.1}$** +5.5 (c 0.9, $CHCl_3$); **SFC conditions**: 10% IPA, 2.5 mL/min, Chiralpak AD-H column, λ = 254 nm, t_R (min): major = 5.591, minor = 6.372.

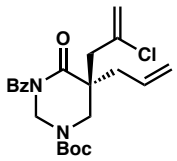

***tert*-butyl (*S*)-5-allyl-3-benzoyl-5-(2-chloroallyl)-4-oxotetrahydropyrimidine-1(2H)-carboxylate (1.6d)**. Following the general procedure, 2-chloropropenyl allyl ester **5d** (20 mg, 0.049 mmol, 1.0 equiv) in hexanes/toluene (2:1, 3.0 mL) was added to a solution of $Pd_2(pmdba)_3$ (2.1 mg, 0.0020 mmol, 4 mol %) and (*S*)-$(CF_3)_3$-*t*Bu-PHOX (2.9 mg, 0.0049

mmol, 10 mol %) in hexanes/toluene (2:1, 0.5 mL). Purification by flash chromatography (EtOAc/hexanes 15%) gave di-substituted oxopiperazine **1.6d** as a yellow oil (17 mg, 94% yield, 94% ee); **^{1}H NMR (400 MHz, $CDCl_3$)** δ (a mixture of two rotamers) 7.65 – 7.45 (m, 3H), 7.40 (t, *J* = 7.6 Hz, 2H), 5.95 – 5.76 (m, 1H), 5.76 – 5.47 (m, 1H), 5.31 (d, *J* = 1.3 Hz, 1H), 5.30 – 5.16 (m, 2H), 4.92 (s, 1H), 4.05 (s, 1H), 3.61 (d, *J* = 14.0 Hz, 1H), 3.06 (d, *J* = 14.8 Hz, 1H), 2.69 – 2.55 (m, 1H), 2.45 (d, *J* = 14.5 Hz, 2H), 1.52 (s, 9H); **^{13}C NMR (101 MHz, $CDCl_3$)** δ (a mixture of two rotamers) 174.4, 173.9, 153.6, 137.5, 135.6, 132.1, 132.0, 128.3, 128.1, 120.8, 118.1, 82.0, 59.1, 48.2, 47.6, 46.6, 42.8, 42.3, 41.7, 28.4; **IR (Neat Film, NaCl)** 2977, 1698, 1630, 1478, 1426, 1368, 1286, 1246, 1140, 902, 802, 765, 724, 695, 636 cm^{-1}; **HRMS (MM: ESI-APCI):** *m/z* calc'd for $C_{22}H_{28}ClN_2O_4$ $[M+H]^+$: 419.1732, found 419.1732; **$[\alpha]_D^{22.6}$** +22.2 (c 1.0, $CHCl_3$); **SFC conditions**: 10% IPA, 2.5 mL/min, Chiralpak AD-H column, λ = 210 nm, t_R (min): major = 4.679, minor = 3.777.

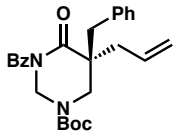

***tert*-butyl (*S*)-5-allyl-3-benzoyl-5-benzyl-4-oxotetrahydropyrimidine-1(2H)-carboxylate (1.6e).** Following the general procedure, benzylated allyl ester **1.5e** (15 mg, 0.031 mmol, 1.0 equiv) in hexanes/toluene (2:1, 1.0 mL) was added to a solution of $Pd_2(pmdba)_3$ (1.4 mg, 0.0013 mmol, 4 mol %) and (*S*)-$(CF_3)_3$-*t*Bu-PHOX (1.9 mg, 0.0031 mmol, 10 mol %) in hexanes/toluene (2:1, 1.2 mL). Purification by silica gel flash chromatography (13% EtOAc/hexanes) gave benzyl tetrahydropyrimidinone **1.6e** as a

colorless oil (11.5 mg, 84% yield, 95% ee); **^{1}H NMR (500 MHz, $CDCl_3$)** δ 7.58 – 7.49 (m, 3H), 7.42 (t, *J* = 7.7 Hz, 2H), 7.31 – 7.24 (m, 3H), 7.20 (d, *J* = 7.2 Hz, 2H), 5.86 (dddd, *J* = 16.8, 10.2, 7.9, 6.6 Hz, 1H), 5.48 – 5.25 (m, 1H), 5.22 (d, *J* = 10.0 Hz, 1H), 5.21 – 5.14 (m, 1H), 4.87 (d, *J* = 11.9 Hz, 1H), 3.89 – 3.72 (m, 1H), 3.55 (d, *J* = 13.7 Hz, 1H), 3.37 – 3.21 (m, 1H), 2.80 – 2.68 (m, 1H), 2.65 (dd, *J* = 14.0, 6.6 Hz, 1H), 2.32 – 2.19 (m, 1H), 1.52 (s, 9H); **^{13}C NMR (101 MHz, $CDCl_3$)** δ (a mixture of two rotamers) 175.4, 173.9, 153.6, 136.1, 135.6, 132.6, 132.1, 131.0, 128.5, 128.3, 128.1, 127.1, 120.2, 81.9, 58.8, 49.5, 47.2, 46.5, 41.1, 40.6, 28.4**; IR (Neat Film, NaCl)** 2978, 2930, 2360, 1698, 1424, 1368, 1288, 1245, 1142, 1029, 924, 856, 802, 718, 696, 636 cm^{-1}; **HRMS (MM: ESI-APCI):** *m/z* calc'd for $C_{26}H_{31}N_2O_4$ $[M+H]^+$: 435.2278, found: 435.2274; **$[\alpha]_D^{22.1}$** –5.6 (c 1.0, $CHCl_3$); **SFC conditions**: 20% IPA, 2.5 mL/min, Chiralpak IC column, λ = 254 nm, t_R (min): major = 4.096, minor = 4.670.

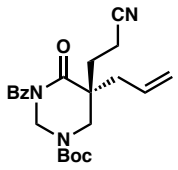

tert-butyl (R)-5-allyl-3-benzoyl-5-(2-cyanoethyl)-4-oxotetrahydropyrimidine-1(2H)-carboxylate (1.6f). Following the general procedure, cyanoethylated tetrahydropyrimidinone **1.5f** (15 mg, 0.034 mmol, 1.0 equiv) in hexanes/toluene (2:1, 1.0 mL) was added to a solution of $Pd_2(pmdba)_3$ (1.2 mg, 0.0014 mmol, 4 mol %) and (*S*)-$(CF_3)_3$-*t*Bu-PHOX (2.0 mg, 0.0034 mmol, 10 mol %) in hexanes/toluene (2:1, 1.4 mL). Purification by silica gel flash chromatography (20% EtOAc/hexanes) gave

cyanoethylated tetrahydropyrimidinone **1.6f** as a colorless oil (9.0 mg, 67% yield, 74% ee): **^{1}H NMR (500 MHz, $CDCl_3$)** δ 7.56 – 7.49 (m, 3H), 7.43 (t, *J* = 7.6 Hz, 2H), 5.75 (dddd, *J* = 16.8, 10.2, 7.9, 6.6 Hz, 1H), 5.35 – 5.13 (m, 4H), 3.86 – 3.55 (m, 2H), 2.57 – 2.51 (m, 1H), 2.44 (dd, *J* = 10.0, 5.9 Hz, 2H), 2.32 (dd, *J* = 14.1, 8.0 Hz, 1H), 2.09 (dt, *J* = 14.6, 8.5 Hz, 1H), 1.96 (ddd, *J* = 14.3, 9.8, 6.2 Hz, 1H), 1.53 (s, 9H); **^{13}C NMR (101 MHz, $CDCl_3$)** δ 174.6, 173.7, 153.4, 135.4, 132.4, 131.2, 128.5, 127.8, 121.2, 119.2, 82.5, 59.4, 48.3, 47.7, 39.1, 31.0, 28.4, 12.6; **IR (Neat Film, NaCl)** 2977, 2931, 2248, 1694, 1601, 1478, 1427,1368, 1285, 1263, 1246, 1141, 1027, 926,901, 857, 802, 763, 721, 696, 636, cm^{-1}; **HRMS (MM: ESI-APCI):** *m/z* calc'd for $C_{22}H_{28}N_3O_4$ $[M+H]^+$: 398.2074, found 398.2071; **$[\alpha]_D^{23.2}$** +10.0 (c 1.0, $CHCl_3$); **SFC conditions**: 30% IPA, 2.5 mL/min, Chiralpak IC column, λ = 254 nm, t_R (min): major = 3.148, minor = 4.927.

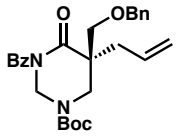

tert-butyl (*R*)-5-allyl-3-benzoyl-5-((benzyloxy)methyl)-4-oxotetrahydropyrimidine-1(2*H*)-carboxylate (1.6g). Following the general procedure, allyl ester **1.5g** (15 mg, 0.029 mmol, 1.0 equiv) in hexanes/toluene (2:1, 1.6 mL) was added to a solution of $Pd_2(pmdba)_3$ (1.3 mg, 0.0012 mmol, 4 mol %) and (*S*)-$(CF_3)_3$-*t*Bu-PHOX (1.7 mg, 0.0029 mmol, 10 mol %) in hexanes/toluene (2:1, 0.5 mL). Purification by flash chromatography (10 → 15% EtOAc/hexanes) gave di-substituted oxopiperazine **1.6g** as a yellow oil (13 mg, 87% yield, 87% ee): **^{1}H NMR (400 MHz, $CDCl_3$)** δ 7.69 – 7.51 (m, 2H), 7.51 – 7.42

(m, 1H), 7.42 – 7.22 (m, 7H), 5.77 (ddt, *J* = 15.0, 10.3, 7.4 Hz, 1H), 5.54 – 5.49 (m, 1H), 5.28 – 5.10 (m, 2H), 5.06 (d, *J* = 12.1 Hz, 1H), 4.63 – 4.40 (m, 2H), 3.94 (m, 1H), 3.82 (d, *J* = 13.9 Hz, 1H), 3.75 (d, *J* = 8.9 Hz, 1H), 3.40 (d, *J* = 9.0 Hz, 1H), 2.42 (m, 2H), 1.50 (s, 9H); **^{13}C NMR (101 MHz, $CDCl_3$)** δ 174.7, 173.5, 153.6, 137.8, 135.5, 132.0, 128.6, 128.3, 128.2, 127.9, 127.7, 112.0, 81.8, 73.8, 58.8, 50.0, 46.9, 46.3, 38.6, 28.4; **IR (Neat Film, NaCl)** 2977, 2926, 2283, 1698, 1641, 1478, 1451, 1426, 1367, 1287, 1246, 1151, 1028, 906, 857, 801, 740, 697, 635 cm^{-1}; **HRMS (MM: ESI-APCI):** *m/z* calc'd for C27H32N2O5 $[M+H]^+$: 465.2384, found 465.2378; **$[\alpha]_D^{23.4}$** +11.9 (c 0.67, $CHCl_3$); **SFC conditions:** 20% IPA, 2.5 mL/min, Chiralpak IC column, λ = 210 nm, t_R (min): major = 5.131, minor = 4.419.

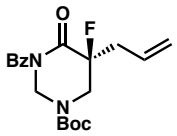

***tert*-butyl (*S*)-5-allyl-3-benzoyl-5-fluoro-4-oxotetrahydropyrimidine-1(2H)-carboxylate (1.6h)**. Following the general procedure, fluorinated tetrahydropyrimidinone **1.5h** (300 mg, 0.74 mmol, 1.0 equiv) in hexanes/toluene (2:1, 39 mL) was added to a solution of $Pd_2(pmdba)_3$ (24 mg, 0.022 mmol, 3 mol %) and (*S*)-$(CF_3)_3$-*t*Bu-PHOX (35 mg, 0.059 mmol, 10 mol %) in hexanes/toluene (2:1, 15 mL). Purification by silica gel flash chromatography (15% EtOAc/hexanes) gave fluorinated tetrahydropyrimidinone **1.6h** as a pale yellow oil (250 mg, 93% yield, 92% ee); **^{1}H NMR (400 MHz, $CDCl_3$)** δ

7.59 (dd, J = 8.3, 1.3 Hz, 2H), 7.54 (t, J = 7.4 Hz, 1H), 7.42 (t, J = 7.8 Hz, 2H), 5.82 (ddt, J = 14.9, 9.6, 7.2 Hz, 1H), 5.66 – 5.34 (m, 1H), 5.29 (s, 1H), 5.25 (d, J = 5.3 Hz, 1H), 5.24 – 5.13 (m, 1H), 4.13 – 3.72 (m, 2H), 2.81 (td, J = 14.3, 6.9 Hz, 1H), 2.67 (ddd, J = 22.4, 14.5, 7.6 Hz, 1H), 1.51 (s, 9H); **^{13}C NMR (101 MHz, $CDCl_3$)** δ (a mixture of two rotamers) 172.5, 168.23 (d, J_{CF} = 23.6 Hz), 153.4, 134.3, 132.7, 129.7, 129.6, 128.5, 128.5, 128.3, 128.0, 121.4, 92.2 (d, J_{CF} = 197.0 Hz, appears as four peaks due to the presence of two rotamers and coupling with fluorine), 82.4, 57.7, 49.4 (appears as four poorly resolved peaks due to the presence of two rotamers and coupling with fluorine), 38.2 (d, J_{CF} = 22.8 Hz), 28.3; **IR (Neat Film, NaCl)** 2978, 1710, 1416, 1368, 1286, 1245, 1158, 1137, 906, 858, 801, 749, 723, 694, 662 cm^{-1}; **HRMS (MM: ESI-APCI):** *m/z* calc'd for $C_{19}H_{24}N_2O_4$ $[M+H]^+$: 363.1715, found: 363.1713; **$[\alpha]_D^{21.8}$** –28.6 (c 0.96, $CHCl_3$); **SFC conditions**: 10% IPA, 2.5 mL/min, Chiralpak IC column, λ = 254 nm, t_R (min): major = 6.226, minor = 5.041.

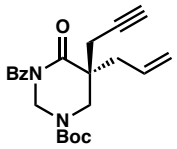

***tert*-butyl (*S*)-5-allyl-3-benzoyl-4-oxo-5-(prop-2-yn-1-yl)tetrahydropyrimidine-1(2H)-carboxylate (1.6i)**. Following the general procedure, propargylated allyl ester **1.5i** (20 mg, 0.047 mmol, 1.0 equiv) in hexanes/toluene (2:1, 2.8 mL) was added to a solution of $Pd_2(pmdba)_3$ (2.1 mg, 0.0019 mmol, 4 mol %) and (*S*)-$(CF_3)_3$-*t*Bu-PHOX (2.8 mg, 0.0047 mmol, 10 mol %) in hexanes/toluene (2:1, 0.5 mL). Purification by flash chromatography (EtOAc/hexanes 5% → 10% → 15%) gave propargyl

tetrahydropyrimidinone **1.6i** as a yellow oil (15 mg, 83% yield, 90% ee): **^{1}H NMR (400 MHz, $CDCl_3$)** δ 7.58 (s, 1H), 7.50 (t, *J* = 7.4 Hz, 2H), 7.39 (t, *J* = 7.5 Hz, 2H), 5.89 – 5.68 (m, 1H), 5.42 (s, 1H), 5.31 – 4.98 (m, 3H), 4.15 – 3.57 (m, 2H), 2.61 (dd, *J* = 16.9, 2.7 Hz, 2H), 2.42 (dd, *J* = 16.9, 2.7 Hz, 2H), 2.11 (t, *J* = 2.6 Hz, 1H), 1.54 (s, 9H); **^{13}C NMR (101 MHz, $CDCl_3$)** δ (a mixture of two rotamers) 174.3, 173.7, 153.6, 135.4, 132.2, 131.8, 128.3, 128.2, 120.6, 82.0, 79.6, 72.4, 59.3, 58.9, 48.2, 47.8, 40.1, 39.6, 28.4, 25.1; **IR (Neat Film, NaCl)** 3271, 2978, 2930, 1698, 1478, 1450, 1425, 1368, 1284, 1247, 1139, 1028, 927, 854, 802, 764, 720, 695, 635 cm^{-1}; **HRMS (MM: ESI-APCI):** *m/z* calc'd for C22H27N2O4 $[M+H]^+$: 383.1965, found 383.1973; **$[\alpha]_D^{23.0}$** +22.1 (c 0.47, $CHCl_3$); **SFC conditions:** 10% IPA, 2.5 mL/min, Chiralpak AD-H column, λ = 210 nm, t_R (min): major = 4.769, minor = 4.399.

1.4.2.7 Experimental Procedure for the Gram Scale Decarboxylative Asymmetric Allylic Alkylation of Benzyl Tetrahydropyrimidinone 1.5e

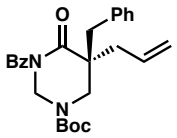

***tert*-butyl (*S*)-5-allyl-3-benzoyl-5-benzyl-4-oxotetrahydropyrimidine-1(2H)-carboxylate (1.6e).** In a nitrogen-filled glovebox, a 250 mL schlenk flask was charged with $Pd_2(pmdba)_3$ (69 mg, 0.063 mmol, 4 mol %), (*S*)-$(CF_3)_3$-*t*Bu-PHOX (99 mg, 0.17 mmol, 8 mol %), hexane/toluene (2:1, 50 mL), and a magnetic stir bar. The flask was

stirred at ambient glovebox temperature (27 °C) for 30 min and then **1.5e** (1g, 2.1 mmol, 1.0 equiv) was added as a solution in hexane/toluene (2:1, 100 mL, total concentration 0.014M). The flask was sealed with a Kontes valve, removed from the glovebox, and heated to 40 °C for 16 h. The solution was concentrated under reduced pressure and purified by silica gel flash chromatography (15% EtOAc/hexanes) to give benzyl tetrahydropyrimidinone **1.6e** as a yellow oil (780 mg, 87% yield, 95% ee); spectroscopic data vide supra.

1.4.2.8 Experimental Procedures for the Transformations of Decarboxylative Allylic Alkylation Products

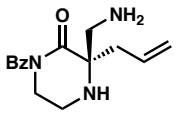

***tert*-butyl (*R*)-((2-allyl-4-benzoyl-3-oxopiperazin-2-yl)methyl)carbamate (1.8)**. Trifluoroacetic acid (114 μL, 1.5 mmol, 20 equiv) was added dropwise to a solution of methylcarbamate oxopiperazine **1.4m** (35 mg, 0.07 mmol, 1.0 equiv) in CH_2Cl_2 (0.74 mL) at 0 °C. The reaction mixture was allowed to warm up to room temperature, stirred for 3 h and concentrated under reduced pressure. The residue was repeatedly taken up in CH_2Cl_2 (1.0 mL) and concentrated, four times. The crude residue was then purified by silica gel flash chromatography (10% MeOH/CH_2Cl_2) to yield deprotected oxopiperazine **1.8** as a pale yellow foam (27 mg, 73% yield); **^{1}H NMR (400 MHz, $CDCl_3$)** δ 7.48 (t, *J* =

8.0 Hz, 3H), 7.37 (t, *J* = 7.4 Hz, 2H), 5.66 (dd, *J* = 16.0, 8.8 Hz, 1H), 5.30 (d, *J* = 9.8 Hz, 1H), 5.25 (d, *J* = 16.8 Hz, 1H), 3.99 – 3.79 (m, 1H), 3.73 – 3.55 (m, 1H), 3.44 – 3.16 (m, 2H), 3.05 (d, *J* = 13.2 Hz, 1H), 2.89 (d, *J* = 11.6 Hz, 1H), 2.76 (dd, *J* = 14.0, 7.0 Hz, 1H), 2.45 (dd, *J* = 14.2, 7.1 Hz, 1H); **^{13}C NMR (101 MHz, $CDCl_3$)** δ 173.7, 172.4, 135.5, 132.2, 129.7, 128.4, 128.0, 122.5, 62.0, 47.0, 43.5, 39.7, 38.1; **IR (Neat Film, NaCl)** 2976, 1682, 1470, 1282, 1203, 1135, 926, 836, 799, 722, 696 cm^{-1}; **HRMS (MM: ESI-APCI):** *m/z* calc'd for C15H20N3O4 $[M+H]^+$: 274.1550, found 274.1555; **$[\alpha]_D^{22.3}$** +15.1 (c 1.0, $CHCl_3$).

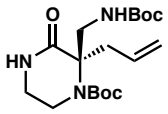

***tert*-butyl (*R*)-2-allyl-2-(((*tert*-butoxycarbonyl)amino)methyl)-3-oxopiperazine-1-carboxylate** (**1.9**). LiOH monohydrate (2.5 mg, 0.06 mmol, 1.4 equiv) was added in one portion to a solution of methylcarbamate oxopiperazine **1.4m** (20 mg, 0.04 mmol, 1.0 equiv) in methanol/water (1:1, 1.8 mL) at room temperature. The reaction mixture was stirred for 1 h, diluted with EtOAc (2 mL) and washed with saturated aqueous $NaHCO_3$ (2 mL). The aqueous phase was extracted with EtOAc (3x3 mL) and the combined organic phases were washed with brine (3 mL), dried over anhydrous Na_2SO_4, decanted, and concentrated under reduced pressure onto silica gel. The silica-loaded residue was purified by silica gel flash chromatography (hexanes/EtOAc 1:1) to yield lactam **1.9** as a white foam (14 mg, 92% yield): **^{1}H NMR (400 MHz, $CDCl_3$)** δ 6.96 (s, 1H), 5.72 (ddt, *J* = 17.2, 10.2, 7.4 Hz, 1H), 5.16 – 5.04 (m, 2H), 4.88 (t, *J* = 6.9 Hz, 1H), 4.26 – 3.91 (m, 1H), 3.82 (s, 1H), 3.60 (dd, *J* = 14.0, 5.9 Hz, 1H), 3.50 (s, 1H), 3.39 – 2.83 (m, 3H), 2.62

(s, 1H), 1.52 (s, 9H), 1.41 (s, 9H); **^{13}C NMR (101 MHz, $CDCl_3$)** δ 172.7, 155.7, 153.9, 132.7, 119.2, 81.2, 79.3, 69.1, 46.0, 43.1, 40.9, 38.9, 28.6, 28.5; **IR (Neat Film, NaCl)** 3337, 2977, 2360, 1698, 1520, 1367, 1243, 1168, 1085, 1058, 919, 866, 768, 733 cm^{-1}; **HRMS (MM: ESI-APCI):** *m/z* calc'd for $C_{18}H_{32}N_3O_5$ $[M+H]^+$: 370.2336, found 370.2337; **$[\alpha]_D^{21.9}$** –5.7 (c 1.0, $CHCl_3$).

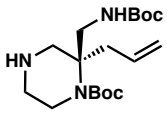

***tert*-butyl (*S*)-2-allyl-2-(((tert-butoxycarbonyl)amino)methyl)piperazine-1-carboxylate** (**1.10**). To a solution of lactam **1.9** (50 mg, 0.14 mmol, 1 equiv) in THF (1.4 mL) at 0 °C was quickly added LAH (8 mg, 0.2 mmol, 1.5 equiv) in one portion. The mixture was stirred at room temperature and three portions of LAH (8 mg, 0.2 mmol, 1.5 equiv) were added over four hours until all starting material was consumed as determined by TLC analysis. The reaction mixture was then cooled to 0 °C and diluted with Et_2O. H_2O (40 μL), 15% aqueous NaOH (40 μL), and H_2O (120 μL) were added successively at 0 °C. The mixture was stirred for 5 minutes at room temperature and then $MgSO_4$ was added. The mixture was stirred for another 5 minutes at room temperature and then filtered over a pad of celite, rinsing with EtOAc. The solvent was concentrated under reduced pressure and the crude residue was purified by silica gel flash chromatography ($MeOH/CH_2Cl_2$, 1 → 2 → 4%) to afford piperazine **1.10** as a colorless oil (30 mg, 63% yield); **^{1}H NMR (400 MHz, $CDCl_3$)** δ 5.84 – 5.66 (m, 1H), 5.28 – 5.01 (m, 3H), 3.75 (dd, *J* = 14.1, 5.6 Hz, 1H), 3.62 (dt, *J* = 13.6, 4.2 Hz, 1H), 3.35 (dd, *J* = 14.1, 7.3 Hz, 1H), 3.24 (ddd, *J* = 13.6, 9.8, 3.8 Hz, 1H), 3.02 – 2.91 (m, 1H), 2.85 (t, *J* = 11.1 Hz, 2H), 2.79

– 2.63 (m, 2H), 2.57 – 2.26 (m, 2H), 1.46 (s, 9H), 1.44 (s, 9H); **^{13}C NMR (101 MHz, $CDCl_3$)** δ 156.8, 156.0, 133.1, 119.1, 80.6, 79.6, 59.9, 50.8, 46.2, 45.1, 42.3, 38.1, 28.6, 28.5; **IR (Neat Film, NaCl)** 3789, 3662, 3451, 3341, 3074, 2976, 2930, 2284, 1693, 1641, 1502, 1453, 1391, 1365, 1298, 1249, 1169, 1085, 996, 914, 859, 771 cm^{-1}; **HRMS (MM: ESI-APCI):** *m/z* calc'd for $C_{18}H_{34}N_3O_4$ $[M+H]^+$: 356.2544, found 356.2549; **$[\alpha]_D^{22.8}$** +5.3 (c 0.67, $CHCl_3$).

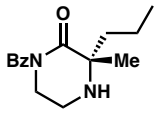

(*S*)-1-benzoyl-3-methyl-3-propylpiperazin-2-one 1.11. Piperazinone **1.4e** (80 mg, 0.22 mmol, 1 equiv) was dissolved in MeOH (2.2 mL). The reaction flask was purged with Argon before adding Pd/C (10%, 24 mg, 0.022 mmol, 0.1 equiv). The flask was evacuated and filled with H_2 three times, and then sparged with H_2 for 5 minutes. The reaction was stirred at room temperature for 6 hours before being filtered through a pad of silica gel while rinsing with EtOAc. The crude hydrogenated product was then dissolved in CH_2Cl_2 (2.2 mL) and TFA (171 μL, 2.23 mmol, 10 equiv) was added. The reaction was stirred for 16 hours and then quenched with saturated aqueous $NaHCO_3$ (5 mL). The solution was extracted with EtOAc (3x5 mL), dried over Na_2SO_4, decanted, and concentrated under reduced pressure. The crude piperazinone was purified by silica gel flash chromatography (2.5 → 5% MeOH/CH_2Cl_2) to afford the desired product **1.11** (55 mg, 94% yield over two steps): **^{1}H NMR (400 MHz, $CDCl_3$)** δ 7.58 – 7.50 (m, 2H), 7.54 – 7.46 (m, 1H), 7.46 – 7.36 (m, 2H), 3.92 (ddd, J = 12.6, 5.4, 4.6 Hz, 1H), 3.81 (ddd,

J = 12.5, 6.7, 5.4 Hz, 1H), 3.32 – 3.18 (m, 2H), 1.92 (ddd, *J* = 13.6, 12.1, 4.7 Hz, 1H), 1.62 (ddd, *J* = 13.6, 12.2, 4.5 Hz, 1H), 1.42 (s, 3H), 1.54 – 1.23 (m, 2H), 0.96 (t, *J* = 7.3 Hz, 3H); **^{13}C NMR (101 MHz, $CDCl_3$)** δ 176.7, 174.7, 136.4, 131.6, 128.3, 127.5, 61.2, 48.2, 41.2, 38.7, 25.0, 16.9, 14.5; **IR (Neat Film, NaCl)** 3331, 2960, 2872, 1681, 1600, 1448, 1378, 1284, 1202, 1176, 1152, 1112, 966, 794, 726, 694, 669 cm^{-1}; **HRMS (MM: ESI-APCI):** *m/z* calc'd for C15H21N2O2 $[M+H]^+$: 261.1598, found 261.1596; **$[\alpha]_D^{22.6}$** – 59.6 (c 1.35, $CHCl_3$).

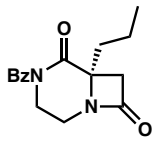

(*R*)-4-benzoyl-6-propyl-1,4-diazabicyclo[4.2.0]octane-5,8-dione (**1.12)**. To a 10 mL round-bottom flask was added $Pd(OPiv)_2$ (3 mg, 0.0096 mmol, 0.1 equiv), AgOPiv[58] (60 mg, 0.29 mmol, 3 equiv), Xantphos (6 mg, 0.0096 mmol, 0.1 equiv), and 1,4-benzoquinone (21 mg, 0.19 mmol, 2 equiv). A solution of piperazine **1.11** (25 mg, 0.096 mmol, 1 equiv) in toluene (1 mL) was then added and the flask was evacuated and filled with carbon monoxide three times. The flask was then stirred at 80 °C for 16 hours. The reaction mixture was allowed to cool to room temperature, diluted with EtOAc, and filtered through celite while rinsing with additional EtOAc. The solvent was concentrated under reduced pressure onto silica gel and then purified by silica gel flash chromatography (2:1 hexanes/EtOAc) to provide the *β*-lactam **1.12** and as a light yellow oil (15 mg, 55% yield): **^{1}H NMR (400 MHz, $CDCl_3$)** δ (5:1 ratio of desired product and an inseparable isomer resulting from insertion into another *β*-C−H) 7.56 – 7.51 (m, 3H), 7.46 – 7.40 (m, 2H), 4.51 (ddd, *J* = 14.0, 6.1, 2.9 Hz, 1H), 3.94 (ddt, *J* = 12.3, 10.8, 5.7 Hz, 1H), 3.78 – 3.67 (m, 1H), 3.40 (dddd, *J* = 12.3, 4.8, 2.8, 1.5 Hz, 1H), 3.27 – 3.10 (m,

2H), 1.98 (ddd, *J* = 14.2, 11.2, 5.5 Hz, 1H), 1.87 (ddd, *J* = 14.2, 11.0, 5.7 Hz, 1H), 1.59 – 1.40 (m, 2H), 1.00 (t, *J* = 7.3 Hz, 3H); **^{13}C NMR (101 MHz, $CDCl_3$)** δ 174.2, 173.2, 169.1, 135.1, 132.6, 128.6, 128.3, 59.7, 46.7, 41.5, 39.7, 37.8, 17.7, 14.3; **IR (Neat Film, NaCl)** 3374, 2961, 1760, 1688, 1600, 1505, 1449, 1350, 1318, 1279, 1228, 1183, 1151, 1110, 963, 936, 796, 726, 694, 662 cm^{-1}; **HRMS (MM: ESI-APCI):** *m/z* calc'd for C16H19N2O3 $[M+H]^+$: 287.1390, found 287.1385; **$[\alpha]_D^{23.5}$** –12.8 (c 0.47, $CHCl_3$).

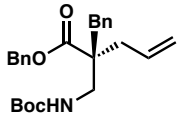

(*S*)-2-benzyl-2-(((tert-butoxycarbonyl)amino)methyl)pent-4-enoic acid (**1.13)**. To a solution of benzyl tetrahydropyrimidinone **1.6e** (200 mg, 0.46 mmol, 1 equiv) in methylene chloride (4.6 mL) was added TFA (352 µL, 4.6 mmol, 10 equiv) dropwise at room temperature. The solution was stirred for 24 hours at room temperature and then quenched with aqueous $NaHCO_3$ (10 mL). The layers were separated and the aqueous layer was extracted with CH_2Cl_2 (4 x 5 mL). The combined organic layers were dried over Na_2SO_4, filtered, and concentrated under reduced pressure. The crude residue was dissolved in MeOH/H_2O (1:1, 5 mL) and LiOH monohydrate (290 mg, 6.9 mmol, 15 equiv) was added. The reaction mixture was heated to 80 °C for 60 hours and then allowed to cool to room temperature. Then, NEt_3 (77 µL, 0.55 mmol, 1.2 equiv) and Boc_2O (110 mg, 0.51 mmol, 1.1 equiv) were added successively at room temperature. The reaction was stirred for 1 hour at room temperature and then acidified with 1 M HCl (4 mL). The solution was extracted with EtOAc (3 x 5 mL). The combined organic layers

were dried over Na_2SO_4. The crude Boc-protected *β*-amino acid was taken up in DMF (2.3 mL). K_2CO_3 (95 mg, 0.69 mmol, 1.5 equiv) and BnBr (66 µL, 0.55 mmol, 1.2 equiv) were added at room temperature. The reaction was stirred at room temperature for 1 hour and then quenched with saturated aqueous NH_4Cl. The solution was extracted with EtOAc (3 x 5 mL) and the combined organic layers were concentrated under reduced pressure and placed under high vacuum until trace DMF had evaporated. The residue was taken up in CH_2Cl_2, concentrated under reduced pressure onto silica gel and purified by silica gel flash chromatography (5 → 10% EtOAc/hexanes) to afford protected $\beta^{2,2}$-amino acid **1.13** as a white solid (80 mg, 40% yield): **^{1}H NMR (400 MHz, $CDCl_3$)** δ 7.42 – 7.27 (m, 5H), 7.20 (dd, *J* = 4.9, 1.9 Hz, 3H), 7.10 – 6.93 (m, 2H), 5.92 – 5.75 (m, 1H), 5.18 – 5.04 (m, 4H), 4.96 – 4.81 (m, 1H), 3.34 (qd, *J* = 14.0, 6.5 Hz, 2H), 2.98 (d, *J* = 13.8 Hz, 1H), 2.86 (d, *J* = 13.8 Hz, 1H), 2.49 (ddt, *J* = 14.2, 6.7, 1.4 Hz, 1H), 2.31 (ddt, *J* = 14.2, 7.9, 1.1 Hz, 1H), 1.43 (s, 9H); **^{13}C NMR (101 MHz, $CDCl_3$)** δ 175.1, 156.1, 136.6, 135.6, 133.4, 130.2, 128.8, 128.6, 128.5, 128.4, 126.9, 119.2, 79.4, 66.8, 51.6, 44.1, 41.0, 38.8, 28.5; **IR (Neat Film, NaCl)** 3452, 3065, 3031, 2977, 2930, 1721, 1640, 1604, 1503, 1454, 1391, 1365, 1245, 1169, 1094, 1030z, 994, 917, 859, 776, 741, 700 cm^{-1}; **HRMS (MM: ESI-APCI):** *m/z* calc'd for C25H32NO4 $[M+H]^+$: 410.2326, found 410.2324; **$[\alpha]_D^{23.4}$** +3.47 (c 1.0, $CHCl_3$).

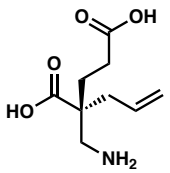

(*R*)-2-allyl-2-(aminomethyl)pentanedioic acid (**1.14**). To a solution of methyl ester tetrahydropyrimidinone **1.6c** (140 mg, 0.325 mmol, 1 equiv) in CH_2Cl_2 (3.1 mL, 0.1 M)

was added TFA (250 μL, 3.25 mmol, 10 equiv) dropwise at room temperature. The solution was stirred for 24 h at room temperature and then concentrated under reduced pressure. Remaining TFA was removed with by azeotroping with CH_2Cl_2 three times. The crude residue was dissolved in MeOH/H_2O (1:1, 3.1 mL, 0.1 M) and LiOH monohydrate (205 mg, 4.89 mmol, 15 equiv) was added. The reaction mixture was heated to 80 °C for 16 h and then allowed to cool to room temperature. The reaction mixture was then acidified with 4 M HCl in dioxanes (~1 mL) until pH 1. Then, the solvent was concentrated under reduced pressure, resulting in precipitation of a white solid. A minimal amount of DMSO (~1 mL) was added to resolvate this precipitate. This solution was subjected to purification by reverse phase preparatory HPLC (0 → 40% MeCN/H_2O gradient over 11 minutes, 20x250 mm C_{18} column, 25 mL/min flow rate) to yield *β*-amino acid **1.14** (30 mg, 46% yield) as a colorless oil. Note: HPLC fractions were spotted onto a silica TLC plate and eluted in (*n*-BuOH/H_2O/EtOAc/AcOH, 1:1:1:1), then stained with ninhydrin to identify product-containing fractions. LC-MS was used to verify the fractions containing product. Note: HPLC H_2O solvent contained 0.25% TFA. **^{1}H NMR (400 MHz, Methanol-d_4)** δ 5.88 – 5.68 (m, 1H), 5.32 – 5.13 (m, 2H), 3.18 – 2.99 (m, 2H), 2.51 (ddt, *J* = 14.4, 7.1, 1.3 Hz, 1H), 2.47 – 2.33 (m, 3H), 1.99 (td, *J* = 7.6, 1.3 Hz, 2H); **^{13}C NMR (101 MHz, MeOD)** δ 176.7, 176.6, 133.1, 120.6, 48.3, 43.5, 39.1, 29.38, 29.35; **IR (Neat Film, NaCl)** 2924, 1678, 1198, 1138 cm^{-1}; **HRMS (MM: ESI-APCI):** *m/z* calc'd for C9H16NO4 $[M+H]^+$: 202.1074, found 202.1075; **$[\alpha]_D^{22.7}$** –3.51 (c 1.0, MeOH).

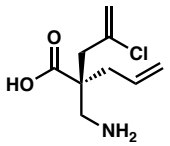

(*S*)-2-allyl-2-(aminomethyl)-4-chloropent-4-enoic acid (1.15). To a solution of chloroallyl tetrahydropyrimidinone **1.6d** (30 mg, 0.072 mmol, 1 equiv) in CH_2Cl_2 (700 μL, 0.1 M) was added TFA (55 μL, 0.72 mmol, 10 equiv) dropwise at room temperature. The solution was stirred for 5 h at room temperature and then concentrated under reduced pressure. Remaining TFA was removed with by azeotroping with CH_2Cl_2 three times. The crude residue was dissolved in MeOH/H_2O (1:1, 700 μL, 0.1 M) and LiOH monohydrate (45 mg, 1.07 mmol, 15 equiv) was added. The reaction mixture was heated to 80 °C for 16 h and then allowed to cool to room temperature. The reaction mixture was then acidified with 4 M HCl in dioxane (~1 mL) until pH 1. Then, the solvent was concentrated under reduced pressure, resulting in precipitation of a white solid. A minimal amount of DMSO (~1 mL) was added to resolvate this precipitate. This solution was subjected to purification by reverse phase preparatory HPLC (10 → 40% MeCN/H_2O gradient over 11 minutes, 20x250 mm C_{18} column, 25 mL/min flow rate) to yield chloroallyl *β*-amino acid **1.15** (10 mg, 69% yield) as a colorless oil. Note: HPLC fractions were spotted onto a silica TLC plate and eluted in (*n*-BuOH/H_2O/EtOAc/AcOH, 1:1:1:1), then stained with ninhydrin to identify product-containing fractions. LC-MS was used to verify the fractions containing product. Note: HPLC H_2O solvent contained 0.25% TFA. **^{1}H NMR (600 MHz, Methanol-d_4)** δ 5.84 (td, *J* = 17.2, 7.3 Hz, 1H), 5.40 (s, 2H), 5.28 – 5.18 (m, 2H), 3.29 (d, *J* = 13.5 Hz, 1H), 3.12 (d, *J* = 13.5 Hz, 1H), 2.94 (d, *J* = 15.1 Hz, 1H), 2.77 (d, *J* = 14.8 Hz, 1H), 2.57 (dd, *J* = 14.5, 7.0 Hz, 1H), 2.47 (dd, *J* = 14.5, 7.8 Hz, 1H); **^{13}C NMR (101 MHz, MeOD)** δ 176.6, 138.2, 133.1, 120.8, 118.7,

48.4, 44.2, 43.5, 39.6. Note: A ^{1}H-^{13}C HMBC experiment revealed the chemical shift of the chiral quaternary carbon to be at 48.4 ppm, obscured by the CD_3OD resonance. **IR (Neat Film, NaCl)** 2926, 1673, 1432, 1200, 1140, 900, 836, 800, 722 cm^{-1}; **HRMS (MM: ESI-APCI):** *m/z* calc'd for C9H15ClNO2 $[M+H]^+$: 204.0786, found 204.0787; **$[\alpha]_D^{22.5}$** –4.64 (c 0.67, MeOH).

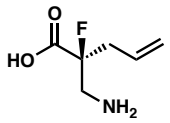

(*S*)-2-(aminomethyl)-2-fluoropent-4-enoic acid (**1.16)**. To a solution of fluoro tetrahydropyrimidinone **1.6h** (20 mg, 0.055 mmol, 1 equiv) in 1:1 MeOH/H_2O (550 µL, 0.1 M) at room temperature was added KOH (31 mg, 0.55 mmol, 10 equiv). The cloudy solution became clear over seconds and was stirred for 5 min at room temperature until TLC analysis showed complete consumption of starting material. AcOH (~100 µL) was added to acidify the solution, which was then extracted with CH_2Cl_2 three times. The combined organic layers were dried with Na_2SO_4 and then concentrated under reduced pressure. HCl was generated *in situ* by adding AcCl (205 µL, 2.87 mmol, 52 equiv) dropwise to a separate 1 dram vial containing MeOH (550 µL) at 0 °C. This HCl solution was stirred for 5 min at 0 °C and was then transferred by pipette into a 1 dram vial containing the crude saponified residue. The reaction was stirred at rt for 2 h and was then concentrated under reduced pressure. The crude residue was dissolved in 1:1 H_2O/MeCN (2.5 mL) and was then subjected to purification by reverse phase preparatory HPLC (0 → 40% MeCN/H_2O gradient over 11 minutes, 20x250 mm C_{18} column, 25 mL/min flow rate) to yield fluoro *β*-amino acid **1.16** (5.0 mg, 65% yield) as a colorless

oil. Note: HPLC fractions were spotted onto a silica TLC plate and eluted in (*n*-BuOH/H_2O/EtOAc/AcOH, 1:1:1:1), then stained with ninhydrin to identify product-containing fractions. LC-MS was used to verify the fractions containing product. Note: HPLC H_2O solvent contained 0.25% TFA. **^{1}H NMR (600 MHz, Methanol-d_4)** δ 5.80 (ddt, J = 17.3, 10.1, 7.2 Hz, 1H), 5.30 – 5.17 (m, 2H), 3.51 (dd, J = 26.1, 13.9 Hz, 1H), 3.38 – 3.32 (dd, J = 26.1, 13.9 Hz, 1H), 2.81 – 2.63 (m, 2H); **^{13}C NMR (101 MHz, MeOD)** δ 171.1 (d, J_{CF} = 26.2 Hz), 130.7, 121.3, 95.0 (d, J_{CF} = 190.2 Hz), 44.74 (d, J_{CF} = 22.1 Hz), 40.44 (d, J_{CF} = 22.1 Hz); **IR (Neat Film, NaCl)** 2924, 1674, 1422, 1202, 1141, 931, 798, 722 cm^{-1}; **HRMS (MM: ESI-APCI):** *m/z* calc'd for C6H11NO2 $[M+H]^+$: 148.0768, found 148.0770; **$[\alpha]_D^{22.5}$** –2.47 (c 0.33, MeOH).

1.4.2.9 Determination of Enantiomeric Excess

Please note racemic products were synthesized according to the general procedure, using achiral GlyPHOX ligand instead of (*S*)-$(CF_3)_3$-*t*Bu-PHOX.[4,55]

Entry	Product	Assay Conditions	Retention time of major isomer (min)	Retention time of minor isomer (min)	%ee
1	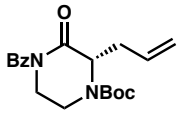	SFC Chiralpak AD-H 15% *i*PrOH isocratic, 2.5 mL/min	3.741	2.682	92%
2	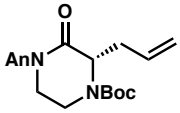	SFC Chiralpak AD-H 15% *i*PrOH isocratic, 2.5 mL/min	4.708	3.998	96%
3	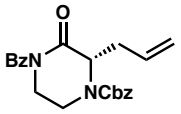	SFC Chiralpak IC 30% *i*PrOH isocratic, 2.5 mL/min	4.873	6.748	99%
4	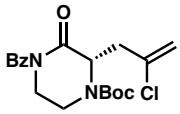	SFC Chiralpak AD-H 15% *i*PrOH isocratic, 2.5 mL/min	4.482	3.224	98%
5	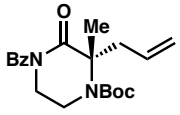	SFC Chiralpak AD-H 7% *i*PrOH isocratic, 2.5 mL/min	7.208	4.714	96%
6	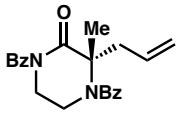	SFC Chiralpak OJ-H 10% MeOH isocratic, 2.5 mL/min	5.574	6.659	70%
7	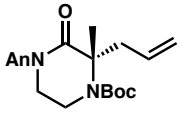	SFC Chiralpak AD-H 10% *i*PrOH isocratic, 2.5 mL/min	5.370	4.278	96%
8	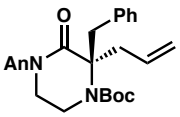	SFC Chiralpak AD-H 15% *i*PrOH isocratic, 2.5 mL/min	7.471	5.802	96%

Entry	Product	Assay Conditions	Retention time of major isomer (min)	Retention time of minor isomer (min)	%ee
9	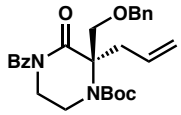	SFC Chiralpak OJ-H 7% *i*PrOH isocratic, 2.5 mL/min	3.737	4.398	92%
10	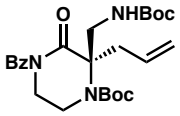	SFC Chiralpak OD-H 10% *i*PrOH isocratic, 2.5 mL/min	4.429	3.910	93%
11	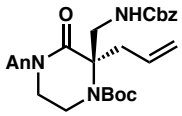	SFC Chiralpak OD-H 15% MeOH isocratic, 2.5 mL/min	8.425	7.817	92%
12	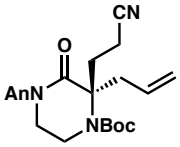	SFC Chiralpak OD-H 15% *i*PrOH isocratic, 2.5 mL/min	6.049	5.143	97%
13	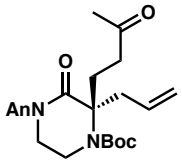	SFC Chiralpak OD-H 7% *i*PrOH isocratic, 2.5 mL/min	9.712	10.434	97%

Entry	Product	Assay Conditions	Retention time of major isomer (min)	Retention time of minor isomer (min)	%ee
14	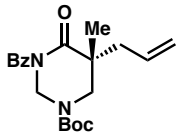	SFC Chiralpak OJ-H 7% *i*PrOH isocratic, 2.5 mL/min	3.209	2.569	93%
15	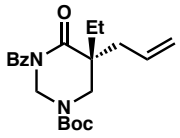	SFC Chiralpak OJ-H 7% *i*PrOH isocratic, 2.5 mL/min	3.956	2.585	94%
16	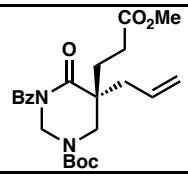	SFC Chiralpak AD-H 10% *i*PrOH isocratic, 2.5 mL/min	5.591	6.372	95%
17	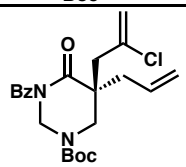	SFC Chiralpak AD-H 10% *i*PrOH isocratic, 2.5 mL/min	4.679	3.777	94%
18	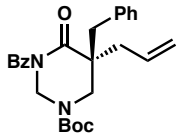	SFC Chiralpak IC 20% iPrOH isocratic, 2.5 mL/min	4.096	4.670	95%
19	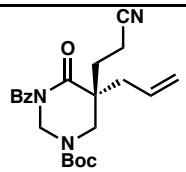	SFC Chiralpak IC 30% *i*PrOH isocratic, 2.5 mL/min	3.148	4.927	74%
20	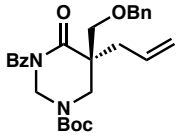	SFC Chiralpak IC 20% *i*PrOH isocratic, 2.5 mL/min	5.131	4.419	87%
21	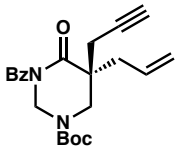	SFC Chiralpak AD-H 10% *i*PrOH isocratic, 2.5 mL/min	4.769	4.399	90%
22	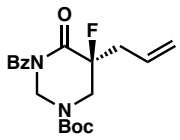	SFC Chiralpak IC 10% *i*PrOH isocratic, 2.5 mL/min	6.226	5.041	92%

1.5 REFERENCES AND NOTES

(1) Shimizu, I.; Yamada, T.; Tsuji, J. Palladium-Catalyzed Rearrangement of Allylic Esters of Acetoacetic Acid to Give γ,δ-Unsaturated Methyl Ketones. *Tetrahedron Lett.* **1980**, *21*, 3199–3202.

(2) Tsuda, T.; Chujo, Y.; Nishi, S.; Tawara, K.; Saegusa, T. Facile Generation of a Reactive Palladium(II) Enolate Intermediate by the Decarboxylation of Palladium(II) .Beta.-Ketocarboxylate and Its Utilization in Allylic Acylation. *J. Am. Chem. Soc.* **1980**, *102*, 6381–6384.

(3) Burger, E. C.; Tunge, J. A. Asymmetric Allylic Alkylation of Ketone Enolates: An Asymmetric Claisen Surrogate. *Org. Lett.* **2004**, *6*, 4113–4115.

(4) Behenna, D. C.; Stoltz, B. M. The Enantioselective Tsuji Allylation. *J. Am. Chem. Soc.* **2004**, *126*, 15044–15045.

(5) Trost, B. M.; Xu, J. Regio- and Enantioselective Pd-Catalyzed Allylic Alkylation of Ketones through Allyl Enol Carbonates. *J. Am. Chem. Soc.* **2005**, *127*, 2846–2847.

(6) Trost, Cb.-C.; Jiang, C. Catalytic Enantioselective Construction of All-Carbon Quaternary Stereocenters. *New York* **2006**, No. 3, 28.

(7) Mohr, J. T.; Behenna, D. C.; Harned, A. M.; Stoltz, B. M. Deracemization of Quaternary Stereocenters by Pd-Catalyzed Enantioconvergent Decarboxylative Allylation of Racemic β-Ketoesters. *Angew. Chem. Int. Ed.* **2005**, *44*, 6924–6927.

(8) Trost, B. M. Metal Catalyzed Allylic Alkylation: Its Development in the Trost Laboratories. *Tetrahedron* **2015**, *71*, 5708–5733.

(9) James, J.; Jackson, M.; Guiry, P. Pd-Catalyzed Decarboxylative Asymmetric Allylic Alkylation: Development, Mechanistic Understanding and Recent Advances. *Adv. Synth. Cat.* In Press.

(10) Reeves, C. M.; Eidamshaus, C.; Kim, J.; Stoltz, B. M. Enantioselective Construction of α-Quaternary Cyclobutanones by Catalytic Asymmetric Allylic Alkylation. *Angew. Chem. Int. Ed.* **2013**, *52*, 6718–6721.

(11) Numajiri, Y.; Pritchett, B. P.; Chiyoda, K.; Stoltz, B. M. Enantioselective Synthesis of α-Quaternary Mannich Adducts by Palladium-Catalyzed Allylic Alkylation: Total Synthesis of (+)-Sibirinine. *J. Am. Chem. Soc.* **2015**, *137*, 1040–1043.

(12) Hong, A. Y.; Krout, M. R.; Jensen, T.; Bennett, N. B.; Harned, A. M.; Stoltz, B. M. Ring-Contraction Strategy for the Practical, Scalable, Catalytic Asymmetric Synthesis of Versatile Γ-Quaternary Acylcyclopentenes. *Angew. Chem. Int. Ed.* **2011**, *50*, 2756–2760.

(13) Behenna, D. C.; Liu, Y.; Yurino, T.; Kim, J.; White, D. E.; Virgil, S. C.; Stoltz, B. M. Enantioselective Construction of Quaternary *N*-Heterocycles by Palladium-Catalysed Decarboxylative Allylic Alkylation of Lactams. *Nat. Chem.* **2012**, *4*, 130–133.

(14) Numajiri, Y.; Jiménez-Osés, G.; Wang, B.; Houk, K. N.; Stoltz, B. M. Enantioselective Synthesis of Dialkylated *N* -Heterocycles by Palladium-Catalyzed Allylic Alkylation. *Org. Lett.* **2015**, *17*, 1082–1085.

(15) Korch, K. M.; Eidamshaus, C.; Behenna, D. C.; Nam, S.; Horne, D.; Stoltz, B. M. Enantioselective Synthesis of α-Secondary and α-Tertiary Piperazin-2-Ones and

Piperazines by Catalytic Asymmetric Allylic Alkylation. *Angew. Chem. Int. Ed.* *54*, 179–183.

(16) Alexy, E. J.; Virgil, S. C.; Bartberger, M. D.; Stoltz, B. M. Enantioselective Pd-Catalyzed Decarboxylative Allylic Alkylation of Thiopyranones. Access to Acyclic, Stereogenic α-Quaternary Ketones. *Org. Lett.* **2017**, *19*, 5007–5009.

(17) Alexy, E. J.; Zhang, H.; Stoltz, B. M. Catalytic Enantioselective Synthesis of Acyclic Quaternary Centers: Palladium-Catalyzed Decarboxylative Allylic Alkylation of Fully Substituted Acyclic Enol Carbonates. *J. Am. Chem. Soc.* **2018**, *140*, 10109–10112.

(18) Vitaku, E.; Smith, D. T.; Njardarson, J. T. Analysis of the Structural Diversity, Substitution Patterns, and Frequency of Nitrogen Heterocycles among U.S. FDA Approved Pharmaceuticals. *J. Med. Chem.* **2014**, *57*, 10257–10274.

(19) Herquline A, produced by Penicillium herquei FKI-7215, exhibits anti-influenza virus properties: Bioscience, Biotechnology, and Biochemistry: Vol 81, No 1

(20) Grady, M. A.; Gasperoni, T. L.; Kirkpatrick, P. Aripiprazole. *Nature Reviews Drug Discovery* **2003**, *2*, 427.

(21) Wang, H.; Kowalski, M. D.; Lakdawala, A. S.; Vogt, F. G.; Wu, L. An Efficient and Highly Diastereoselective Synthesis of GSK1265744, a Potent HIV Integrase Inhibitor. *Org. Lett.* **2015**, *17*, 564–567.

(22) Ziegler, R. E.; Desai, B. K.; Jee, J.-A.; Gupton, B. F.; Roper, T. D.; Jamison, T. F. 7-Step Flow Synthesis of the HIV Integrase Inhibitor Dolutegravir. *Angew. Chem. Int. Ed.* **2018**, *57*, 7181–7185.

(23) Hirata, K.; Kotoku, M.; Seki, N.; Maeba, T.; Maeda, K.; Hirashima, S.; Sakai, T.; Obika, S.; Hori, A.; Hase, Y.; et al. SAR Exploration Guided by LE and Fsp3: Discovery of a Selective and Orally Efficacious RORγ Inhibitor. *ACS Med. Chem. Lett.* **2016**, *7*, 23–27.

(24) Hung, A. W.; Ramek, A.; Wang, Y.; Kaya, T.; Wilson, J. A.; Clemons, P. A.; Young, D. W. Route to Three-Dimensional Fragments Using Diversity-Oriented Synthesis. *Proc. Natl. Acad. Sci.*. **2011**, *108*, 6799–6804.

(25) Lovering, F.; Bikker, J.; Humblet, C. Escape from Flatland: Increasing Saturation as an Approach to Improving Clinical Success. *Journal of Medicinal Chemistry* **2009**, *52*, 6752–6756.

(26) Lovering, F. Escape from Flatland 2: Complexity and Promiscuity. *Med. Chem. Commun.* **2013**, *4*, 515–519.

(27) Monteleone, S.; Fuchs, J. E.; Liedl, K. R. Molecular Connectivity Predefines Polypharmacology: Aliphatic Rings, Chirality, and Sp3 Centers Enhance Target Selectivity. *Frontiers in Pharmacology* **2017**, *8*, 552.

(28) Wishart, D. S.; Feunang, Y. D.; Guo, A. C.; Lo, E. J.; Marcu, A.; Grant, J. R.; Sajed, T.; Johnson, D.; Li, C.; Sayeeda, Z.; et al. DrugBank 5.0: A Major Update to the DrugBank Database for 2018. *Nucleic Acids Res.* **2018**, *46* (D1), D1074–D1082.

(29) Holl, R.; Schepmann, D.; Wünsch, B. Homologous Piperazine-Alcanols: Chiral Pool Synthesis and Pharmacological Evaluation. *Med. Chem. Commun.* **2012**, *3*, 673–679.

(30) Sudhakar, G.; Bayya, S.; Reddy, K. J.; Sridhar, B.; Sharma, K.; Bathula, S. R. Synthesis and Cytotoxicity of the Proposed Structure of Piperazirum, Its Stereoisomers and Analogues. *Euro. J. Org. Chem.* **2014**, 1253–1265.

(31) Chamakuri, S.; Jain, P.; Reddy Guduru, S. K.; Arney, J. W.; MacKenzie, K. R.; Santini, C.; Young, D. W. Synthesis of Enantiomerically Pure 6-Substituted-Piperazine-2-Acetic Acid Esters as Intermediates for Library Production. *J. Org. Chem.* **2018**.

(32) Kuwano, R.; Ito, Y. Asymmetric Hydrogenation of 1,4,5,6-Tetrahydropyrazine-2-(N-Tert-Butyl)Carboxamide Catalyzed by Trans-Chelating Chiral Diphosphine−Rhodium Complexes. *J. Org. Chem.* **1999**, *64*, 1232–1237.

(33) Huang, W.-X.; Liu, L.-J.; Wu, B.; Feng, G.-S.; Wang, B.; Zhou, Y.-G. Synthesis of Chiral Piperazines via Hydrogenation of Pyrazines Activated by Alkyl Halides. *Org. Lett.* **2016**, *18*, 3082–3085.

(34) Montgomery, T. D.; Rawal, V. H. Palladium-Catalyzed Modular Synthesis of Substituted Piperazines and Related Nitrogen Heterocycles. *Org. Lett.* **2016**, *18*, 740–743.

(35) Nakhla, J. S.; Wolfe, J. P. A Concise Asymmetric Synthesis of Cis-2,6-Disubstituted N-Aryl Piperazines via Pd-Catalyzed Carboamination Reactions. *Org. Lett.* **2007**, *9*, 3279–3282.

(36) Cochran, B. M.; Michael, F. E. Synthesis of 2,6-Disubstituted Piperazines by a Diastereoselective Palladium-Catalyzed Hydroamination Reaction. *Org. Lett.* **2008**, *10*, 329–332.

(37) McDermott, B. P.; Campbell, A. D.; Ertan, A. First Example of S-BuLi/(-)-Sparteine-Mediated Chiral Deprotonation of a Piperazine and Proof of the Sense of Induction. *Synlett* **2008**, *2008*, 875–879.

(38) Firth, J. D.; O'Brien, P.; Ferris, L. Synthesis of Enantiopure Piperazines via Asymmetric Lithiation–Trapping of N-Boc Piperazines: Unexpected Role of the Electrophile and Distal N-Substituent. *J. Am. Chem. Soc.* **2016**, *138*, 651–659.

(39) Gettys, K. E.; Ye, Z.; Dai, M. Recent Advances in Piperazine Synthesis. *Synthesis* **2017**, *49*, 2589–2604.

(40) Meyers, J.; Carter, M.; Mok, N. Y.; Brown, N. On the Origins of Three-Dimensionality in Drug-like Molecules. *Future Medicinal Chemistry* **2016**, *8*, 1753–1767.

(41) Marson, C. M. Chapter Two - Saturated Heterocycles with Applications in Medicinal Chemistry. In *Advances in Heterocyclic Chemistry*; Scriven, E. F. V., Ramsden, C. A., Eds.; Heterocyclic Chemistry in the 21st Century; Academic Press, 2017; Vol. 121, pp 13–33.

(42) Vo, C.-V. T.; Bode, J. W. Synthesis of Saturated N-Heterocycles. *J. Org. Chem.* **2014**, *79*, 2809–2815.

(43) Ruider, S. A.; Müller, S.; Carreira, E. M. Ring Expansion of 3-Oxetanone-Derived Spirocycles: Facile Synthesis of Saturated Nitrogen Heterocycles. *Angew. Chem. Int. Ed. 52*, 11908–11911.

(44) Weiner, B.; Szymański, W.; Janssen, D. B.; Minnaard, A. J.; Feringa, B. L. Recent Advances in the Catalytic Asymmetric Synthesis of β-Amino Acids. *Chem. Soc. Rev.* **2010**, *39*, 1656–1691.

(45) Steer, D. L.; Lew, R. A.; Perlmutter, P.; Smith, A. I.; Aguilar, M.-I. Beta-Amino Acids: Versatile Peptidomimetics. *Curr. Med. Chem.* **2002**, *9*, 811–822.

(46) Seebach, D.; Beck, A. K.; Bierbaum, D. J. The World of Beta- and Gamma-Peptides Comprised of Homologated Proteinogenic Amino Acids and Other Components. *Chem. Biodivers.* **2004**, *1*, 1111–1239.

(47) Yu, J.-S.; Noda, H.; Shibasaki, M. Quaternary B2,2-Amino Acids: Catalytic Asymmetric Synthesis and Incorporation into Peptides by Fmoc-Based Solid Phase Peptide Synthesis. *Angew. Chem. Int. Ed.* **2018**, *57*, 818–822.

(48) Nascimento de Oliveira, M.; Arseniyadis, S.; Cossy, J. Palladium-Catalyzed Asymmetric Allylic Alkylation of 4-Substituted Isoxazolidin-5-Ones: A Straightforward Access to B2,2-Amino Acids. *Chem. Eur. J.* **2018**, *24*, 4810–4814.

(49) Guggisberg, A.; Drandarov, K.; Hesse, M. Protoverbine, the Parent Member of a Class of Macrocyclic Spermine Alkaloids. *Helvetica Chimica Acta* **2000***, 83*, 3035–3042.

(50) Drandarov, K.; Guggisberg, A.; Hesse, M. Asymmetric Syntheses of the Macrocyclic Spermine Alkaloids (−)-(S)-Protoverbine, (−)-(S)-Buchnerine, and Their Naturally Occurring Congenial Alkaloids. *Helvetica Chimica Acta* **2002***, 85,* 979–989.

(51) Cabrera-Pardo, J. R.; Trowbridge, A.; Nappi, M.; Ozaki, K.; Gaunt, M. J. Selective Palladium(II)-Catalyzed Carbonylation of Methylene β-C−H Bonds in Aliphatic Amines. *Angew. Chem. Int. Ed.* **2017**, *56*, 11958–11962.

(52) Seto, M.; Roizen, J. L.; Stoltz, B. M. Catalytic Enantioselective Alkylation of Substituted Dioxanone Enol Ethers: Ready Access to C(α)-Tetrasubstituted Hydroxyketones, Acids, and Esters. *Angew. Chem.* **2008**, *120*, 6979–6982.

(53) McDougal, N. T.; Streuff, J.; Mukherjee, H.; Virgil, S. C.; Stoltz, B. M. Rapid Synthesis of an Electron-Deficient t-BuPHOX Ligand: Cross-Coupling of Aryl Bromides with Secondary Phosphine Oxides. *Tetrahedron Lett.* **2010**, *51*, 5550–5554.

(54) Childs, M. E.; Weber, W. P. Preparation of Cyanoformates. Crown Ether Phase Transfer Catalysis. *J. Org. Chem.* **1976**, *41*, 3486–3487.

(55) Tani, K.; Behenna, D. C.; McFadden, R. M.; Stoltz, B. M. A Facile and Modular Synthesis of Phosphinooxazoline Ligands. *Org. Lett.* **2007**, *9*, 2529–2531.

(56) Ukai, T.; Kawazura, H.; Ishii, Y.; Bonnet, J. J.; Ibers, J. A. Chemistry of Dibenzylideneacetone-Palladium(0) Complexes: I. Novel Tris(Dibenzylideneacetone)Dipalladium(Solvent) Complexes and Their Reactions with Quinones. *J. Organomet. Chem.* ***1999****, 65, 253–266.*

(57) Fairlamb, I. J. S.; Kapdi, A. R.; Lee, A. F. H2-Dba Complexes of Pd(0): The Substituent Effect in Suzuki−Miyaura Coupling. *Org. Lett.* **2004**, *6*, 4435–4438.

(58) Endo, K.; Grubbs, R. H. Chelated Ruthenium Catalysts for Z-Selective Olefin Metathesis. *J. Am. Chem. Soc.* **2011**, *133*, 8525–8527.

(59) Klepacz, A.; Zwierzak, A. An Expeditious One-Pot Synthesis of Diethyl N-Boc-1-Aminoalkylphosphonates. *Tetrahedron Lett.* **2002**, *43*, 1079–1080.

(60) Sikriwal, D.; Kant, R.; Maulik, P. R.; Dikshit, D. K. A Short Formal Synthesis of Three Epimers of Penmacric Acid. *Tetrahedron* **2010**, *66*, 6167–6173.

(61) Taylor, R. R. R.; Twin, H. C.; Wen, W. W.; Mallot, R. J.; Lough, A. J.; Gray-Owen, S. D.; Batey, R. A. Substituted 2,5-Diazabicyclo[4.1.0]Heptanes and Their Application as General Piperazine Surrogates: Synthesis and Biological Activity of a Ciprofloxacin Analogue. *Tetrahedron* **2010**, *66*, 3370–3377.

(62) White, D. E.; Stewart, I. C.; Grubbs, R. H.; Stoltz, B. M. The Catalytic Asymmetric Total Synthesis of Elatol. *J. Am. Chem. Soc.* **2008**, *130*, 810–811.

(63) Chollet, A.; Mori, G.; Menendez, C.; Rodriguez, F.; Fabing, I.; Pasca, M. R.; Madacki, J.; Korduláková, J.; Constant, P.; Quémard, A.; et al. Design, Synthesis and Evaluation of New GEQ Derivatives as Inhibitors of InhA Enzyme and Mycobacterium Tuberculosis Growth. *Eur. J. Med. Chem.* **2015**, *101*, 218–235.

APPENDIX 1

Spectra Relevant to Chapter 1:

Enantioselective Synthesis of gem-Disubstituted N-Boc

Diazaheterocycles via Decarboxylative Asymmetric Allylic Alkylation

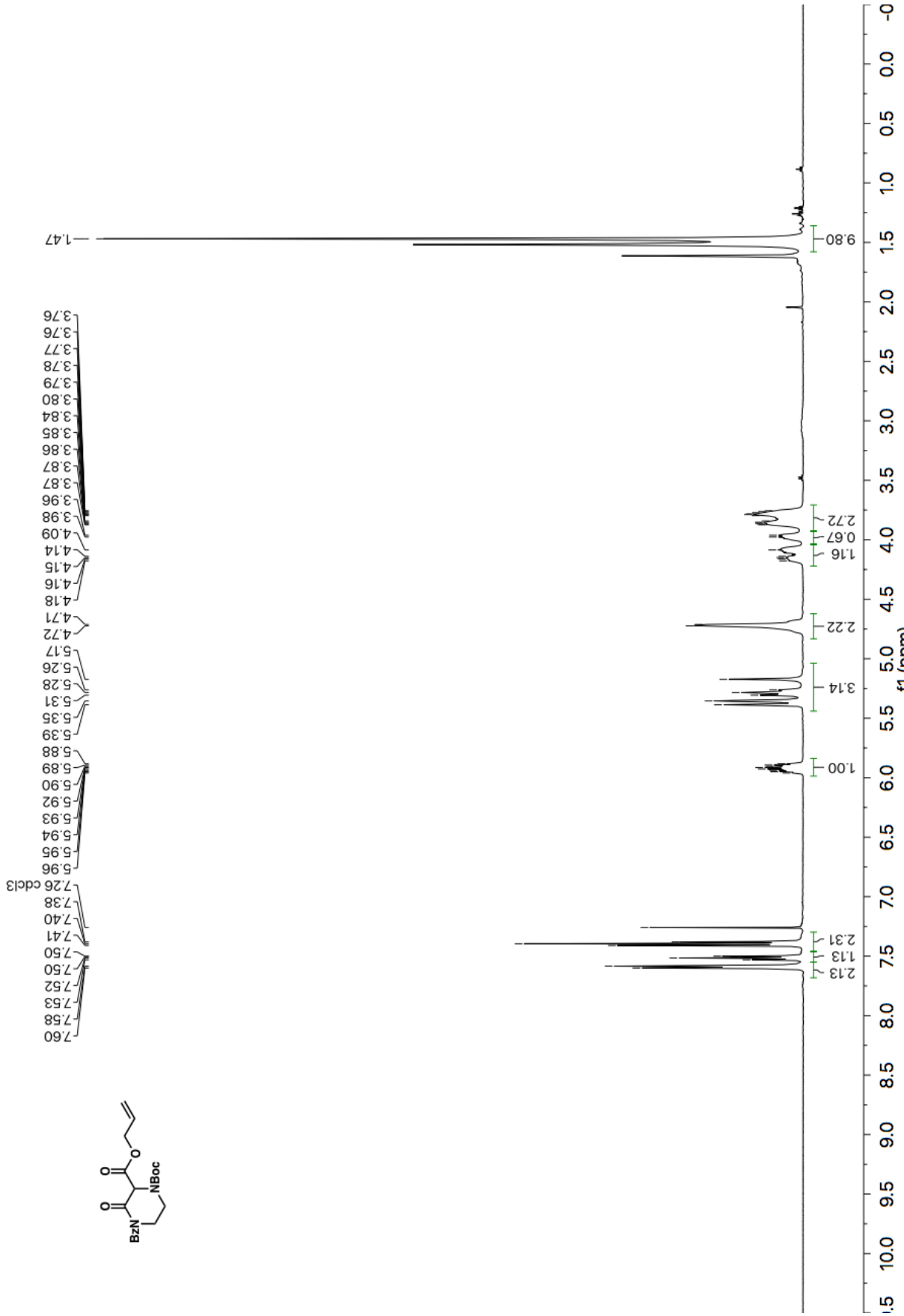

Figure A1.1 ^{1}H NMR (500 MHz, $CDCl_3$) of compound **1.2.**

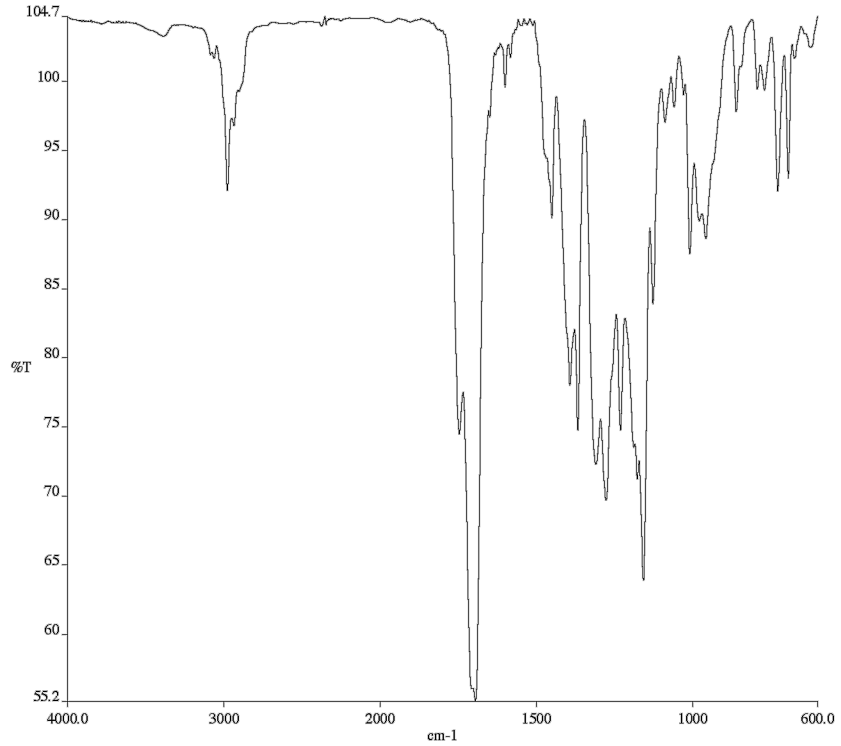

Figure A1.2 Infrared spectrum (Thin Film, NaCl) of compound **1.2**.

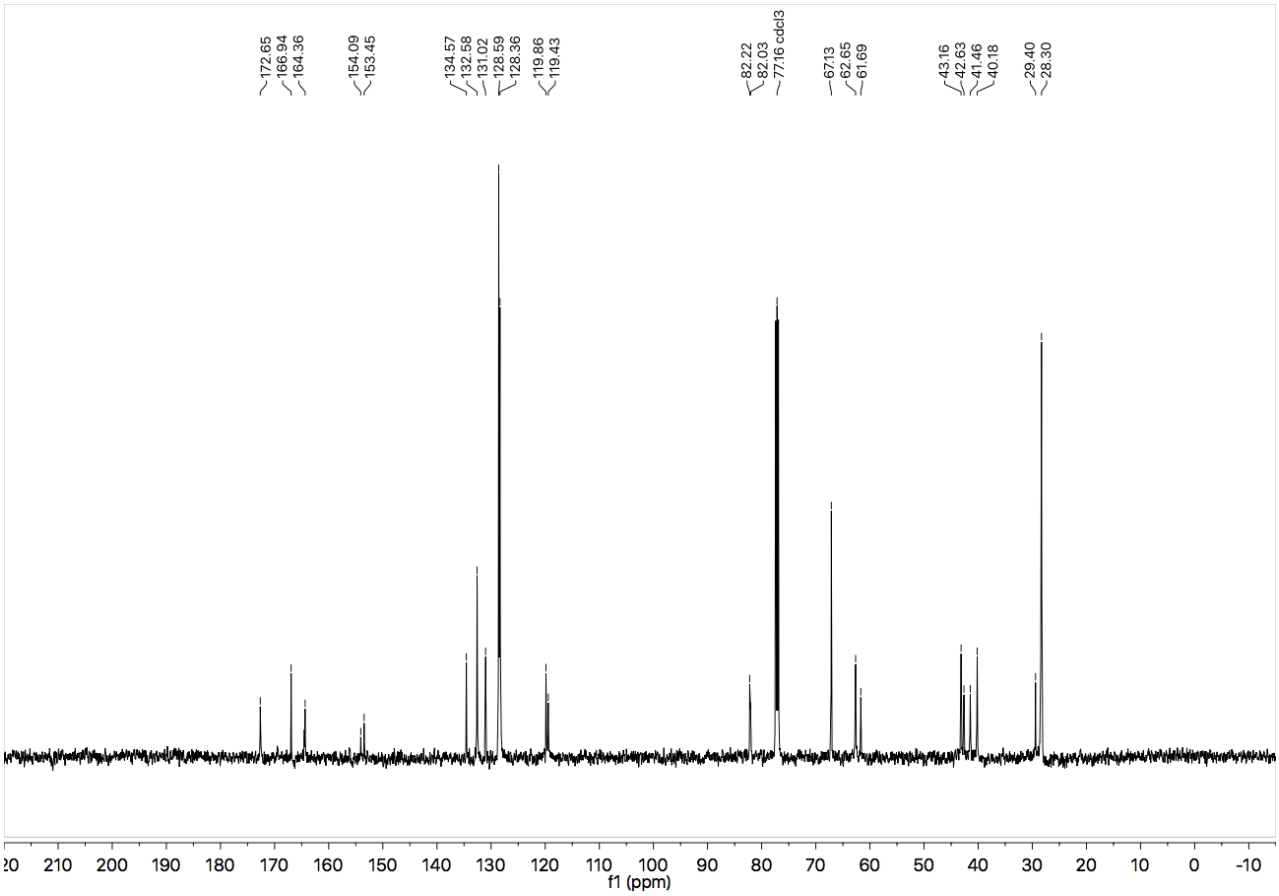

Figure A1.3 ^{13}C NMR (126 MHz, $CDCl_3$) of compound **1.2**.

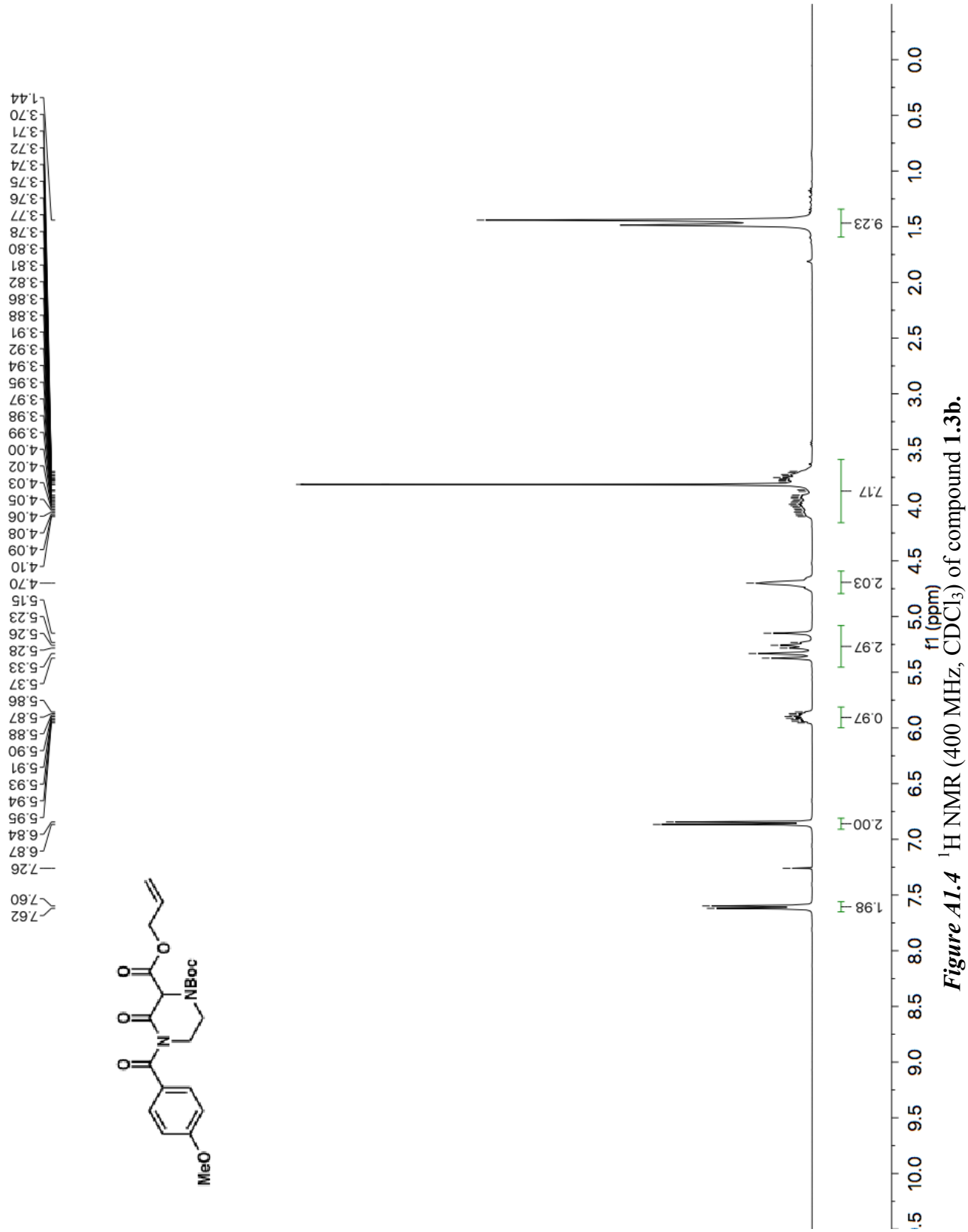

Figure A1.4 ^{1}H NMR (400 MHz, $CDCl_3$) of compound **1.3b.**

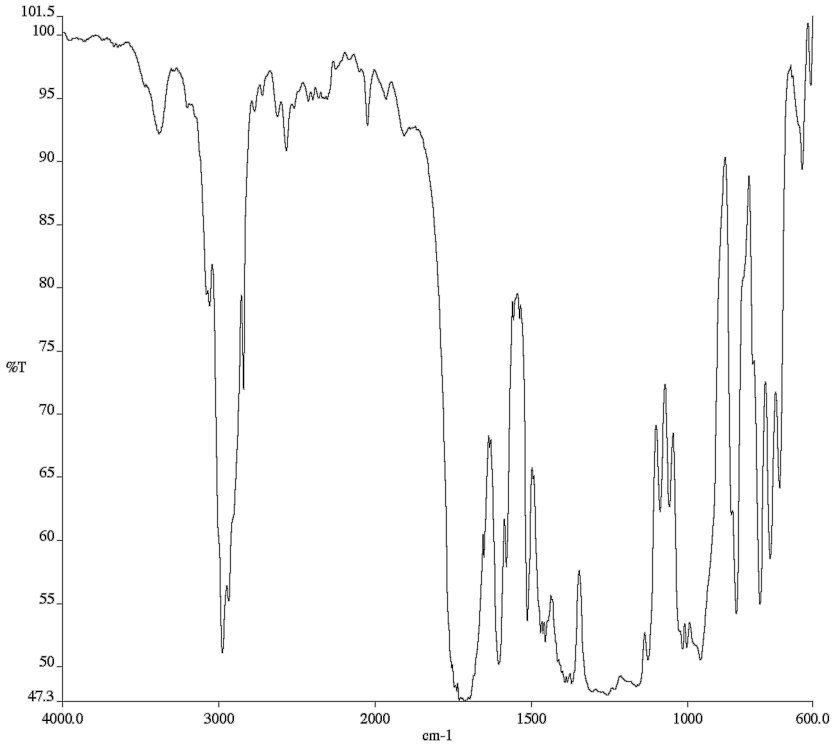

Figure A1.5 Infrared spectrum (Thin Film, NaCl) of compound **1.3b**.

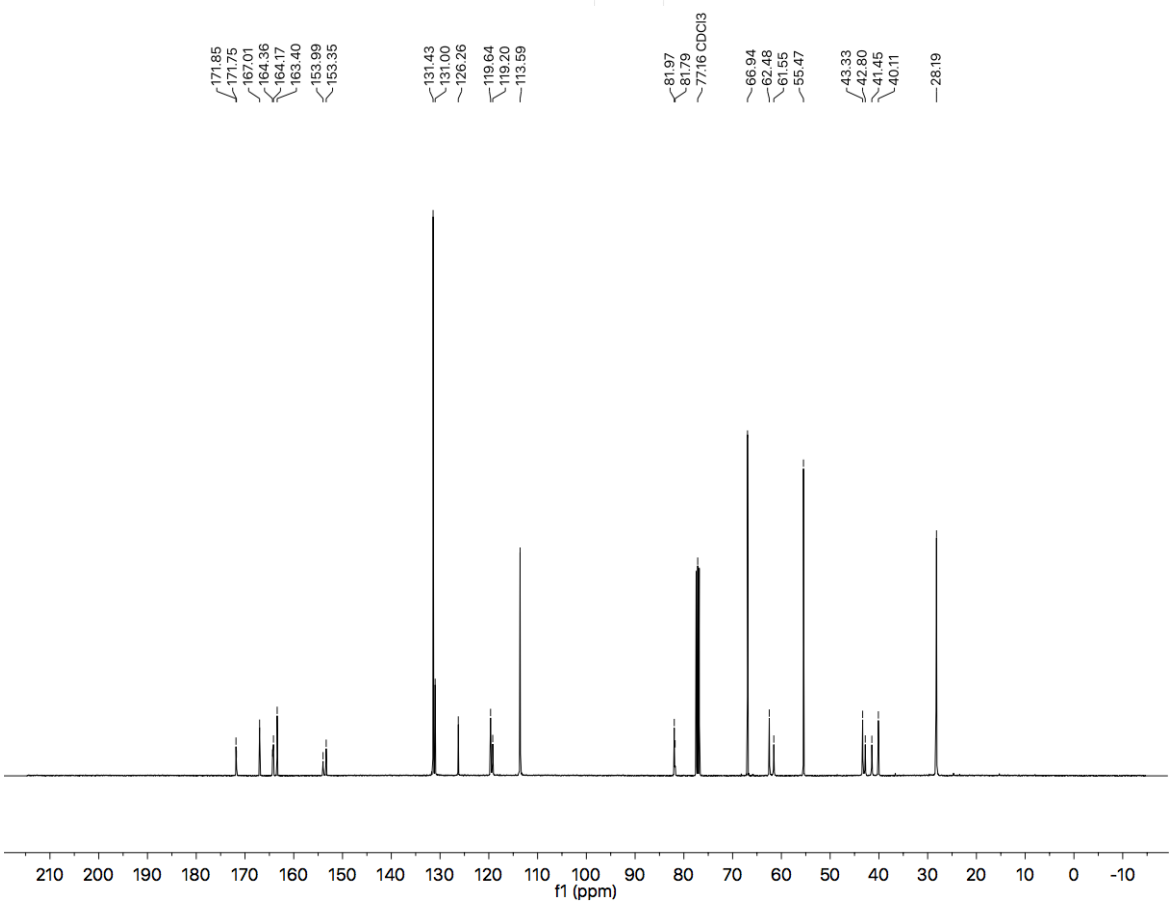

Figure A1.6 ^{13}C NMR (101 MHz, $CDCl_3$) of compound **1.3b**.

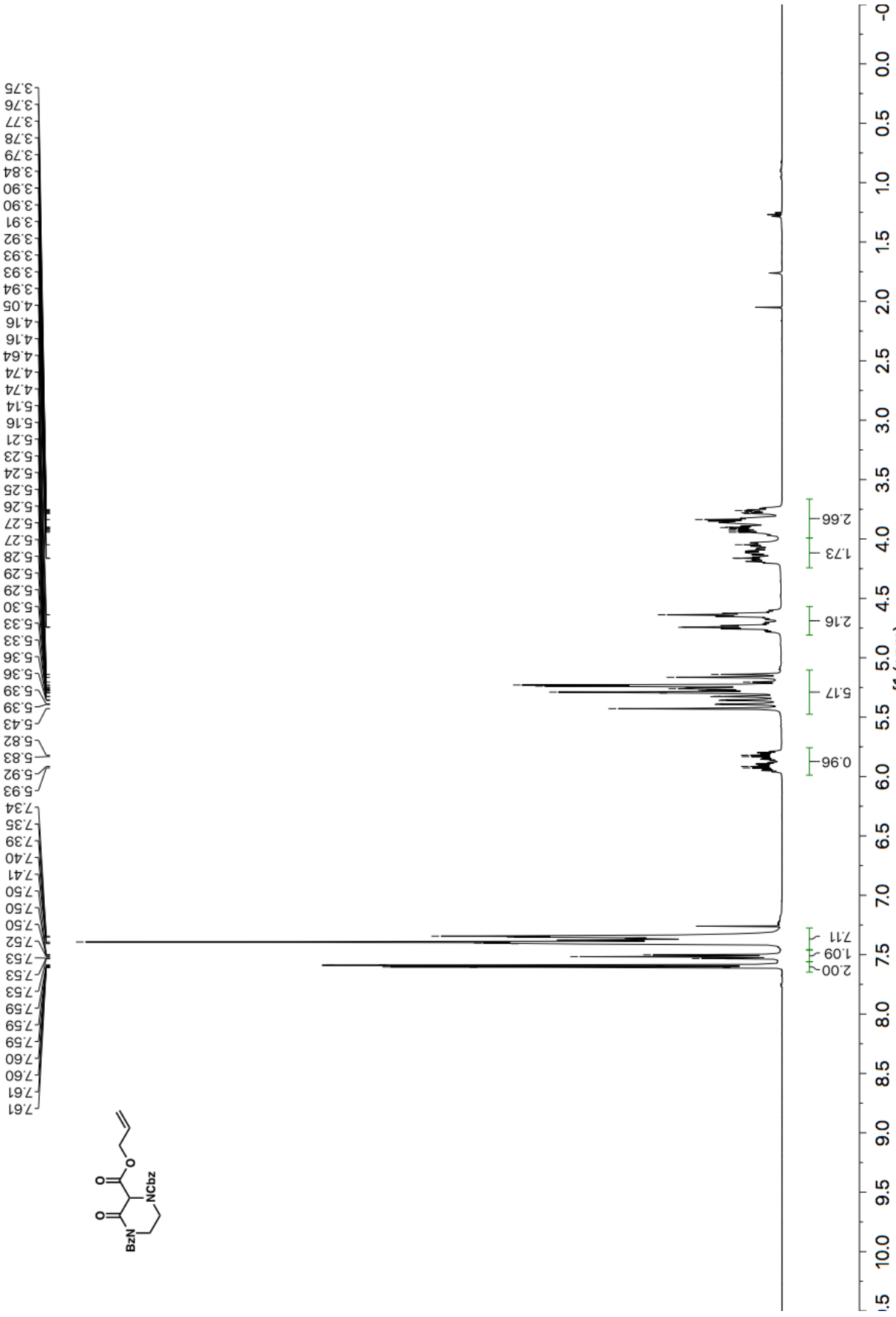

Figure A1.7 ^{1}H NMR (500 MHz, $CDCl_3$) of compound **1.3c.**

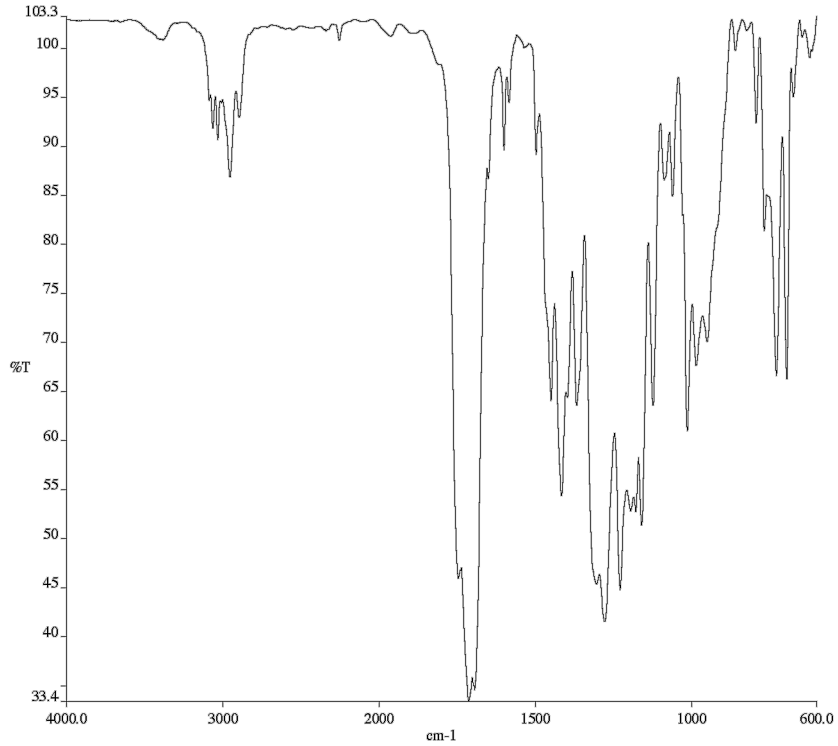

Figure A1.8 Infrared spectrum (Thin Film, NaCl) of compound **1.3c**.

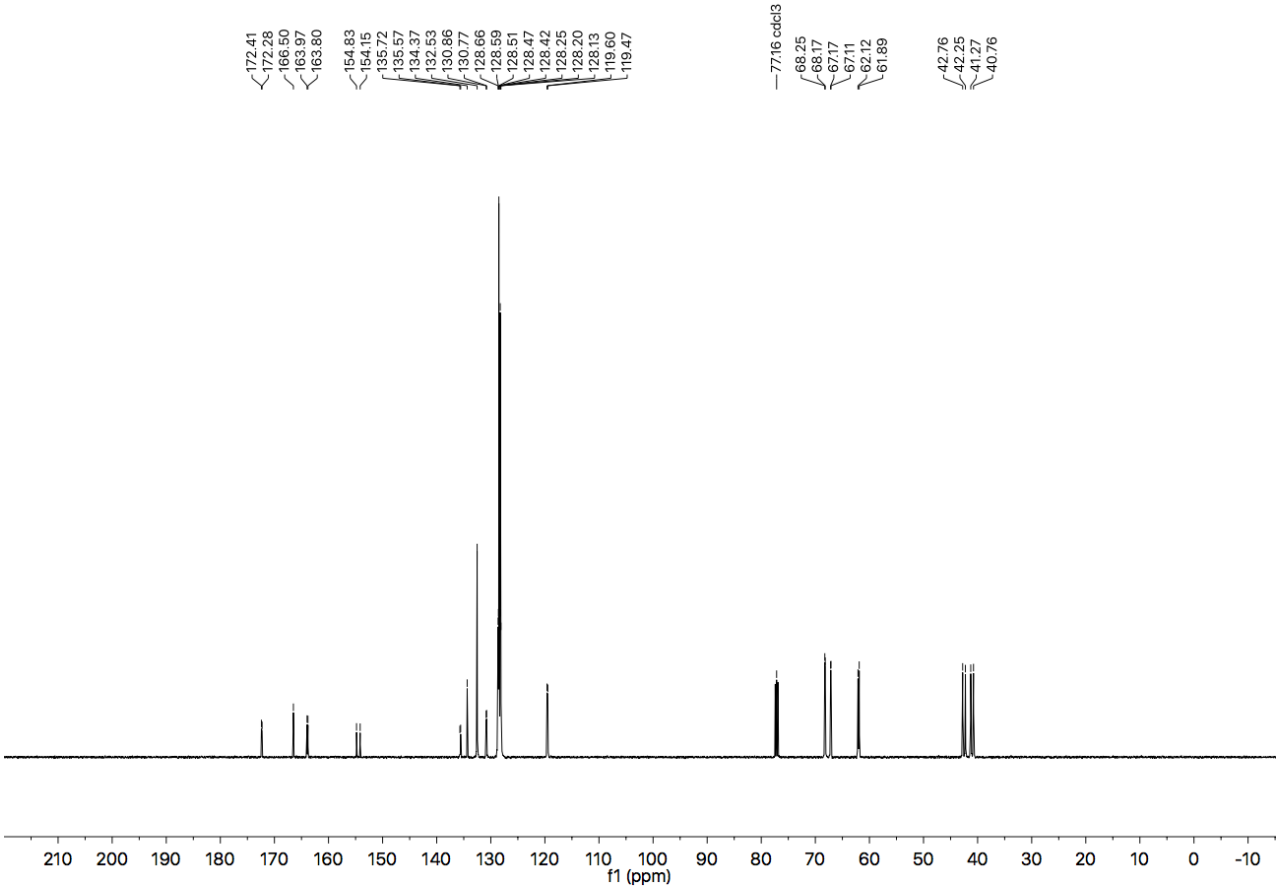

Figure A1.9 ^{13}C NMR (126 MHz, $CDCl_3$) of compound **1.3c**.

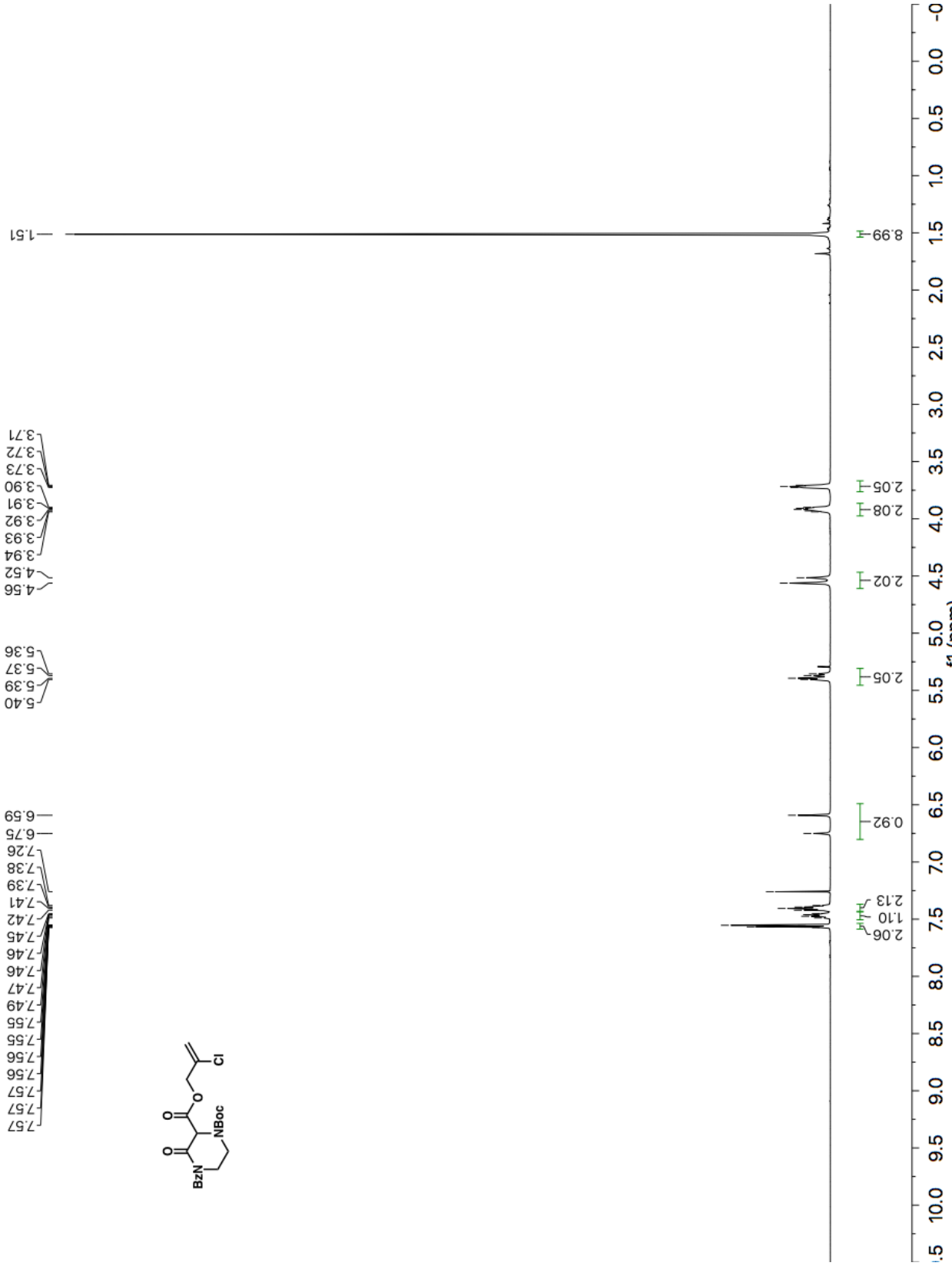

Figure A1.10 ^{1}H NMR (400 MHz, $CDCl_3$) of compound **1.3d.**

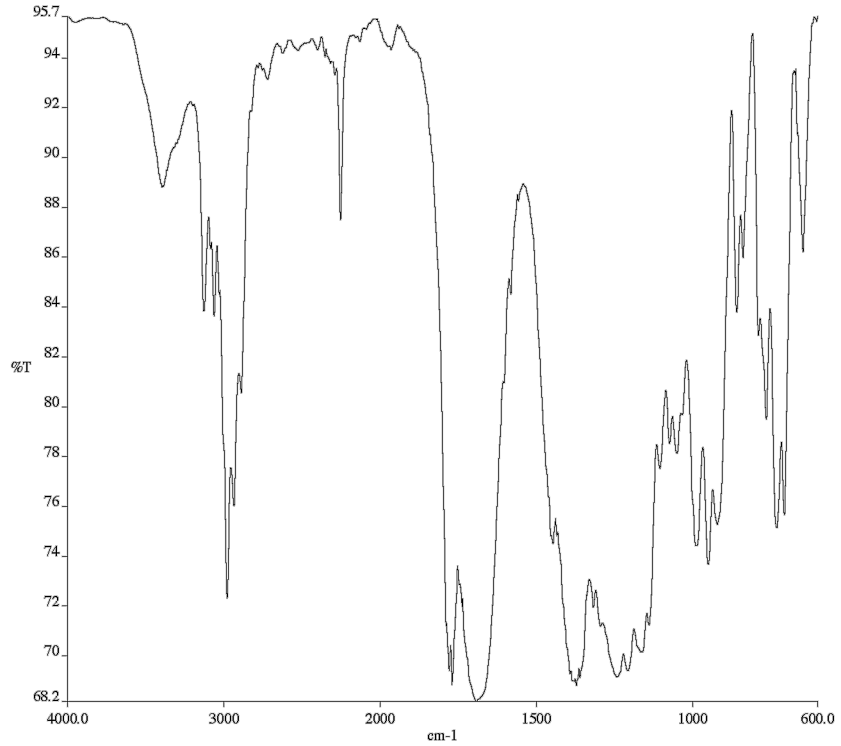

Figure A1.11 Infrared spectrum (Thin Film, NaCl) of compound **1.3d**.

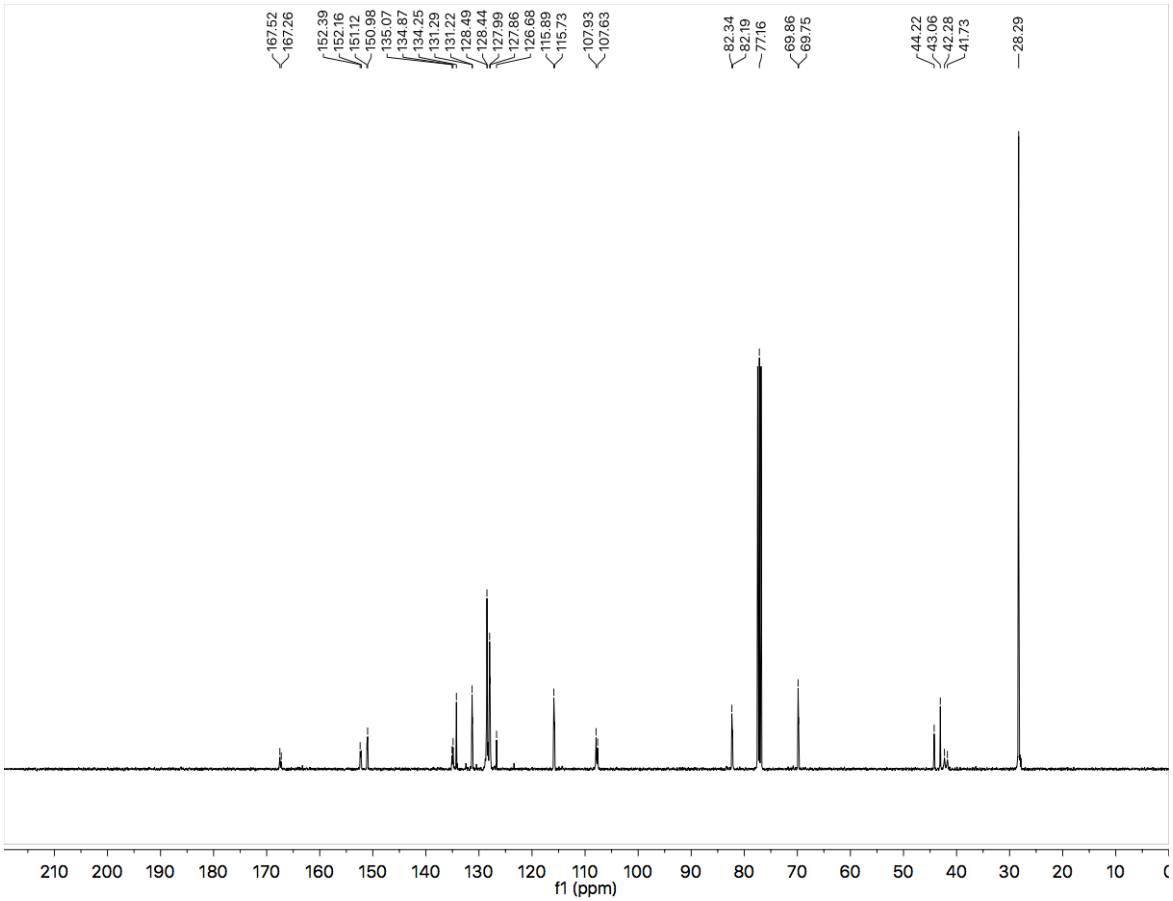

Figure A1.12 ^{13}C NMR (101 MHz, $CDCl_3$) of compound **1.3d**.

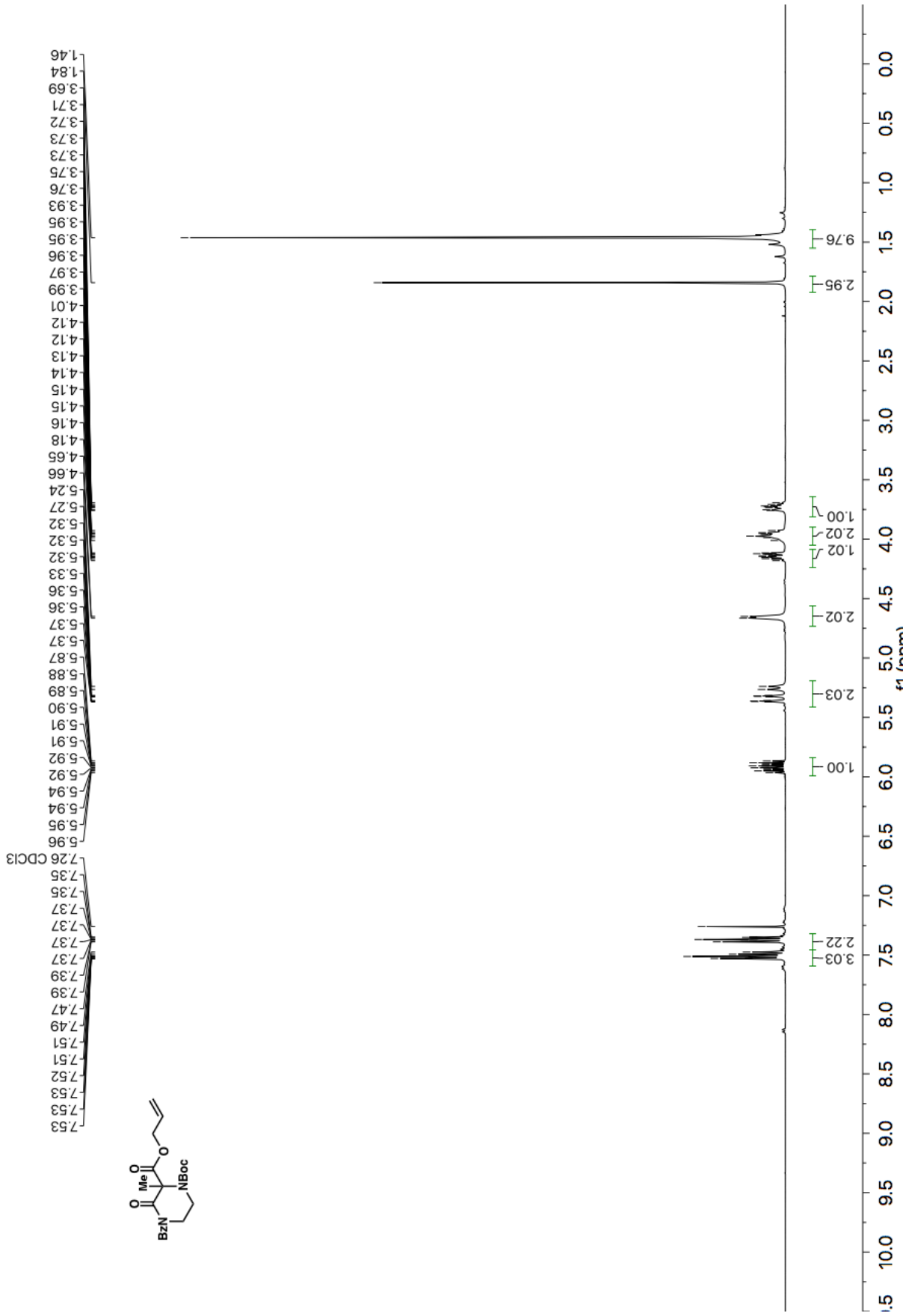

Figure A1.13 ^{1}H NMR (400 MHz, $CDCl_3$) of compound **1.3e.**

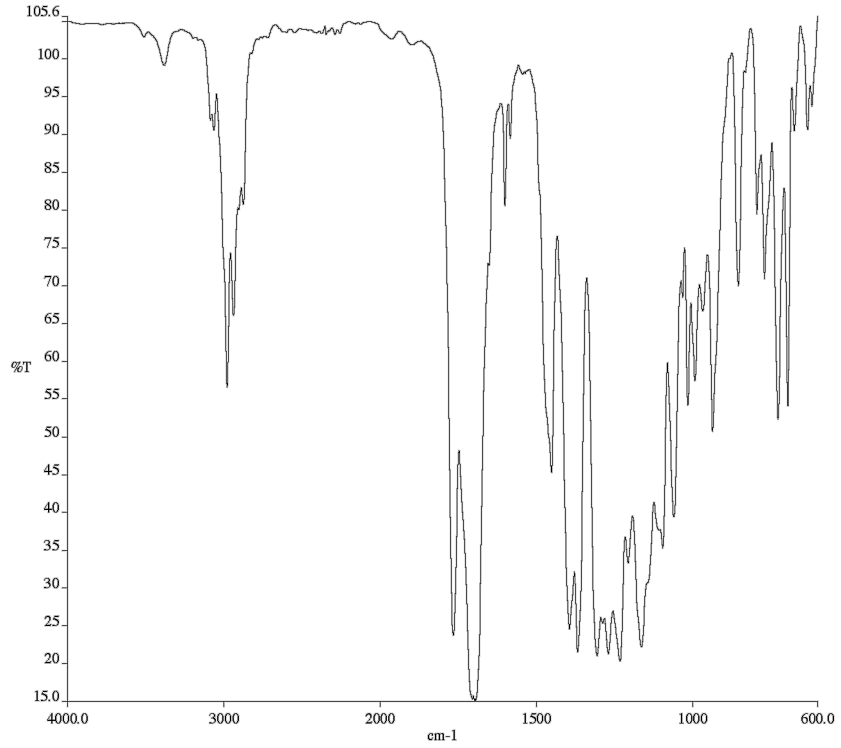

Figure A1.14 Infrared spectrum (Thin Film, NaCl) of compound **1.3e**.

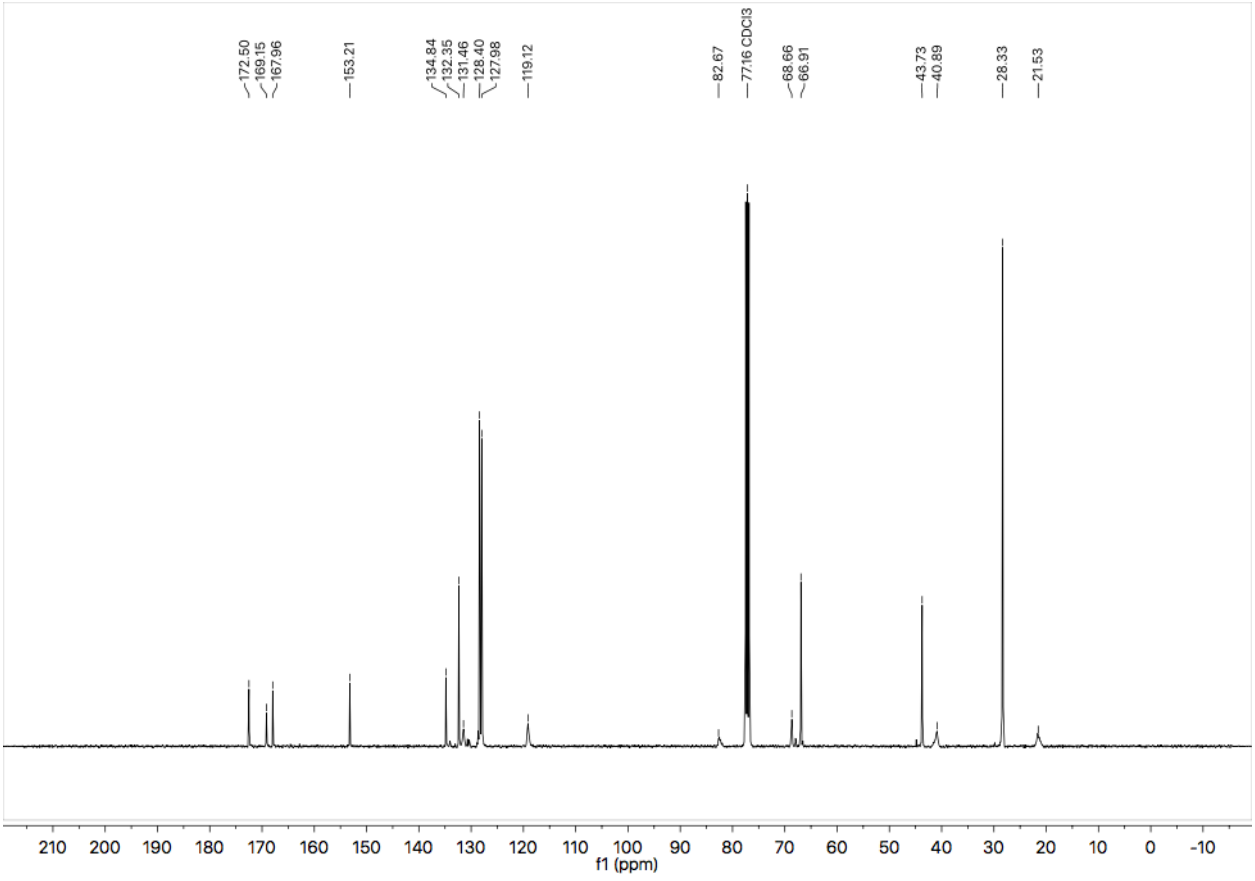

Figure A1.15 ^{13}C NMR (101 MHz, $CDCl_3$) of compound **1.3e**.

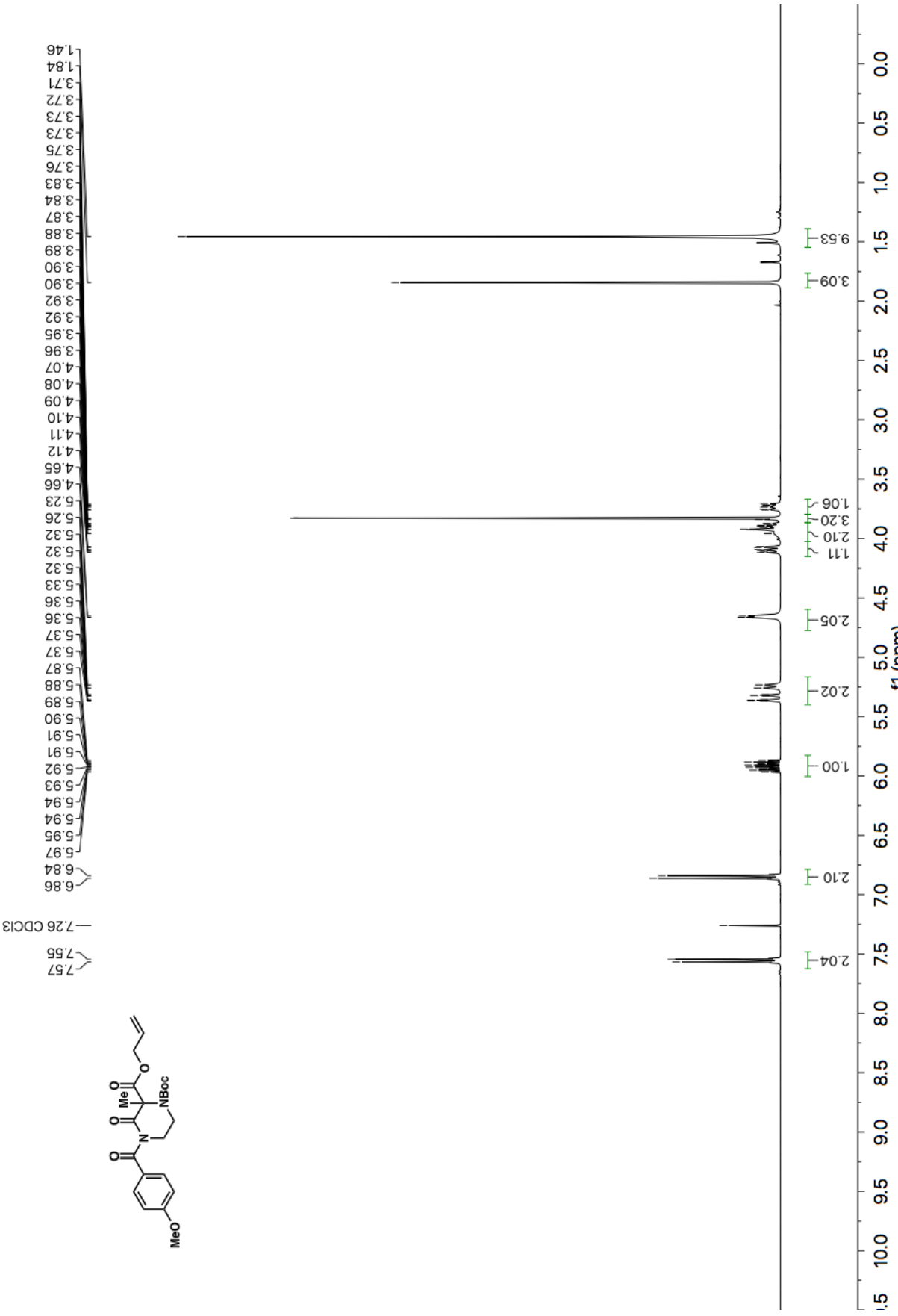

Figure A1.16 ^{1}H NMR (400 MHz, $CDCl_3$) of compound **1.3f.**

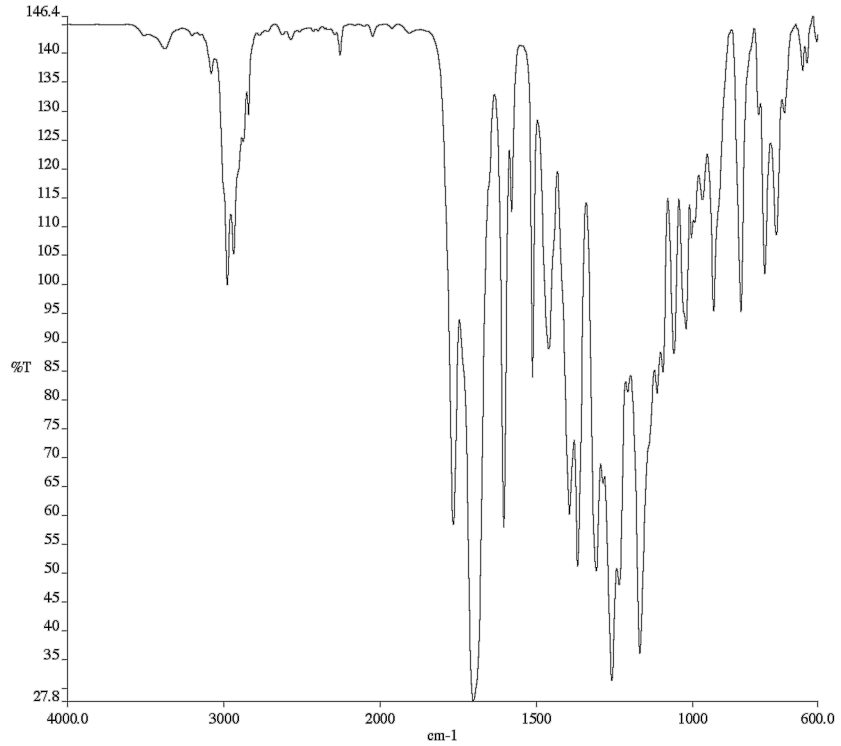

Figure A1.17 Infrared spectrum (Thin Film, NaCl) of compound **1.3f**.

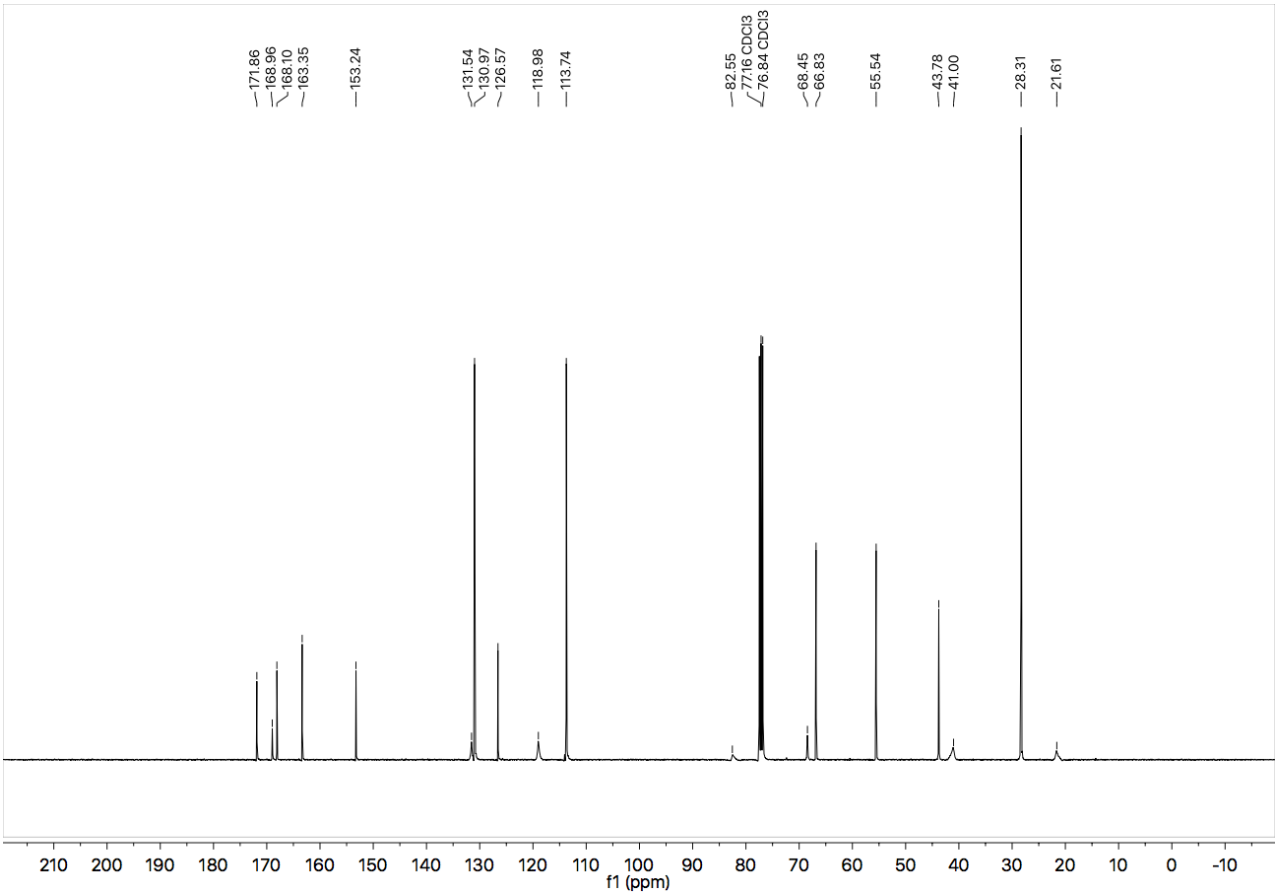

Figure A1.18 ^{13}C NMR (101 MHz, $CDCl_3$) of compound **1.3f**.

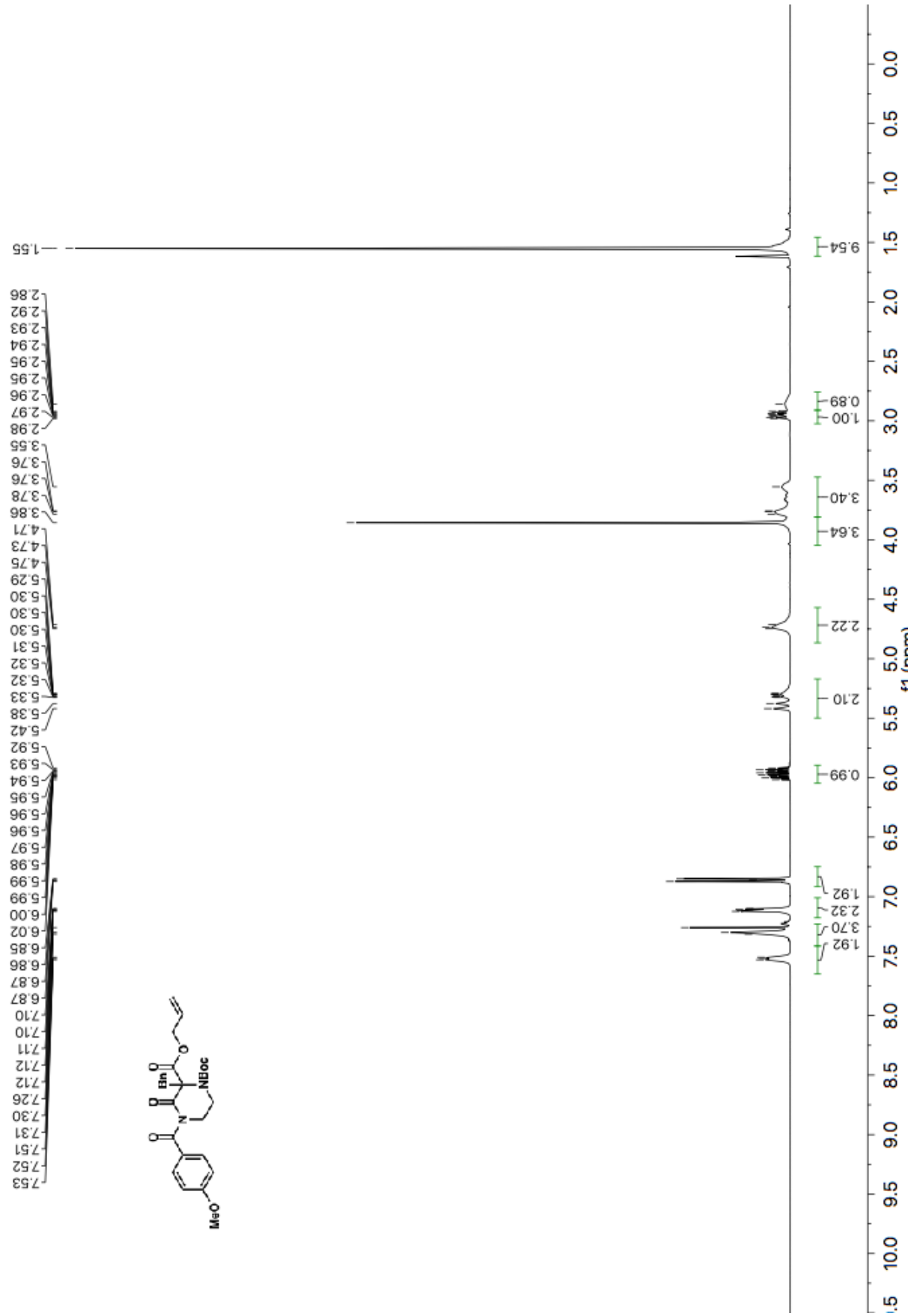

Figure A1.19 ^{1}H NMR (400 MHz, $CDCl_3$) of compound **1.3h.**

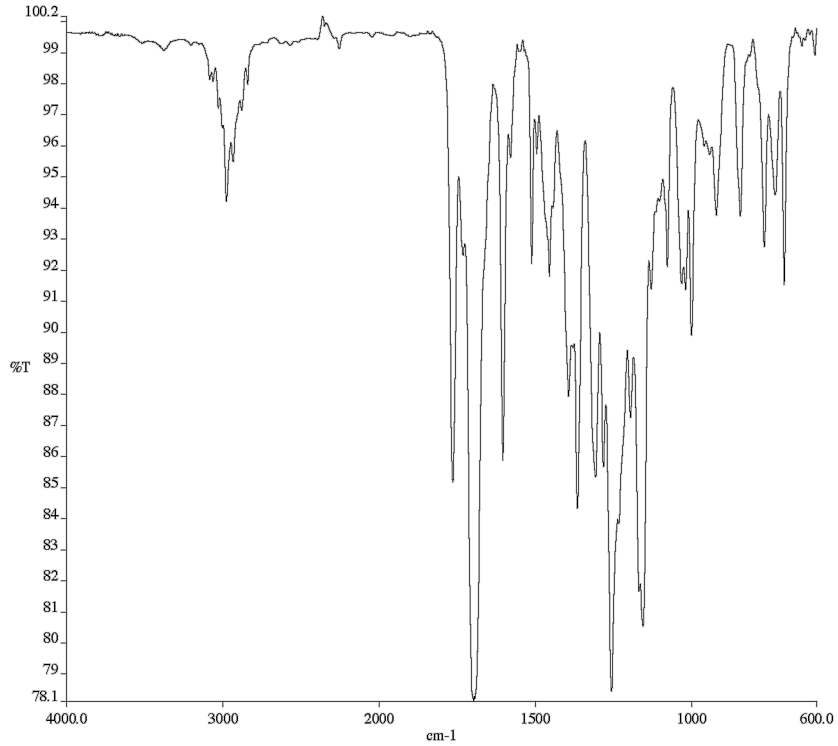

Figure A1.20 Infrared spectrum (Thin Film, NaCl) of compound **1.3h**.

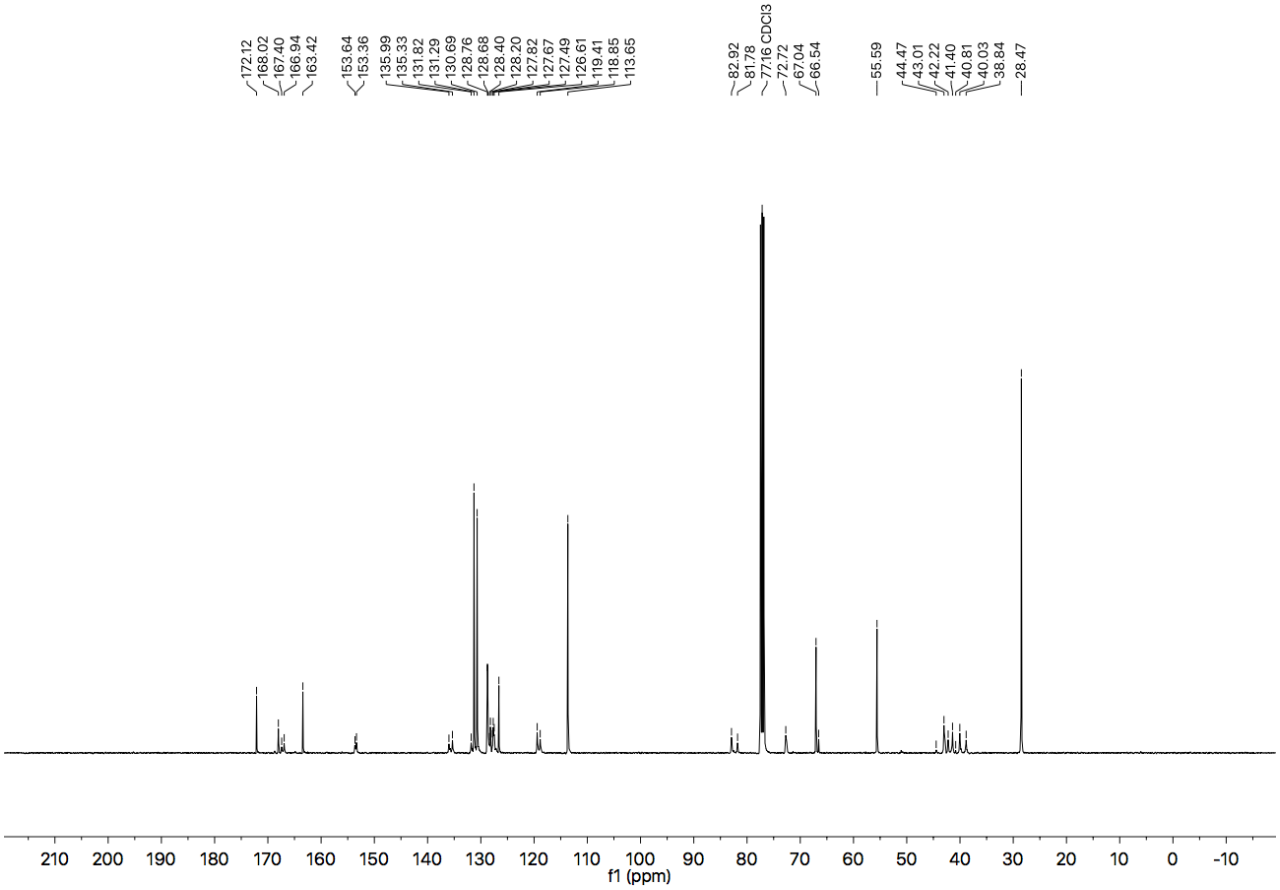

Figure A1.21 ^{13}C NMR (101 MHz, $CDCl_3$) of compound **1.3h**.

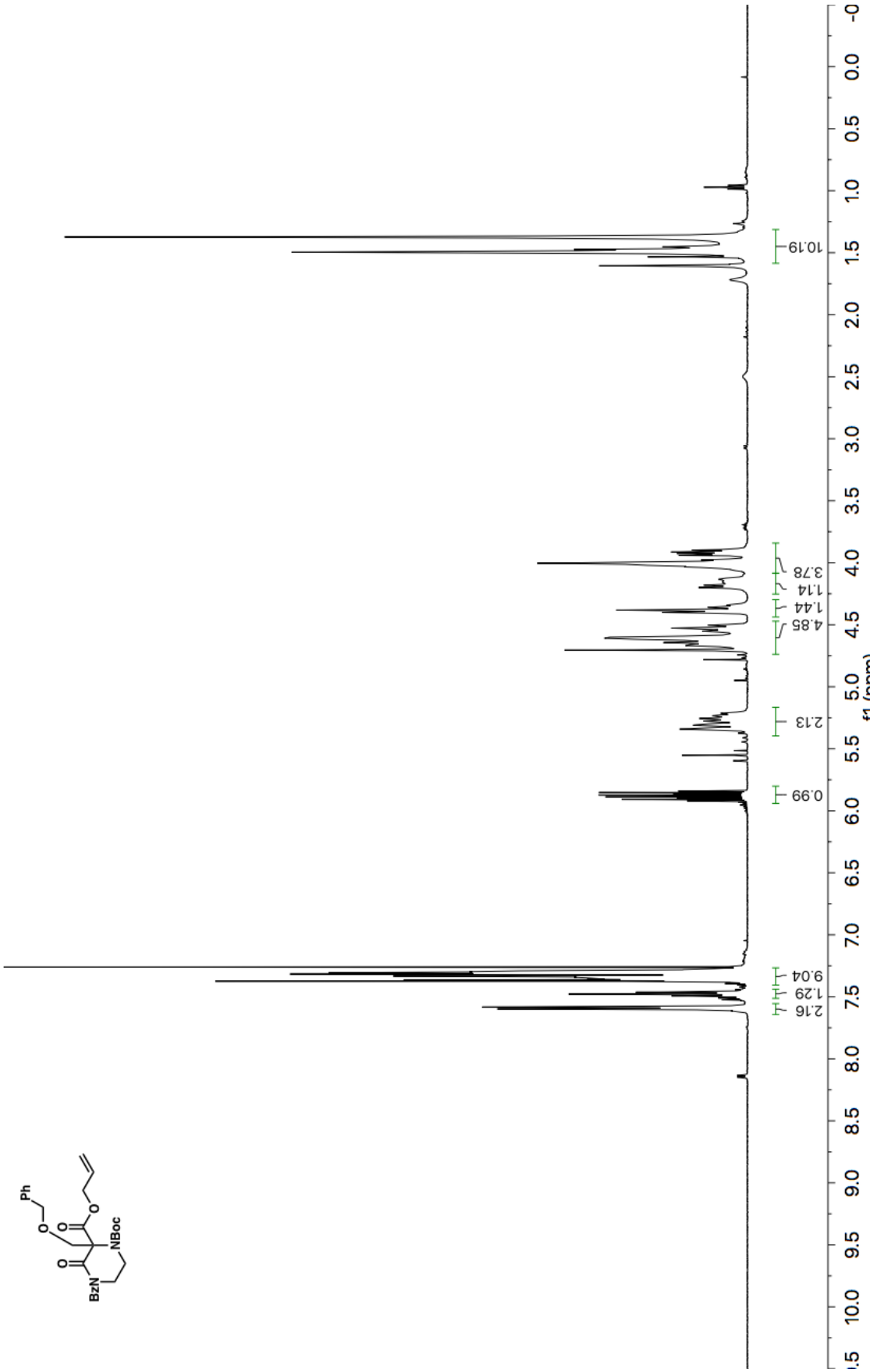

Figure A1.22 ^{1}H NMR (500 MHz, $CDCl_3$) of compound **1.3i.**

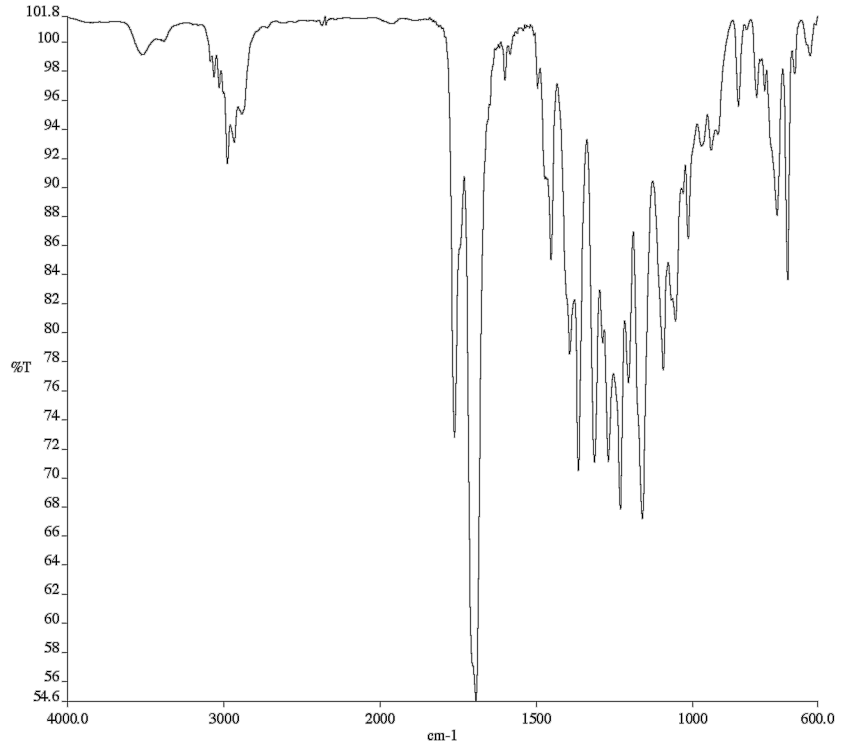

Figure A1.23 Infrared spectrum (Thin Film, NaCl) of compound **1.3i**.

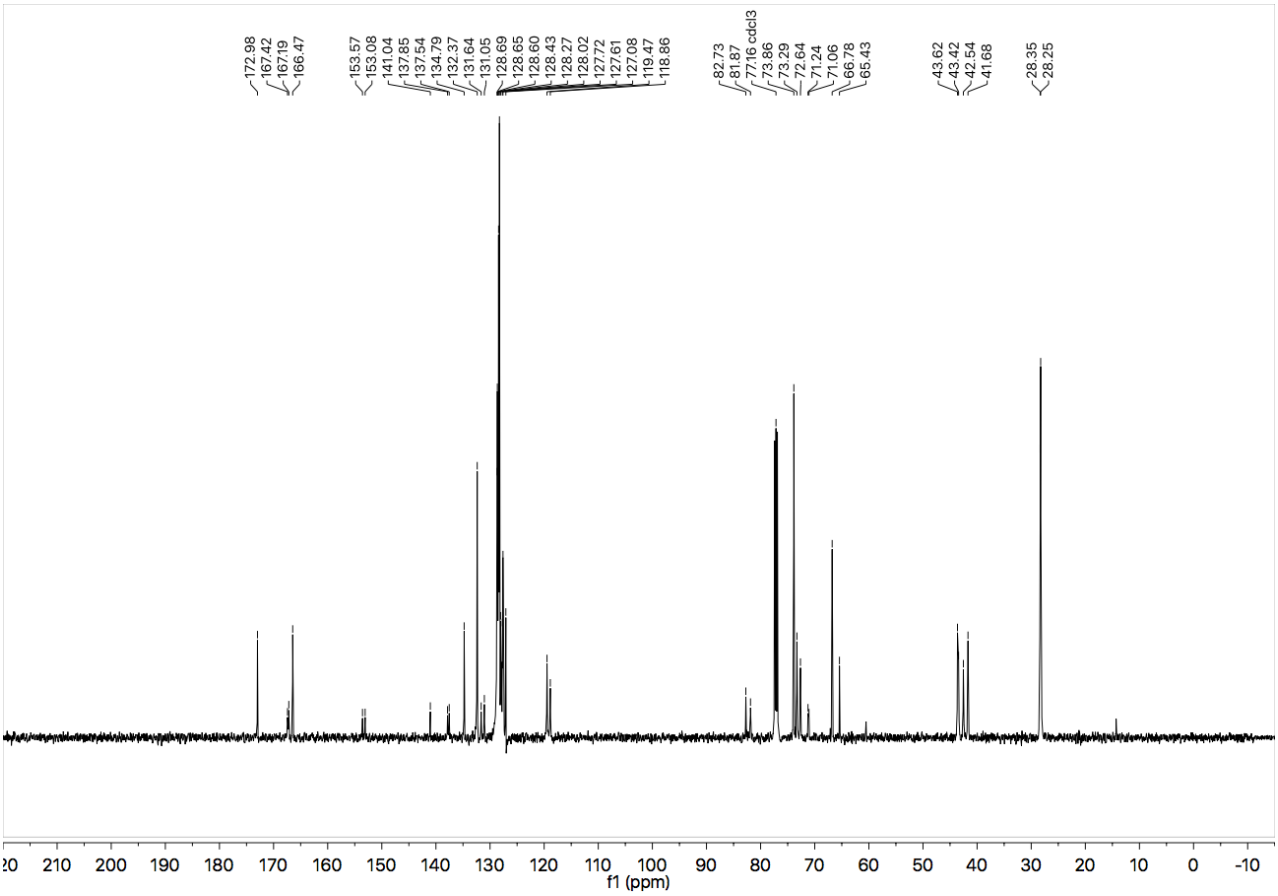

Figure A1.24 ^{13}C NMR (126 MHz, $CDCl_3$) of compound **1.3i**.

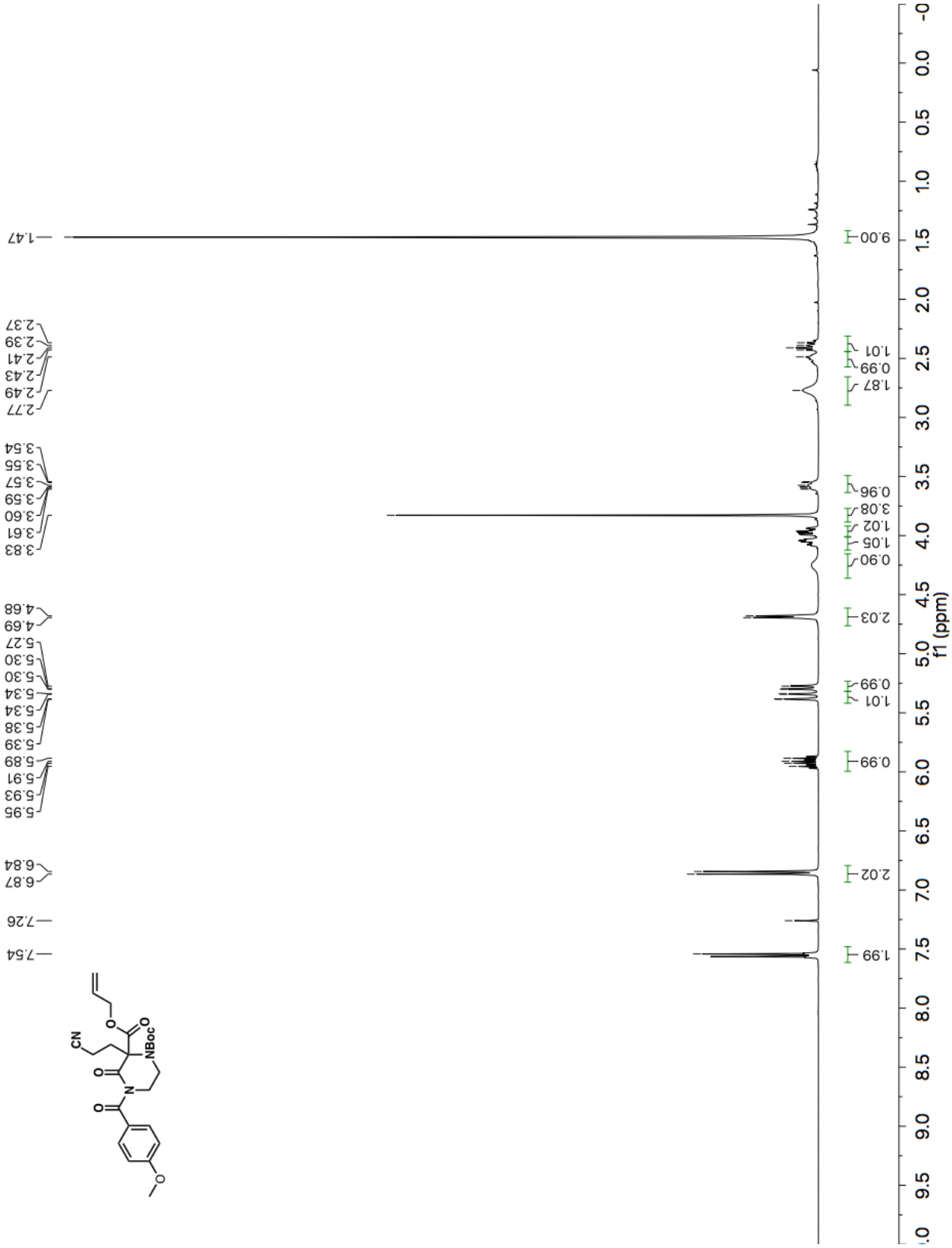

Figure A1.25 ^{1}H NMR (400 MHz, $CDCl_3$) of compound **1.3j.**

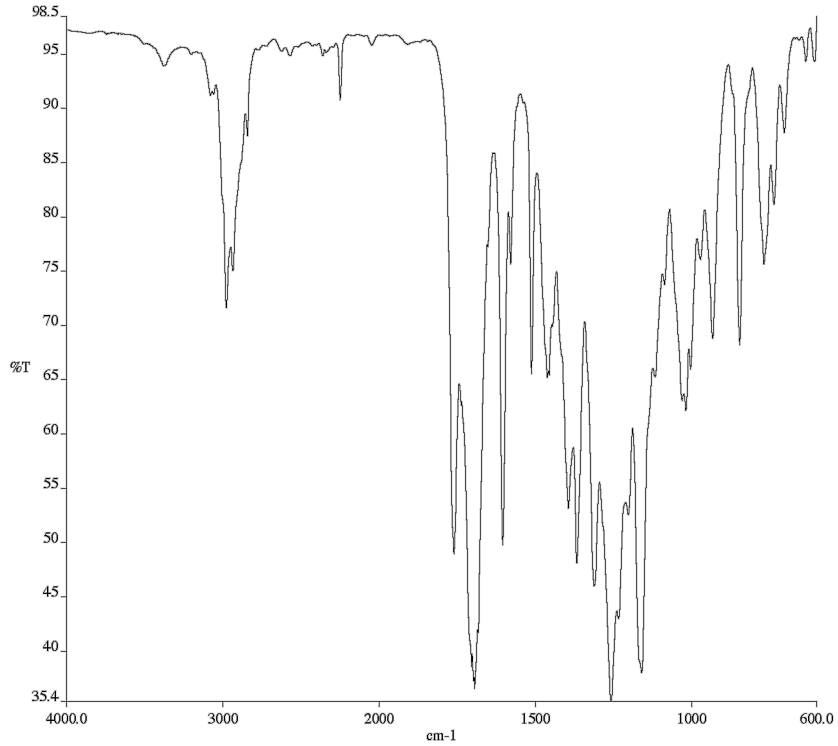

Figure A1.26 Infrared spectrum (Thin Film, NaCl) of compound **1.3j**.

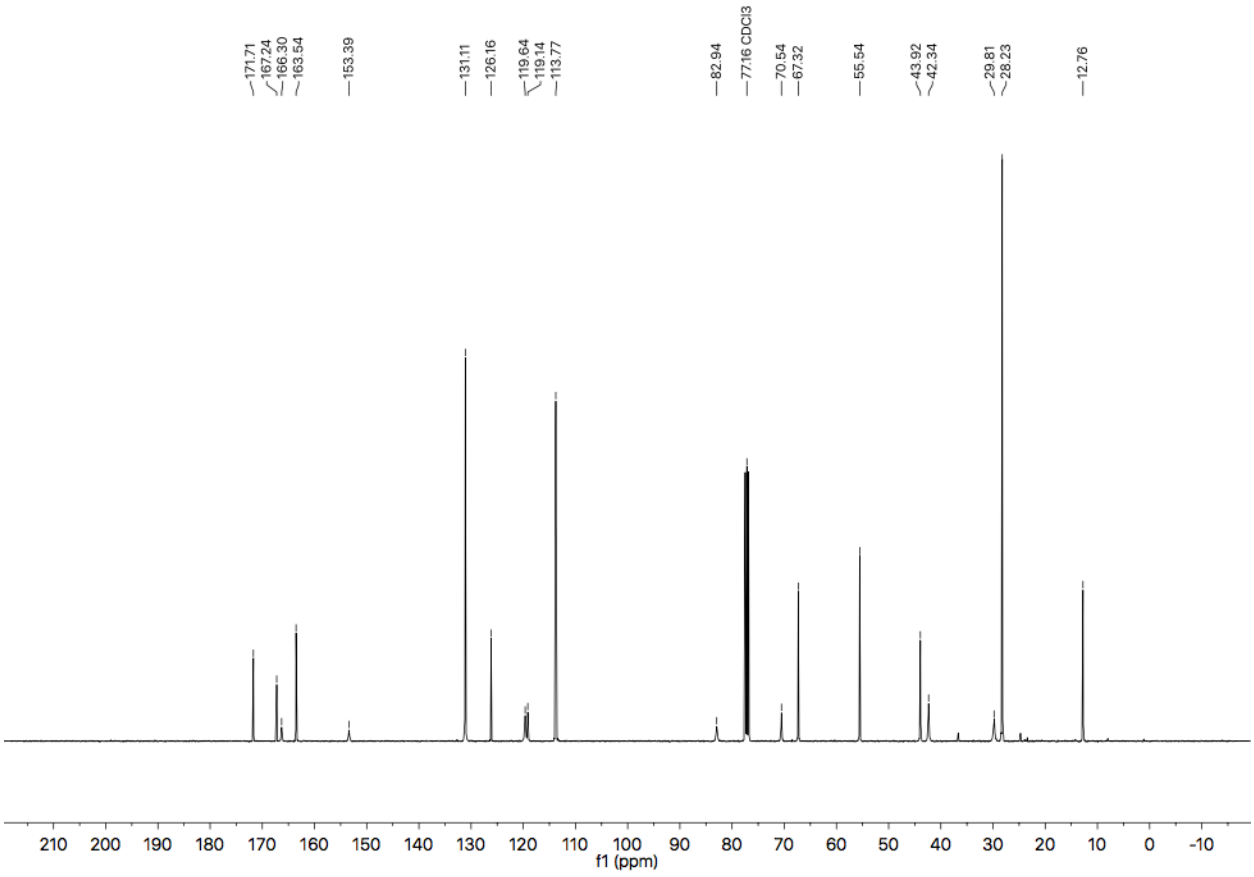

Figure A1.27 ^{13}C NMR (101 MHz, $CDCl_3$) of compound **1.3j**.

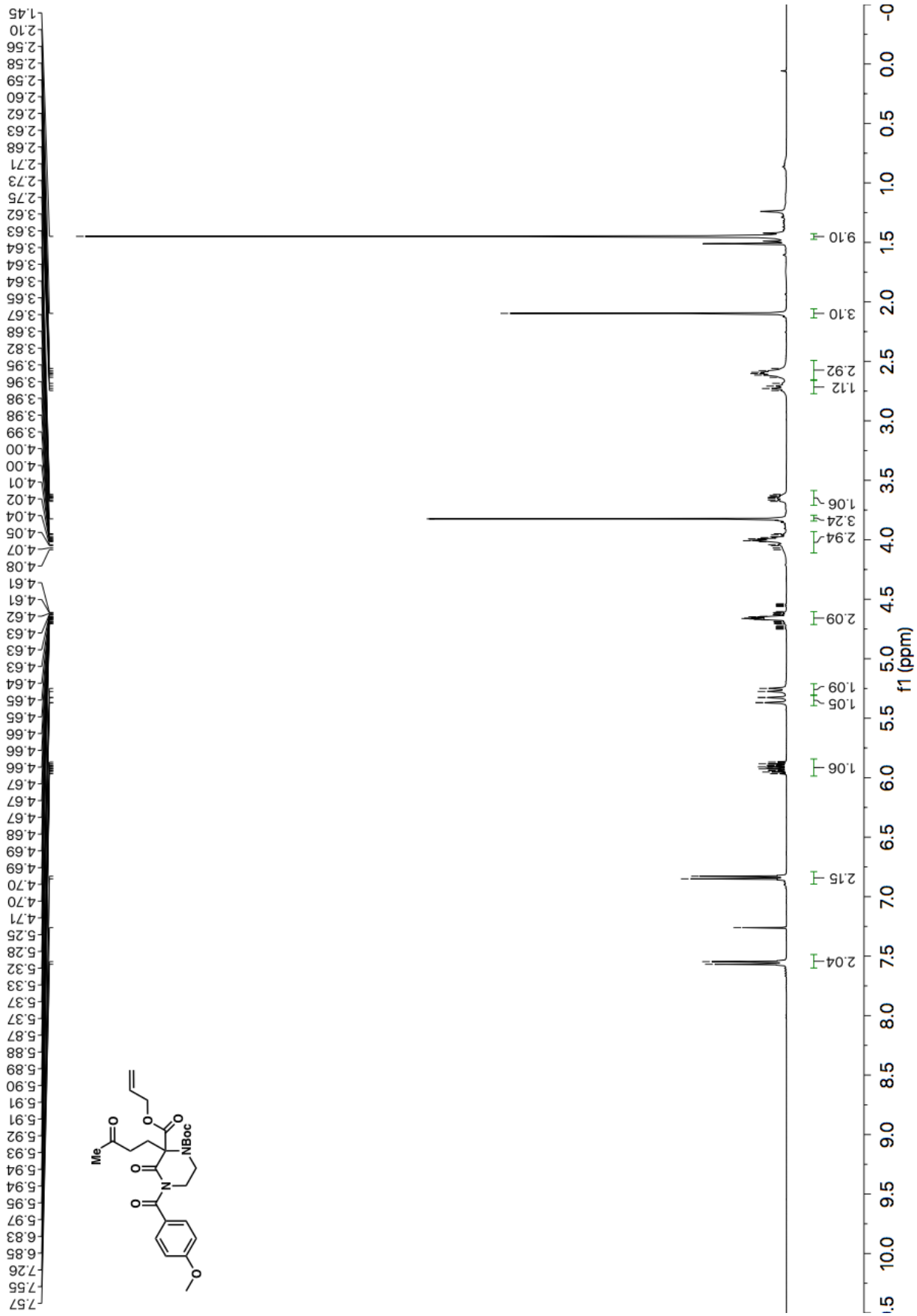

Figure A1.28 ^{1}H NMR (400 MHz, $CDCl_3$) of compound **1.3k.**

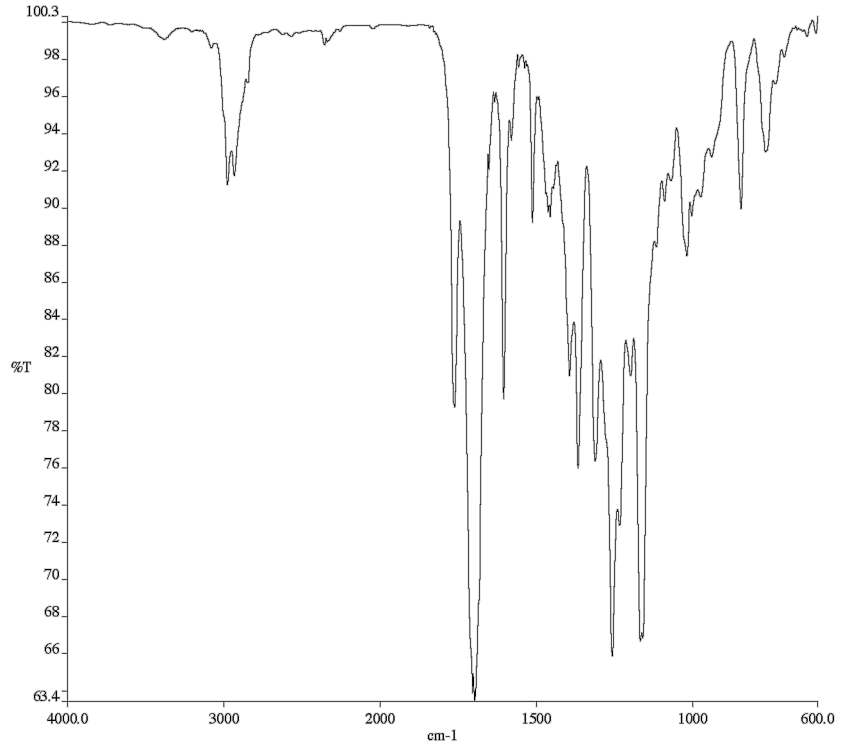

Figure A1.29 Infrared spectrum (Thin Film, NaCl) of compound **1.3k**.

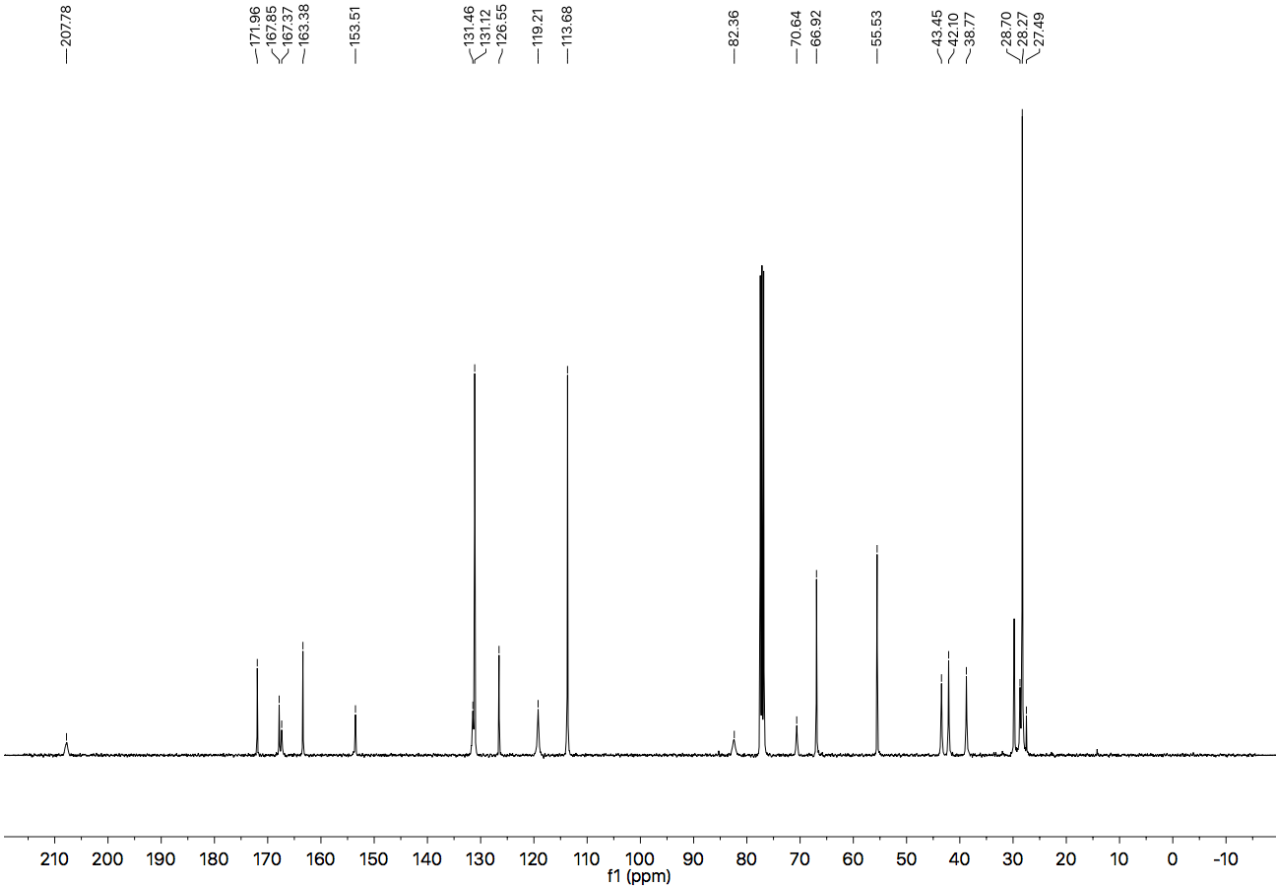

Figure A1.30 ^{13}C NMR (101 MHz, $CDCl_3$) of compound **1.3k**.

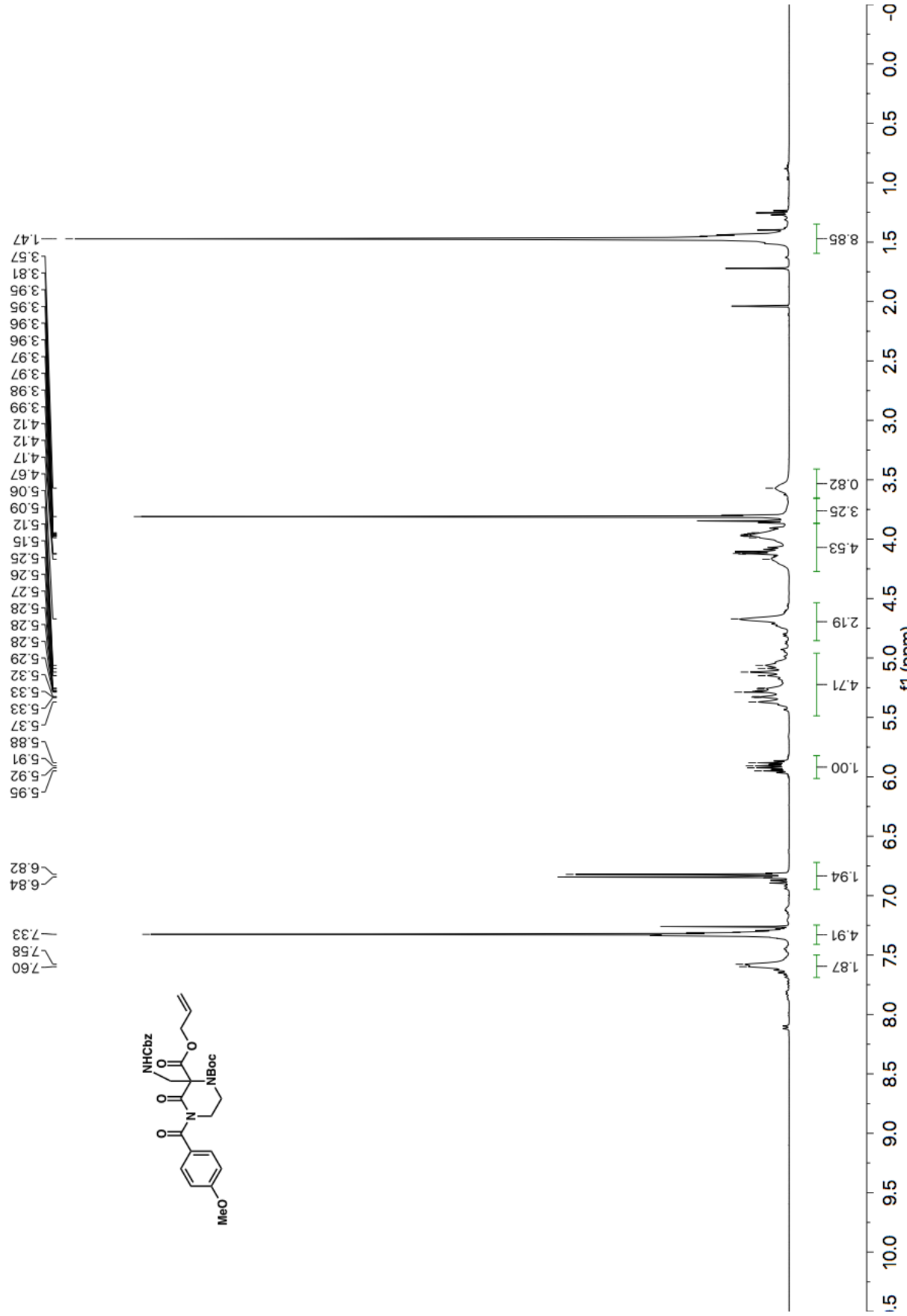

Figure A1.31 ^{1}H NMR (400 MHz, $CDCl_3$) of compound **1.31.**

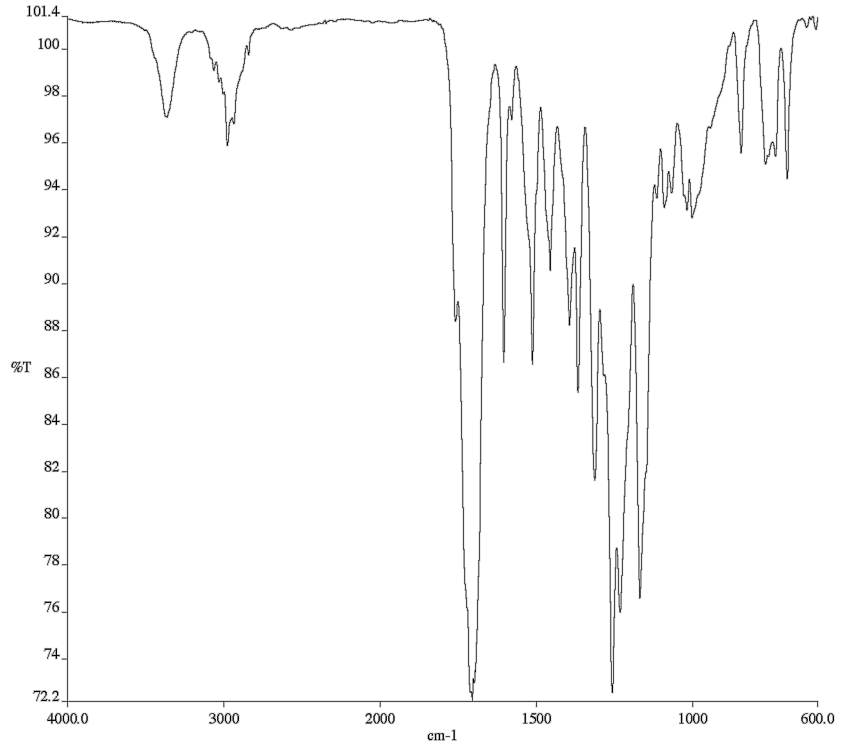

Figure A1.32 Infrared spectrum (Thin Film, NaCl) of compound **1.3l**.

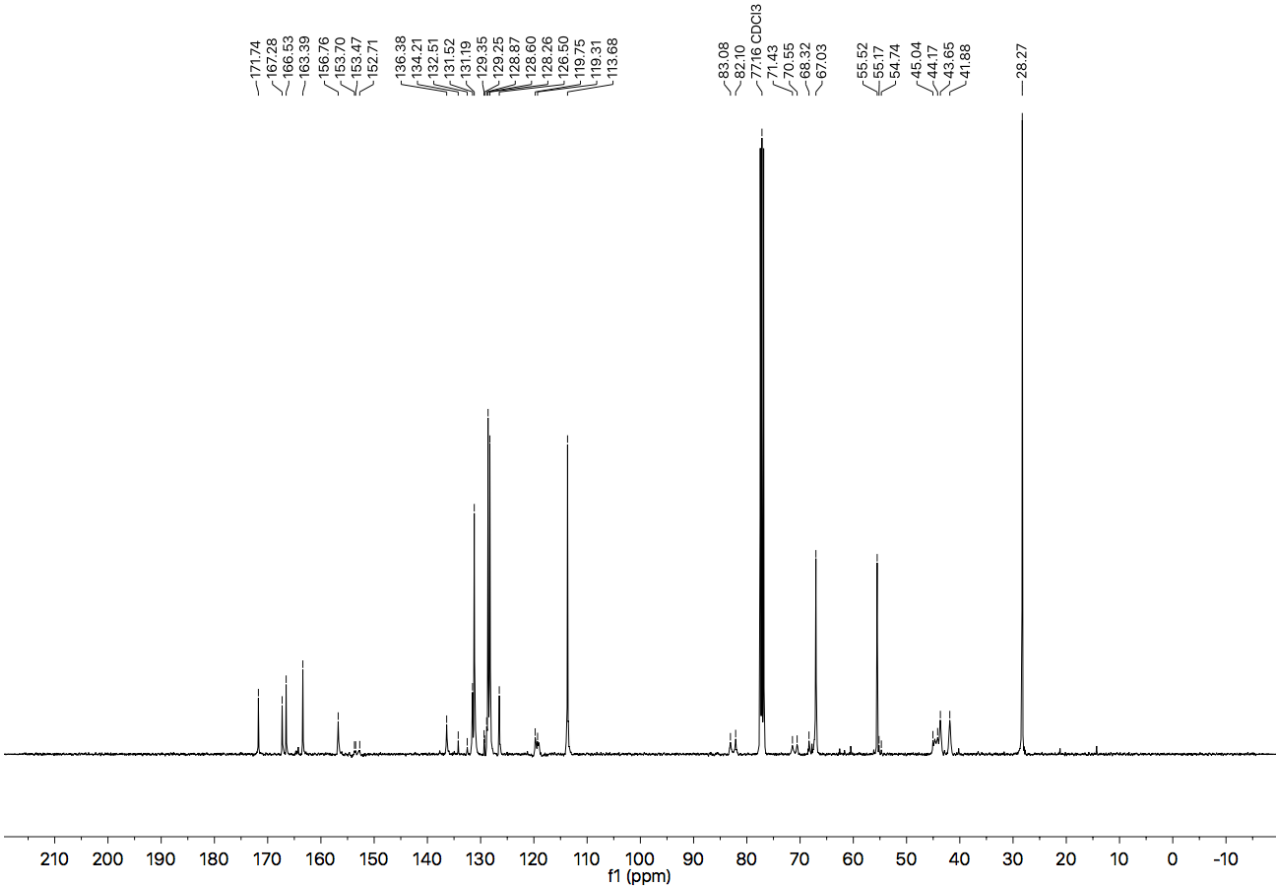

Figure A1.33 ^{13}C NMR (101 MHz, $CDCl_3$) of compound **1.3l**.

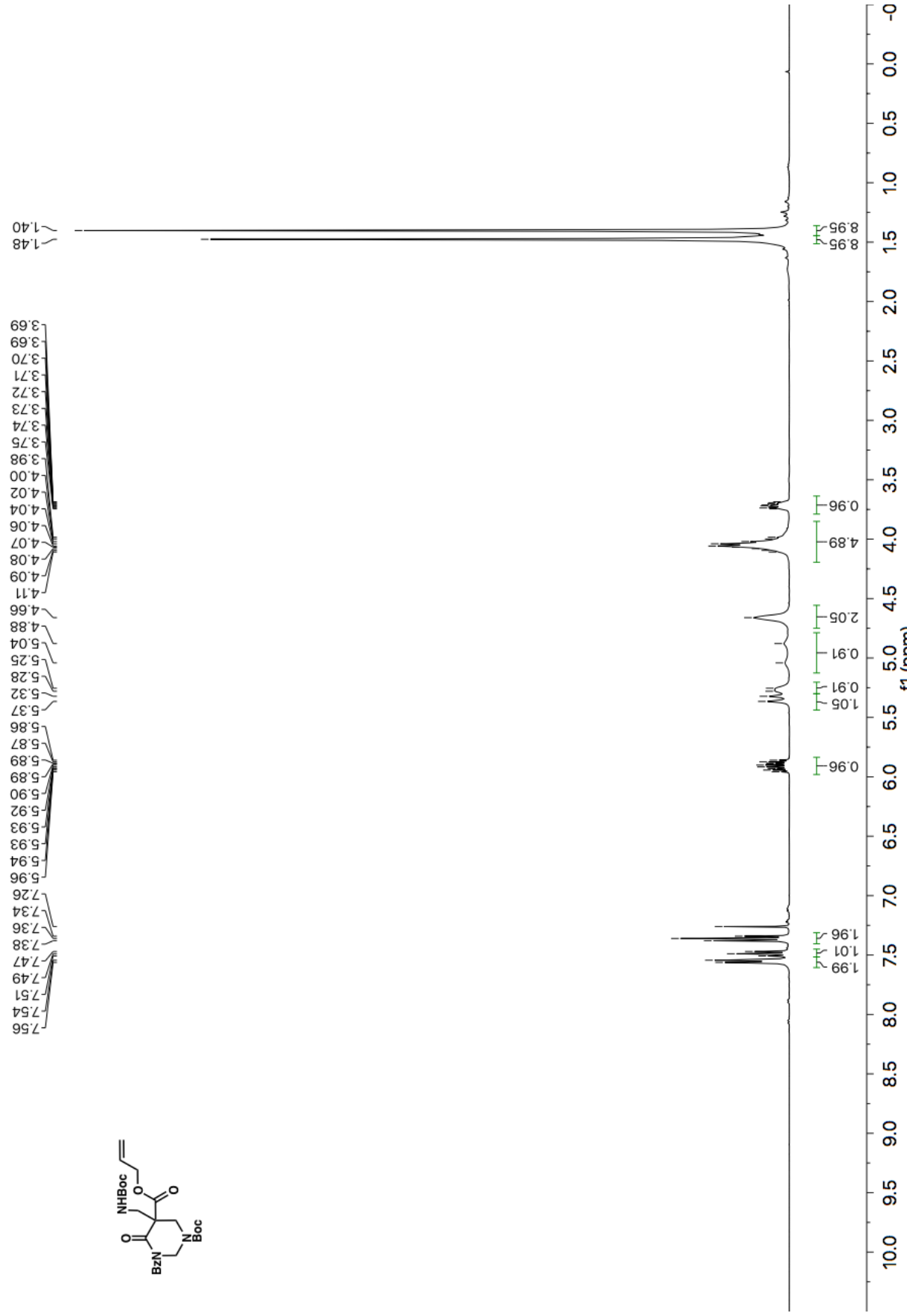

Figure A1.34 ^{1}H NMR (400 MHz, $CDCl_3$) of compound **1.3m.**

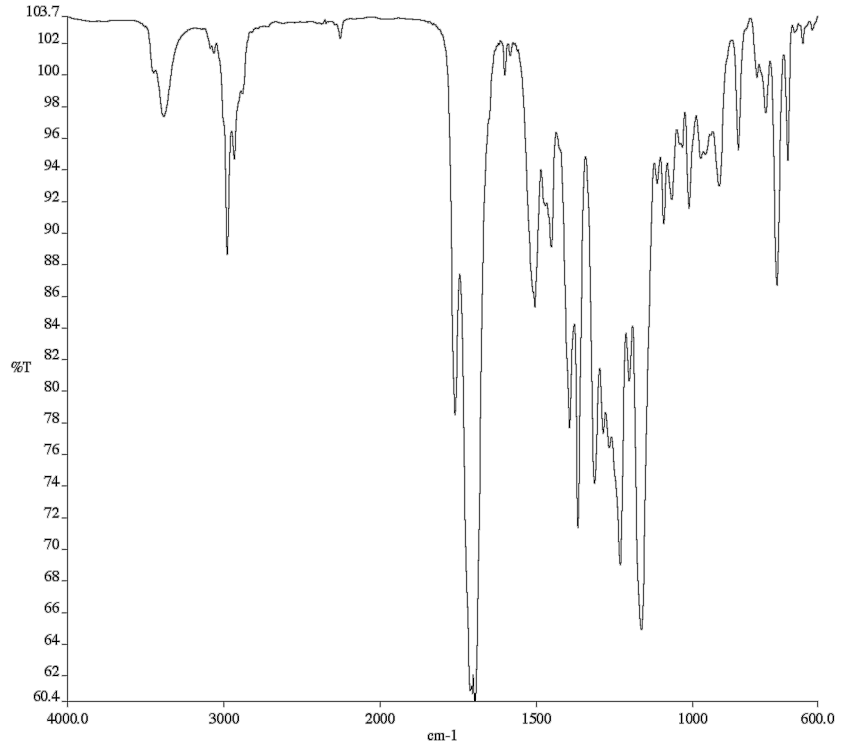

Figure A1.35 Infrared spectrum (Thin Film, NaCl) of compound **1.3m**.

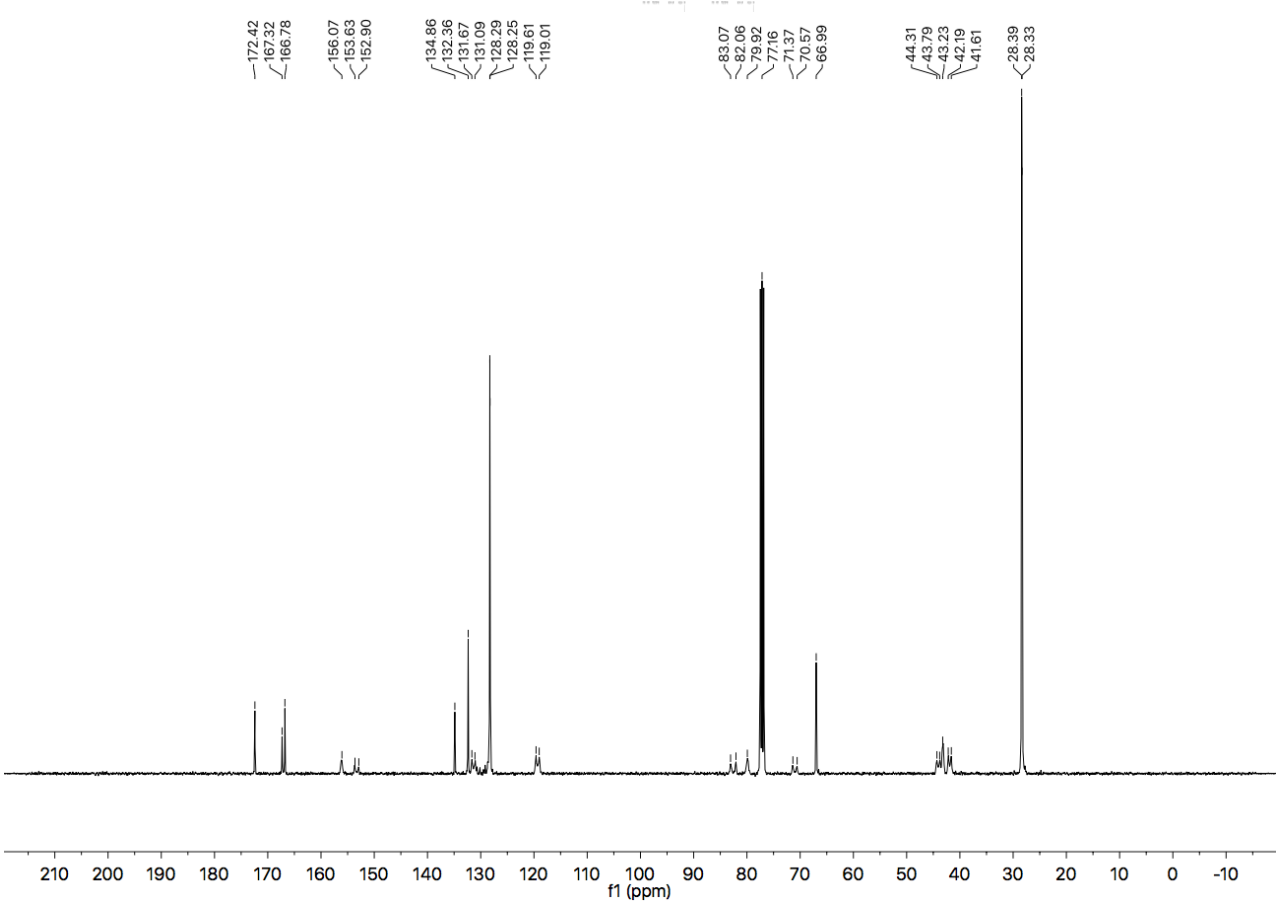

Figure A1.36 ^{13}C NMR (101 MHz, $CDCl_3$) of compound **1.3m**.

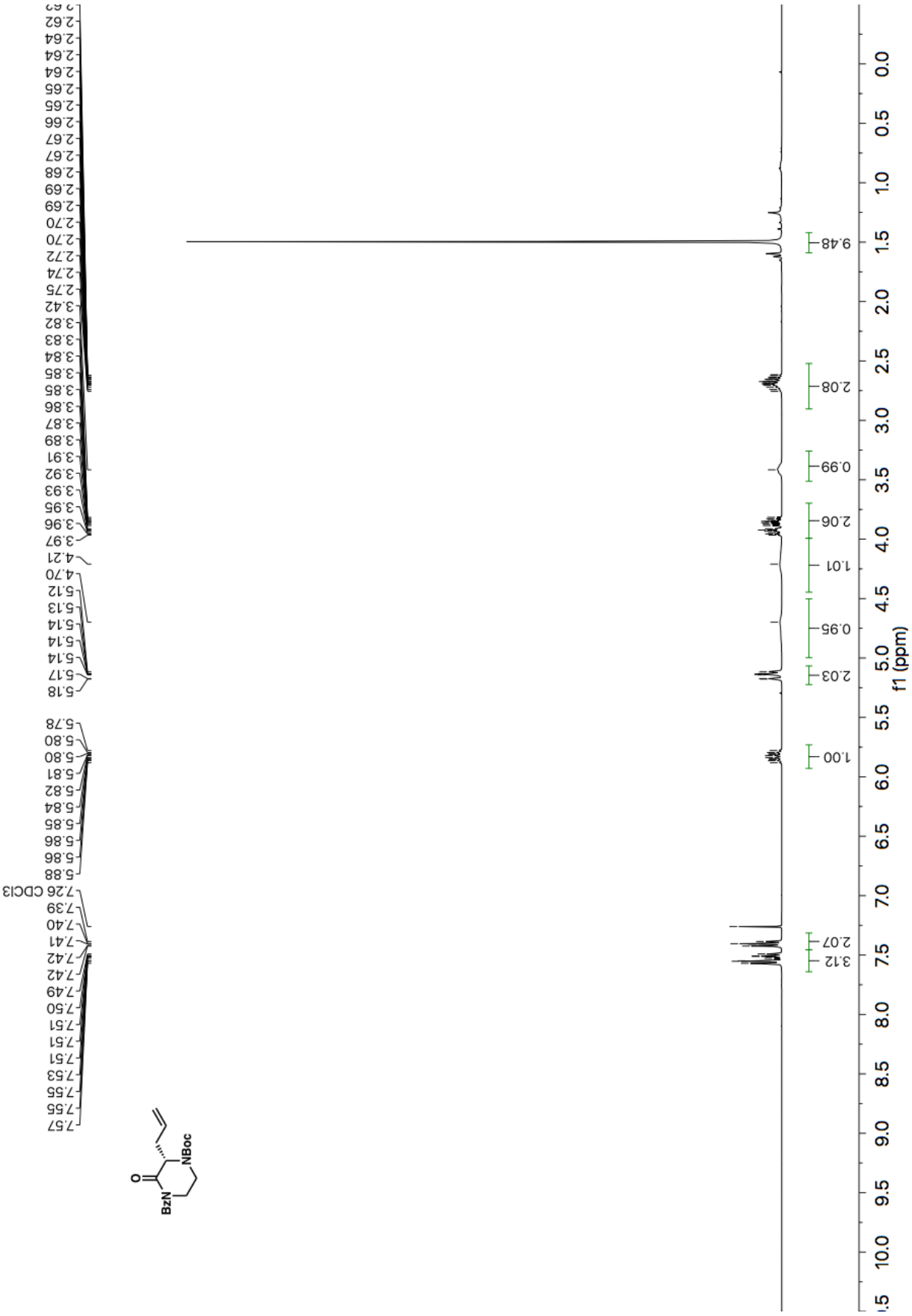

Figure A1.37 ^{1}H NMR (400 MHz, $CDCl_3$) of compound **1.4a.**

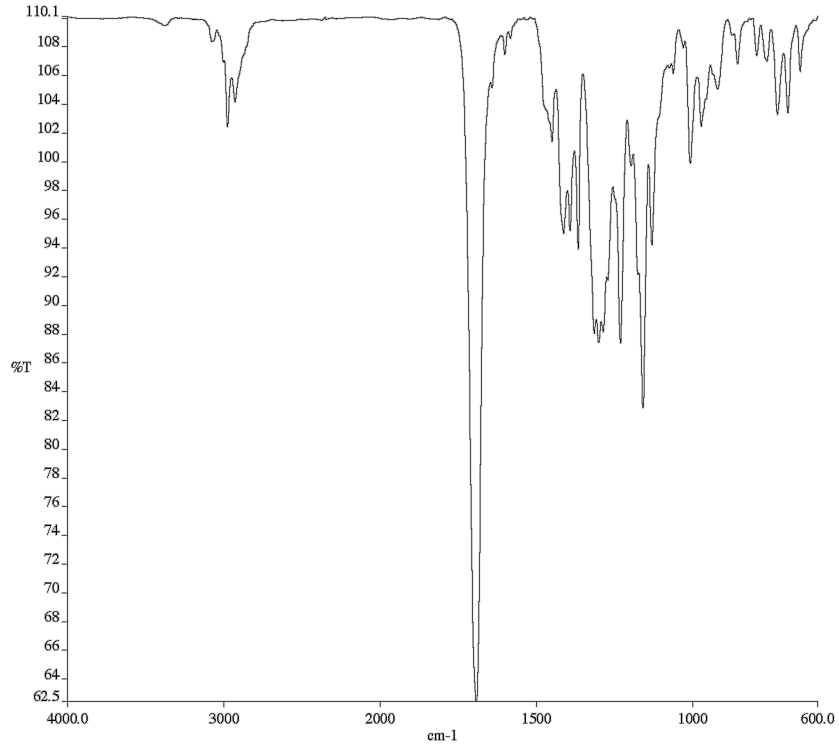

Figure A1.37 Infrared spectrum (Thin Film, NaCl) of compound **1.4a**.

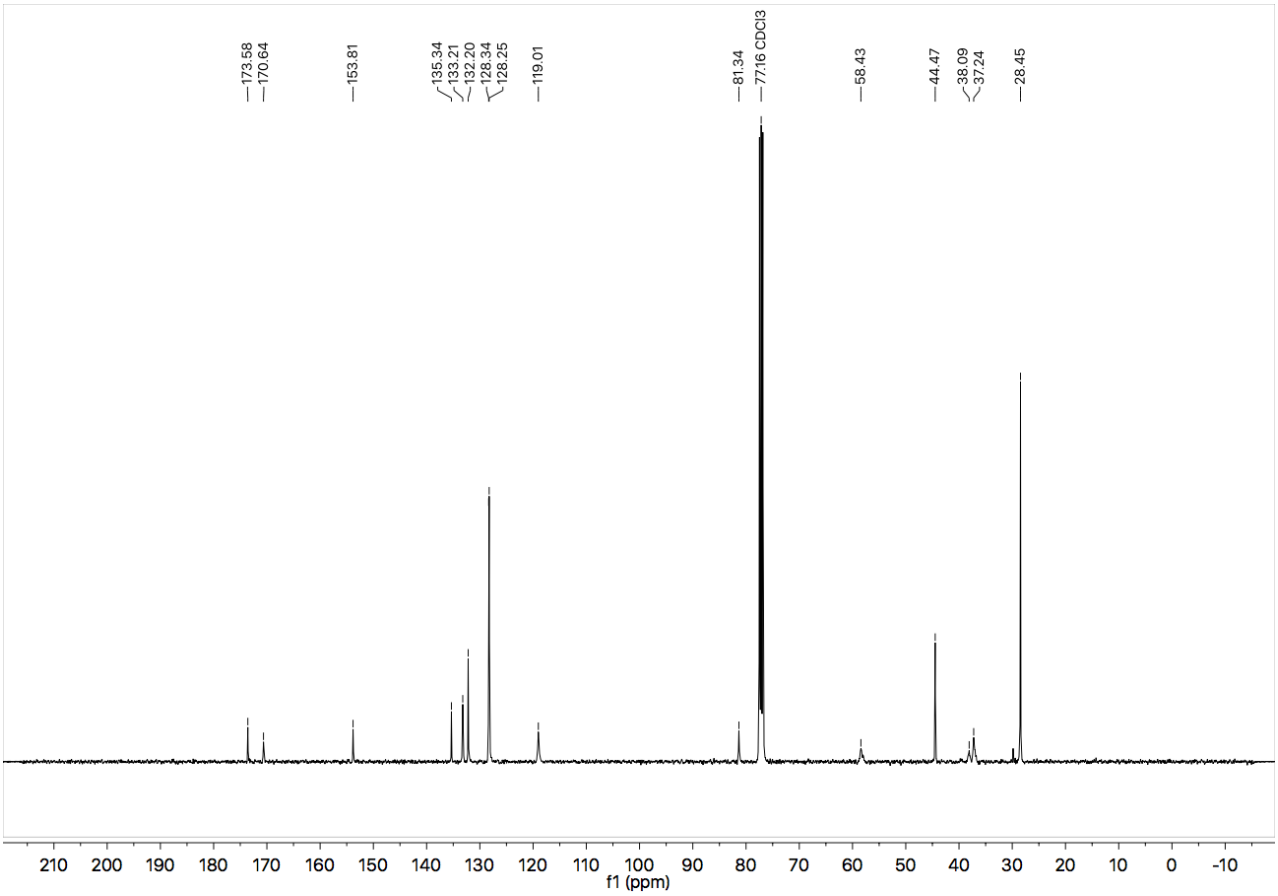

Figure A1.39 ^{13}C NMR (101 MHz, $CDCl_3$) of compound **1.4a**.

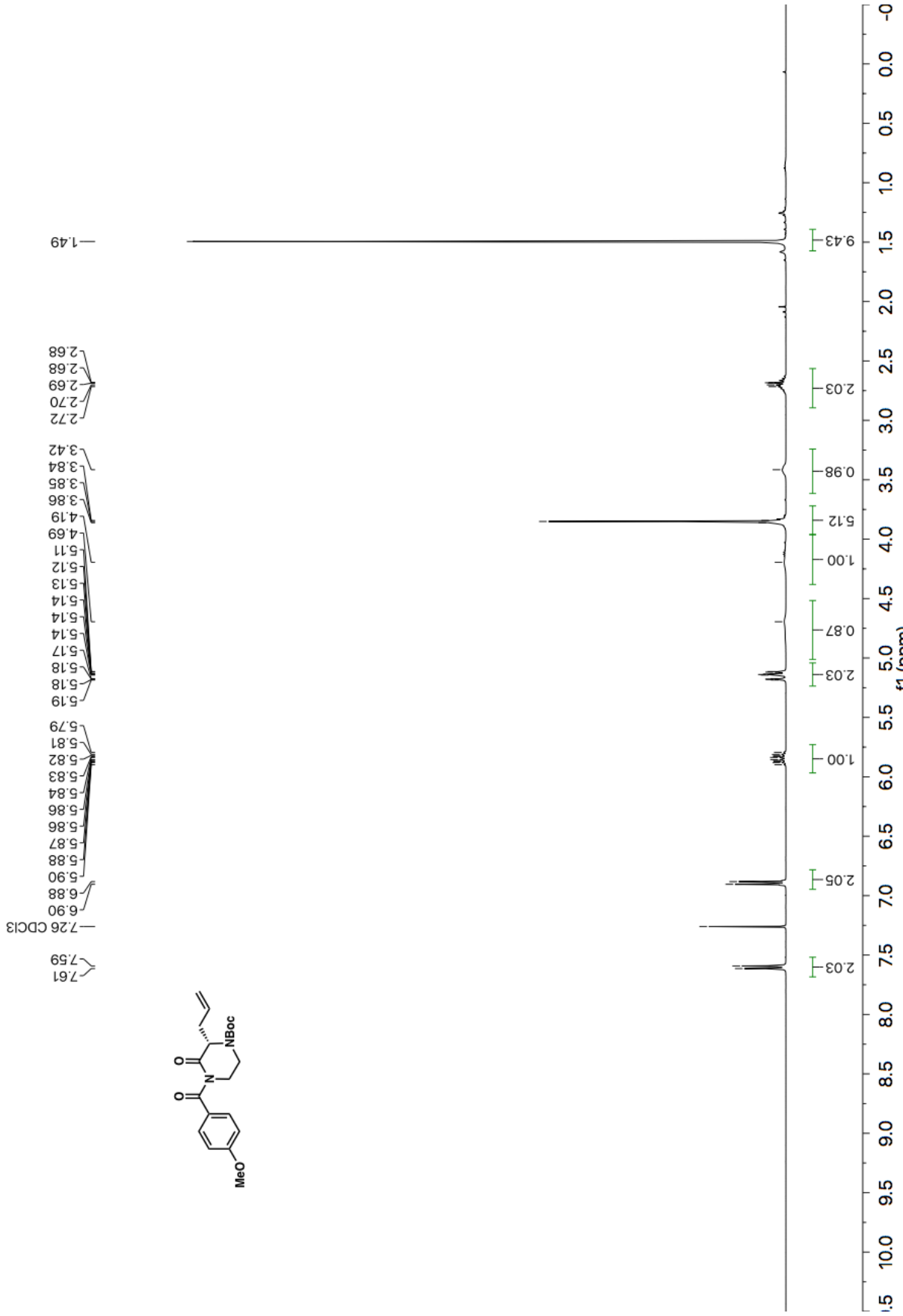

Figure A1.40 ^{1}H NMR (400 MHz, $CDCl_3$) of compound **1.4b.**

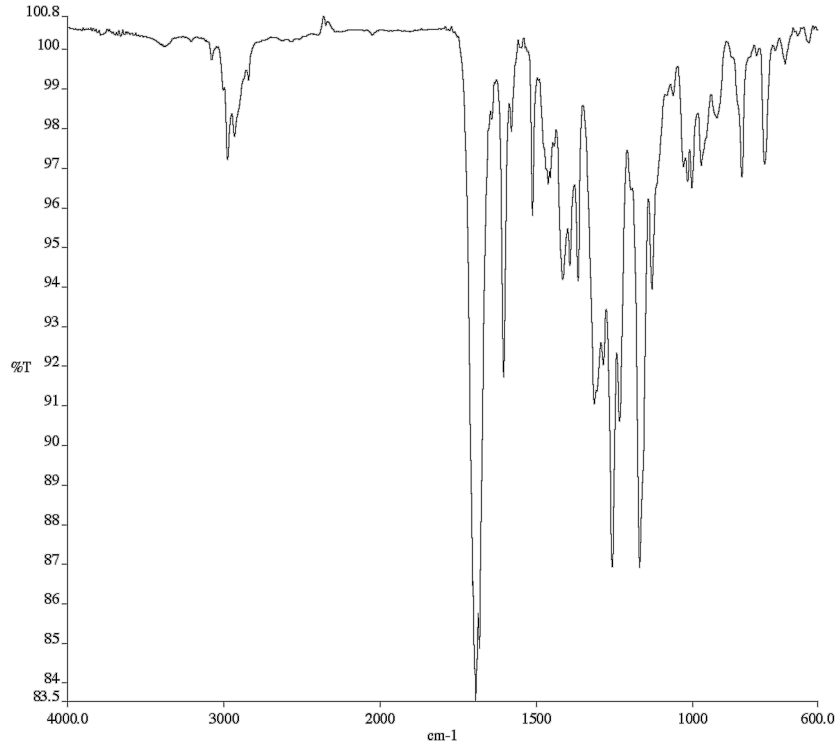

Figure A1.41 Infrared spectrum (Thin Film, NaCl) of compound **1.4b**.

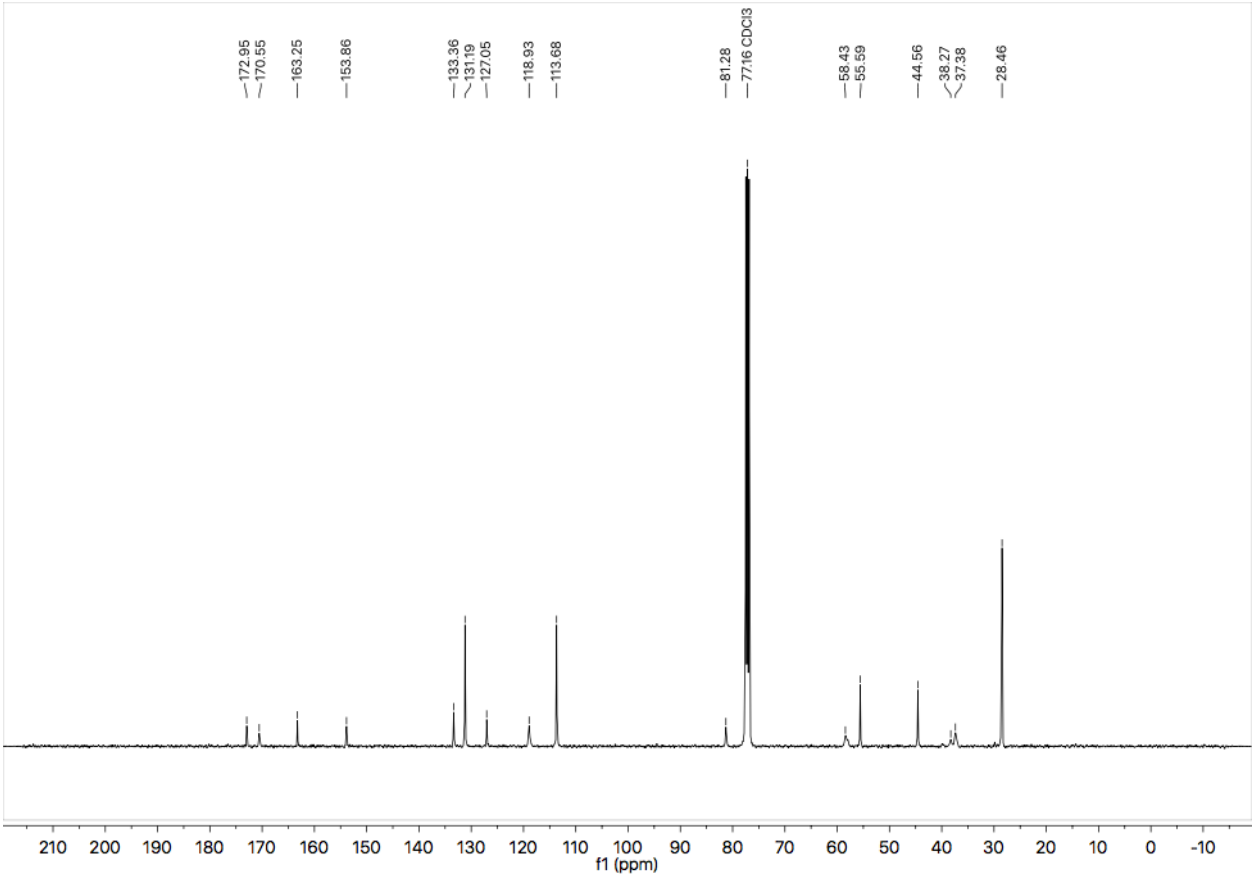

Figure A1.42 ^{13}C NMR (101 MHz, $CDCl_3$) of compound **1.4b**.

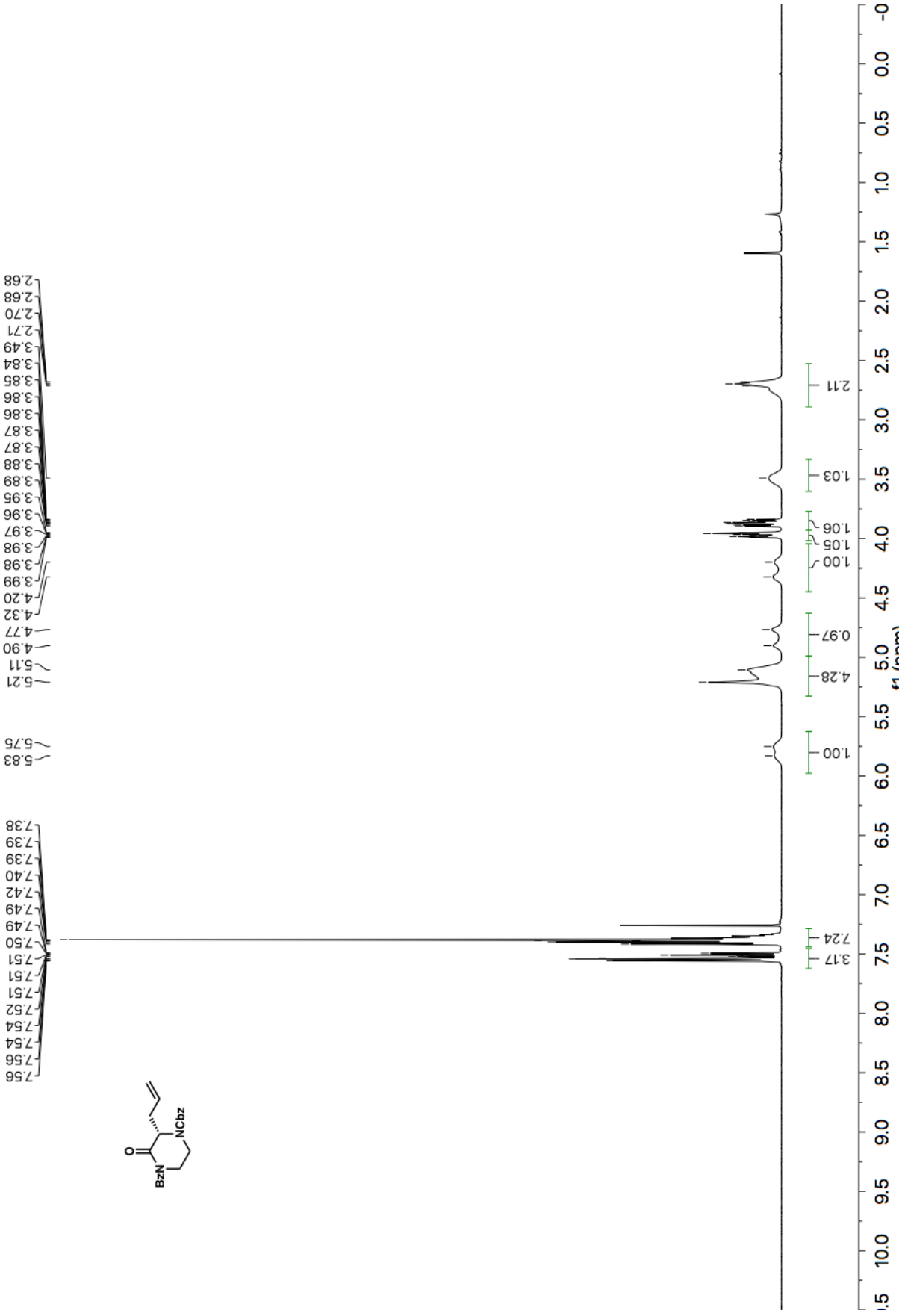

Figure A1.43 ^{1}H NMR (400 MHz, $CDCl_3$) of compound **1.4c.**

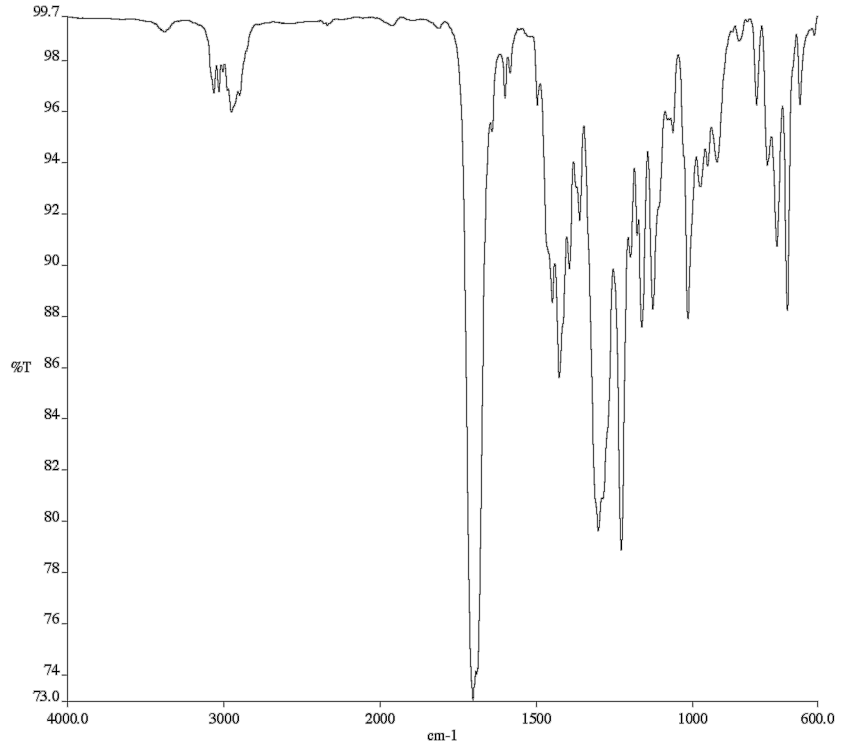

Figure A1.44 Infrared spectrum (Thin Film, NaCl) of compound **1.4c**.

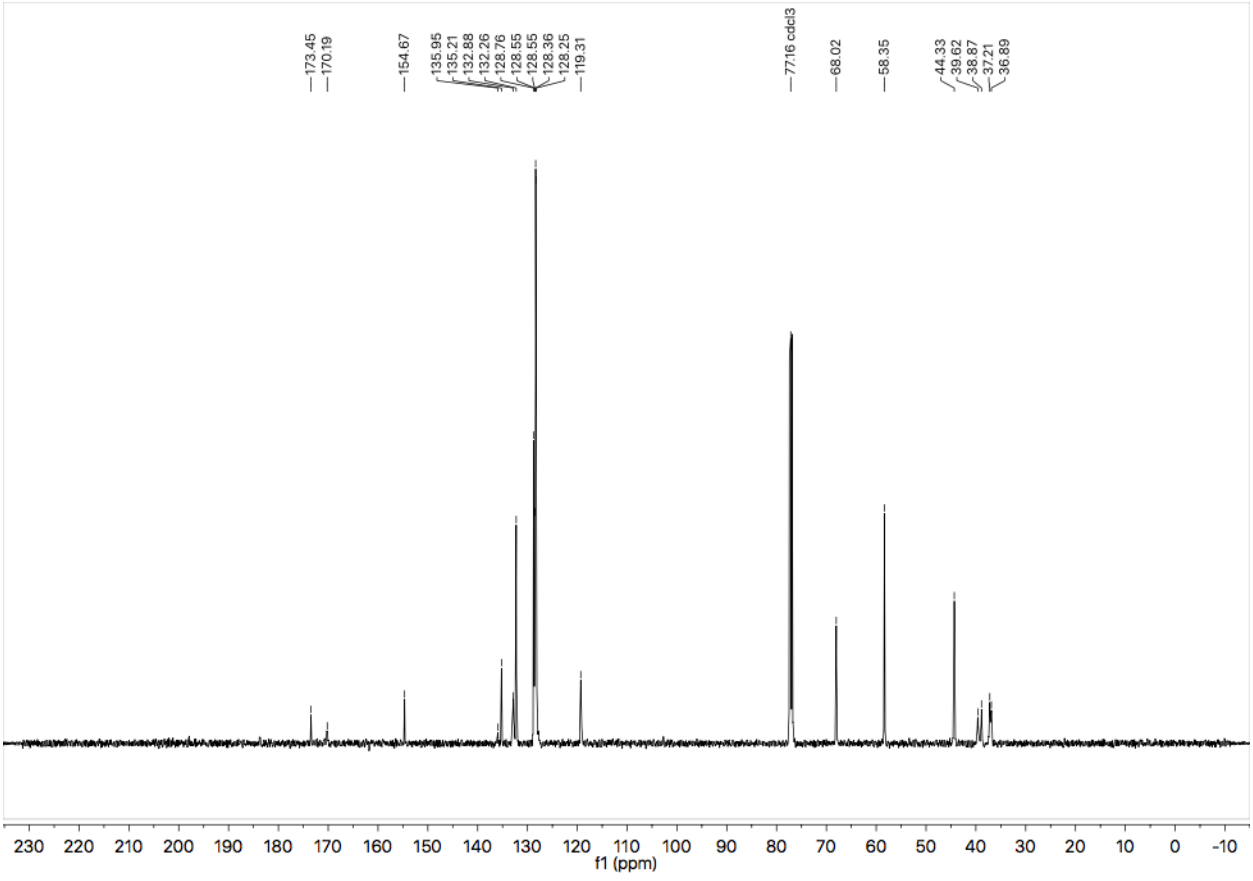

Figure A1.45 ^{13}C NMR (101 MHz, $CDCl_3$) of compound **1.4c**.

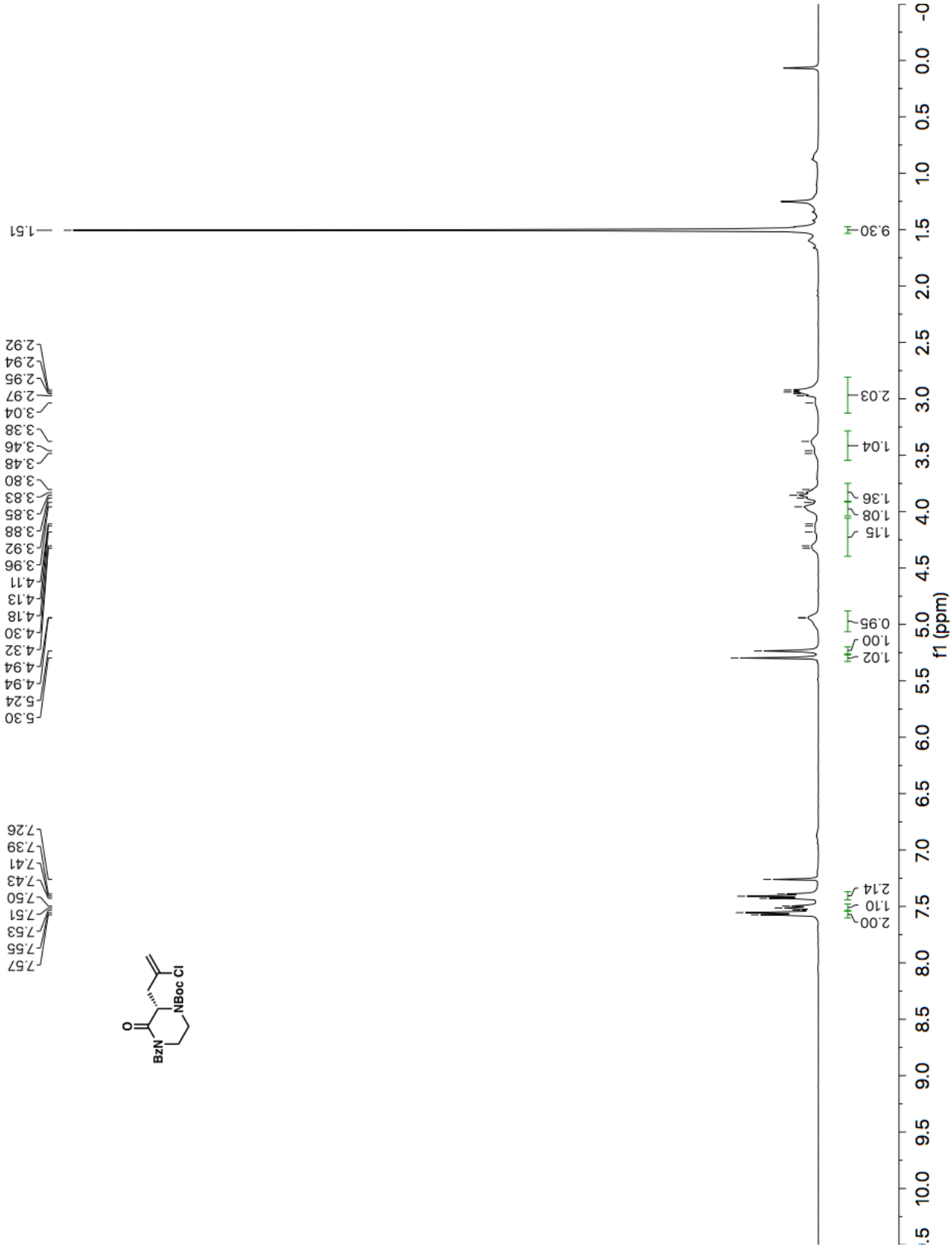

Figure A1.46 ^{1}H NMR (500 MHz, $CDCl_3$) of compound **1.4d.**

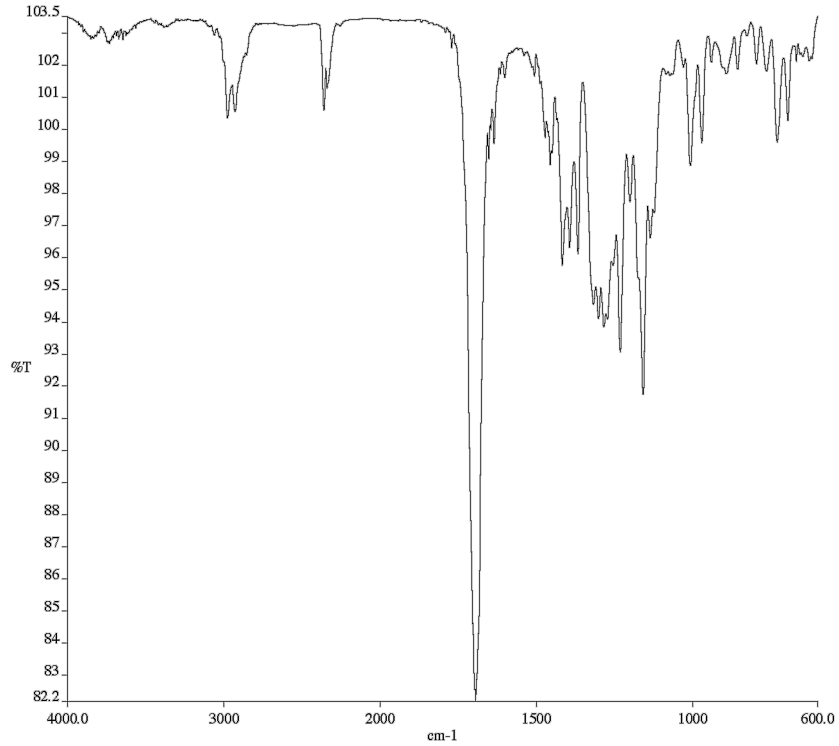

Figure A1.47 Infrared spectrum (Thin Film, NaCl) of compound **1.4d**.

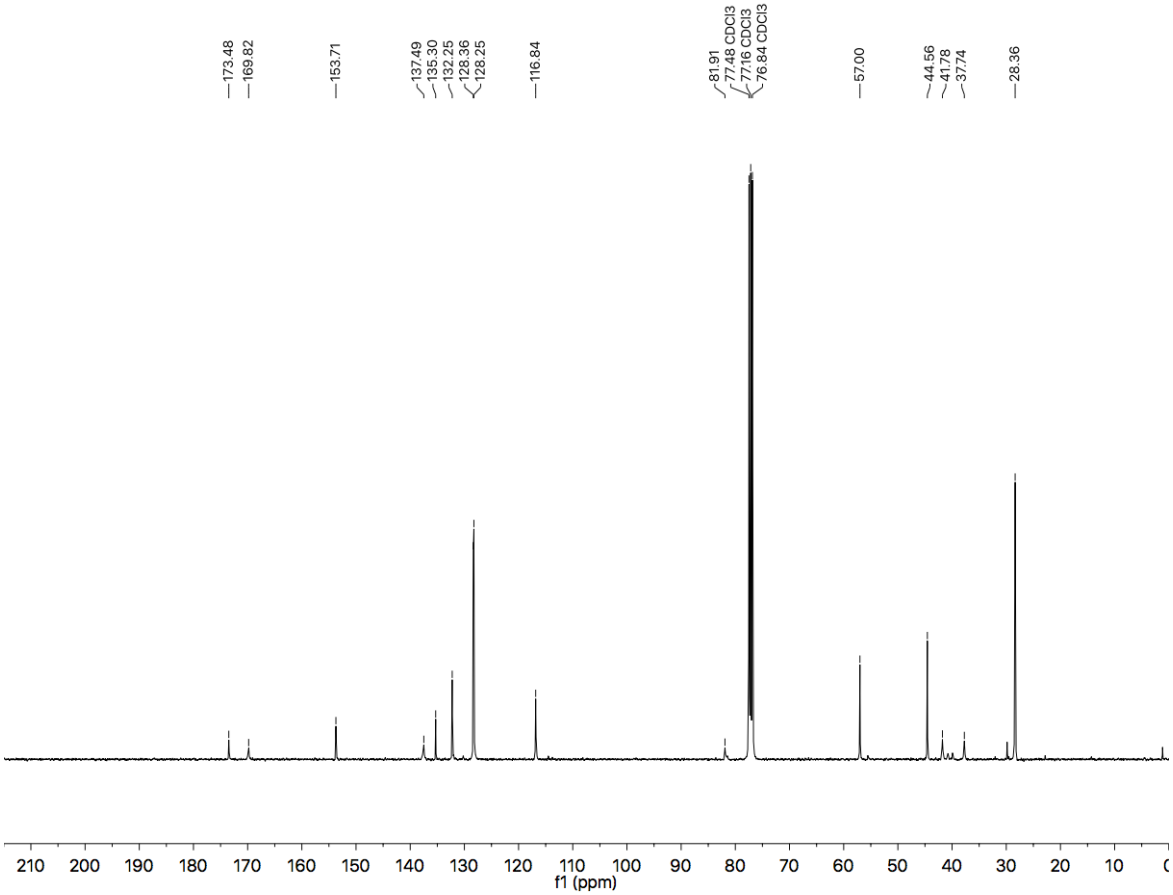

Figure A1.48 ^{13}C NMR (126 MHz, $CDCl_3$) of compound **1.4d**.

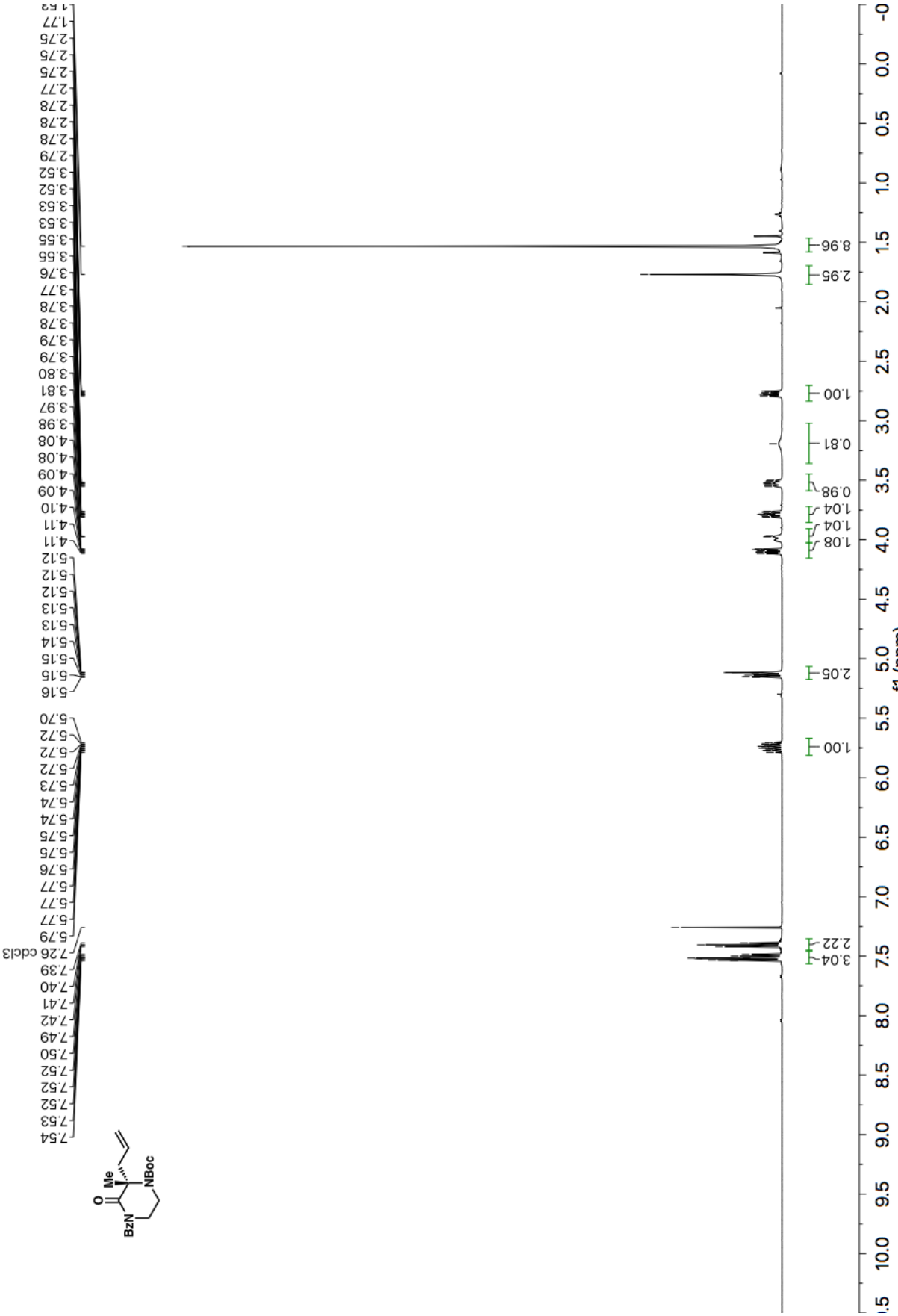

Figure A1.49 ^{1}H NMR (500 MHz, $CDCl_3$) of compound **1.4e.**

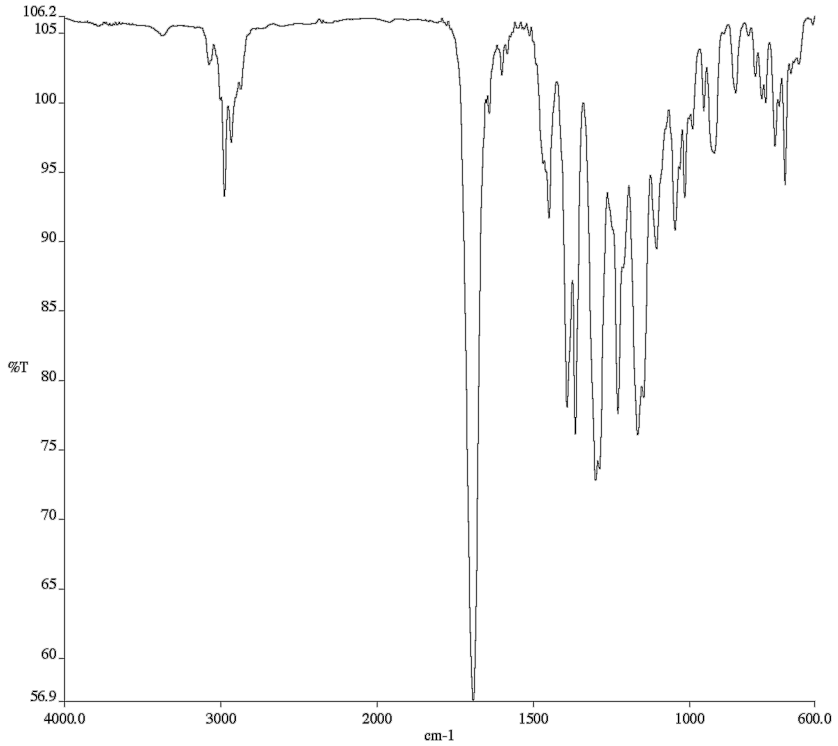

Figure A1.50 Infrared spectrum (Thin Film, NaCl) of compound **1.4e**.

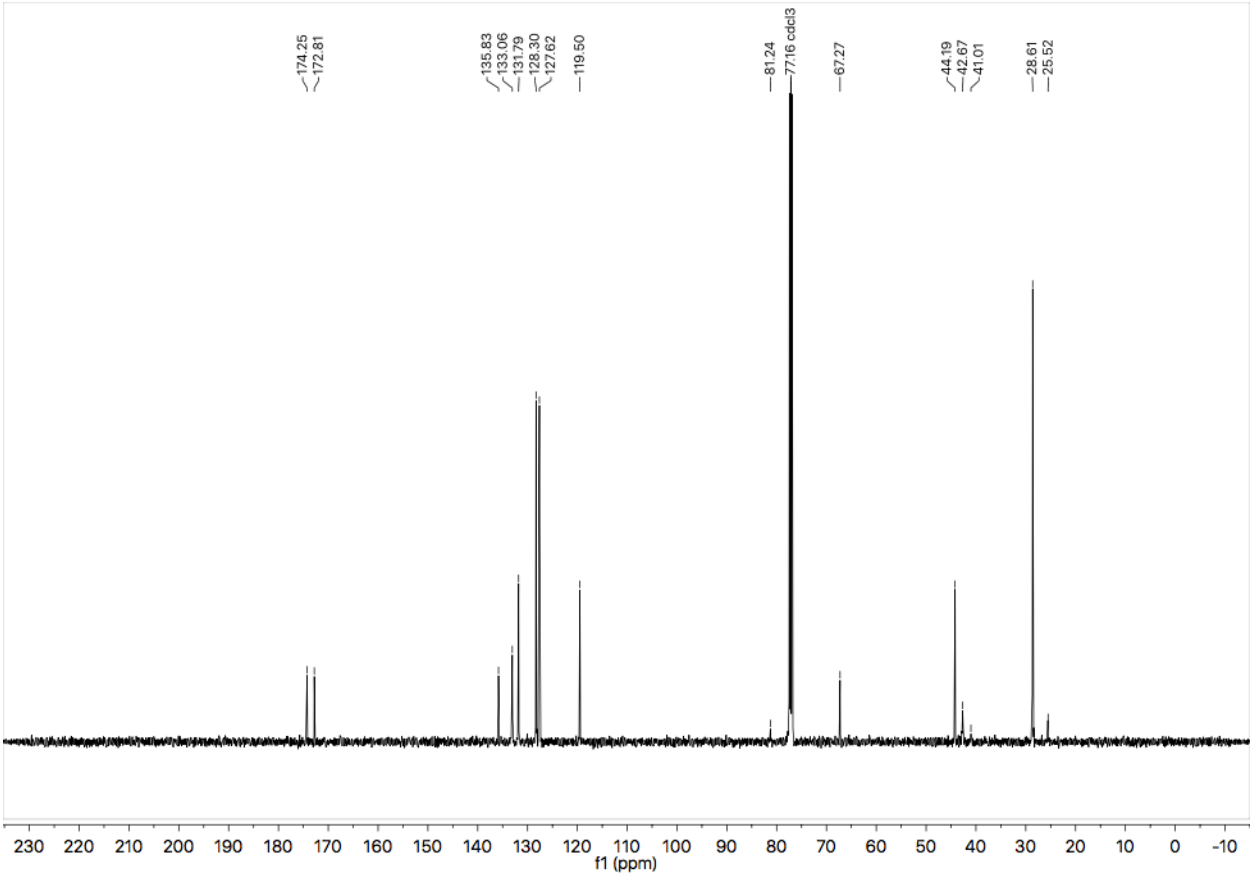

Figure A1.51 ^{13}C NMR (126 MHz, $CDCl_3$) of compound **1.4e**.

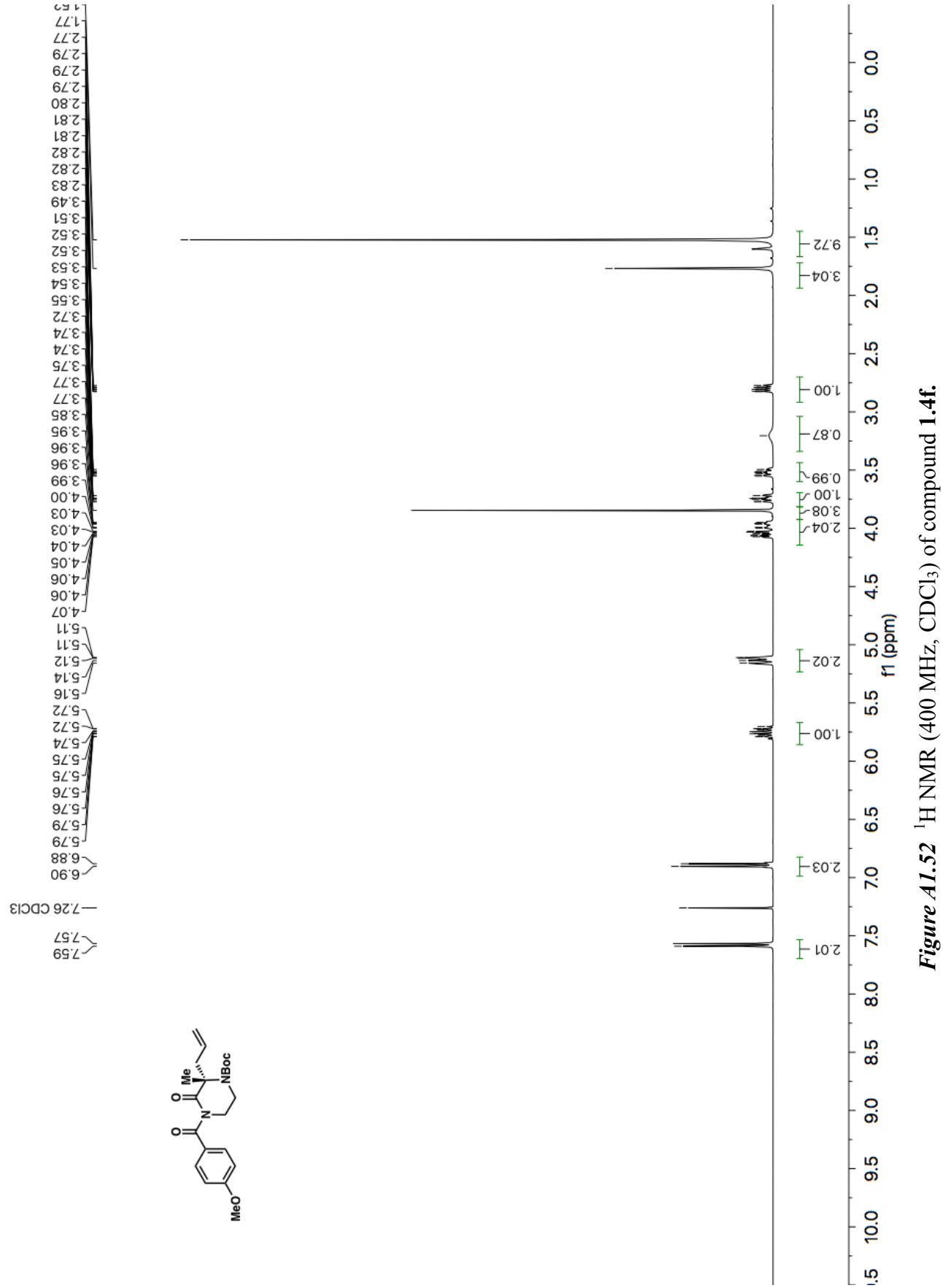

Figure A1.52 ^{1}H NMR (400 MHz, $CDCl_3$) of compound **1.4f.**

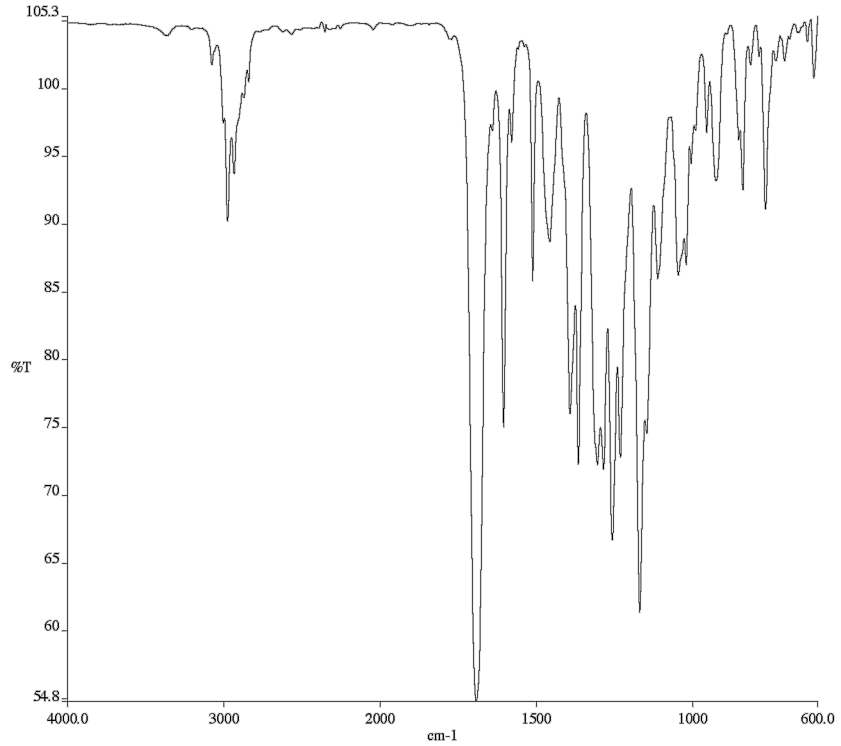

Figure A1.53 Infrared spectrum (Thin Film, NaCl) of compound **1.4f**.

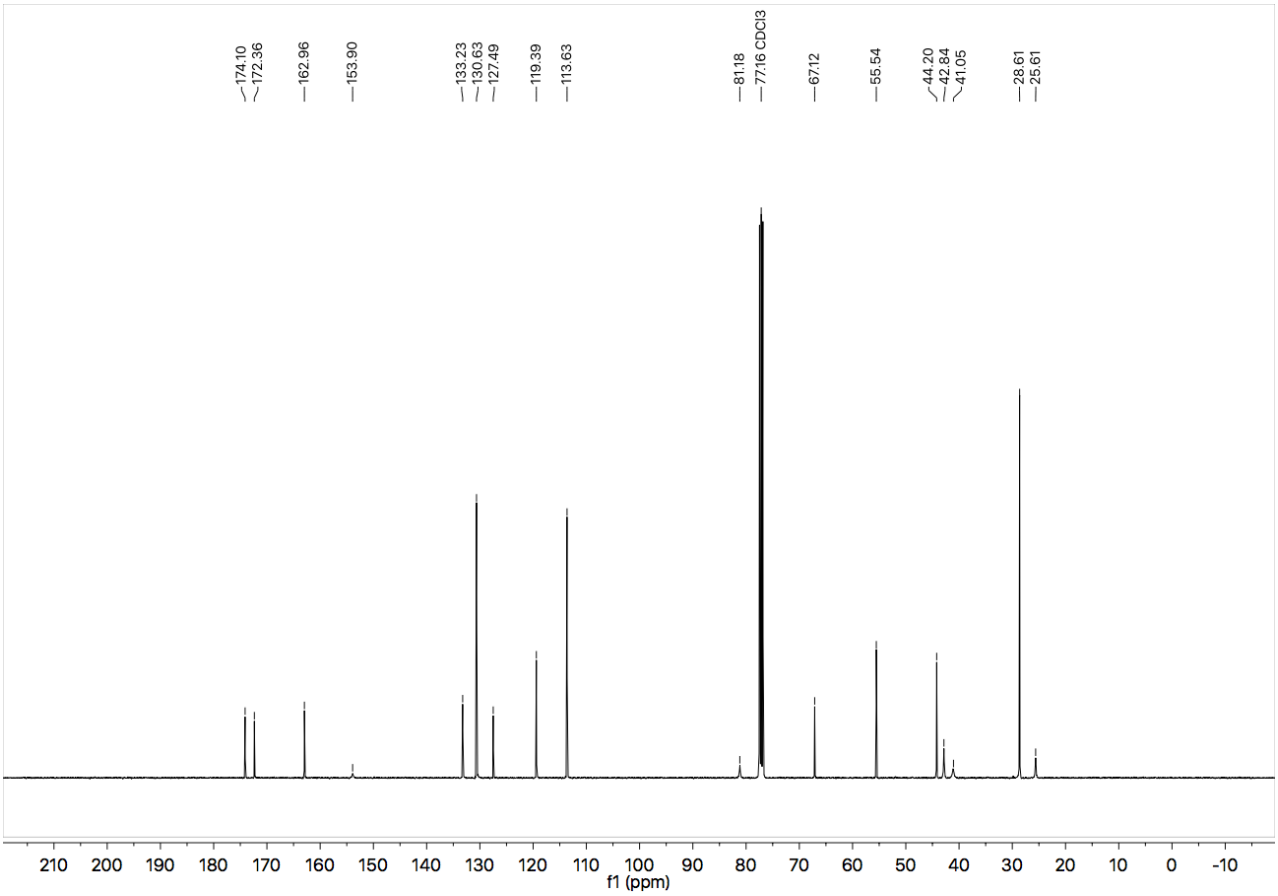

Figure A1.54 ^{13}C NMR (101 MHz, $CDCl_3$) of compound **1.4f**.

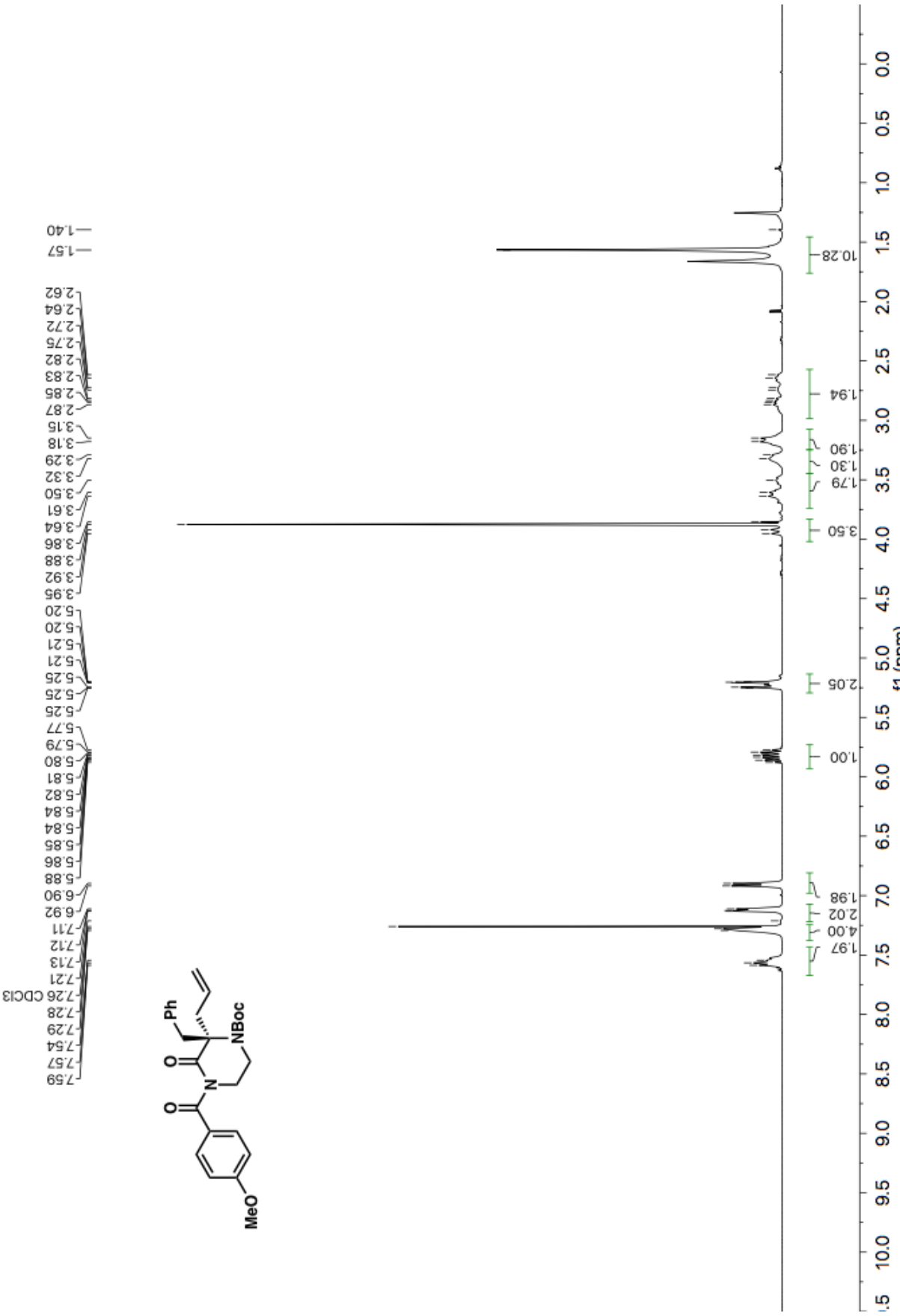

Figure A1.55 ^{1}H NMR (400 MHz, $CDCl_3$) of compound **1.4h.**

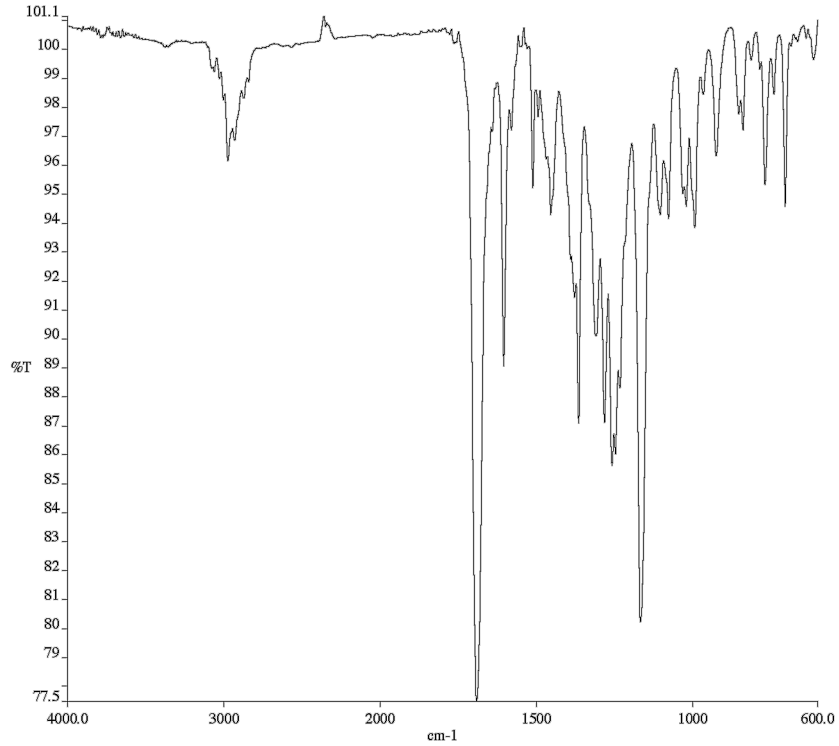

Figure A1.56 Infrared spectrum (Thin Film, NaCl) of compound **1.4h**.

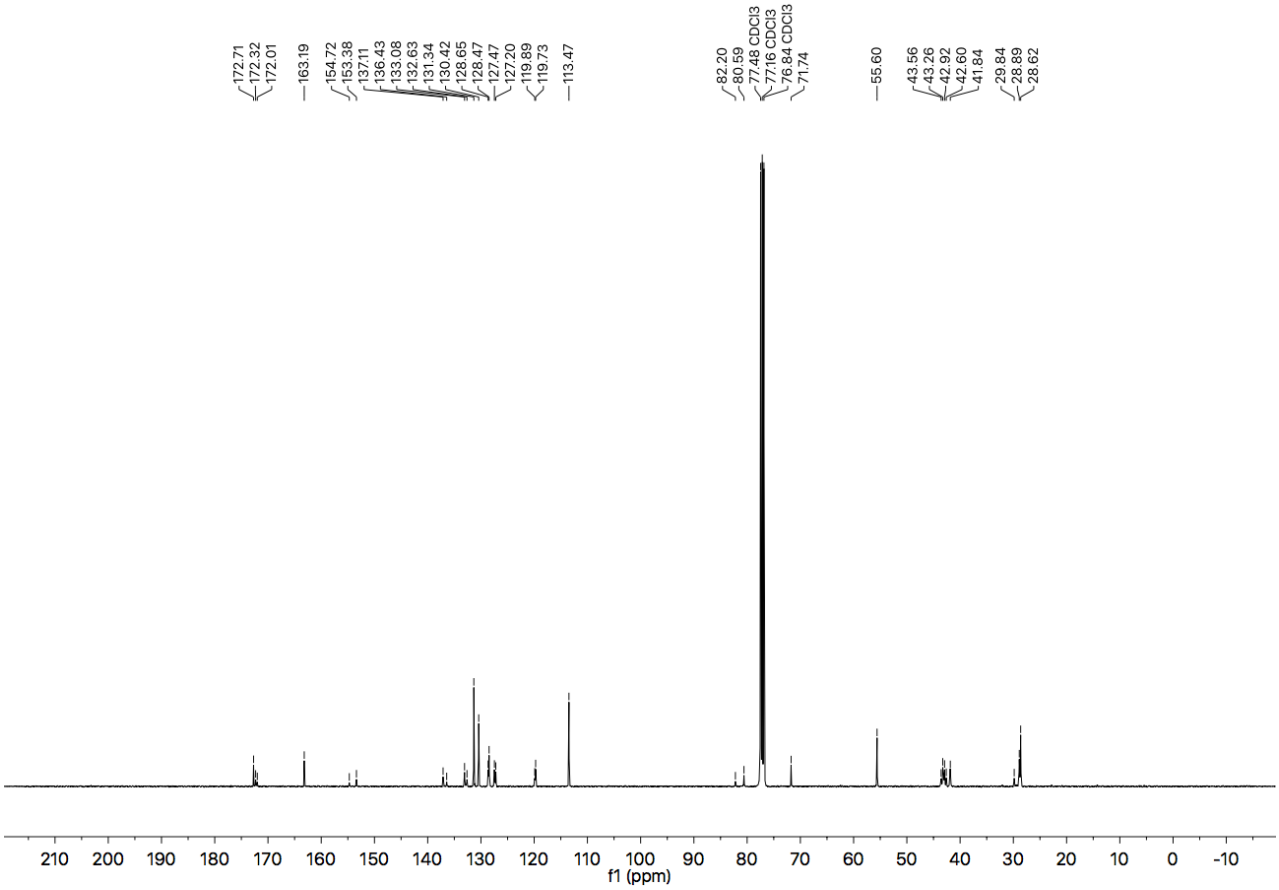

Figure A1.57 ^{13}C NMR (101 MHz, $CDCl_3$) of compound **1.4h**.

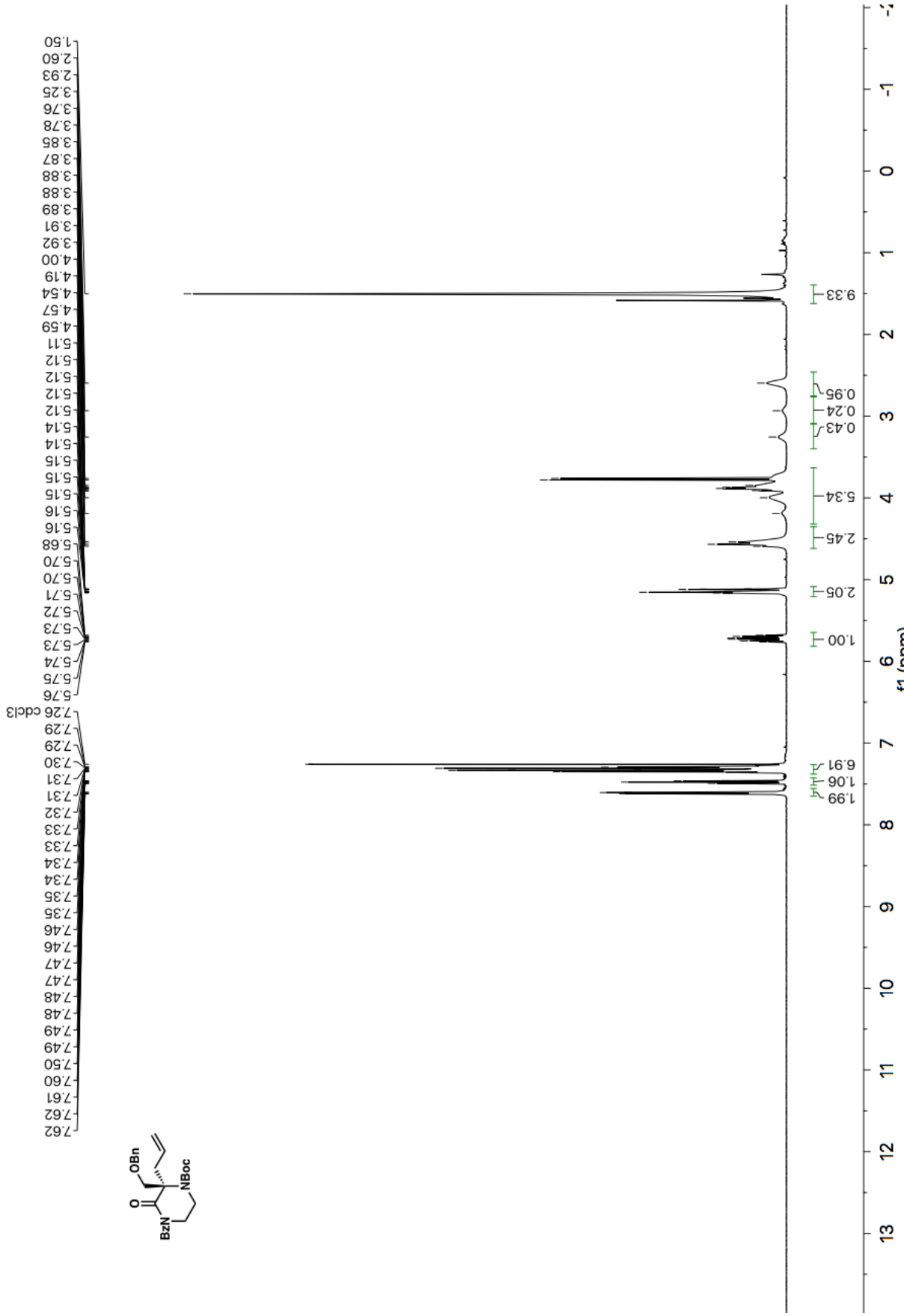

Figure A1.58 ^{1}H NMR (500 MHz, $CDCl_3$) of compound **1.4i.**

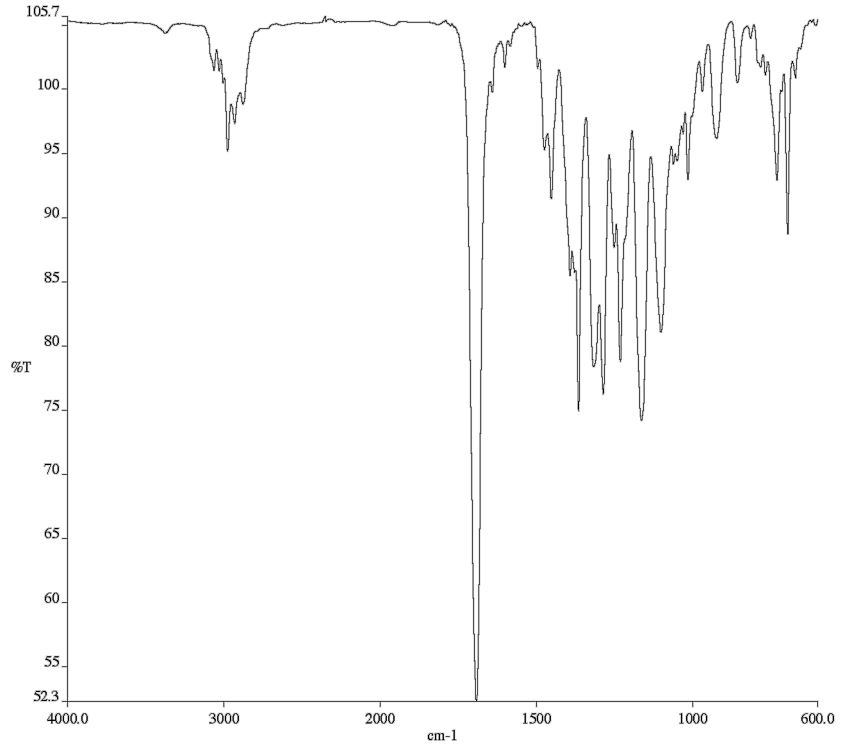

Figure A1.59 Infrared spectrum (Thin Film, NaCl) of compound **1.4i**.

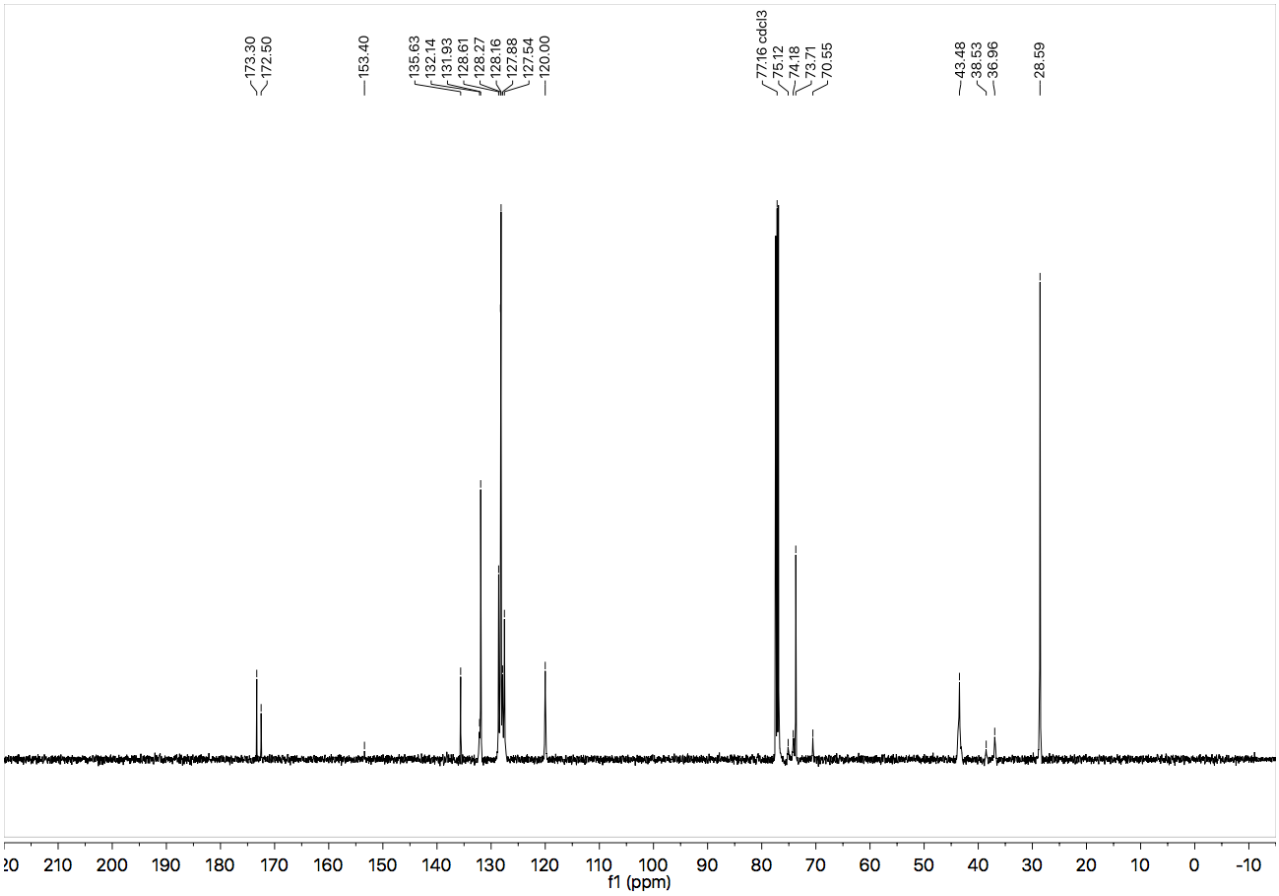

Figure A1.60 ^{13}C NMR (126 MHz, $CDCl_3$) of compound **1.4i**.

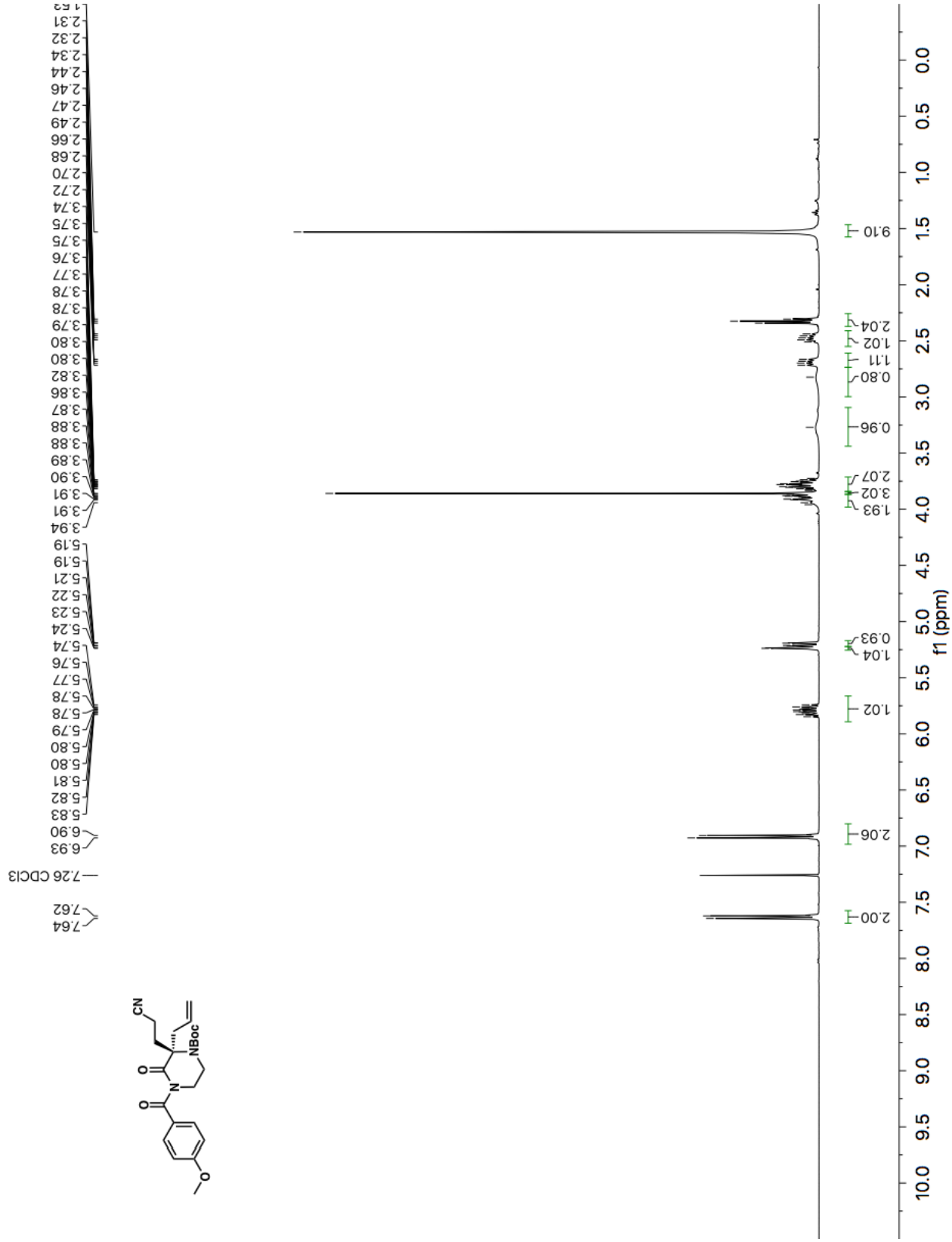

Figure A1.61 ^{1}H NMR (400 MHz, $CDCl_3$) of compound **1.4j.**

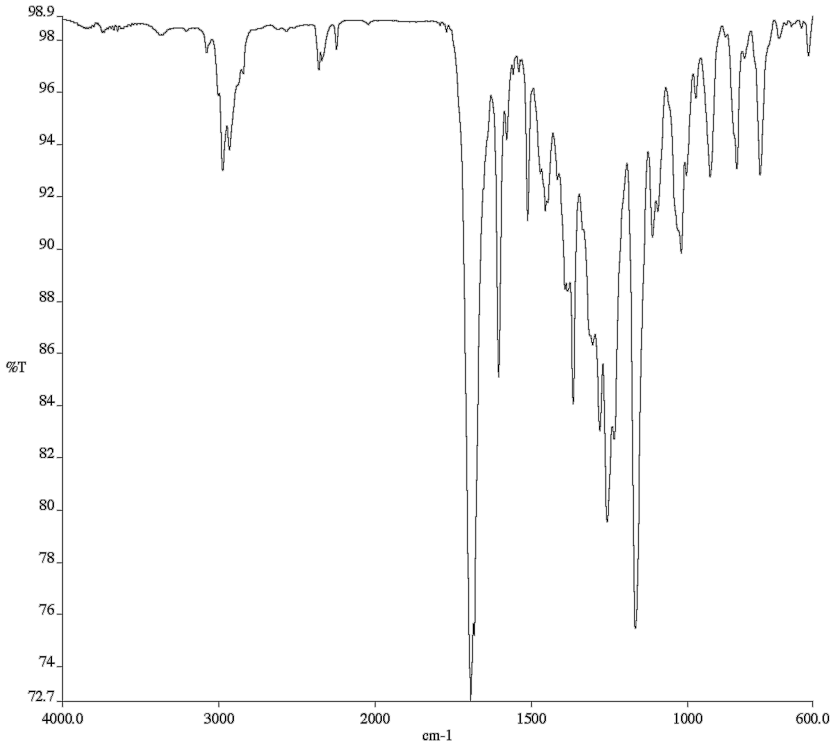

Figure A1.62 Infrared spectrum (Thin Film, NaCl) of compound **1.4j**.

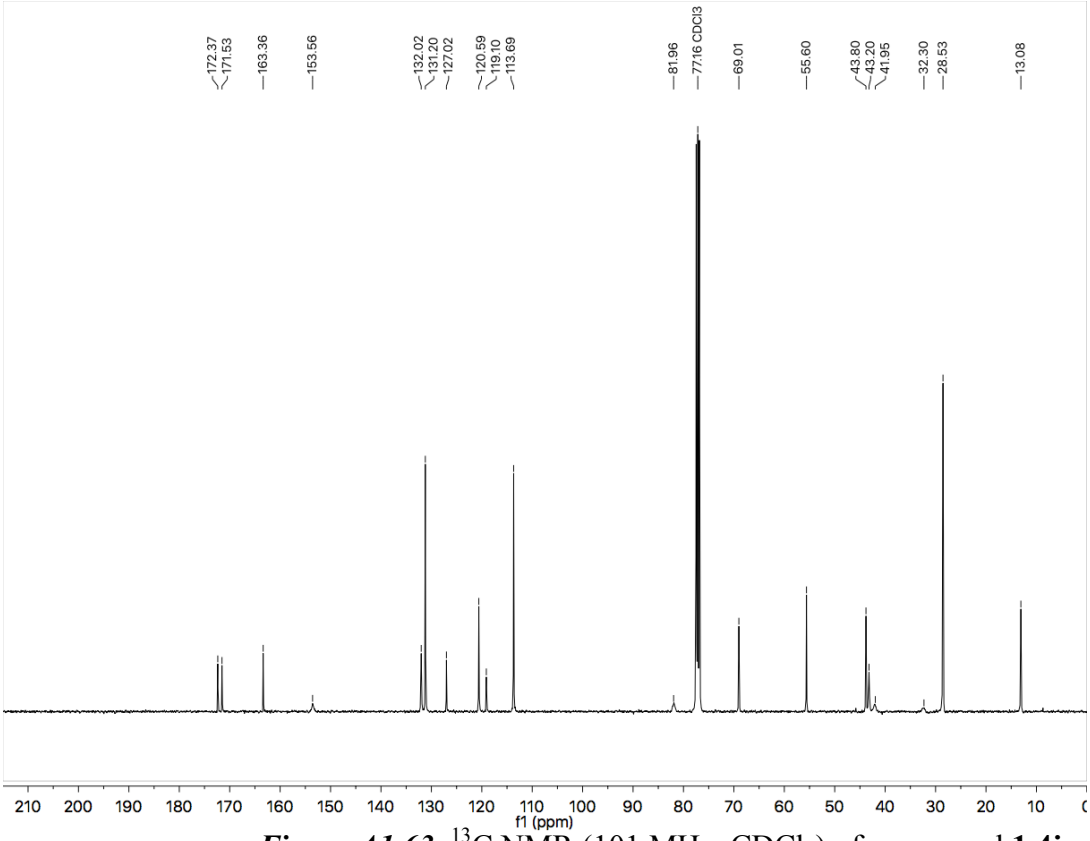

Figure A1.63 ^{13}C NMR (101 MHz, $CDCl_3$) of compound **1.4j**.

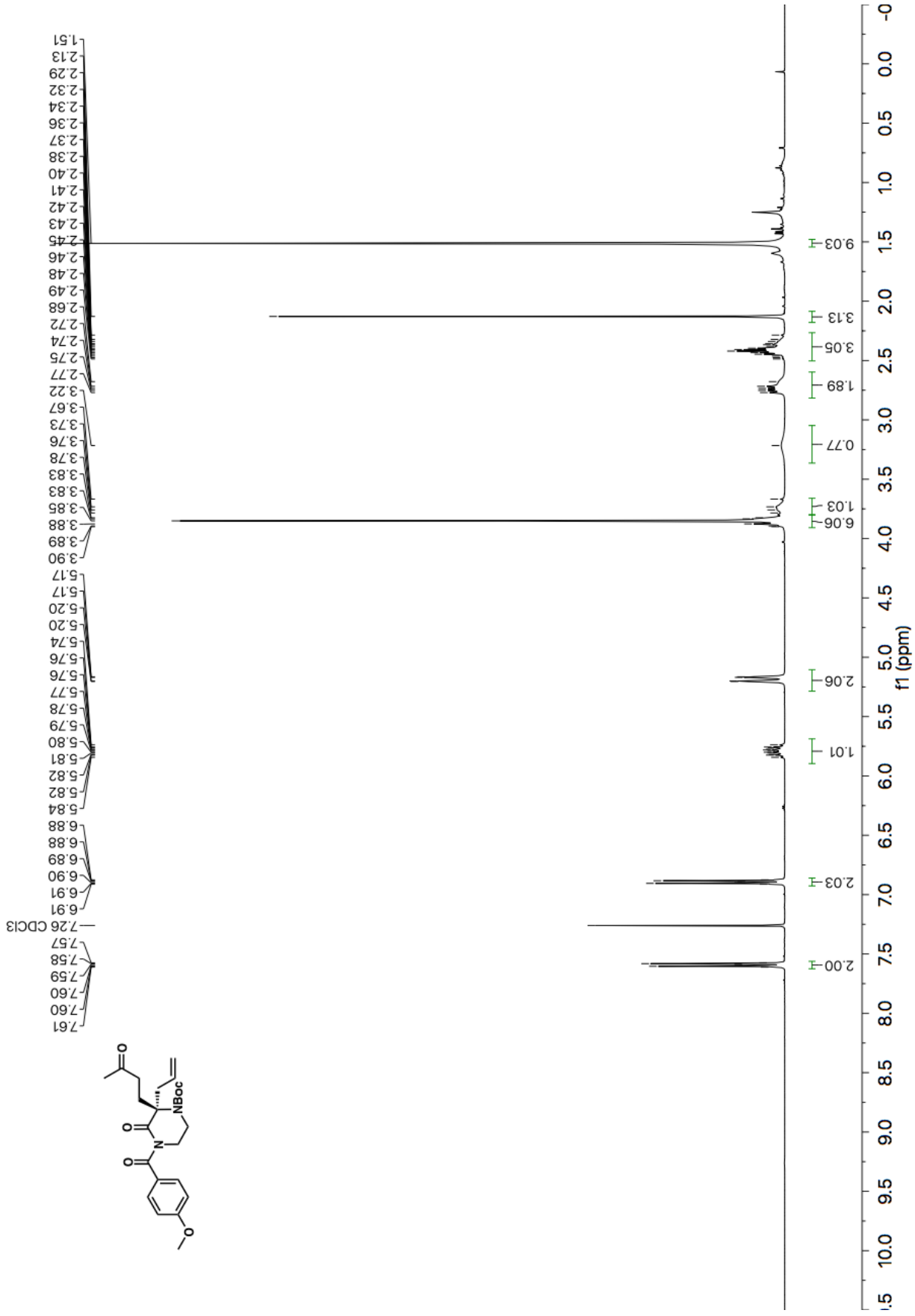

Figure A1.64 ^{1}H NMR (400 MHz, $CDCl_3$) of compound **1.4k.**

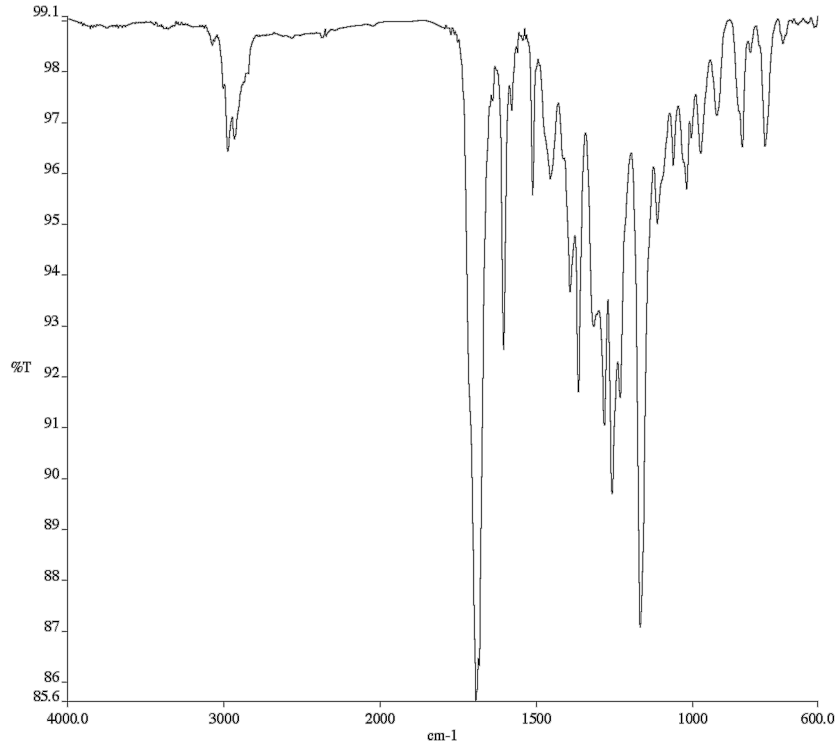

Figure A1.65 Infrared spectrum (Thin Film, NaCl) of compound **1.4k**.

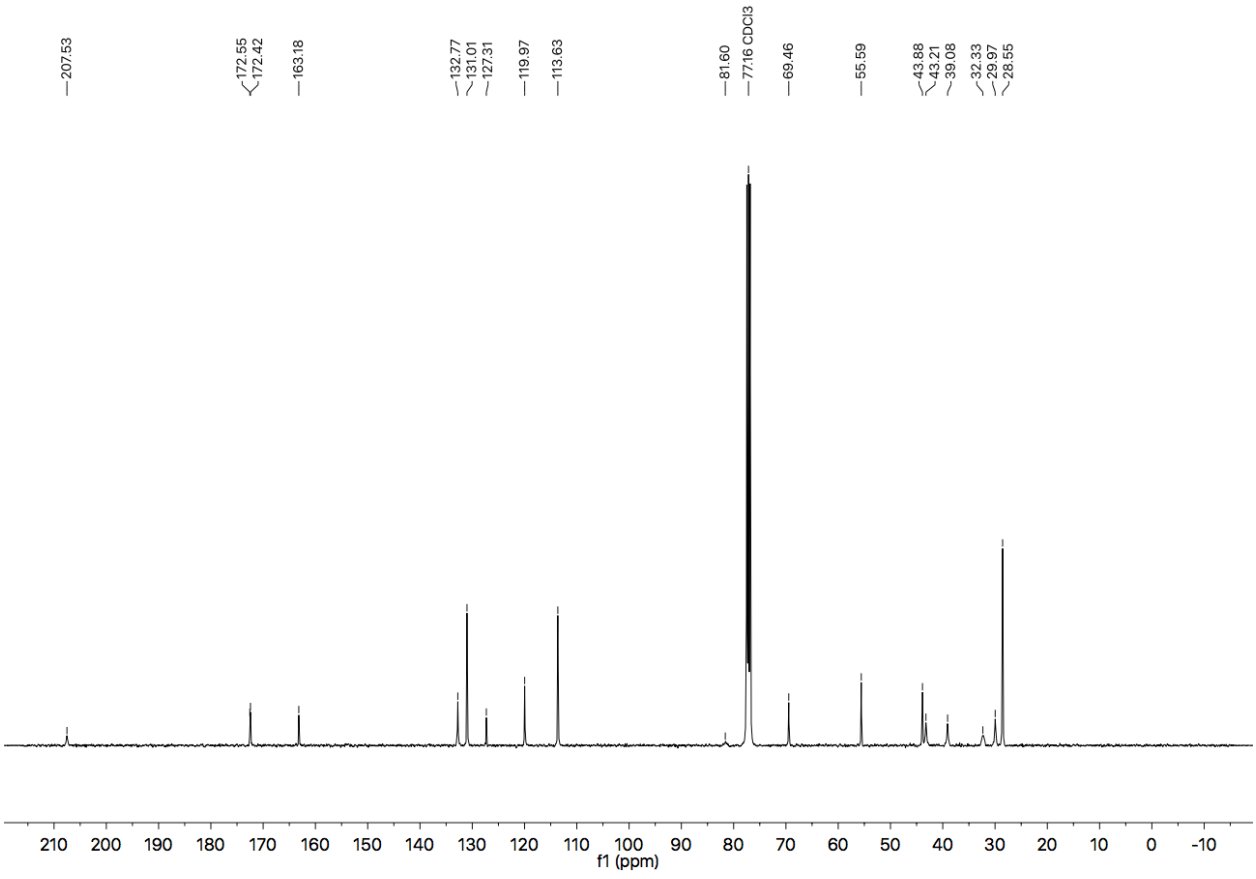

Figure A1.66 ^{13}C NMR (101 MHz, $CDCl_3$) of compound **1.4k**.

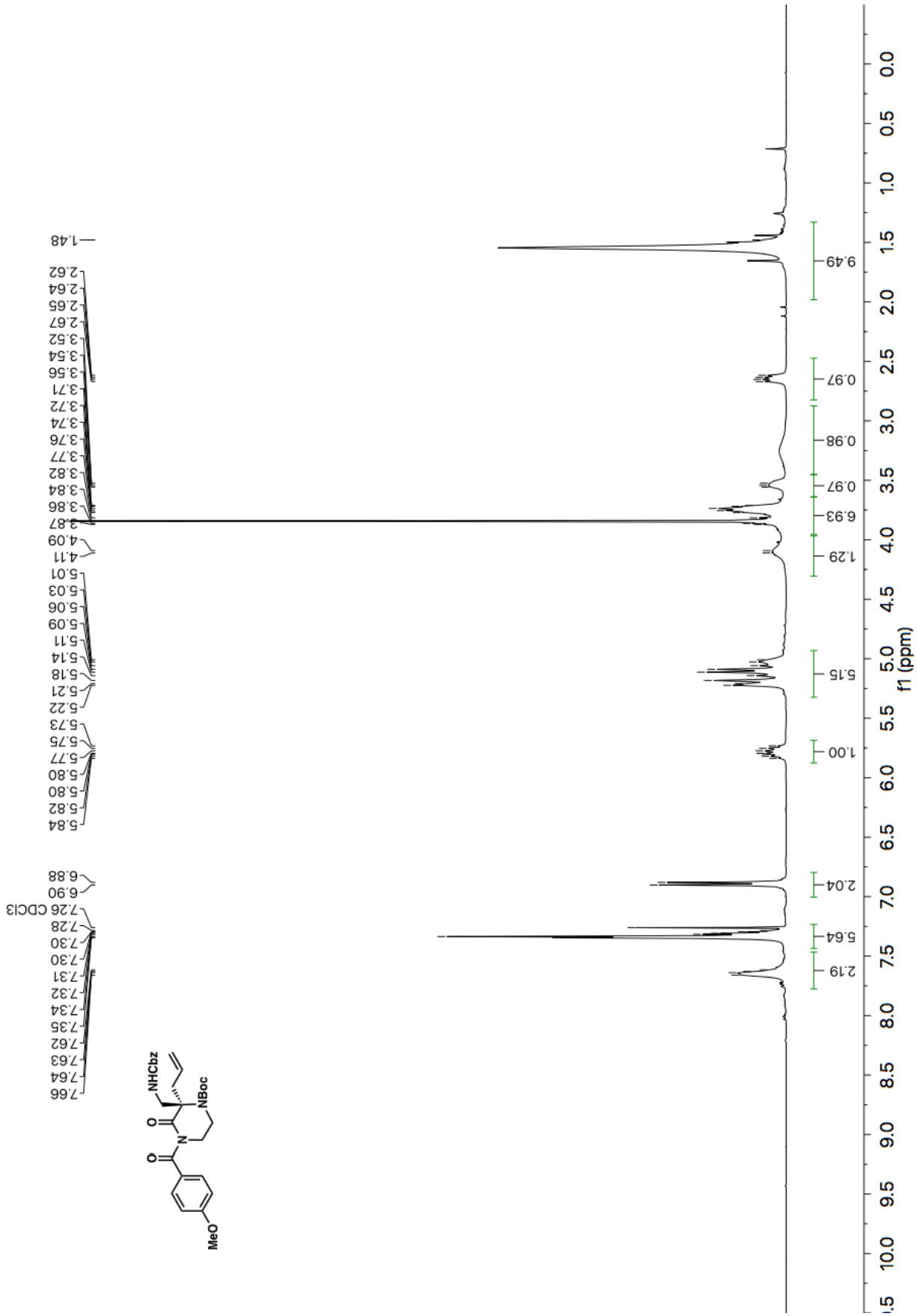

Figure A1.67 ^{1}H NMR (400 MHz, $CDCl_3$) of compound **1. 4l.**

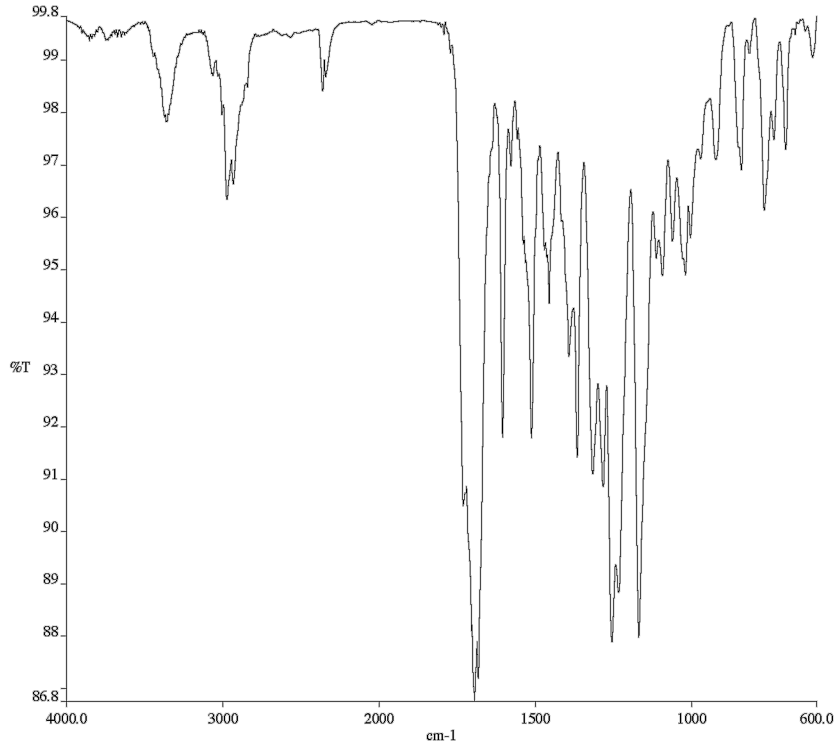

Figure A1.68 Infrared spectrum (Thin Film, NaCl) of compound **1.4l**.

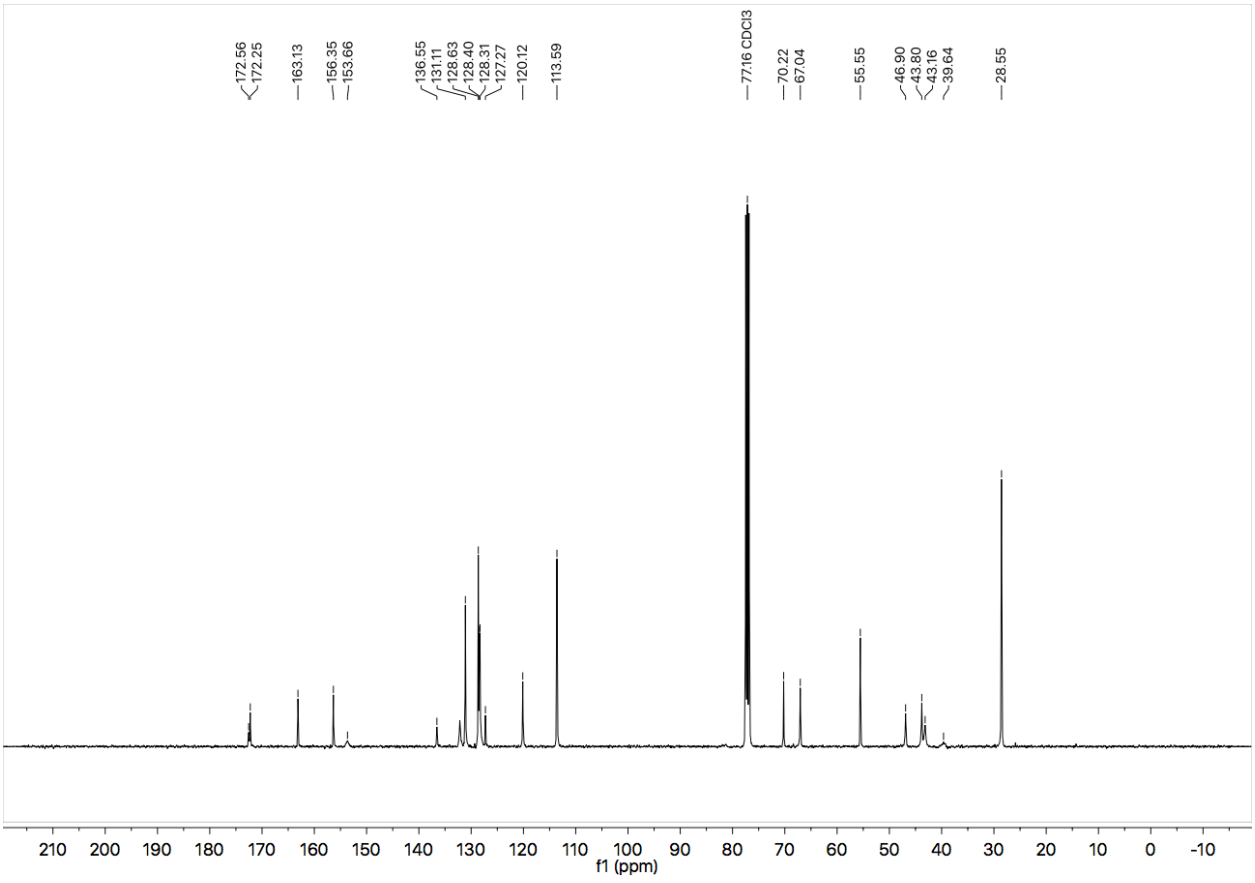

Figure A1.69 ^{13}C NMR (101 MHz, $CDCl_3$) of compound **1.4l**.

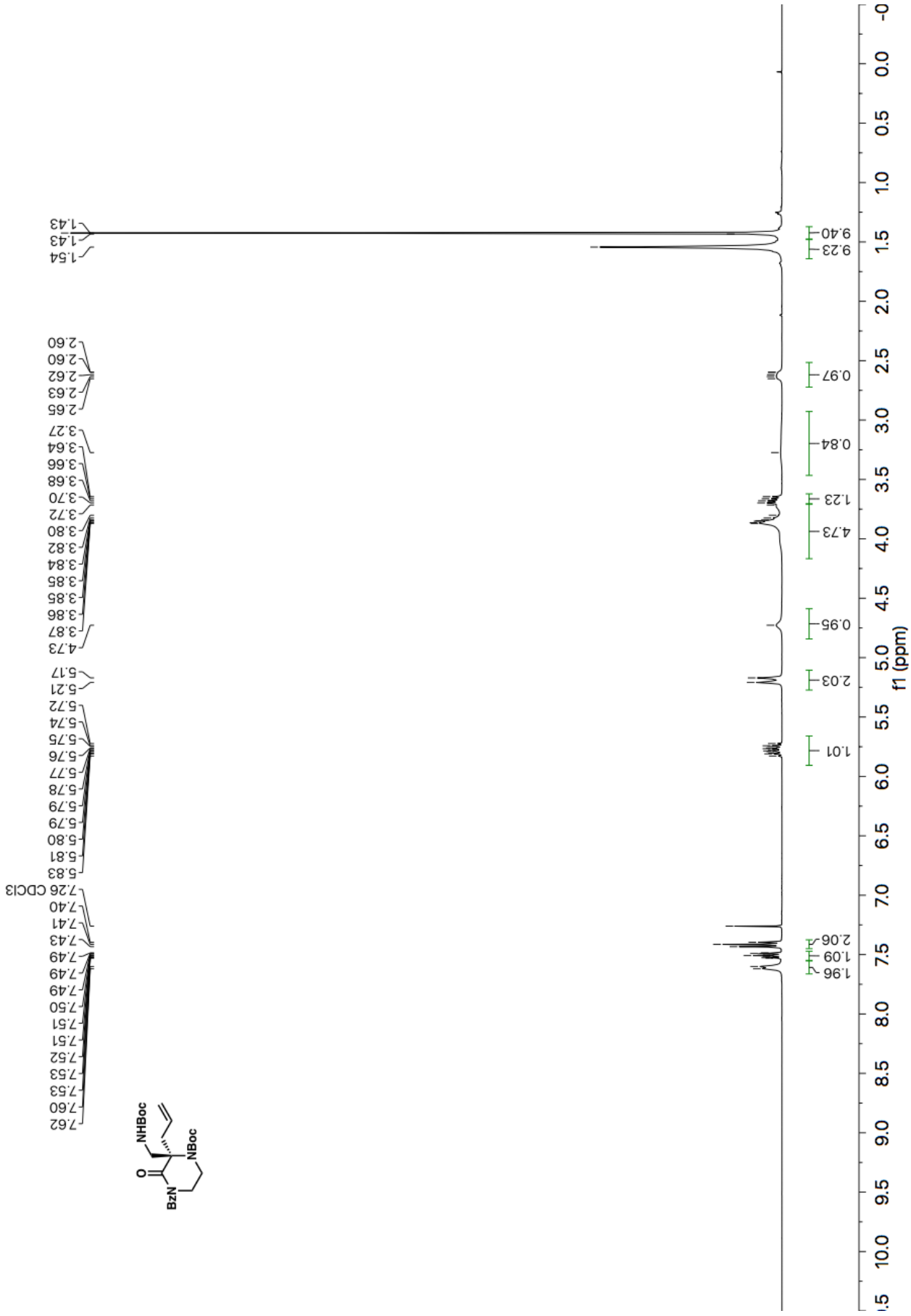

Figure A1.70 ^{1}H NMR (400 MHz, $CDCl_3$) of compound **1.4m.**

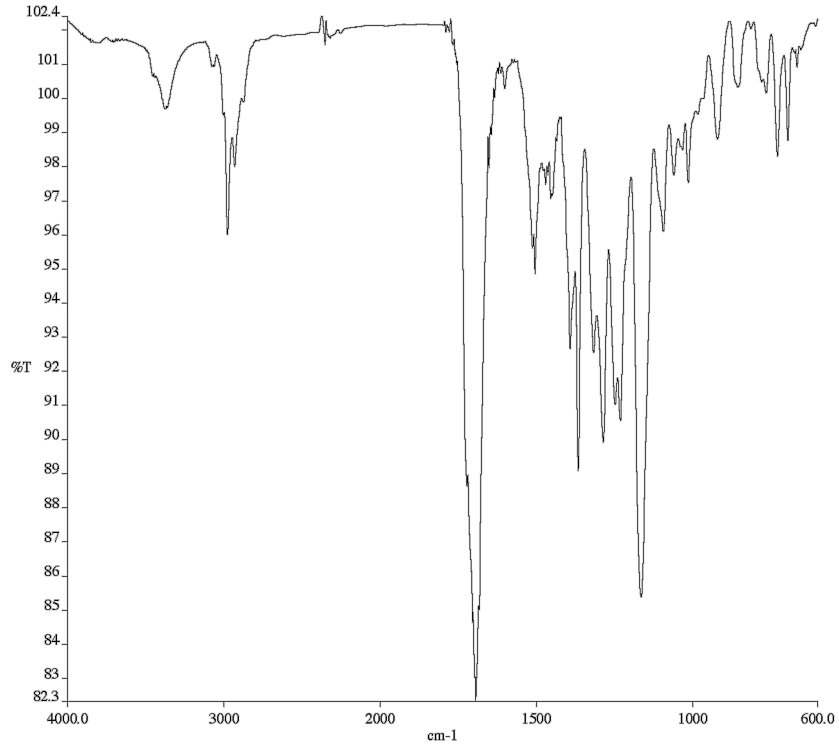

Figure A1.71 Infrared spectrum (Thin Film, NaCl) of compound **1.4m**.

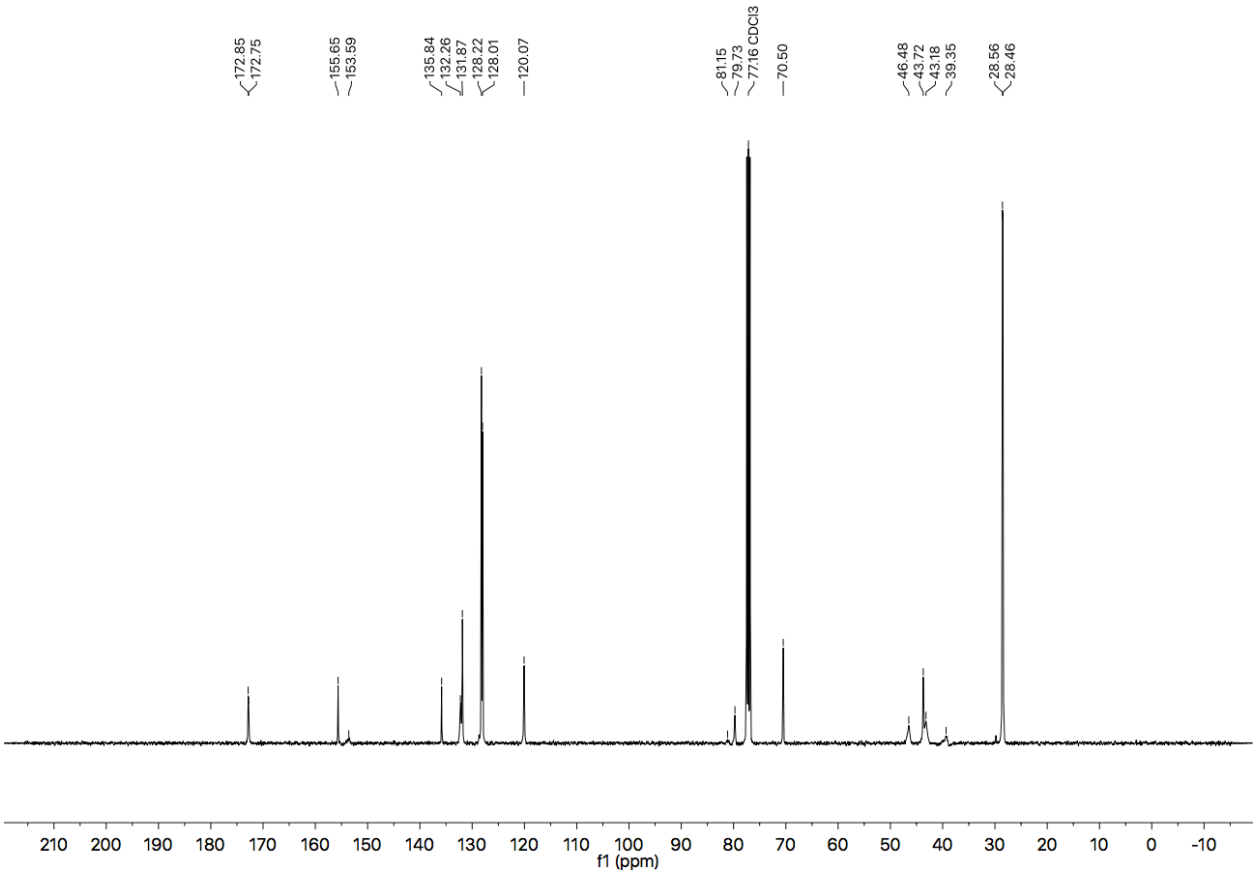

Figure A1.72 ^{13}C NMR (101 MHz, $CDCl_3$) of compound **1.4m**.

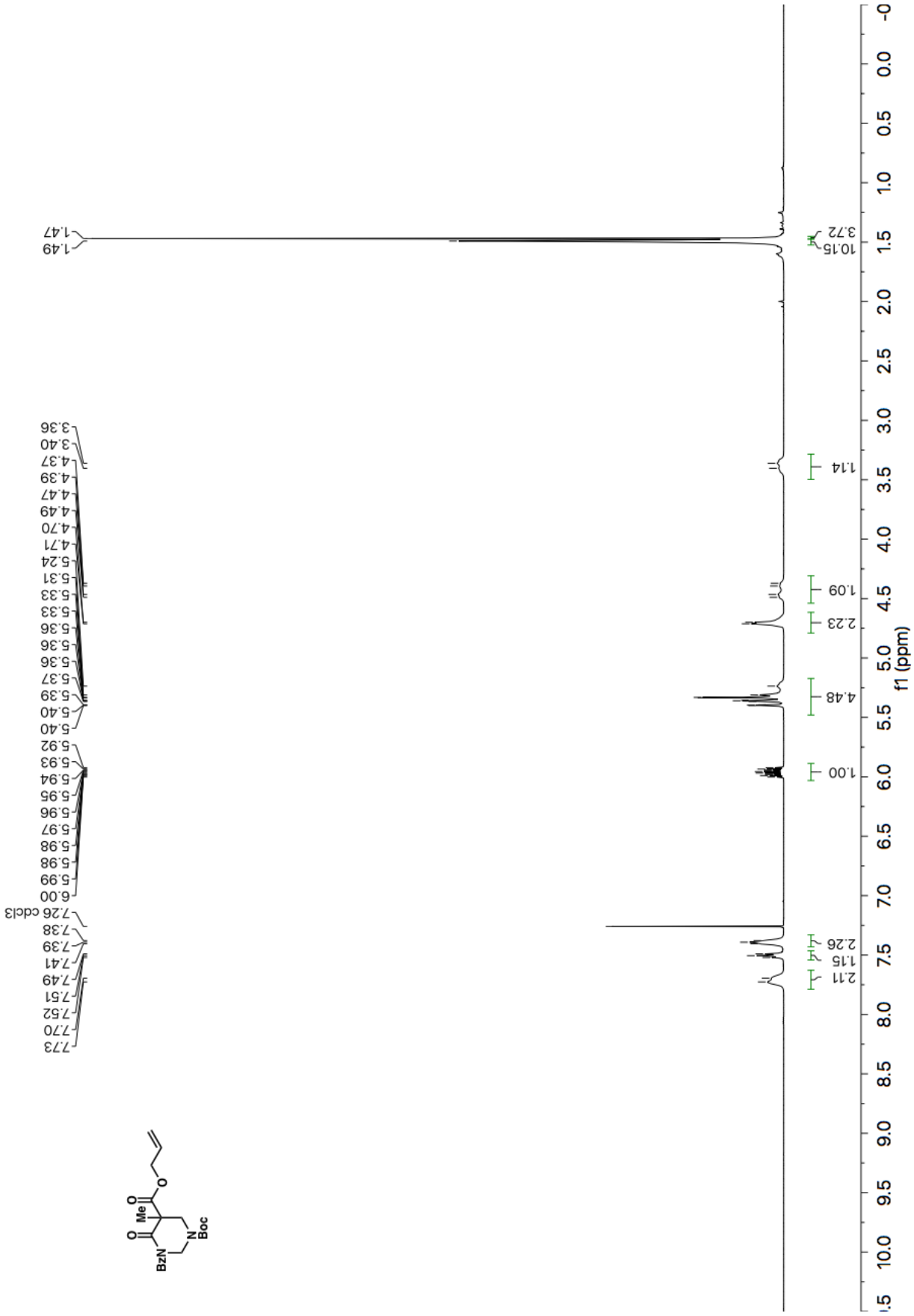

Figure A1.73 ^{1}H NMR (500 MHz, $CDCl_3$) of compound **1.5a.**

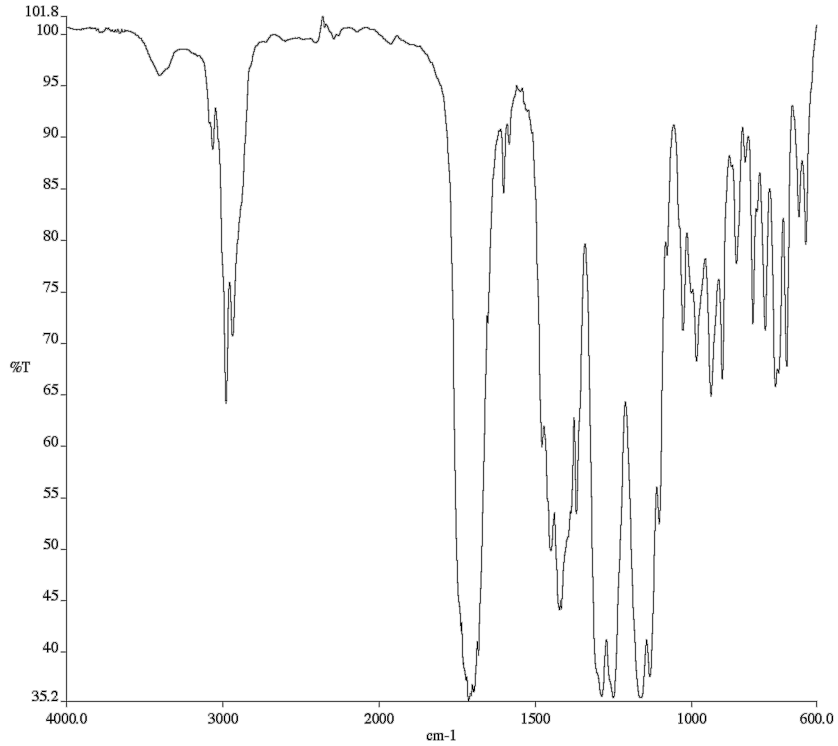

Figure A1.71 Infrared spectrum (Thin Film, NaCl) of compound **1.5a**.

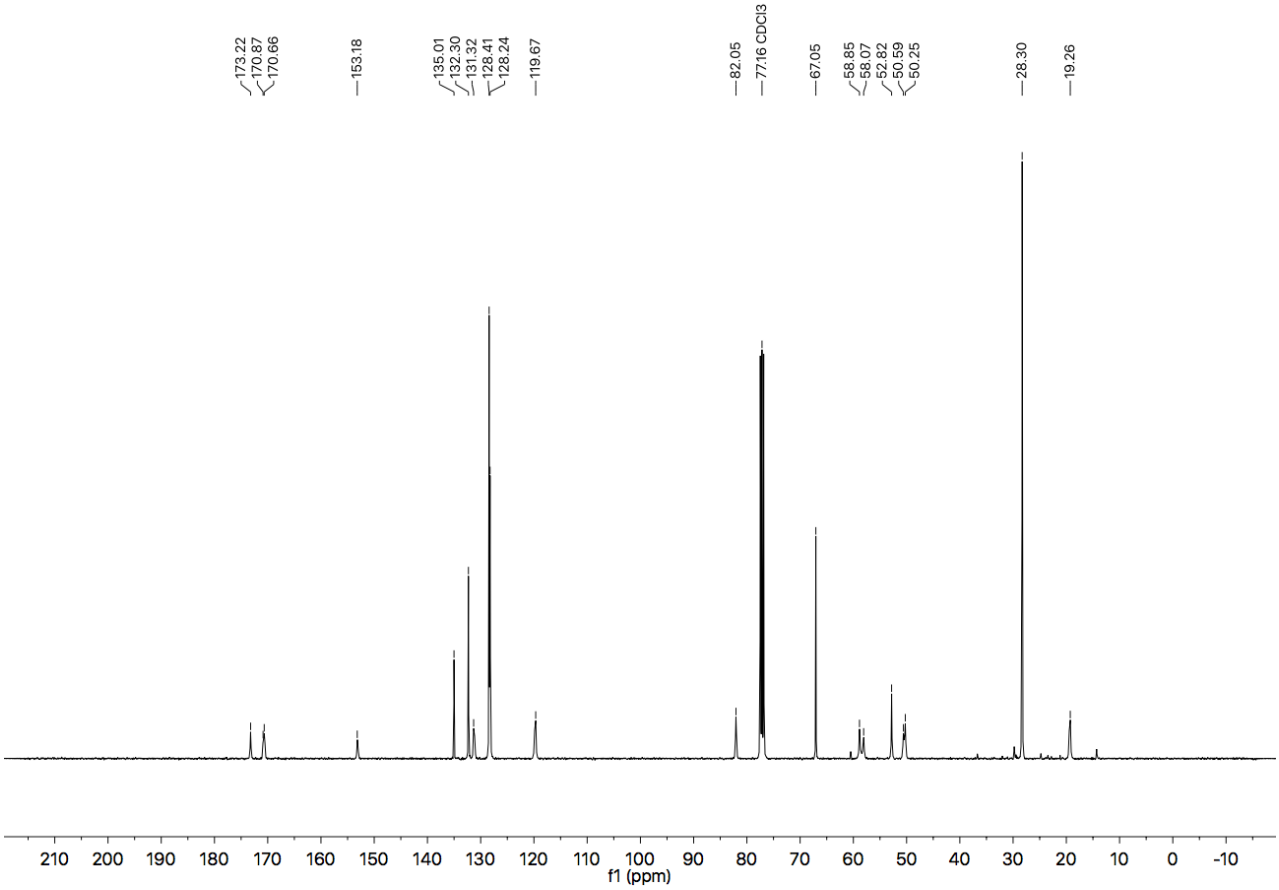

Figure A1.72 ^{13}C NMR (101 MHz, $CDCl_3$) of compound **1.5a**.

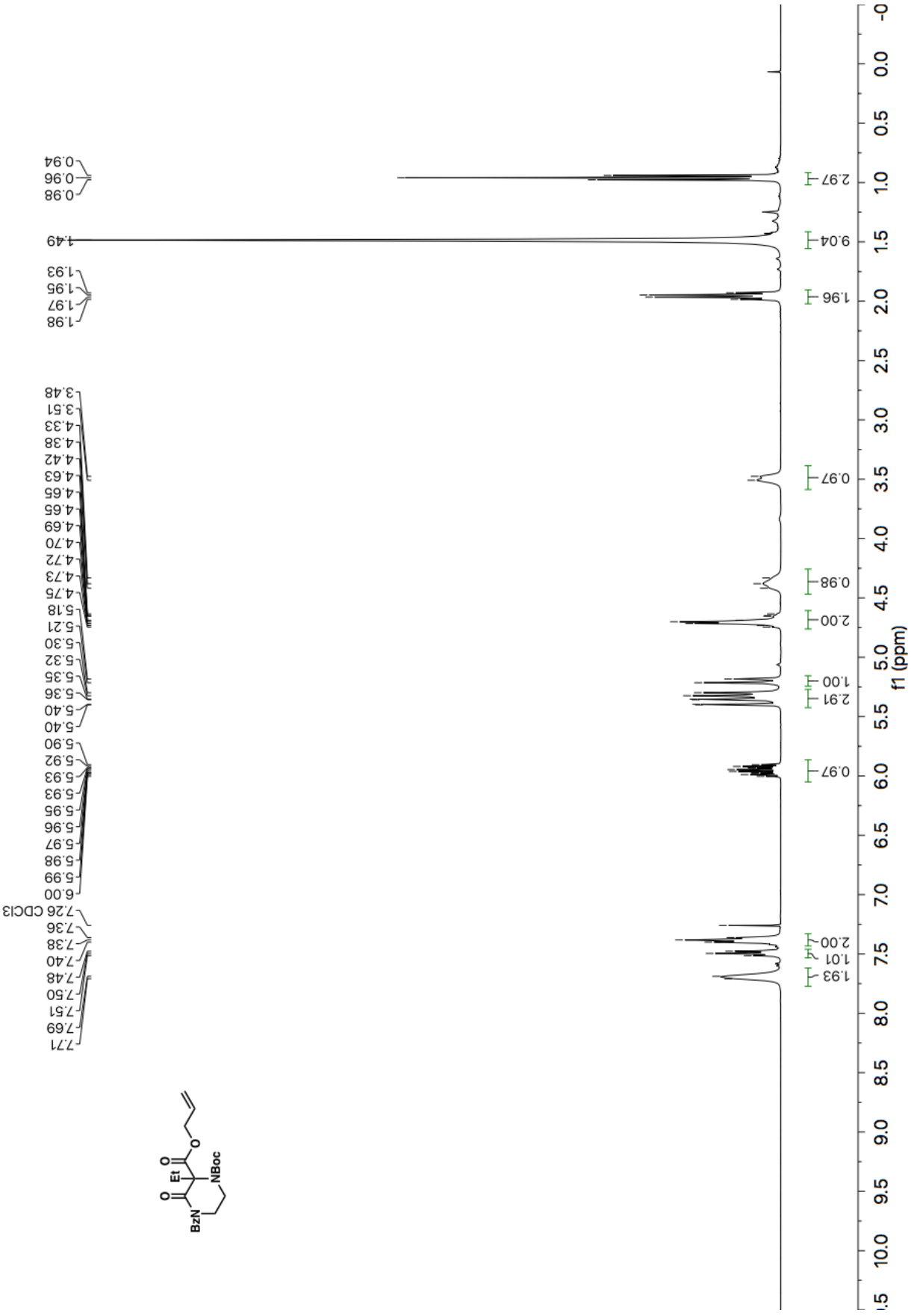

Figure A1.73 ^{1}H NMR (400 MHz, $CDCl_3$) of compound **1.5b.**

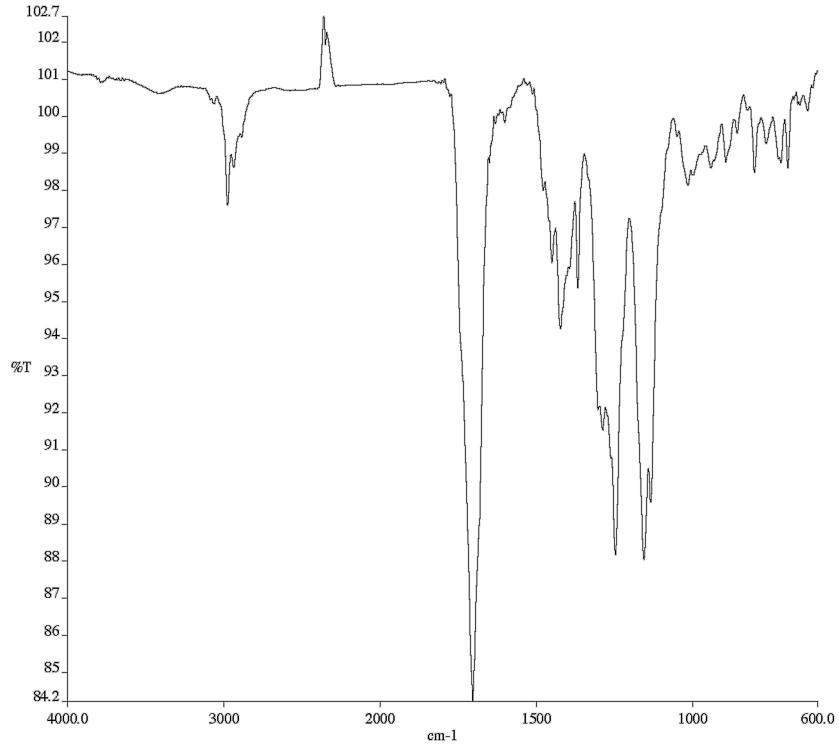

Figure A1.74 Infrared spectrum (Thin Film, NaCl) of compound **1.5b**.

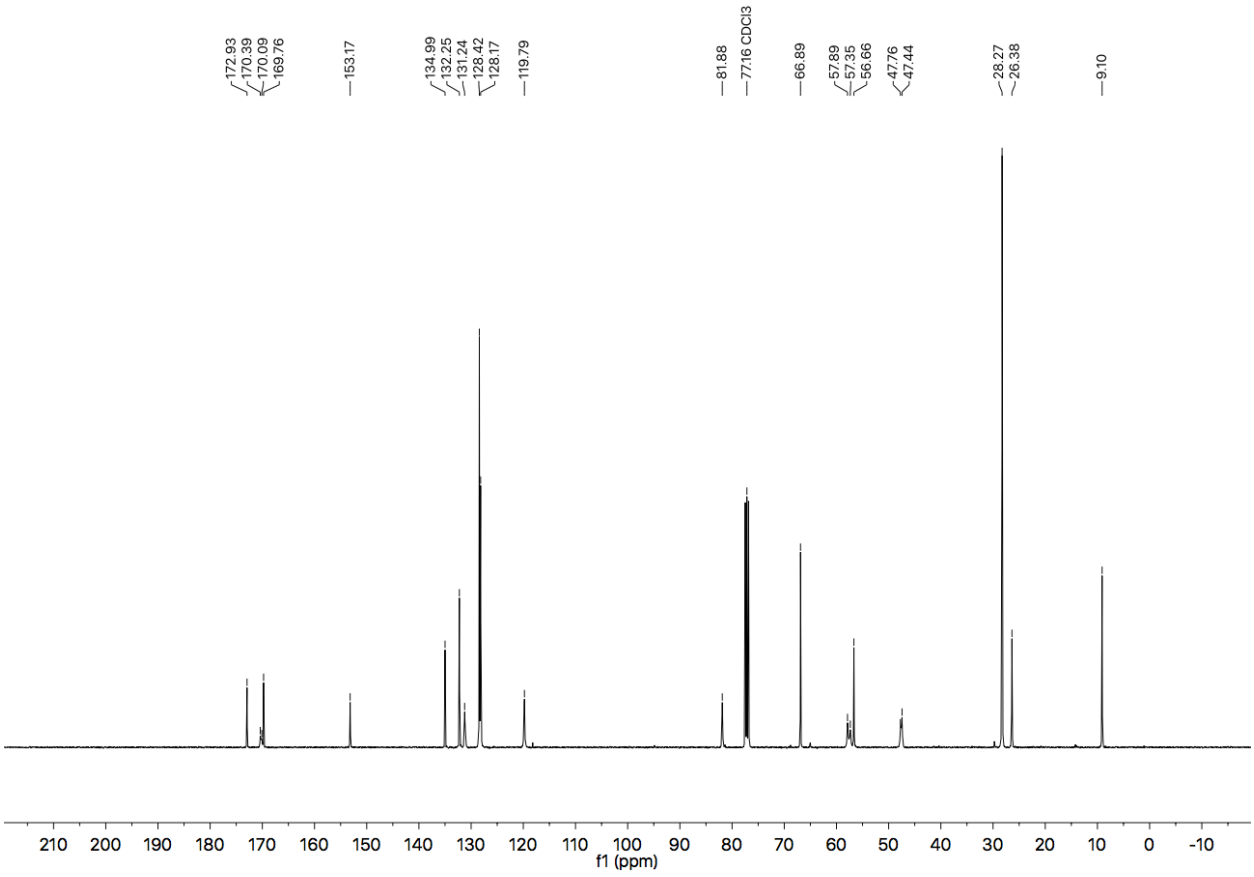

Figure A1.75 ^{13}C NMR (101 MHz, $CDCl_3$) of compound **1.5b**.

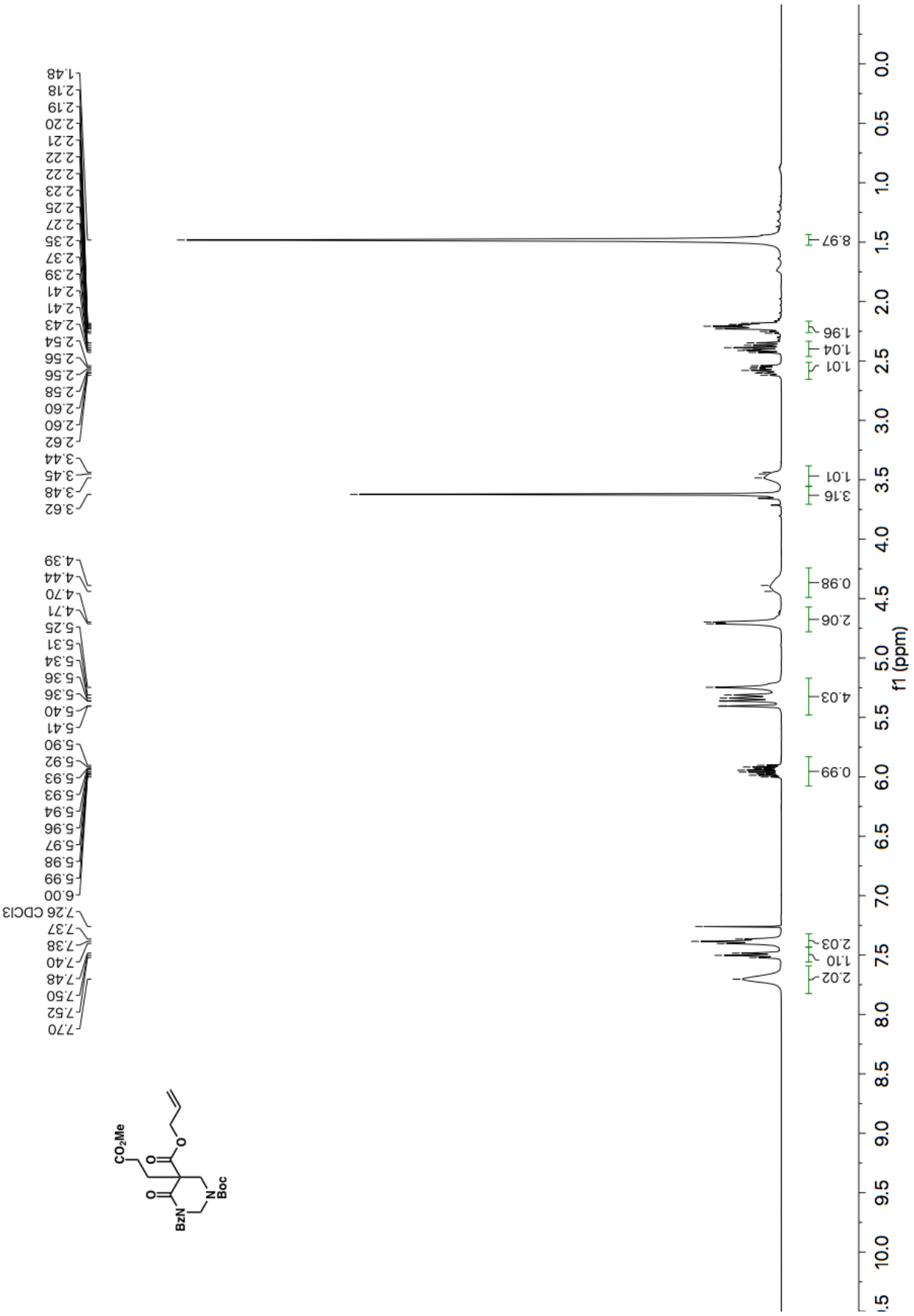

Figure A1.76 ^{1}H NMR (400 MHz, $CDCl_3$) of compound **1.5c.**

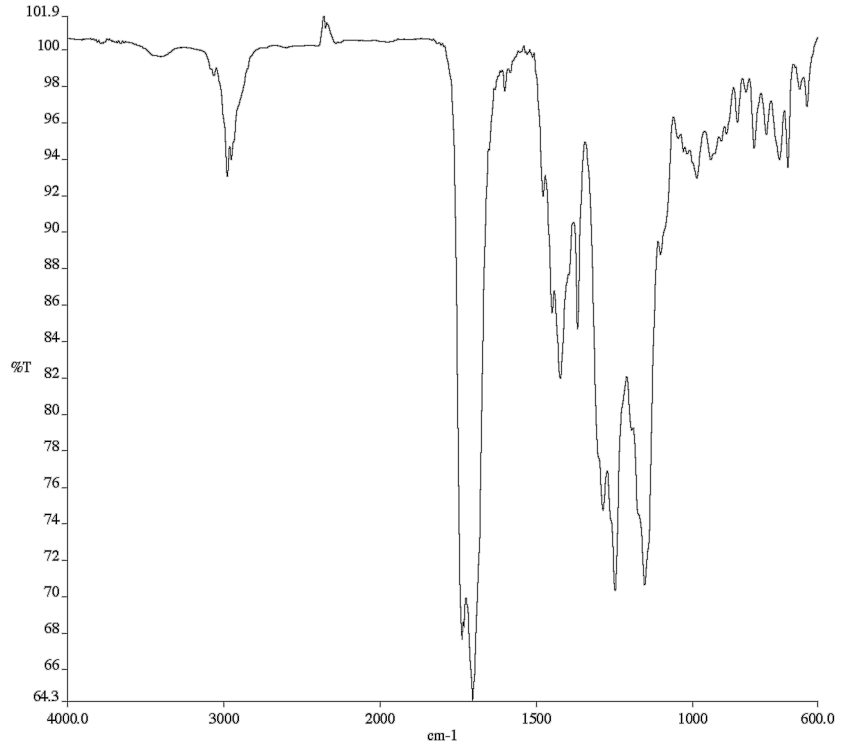

Figure A1.77 Infrared spectrum (Thin Film, NaCl) of compound **1.5c**.

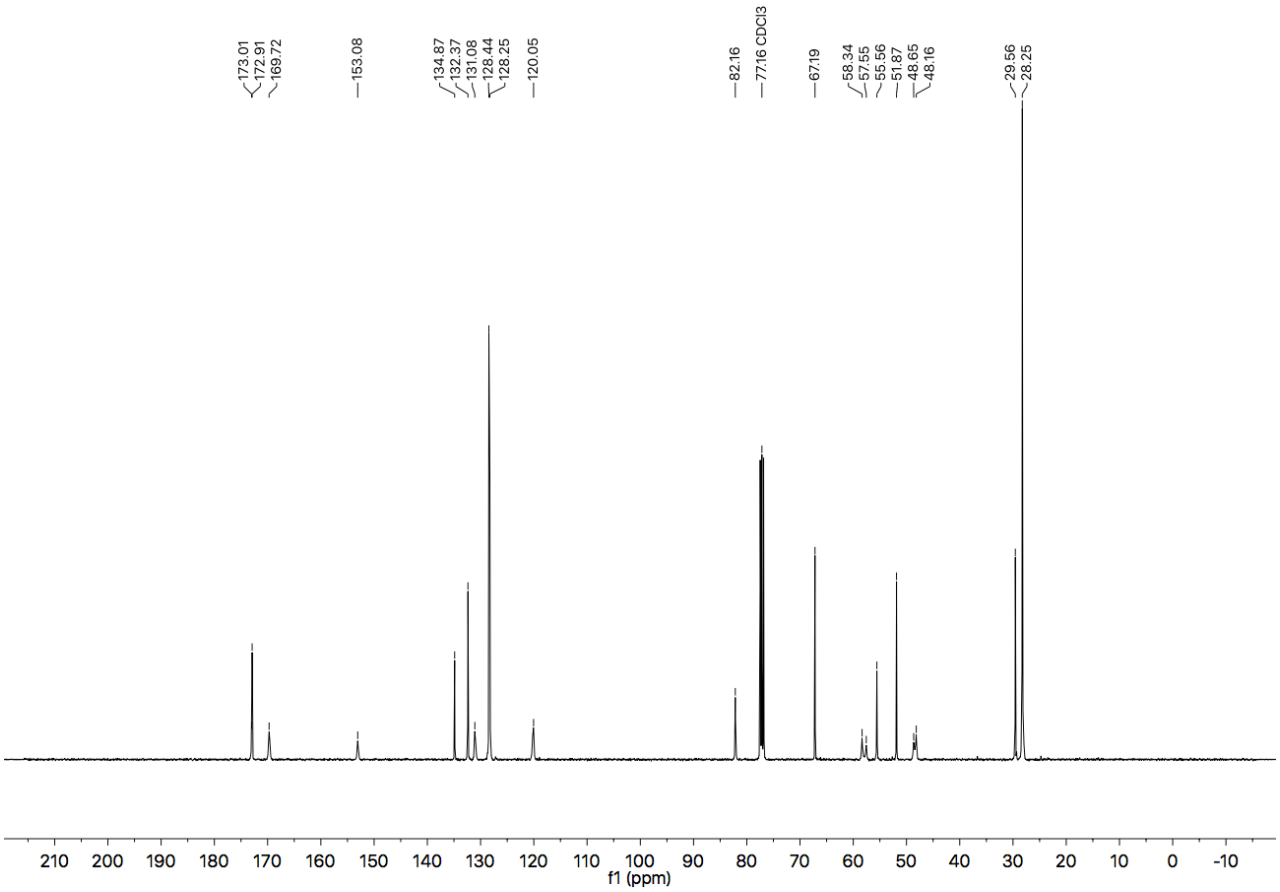

Figure A1.78 ^{13}C NMR (101 MHz, $CDCl_3$) of compound **1.5c**.

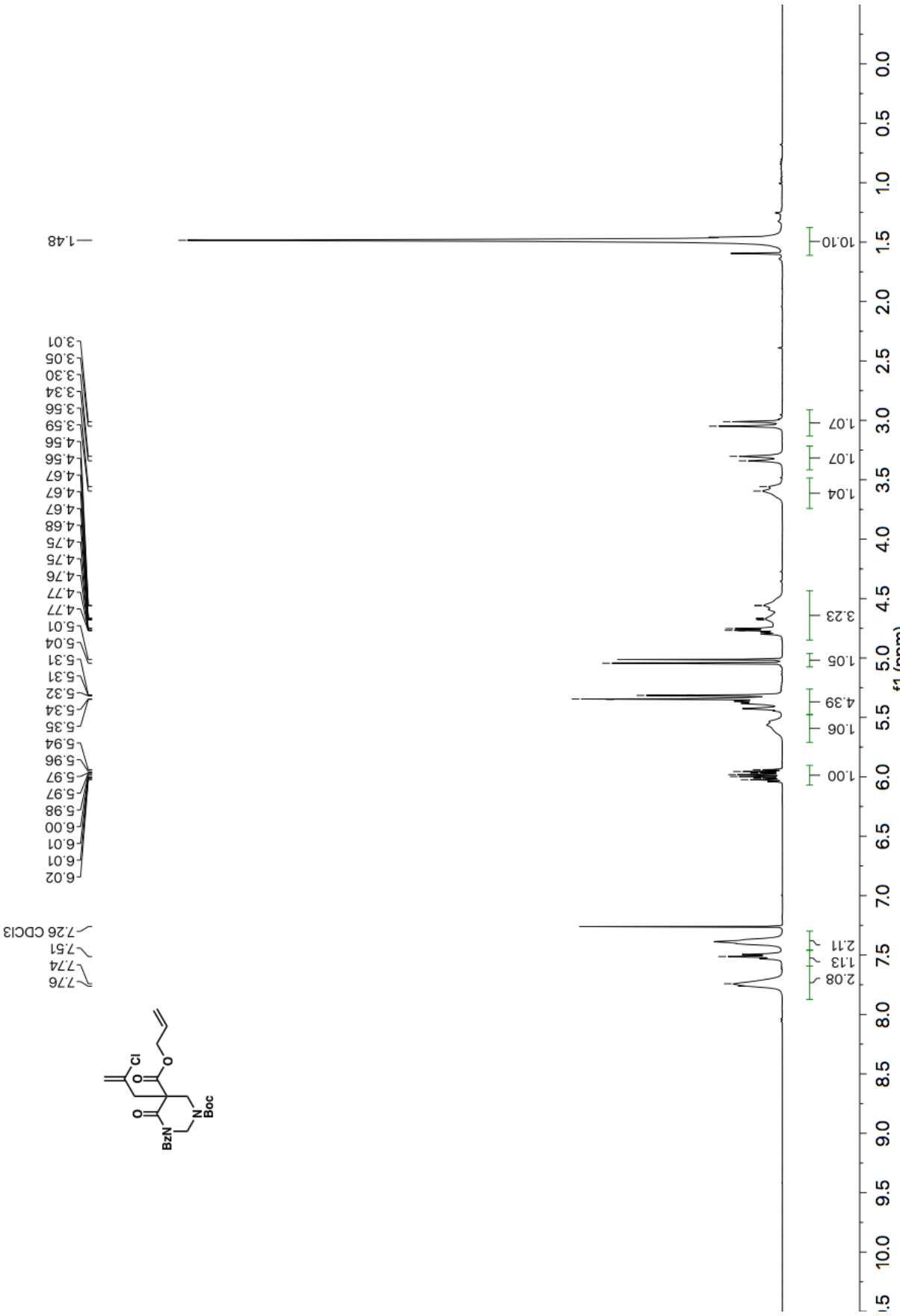

Figure A1.79 ^{1}H NMR (400 MHz, $CDCl_3$) of compound **1.5d.**

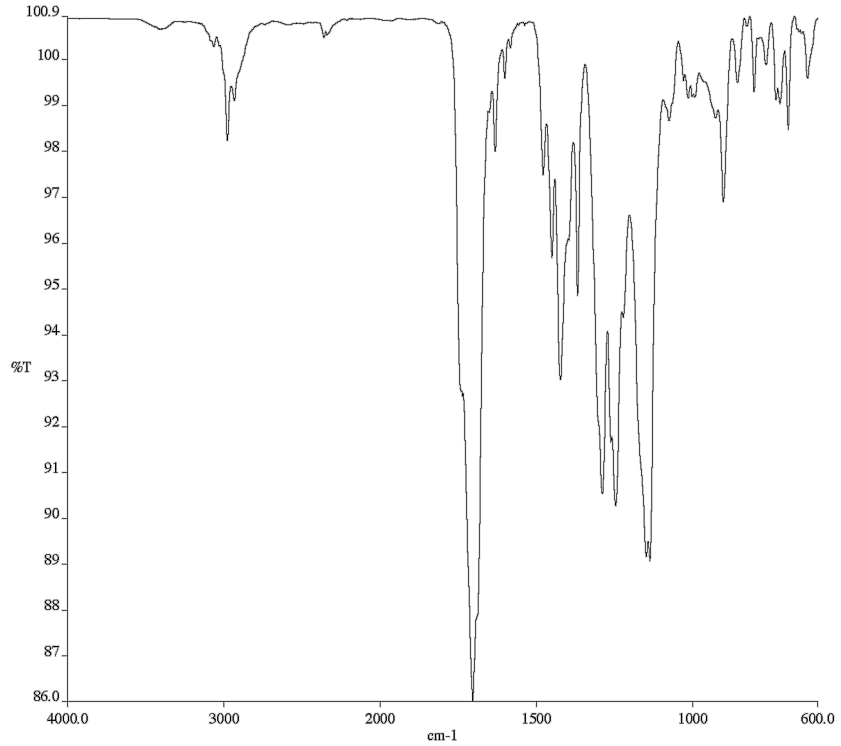

Figure A1.80 Infrared spectrum (Thin Film, NaCl) of compound **1.5d**.

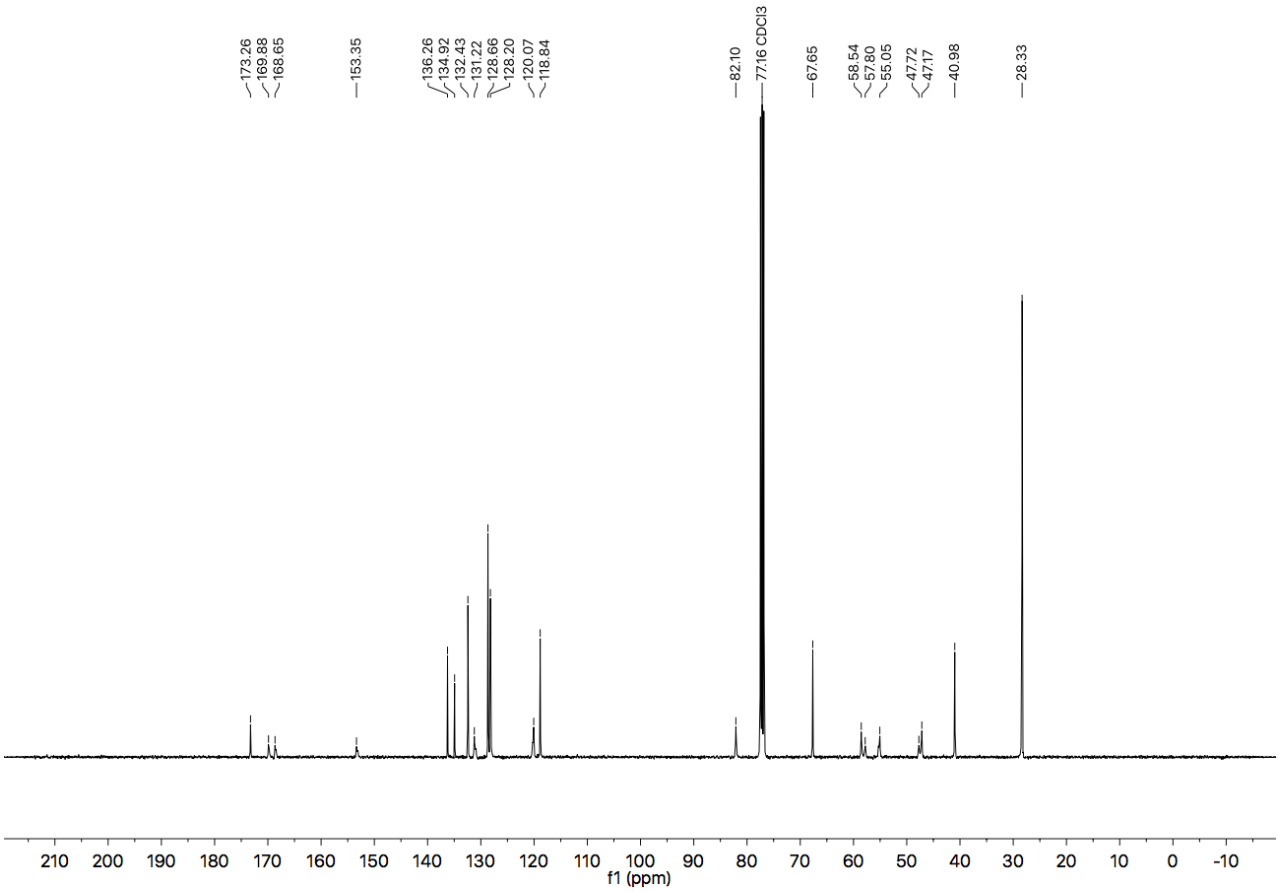

Figure A1.81 ^{13}C NMR (101 MHz, $CDCl_3$) of compound **1.5d**.

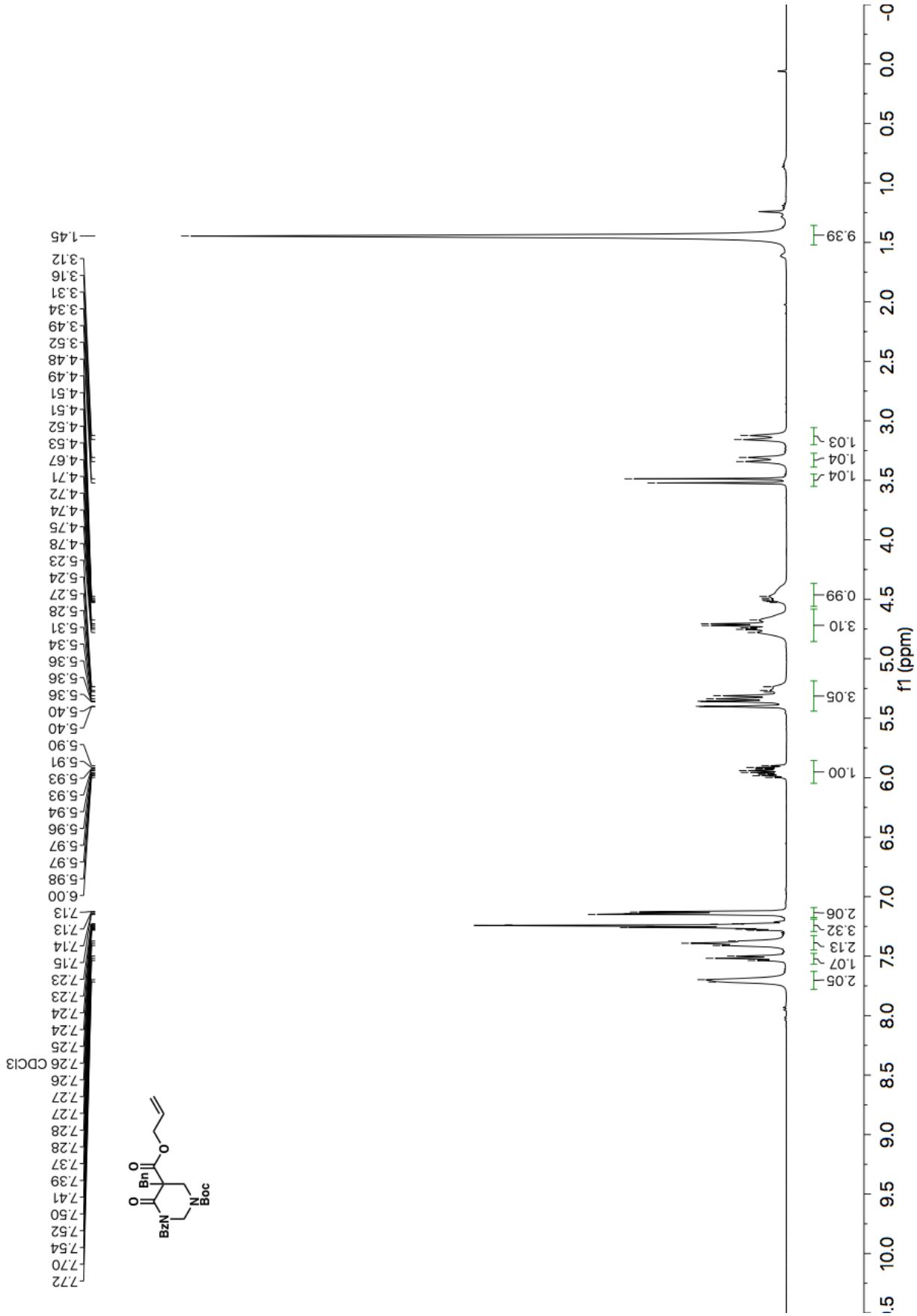

Figure A1.82 ^{1}H NMR (400 MHz, $CDCl_3$) of compound **1.5e.**

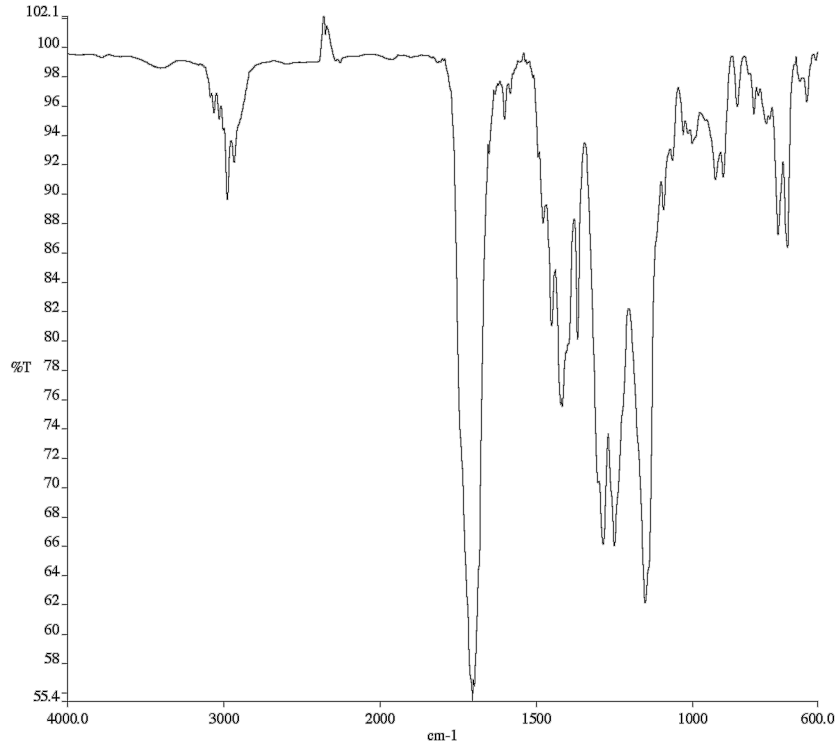

Figure A1.83 Infrared spectrum (Thin Film, NaCl) of compound **1.5e**.

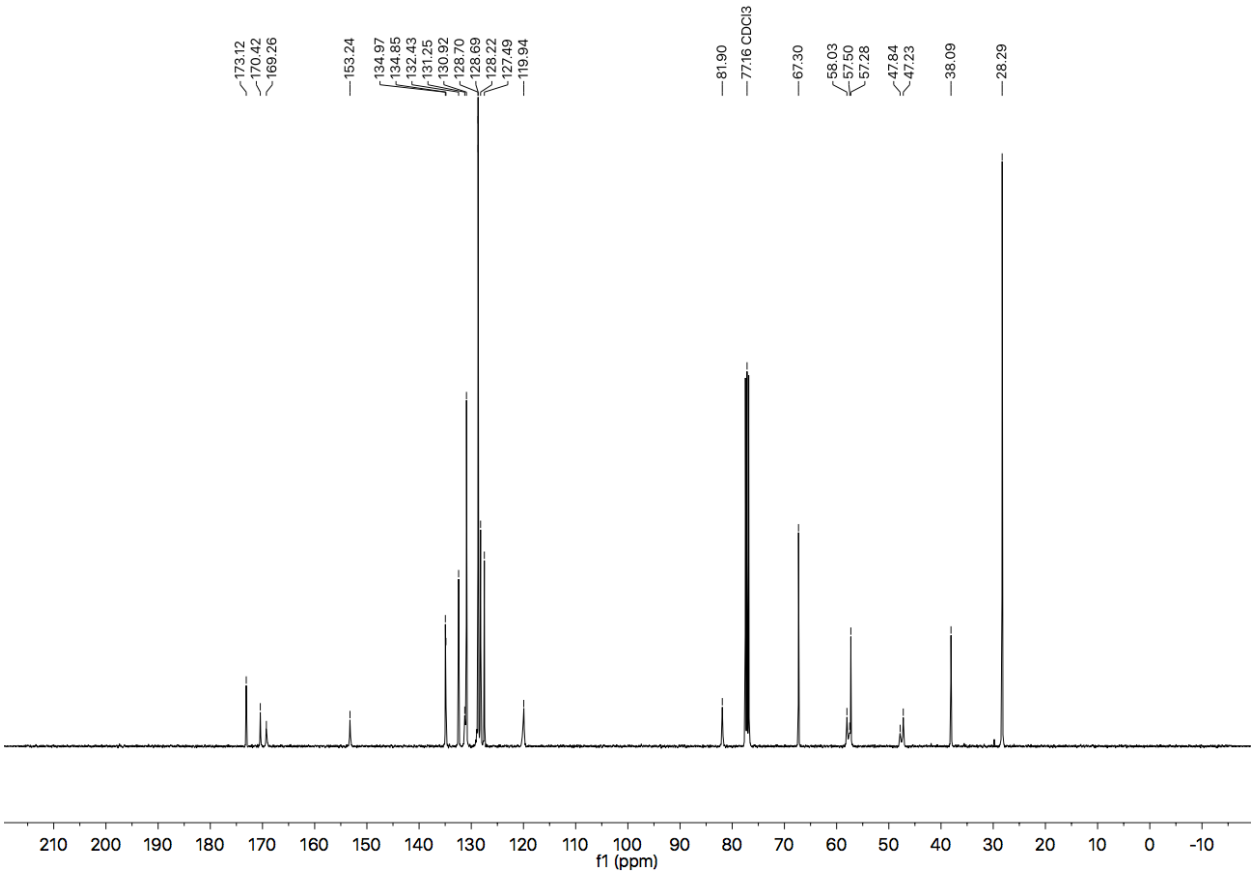

Figure A1.84 ^{13}C NMR (101 MHz, $CDCl_3$) of compound **1.5e**.

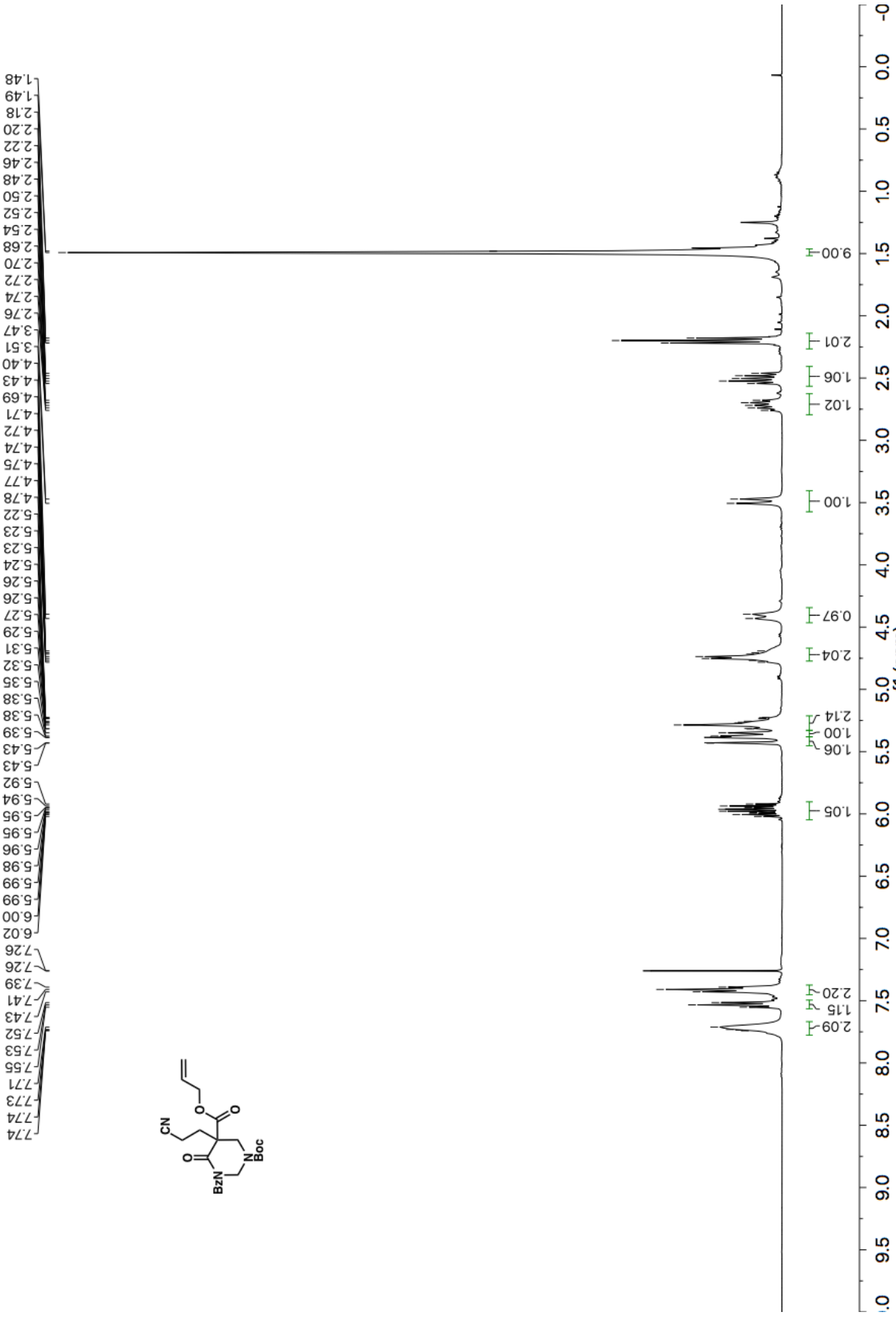

Figure A1.85 ^{1}H NMR (400 MHz, $CDCl_3$) of compound **1. 5f.**

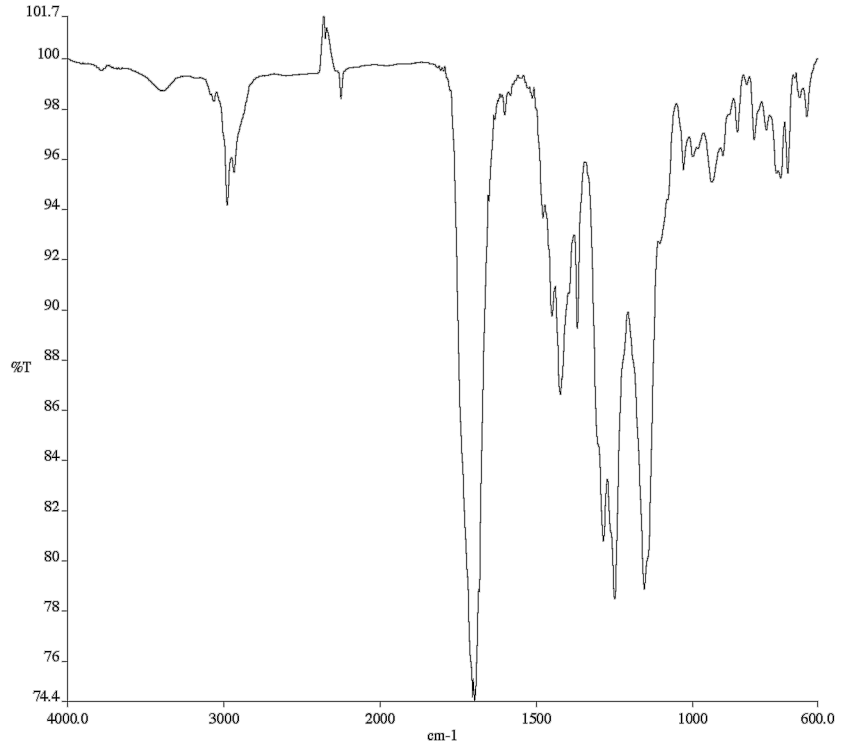

Figure A1.86 Infrared spectrum (Thin Film, NaCl) of compound **1.5f**.

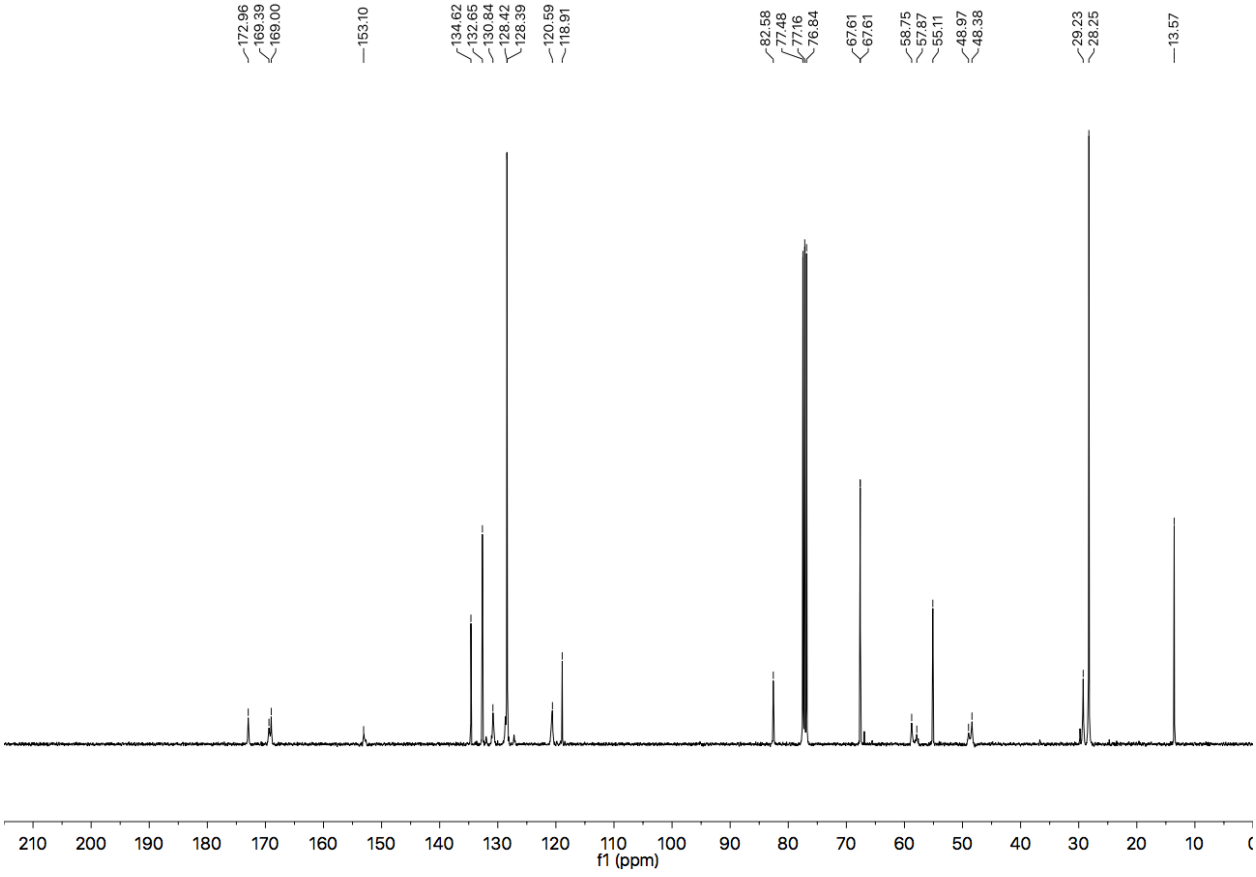

Figure A1.87 ^{13}C NMR (101 MHz, $CDCl_3$) of compound **1.5f**.

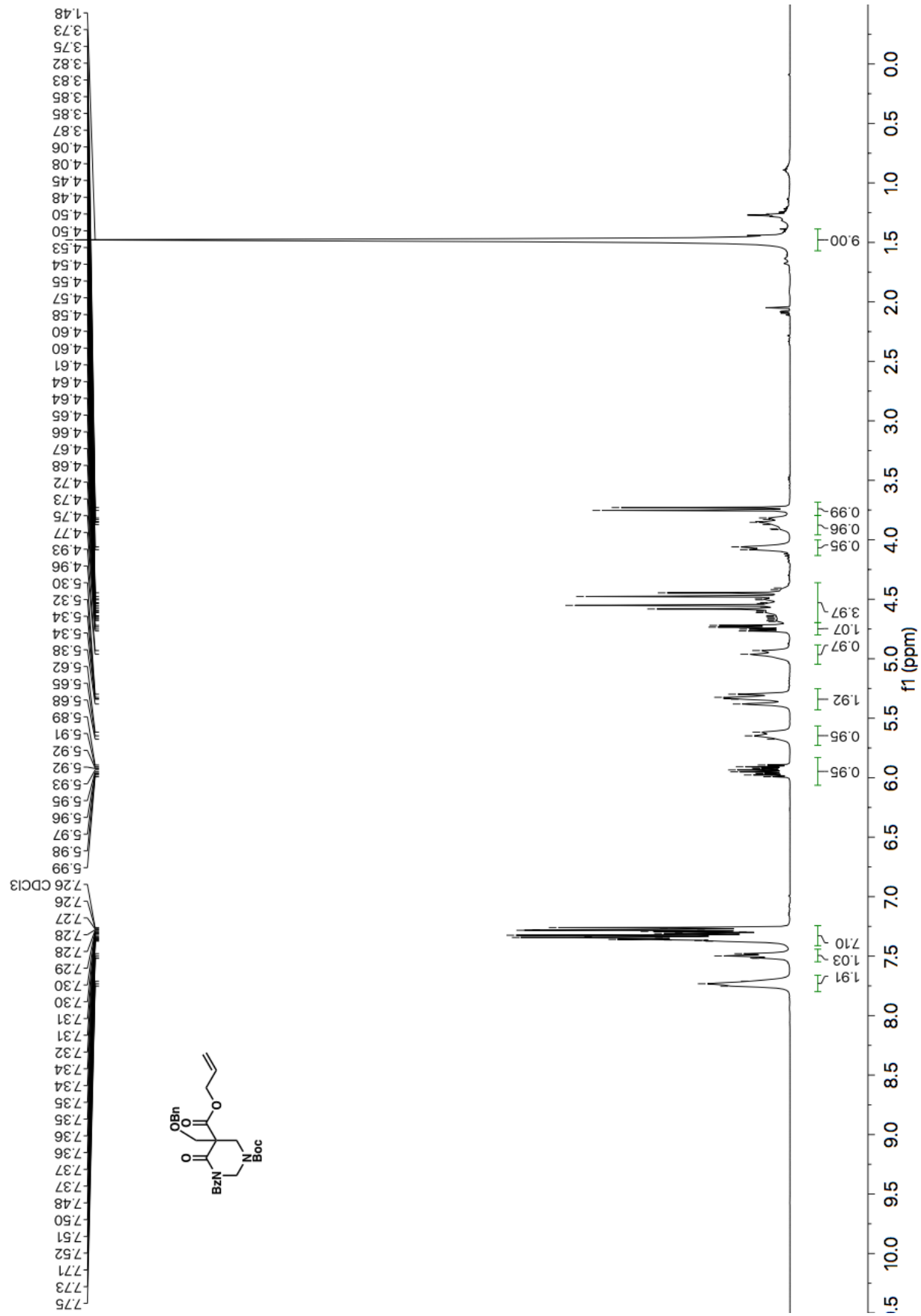

Figure A1.88 ^{1}H NMR (400 MHz, $CDCl_3$) of compound **1.5g.**

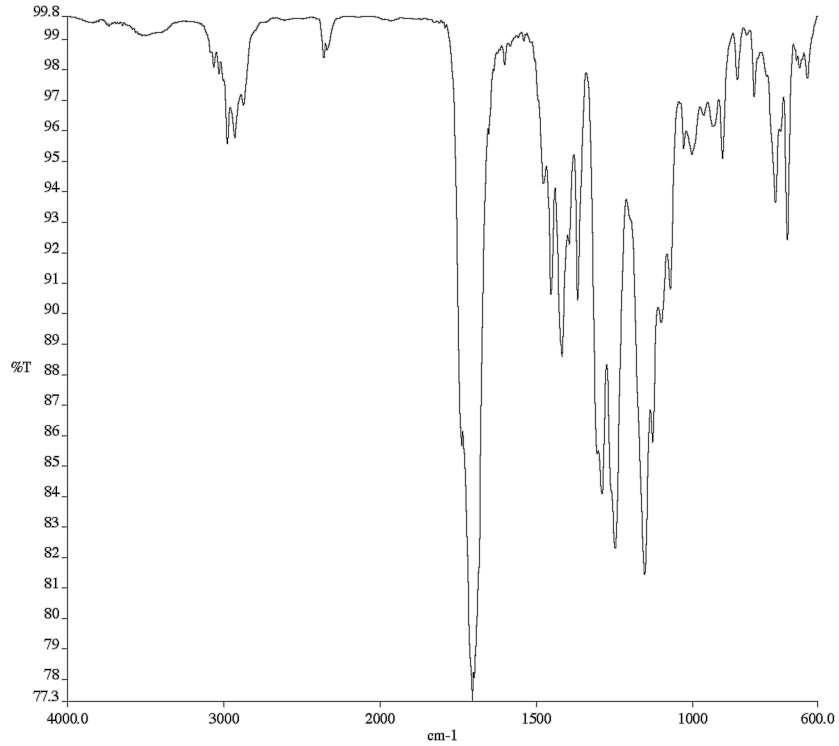

Figure A1.89 Infrared spectrum (Thin Film, NaCl) of compound **1.6**.

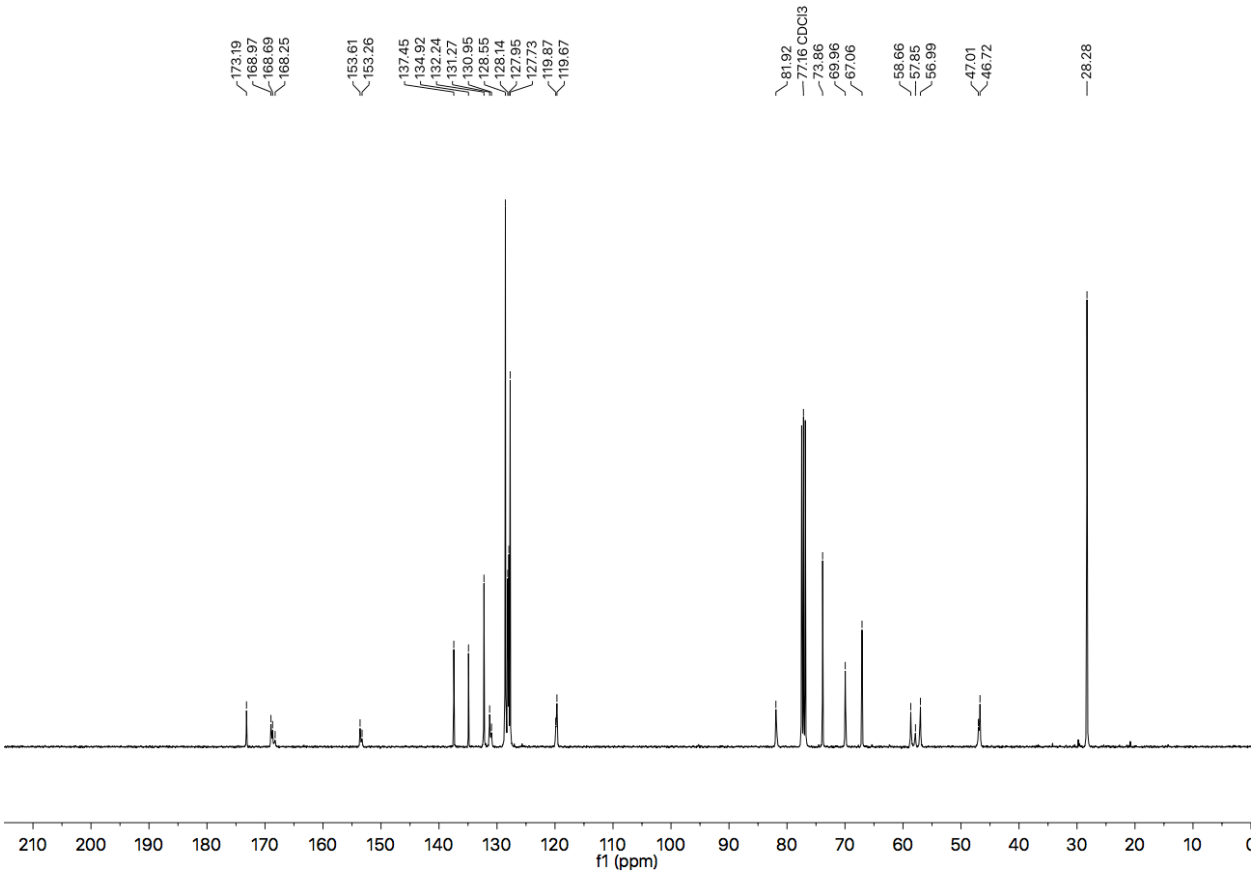

Figure A1.90 ^{13}C NMR (101 MHz, $CDCl_3$) of compound **1.5g**.

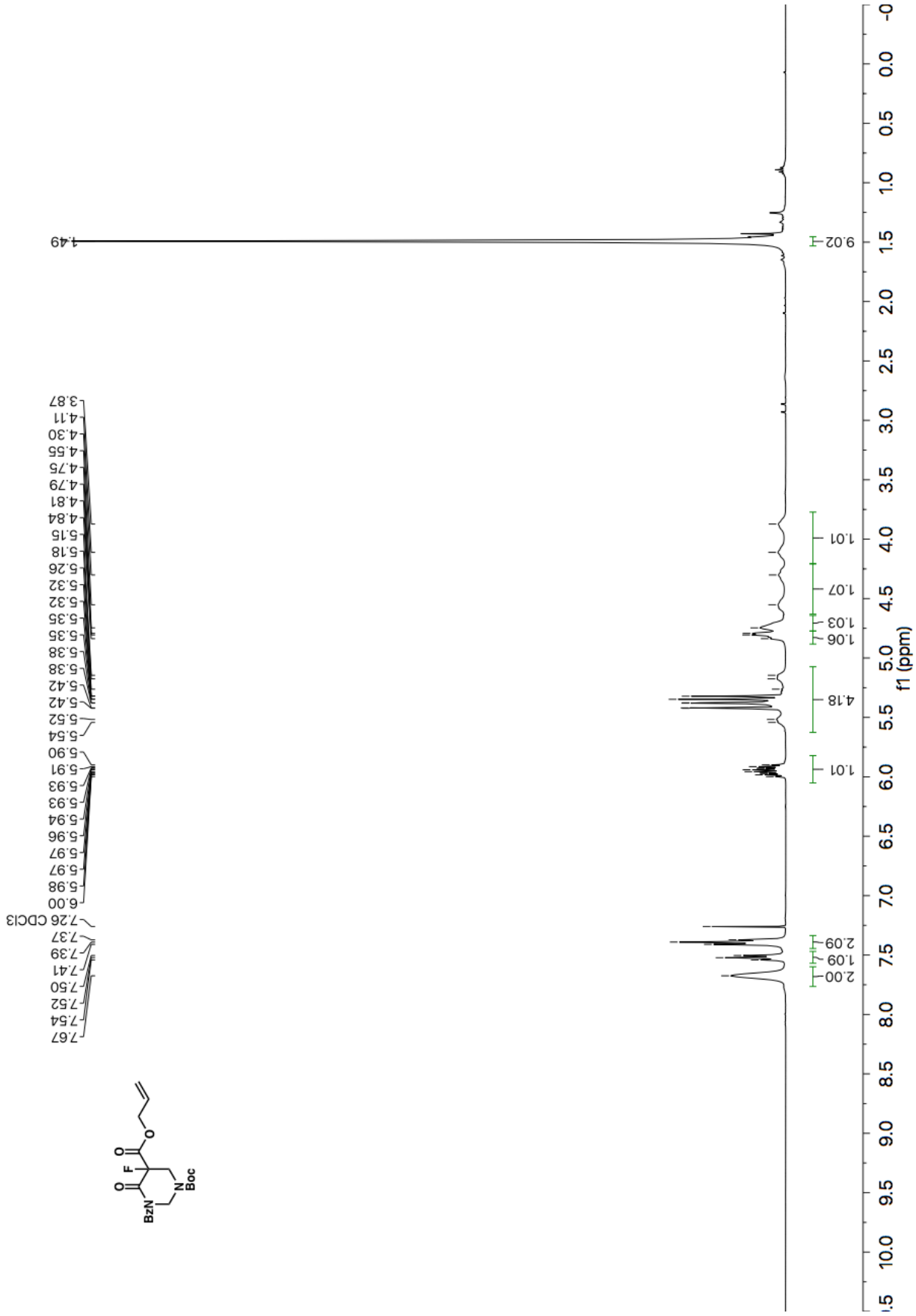

Figure A1.91 ^{1}H NMR (400 MHz, $CDCl_3$) of compound **1.5h.**

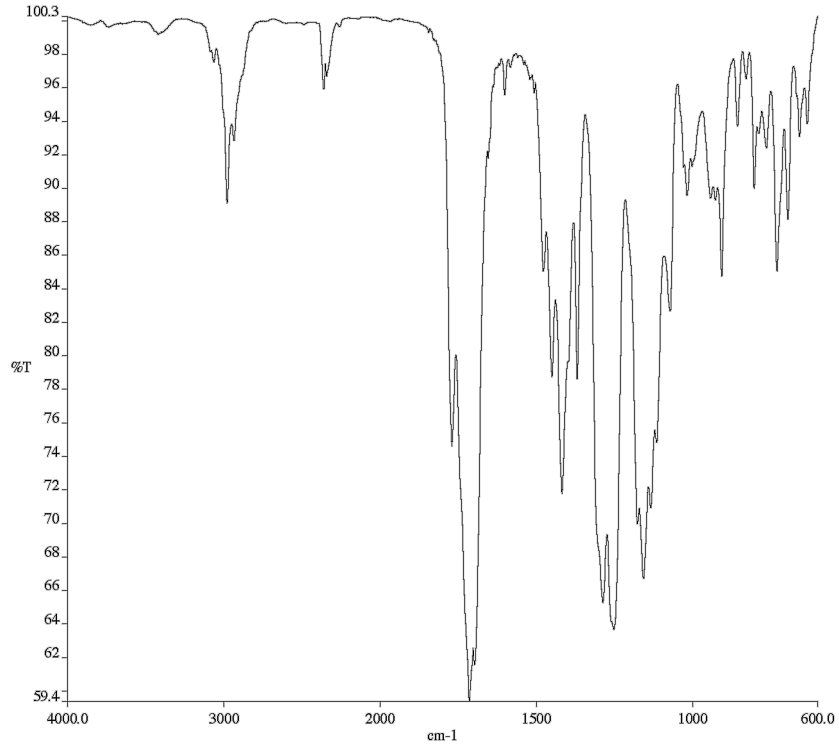

Figure A1.92 Infrared spectrum (Thin Film, NaCl) of compound **1.5h**.

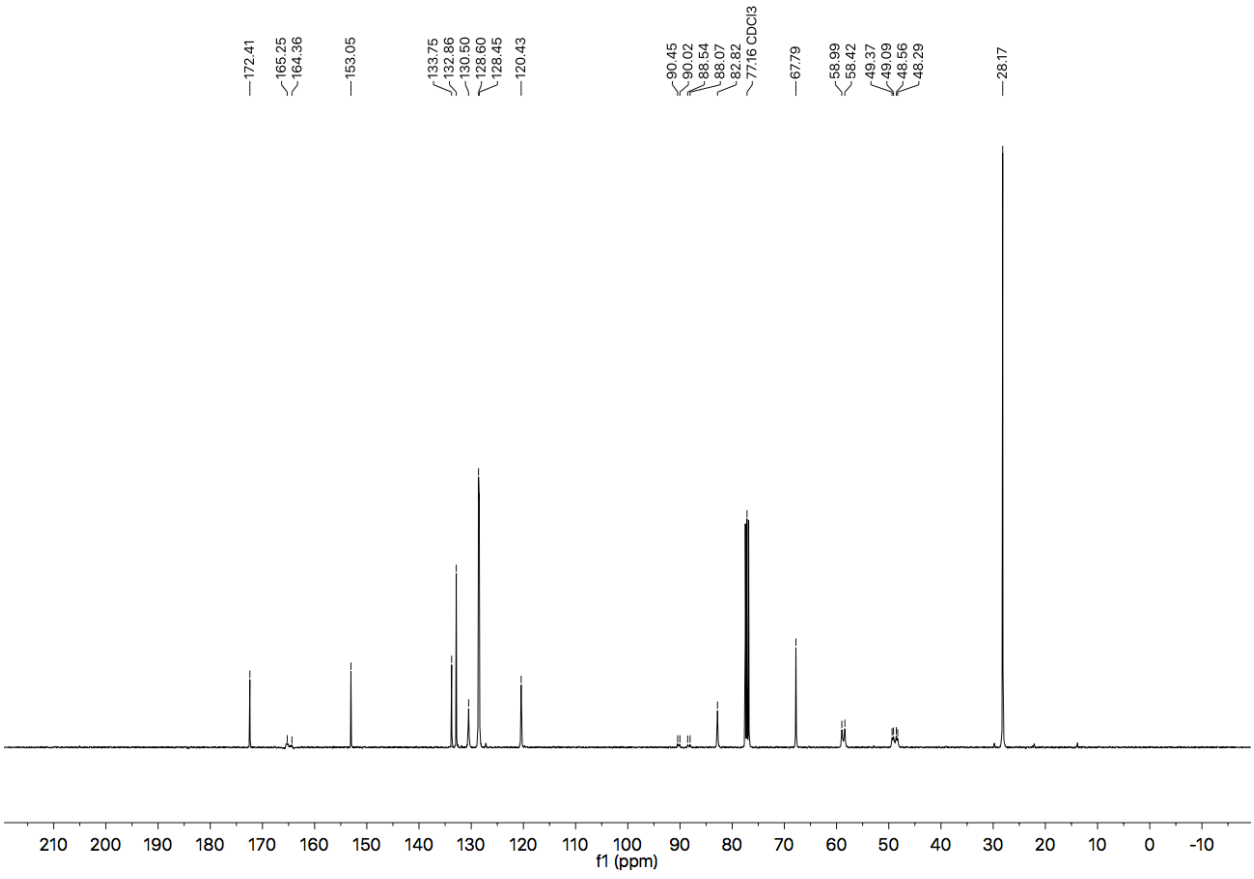

Figure A1.93 ^{13}C NMR (101 MHz, $CDCl_3$) of compound **1.5h**.

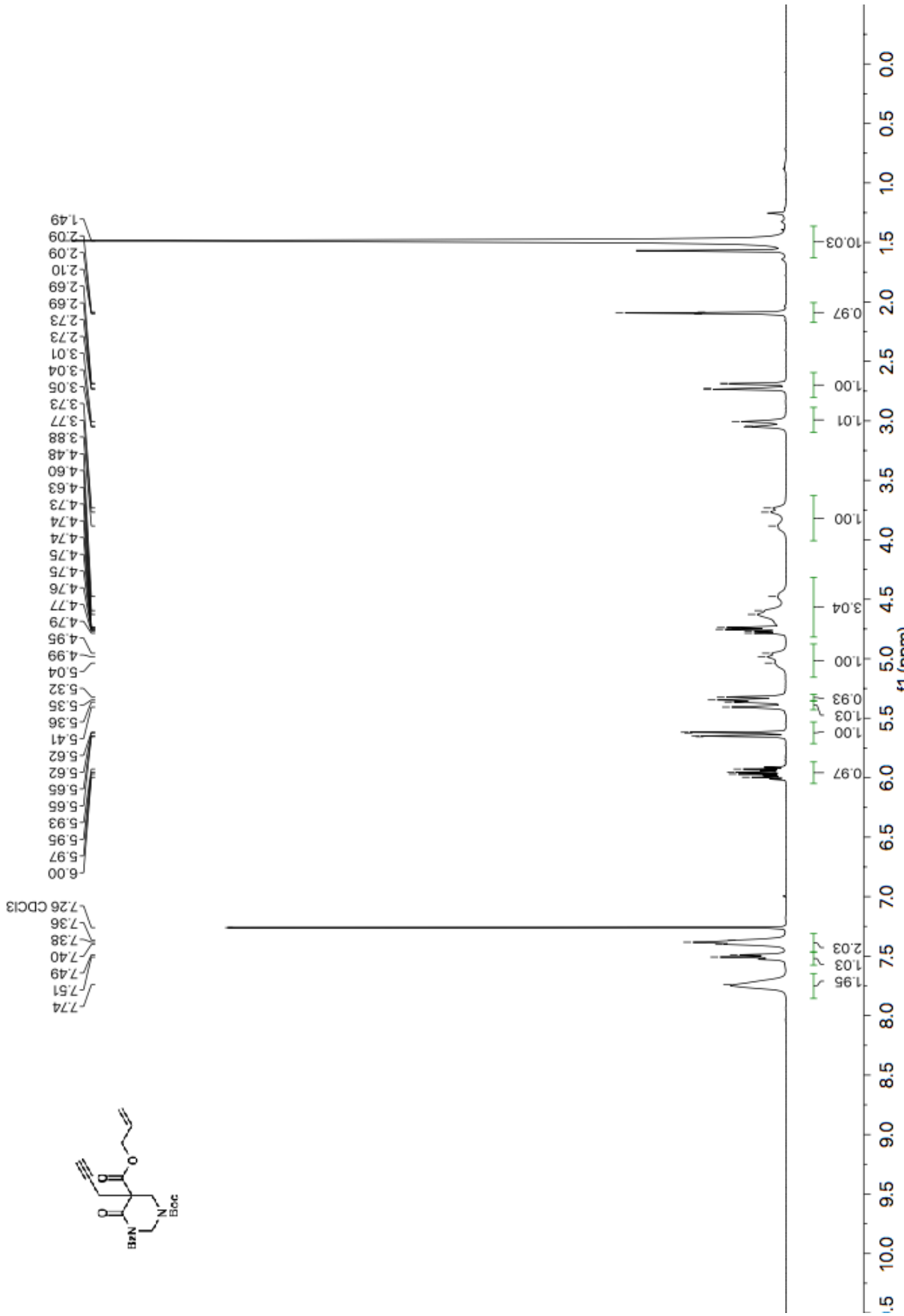

Figure A1.94 ^{1}H NMR (400 MHz, $CDCl_3$) of compound **1.5i.**

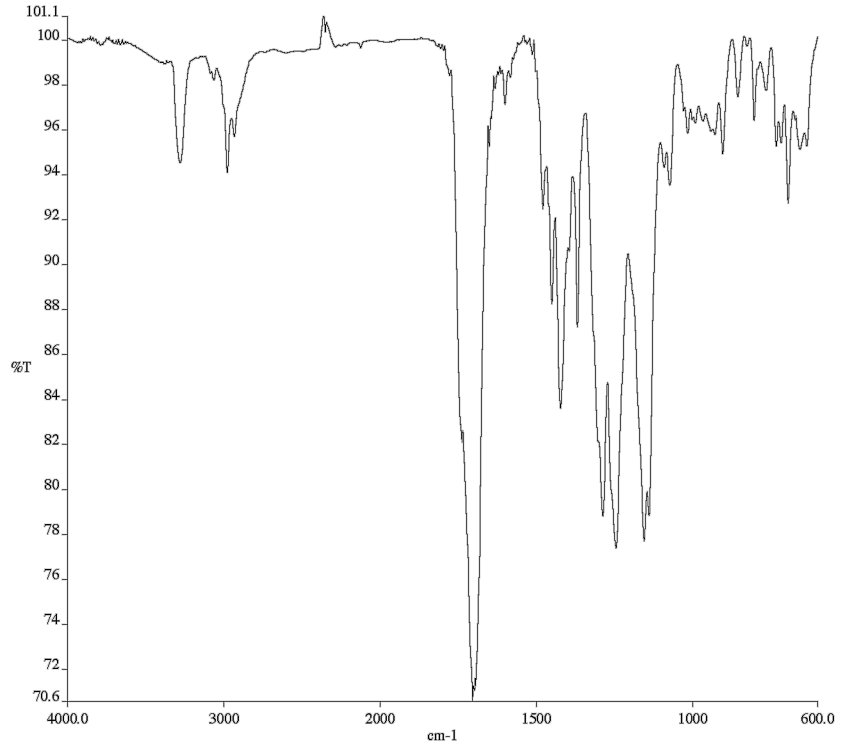

Figure A1.95 Infrared spectrum (Thin Film, NaCl) of compound **1.5i**.

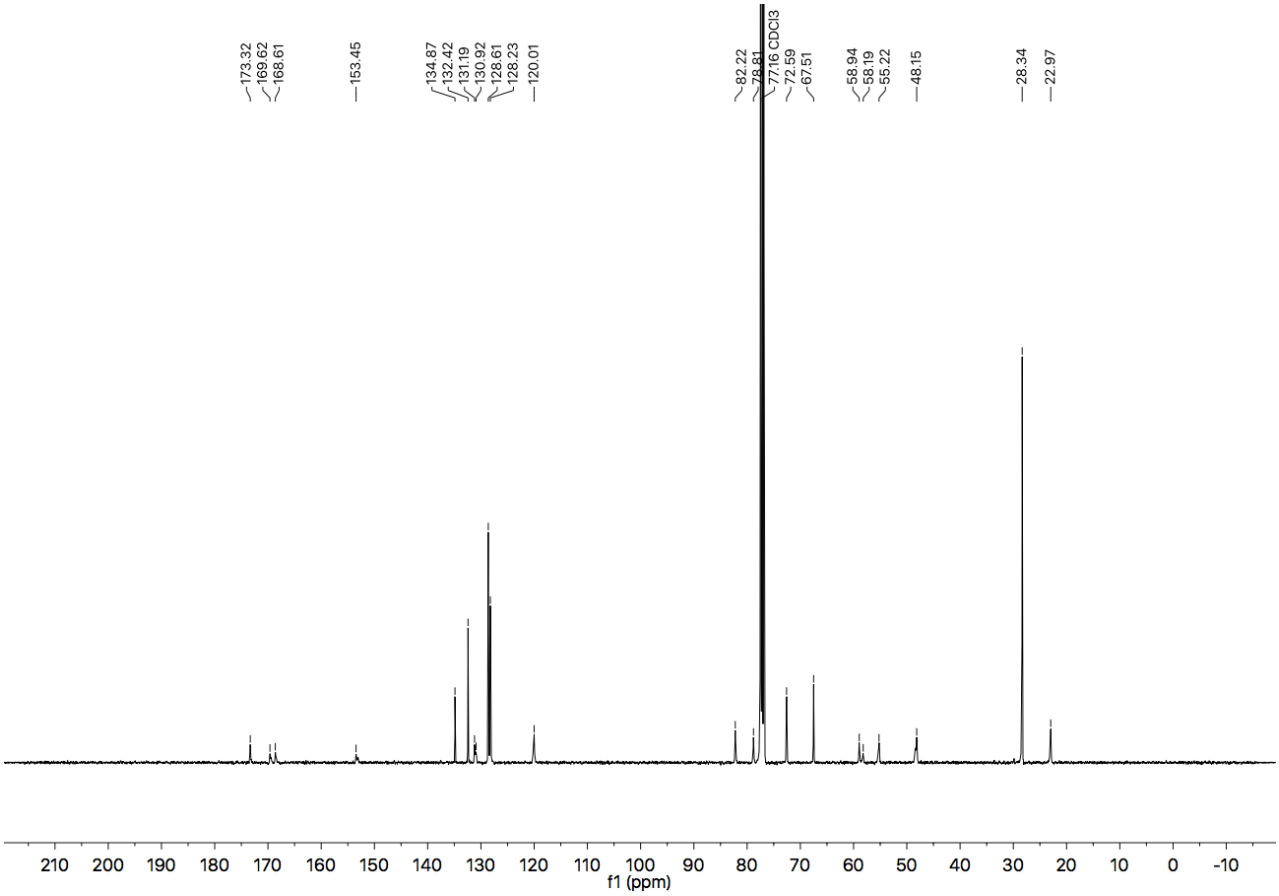

Figure A1.96 ^{13}C NMR (101 MHz, $CDCl_3$) of compound **1.5i**.

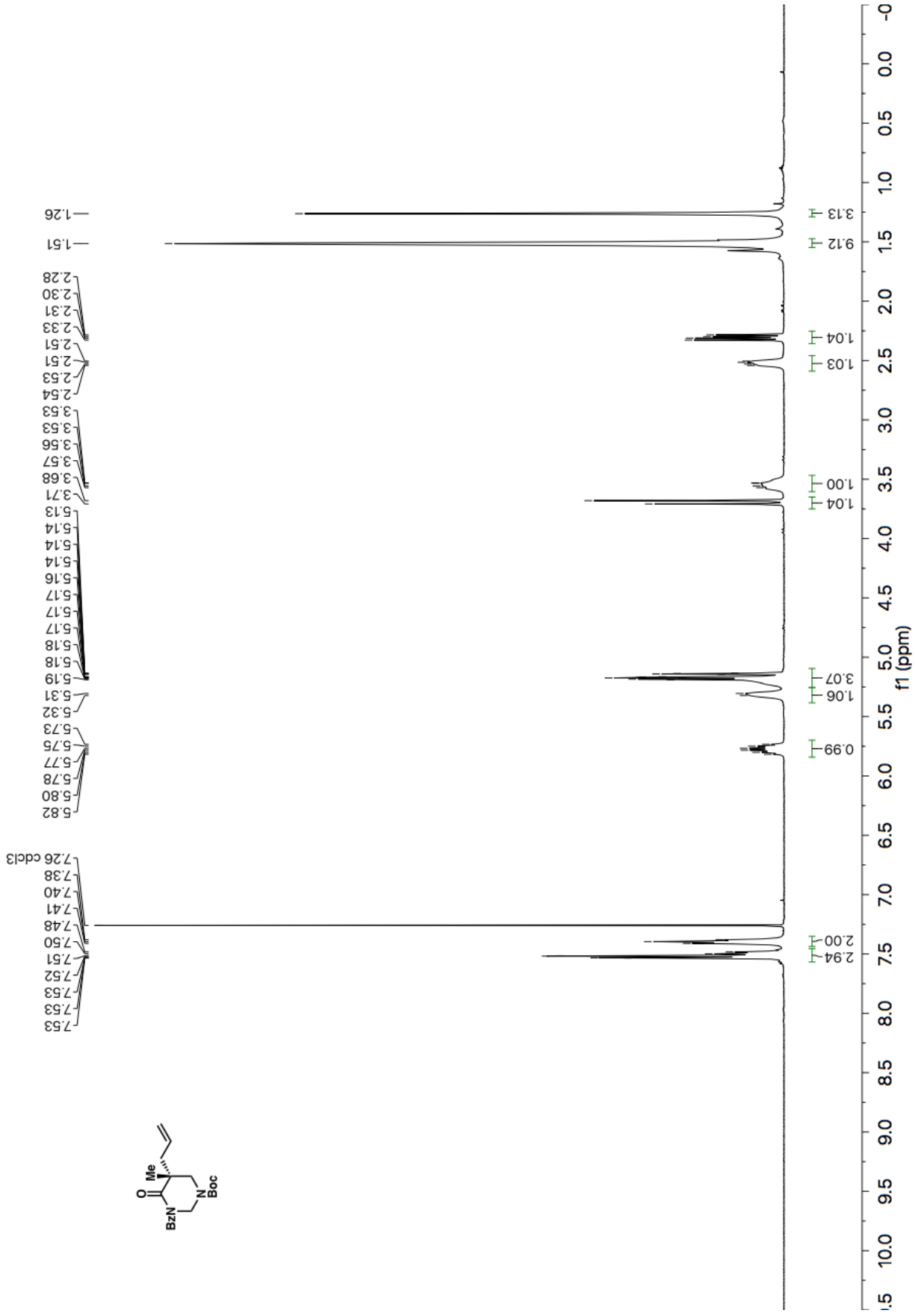

Figure A1.97 ^{1}H NMR (500 MHz, $CDCl_3$) of compound **1.6a.**

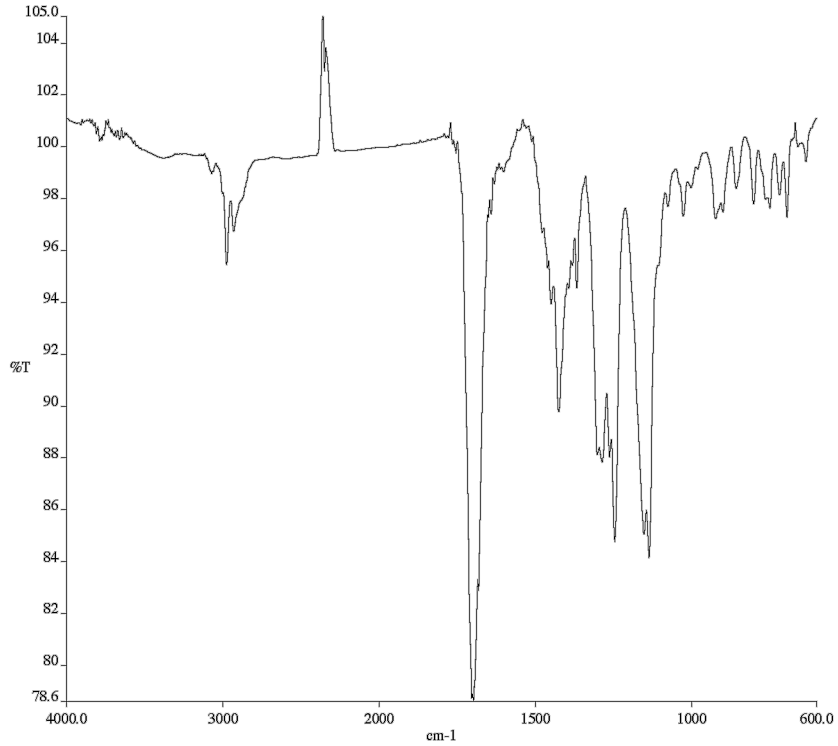

Figure A1.98 Infrared spectrum (Thin Film, NaCl) of compound **1.6a**.

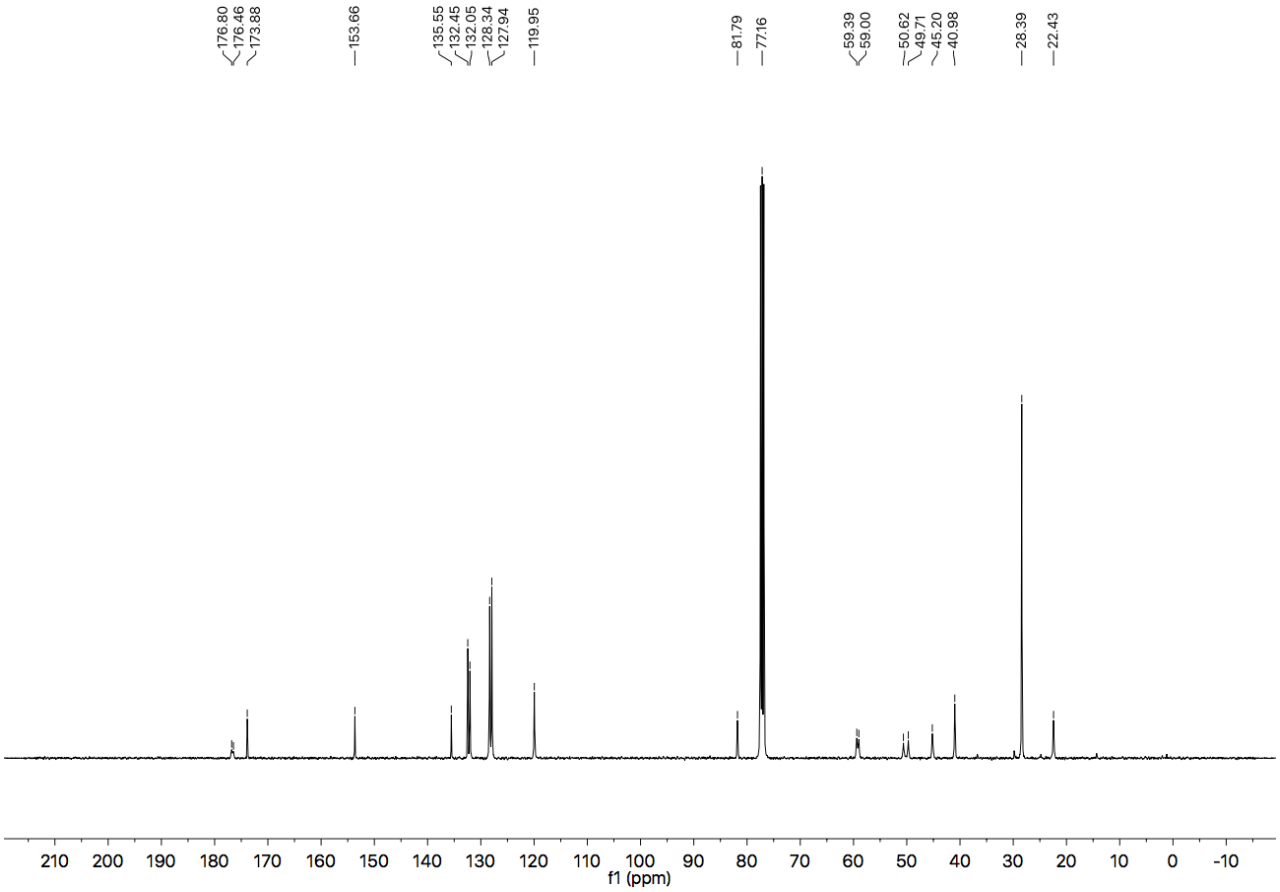

Figure A1.99 ^{13}C NMR (101 MHz, $CDCl_3$) of compound **1.6a**.

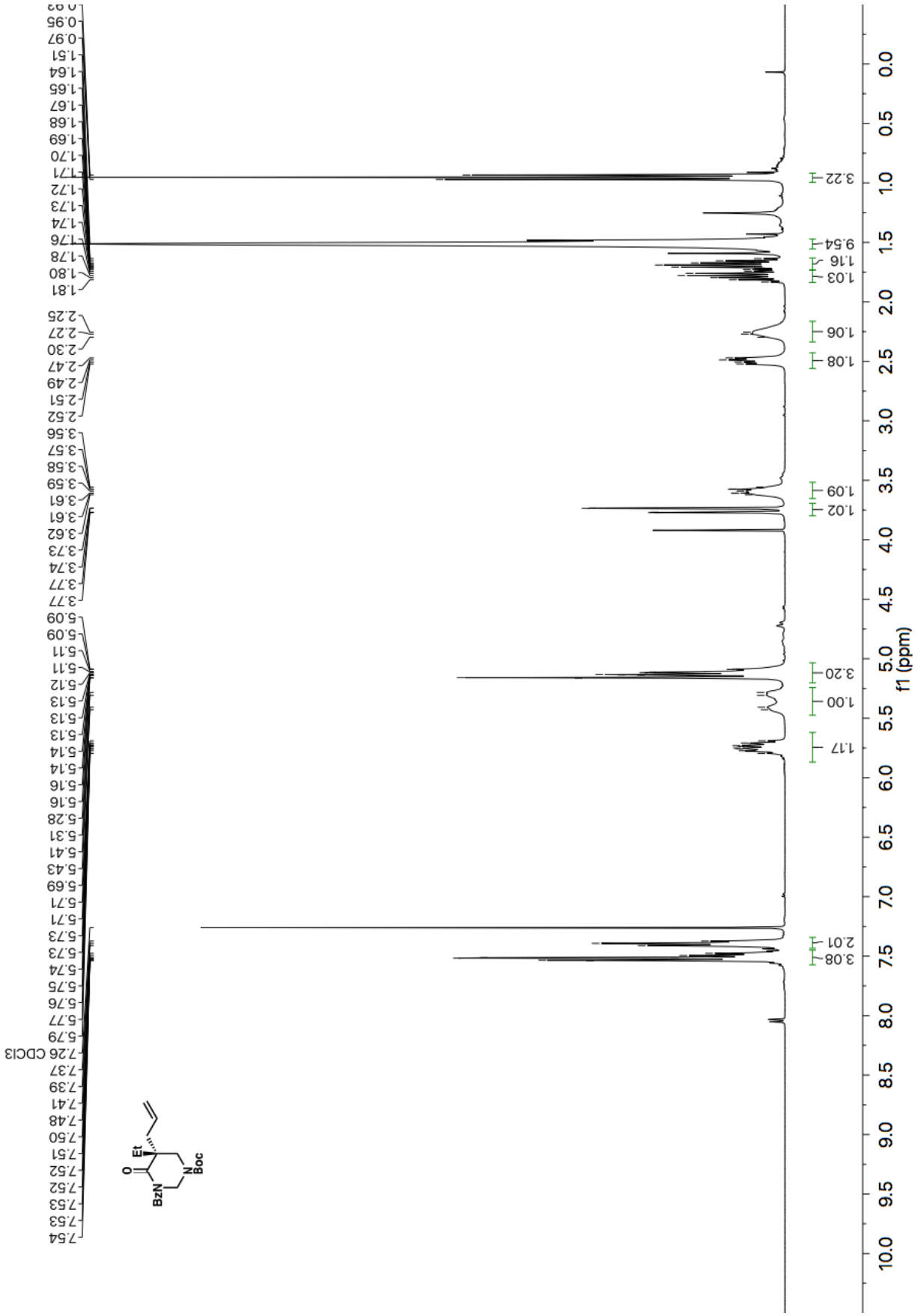

Figure A1.100 ^{1}H NMR (400 MHz, $CDCl_3$) of compound **1.6b.**

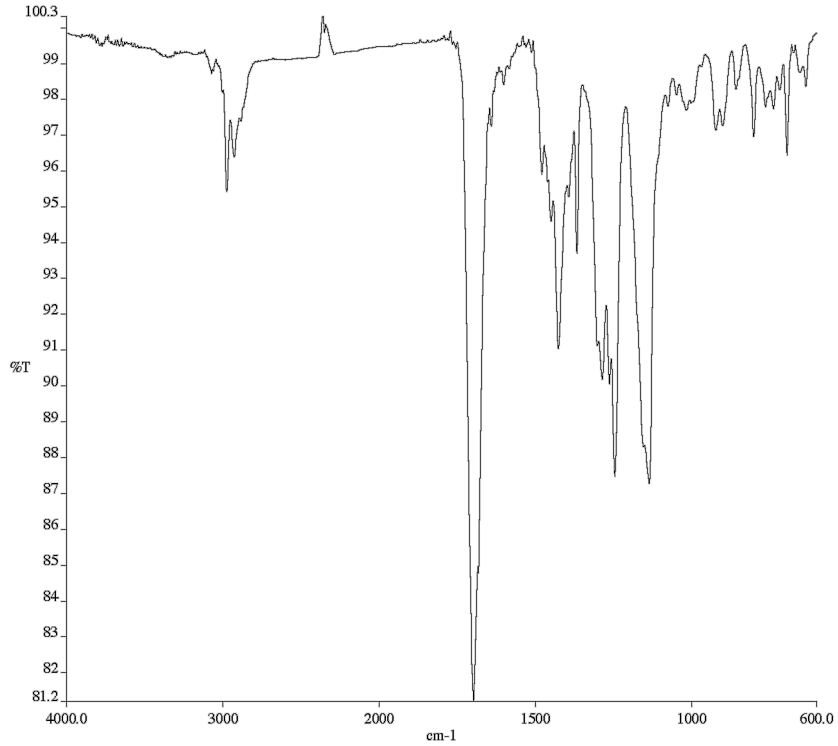

Figure A1.101 Infrared spectrum (Thin Film, NaCl) of compound **1.6b**.

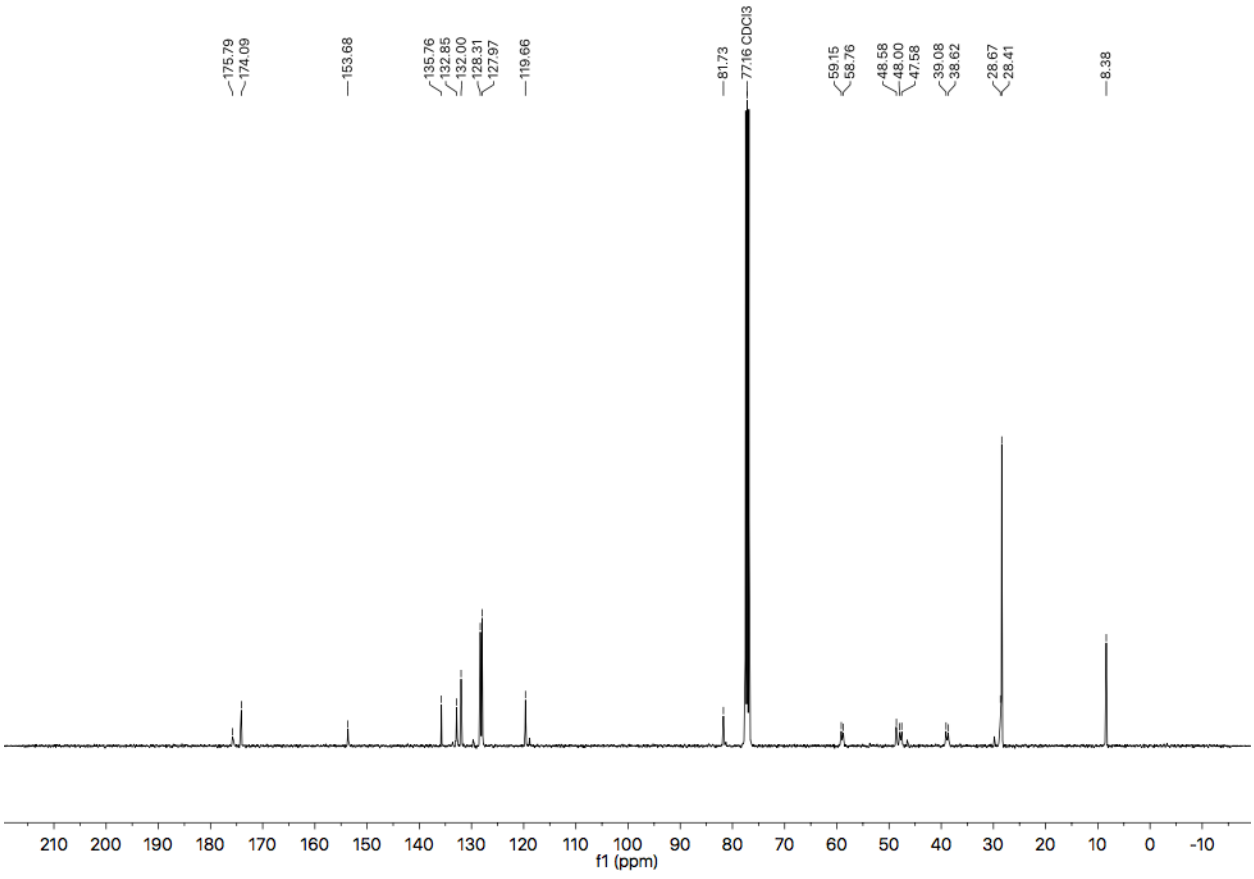

Figure A1.102 ^{13}C NMR (101 MHz, $CDCl_3$) of compound **1.6b**.

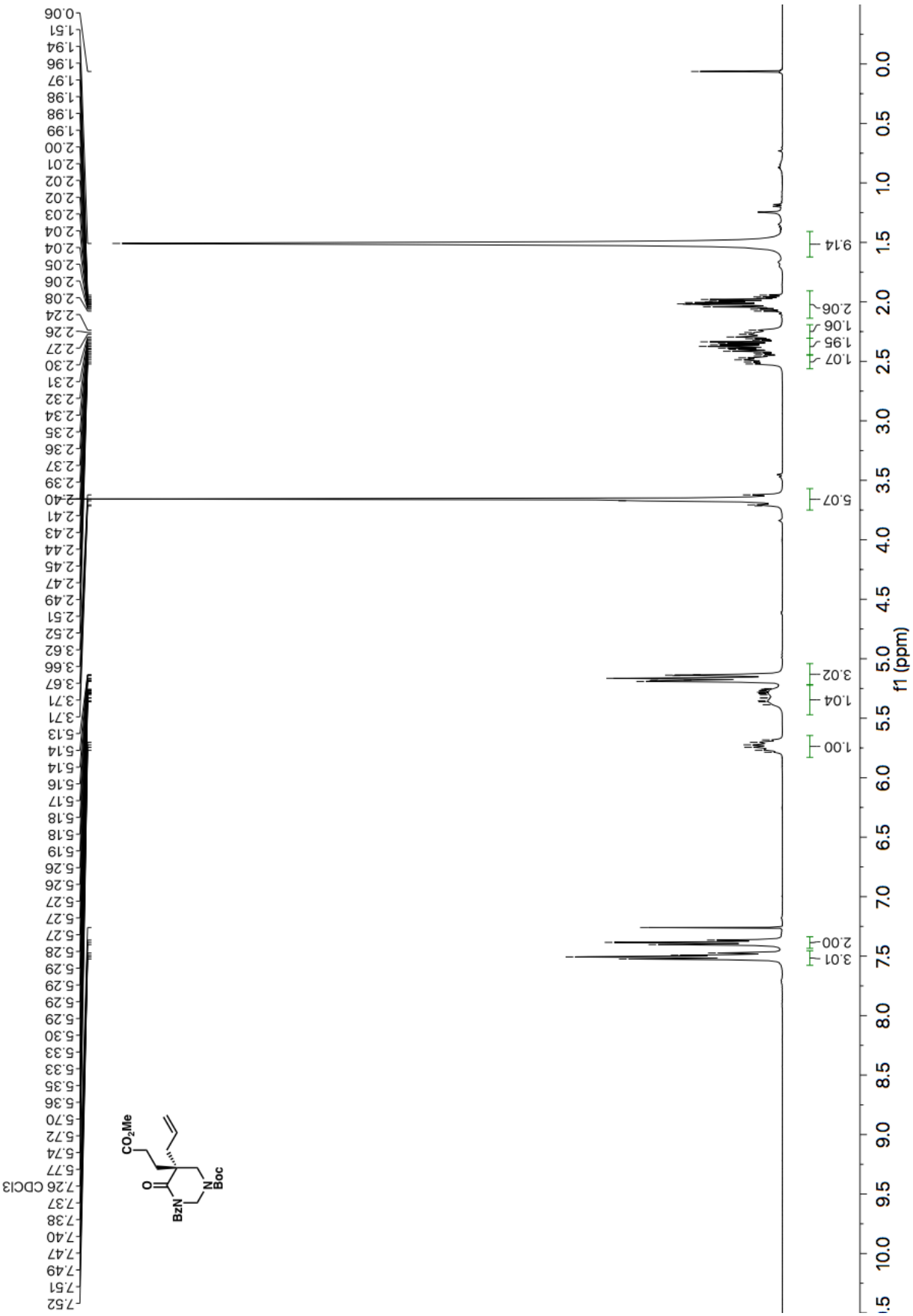

Figure A1.103 ^{1}H NMR (400 MHz, $CDCl_3$) of compound **1.6c.**

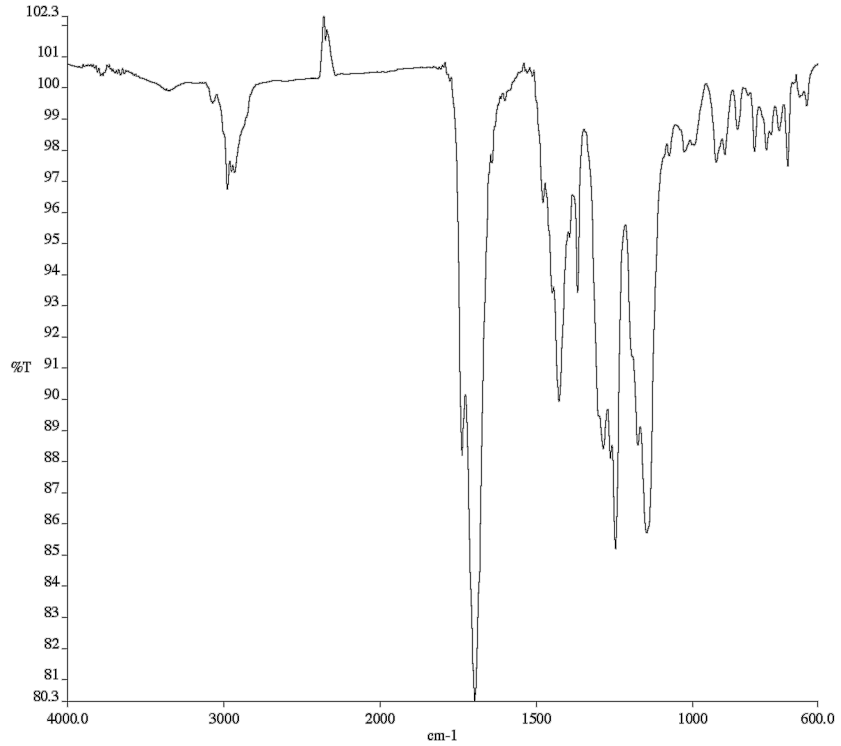

Figure A1.104 Infrared spectrum (Thin Film, NaCl) of compound **1.6c**.

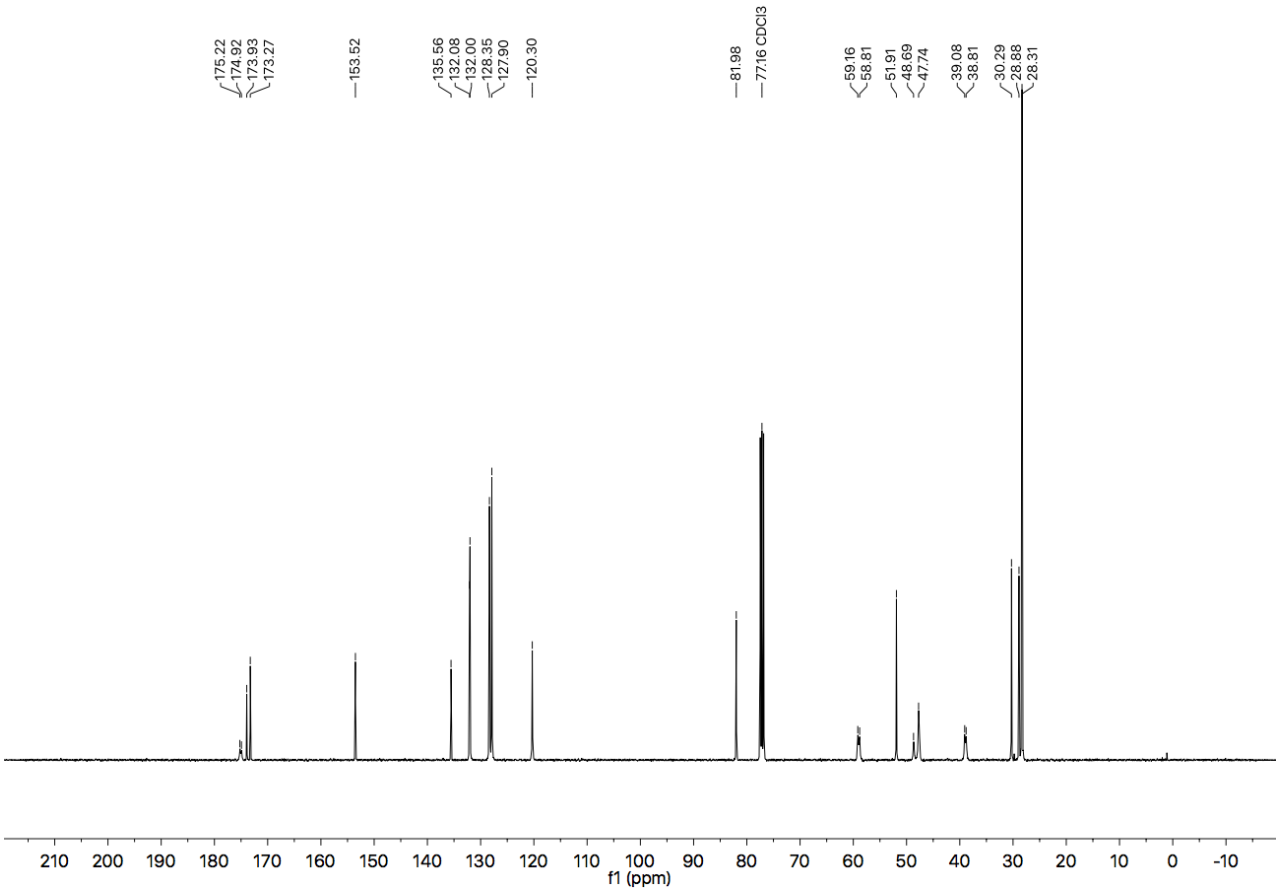

Figure A1.105 ^{13}C NMR (101 MHz, $CDCl_3$) of compound **1.6c**.

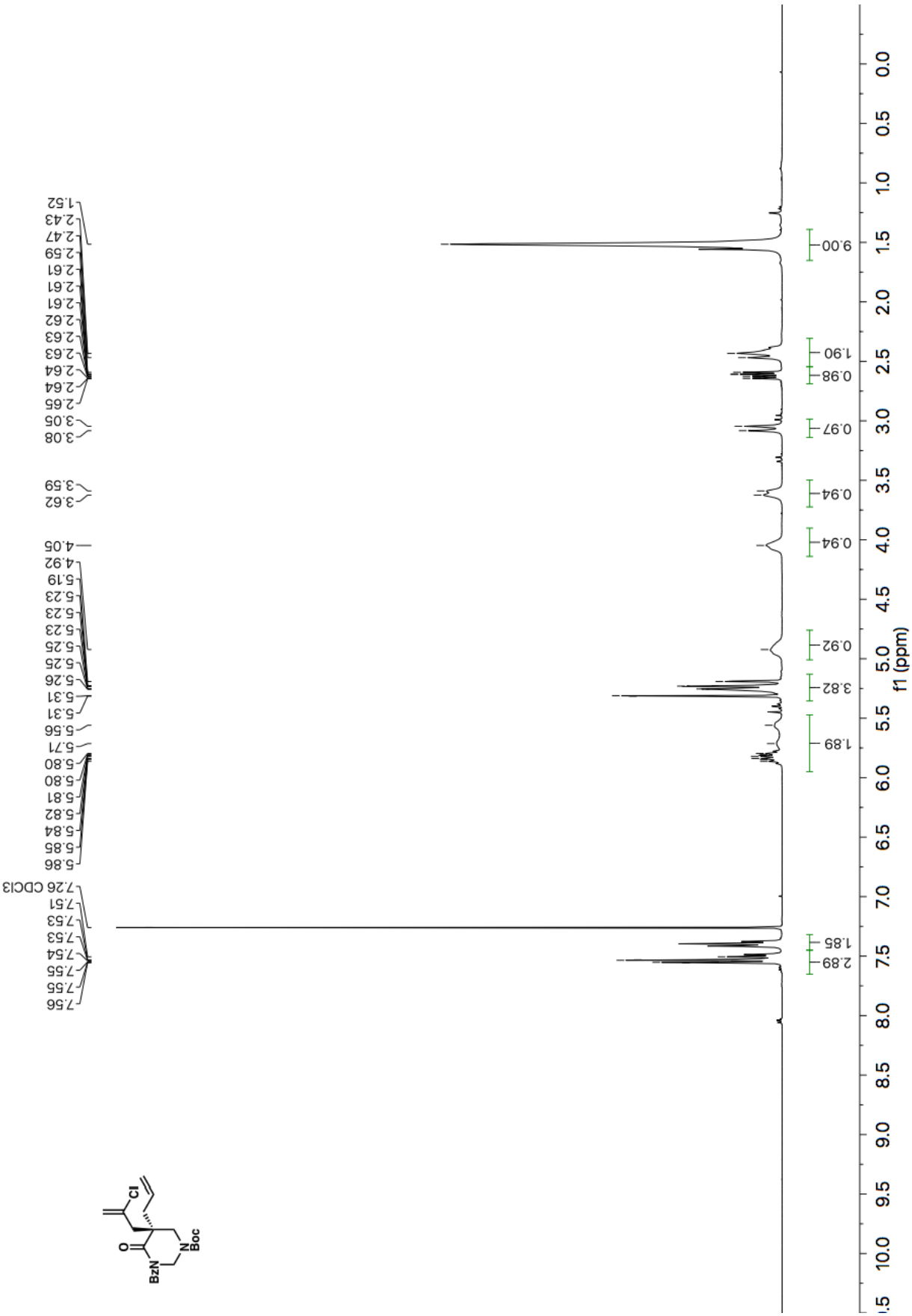

Figure A1.106 ^{1}H NMR (400 MHz, $CDCl_3$) of compound **1.6d.**

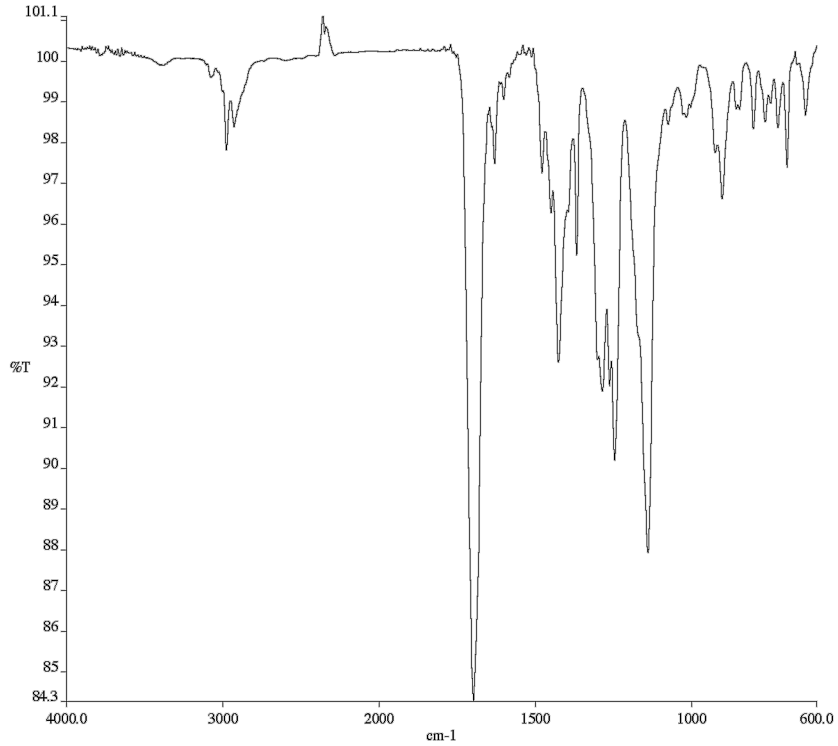

Figure A1.107 Infrared spectrum (Thin Film, NaCl) of compound **1.6d**.

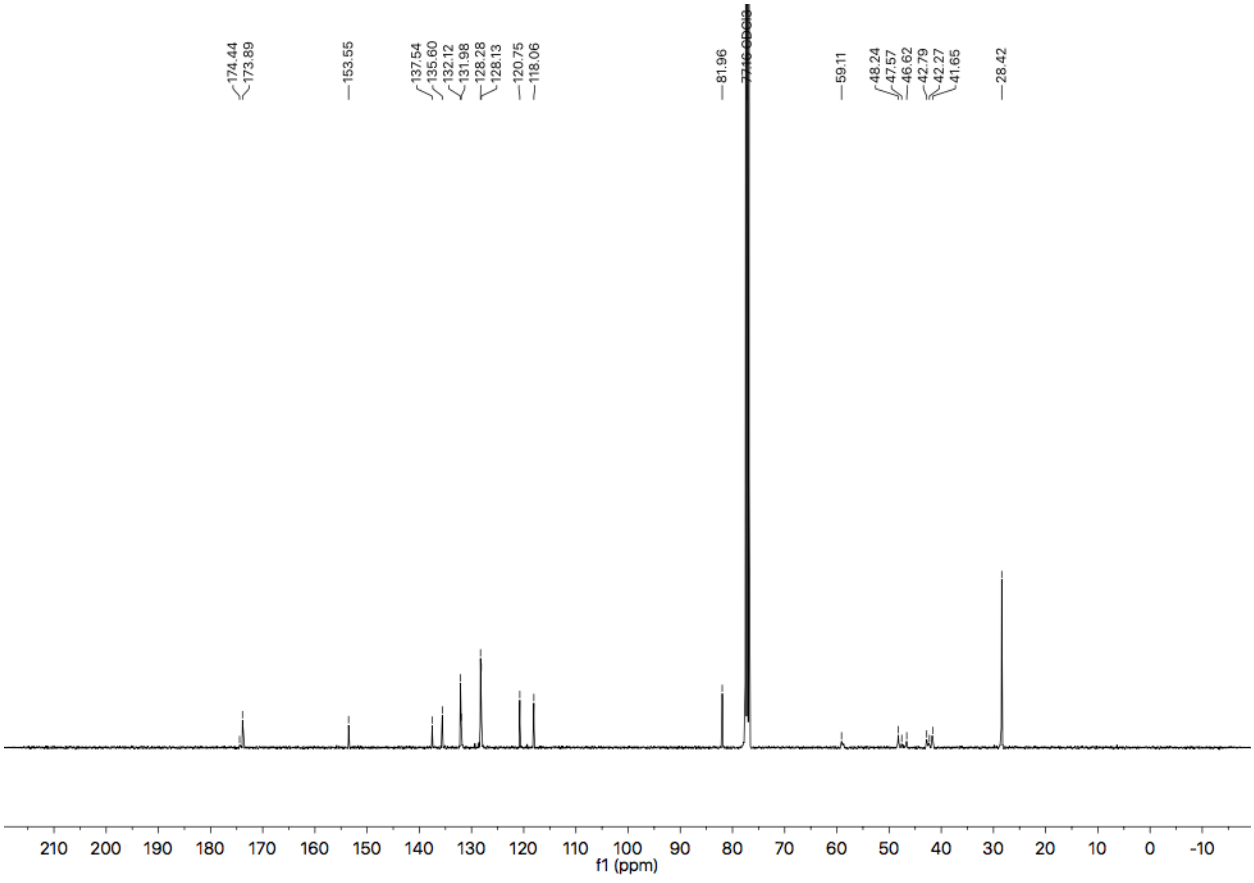

Figure A1.108 ^{13}C NMR (101 MHz, $CDCl_3$) of compound **1.6d**.

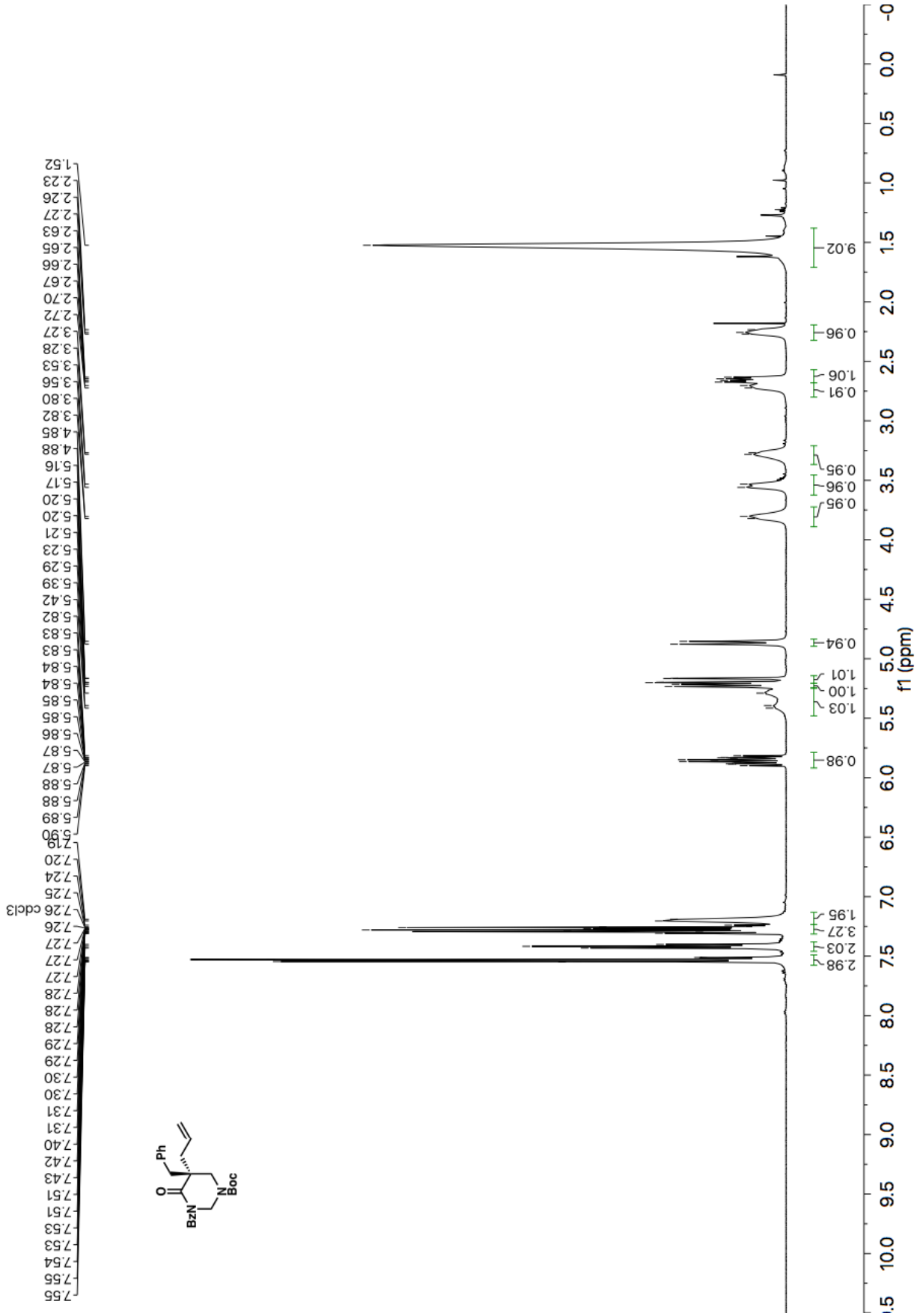

Figure A1.109 ^{1}H NMR (500 MHz, $CDCl_3$) of compound **1.6e.**

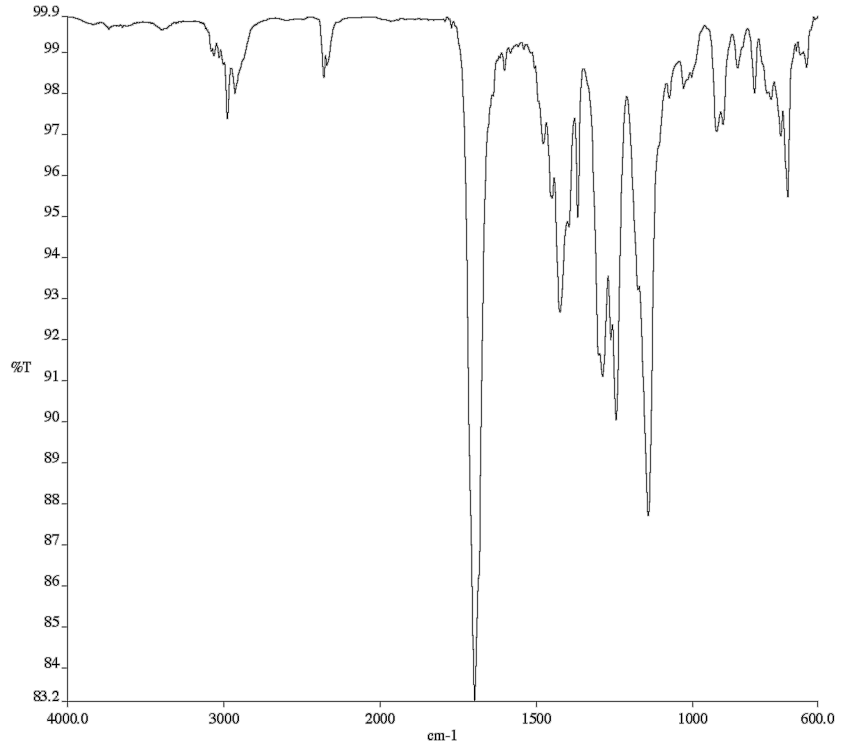

Figure A1.110 Infrared spectrum (Thin Film, NaCl) of compound **1.6e**.

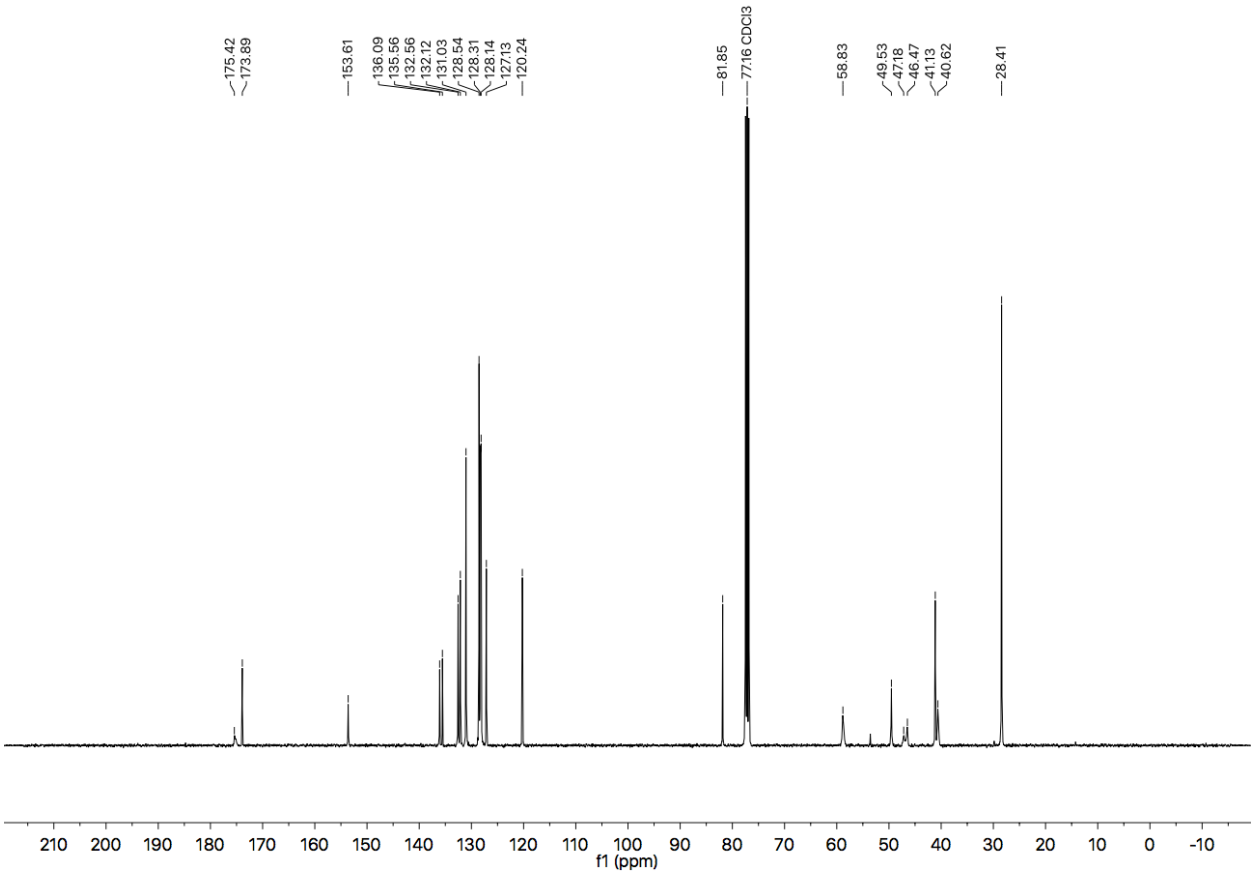

Figure A1.111 ^{13}C NMR (101 MHz, $CDCl_3$) of compound **1.6e**.

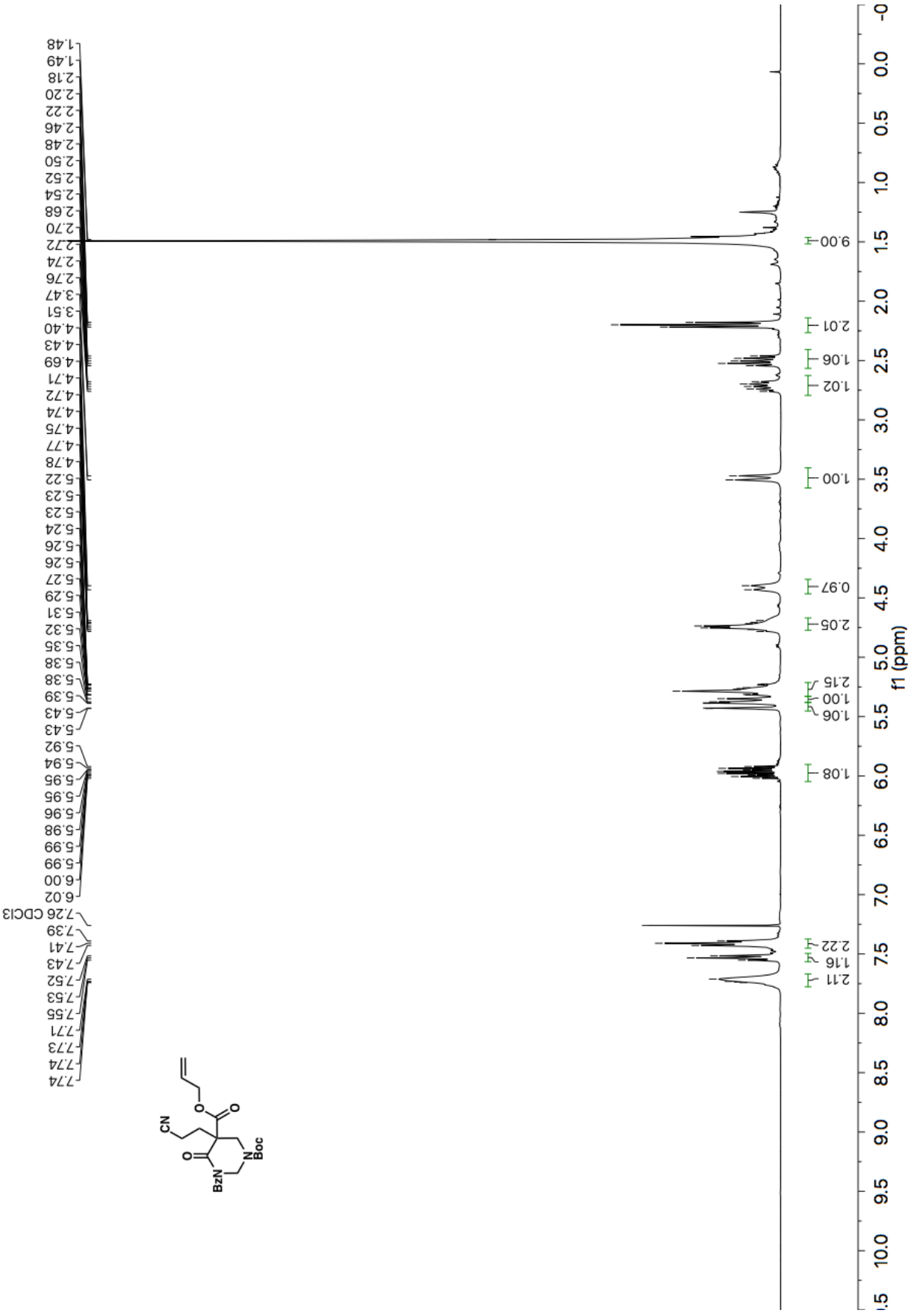

Figure A1.112 ^{1}H NMR (500 MHz, $CDCl_3$) of compound **1.6f.**

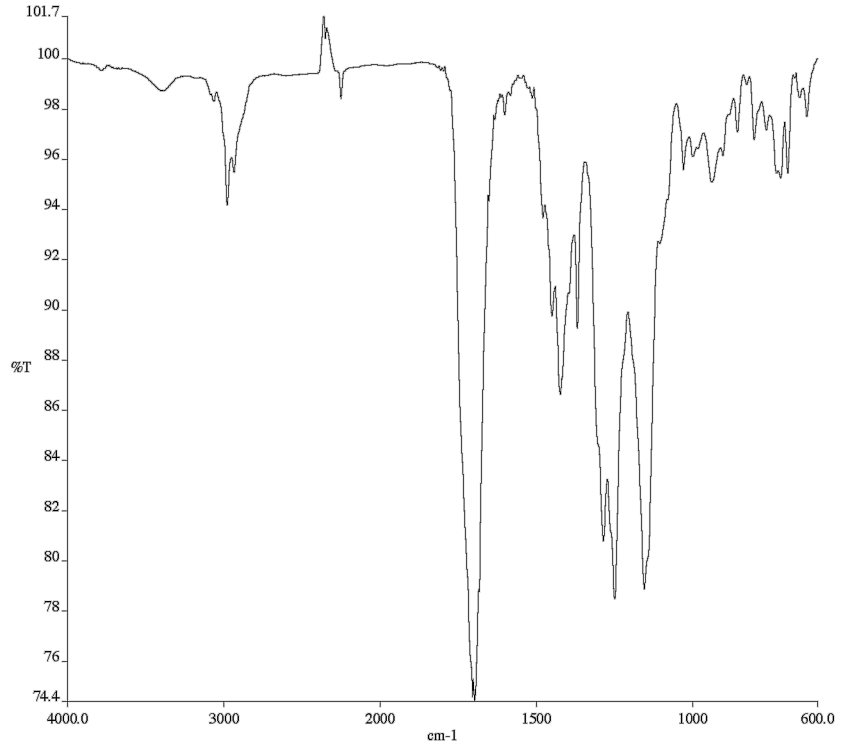

Figure A1.113 Infrared spectrum (Thin Film, NaCl) of compound **1.6f**.

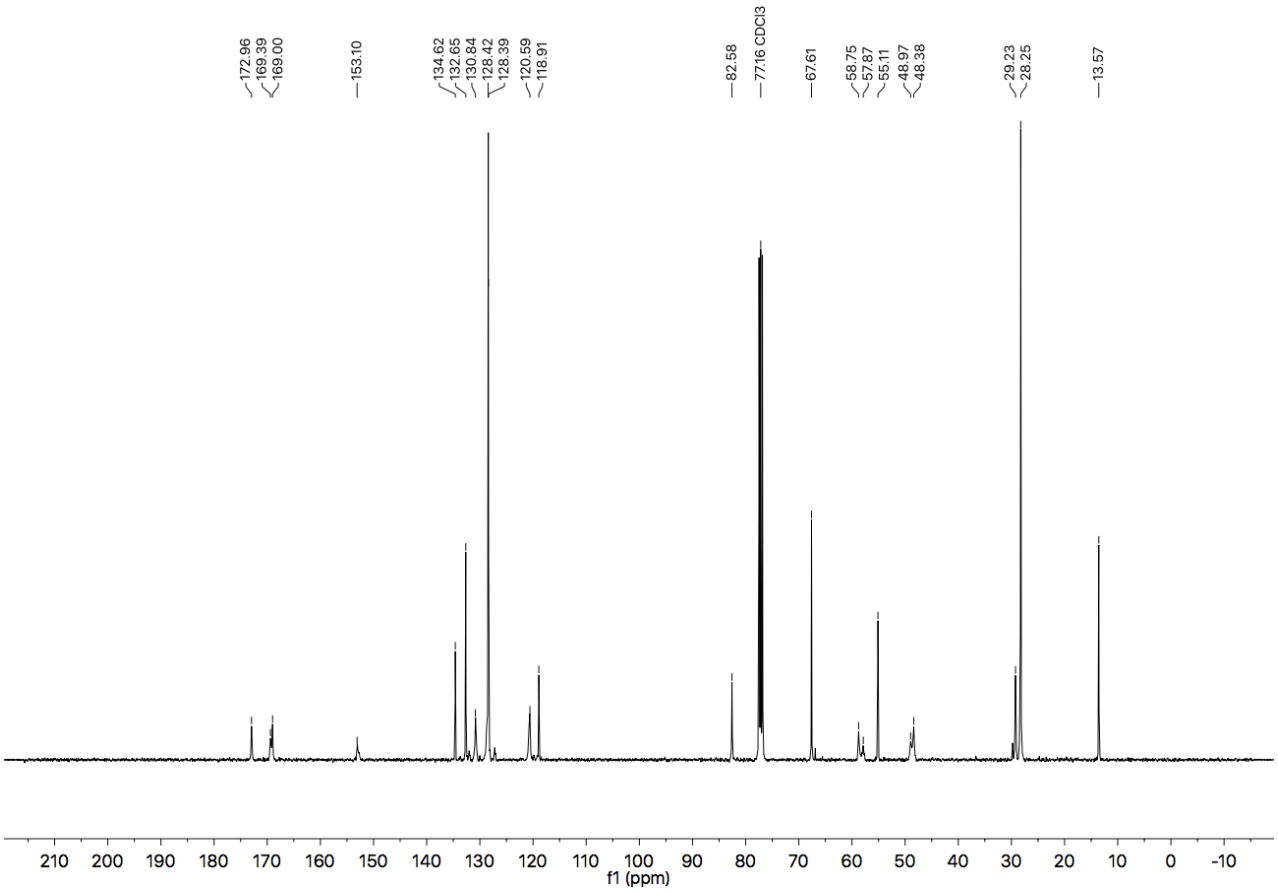

Figure A1.114 ^{13}C NMR (101 MHz, $CDCl_3$) of compound **1.6f**.

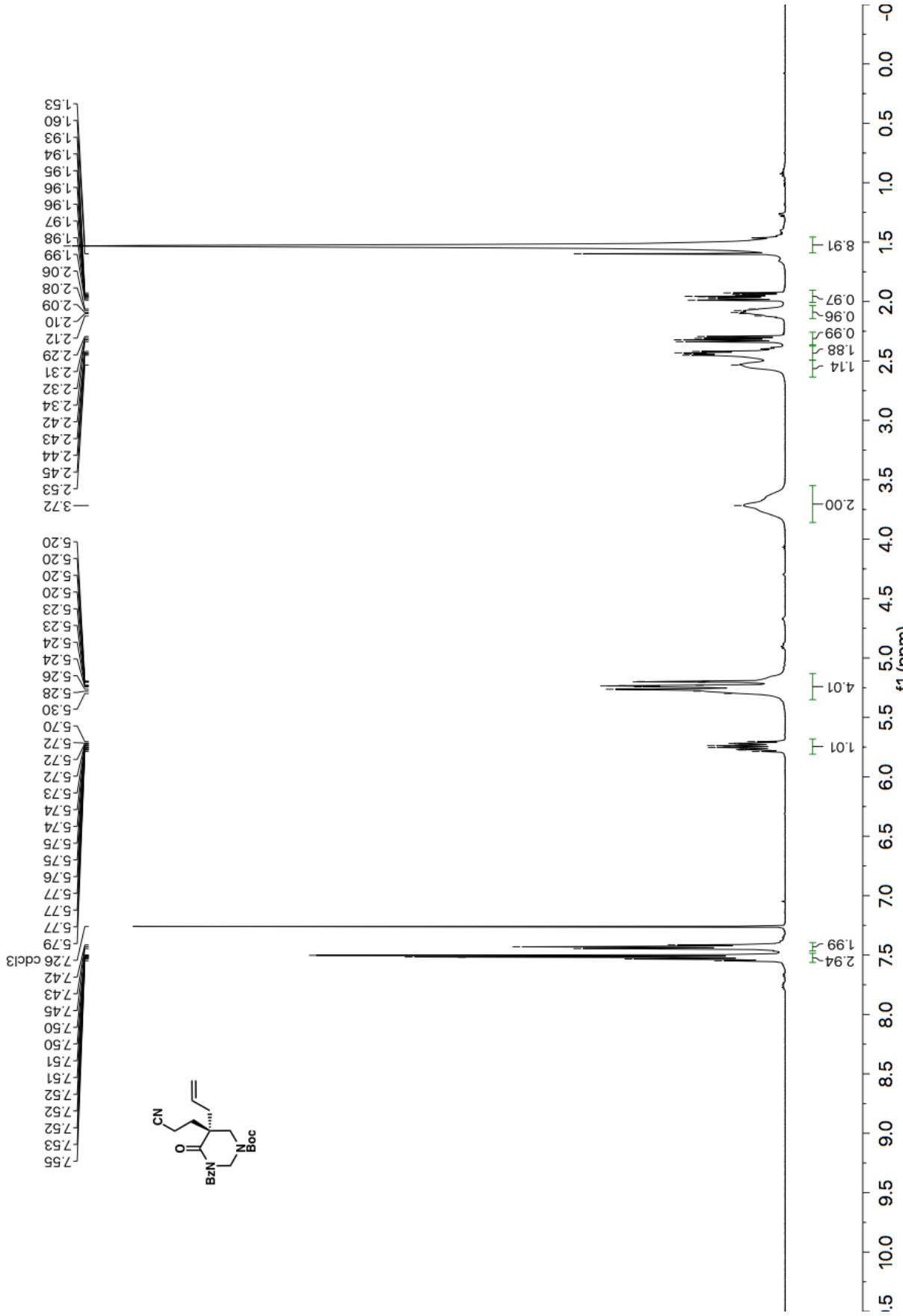

Figure A1.115 ^{1}H NMR (500 MHz, $CDCl_3$) of compound **1.6f.**

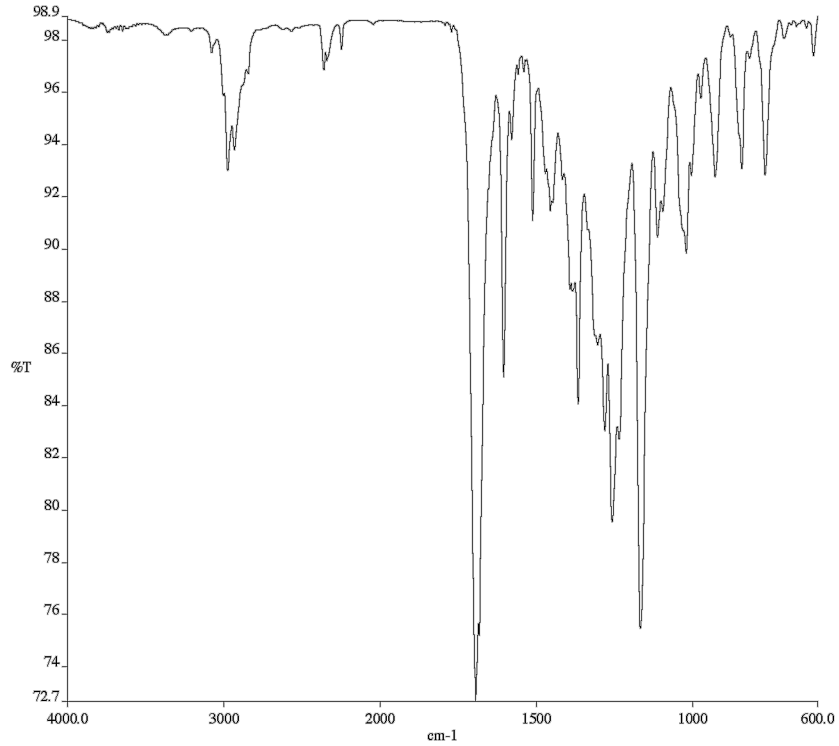

Figure A1.116 Infrared spectrum (Thin Film, NaCl) of compound **1.6f**.

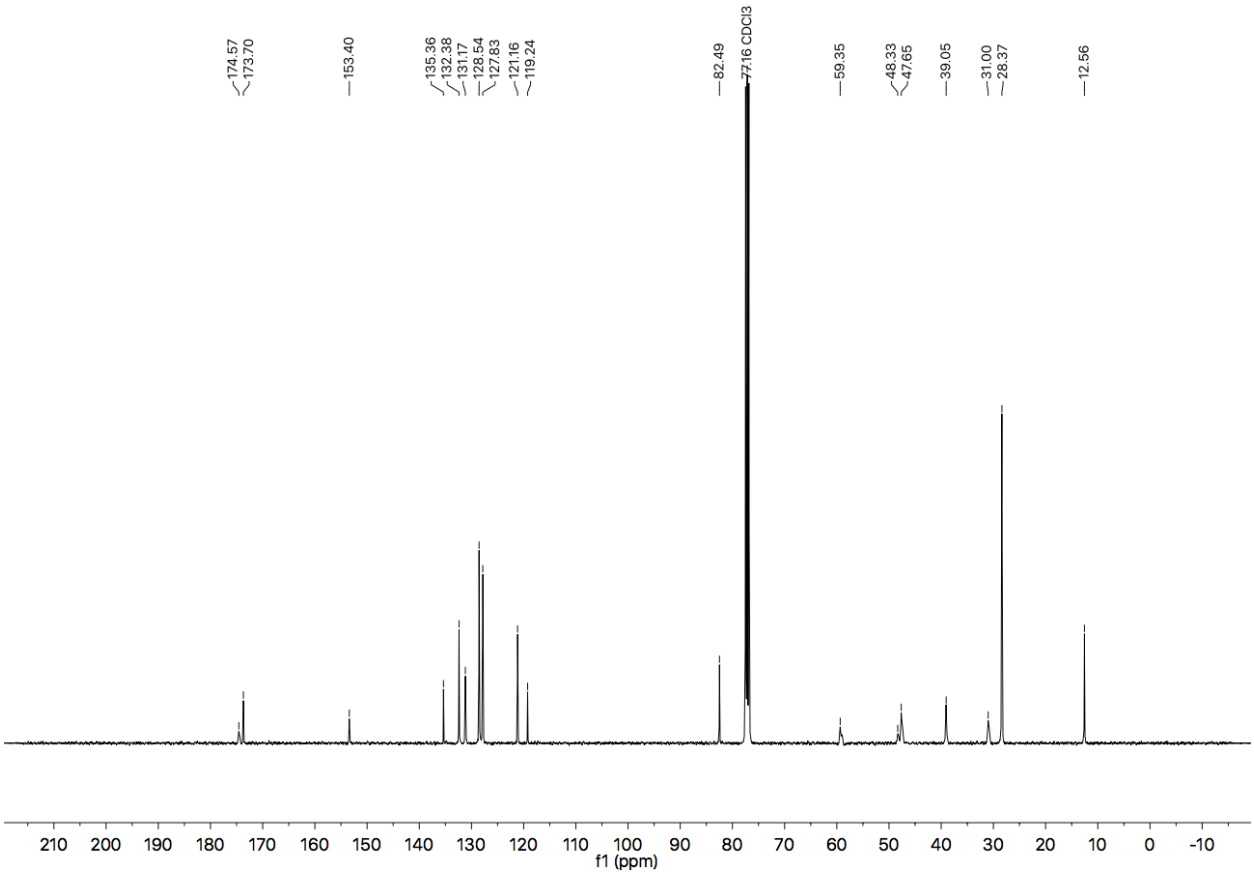

Figure A1.117 ^{13}C NMR (101 MHz, $CDCl_3$) of compound **1.6f**.

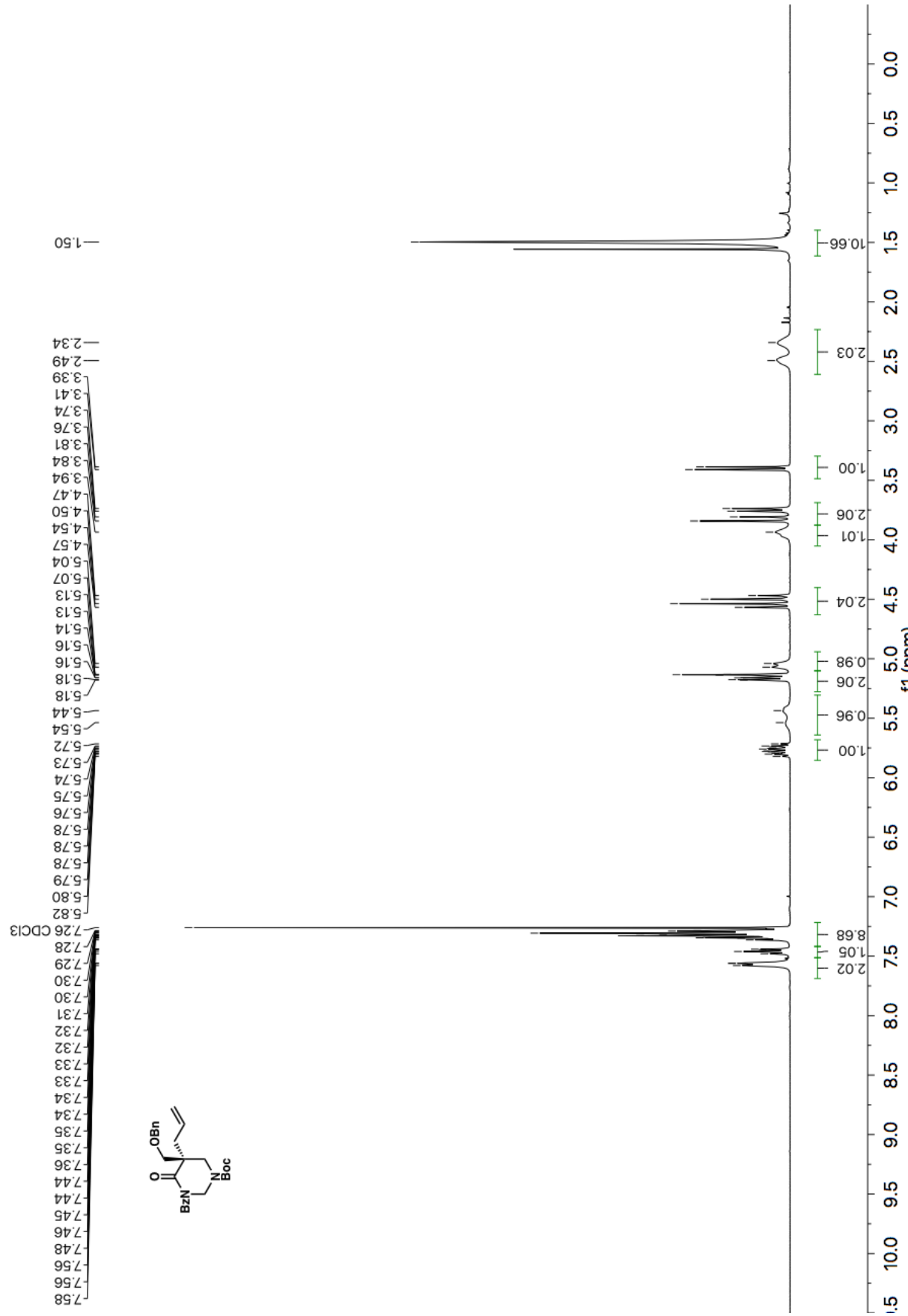

Figure A1.118 ^{1}H NMR (400 MHz, $CDCl_3$) of compound **1.6g.**

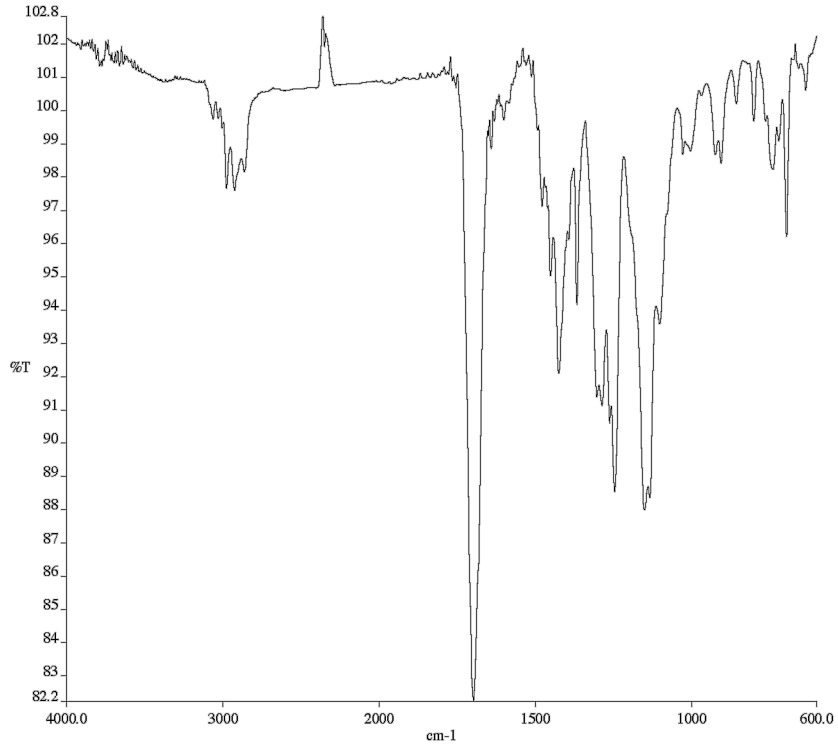

Figure A1.119 Infrared spectrum (Thin Film, NaCl) of compound **1.6g**.

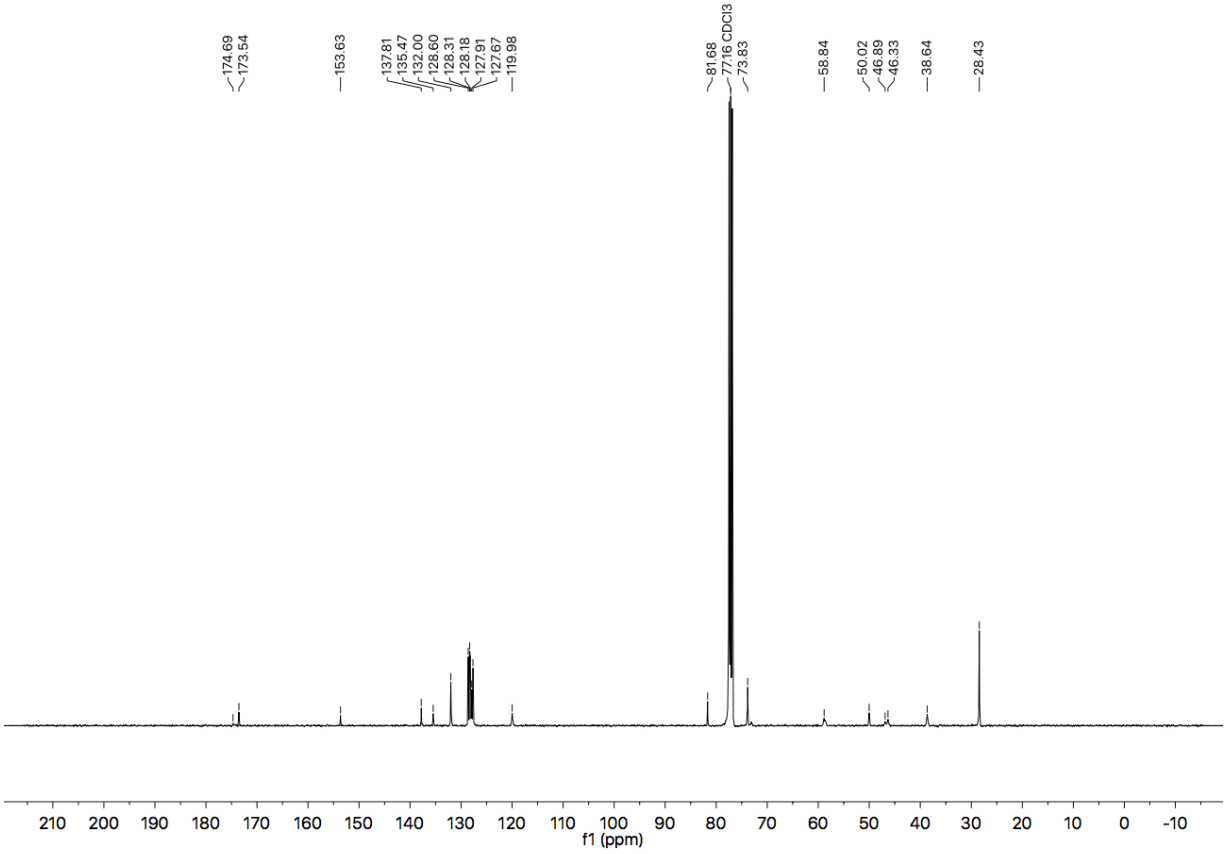

Figure A1.120 ^{13}C NMR (101 MHz, $CDCl_3$) of compound **1.6g**.

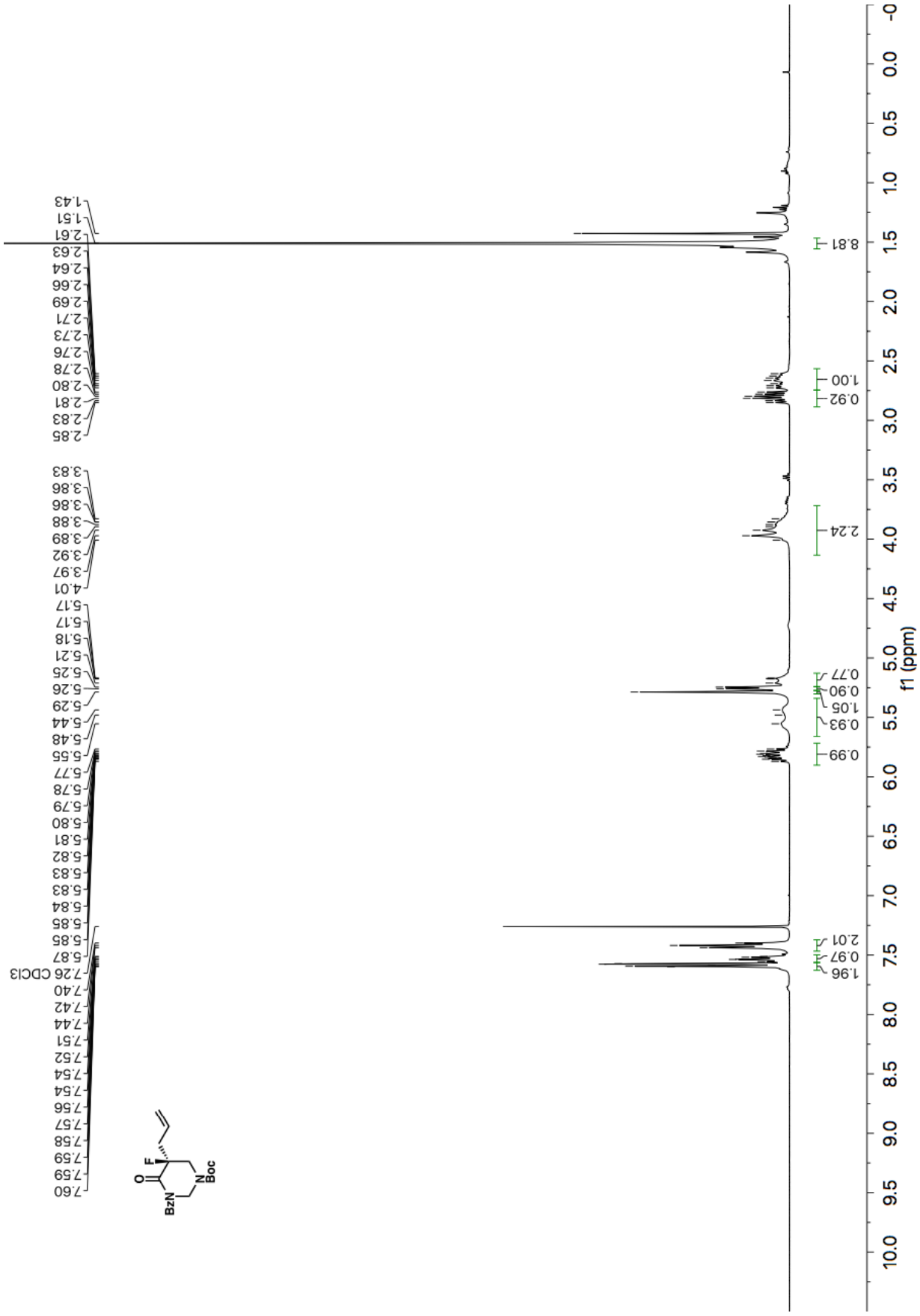

Figure A1.121 ^{1}H NMR (400 MHz, $CDCl_3$) of compound **1.6h**

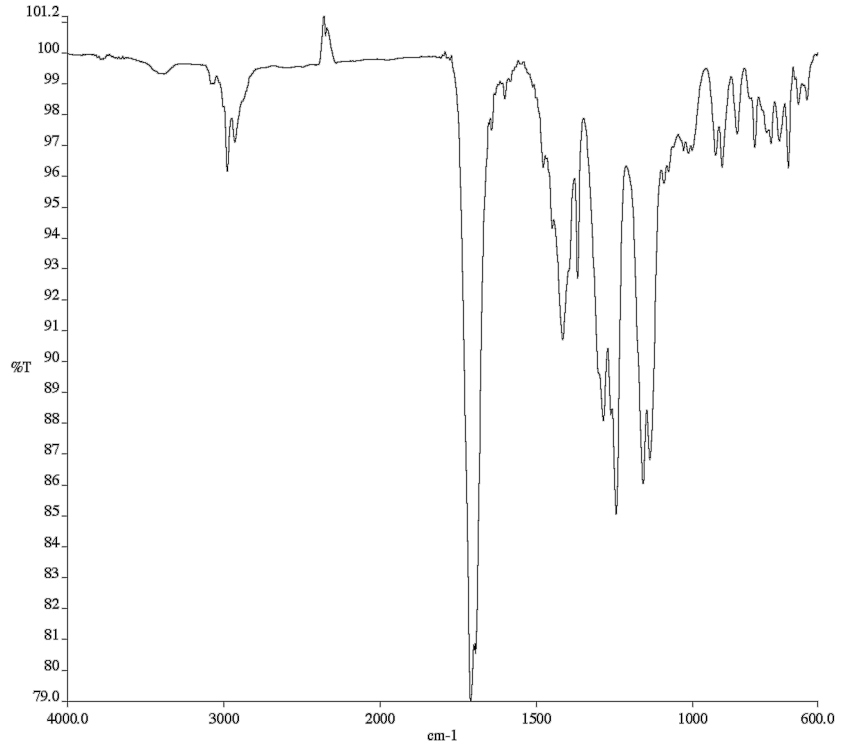

Figure A1.122 Infrared spectrum (Thin Film, NaCl) of compound **1.6h**.

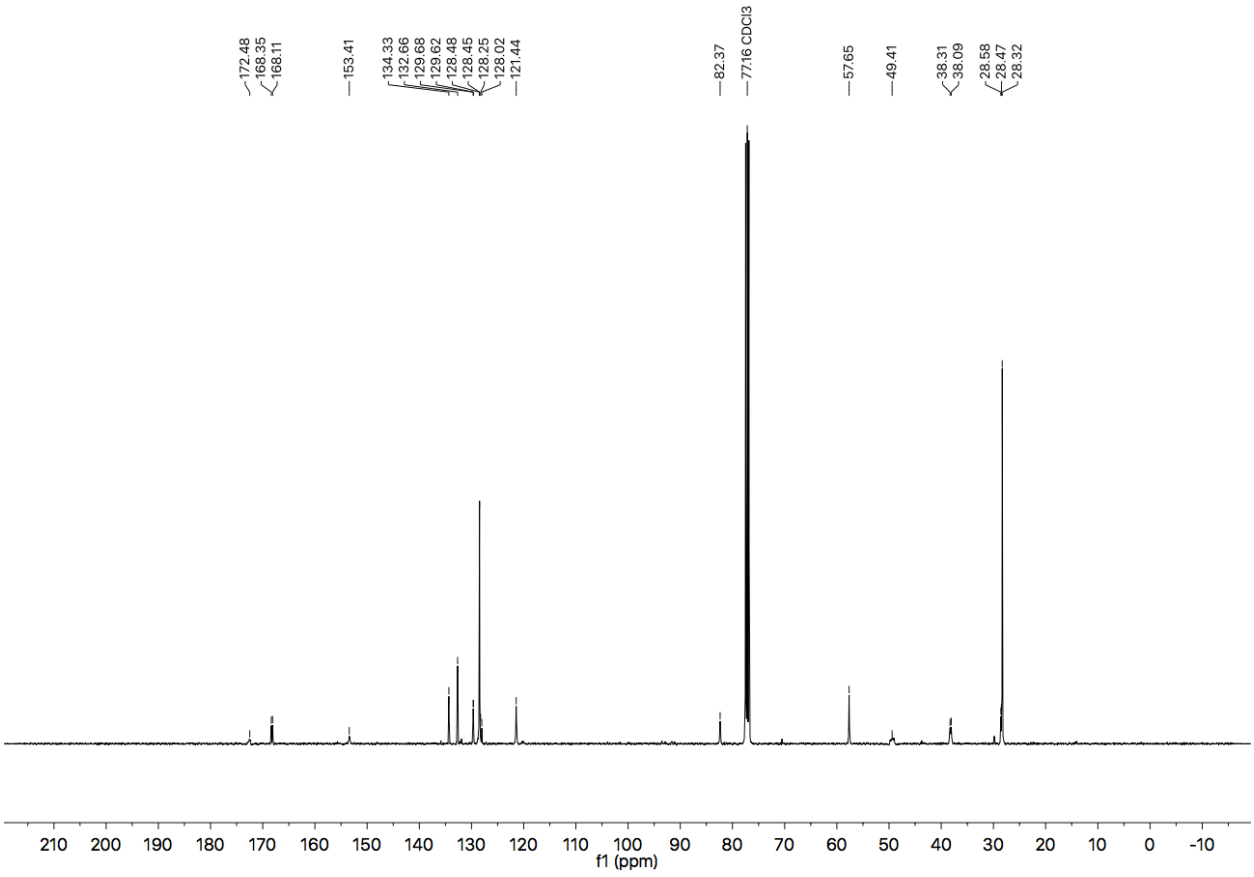

Figure A1.123 ^{13}C NMR (101 MHz, $CDCl_3$) of compound **1.6h**.

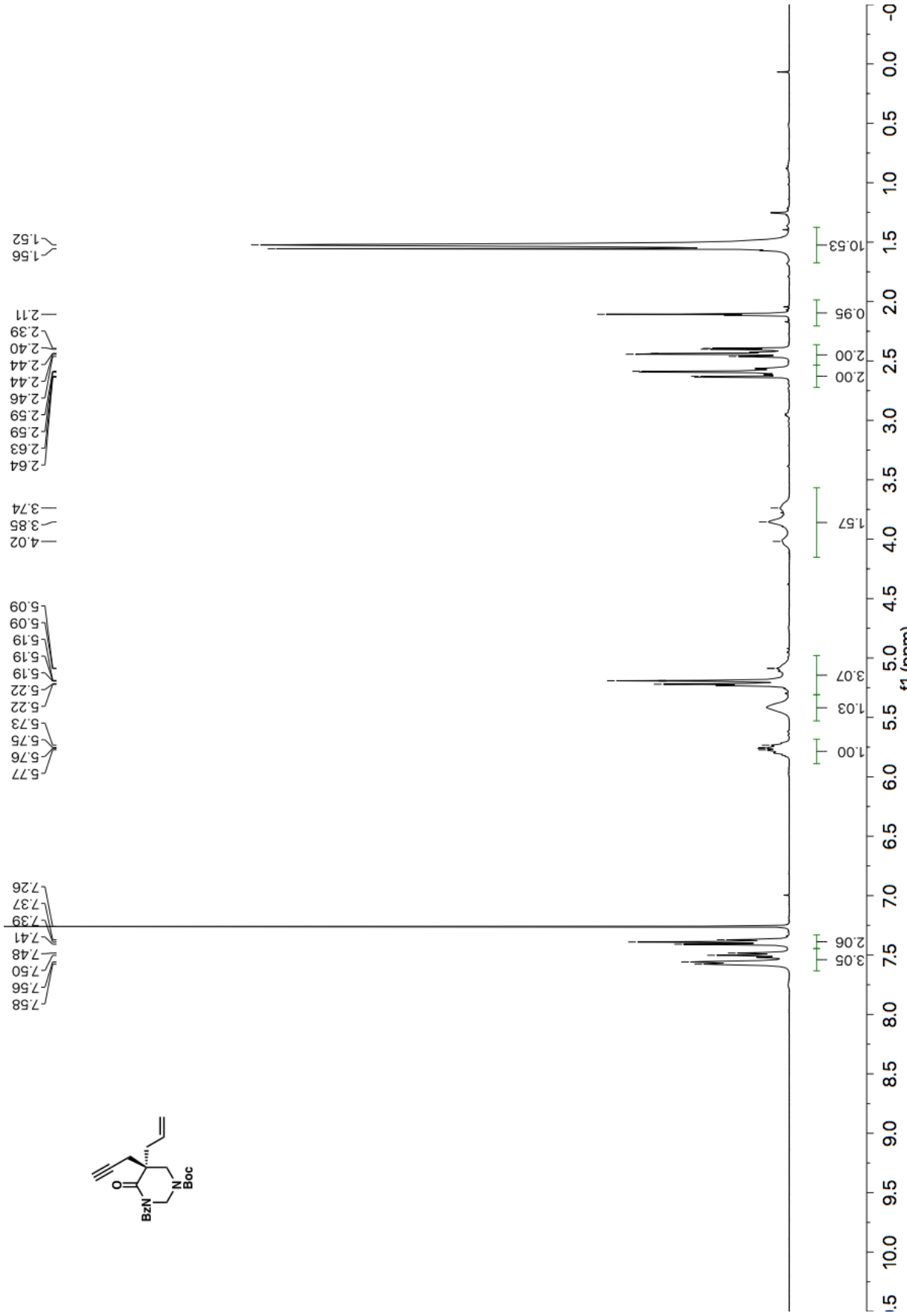

Figure A1.124 ^{1}H NMR (400 MHz, $CDCl_3$) of compound **1.6i.**

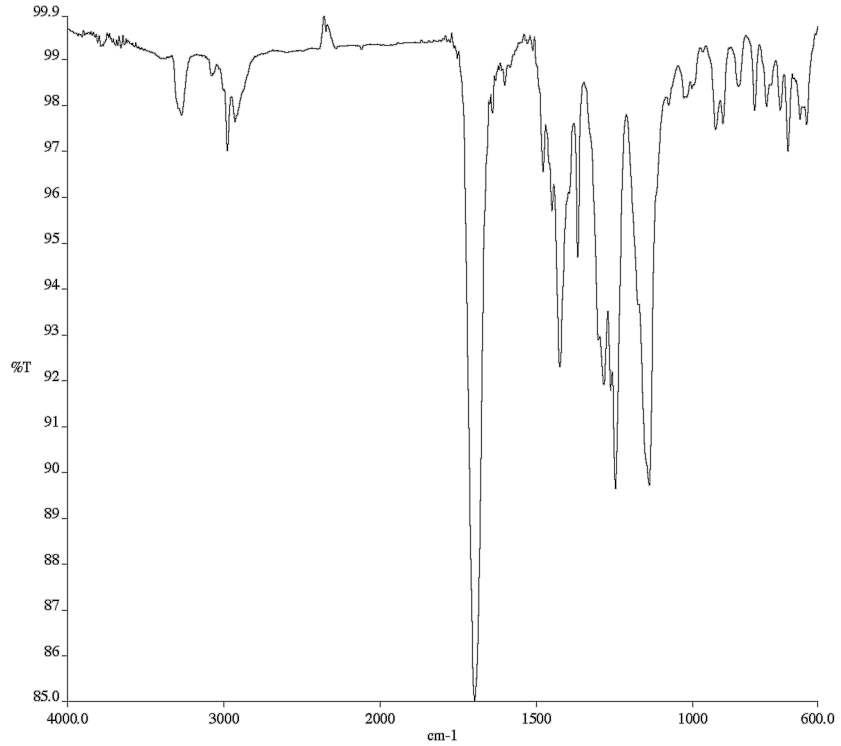

Figure A1.125 Infrared spectrum (Thin Film, NaCl) of compound **1.6i**.

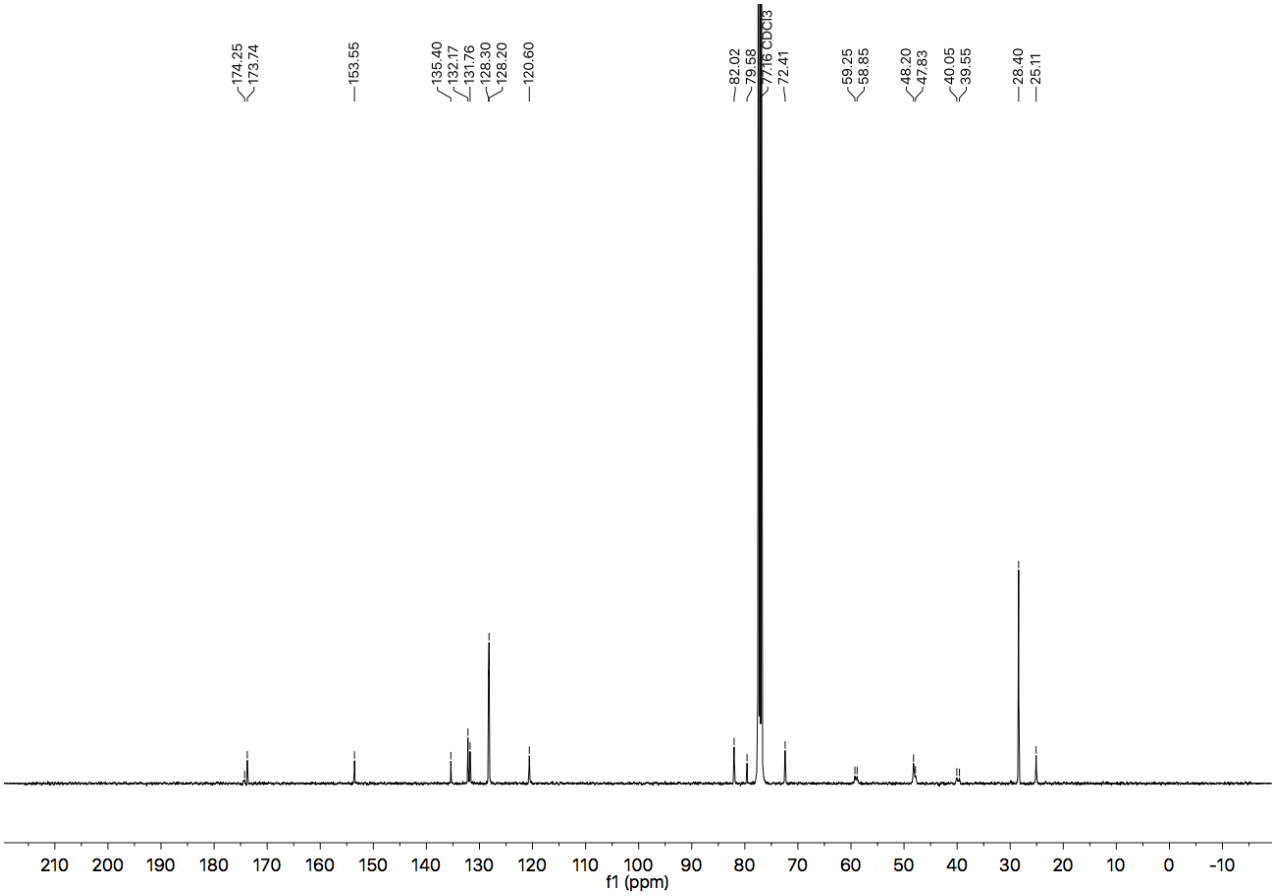

Figure A1.126 ^{13}C NMR (101 MHz, $CDCl_3$) of compound **1.6i**.

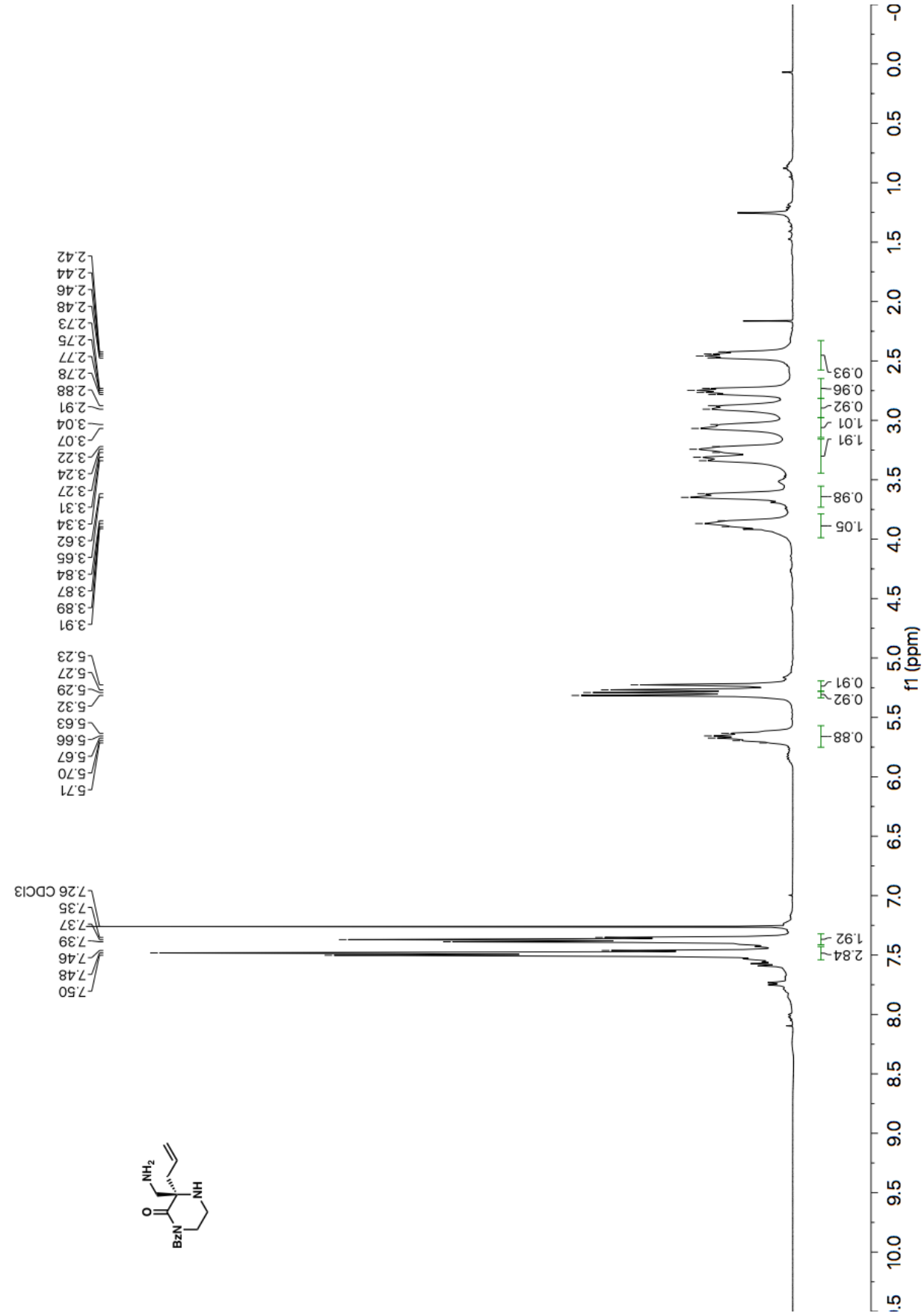

Figure A1.127 ^{1}H NMR (400 MHz, $CDCl_3$) of compound **1.8.**

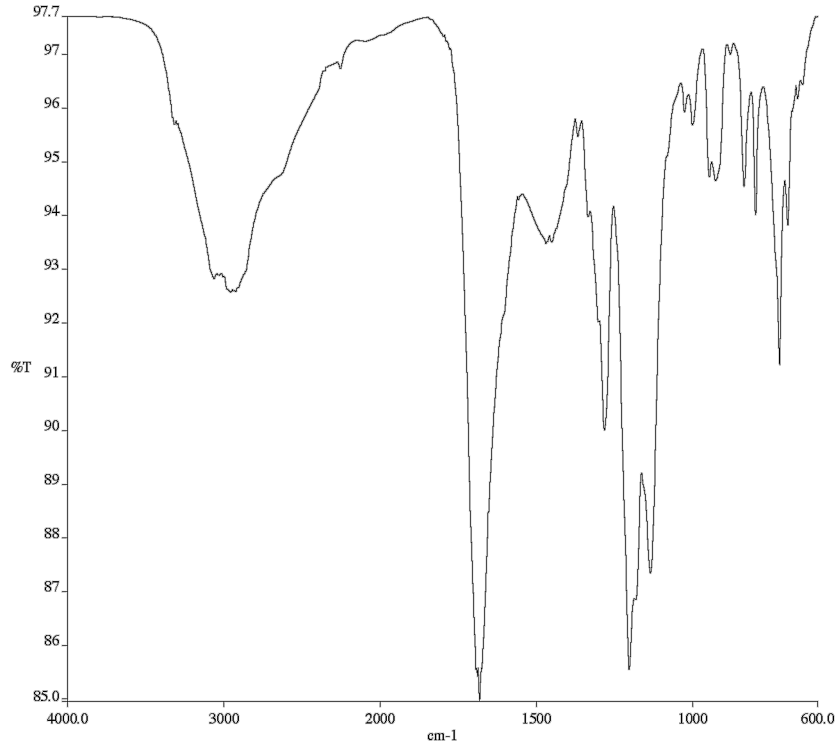

Figure A1.128 Infrared spectrum (Thin Film, NaCl) of compound **1.8**.

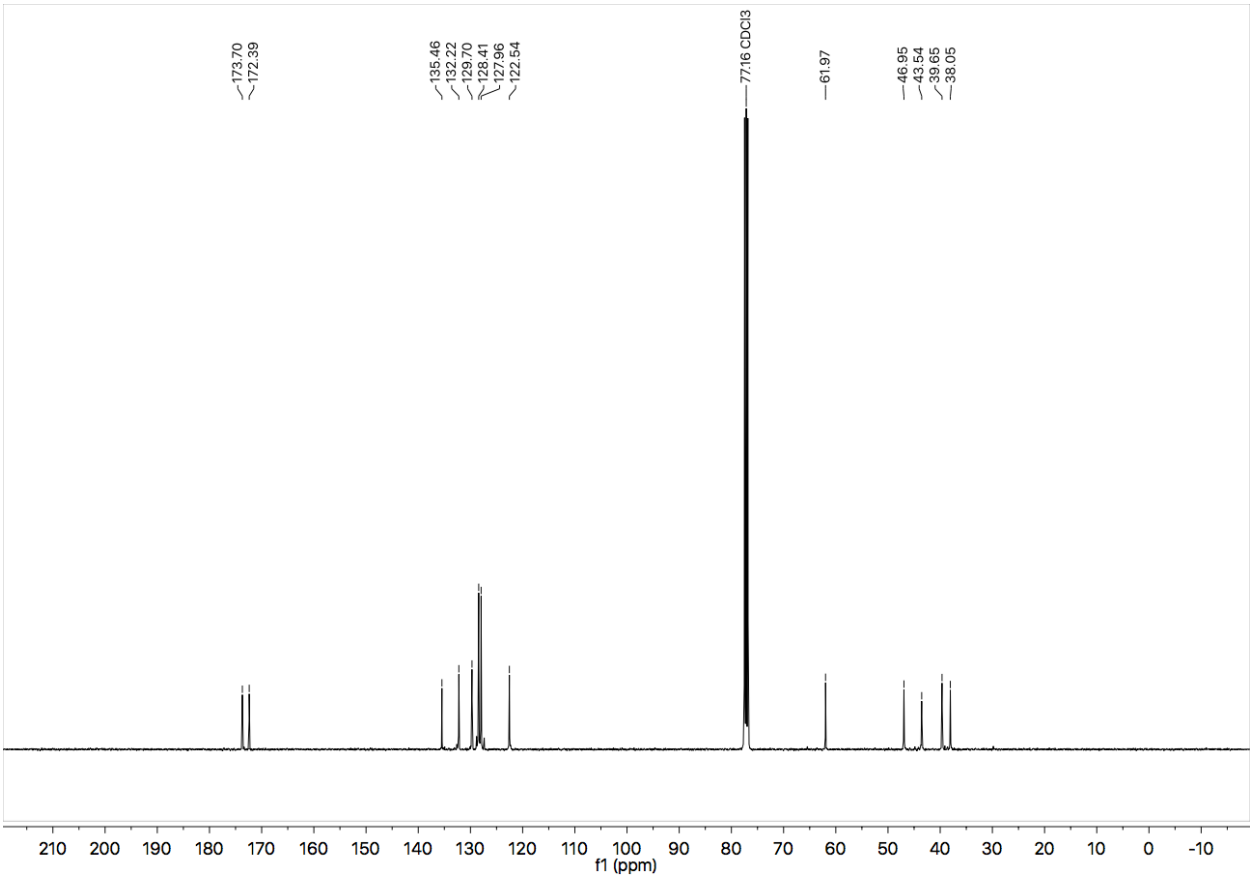

Figure A1.129 ^{13}C NMR (101 MHz, $CDCl_3$) of compound **1.8**.

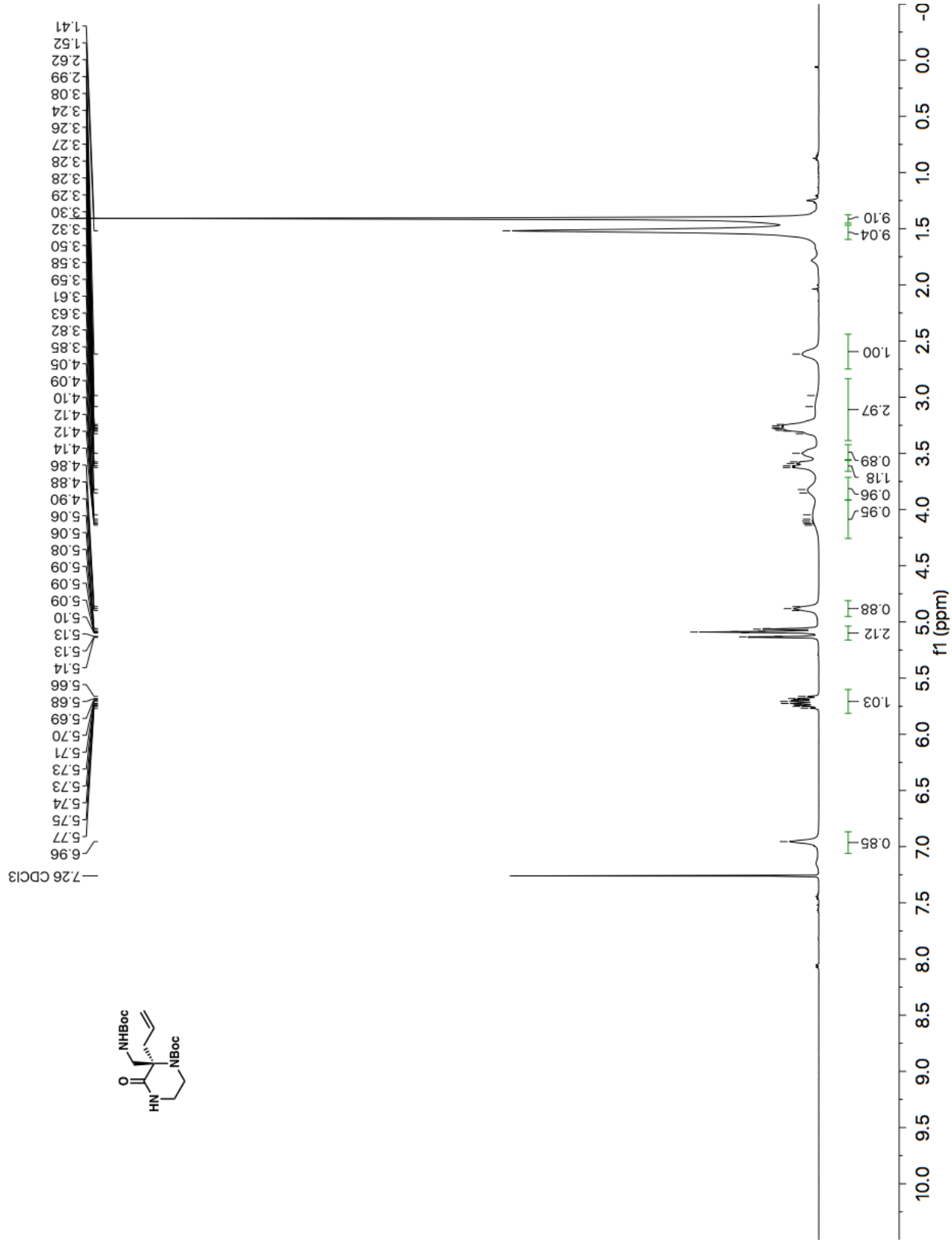

Figure A1.130 ^{1}H NMR (400 MHz, $CDCl_3$) of compound **1.9.**

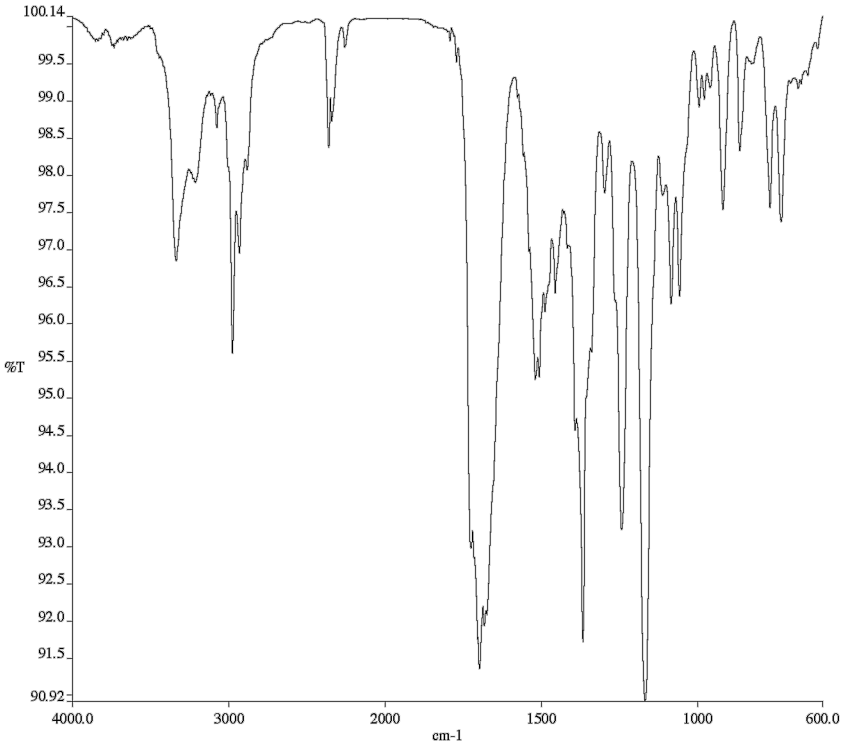

Figure A1.131 Infrared spectrum (Thin Film, NaCl) of compound **1.9**.

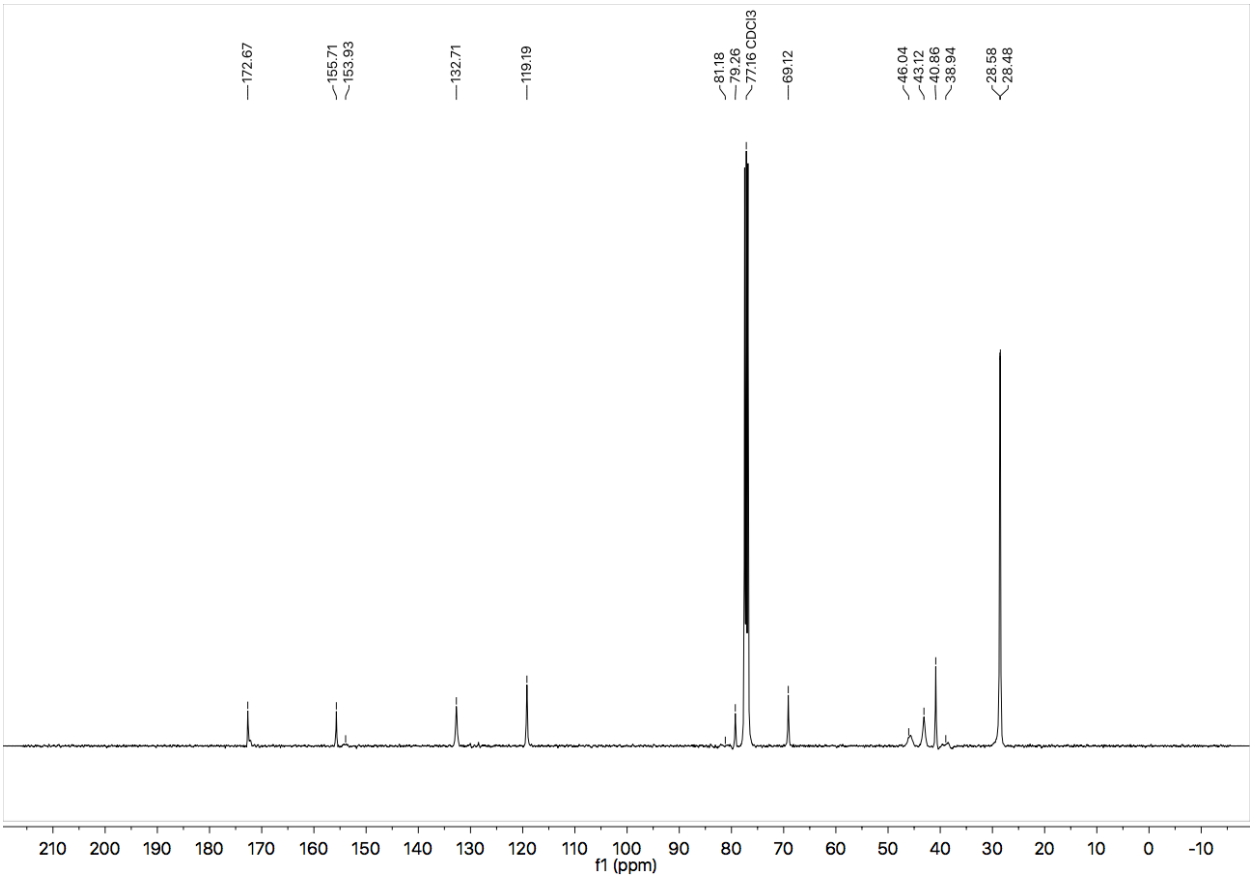

Figure A1.132 ^{13}C NMR (101 MHz, $CDCl_3$) of compound **1.9**.

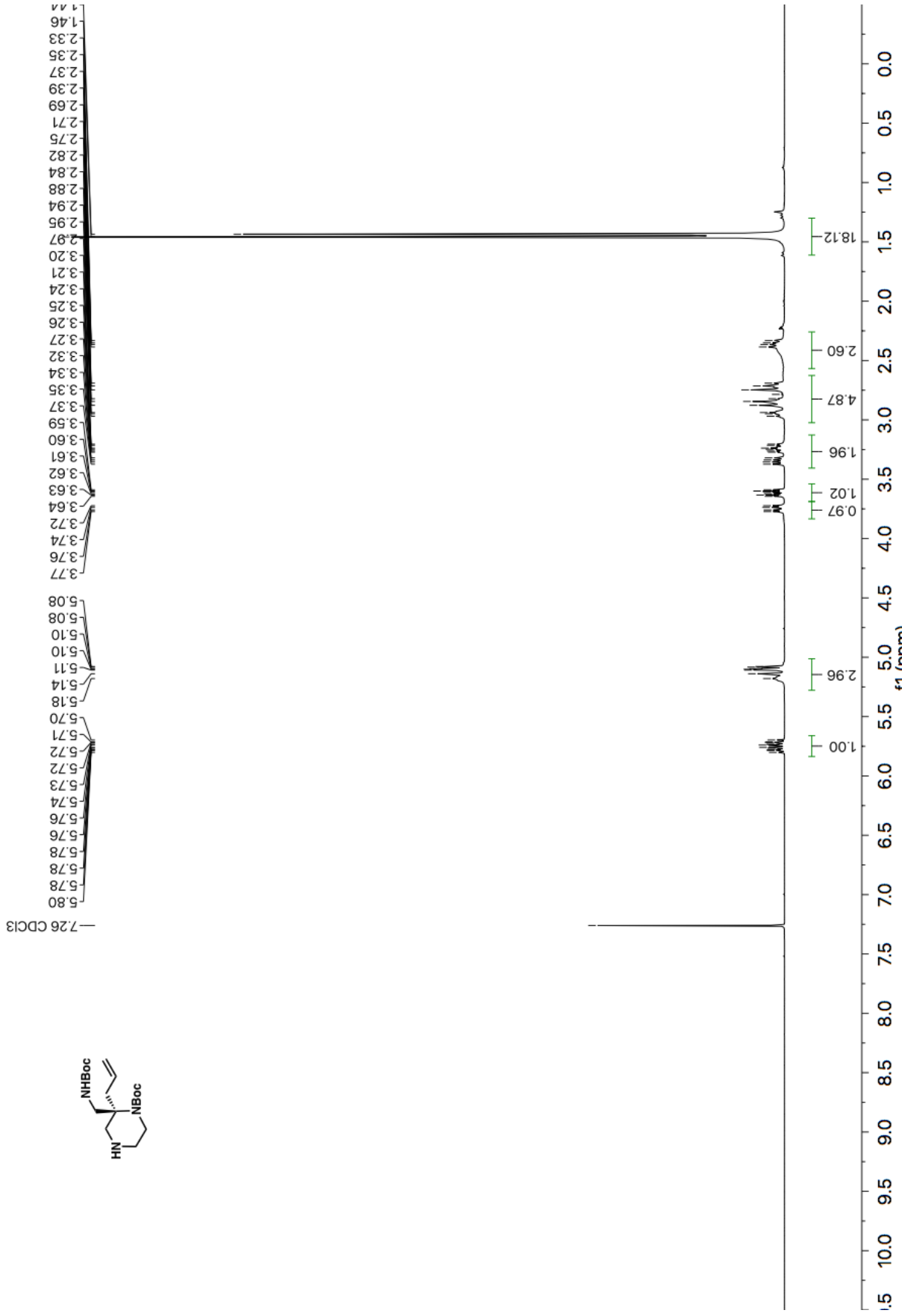

Figure A1.133 ^{1}H NMR (400 MHz, $CDCl_3$) of compound **1.10.**

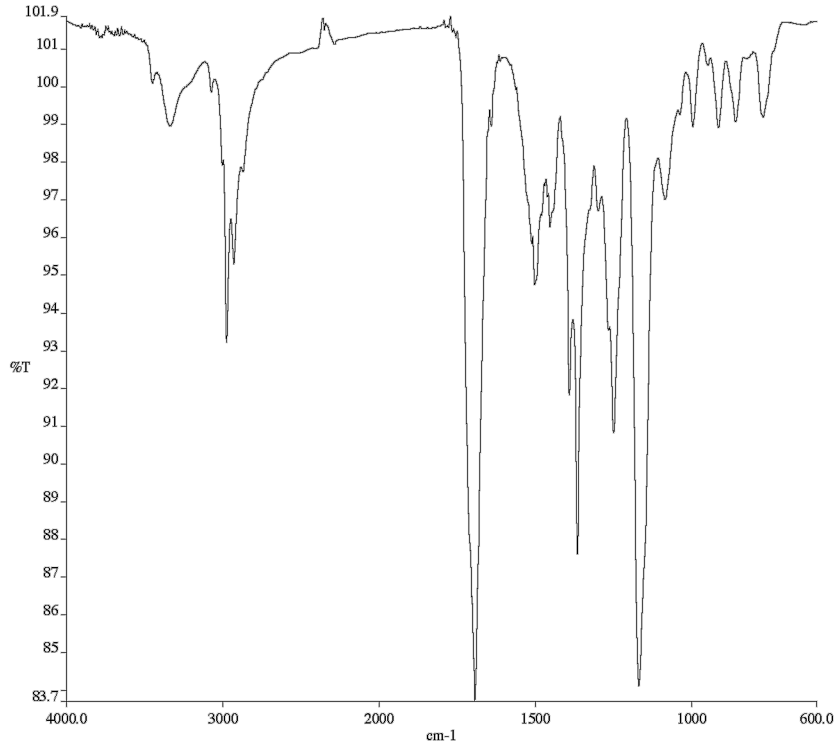

Figure A1.134 Infrared spectrum (Thin Film, NaCl) of compound **1.10**.

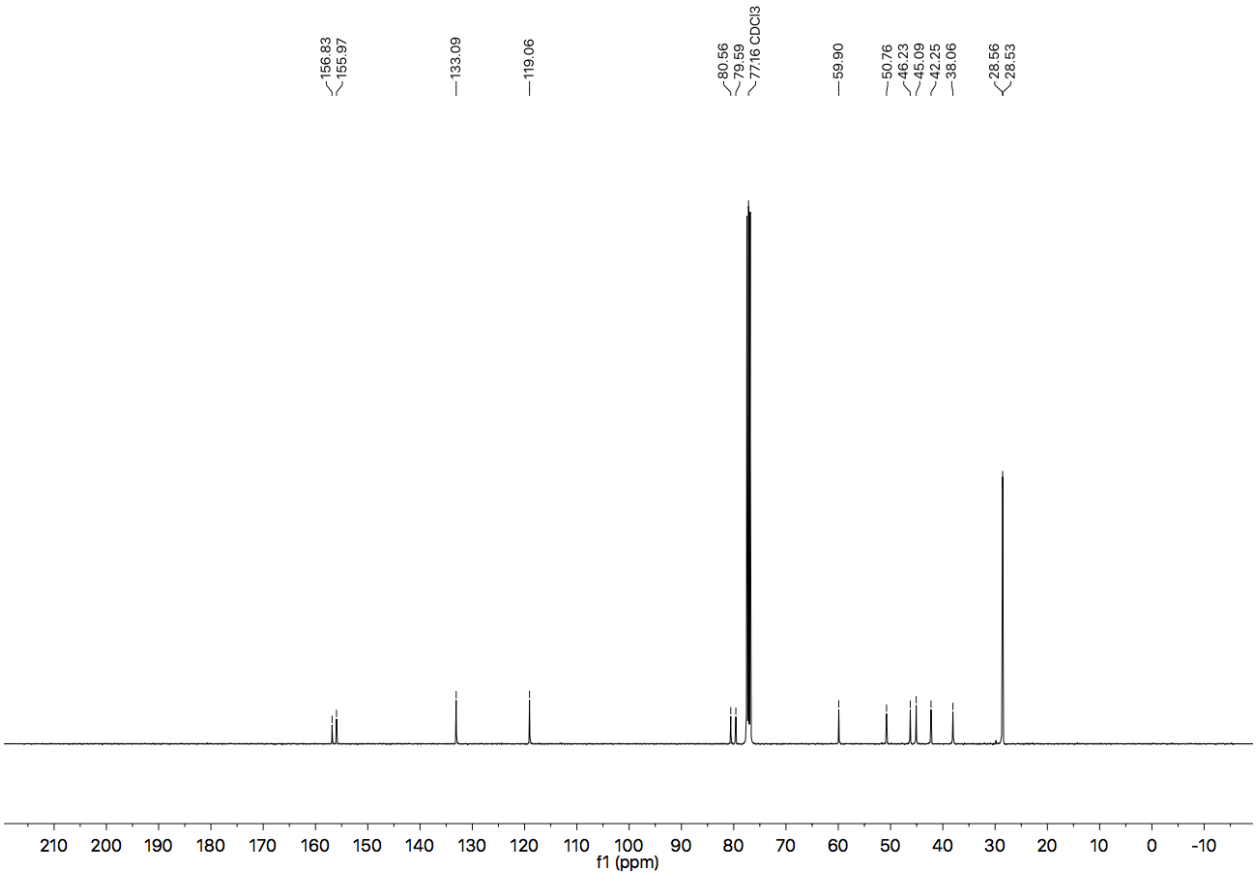

Figure A1.135 ^{13}C NMR (101 MHz, $CDCl_3$) of compound **1.10**.

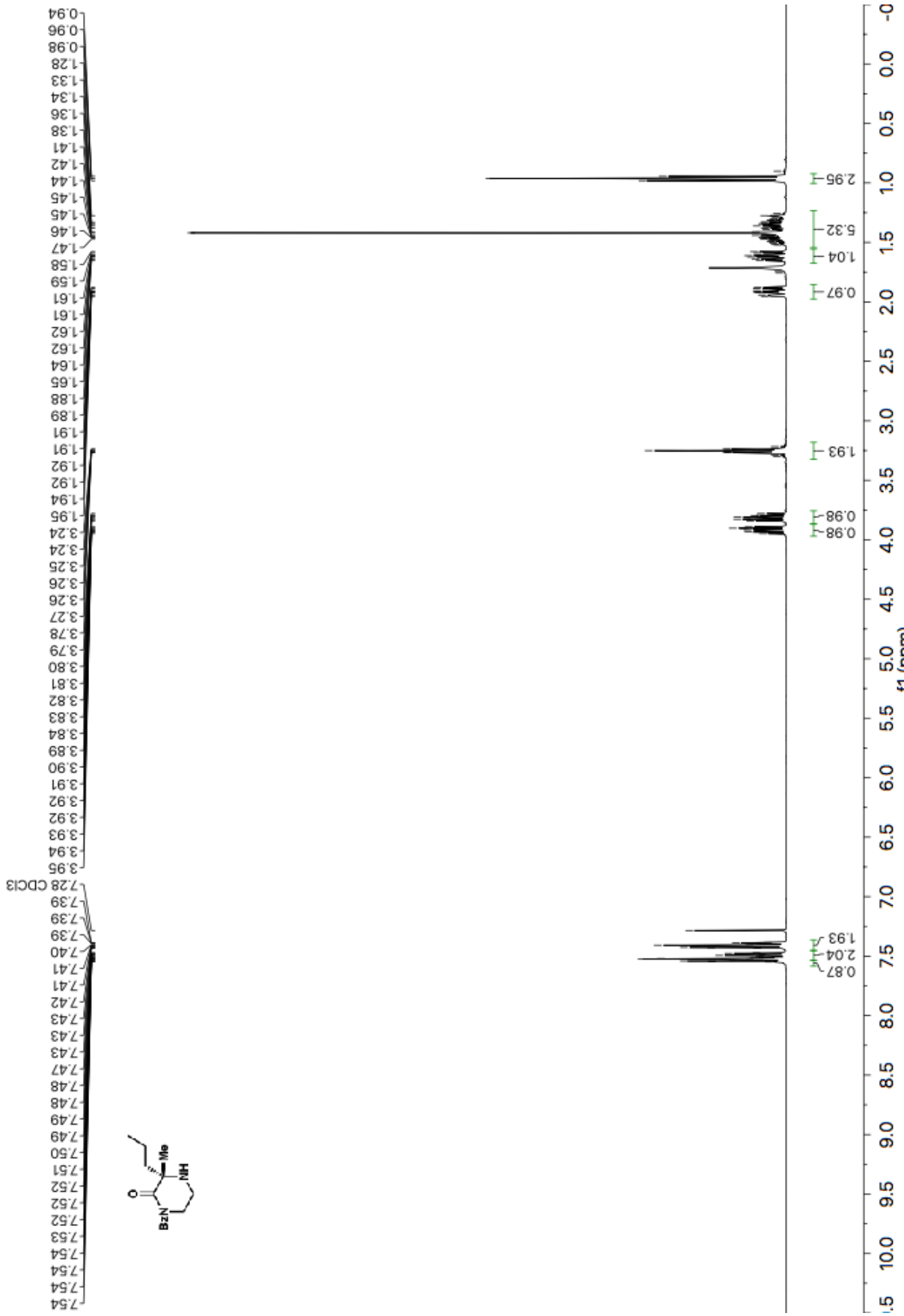

Figure A1.136 ^{1}H NMR (400 MHz, $CDCl_3$) of compound **1.11.**

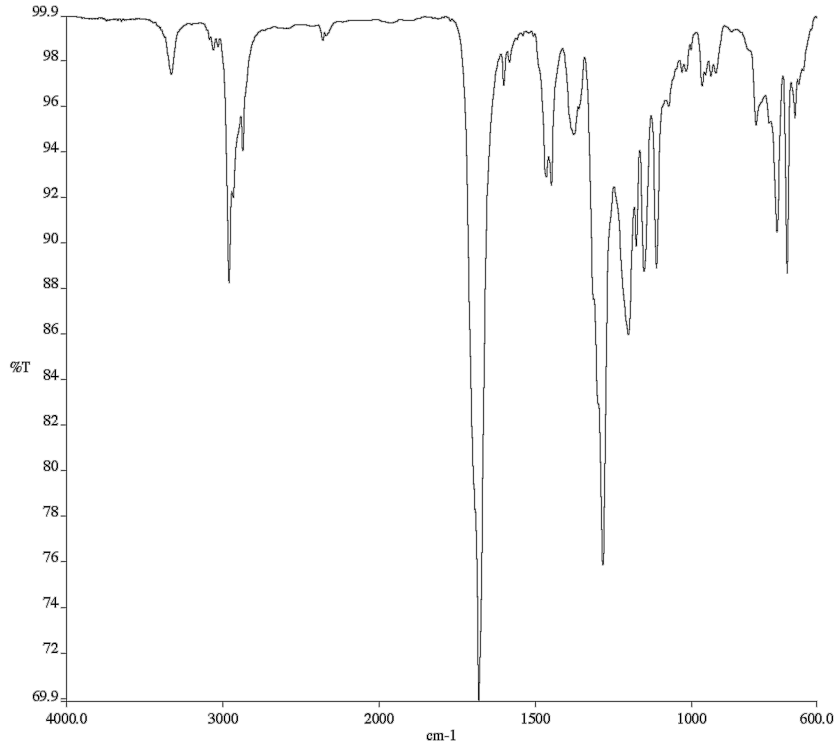

Figure A1.137 Infrared spectrum (Thin Film, NaCl) of compound **1.11**.

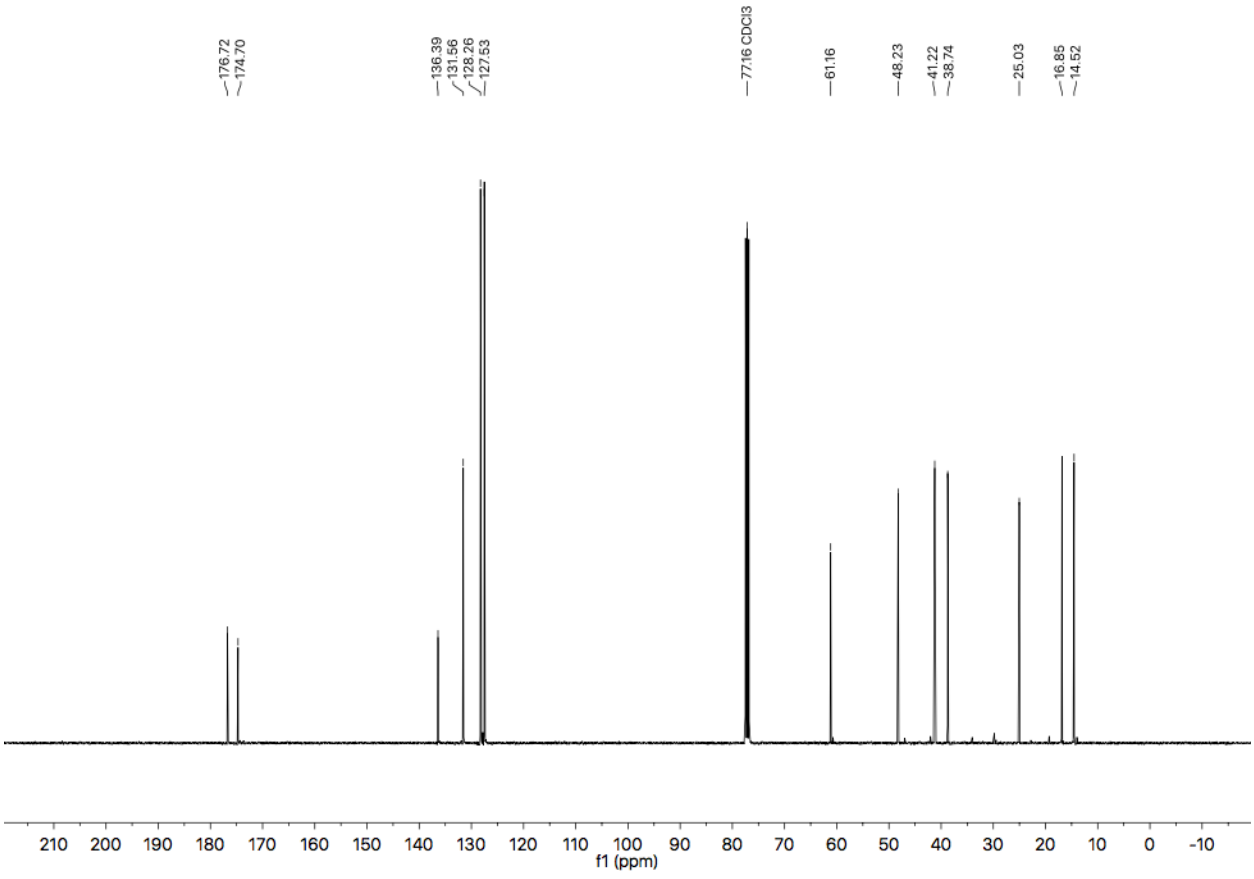

Figure A1.138 ^{13}C NMR (101 MHz, $CDCl_3$) of compound **1.11**.

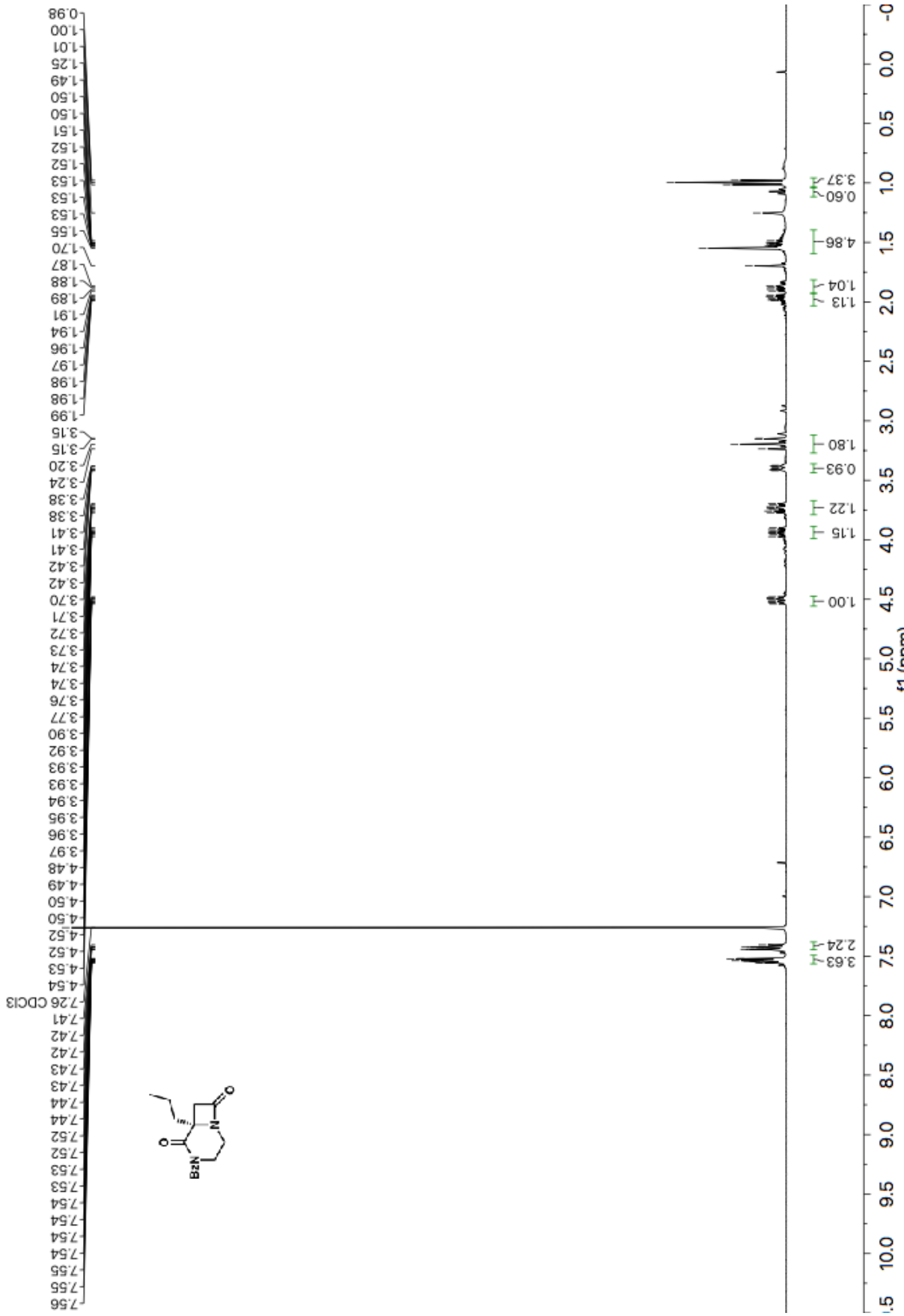

Figure A1.139 ^{1}H NMR (400 MHz, $CDCl_3$) of compound **1.12.**

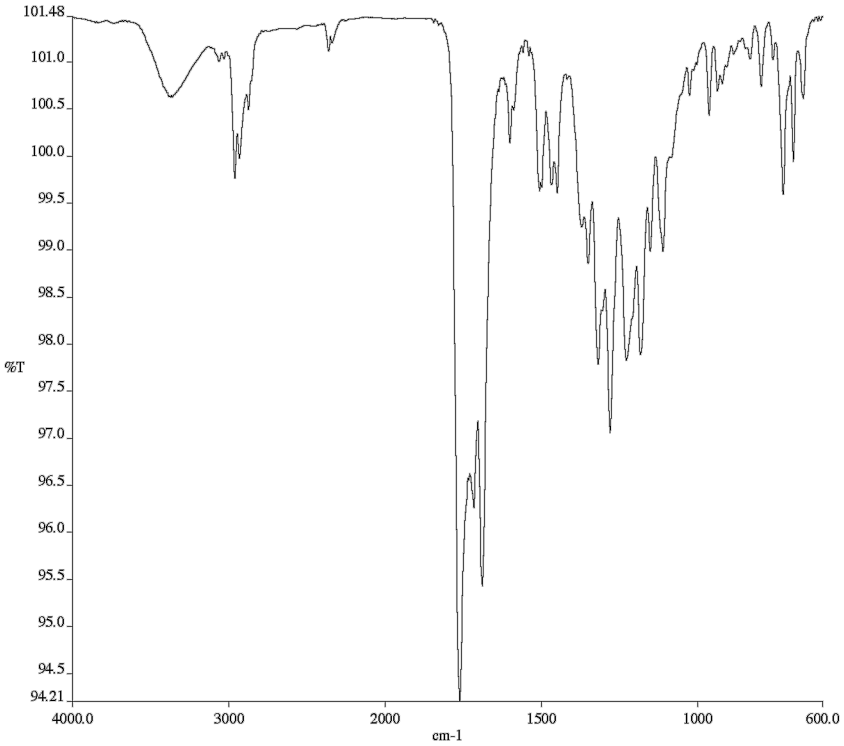

Figure A1.140 Infrared spectrum (Thin Film, NaCl) of compound **1.12**.

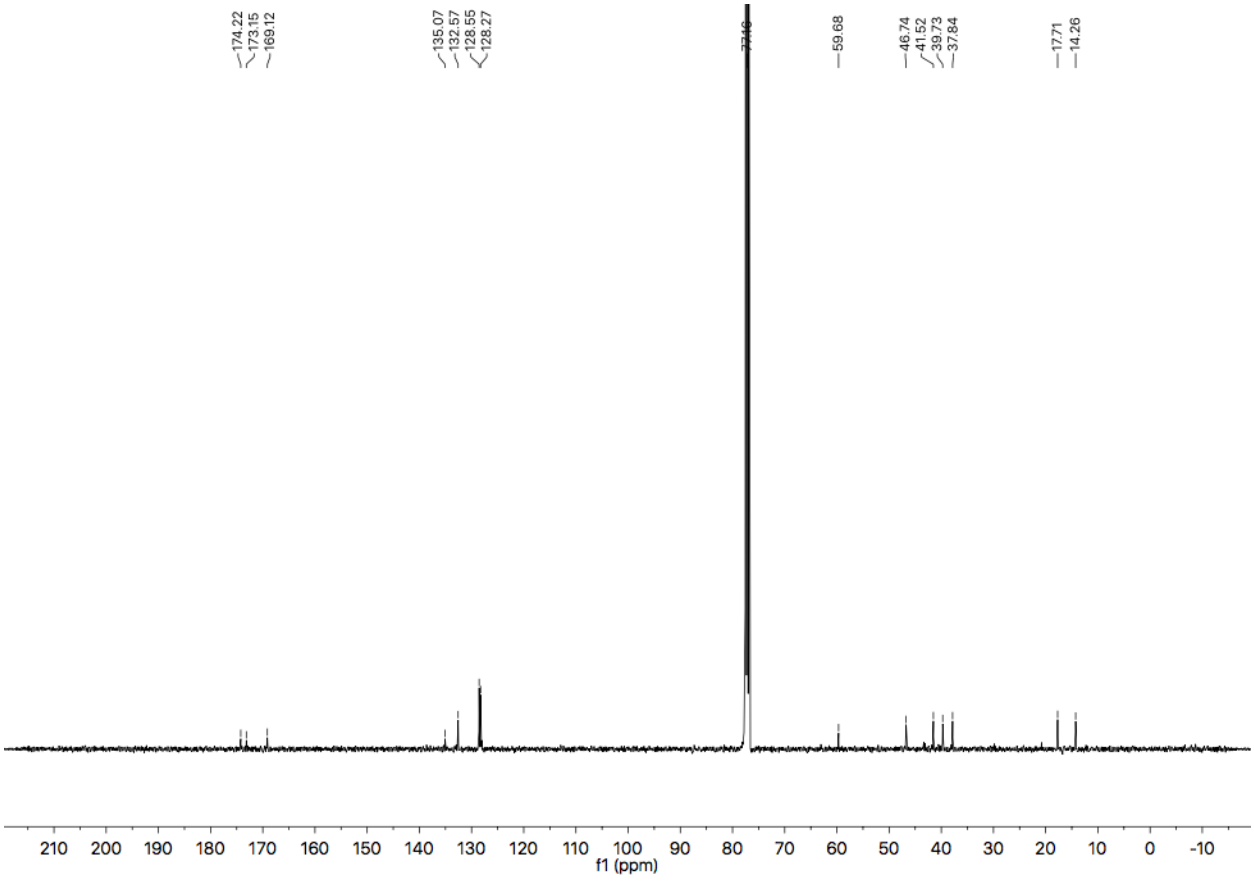

Figure A1.141 ^{13}C NMR (101 MHz, $CDCl_3$) of compound **1.12**.

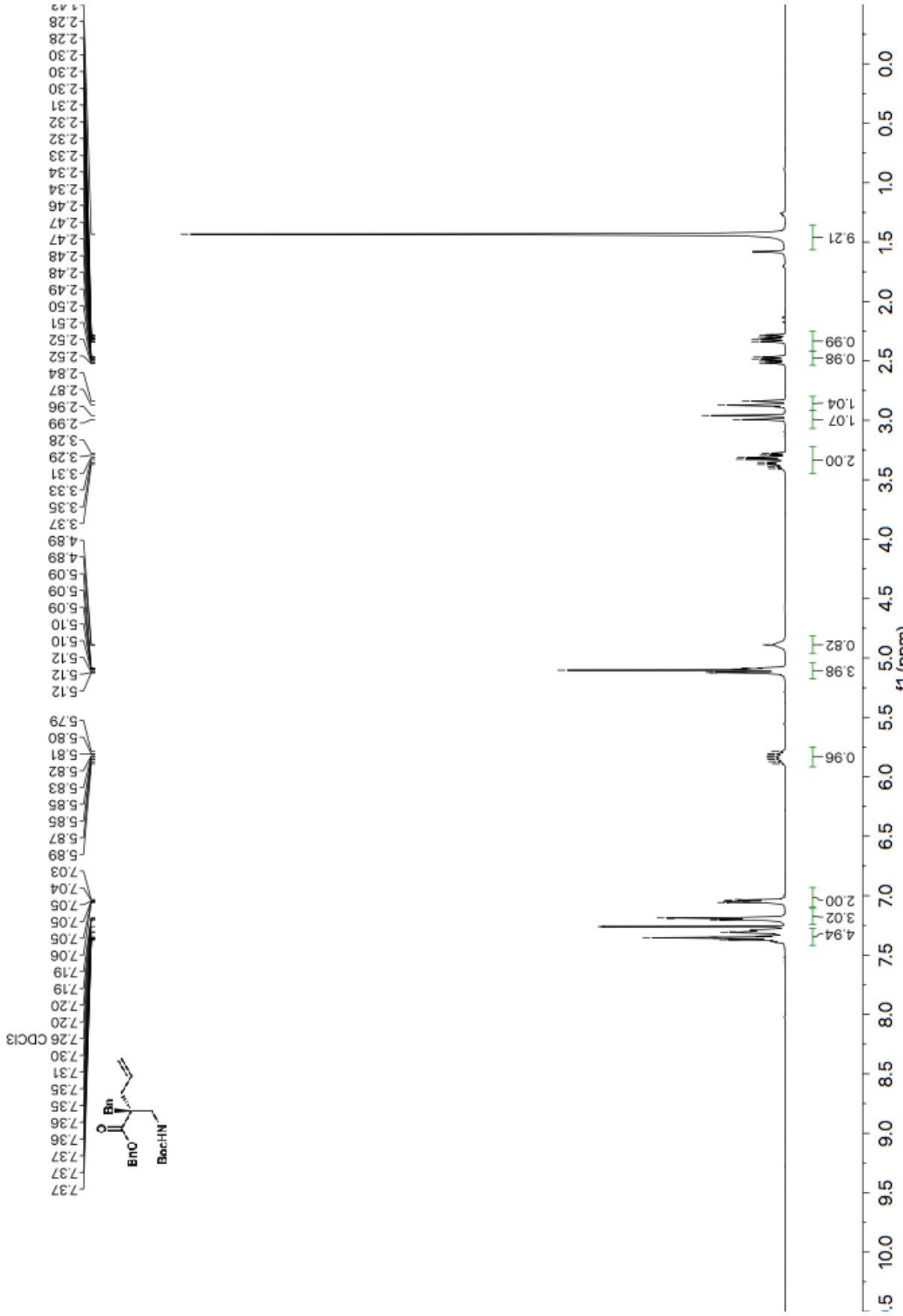

Figure A1.142 ^{1}H NMR (400 MHz, $CDCl_3$) of compound **1.13.**

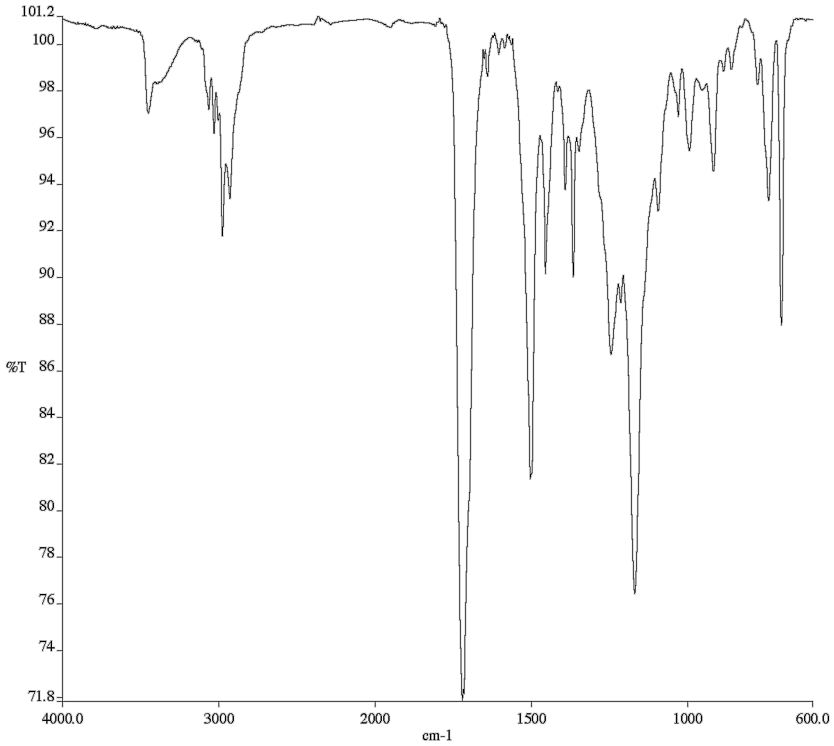

Figure A1.143 Infrared spectrum (Thin Film, NaCl) of compound **1.13**.

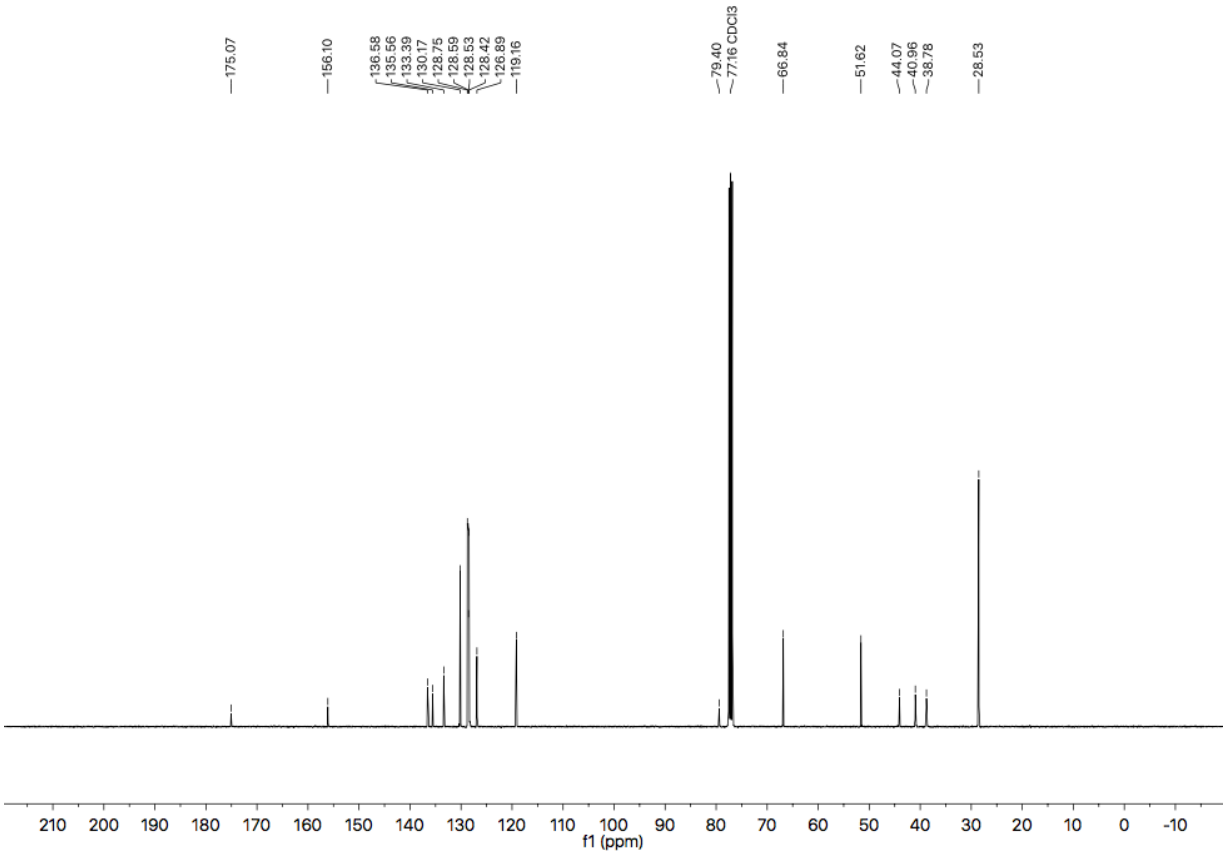

Figure A1.144 ^{13}C NMR (101 MHz, $CDCl_3$) of compound **1.13**.

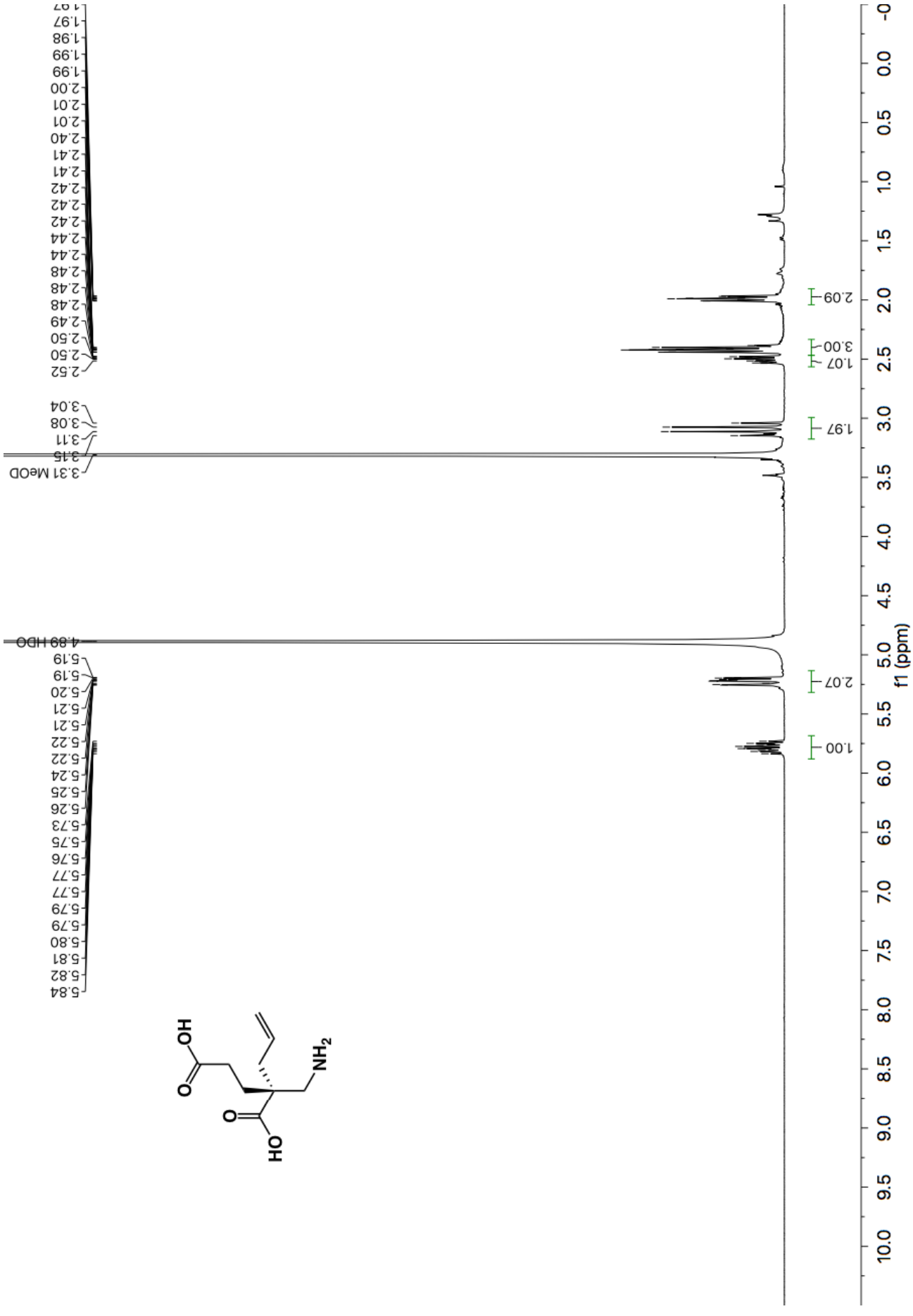

Figure A1.145 ^{1}H NMR (400 MHz, CD_3OD) of compound **1.14.**

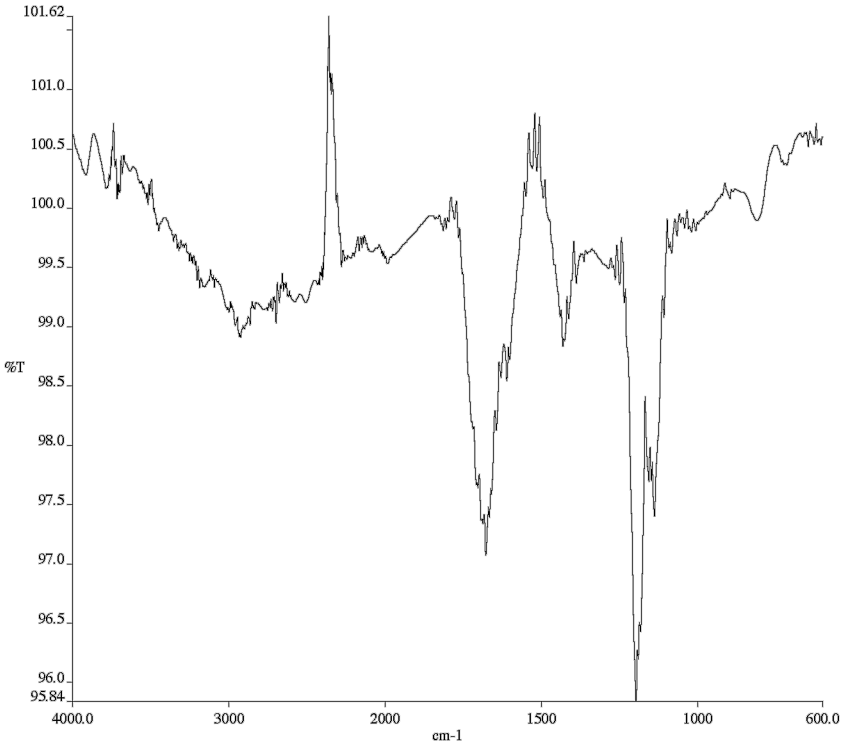

Figure A1.146 Infrared spectrum (Thin Film, NaCl) of compound **1.14**.

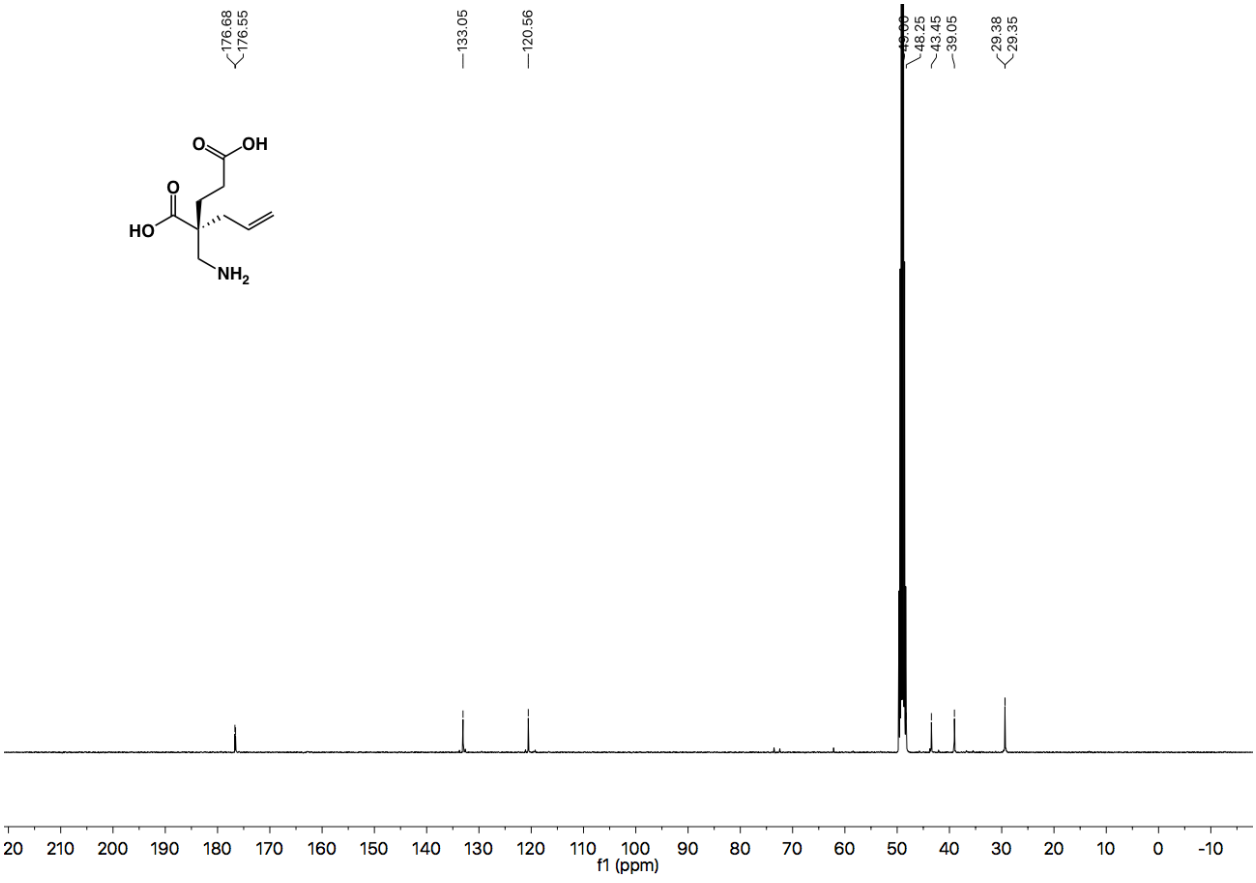

Figure A1.147 ^{13}C NMR (101 MHz, CD_3OD) of compound **1.14**.

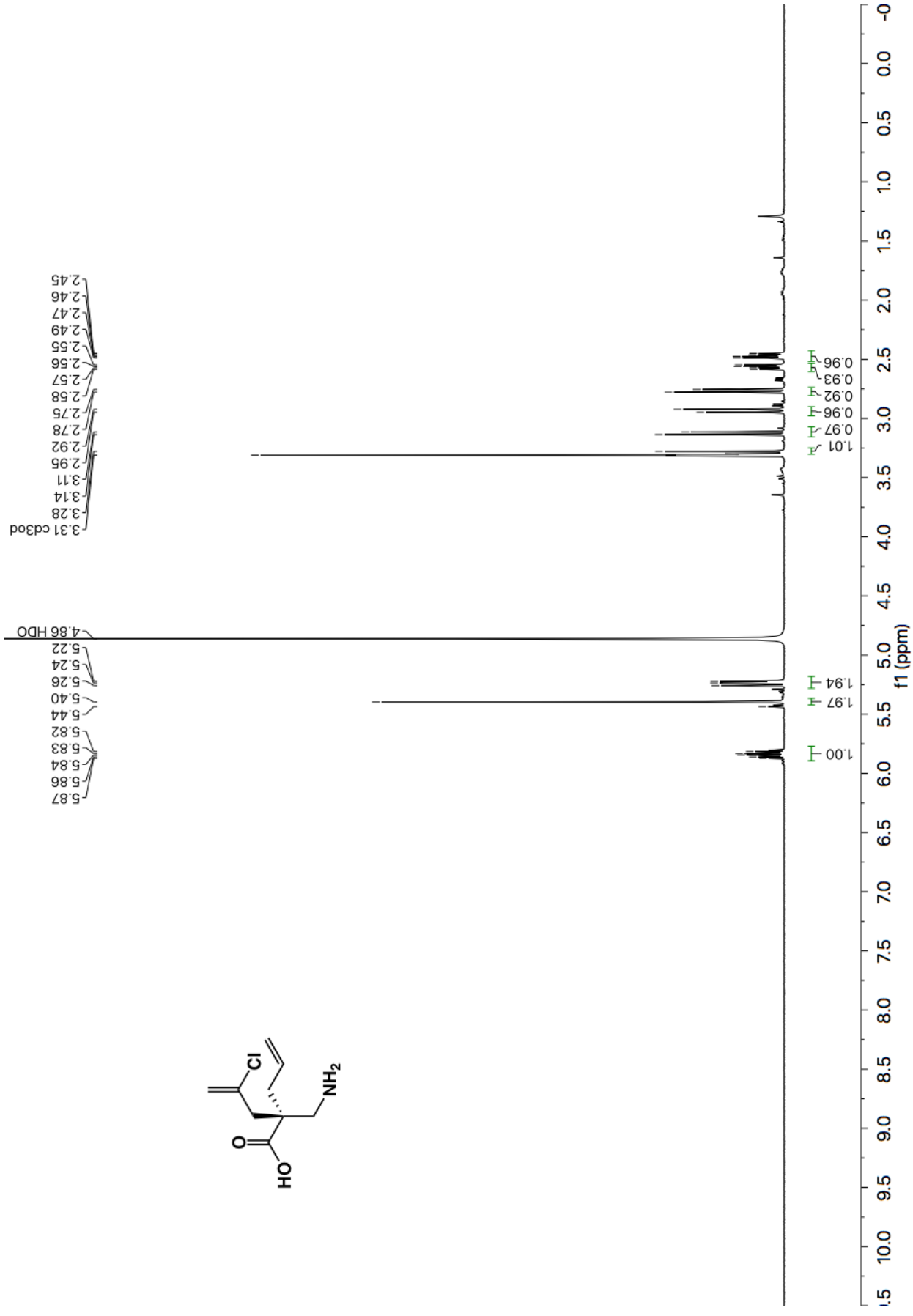

Figure A1.148 ^{1}H NMR (600 MHz, CD_3OD) of compound **1.15.**

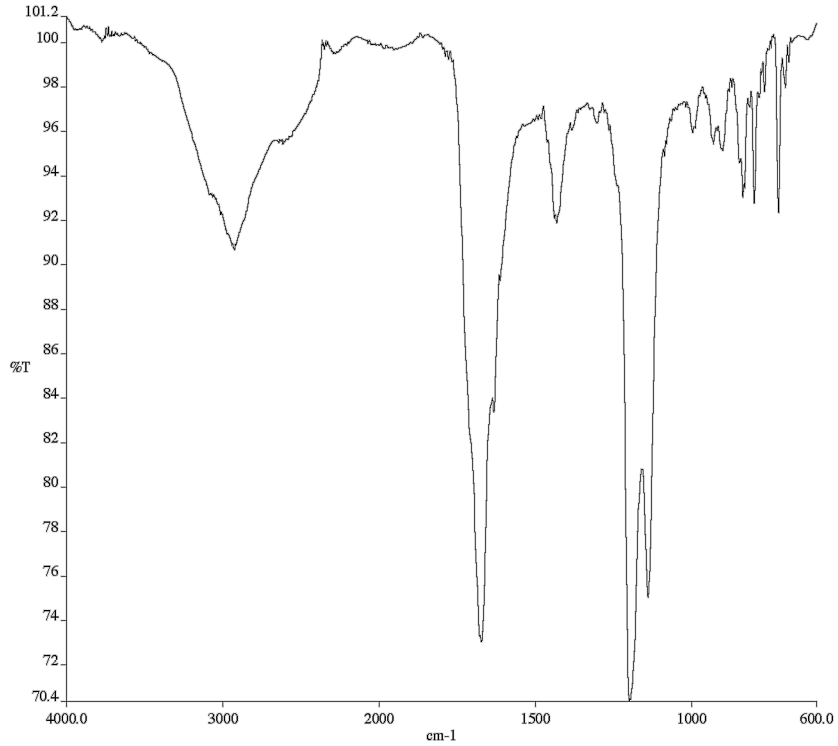

Figure A1.149 Infrared spectrum (Thin Film, NaCl) of compound **1.15**.

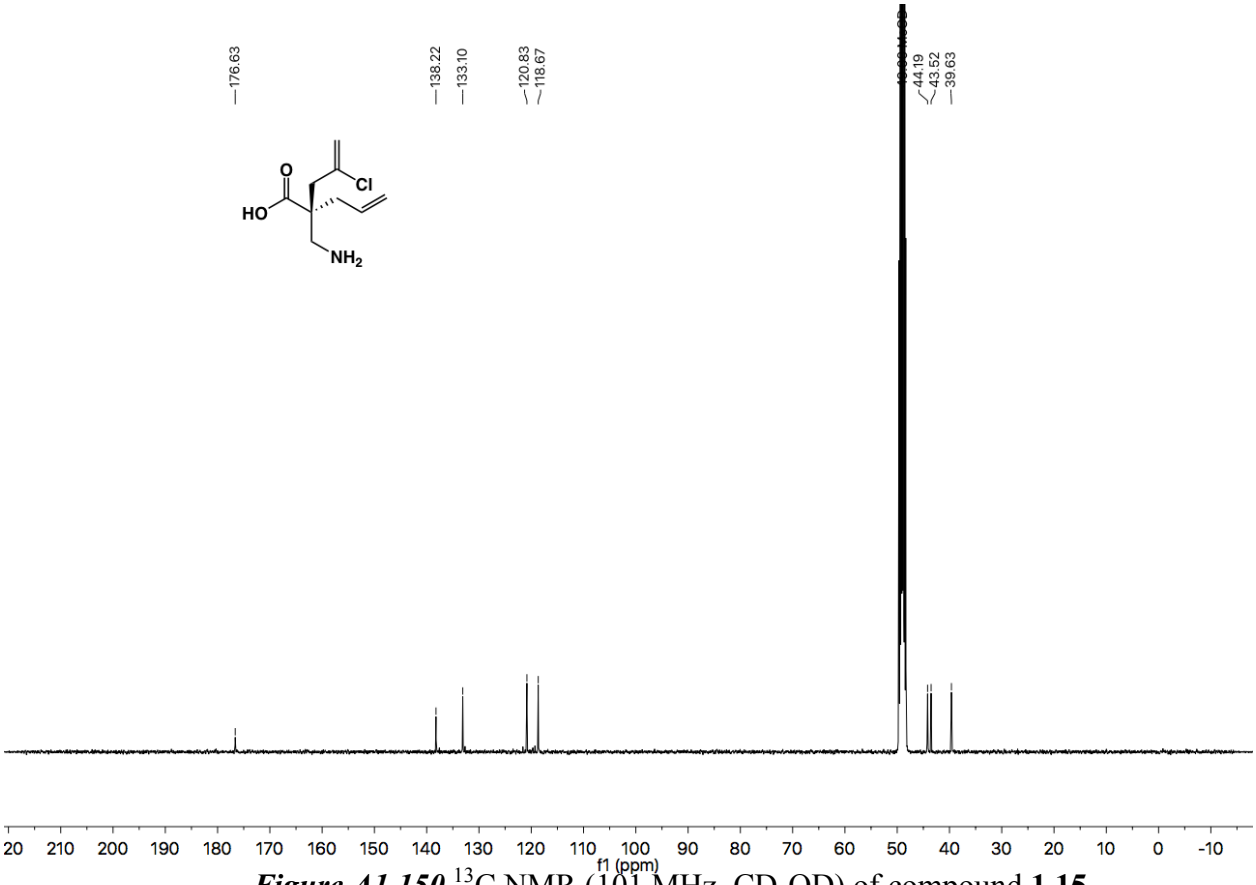

Figure A1.150 ^{13}C NMR (101 MHz, CD_3OD) of compound **1.15**.

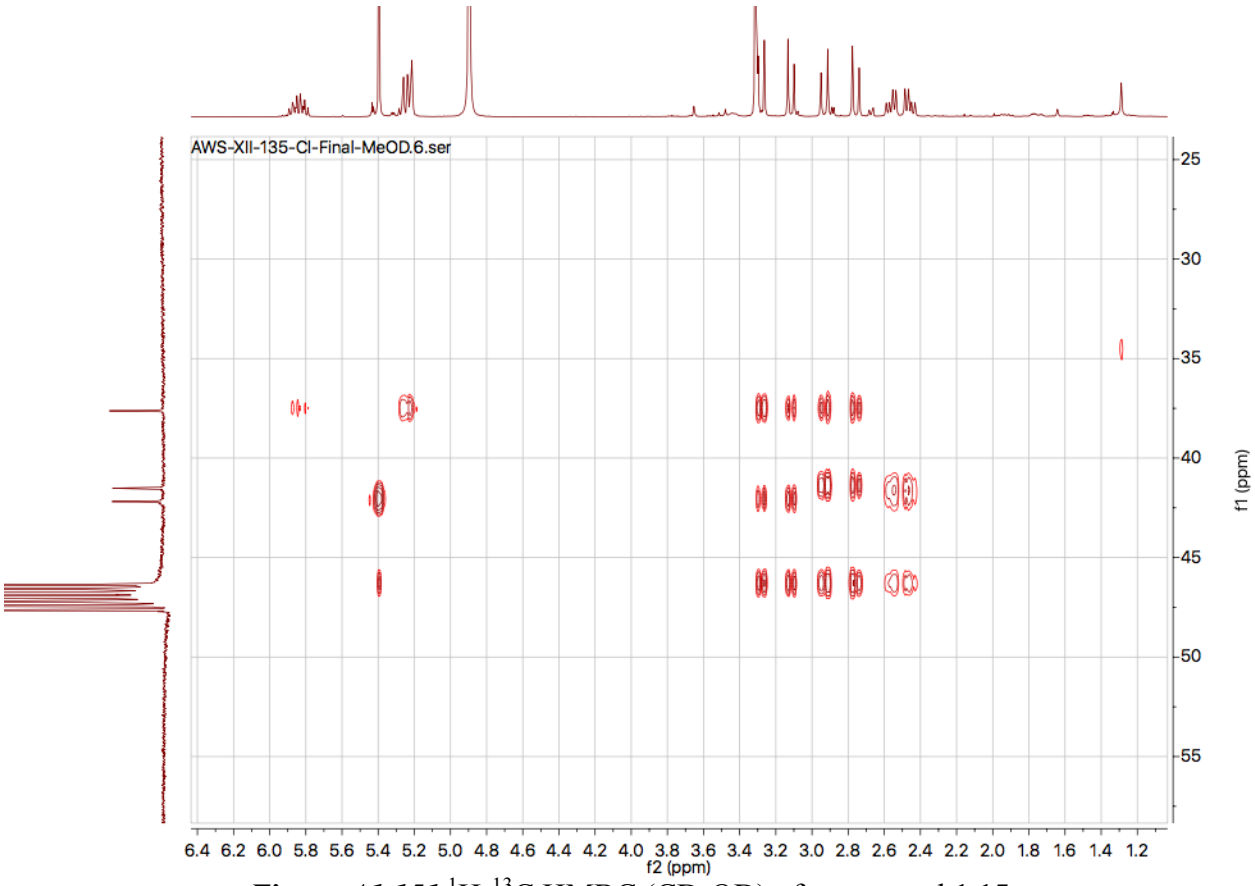

Figure A1.151 ^{1}H-^{13}C HMBC (CD_3OD) of compound **1.15**

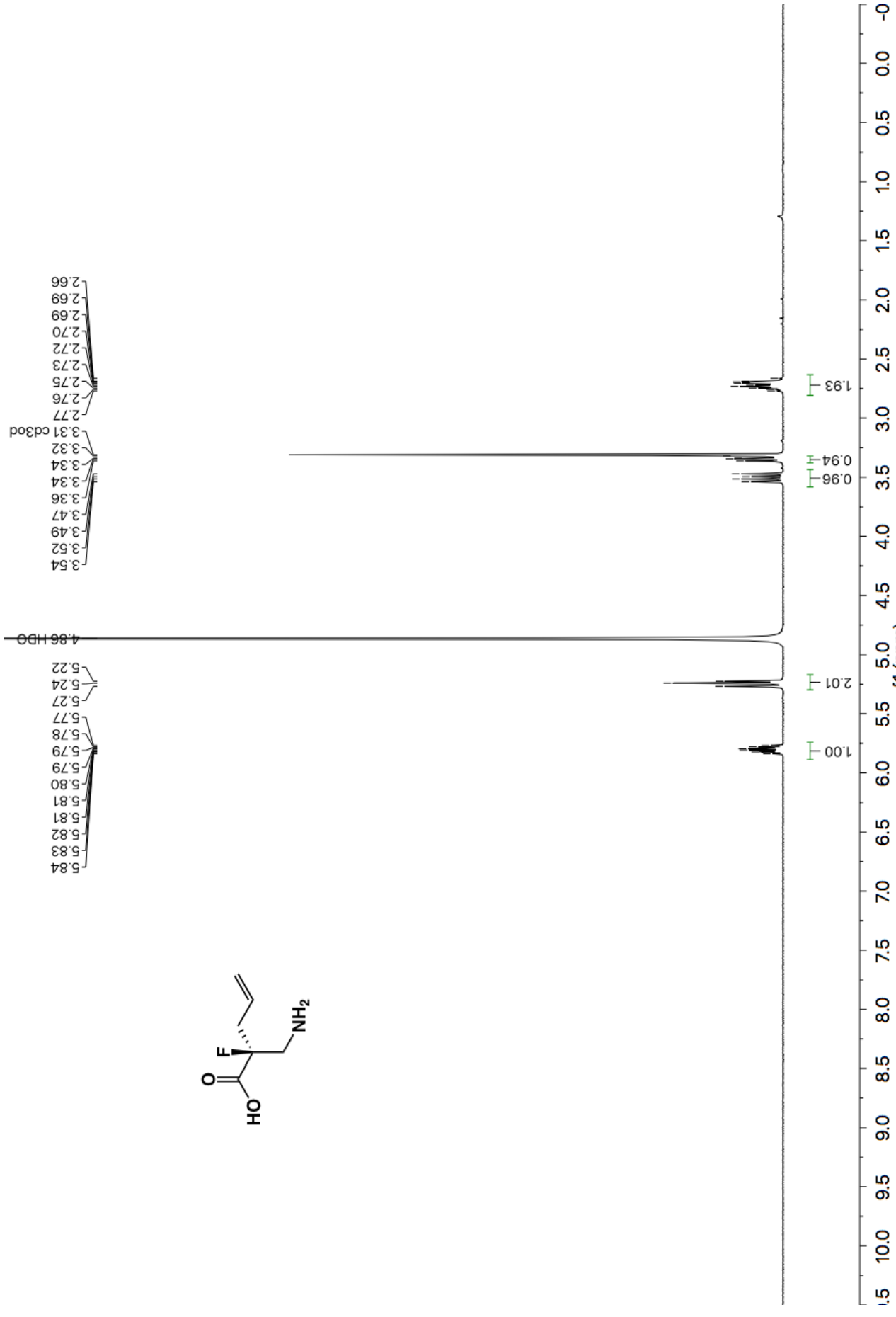

Figure A1.152 ^{1}H NMR (600 MHz, CD_3OD) of compound **1.16.**

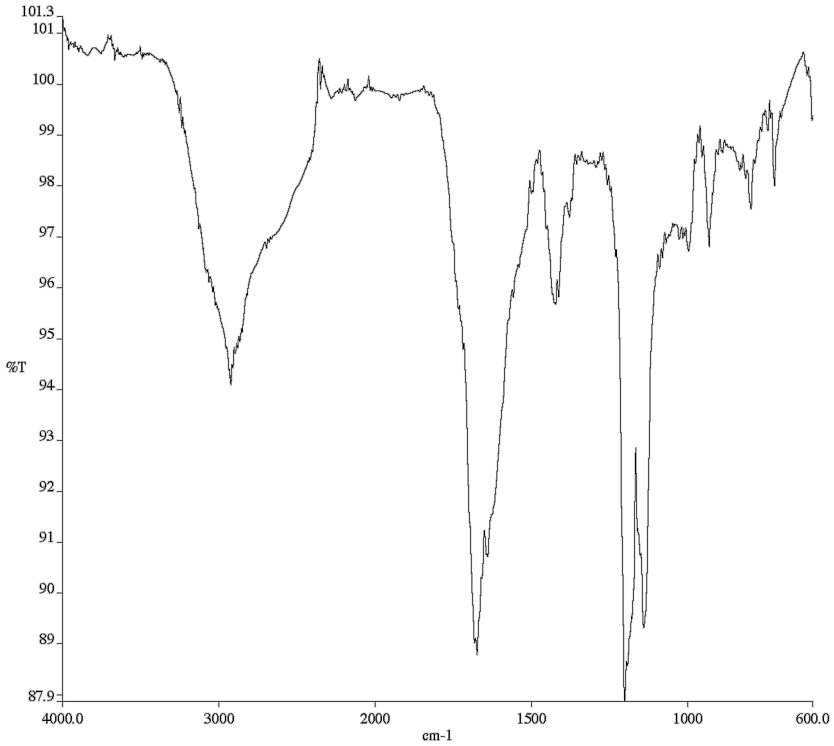

Figure A1.153 Infrared spectrum (Thin Film, NaCl) of compound **1.16**.

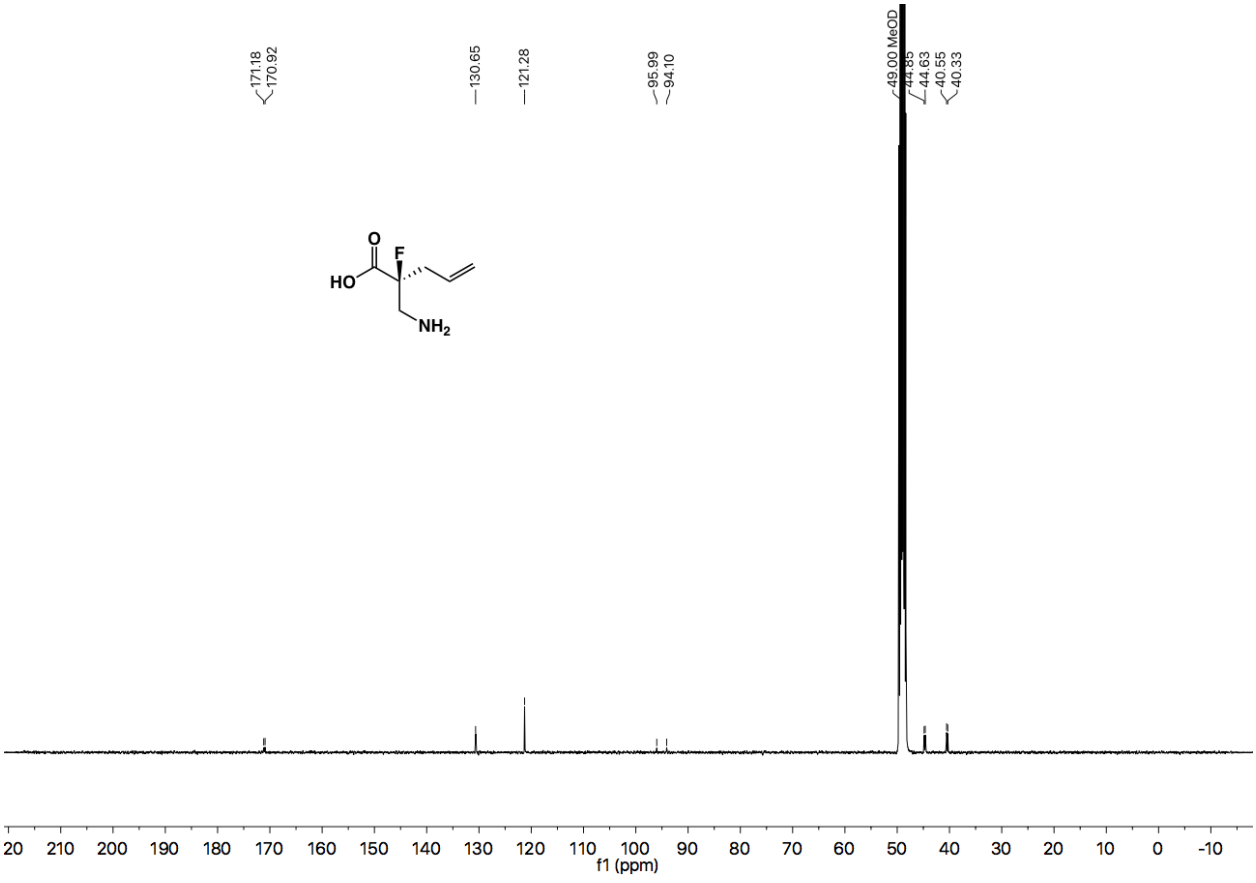

Figure A1.154 ^{13}C NMR (101 MHz, CD_3OD) of compound **1.16**.

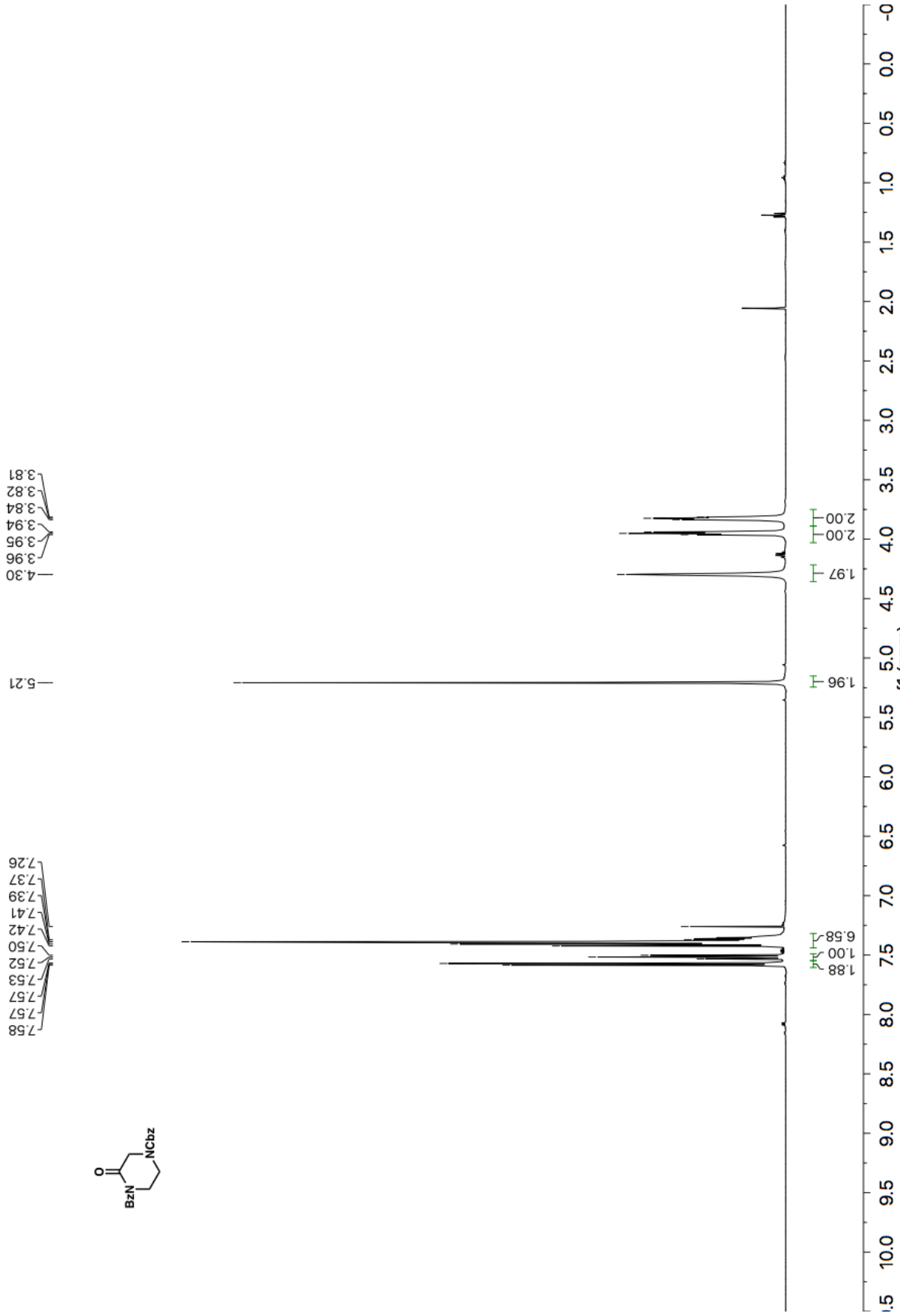

Figure A1.155 ^{1}H NMR (500 MHz, $CDCl_3$) of compound **SI-3.**

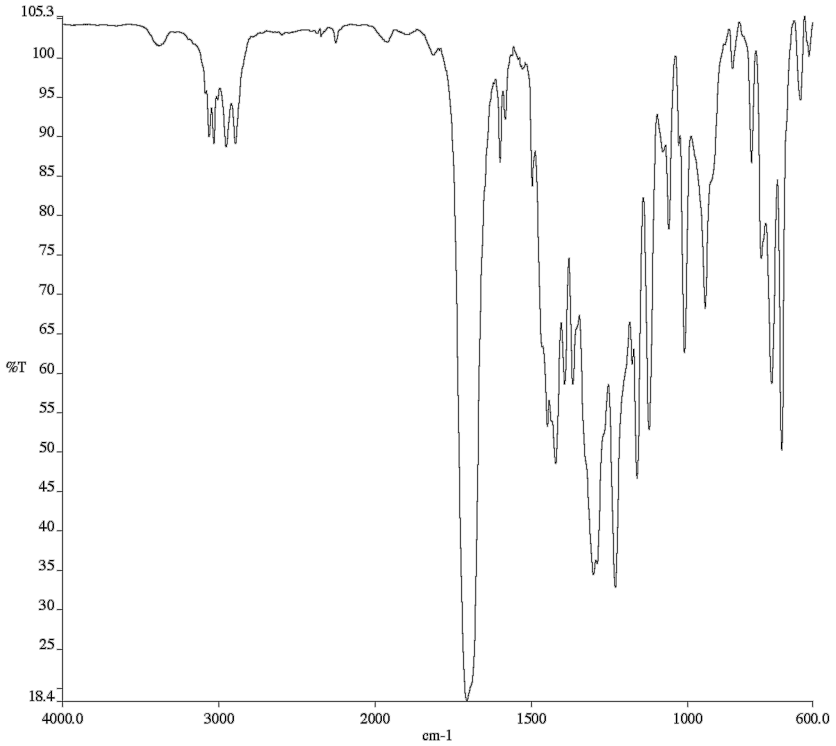

Figure A1.156 Infrared spectrum (Thin Film, NaCl) of compound **SI-3**.

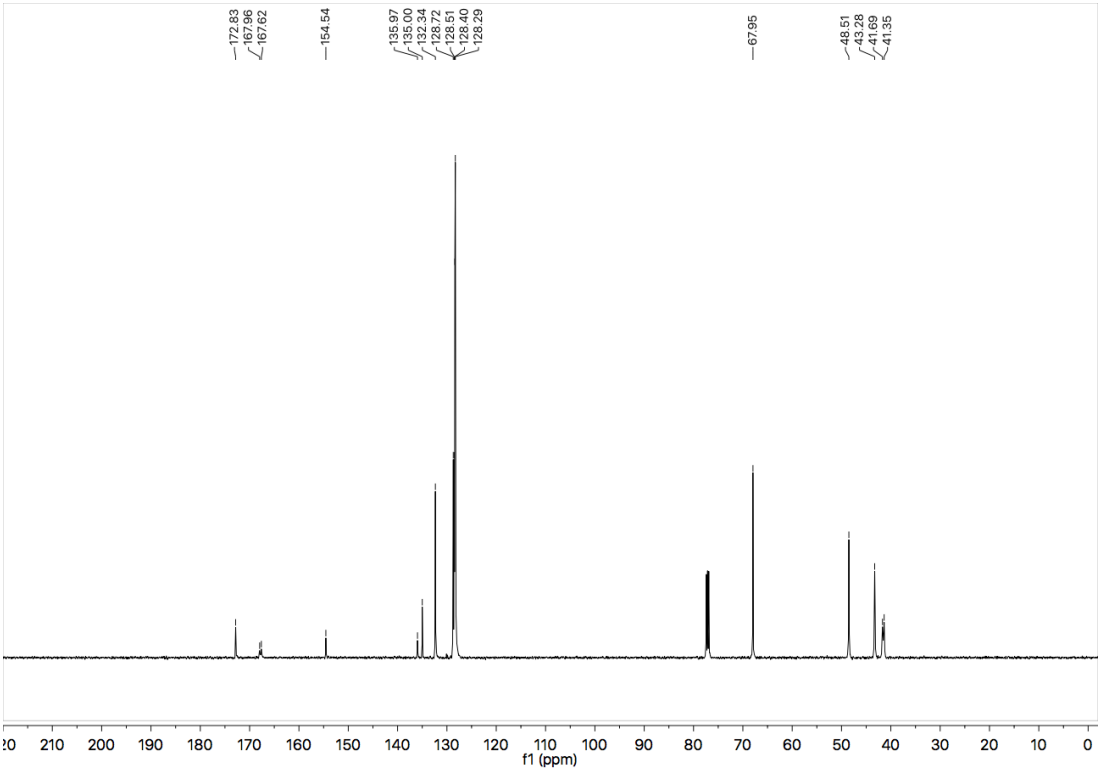

Figure A1.157 ^{13}C NMR (126 MHz, $CDCl_3$) of compound **SI-3**.

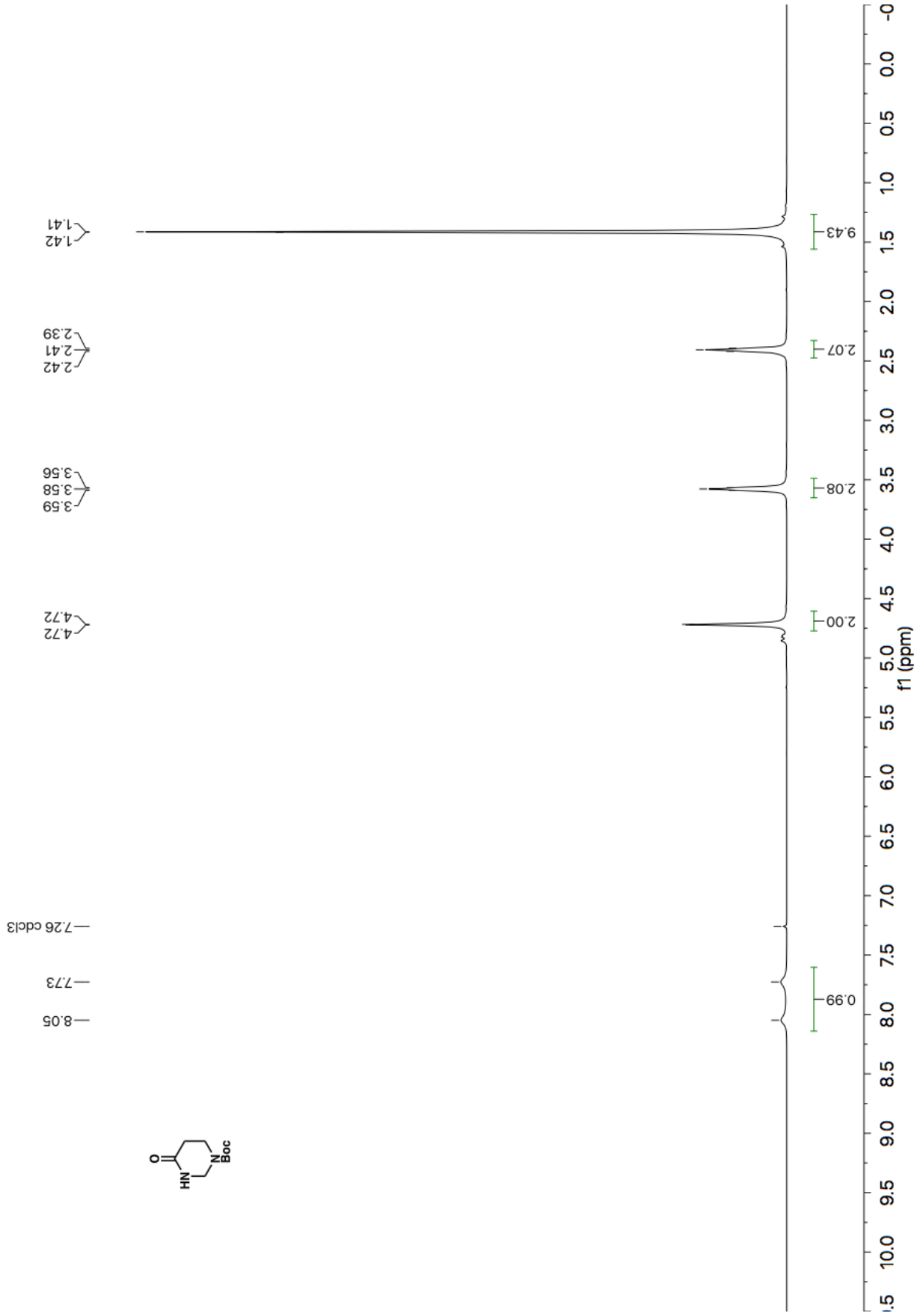

Figure A1.158 ^{1}H NMR (500 MHz, $CDCl_3$) of compound **SI-4.**

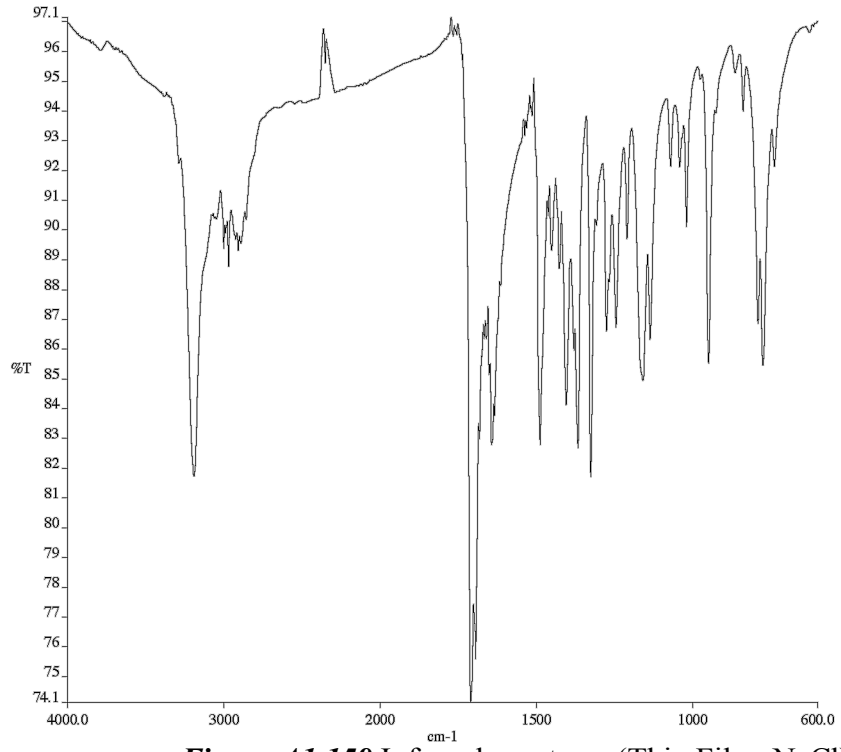

Figure A1.159 Infrared spectrum (Thin Film, NaCl) of compound **SI-4**.

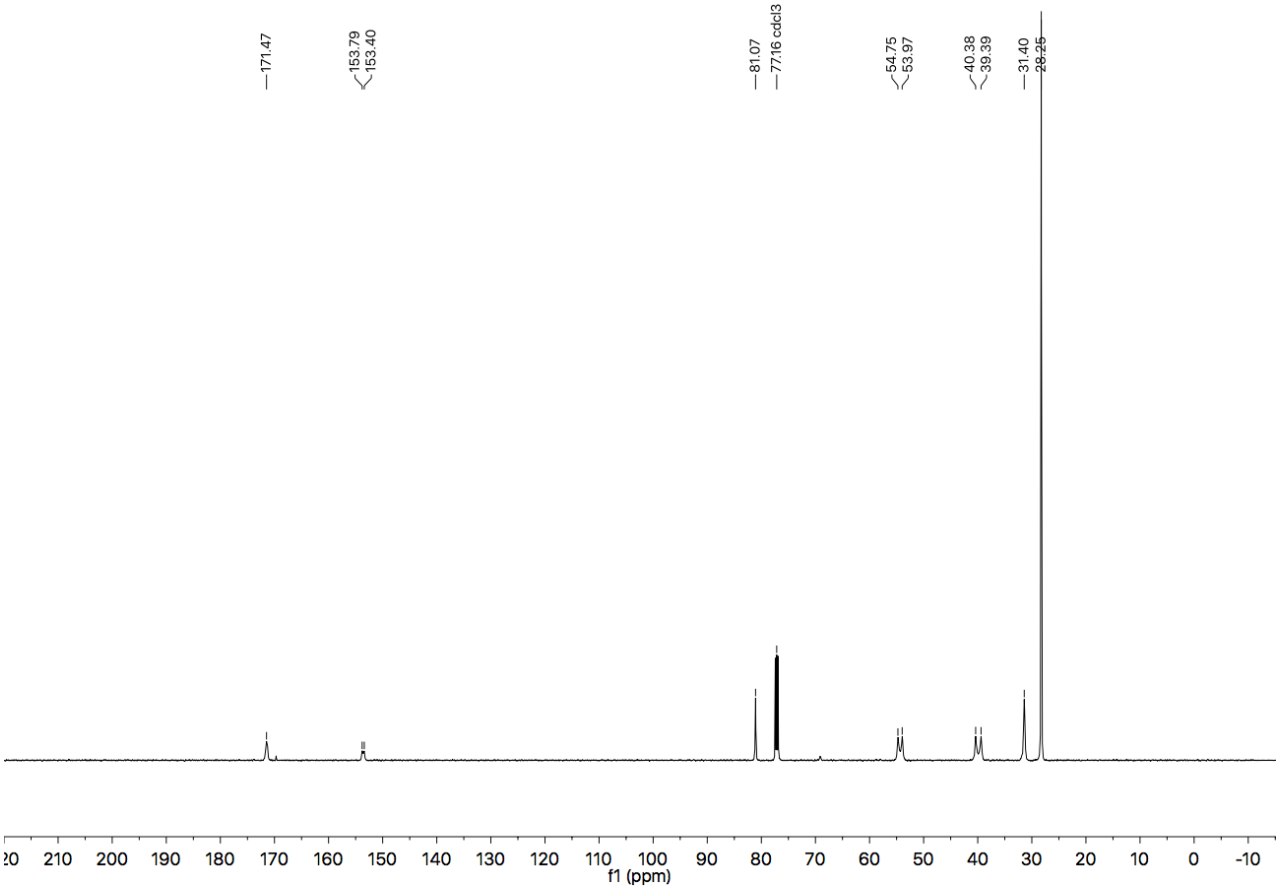

Figure A1.160 ^{13}C NMR (126 MHz, $CDCl_3$) of compound **SI-4**.

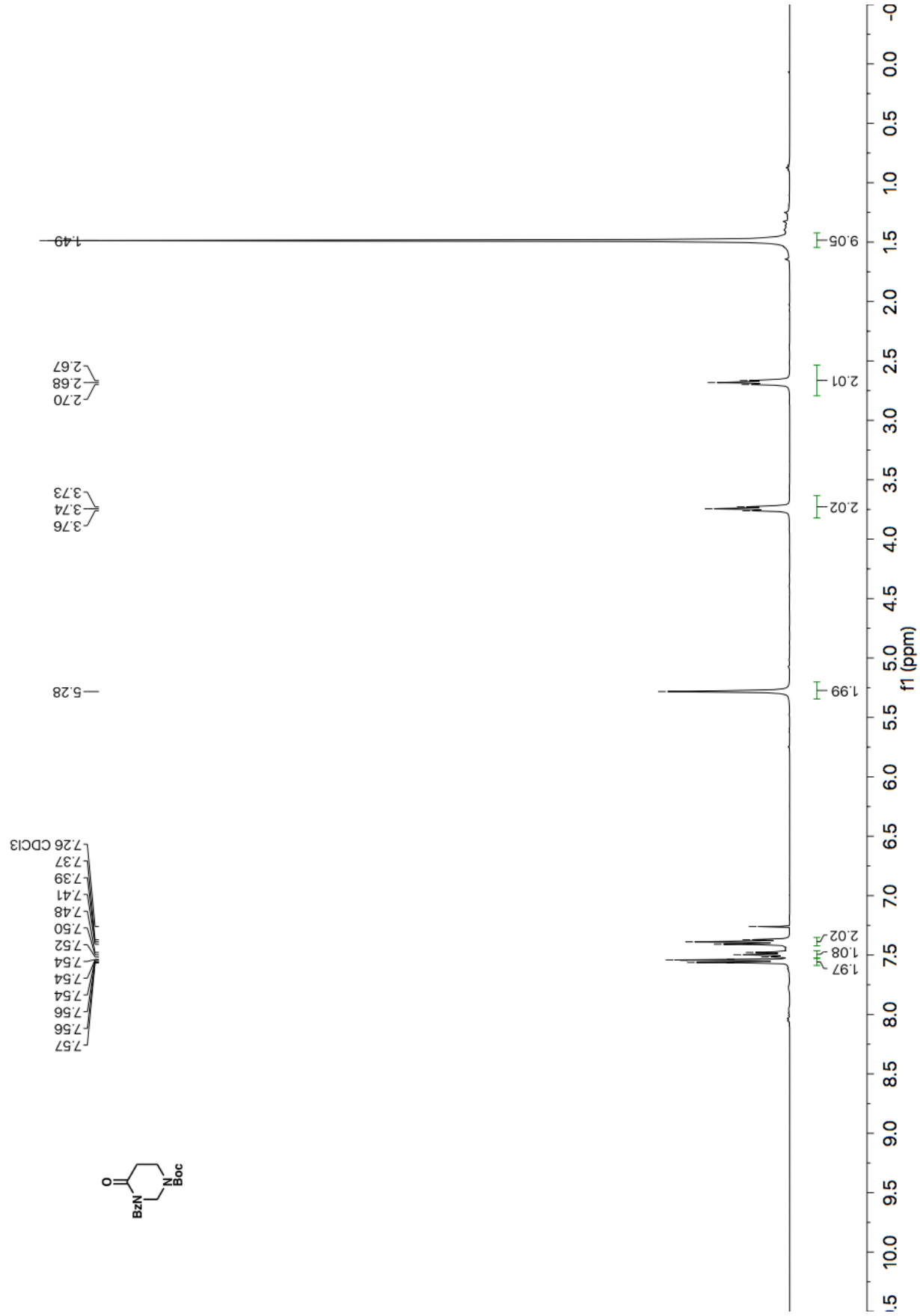

Figure A1.161 ^{1}H NMR (400 MHz, $CDCl_3$) of compound **SI-5.**

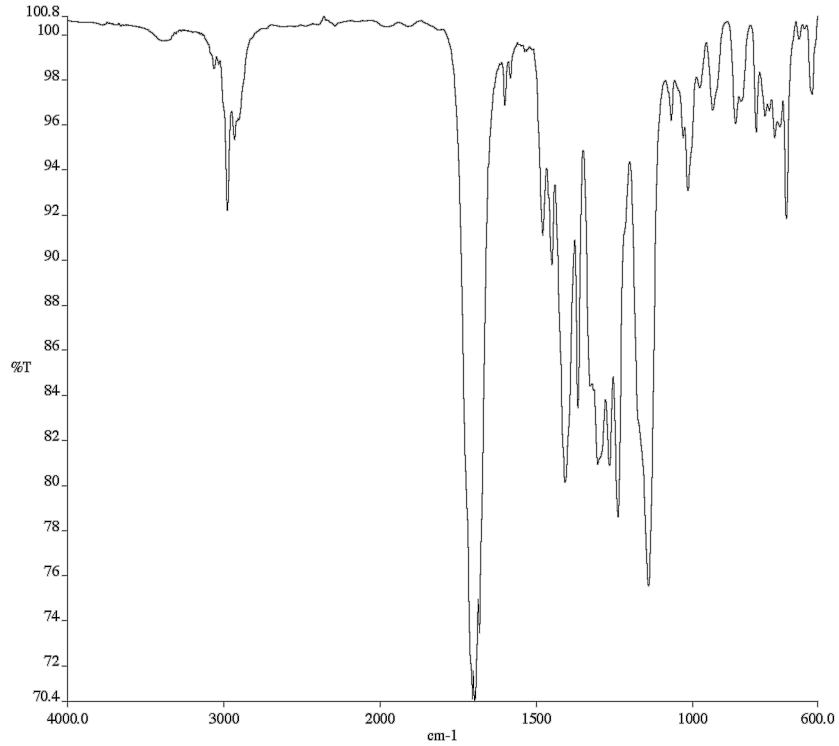

Figure A1.162 Infrared spectrum (Thin Film, NaCl) of compound **SI-5**.

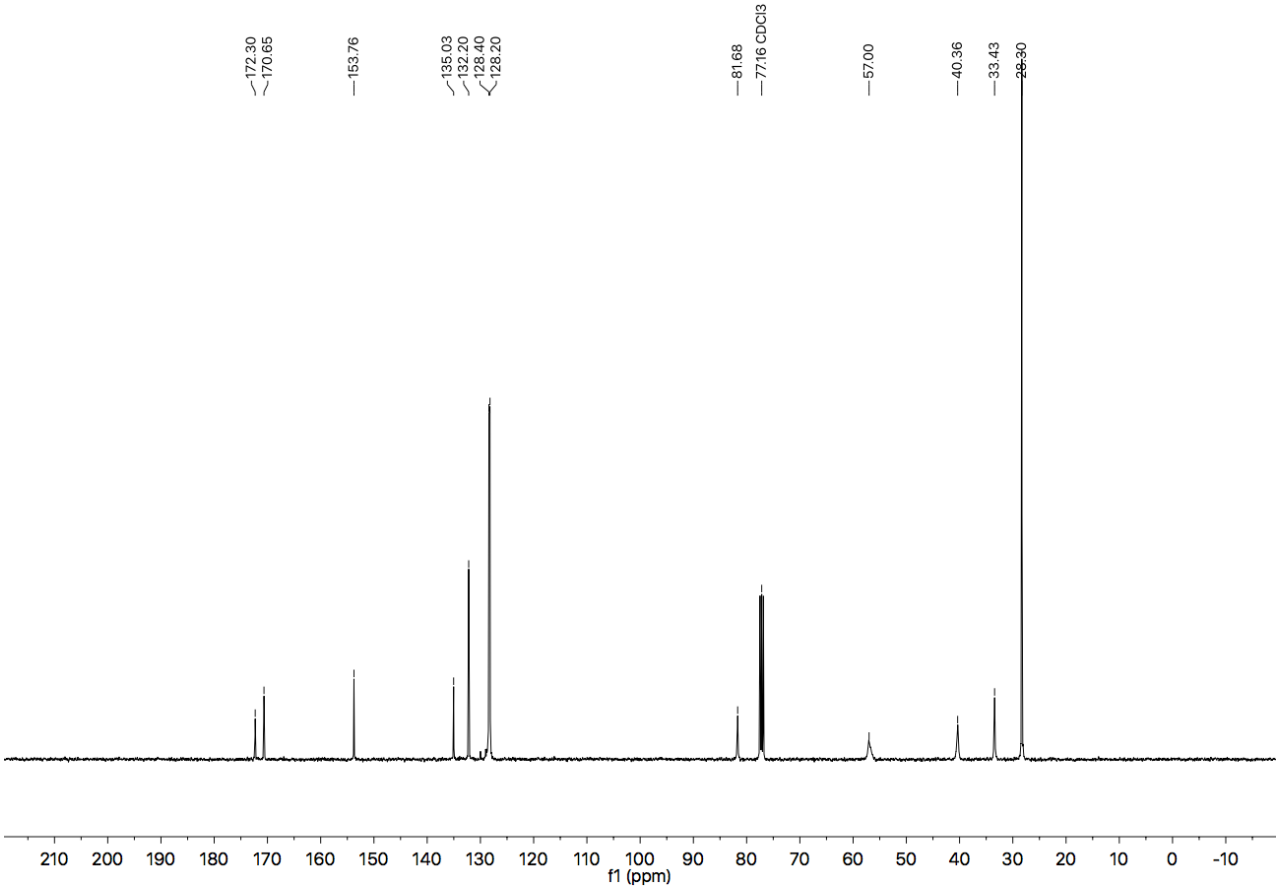

Figure A1.163 ^{13}C NMR (101 MHz, $CDCl_3$) of compound **SI-5**.

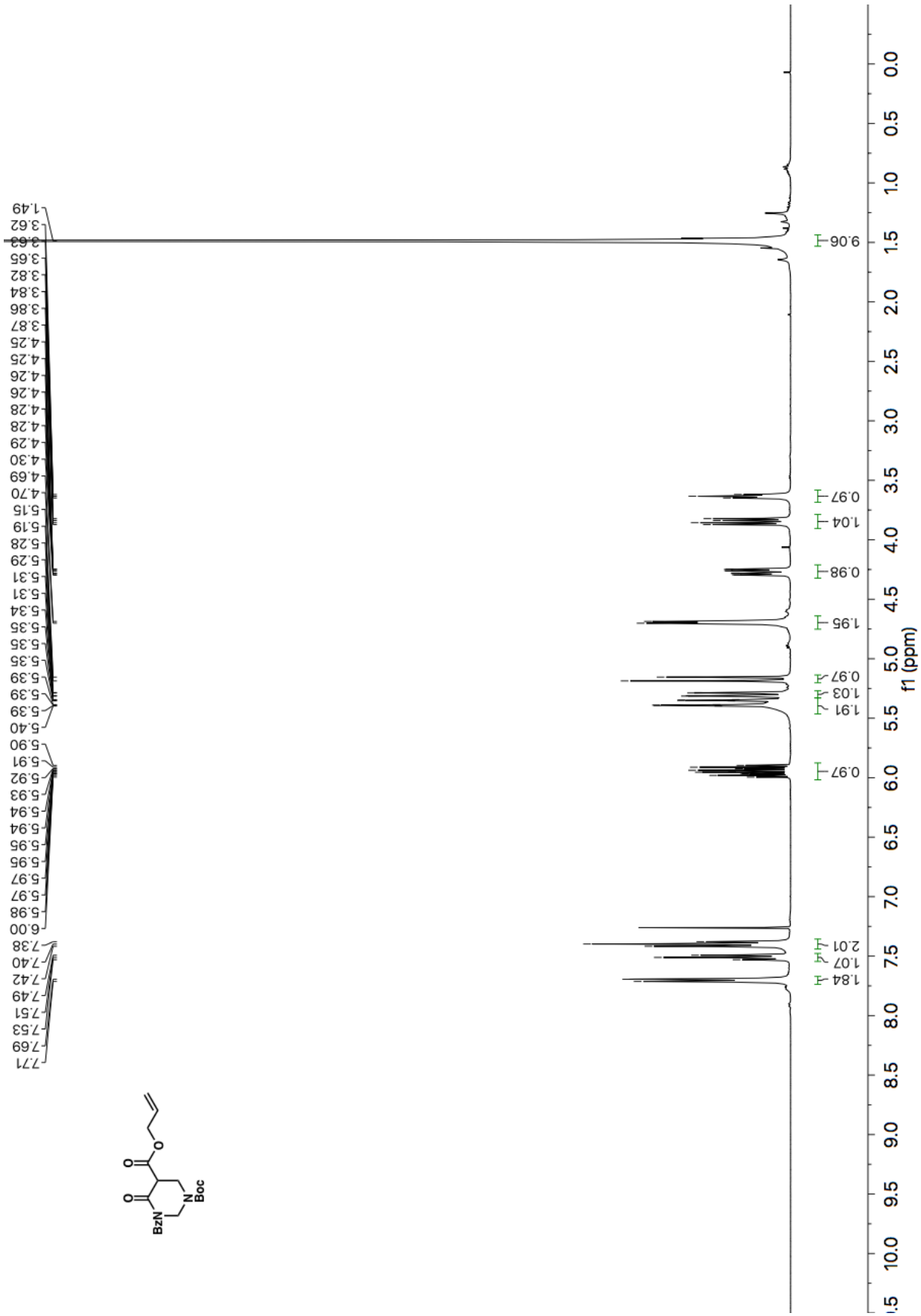

Figure A1.164 ^{1}H NMR (400 MHz, $CDCl_3$) of compound **SI-6.**

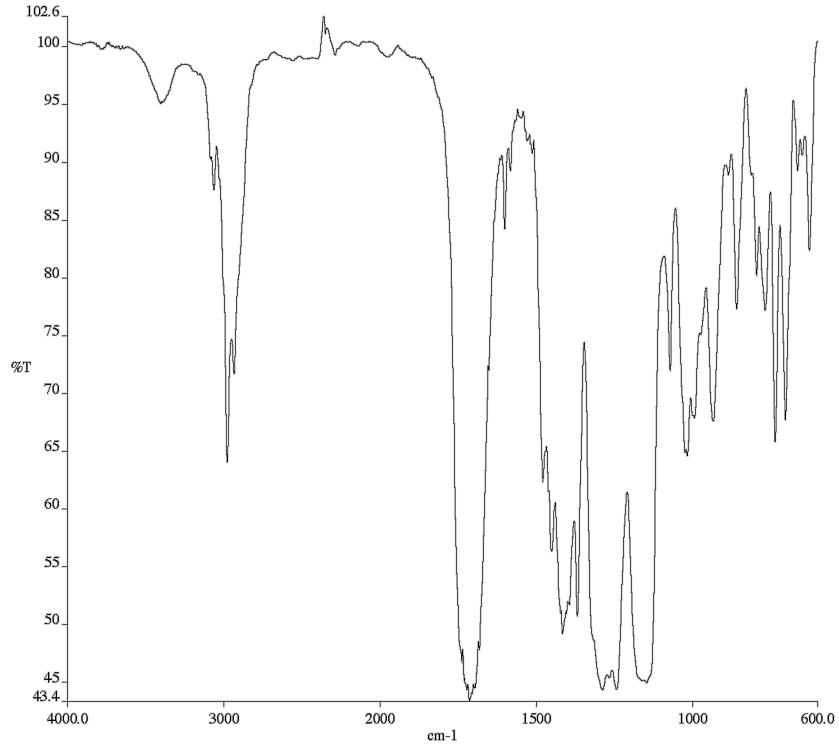

Figure A1.165 Infrared spectrum (Thin Film, NaCl) of compound **SI-6**.

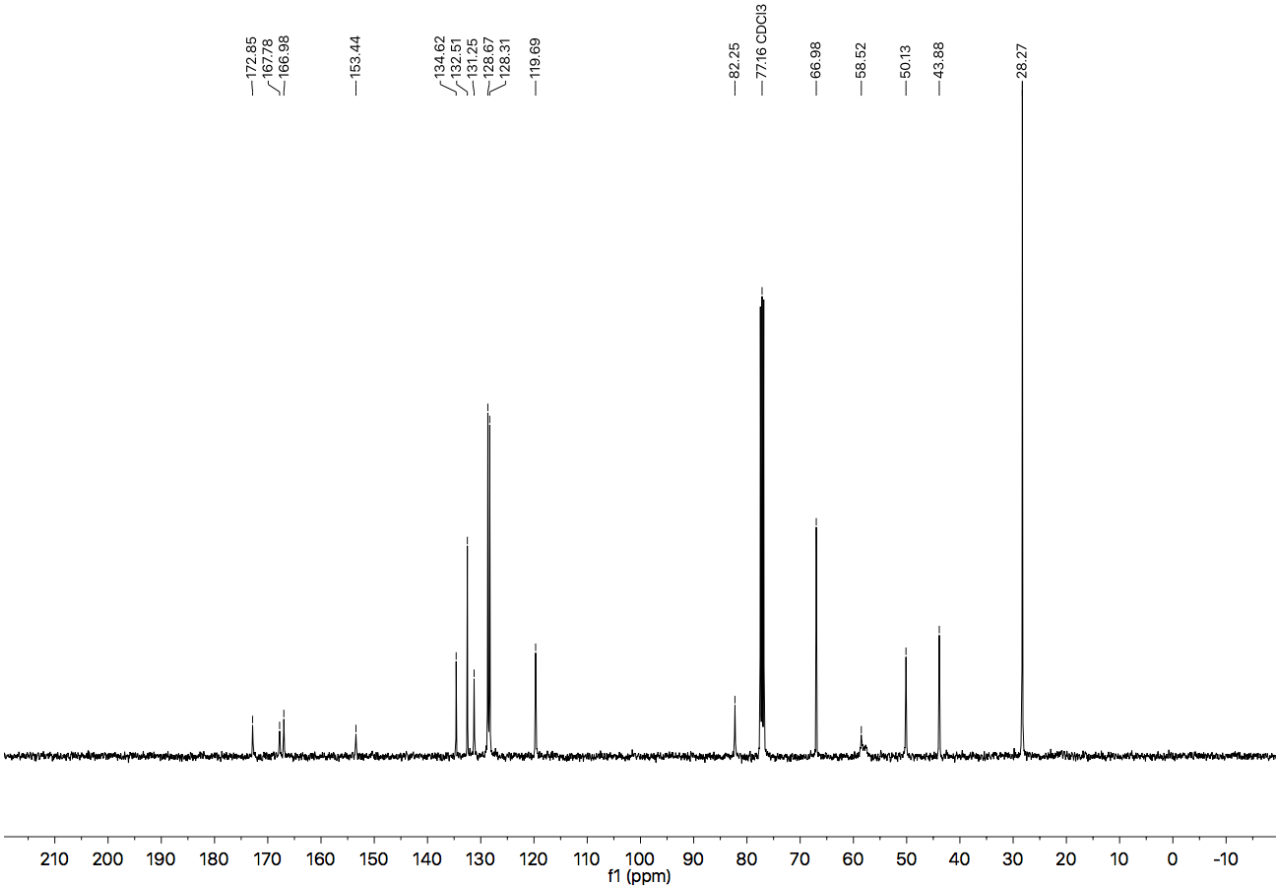

Figure A1.166 ^{13}C NMR (101 MHz, $CDCl_3$) of compound **SI-6**.

APPENDIX 2

Decarboxylative Asymmetric Allylic Alkylation of gem-Disubstituted Diazepanes[†]

A2.1 INTRODUCTION AND BACKGROUND

Diazepanes and benzodiazepines are medicinally important seven-membered diazaheterocycles found in a variety of pharmaceuticals, including the eponymous benzodiazepine class of GABA agonists widely used as anxiolytics, sedatives, and pain relievers. These heterocycles exhibit a range of biological activities, having been tested in cancer therapeutics (BMS-214662) and marketed in FDA-approved drugs for the treatment of various conditions including allergies (Emedastine), hypertension (Bunazosin), and more recently, insomnia (Suvorexant) (Figure A2.1). Merck's Suvorexant, which is the first orexin receptor antagonist of its class, is especially interesting as a mechanistically novel treatment for insomnia.

Figure A2.1 *Diazepines and diazepanes are medicinally important heterocycles*

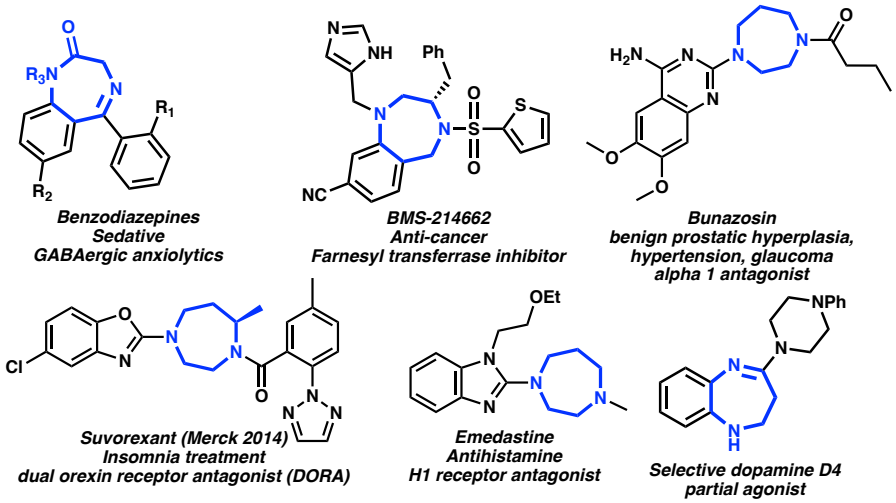

While these diazepane-containing pharmaceuticals may occasionally contain chiral monosubstitutions, chiral *gem*-disubstitutions are absent. In fact, to our knowledge, there are no known stereoselective methods to generate chiral *gem*-disubstituted diazepanes. Such a method would be important, as there is increasing recognition of the correlation between three-dimensional complexity and drug-like properties. This increasing recognition is in part responsible for the resurgent interest in natural-product screening libraries.[1] Thus, including more structurally complex *gem*-disubstituted diazepanes in the synthetic toolkit of medicinal chemistry would enable deeper structure-activity-relationship (SAR) studies of novel molecular space, potentially resulting in new small molecule drugs.

Figure A2.2 *gem-Disubstituted diazepanes can augment biological properties of small molecules*

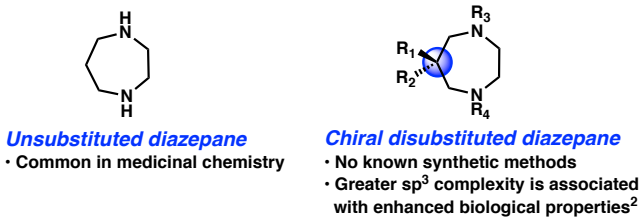

Here we report our preliminary investigations into the stereoselective synthesis of chiral *gem*-disubstituted oxo-diazepanes via the decarboxylative asymmetric allylic alkylation (DAAA) reaction. The resultant *gem*-disubstituted oxo-diazepanes can be reductively transformed into valuable chiral diazapanes. Our laboratory has extensively explored the utility of DAAA in generating all-carbon quaternary and tetrasubstituted centers; it has proven to be a robust method that tolerates an incredible range of substrates, from carbocyclic ketones to lactams to acyclic compounds. Oxodiazepane DAAA substrates can be synthesized beginning from Boc-piperidinone **A2.1** (Scheme A2.1); Beckmann rearrangement[2] of commercially available piperidinone **A2.1** (<$0.50/gram) results in Boc-diazepanone **A2.2**, which can then be benzoylated and acylated to afford dicarbonyl compound **A2.3**. **A2.3** then serves as a divergent point of entry into a variety of DAAA substrates.

Scheme A2.1 *Synthetic route toward diazepane DAAA substrates*

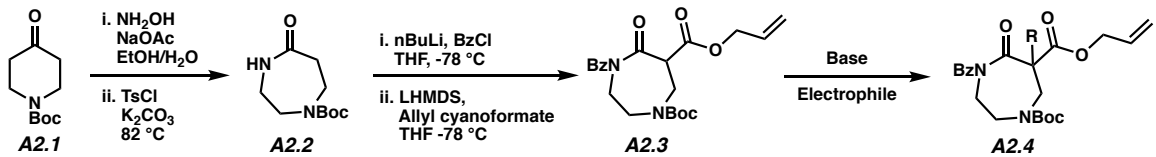

We chose the benzyl substrate **A2.4a** for initial optimizations (Table A2.1). Starting with conditions using (*S*)-$(CF_3)_3$-*t*-Bu-PHOX and 2:1 hexanes/toluene at 0.014 M concentration, which were based on our previous report,[3] we were pleased to obtain the desired oxo-diazepane in 85% *ee*. Polar aprotic ethereal solvents (entries 1 and 2) proved inferior to less polar solvents such as methylcyclohexane. Ultimately, we found that conducting the reaction in methylcyclohexane provided the highest enantioselectivity at 89% *ee* (Entry 6).

Table A2.1 *Optimization studies on the DAAA of benzyl substrate* ***A2.4a***

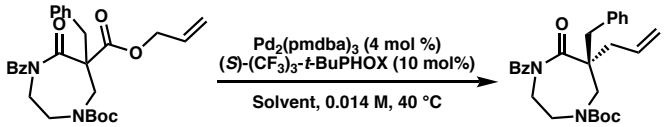

A2.4a ***A2.5a***

Entry	Solvent	ee (%)
1	THF	20
3	Dioxane	38
3	MTBE	70
4	Toluene	69
5	2:1 Hexanes/Toluene	85
6	MeCyclohexane	89

[a] Screens performed on a 0.04 mmol scale. [b] The *ee* values were determined by chiral SFC analysis. Bz = benzoyl, Boc = tert-butoxycarbonyl, pmdba = bis(4-methoxybenzylidene)acetone

With optimal conditions in hand, we began exploring the oxodiazepane DAAA substrate scope (Table A2.2). In substrates **A2.4i-k**, we examined the electronic effect of the N1 protecting group, observing that anisoyl-protection yielded the product **A2.5j** with greater

ee than the *para*-CF_3 and benzoyl versions **A2.5i** and **A2.5k**. The reaction is tolerant of a variety of functional groups such as chloroallyl (**A2.5b**), methyl ester (**A2.5c**), fluoro (**A2.5e**, **A2.5g**), carbamate (**A2.5f**), and alkyne (**A2.5h**), providing the desired products in *ee*'s up to 95% and yields up to >99%. Notably, the nitrile product **A2.5d** was obtained in a reduced 79% ee, suggesting that the seven-membered ring enables the nitrile functionality to adopt a conformation that interferes with the transition state of the reaction; this result contrasts with previous results using piperidinones and morpholinones in which high enantioselectivity was observed with the corresponding nitrile substrates.[4,5]

Table A2.2 *Oxodiazepane substrate scope exploration*

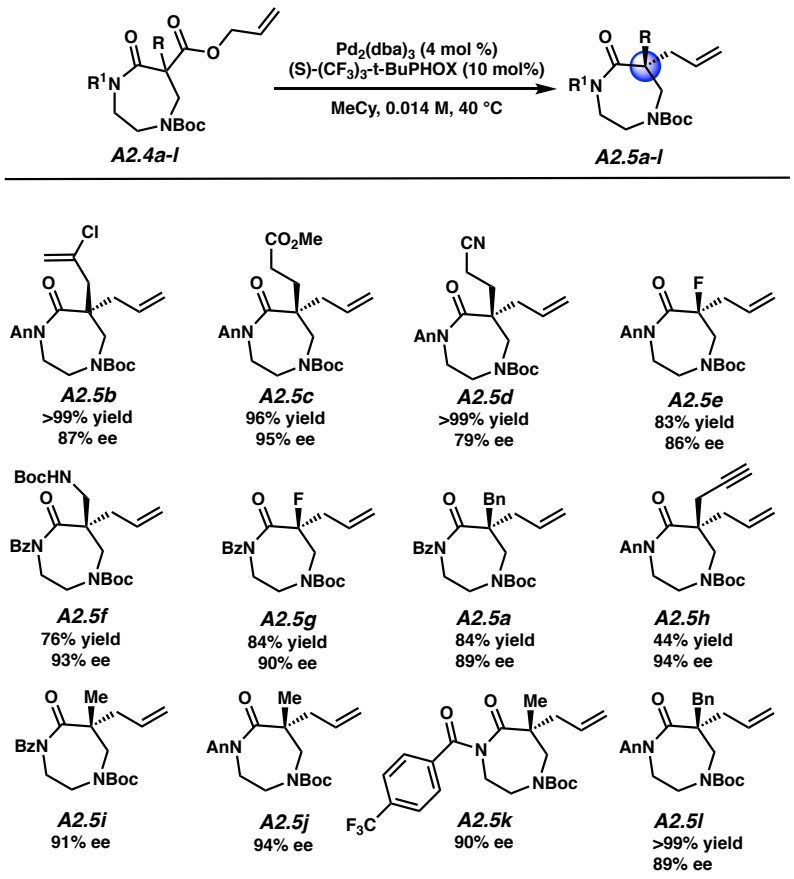

[a] Conditions: oxodiazepane **A2.4a-l** (1.0 equiv), $Pd_2(dba)_3$ (4 mol %), (*S*)-$(CF_3)_3$-*t*BuPHOX (10 mol %), in methylcyclohexane (0.014 M) at 40 °C for 12-24 h. [b] $Pd_2(pmdba)_3$ (4 mol %) instead of $Pd_2(dba)_3$. All reported yields are for isolated products. The *ee* values were determined by chiral SFC analysis. An = 4-methoxybenzoyl, dba = dibenzylideneacetone.

Unfortunately, attempts to synthesize other medicinally important seven-membered diazaheterocycle DAAA substrates using isomeric and benzo-fused intermediates such as **A2.6** and **A2.7** were unsuccessful. With **A2.6**, attempts at acylation to form the dicarbonyl intermediate resulted in degradation of the starting material. With **A2.7**, its corresponding enolate was unreactive and starting material was reisolated.

Scheme A2.2 *Attempted synthesis of other medicinally relevant DAAA substrates*

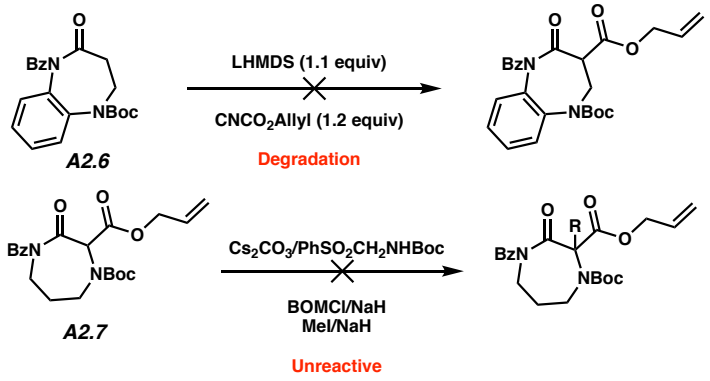

We are currently exploring various product derivatizations and transformations, the results of which we hope will be published shortly.

A2.2 CONCLUSIONS

In summary, we report the enantioselective synthesis of unprecedented *gem*-disubstituted oxodiazepanes using the venerable Pd-catalyzed decarboxylative asymmetric allylic alkylation. The versatile (*S*)-$(CF_3)_3$-*t*-Bu-PHOX ligand performs well,

yielding products in *ee*'s ranging from 79-95%. These novel chiral diazepanes are anticipated to find utility in the design of novel diazepane-containing pharmaceuticals; their added three-dimensional complexity should enable access to new chemical space in the quest for new medicines.

A2.3 EXPERIMENTAL SECTION

A2.3.1 MATERIALS AND METHODS

Unless otherwise stated, reactions were performed in flame-dried glassware under an argon or nitrogen atmosphere using dry, deoxygenated solvents. Solvents were dried by passage through an activated alumina column under argon. *tert*-Butyl 4-oxopiperidine-1-carboxylate **A2.1** was obtained from Combi-Blocks. Commercially obtained reagents were used as received. Chemicals were purchased from Sigma Aldrich/Strem/Alfa Aesar/Combi-Blocks and used as received.

Reaction temperatures were controlled by an IKAmag temperature modulator. Glove box manipulations were performed under a nitrogen atmosphere. Thin-layer chromatography (TLC) was performed using E. Merck silica gel 60 F254 precoated plates (0.25 mm) and visualized by UV fluorescence quenching, iodine on silica, ninhydrin, or $KMnO_4$ staining. Silia*Flash* P60 Academic Silica gel (particle size 0.040–0.063 mm) was used for flash chromatography.

Analytical SFC was performed with a Mettler SFC supercritical CO_2 analytical chromatography system utilizing a Chiralpak IC column (4.6 mm x 25 cm) obtained from Daicel Chemical Industries, Ltd. with visualization at 254 nm. Reverse Phase Preparatory HPLC was performed with a Teledyne ISCO ACCQPrep HP125 preparative liquid chromatography system equipped with a RediSep Prep C18 5 μm column (20 x 250 mm).

^{1}H NMR spectra were recorded on a Varian Inova 600 MHz or 500 MHz spectrometer or a Bruker Avance HD 400 MHz spectrometer and are reported relative to residual $CHCl_3$ (δ 7.26 ppm) or CH_3OH (δ 3.31 ppm). ^{13}C NMR spectra were recorded on a Varian Inova 500 MHz spectrometer or a Bruker Avance HD 400 MHz spectrometer and are reported relative to residual $CDCl_3$ (δ 77.16 ppm) or CD_3OD (δ 49.00 ppm). Data for ^{1}H NMR are reported as follows: s = singlet, d = doublet, t = triplet, q = quartet, p = pentet, sept = septuplet, m = multiplet, br s = broad singlet. Data for ^{13}C NMR are reported in terms of chemical shifts (δ ppm). Some reported spectra include minor solvent impurities of water (δ 1.56 or 4.87 ppm), ethyl acetate (δ 4.12, 2.05, 1.26 ppm), methylene chloride (δ 5.30 ppm), acetone (δ 2.17 ppm), grease (δ 1.26, 0.86 ppm), and/or silicon grease (δ 0.07 ppm), which do not impact product assignments.

IR spectra were obtained using a Perkin Elmer Paragon 1000 spectrometer using thin films deposited on NaCl plates and reported in frequency of absorption (cm^{-1}). High resolution mass spectra (HRMS) were obtained from an Agilent 6200 Series TOF with an Agilent G1978A Multimode source in electrospray ionization (ESI+), atmospheric pressure chemical ionization (APCI+), or mixed ionization mode (MM: ESI-APCI+). Optical rotations were measured with a Jasco P-2000 polarimeter operating on the sodium D-line (589 nm), using a 100 mm pathlength cell and are reported as: $[\alpha]_D^T$ (concentration in g/100 mL, solvent). Stereochemistry is assigned by analogy to previous results. [4,6–10]

A2.3.2 EXPERIMENTAL PROCEDURES AND SPECTROSCOPIC DATA

A2.3.3 Procedures for the Synthesis of Oxodiazepane Allylic Alkylation Substrates

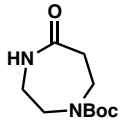

***tert*-butyl 5-oxo-1,4-diazepane-1-carboxylate**. Prepared according to a literature procedure, via Beckmann rearrangement.[2]

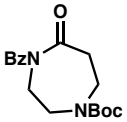

tert-butyl 4-benzoyl-5-oxo-1,4-diazepane-1-carboxylate. To a solution of ***tert*-butyl 5-oxo-1,4-diazepane-1-carboxylate** (5 g, 1 equiv) in THF (230 mL, 0.1 M) at -78 °C was slowly added *n*BuLi (12.8 mL, 2.18 M, 1.2 equiv). The cloudy solution was allowed to warm up at ambient temperature until the solution became clear, at which point it was again cooled to -78 °C. Then, BzCl (3.52 mL, 1.3 equiv) was added and the reaction turned light orange over several minutes. The reaction was stirred for 1 h at -78 °C and was then quenched with sat. NH_4Cl (aq), extracted with EtOAc (3x). The combined organic layers were dried over Na_2SO_4, concentrated onto SiO_2. The silica-adsorbed crude product was purified by silica gel flash chromatography (20% acetone/hexanes) to afford the desired product in quantitative yield (7.43g); **^{1}H NMR (400 MHz, $CDCl_3$)** δ 7.57 – 7.49 (m, 2H), 7.49 – 7.41 (m, 1H), 7.41 – 7.32 (m, 2H), 4.03 – 3.96 (m, 2H), 3.71 (q, *J* = 6.1, 5.1 Hz, 4H), 2.82 – 2.75 (m, 2H), 1.47 (s, 9H); **^{13}C NMR (101 MHz, $CDCl_3$)** δ 175.6, 173.7, 154.5, 135.9, 131.7, 128.2, 127.9, 80.7, (47.7 and 47.10 appear as two peaks due to hindered rotation), 45.4, (41.6 and 41.0 appear as two peaks due to hindered rotation), 40.6, 28.3; **IR (Neat Film, NaCl)** 2976, 2932, 2251, 1682, 1599, 1582, 1450,

1422, 1392, 1366,1327, 1285, 1247, 1229, 1157, 1115, 1032, 1018, 976, 954, 915,862, 793,769, 729, 696, 647 cm^{-1}; **HRMS (MM: ESI-APCI):** *m/z* calc'd for $C_{17}H_{26}N_3O_4$ $[M+NH_4]^+$: 336.1918, found 336.1912.

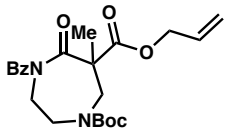

6-allyl 1-(tert-butyl) 4-benzoyl-6-methyl-5-oxo-1,4-diazepane-1,6-dicarboxylate. To a solution of **6-allyl 1-(tert-butyl) 4-benzoyl-5-oxo-1,4-diazepane-1,6-dicarboxylate** (240 mg, 1 equiv) in THF (6 mL, 0.1 M) at 0 °C was added NaH (60% in mineral oil, 26 mg, 1.1 equiv). The solution was stirred at 0 °C for 40 min and then MeI (186 uL, 5 equiv) was added. The reaction was heated to 45 °C for 16 h, then quenched with sat. NH_4Cl (aq), and then extracted with EtOAc (3x). The combined organic layers were dried over Na_2SO_4 and concentrated onto SiO_2. The silica-adsorbed crude product was purified by silica gel flash chromatography (20% EtOAc/hexanes) to afford the desired product in as a light yellow oil (200 mg, 81% yield). **^{1}H NMR (400 MHz, $CDCl_3$)** δ 7.70 – 7.63 (m, 2H), 7.52 – 7.43 (m, 1H), 7.38 (t, *J* = 7.6 Hz, 2H), 5.96 (ddt, *J* = 16.6, 10.4, 6.0 Hz, 1H), 5.40 (dq, *J* = 17.3, 1.5 Hz, 1H), 5.34 (d, *J* = 10.4 Hz, 1H), 4.73 (t, *J* = 6.2 Hz, 2H), 4.33 (s, 1H), 4.10 (d, *J* = 14.8 Hz, 1H), 3.64 (dt, *J* = 14.0, 3.4 Hz, 4H), 1.57 (s, 3H), 1.45 (s, 9H); **^{13}C NMR (101 MHz, $CDCl_3$)** δ (174.5 and 174.1 appear as two peaks due to hindered rotation), 173.0, 171.7, (155.1 and 154.9 appear as two peaks due to hindered rotation), 135.7, 131.9, 131.1, 128.3, 128.2, 120.1, 81.1, 66.8, 57.6, (49.7 and 49.0 appear as two peaks due to hindered rotation), (47.0 and 46.0 appear as two peaks due to hindered rotation), 43.1, 28.4, 23.6. **IR (Neat Film, NaCl)** 2977, 1693, 1449, 1416, 1366, 1325,

1281, 1249, 1139, 1104, 1047, 983, 938, 768, 727, 694 cm^{-1}; **HRMS (MM: ESI-APCI):** *m/z* calc'd for $C_{22}H_{28}N_2O_6$ $[M+H]^+$: 417.2020, found 417.2010.

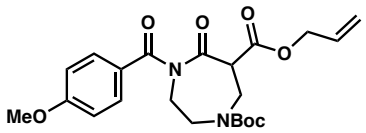

6-allyl 1-(tert-butyl) 4-(4-methoxybenzoyl)-5-oxo-1,4-diazepane-1,6-dicarboxylate.

To a solution of ***tert*-butyl 4-(4-methoxybenzoyl)-5-oxo-1,4-diazepane-1-carboxylate** (1 g, 1.0 equiv) in THF (20 mL, 0.1 M total concentration) at −78 °C was added LiHMDS (528 mg, 1.1 equiv) in THF (9 mL) dropwise. The resulting light yellow reaction mixture was stirred for 15 min at −78 °C. Then, allyl cyanoformate (368 μL, 1.2 equiv) was added dropwise at −78 °C, giving a clear solution. After stirring for 1.5 h at −78 °C, the reaction was quenched with 1 M HCl (10 mL) and diluted with ethyl acetate (20 mL). The aqueous phase was extracted with ethyl acetate (3 x 30 mL). The combined organic layers were dried over anhydrous Na_2SO_4 and solid $NaHCO_3$, decanted, and concentrated under reduced pressure onto silica. The silica-adsorbed crude mixture was purified by silica gel flash chromatography (10% → 20% EtOAc/hexanes) to give **allyl 1-(tert-butyl) 4-(4-methoxybenzoyl)-5-oxo-1,4-diazepane-1,6-dicarboxylate** as a clear oil (600 mg, 48% yield). **^{1}H NMR (400 MHz, $CDCl_3$)** δ 7.72 – 7.60 (m, 2H), 6.91 – 6.79 (m, 2H), 5.92 (ddt, *J* = 17.3, 10.4, 5.9 Hz, 1H), 5.42 – 5.20 (m, 2H), 4.77 – 4.56 (m, 2H), 4.40 – 3.92 (m, 4H), 3.82 (s, 5H), 3.58 – 3.24 (m, 1H), 1.46 (s, 9H); **^{13}C NMR (101 MHz, $CDCl_3$)** δ 173.1, 171.3, 167.6, 163.1, 154.6, 131.3, 131.2, 127.0, 119.4, 113.6, 81.1, 66.5, 55.9, 55.4, (47.7 and 46.7 appear as two peaks due to hindered rotation),

45.12, (43.3 and 42.8 appear as two peaks due to hindered rotation), 28.3. **IR (Neat Film, NaCl)** 2977, 1746, 1693, 1603, 1578, 1511, 1454, 1419, 1392, 1366, 1324, 1255, 1168, 1025, 995, 965, 842, 766 cm^{-1}; **HRMS (MM: ESI-APCI):** *m/z* calc'd for $C_{22}H_{28}N_2O_7$ $[M+H]^+$: 433.1969, found 433.1966.

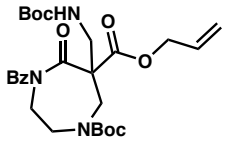

6-allyl 1-(tert-butyl) 4-benzoyl-6-(((tert-butoxycarbonyl)amino)methyl)-5-oxo-1,4-diazepane-1,6-dicarboxylate. A solution of **A2.3** (200 mg, 1 equiv) and *tert*-butyl ((phenylsulfonyl)methyl)carbamate[11,12] (162 mg, 1.2 equiv) in CH_2Cl_2 (2.5 mL, 0.2 M) was stirred for 5 min at rt. Then at room temperature was added Cs_2CO_3 (405 mg, 2.5 equiv). The reaction was stirred at rt for 30 min, then sat. aqueous NH_4Cl (1 mL) was added and the biphasic mixture was vigorously stirred for 20 min. The aqueous phase was extracted with CH_2Cl_2 (3 x 3 mL). The combined organic phases were dried over anhydrous Na_2SO_4, decanted, and concentrated under reduced pressure onto silica gel. The silica-loaded crude reaction mixture was purified by automated silica gel flash chromatography (Teledyne ISCO) (10 → 40% acetone/hexanes) to give methylcarbamate allyl ester **A2.4f** as a white foam (200 mg, 76% yield): **^{1}H NMR (400 MHz, $CDCl_3$)** δ 7.83 – 7.71 (m, 2H), 7.59 – 7.46 (m, 1H), 7.40 (dd, *J* = 8.4, 7.0 Hz, 2H), 6.00 (ddt, *J* = 16.6, 10.3, 6.1 Hz, 1H), 5.51 – 5.25 (m, 2H), 5.17 (s, 1H), 4.81 – 4.62 (m, 2H), 4.36 (dd, *J* = 51.1, 15.8 Hz, 1H), 4.14 – 3.20 (m, 7H), 1.43 (d, *J* = 8.5 Hz, 18H); **^{13}C NMR (101 MHz, $CDCl_3$)** δ (174.1 and 173.8 appear as two peaks due to hindered rotation), 172.7, (170.0 and 169.6 appear as two peaks due to hindered rotation), 155.9, (155.1 and 154.6

appear as two peaks due to hindered rotation), 135.4, 132.2, 131.3, 128.5, 128.3, 120.2, 81.4, 79.5, 67.4, 62.6, 47.0, 46.8, 45.9, 43.2, 28.4, 28.4. **IR (Neat Film, NaCl)** 3457, 2977, 2934, 2253, 1704, 1600, 1503, 1450, 1417, 1392, 1367, 1325, 1283, 1248, 1158, 1042, 980, 913,77 860, 767, 729, 693, 663 cm^{-1}; **HRMS (MM: ESI-APCI):** *m/z* calc'd for $C_{27}H_{37}N_3O_8$ $[M+H]^+$: 532.2653, found 532.2664.

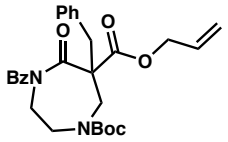

6-allyl 1-(tert-butyl) 4-benzoyl-6-benzyl-5-oxo-1,4-diazepane-1,6-dicarboxylate (A2.4a). Sodium hydride (60% in mineral oil, 22 mg, 1.1 equiv) was added to a solution of allyl ester **A2.3** (200 mg, 1.0 equiv) in THF (5 mL, 0.1 M) at 0 °C. After stirring for 30 min at 0 °C, BnBr (71 μL, 1.2 equiv) was added. The reaction mixture was heated to 50 °C and stirred for 16 h; at the 4 h mark, 2 equiv BnBr was added; at the 12 h mark, 2 equiv more BnBr was added. The reaction was quenched with aqueous NH_4Cl (10 mL) and extracted with EtOAc (3 x 5 mL). The combined organic phases were dried over anhydrous Na_2SO_4, decanted, and concentrated under reduced pressure onto silica gel. The silica-loaded residue was purified by silica gel flash chromatography (20% EtOAc/hexanes) to give benzylated allyl ester **A2.4a** as a white foam (130 mg, 53% yield). **^{1}H NMR (400 MHz, Chloroform-*d*)** δ 7.68 (d, *J* = 7.6 Hz, 2H), 7.55 – 7.46 (m, 1H), 7.37 (t, *J* = 7.7 Hz, 2H), 7.31 – 7.25 (m, 3H), 7.24 – 7.12 (m, 2H), 5.86 (tq, *J* = 22.8, 6.5 Hz, 1H), 5.38 (s, 1H), 5.36 – 5.27 (m, 1H), 4.63 (q, *J* = 6.3, 5.8 Hz, 2H), 4.12 (d, *J* = 15.1 Hz, 1H), 4.01 – 3.89 (m, 1H), 3.69 (q, *J* = 12.0, 9.6 Hz, 2H), 3.61 – 3.35 (m, 3H),

1.45 (s, 9H); **^{13}C NMR (101 MHz, $CDCl_3$)** δ (174.3 and 174.0 appear as two peaks due to hindered rotation), (172.1 and 171.9 appear as two peaks due to hindered rotation), (170.8 and 170.2 appear as two peaks due to hindered rotation), (155.5 and 154.9 appear as two peaks due to hindered rotation), (135.6 & 135.5 appear as two peaks due to hindered rotation), 135.4, 132.0, (131.1 & 130.9 appear as two peaks due to hindered rotation), (130.7 & 130.5 appear as two peaks due to hindered rotation), 128.4, 128.4, 128.2, (127.4 & 127.3 appear as two peaks due to hindered rotation), (120.5 & 120.1 appear as two peaks due to hindered rotation), (81.2 & 80.9 appear as two peaks due to hindered rotation), (66.9 & 66.8 appear as two peaks due to hindered rotation), (62.5 & 62.1 appear as two peaks due to hindered rotation), (47.3 & 46.7 appear as two peaks due to hindered rotation), (46.2 & 45.7 appear as two peaks due to hindered rotation), (42.4 & 42.1 appear as two peaks due to hindered rotation), 42.0, 28.4. **IR (Neat Film, NaCl)** 3062, 3030, 2976, 2933, 1694, 1601, 1583, 1494, 1450, 1415, 1392, 1366, 1325, 1280, 1247, 1154, 1131, 1092, 1041, 1022, 980, 939, 867, 795, 767, 727, 703, 661 cm^{-1}; **HRMS (MM: ESI-APCI):** *m/z* calc'd for $C_{28}H_{32}N_2O_6$ $[M+H]^+$: 437.1707, found 437.1697.

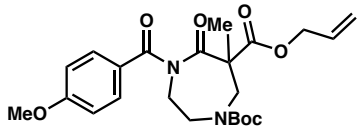

6-allyl 1-(tert-butyl) 4-(4-methoxybenzoyl)-6-methyl-5-oxo-1,4-diazepane-1,6-dicarboxylate (A2.4j). To a solution of anisoyl allyl ester (200 mg, 1 equiv) and Cs_2CO_3 (301 mg, 2 equiv) in MeCN (4.6 mL, 0.1 M) was added MeI (143 uL, 5 equiv). The reaction was heated to 45 °C for 40 min and then quenched with aqueous NH_4Cl (10 mL)

and extracted with EtOAc (3 x 5 mL). The combined organic phases were dried over anhydrous Na_2SO_4, decanted, and concentrated under reduced pressure. The crude product was purified by automated silica gel flash chromatography (Teledyne ISCO) (0 → 90% EtOAc/hexanes) to give methylated allyl ester **A2.4j** as a clear oil (70 mg, 34% yield). **^{1}H NMR (400 MHz, Chloroform-*d*)** δ 7.75 – 7.65 (m, 2H), 6.90 – 6.82 (m, 2H), 5.96 (ddt, *J* = 17.3, 10.4, 6.0 Hz, 1H), 5.40 (dq, *J* = 17.2, 1.4 Hz, 1H), 5.36 – 5.29 (m, 1H), 4.71 (dddd, *J* = 14.2, 7.3, 4.4, 2.1 Hz, 2H), 4.27 – 4.15 (m, 1H), 4.14 – 4.04 (m, 1H), 3.83 (s, 3H), 3.76 (d, *J* = 13.6 Hz, 1H), 3.62 (dt, *J* = 13.9, 3.2 Hz, 2H), 3.56 – 3.46 (m, 1H), 1.60 – 1.55 (m, 3H), 1.44 (d, *J* = 17.8 Hz, 9H); **^{13}C NMR (101 MHz, $CDCl_3$)** (173.9 & 173.6 appear as two peaks due to hindered rotation), 172.8, (172.0 & 171.8 appear as two peaks due to hindered rotation), 162.9, (155.1 & 154.9 appear as two peaks due to hindered rotation), 131.2, 131.2, 130.9, 127.5, (120.1 & 119.9 appear as two peaks due to hindered rotation), 113.6, 80.9, 66.7, 57.5, 55.4, (49.6 & 48.1 appear as two peaks due to hindered rotation), (47.1 & 46.1 appear as two peaks due to hindered rotation), 43.6, 28.3, 23.6. **IR (Neat Film, NaCl)** 2974, 2937, 1698, 1604, 1578, 1511, 1453, 1416, 1392, 1366, 1324, 1280, 1256, 1169, 1139, 1103, 1031, 1001, 983, 929, 840, 768, 733 cm^{-1}; **HRMS (MM: ESI-APCI):** *m/z* calc'd for $C_{23}H_{30}N_2O_7$ $[M+H]^+$: 447.2126, found 447.2128.

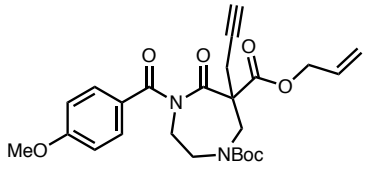

6-allyl 1-(tert-butyl) 4-(4-methoxybenzoyl)-5-oxo-6-(prop-2-yn-1-yl)-1,4-diazepane-1,6-dicarboxylate (A2.4h). Sodium hydride (60% in mineral oil, 25 mg, 1.1 equiv) was added to a solution of anisoyl allyl ester (250 mg, 1.0 equiv) in THF (5.8 mL, 0.1 M) at 0 °C. After stirring for 30 min at 0 °C, propargyl bromide (80% wt/wt in toluene, 125 μL, 2 equiv) was added. The reaction mixture was heated to 50 °C and stirred for 16 h, turning yellow in minutes. The reaction was quenched with aqueous $NaHCO_3$ (10 mL) and extracted with EtOAc (3 x 5 mL). The combined organic phases were dried over anhydrous Na_2SO_4, decanted, and concentrated under reduced pressure. The crude product was purified by automated silica gel flash chromatography (Teledyne ISCO, 0 → 50% acetone/hexanes) to give propargyl allyl ester **A2.4h** as a clear oil (220 mg, 81% yield). **^{1}H NMR (500 MHz, Chloroform-*d*)** δ 7.68 (dt, *J* = 11.9, 4.8 Hz, 2H), 6.84 (d, *J* = 8.6 Hz, 2H), 5.99 (ddt, *J* = 17.3, 10.4, 6.0 Hz, 1H), 5.54 – 5.27 (m, 2H), 4.79 (dd, *J* = 14.0, 5.8 Hz, 2H), 4.33 – 3.96 (m, 3H), 3.82 (s, 4H), 3.78 – 3.56 (m, 1H), 3.48 (dt, *J* = 13.3, 3.1 Hz, 1H), 3.17 – 3.01 (m, 1H), 3.01 – 2.88 (m, 1H), 2.08 (t, *J* = 2.8 Hz, 1H), 1.42 (d, *J* = 14.3 Hz, 9H); **^{13}C NMR (126 MHz, cdcl$_3$)** δ (173.7 & 173.2 appear as two peaks due to hindered rotation), (170.5 & 170.3 appear as two peaks due to hindered rotation), (169.7 & 169.2 appear as two peaks due to hindered rotation), 163.0, (155.5 & 154.9 appear as two peaks due to hindered rotation), 131.1, 131.0, 127.1, 120.2, 120.0, 113.5, (81.1 & 81.0 appear as two peaks due to hindered rotation), (78.9 & 78.6 appear as two peaks due to hindered rotation), 72.3, 67.3, (60.7 & 60.4 appear as two peaks due to hindered rotation), 55.4, (47.0 & 46.5 appear as two peaks due to hindered rotation), (46.1 & 46.0 appear as two peaks due to hindered rotation), 43.0, 28.3, (27.0 & 26.8

appear as two peaks due to hindered rotation). **HRMS (MM: ESI-APCI):** *m/z* calc'd for $C_{25}H_{31}N_2O_7$ $[M+H]^+$: 471. 2126, found 471.2130.

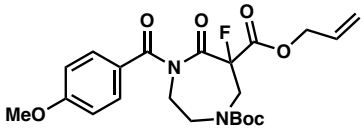

6-allyl 1-(tert-butyl) 6-fluoro-4-(4-methoxybenzoyl)-5-oxo-1,4-diazepane-1,6-dicarboxylate (A2.4e). Sodium hydride (60% in mineral oil, 32 mg, 1.1 equiv) was added to a solution of anisoyl allyl ester (320 mg, 1.0 equiv) in THF (7.4 mL, 0.1 M) at 0 °C. After stirring for 30 min at rt, Selectfluor (315 mg 1.2 equiv) was added. The reaction mixture was heated to 50 °C and stirred for 16 h. The reaction was quenched with aqueous $NaHCO_3$ (10 mL) and extracted with EtOAc (3 x 5 mL). The combined organic phases were dried over anhydrous Na_2SO_4, decanted, and concentrated under reduced pressure. The crude product was purified by automated silica gel flash chromatography (Teledyne ISCO, 0 → 50% acetone/hexanes) to give fluorinated allyl ester **A2.4e** as a clear oil (290 mg, 87% yield). **^{1}H NMR (400 MHz, Chloroform-*d*)** δ 7.66 – 7.58 (m, 2H), 6.90 – 6.82 (m, 2H), 5.91 (ddt, *J* = 16.3, 10.9, 5.7 Hz, 1H), 5.42 – 5.32 (m, 1H), 5.29 (d, *J* = 9.6 Hz, 1H), 4.71 (dt, *J* = 21.0, 13.8 Hz, 3H), 4.52 – 4.40 (m, 1H), 4.39 – 4.19 (m, 2H), 3.94 (ddd, *J* = 21.1, 14.6, 9.4 Hz, 1H), 3.82 (s, 3H), 3.77 – 3.56 (m, 1H), 3.22 – 3.09 (m, 1H), 1.47 (s, 9H); **^{13}C NMR (101 MHz, $CDCl_3$)** δ 172.5, 169.6 (dd, *J* = 48.2, 25.4 Hz), 164.9 (d, *J* = 25.8 Hz), 163.4, 154.9, 131.2, 130.8, 126.0, 119.7, 113.8, 95.66 (dd, *J* = 205.6, 14.6 Hz), 81.4, 67.2, 55.5, 47.5 (dd, *J* = 109.0, 23.7 Hz), 47.1

(d, J = 92.2 Hz), 43.3, 28.2. **IR (Neat Film, NaCl)** cm^{-1}; **HRMS (MM: ESI-APCI):** *m/z* calc'd for $C_{22}H_{28}FN_2O_7$ $[M+H]^+$: 451.1875, found 451.1877.

A2.3.4 General Procedure for Allylic Alkylation Optimization Screen

In a nitrogen-filled glovebox, an oven-dried 1 dram vial was charged with $Pd_2(pmdba)_3$ (4 mol %), ligand (10 mol %), solvent (1 mL), and a magnetic stir bar. The vial was stirred at ambient glovebox temperature (27 °C) for 30 min and then substrate **A2.4a** (20 mg, 1.0 equiv) was added as a solution in solvent (1.8 mL, total concentration 0.014 M). The vial was sealed with a teflon cap and heated to 40 °C. When complete consumption of the starting material was observed by thin layer chromatography, the reaction mixture was removed from the glovebox and concentrated under reduced pressure. The residue was purified by silica gel flash chromatography to afford the oxodiazepane **A2.5a**.

A2.3.5 General Procedure for Pd-Catalyzed Decarboxylative Allylic Alkylation Reactions

<u>*Please note*</u> The absolute configuration for all other products has been inferred by analogy.[4,6–10] For respective SFC conditions, please refer to the section **Determination of Enantiomeric Excess**.

In a nitrogen-filled glovebox, an oven-dried 1 dram vial or 20 mL scintillation vial was charged with $Pd_2(pmdba)_3$ or $Pd_2(dba)_3$ (4 mol %), (*S*)-$(CF_3)_3$-*t*Bu-PHOX (10 mol %), methylcyclohexane, and a magnetic stir bar. The vial was stirred at ambient glovebox temperature (27 °C) for 30 min and then the substrate (1.0 equiv) was added as

a solution in methylcyclohexane (total concentration 0.014 M). The vial was sealed with a teflon cap and heated to 40 °C. When complete consumption of the starting material was observed by thin layer chromatography, the reaction mixture was removed from the glovebox and concentrated under reduced pressure. The residue was purified by silica gel flash chromatography to afford the desired oxopiperazine.

A2.3.6 Experimental Procedures and Spectroscopic data for the Pd-Catalyzed Decarboxylative Asymmetric Allylic Alkylation of Oxodiazepane Substrates

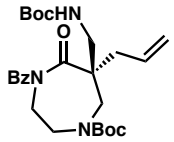

tert-butyl (*S*)-6-allyl-4-benzoyl-6-(((tert-butoxycarbonyl)amino)methyl)-5-oxo-1,4-diazepane-1-carboxylate (A2.5f). Following the general procedure, allyl ester **A2.4f** (53 mg, 1.0 equiv) in MeCy (1 mL) was added to a solution of $Pd_2(dba)_3$ (3.7 mg, 4 mol %) and (*S*)-$(CF_3)_3$-*t*Bu-PHOX (5.9 mg, 10 mol %) in MeCy (7.1 mL). Purification by automated silica gel flash chromatography (0 → 50% EtOAc/hexanes) gave methyl carbamate oxodiazepane **A2.5f** as a white foam (37 mg, 76% yield, 93% ee). **^{1}H NMR (400 MHz, Chloroform-*d*)** δ 7.71 – 7.31 (m, 5H), 5.74 (ddt, *J* = 15.7, 10.5, 7.4 Hz, 1H), 5.21 – 5.05 (m, 2H), 4.38 (dd, *J* = 15.2, 5.3 Hz, 1H), 4.09 – 3.13 (m, 7H), 2.67 – 2.09 (m, 2H), 1.47 (d, *J* = 24.6 Hz, 18H); **^{13}C NMR (101 MHz, $CDCl_3$)** δ (179.3 and 178.8 appear as two peaks due to hindered rotation), 174.5, 156.2, (155.9 and 155.0 appear as two peaks due to hindered rotation), 136.2, (132.5 and 132.0 appear as two peaks due to

hindered rotation), 131.7, 128.5, 127.7, 120.0, (81.3 and 81.1 appear as two peaks due to hindered rotation), 79.5, 54.7, 48.8, (47.2 and 46.7 appear as two peaks due to hindered rotation), 46.2, (42.6 and 41.1 appear as two peaks due to hindered rotation), (38.7 and 37.1 appear as two peaks due to hindered rotation), 28.5, 28.4. **IR (Neat Film, NaCl)** 2977, 1687, 1502, 1422, 1391, 1365, 1322, 1282, 1245, 1168, 978, 916, 753 cm^{-1}; **HRMS (MM: ESI-APCI):** *m/z* calc'd for $C_{26}H_{37}N_3O_6$ $[M+H]^+$: 488.2755, found 488.2747; $\mathbf{[\alpha]_D^{23.2}}$ –3.70 (c 1.85, $CHCl_3$); **SFC conditions**: 20% IPA, 2.5 mL/min, Chiralpak IC column, λ = 254 nm, t_R (min): major = 5.684, minor = 4.539.

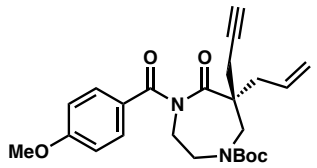

tert-butyl (S)-6-allyl-4-(4-methoxybenzoyl)-5-oxo-6-(prop-2-yn-1-yl)-1,4-diazepane-1-carboxylate (A2.5h). Following the general procedure, allyl ester **A2.4h** (70 mg, 1.0 equiv) in MeCy (1 mL) was added to a solution of $Pd_2(dba)_3$ (5.4 mg, 4 mol %) and (*S*)-$(CF_3)_3$-*t*Bu-PHOX (8.8 mg, 10 mol %) in MeCy (7.3 mL). **Note: Reaction performed at 50 °C because no reaction occurred at 40 °C**. Purification by automated silica gel flash chromatography (Teledyne ISCO, 0 → 40% acetone/hexanes) gave propargyl oxodiazepane **A2.5h** as a clear oil (28 mg, 44% yield, 94% ee); **^{1}H NMR (400 MHz, Chloroform-*d*)** δ 7.59 (d, *J* = 8.2 Hz, 2H), 6.96 – 6.80 (m, 2H), 5.93 – 5.63 (m, 1H), 5.30 – 5.10 (m, 2H), 4.28 (d, *J* = 15.2 Hz, 1H), 3.83 (s, 7H), 3.50 (d, *J* = 11.6 Hz, 1H), 2.60 (dq, *J* = 30.2, 17.2, 16.6 Hz, 4H), 2.20 – 1.99 (m, 1H), 1.55 (d, *J* = 38.4 Hz, 9H); **^{13}C NMR (101 MHz, $CDCl_3$)** δ 177.5, 174.6, 162.8, (155.6 & 155.2 appear as two peaks due

to hindered rotation), 132.1, 130.7, 127.9, 120.0, 113.7, (81.1 & 80.9 appear as two peaks due to hindered rotation), 80.5, 72.0, 55.5, 52.6, (49.1 & 46.9 appear as two peaks due to hindered rotation), 47.6, (43.0 & 42.33 appear as two peaks due to hindered rotation), (39.11 & 37.4 appear as two peaks due to hindered rotation), 28.5, (26.5 & 25.9 appear as two peaks due to hindered rotation). **IR (Neat Film, NaCl)** 3283, 2972, 2922, 1692, 1603, 1511, 1454, 1418, 1365, 1322, 1255, 1169, 1031, 980, 926, 839, 766, 670 cm^{-1}; **HRMS (MM: ESI-APCI):** *m/z* calc'd for $C_{24}H_{31}N_2O_5$ $[M+H]^+$: 427.2227, found 427.2238; **$[\alpha]_D^{22.1}$** –7.69 (c 1.0, $CHCl_3$); **SFC conditions**: 10% IPA, 2.5 mL/min, Chiralpak AD-H column, λ = 254 nm, t_R (min): major = 11.163, minor = 10.615.

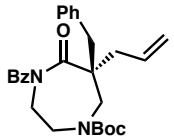

tert-butyl (*S*)-6-allyl-4-benzoyl-6-benzyl-5-oxo-1,4-diazepane-1-carboxylate (A2.5a). Following the general procedure, allyl ester **A2.4a** (42 mg, 1.0 equiv) in MeCy (1 mL) was added to a solution of $Pd_2(dba)_3$ (3.7 mg, 4 mol %) and (*S*)-$(CF_3)_3$-*t*Bu-PHOX (6.0 mg, 10 mol %) in MeCy (6.2 mL). Purification by silica gel flash chromatography (0 → 20% EtOAc/hexanes) gave benzyl oxodiazepane **A2.5a** as a light pink oil (28 mg, 86% yield, 89% ee); **^{1}H NMR (400 MHz, Chloroform-*d*)** δ 7.56 – 7.40 (m, 3H), 7.40 – 7.32 (m, 2H), 7.32 – 7.19 (m, 3H), 7.19 – 7.00 (m, 2H), 5.88 (s, 1H), 5.26 – 5.07 (m, 2H), 4.26 – 4.03 (m, 1H), 3.94 (d, *J* = 15.4 Hz, 1H), 3.73 (d, *J* = 42.2 Hz, 1H), 3.54 (d, *J* = 15.3 Hz, 1H), 3.40 (s, 2H), 3.09 (dd, *J* = 61.0, 13.7 Hz, 1H), 2.94 – 2.34 (m, 3H), 1.48 (s, 10H); **^{13}C NMR (101 MHz, $CDCl_3$)** δ 179.1, 174.8, (156.0 & 155.3 appear as two peaks due to

hindered rotation), 136.6, 136.3, 133.0, 131.5, 130.8, 128.5, 128.4, 127.8, 127.1, (120.0 & 119.6 appear as two peaks due to hindered rotation), 80.8, (54.2 & 53.8 appear as two peaks due to hindered rotation), 49.1, 47.3, 46.8, (42.5 & 42.0 appear as two peaks due to hindered rotation), (41.4 & 40.3 appear as two peaks due to hindered rotation), 28.5. **IR (Neat Film, NaCl)** 3062, 2975, 2928, 1693, 1682, 1601, 1452, 1415, 1392, 1365, 1322, 1283, 1246, 1156, 1044, 978, 917, 865, 728, 697 cm^{-1}; **HRMS (MM: ESI-APCI):** *m/z* calc'd for $C_{27}H_{33}N_2O_4$ $[M+H]^+$: 449.2435, found 449.2429; $\mathbf{[\alpha]_D^{22.4}}$ +14.19 (c .66, $CHCl_3$); **SFC conditions**: 20% IPA, 2.5 mL/min, Chiralpak AD-H column, λ = 254 nm, t_R (min): major = 3.572, minor = 2.789.

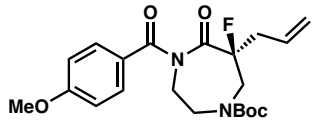

tert-butyl (S)-6-allyl-6-fluoro-4-(4-methoxybenzoyl)-5-oxo-1,4-diazepane-1-carboxylate (A2.5e). Following the general procedure, allyl ester **A2.4e** (45 mg, 1.0 equiv) in MeCy (1 mL) was added to a solution of $Pd_2(dba)_3$ (3.7 mg, 4 mol %) and (*S*)-$(CF_3)_3$-*t*Bu-PHOX (5.9 mg, 10 mol %) in MeCy (6.1 mL). Purification by automated silica gel flash chromatography (0 → 50% acetone/hexanes) gave fluorinated oxodiazepane **A2.5e** as a clear pink oil (45 mg, 83% yield, 86% ee); **^{1}H NMR (400 MHz, Chloroform-*d*)** δ 7.61 – 7.53 (m, 2H), 6.92 – 6.84 (m, 2H), 5.93 – 5.78 (m, 1H), 5.30 – 5.21 (m, 2H), 4.35 (t, *J* = 16.0 Hz, 1H), 4.22 – 4.02 (m, 2H), 3.96 – 3.85 (m, 1H), 3.84 (s, 3H), 3.40 – 3.19 (m, 2H), 2.94 – 2.78 (m, 1H), 2.71 – 2.48 (m, 1H), 1.47 (s, 9H); **^{13}C NMR (101 MHz, $CDCl_3$)** δ 173.9, 173.7, 163.1, 155.2, 131.0, 130.6, 127.1, 120.9, 113.8,

97.8 (dd, J = 193.7, 52.5 Hz), 81.1, 55.5, 49.8 (dd, J = 33.5, 23.3 Hz), (47.5 & 46.94 appear as two peaks due to hindered rotation), 43.2, 39.8 (dd, J = 32.1, 21.8 Hz), 28.3. **IR (Neat Film, NaCl)** 2977, 2932,1696, 1603,1578, 1511, 1448, 1413, 1366, 1327, 1256, 1169, 1152, 1029, 1000, 977, 923, 835, 766 cm^{-1}; **HRMS (MM: ESI-APCI):** *m/z* calc'd for $C_{21}H_{28}FN_2O_5$ $[M+H]^+$: 407.1977, found 407.1973; $\mathbf{[\alpha]_D^{22.5}}$ +46.99 (c 1.7, $CHCl_3$); **SFC conditions**: 20% IPA, 2.5 mL/min, Chiralpak OD-H column, λ = 254 nm, t_R (min): major = 2.692, minor = 3.253.

A2.3.7 REFERENCES AND NOTES

(1) Kearney, S. E.; Zahoránszky-Kőhalmi, G.; Brimacombe, K. R.; Henderson, M. J.; Lynch, C.; Zhao, T.; Wan, K. K.; Itkin, Z.; Dillon, C.; Shen, M.; et al. Canvass: A Crowd-Sourced, Natural-Product Screening Library for Exploring Biological Space. *ACS Cent. Sci.* **2018**, *4*, 1727–1741.

(2) Ferreira, M. del R. R.; Cecere, G.; Pace, P.; Summa, V. Routes to HIV-Integrase Inhibitors: Efficient Synthesis of Bicyclic Pyrimidones by Ring Expansion or Amination at a Benzylic Position. *Tetrahedron Lett.* **2009**, *50*, 148–151.

(3) Sun, A. W.; Hess, S. N.; Stoltz, B. M. Enantioselective Synthesis of Gem-Disubstituted N-Boc Diazaheterocycles via Decarboxylative Asymmetric Allylic Alkylation. *Chem. Sci.* **2019**, *10*, 788–792.

(4) Behenna, D. C.; Liu, Y.; Yurino, T.; Kim, J.; White, D. E.; Virgil, S. C.; Stoltz, B. M. Enantioselective Construction of Quaternary *N*-Heterocycles by Palladium-Catalysed Decarboxylative Allylic Alkylation of Lactams. *Nat. Chem.* **2012**, *4*, 130–133.

(5) Numajiri, Y.; Jiménez-Osés, G.; Wang, B.; Houk, K. N.; Stoltz, B. M. Enantioselective Synthesis of Dialkylated *N* -Heterocycles by Palladium-Catalyzed Allylic Alkylation. *Org. Lett.* **2015**, *17*, 1082–1085.

(6) Behenna, D. C.; Stoltz, B. M. The Enantioselective Tsuji Allylation. *J. Am. Chem. Soc.* **2004**, *126*, 15044–15045.

(7) Mohr, J. T.; Behenna, D. C.; Harned, A. M.; Stoltz, B. M. Deracemization of Quaternary Stereocenters by Pd-Catalyzed Enantioconvergent Decarboxylative Allylation of Racemic β-Ketoesters. *Angew. Chem. Int. Ed.* **2005**, *44*, 6924–6927.

(8) Reeves, C. M.; Eidamshaus, C.; Kim, J.; Stoltz, B. M. Enantioselective Construction of α-Quaternary Cyclobutanones by Catalytic Asymmetric Allylic Alkylation. *Angew. Chem. Int. Ed.* **2013**, *52*, 6718–6721.

(9) Seto, M.; Roizen, J. L.; Stoltz, B. M. Catalytic Enantioselective Alkylation of Substituted Dioxanone Enol Ethers: Ready Access to C(α)-Tetrasubstituted Hydroxyketones, Acids, and Esters. *Angew. Chem.* **2008**, *120*, 6979–6982.

(10) McDougal, N. T.; Streuff, J.; Mukherjee, H.; Virgil, S. C.; Stoltz, B. M. Rapid Synthesis of an Electron-Deficient t-BuPHOX Ligand: Cross-Coupling of Aryl Bromides with Secondary Phosphine Oxides. *Tetrahedron Lett.* **2010**, *51*, 5550–5554.

(11) Klepacz, A.; Zwierzak, A. An Expeditious One-Pot Synthesis of Diethyl N-Boc-1-Aminoalkylphosphonates. *Tetrahedron Lett.* **2002**, *43*, 1079–1080.

(12) Sikriwal, D.; Kant, R.; Maulik, P. R.; Dikshit, D. K. A Short Formal Synthesis of Three Epimers of Penmacric Acid. *Tetrahedron* **2010**, *66*, 6167–6173.

APPENDIX 3

Spectra Relevant to Appendix 2:

Decarboxylative Asymmetric Allylic Alkylation

of gem-Disubstituted Diazepanes

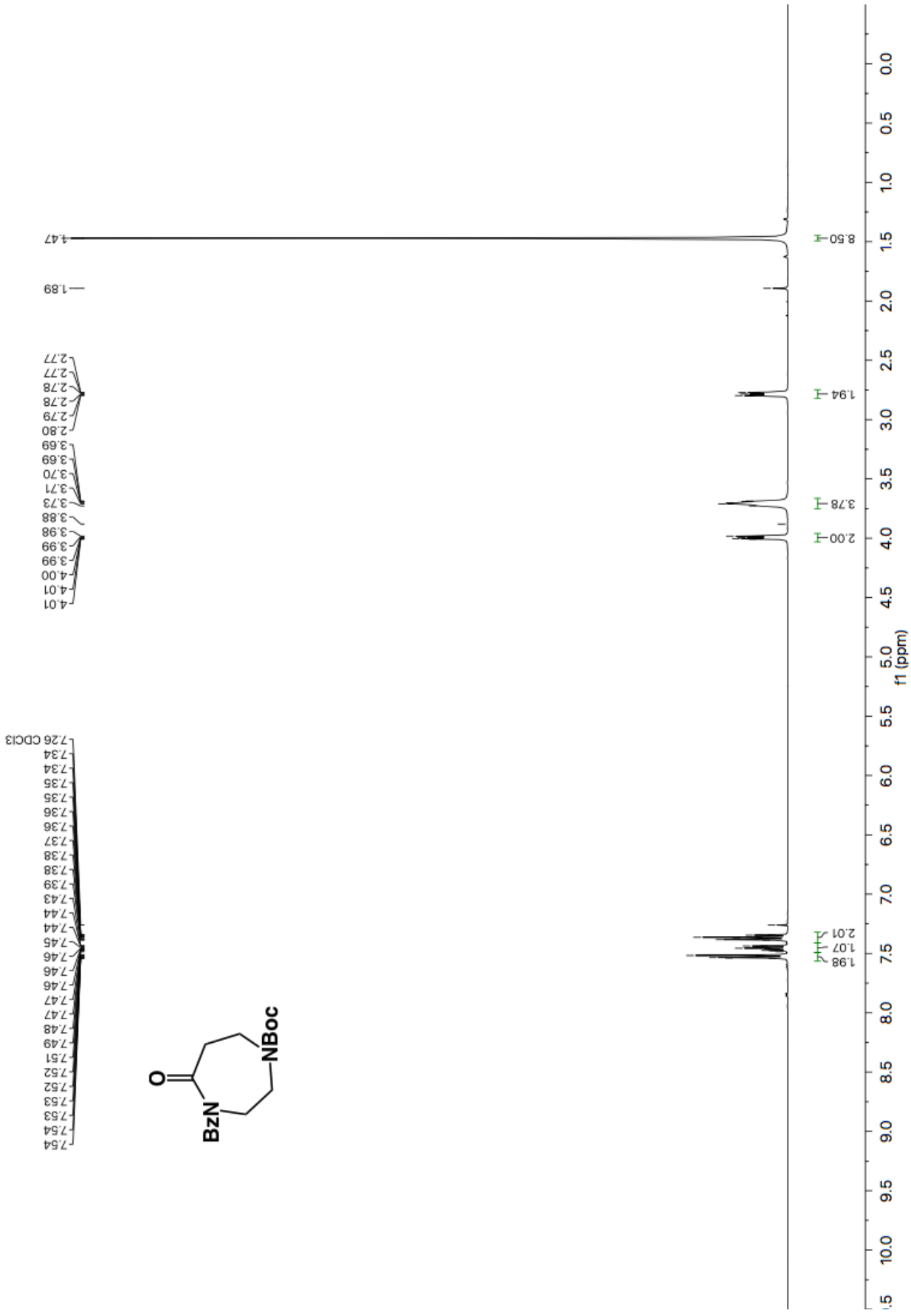

Figure A3.1 ^{1}H NMR (600 MHz, $CDCl_3$) of compound **A2S1.**

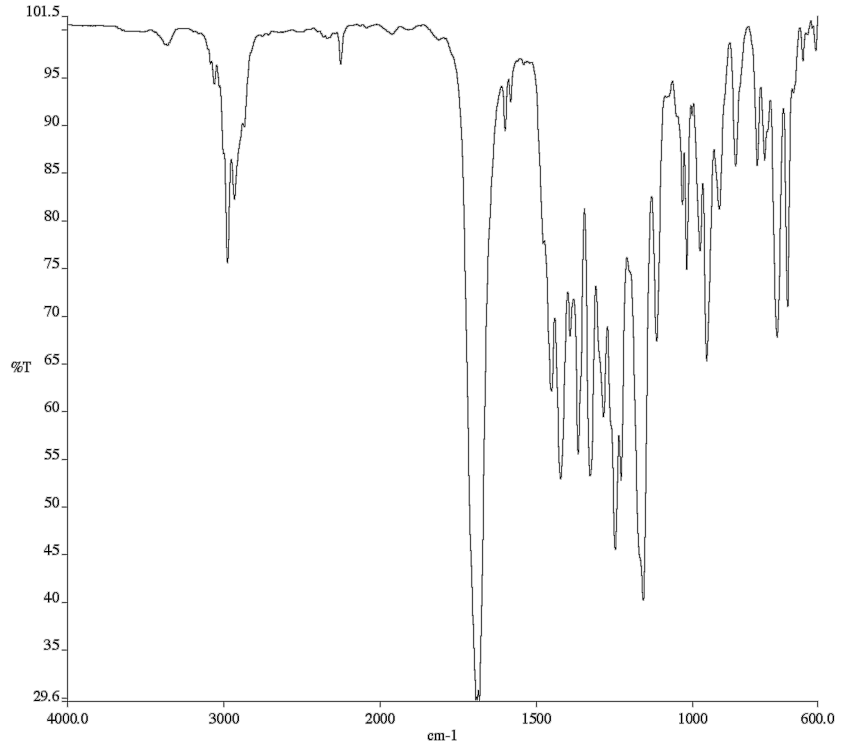

Figure A3.2 Infrared spectrum (Thin Film, NaCl) of compound **A2S1**.

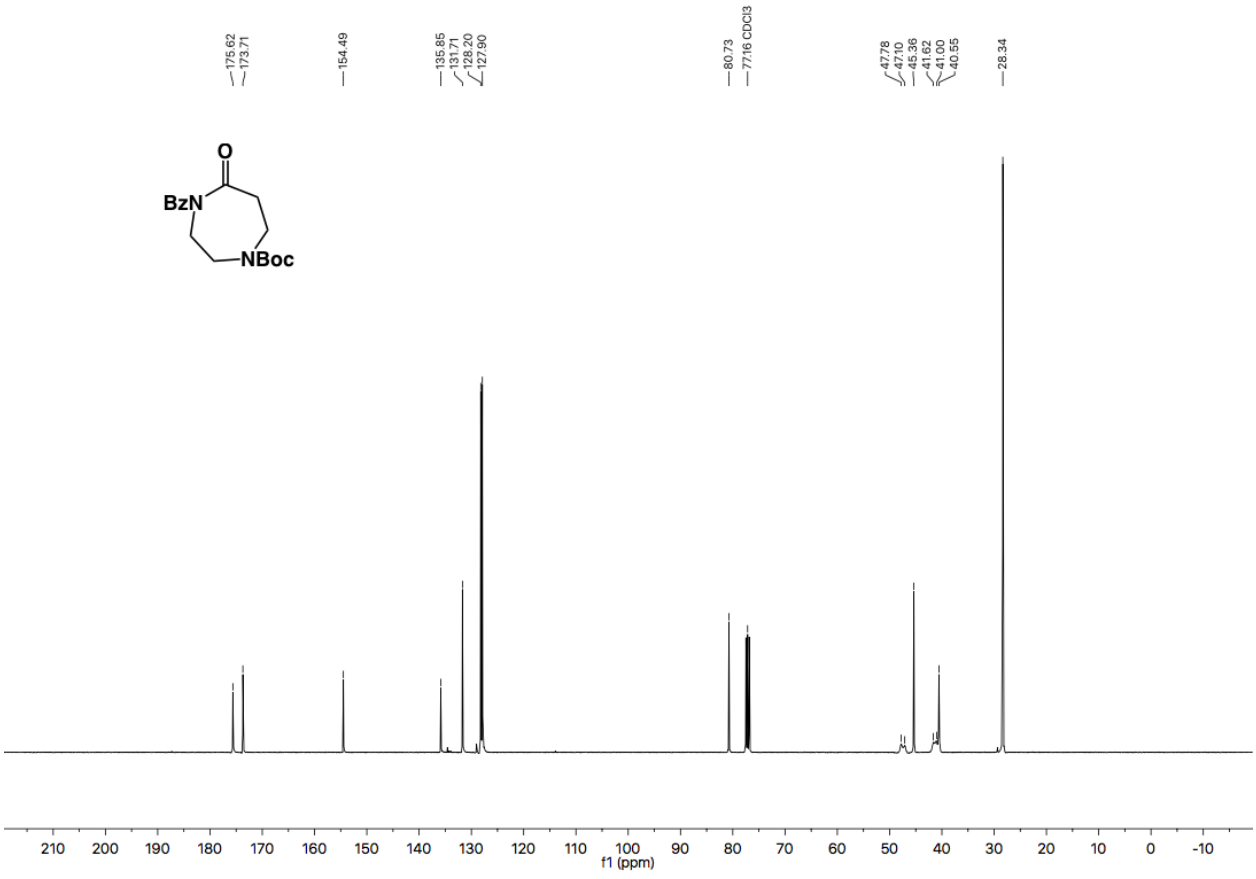

Figure A3.3 ^{13}C NMR (101 MHz, $CDCl_3$) of compound **A2S1**.

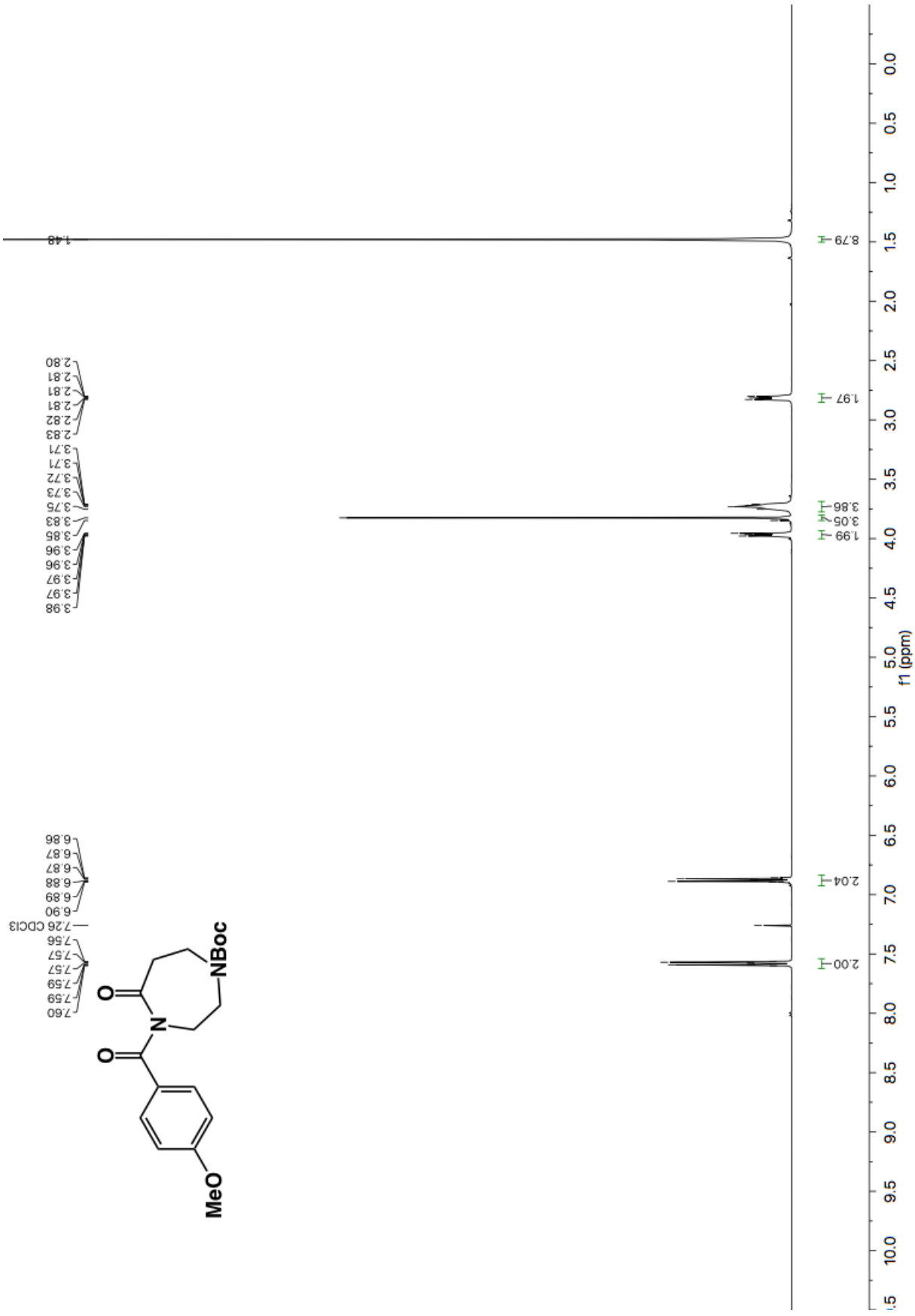

Figure A3.4 ^{1}H NMR (600 MHz, $CDCl_3$) of compound **A2S3.**

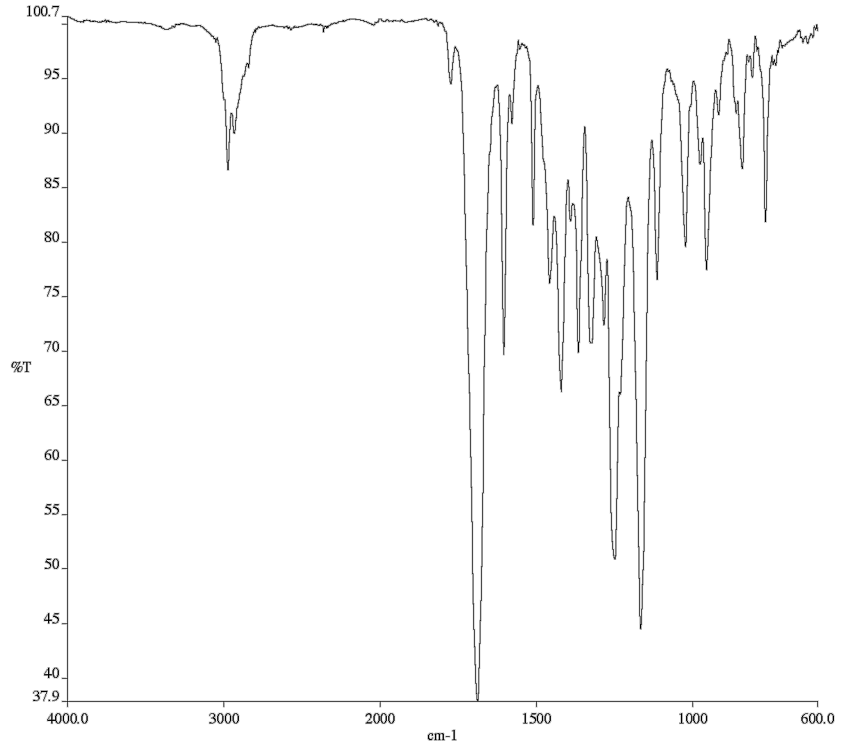

Figure A3.5 Infrared spectrum (Thin Film, NaCl) of compound **A2S3**.

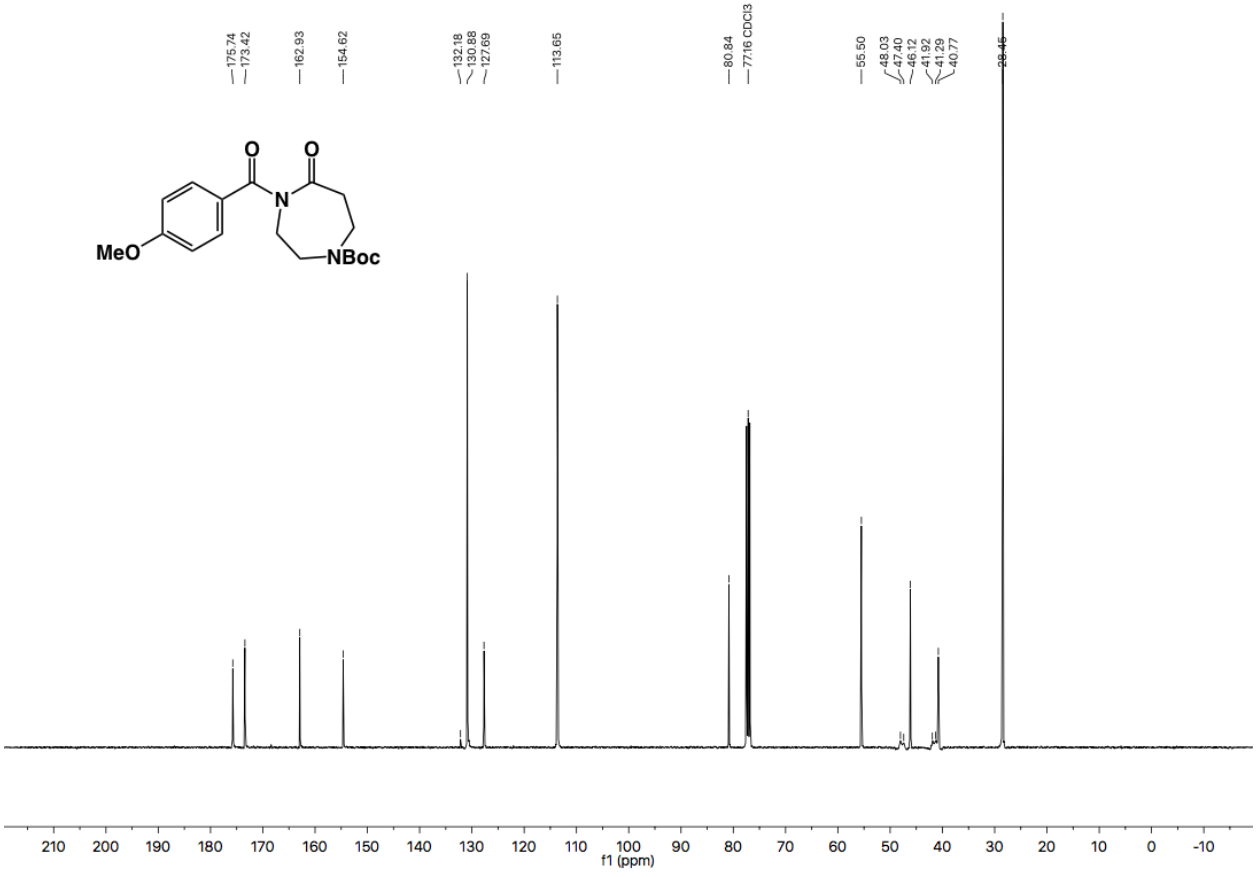

Figure A3.6 ^{13}C NMR (101 MHz, $CDCl_3$) of compound **A2S3**.

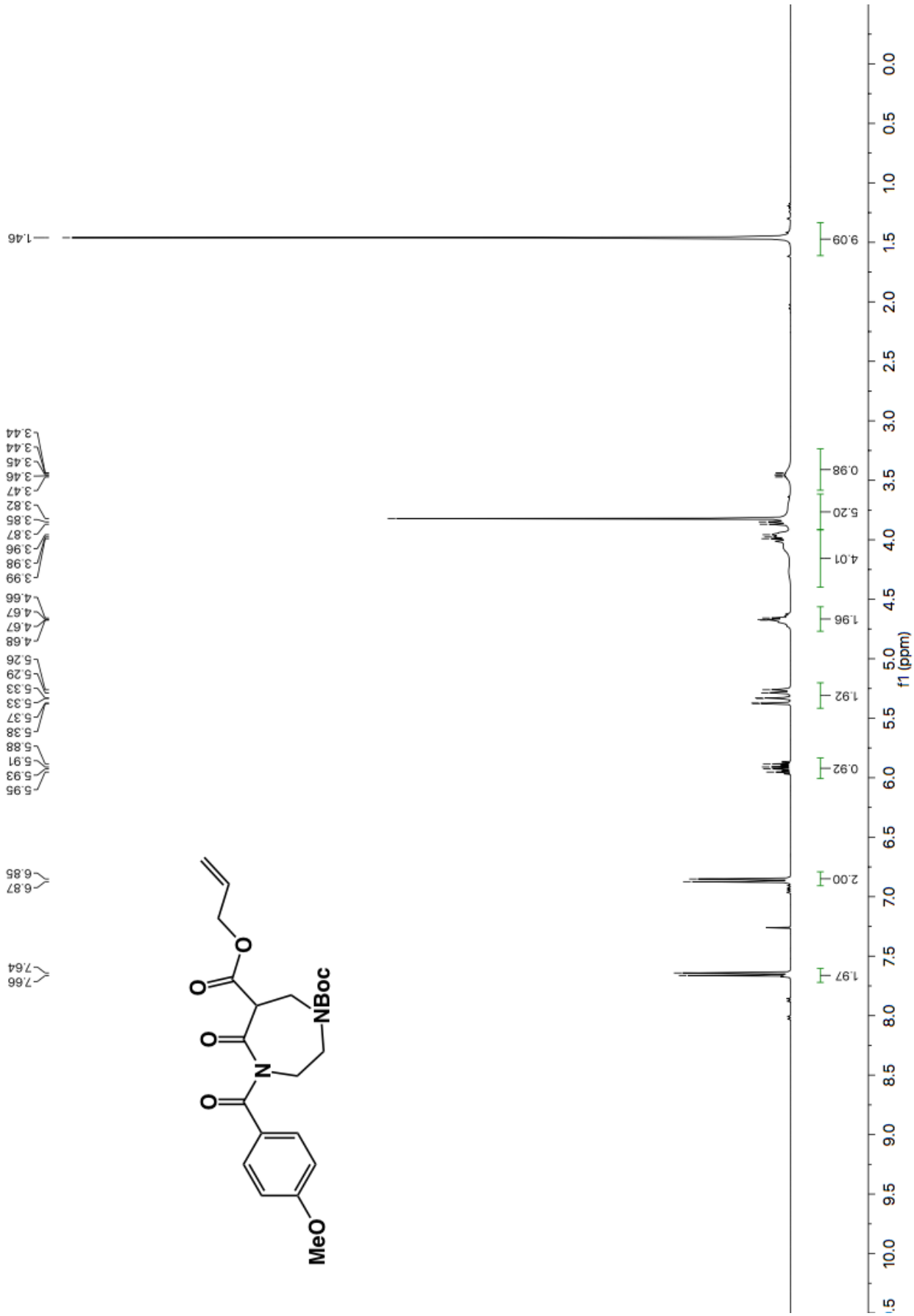

Figure A3.7 ^{1}H NMR (600 MHz, $CDCl_3$) of compound **A2S4.**

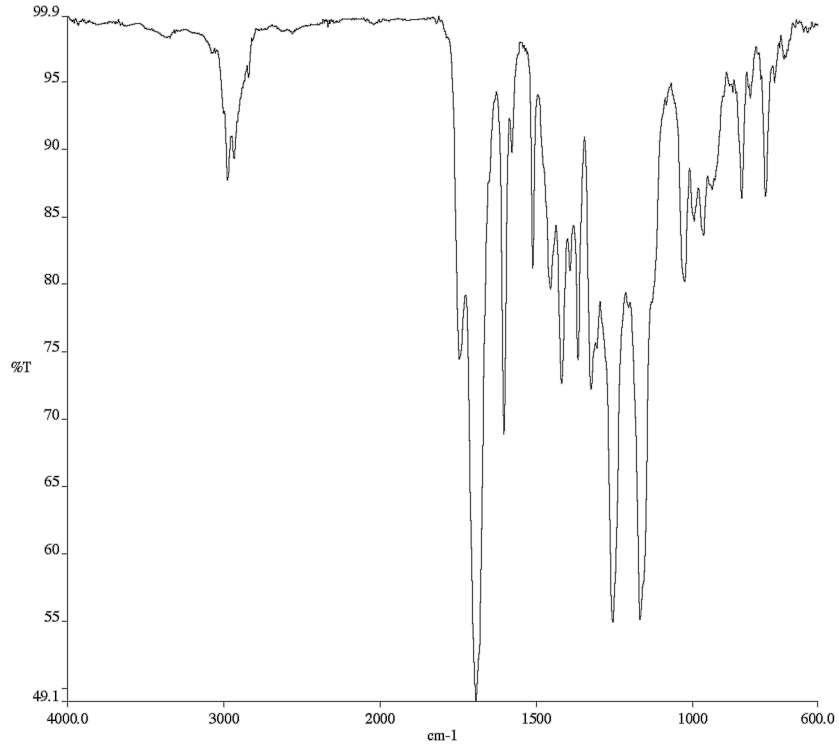

Figure A3.8 Infrared spectrum (Thin Film, NaCl) of

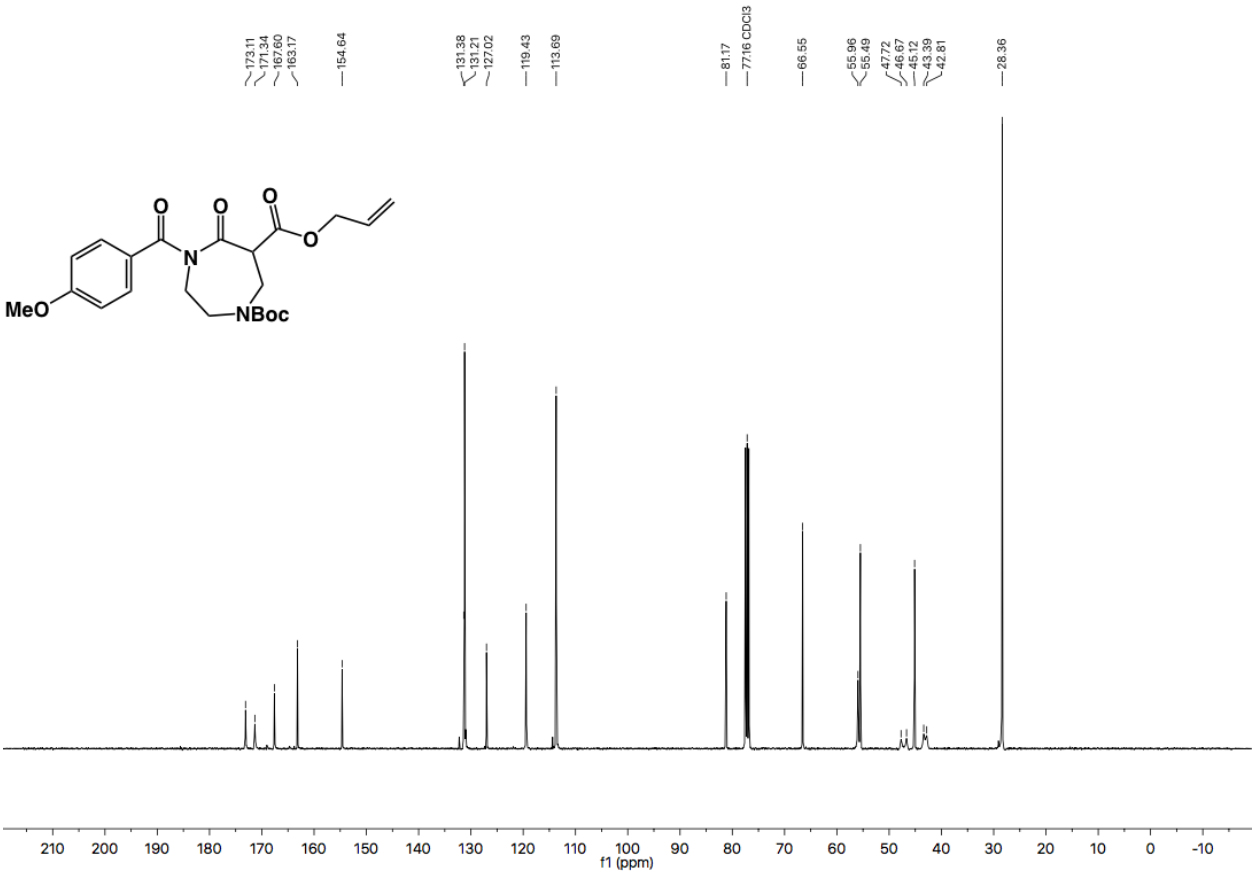

Figure A3.9 ^{13}C NMR (101 MHz, $CDCl_3$) of compound **A2S4**.

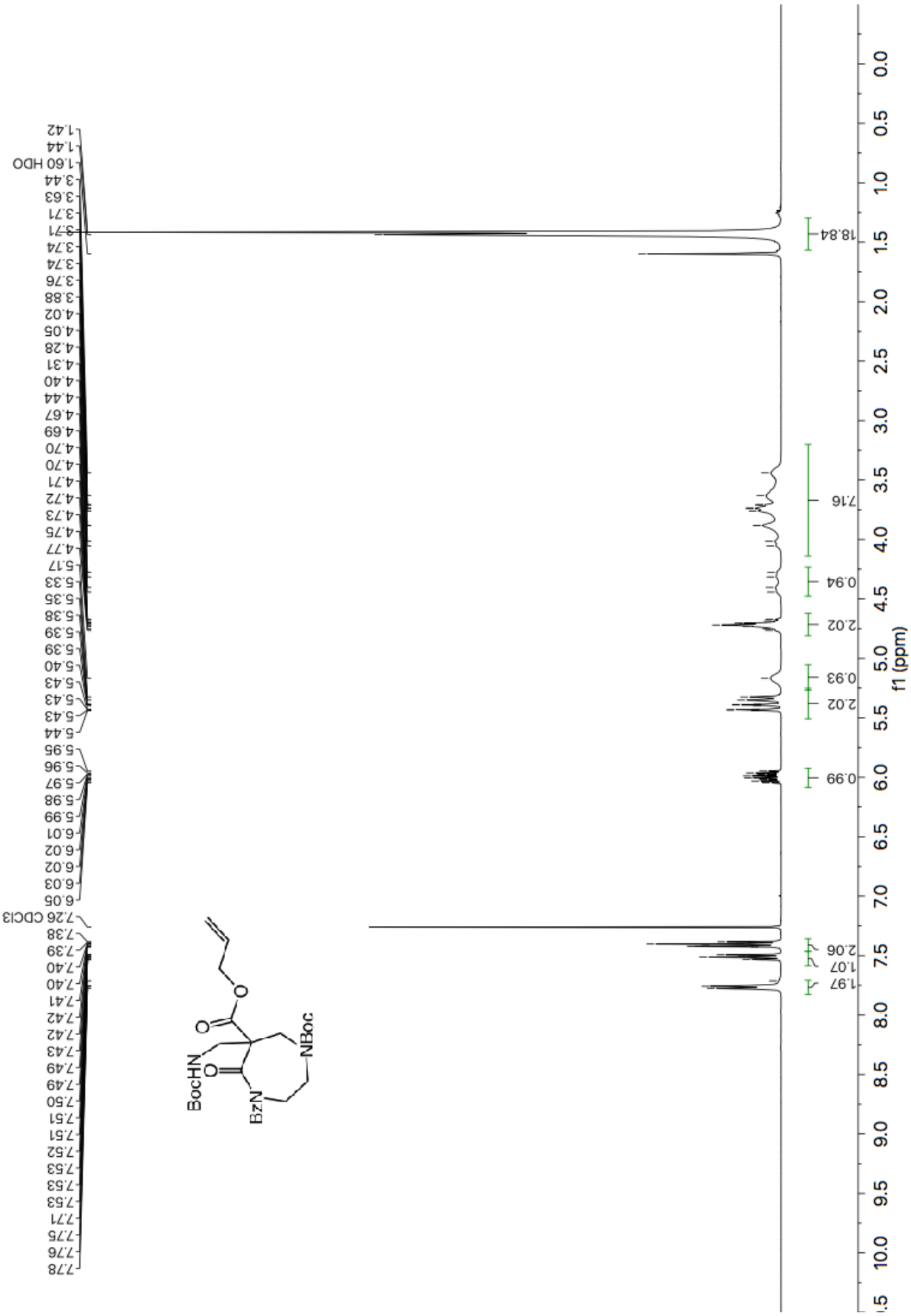

Figure A3.10 ^{1}H NMR (600 MHz, $CDCl_3$) of compound **A2.4f.**

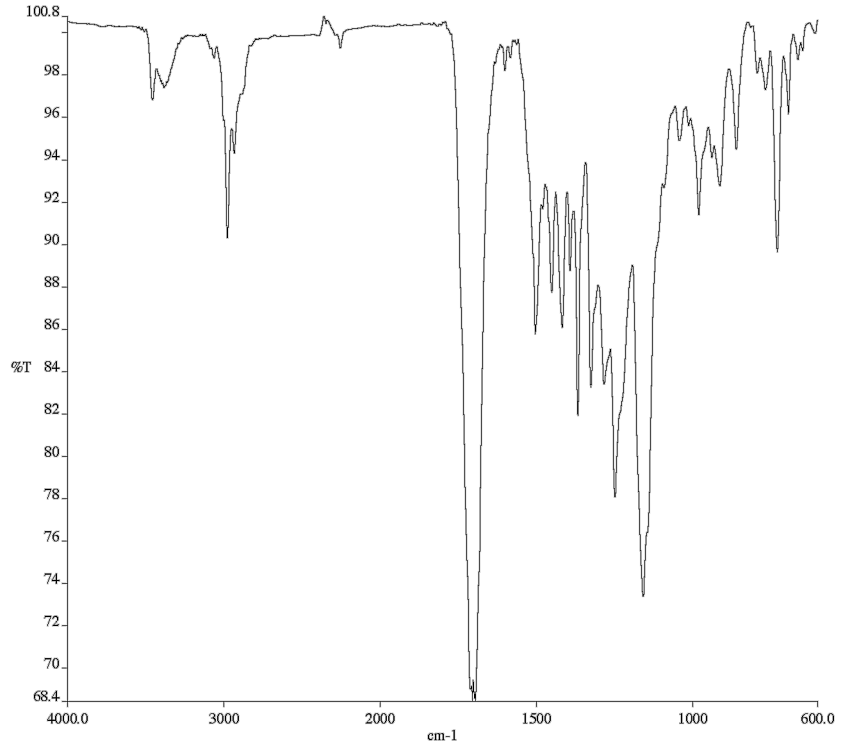

Figure A3.11 Infrared spectrum (Thin Film, NaCl) of compound **A2.4f**.

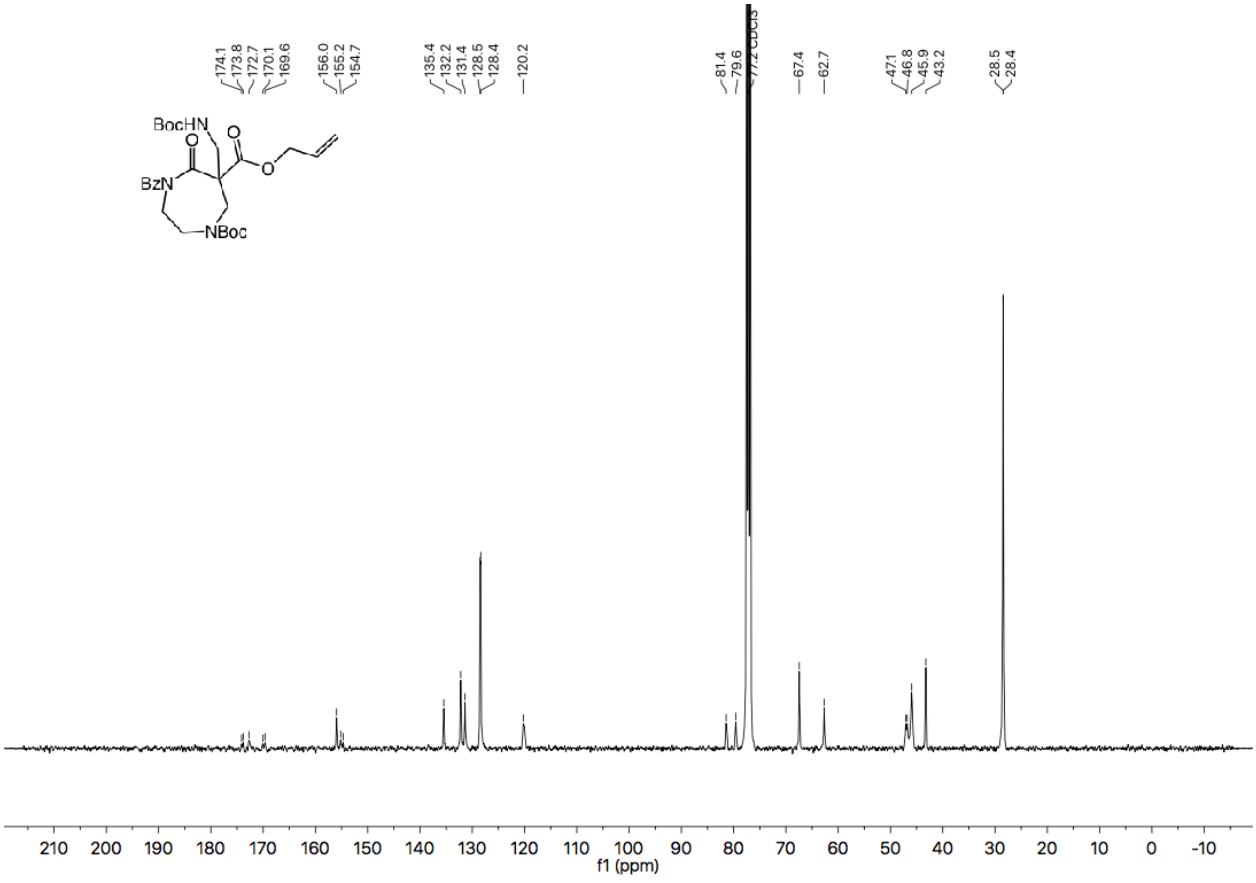

Figure A3.12 ^{13}C NMR (101 MHz, $CDCl_3$) of compound **A2.4f**.

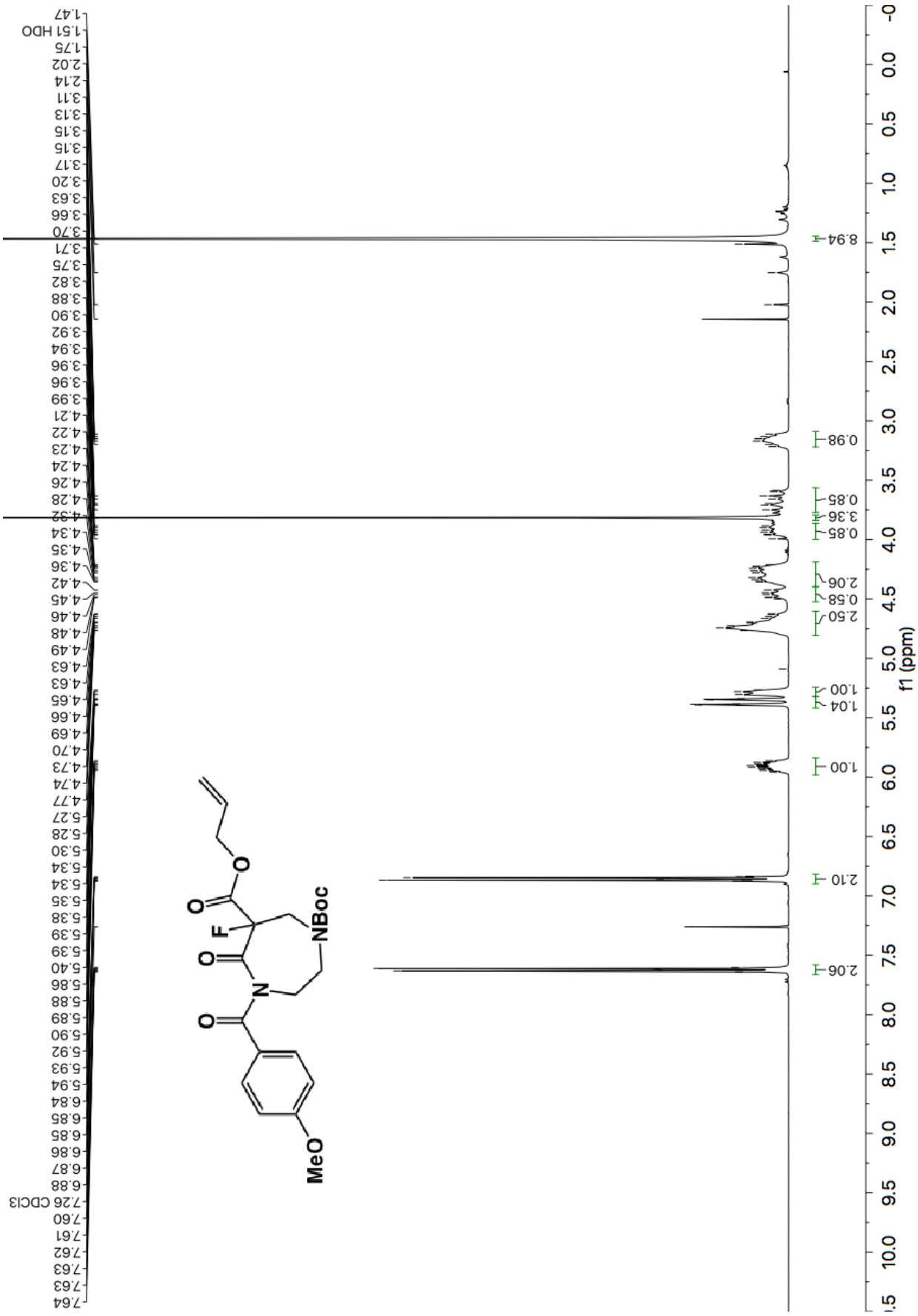

Figure A3.13 ^{1}H NMR (600 MHz, $CDCl_3$) of compound **A2.4g.**

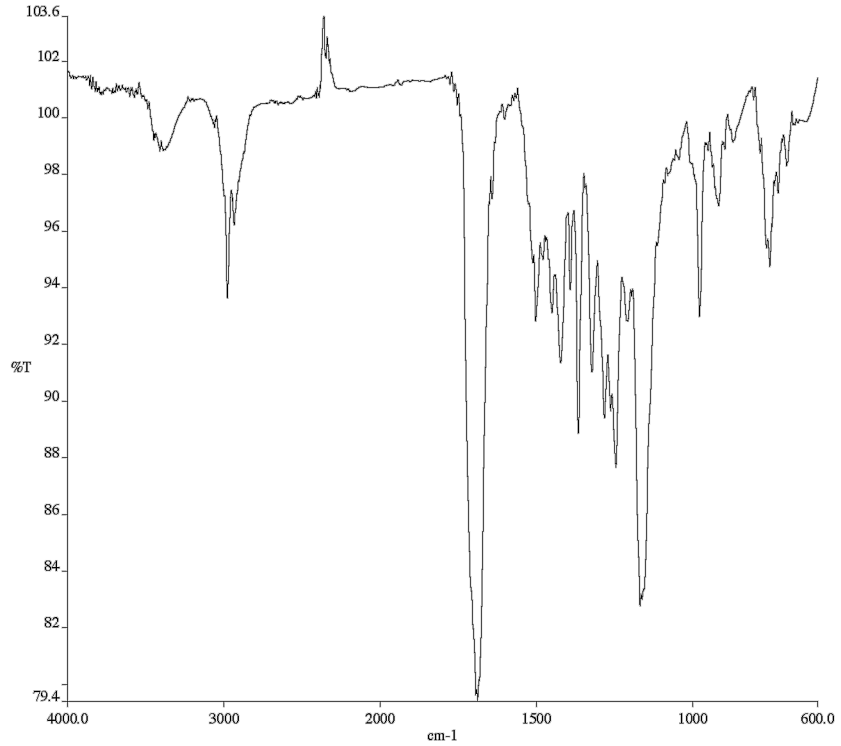

Figure A3.14 Infrared spectrum (Thin Film, NaCl) of compound **A2.4g**.

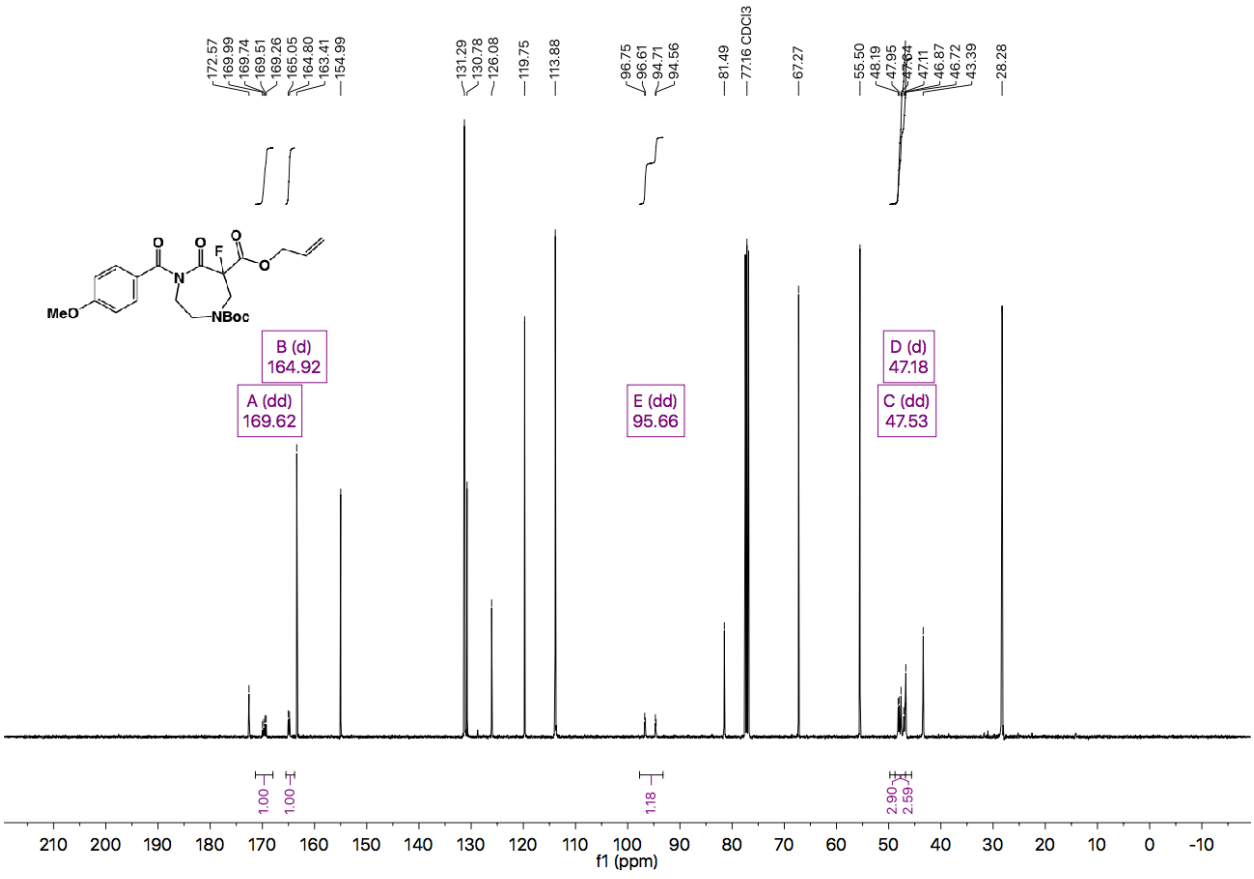

Figure A3.15 ^{13}C NMR (101 MHz, $CDCl_3$) of compound **A2.4g**.

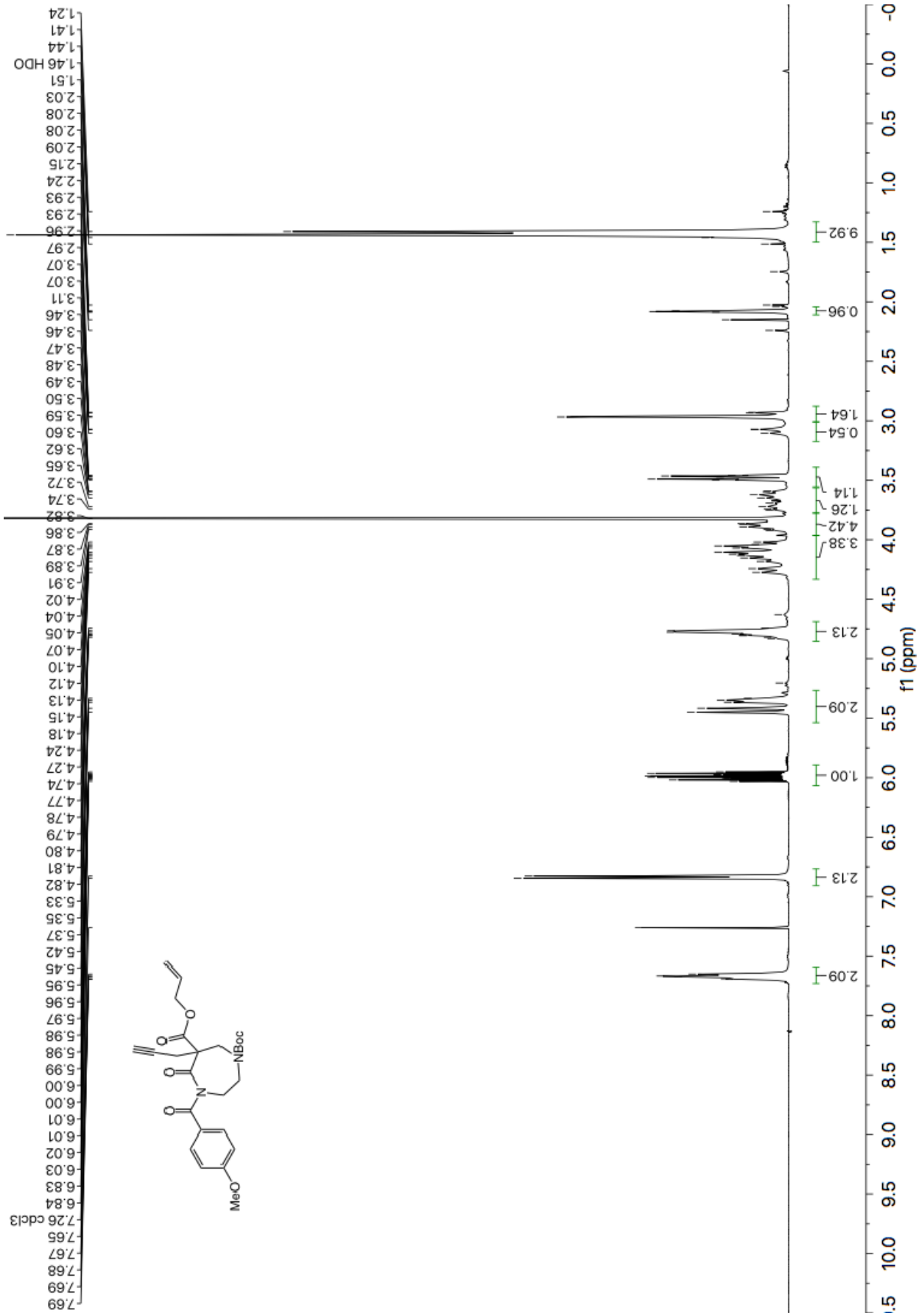

Figure A3.16 ^{1}H NMR (600 MHz, $CDCl_3$) of compound **A2.4h.**

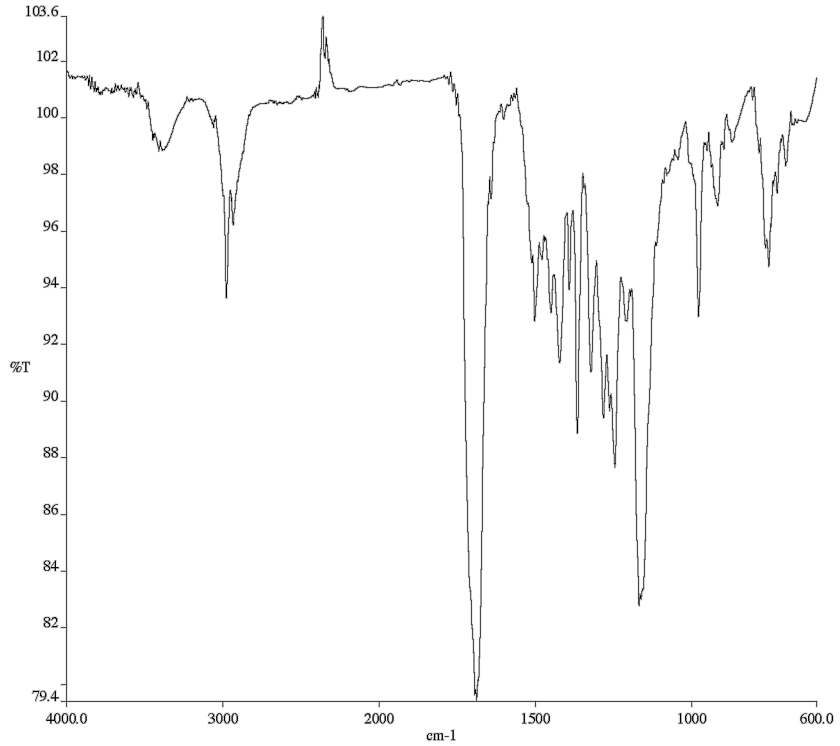

Figure A3.17 Infrared spectrum (Thin Film, NaCl) of compound **A2.4h**.

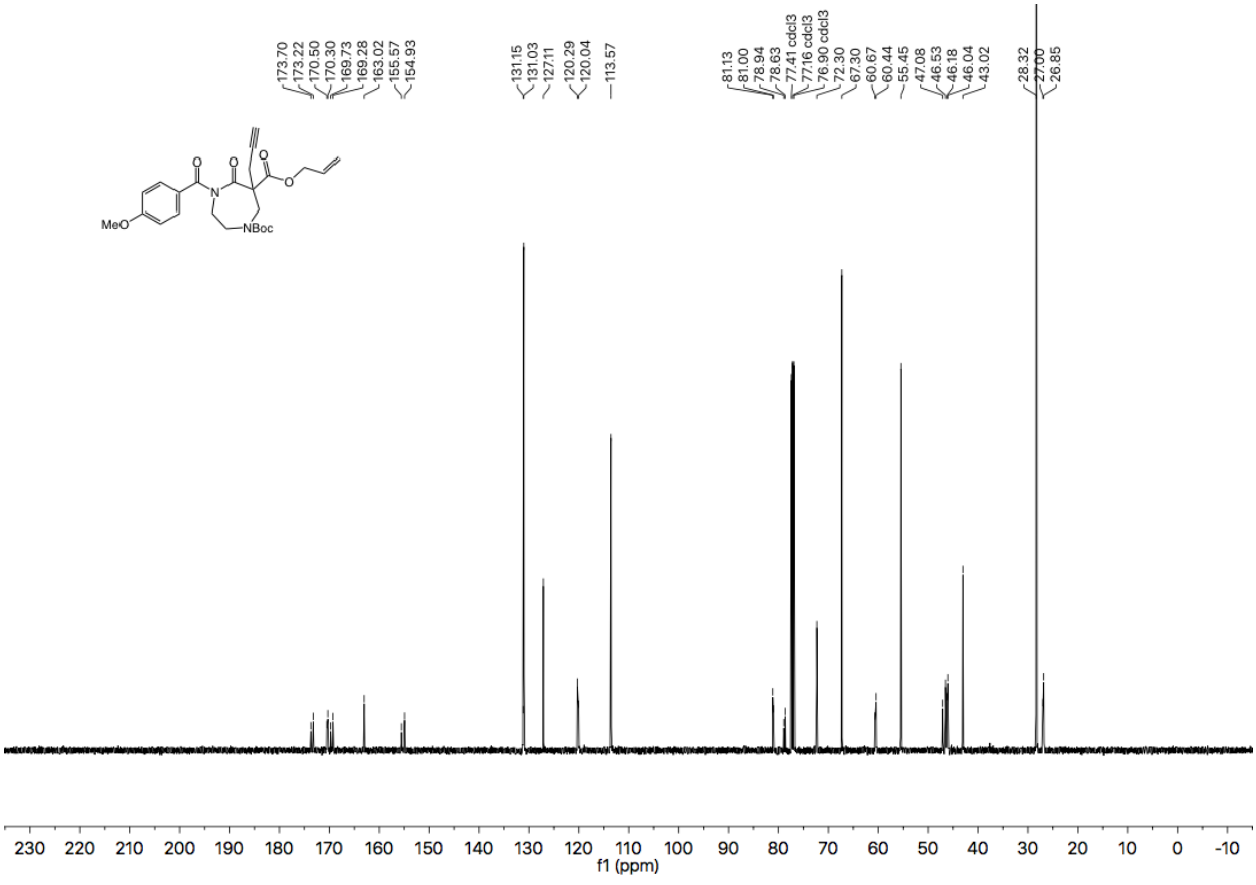

Figure A3.18 ^{13}C NMR (101 MHz, $CDCl_3$) of compound **A2.4h**.

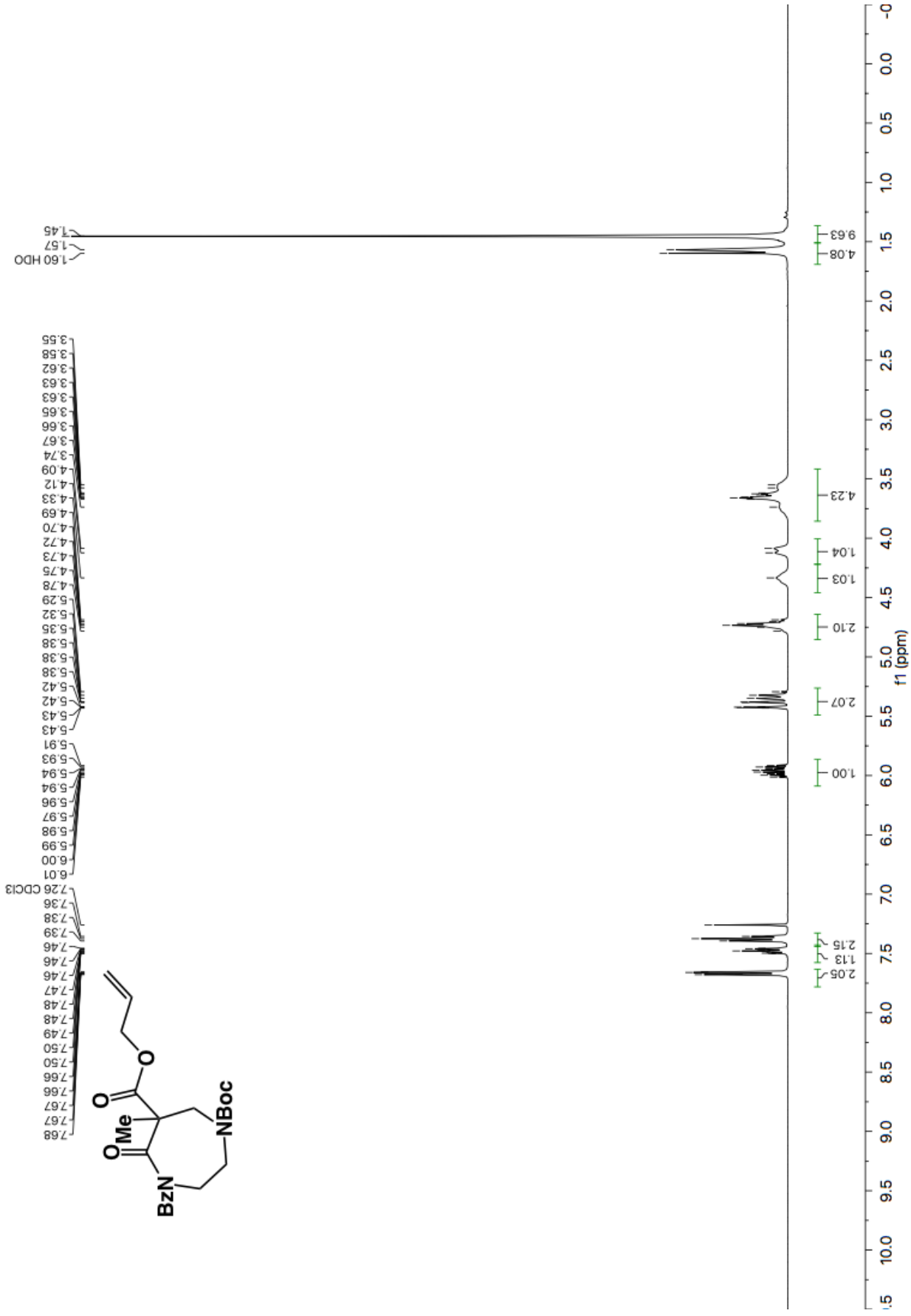

Figure A3.19 ^{1}H NMR (600 MHz, $CDCl_3$) of compound **A2.4i.**

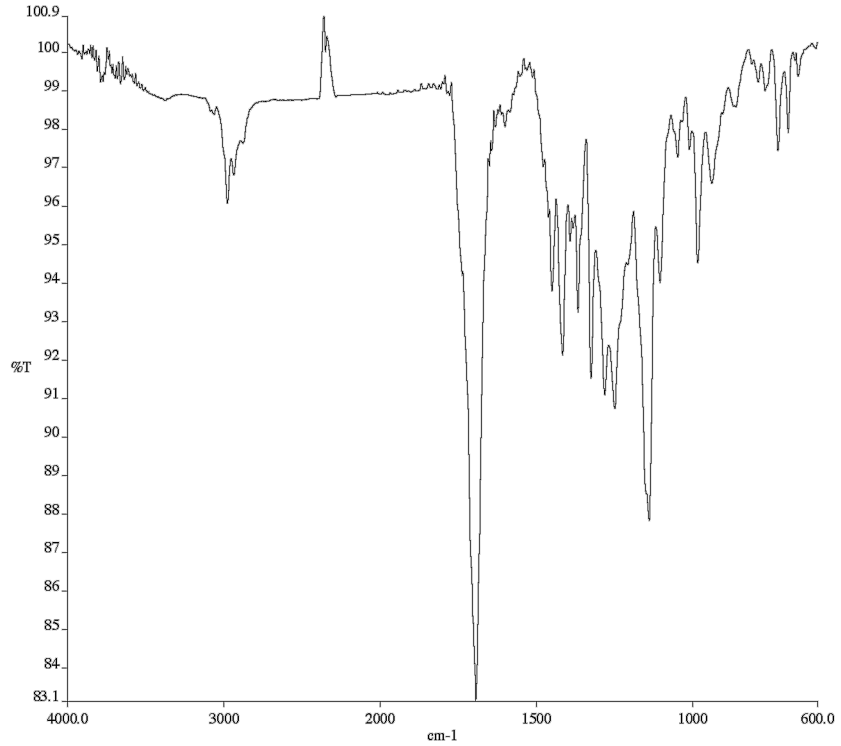

Figure A3.20 Infrared spectrum (Thin Film, NaCl) of compound **A2.4i**.

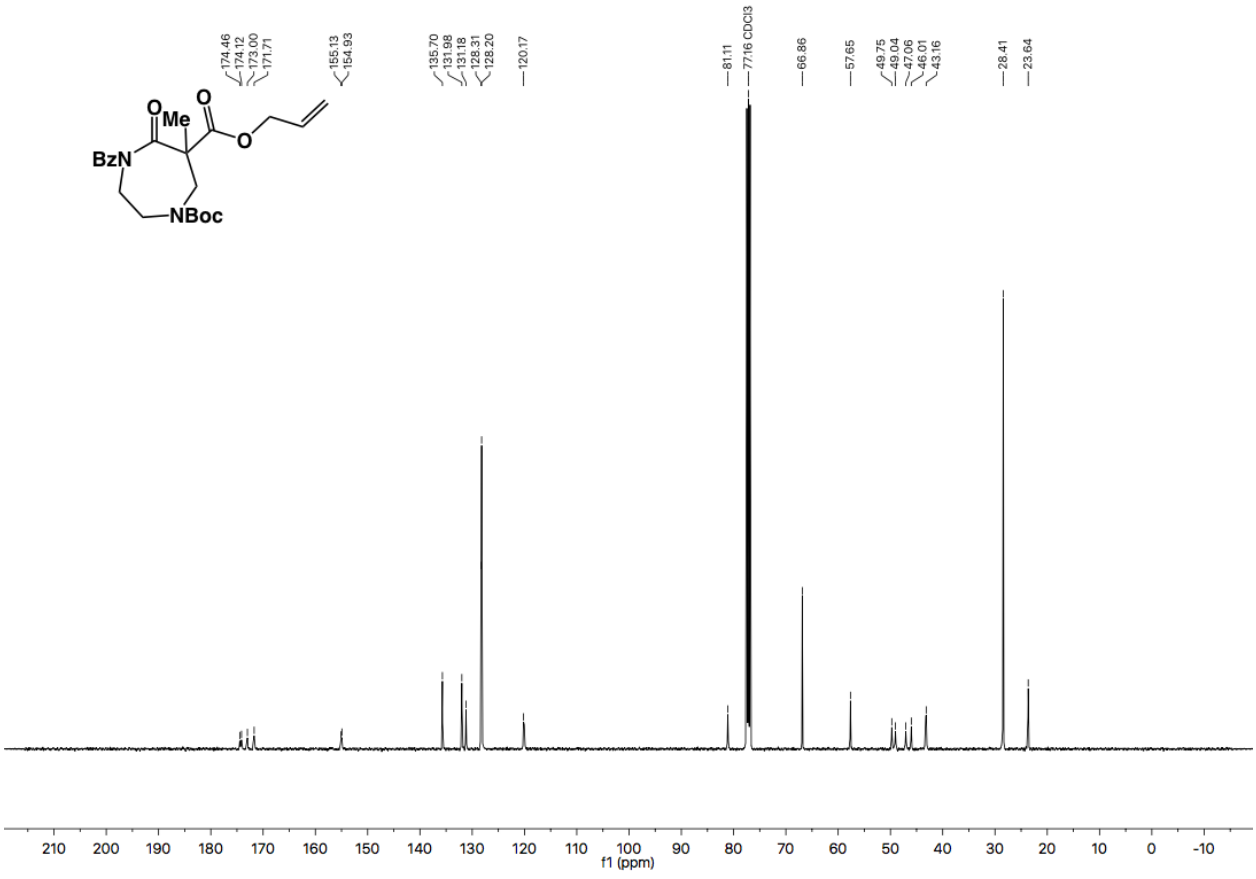

Figure A3.21 ^{13}C NMR (101 MHz, $CDCl_3$) of compound **A2.4i**.

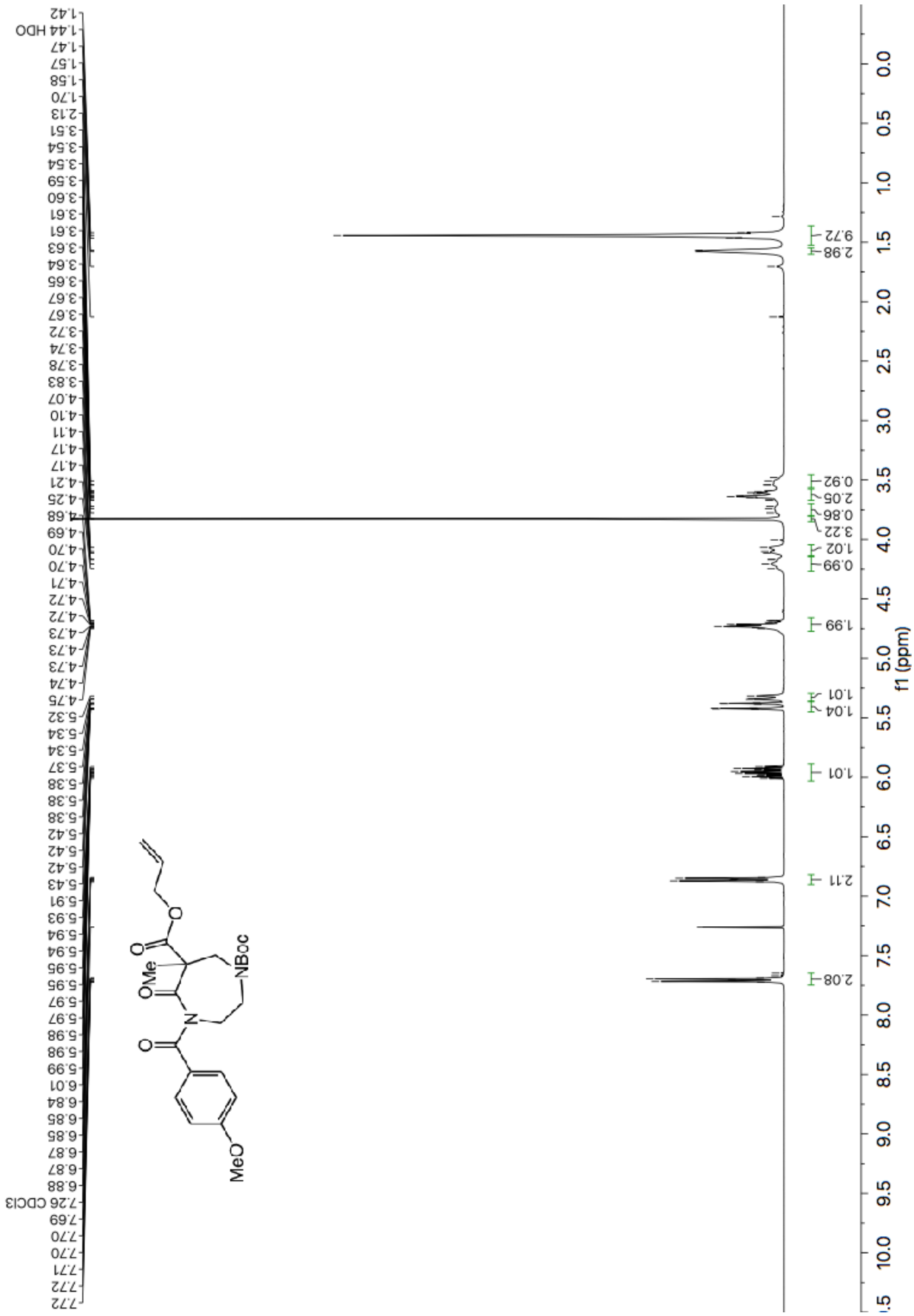

Figure A3.22 ^{1}H NMR (600 MHz, $CDCl_3$) of compound **A2.4j.**

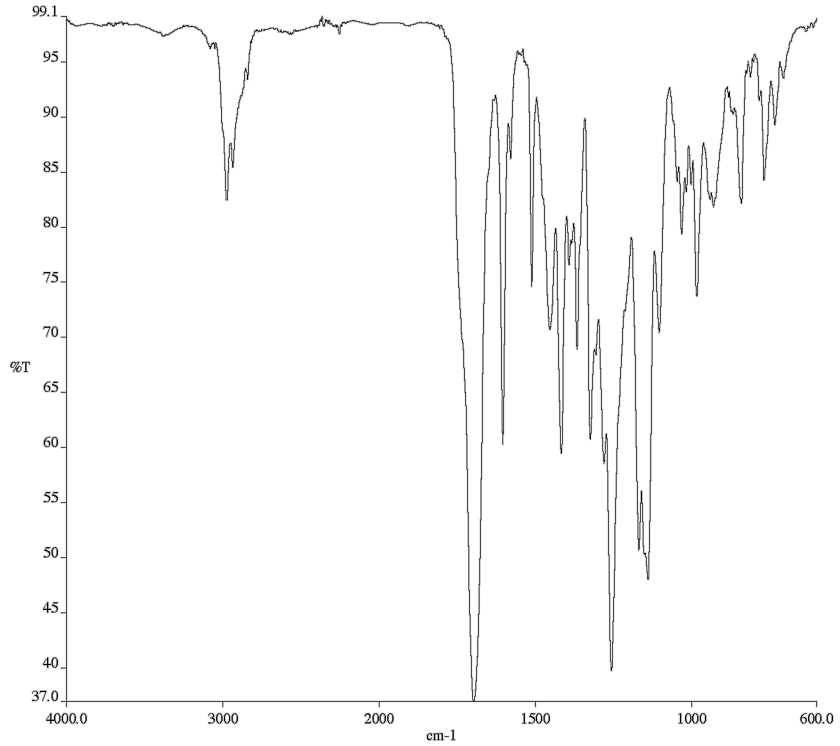

Figure A3.23 Infrared spectrum (Thin Film, NaCl) of compound **A2.4j**.

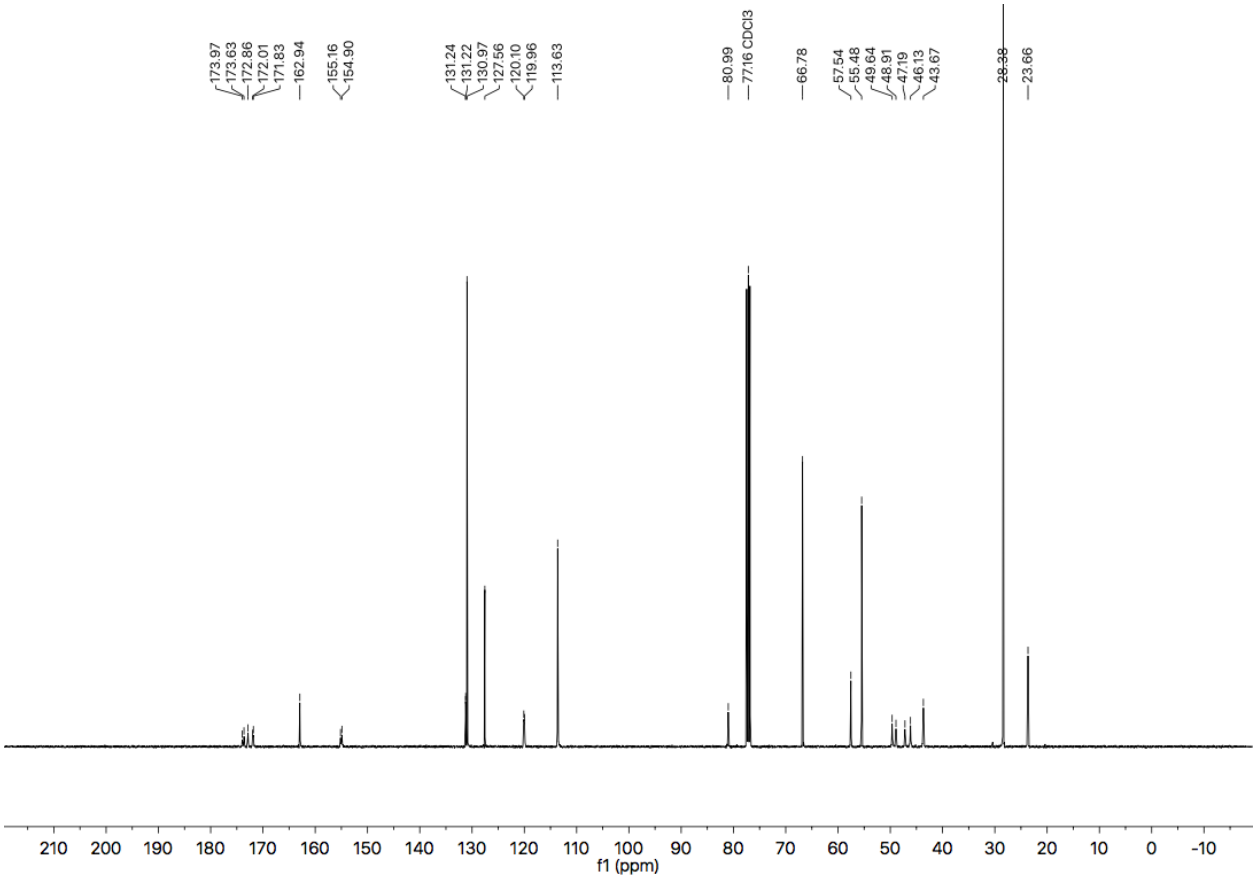

Figure A3.24 ^{13}C NMR (101 MHz, $CDCl_3$) of compound **A2.4j**.

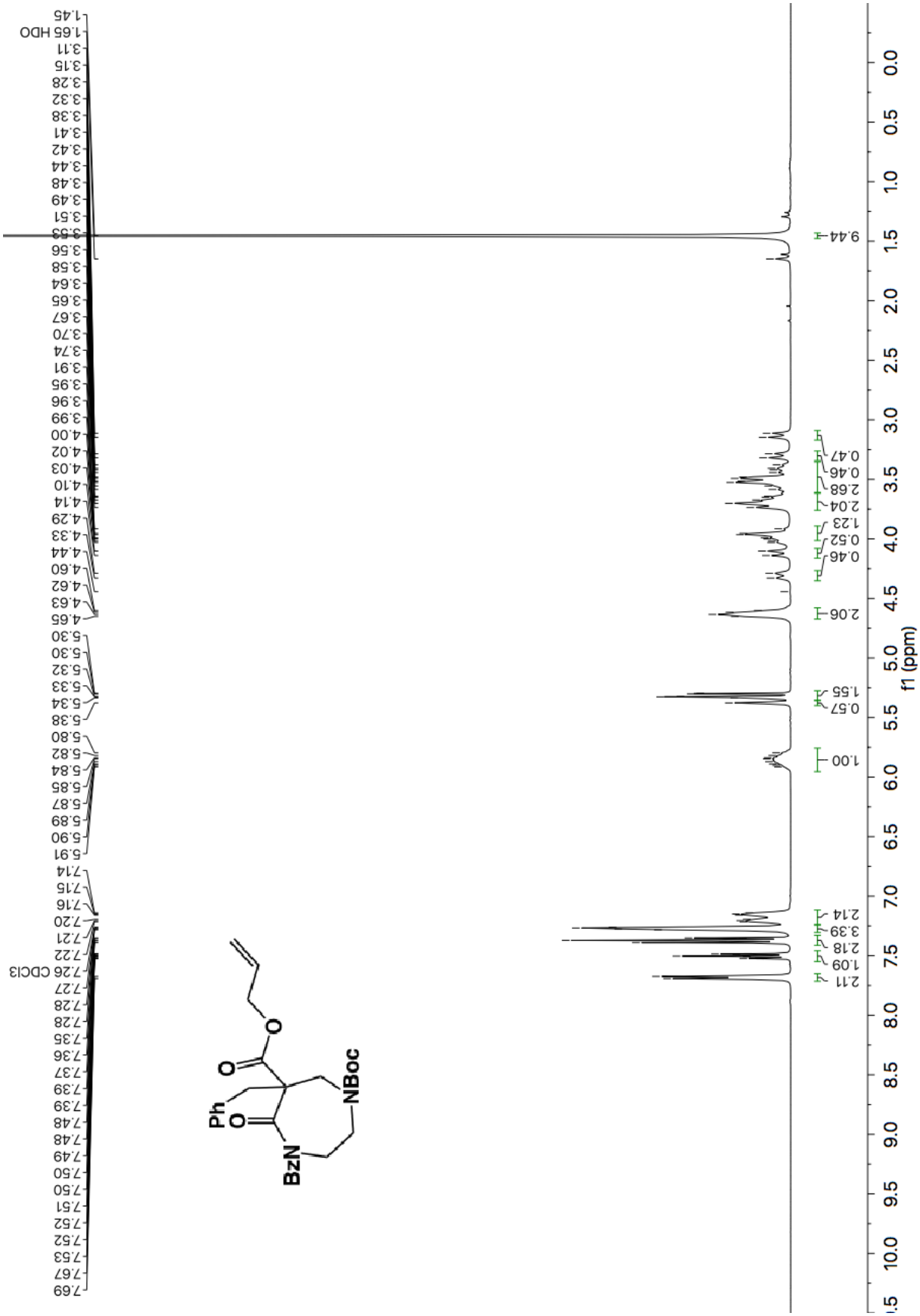

Figure A3.25 ^{1}H NMR (600 MHz, $CDCl_3$) of compound **A2.4l.**

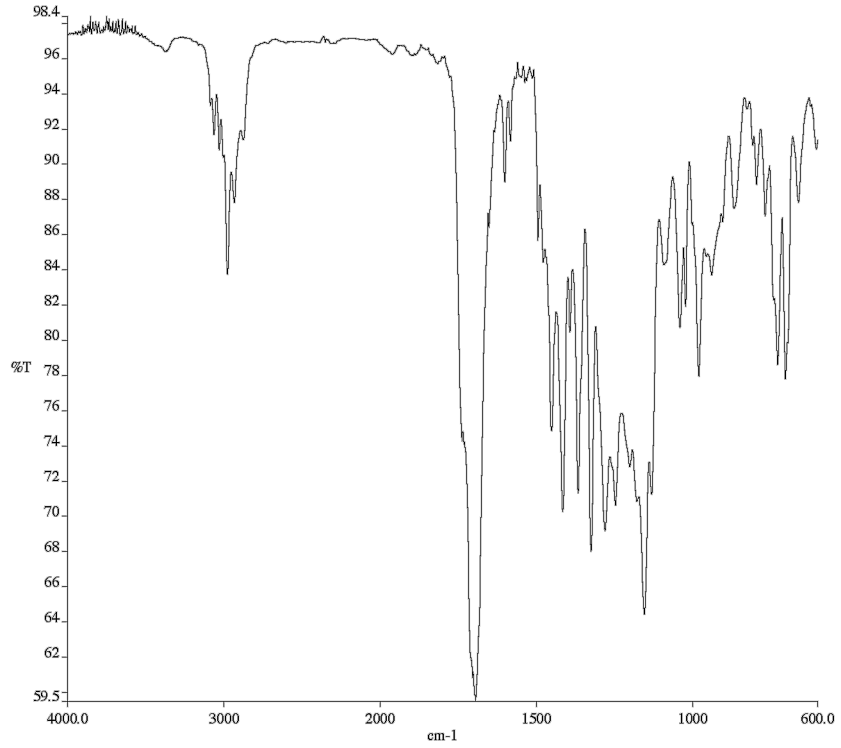

Figure A3.26 Infrared spectrum (Thin Film, NaCl) of compound **A2.4l**.

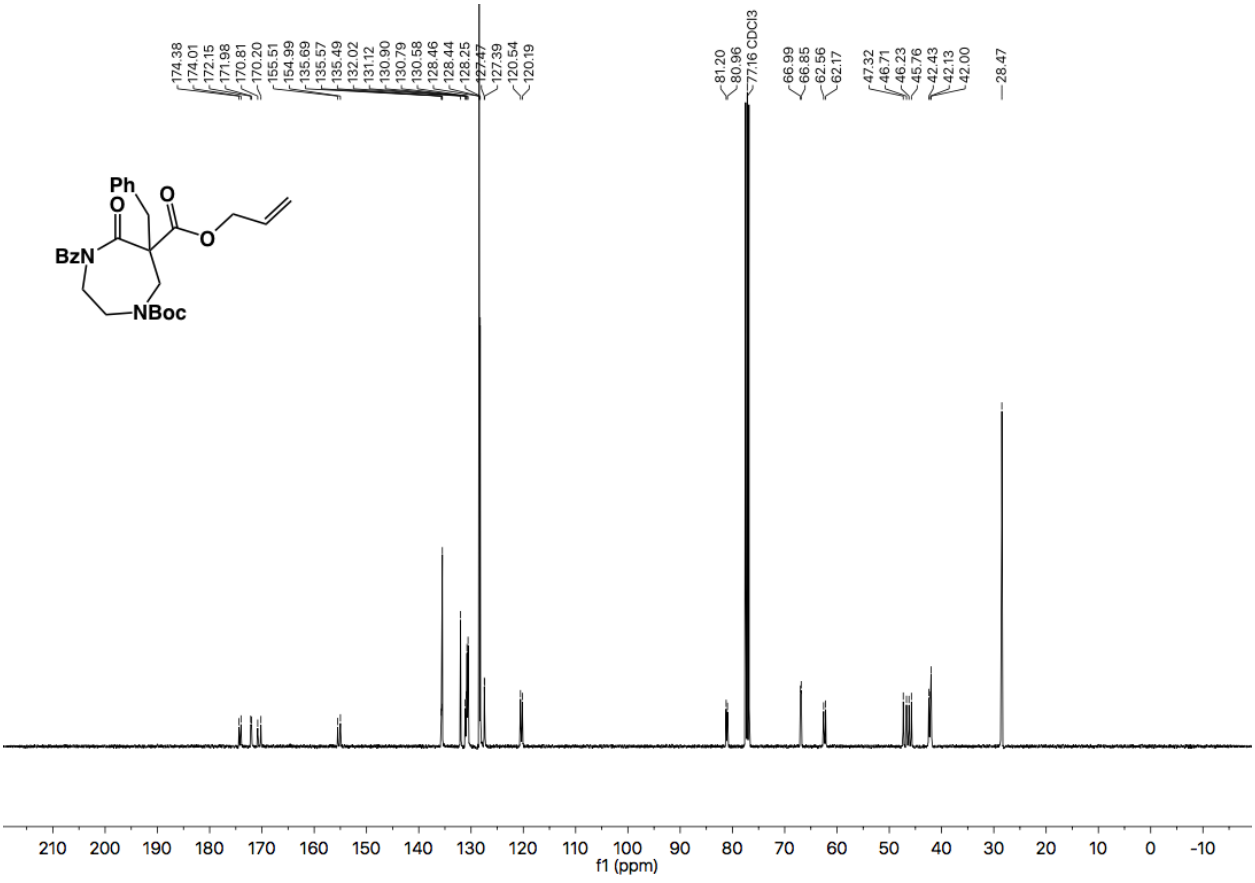

Figure A3.27 ^{13}C NMR (101 MHz, $CDCl_3$) of compound **A2.4l**.

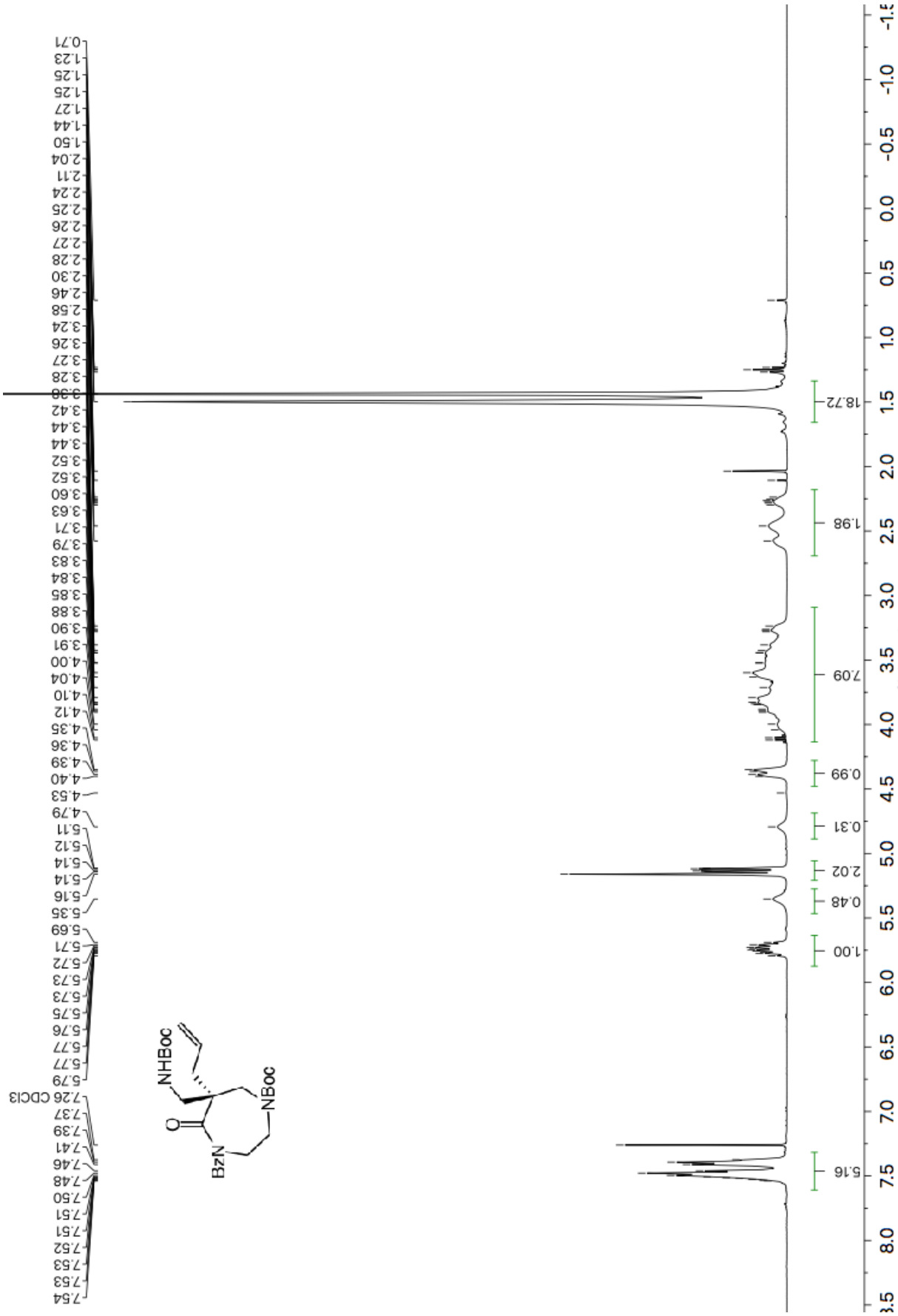

Figure A3.28 ^{1}H NMR (600 MHz, $CDCl_3$) of compound **A2.5f.**

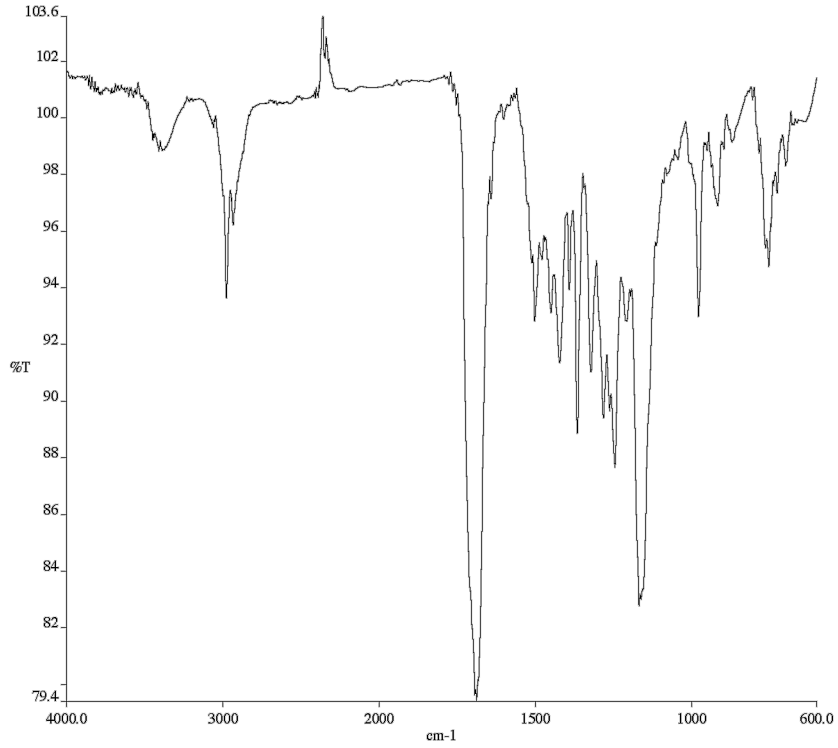

Figure A3.29 Infrared spectrum (Thin Film, NaCl) of compound **A2.5f**.

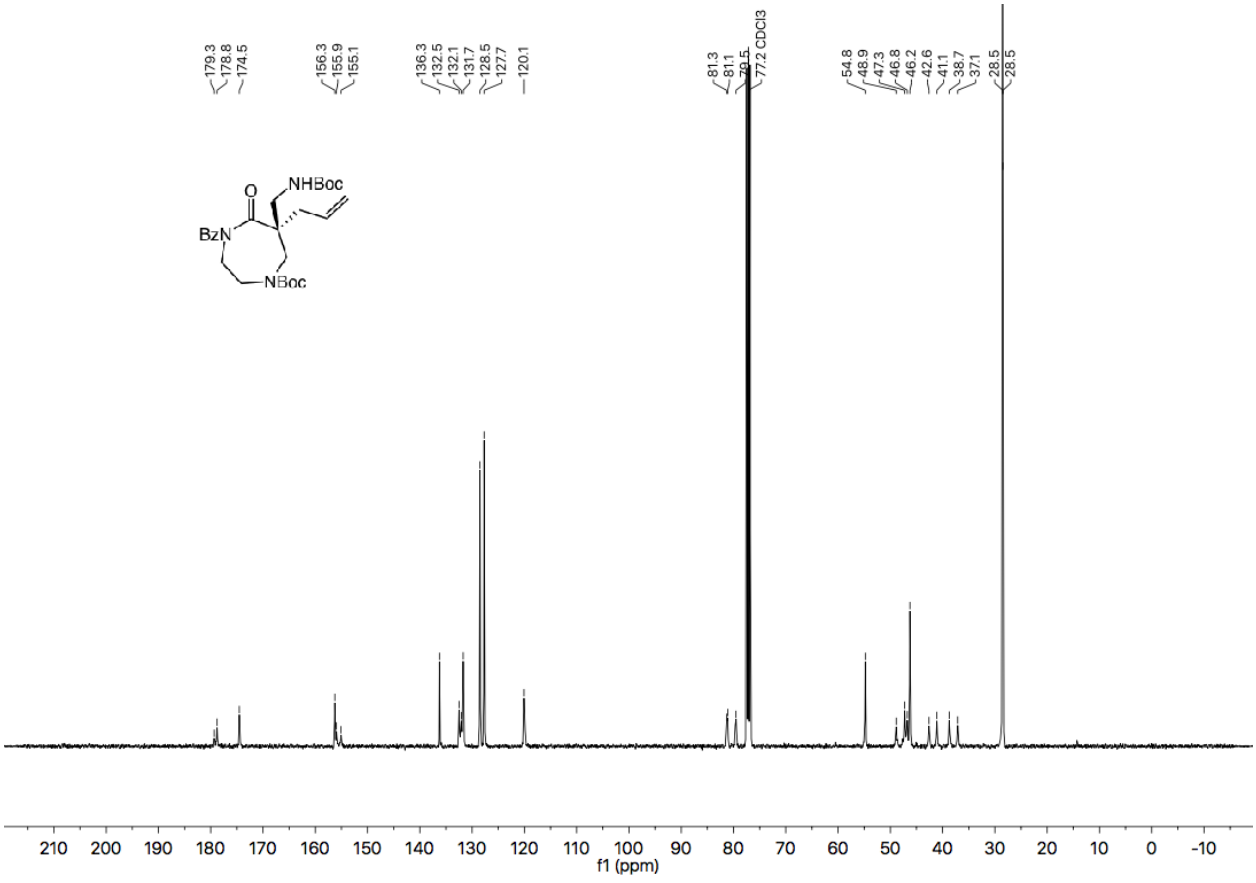

Figure A3.30 ^{13}C NMR (101 MHz, $CDCl_3$) of compound **A2.5f**.

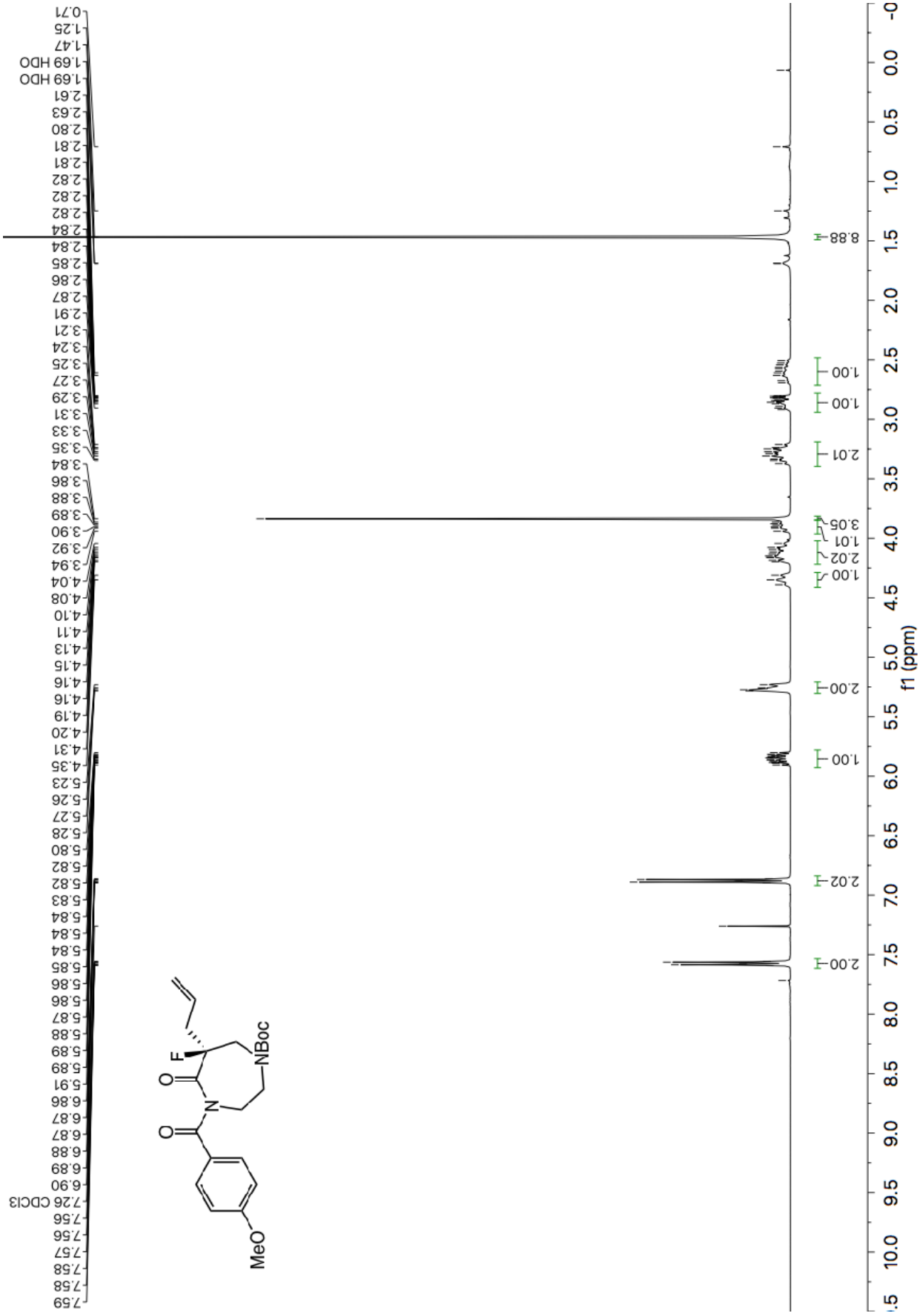

Figure A3.31 ^{1}H NMR (600 MHz, $CDCl_3$) of compound **A2.5g.**

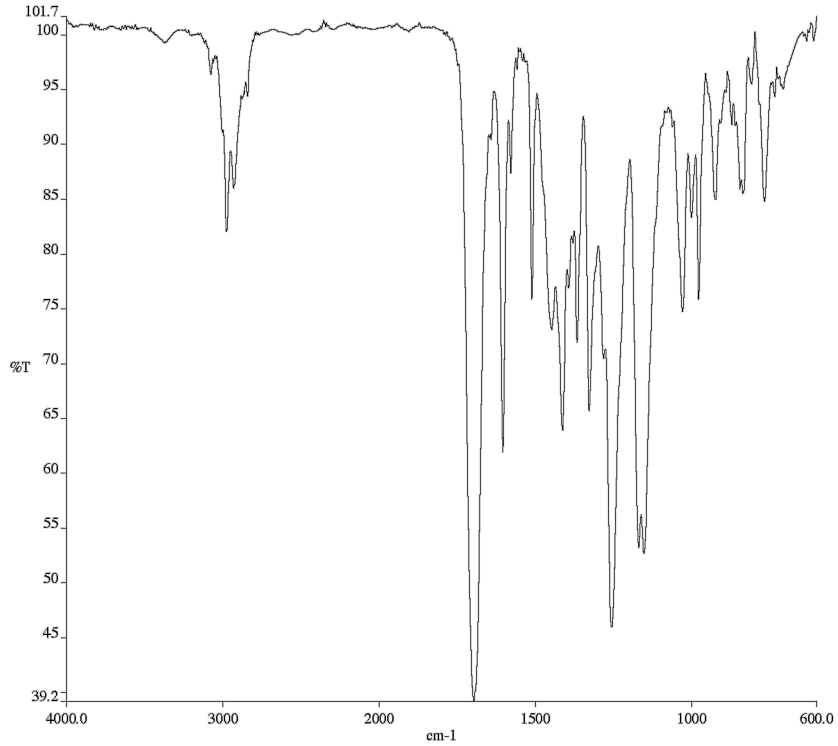

Figure A3.32 Infrared spectrum (Thin Film, NaCl) of compound **A2.5g**.

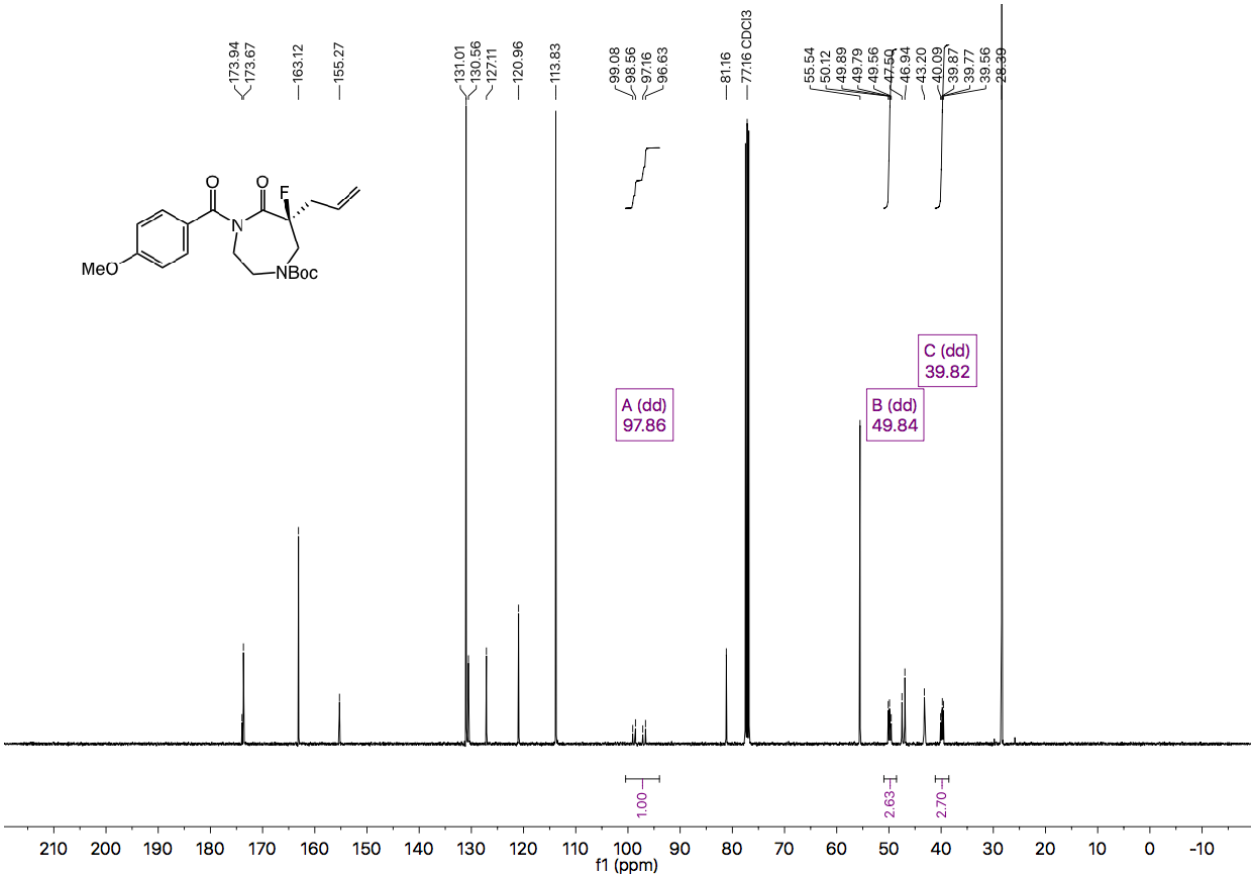

Figure A3.33 ^{13}C NMR (101 MHz, $CDCl_3$) of compound **A2.5g**.

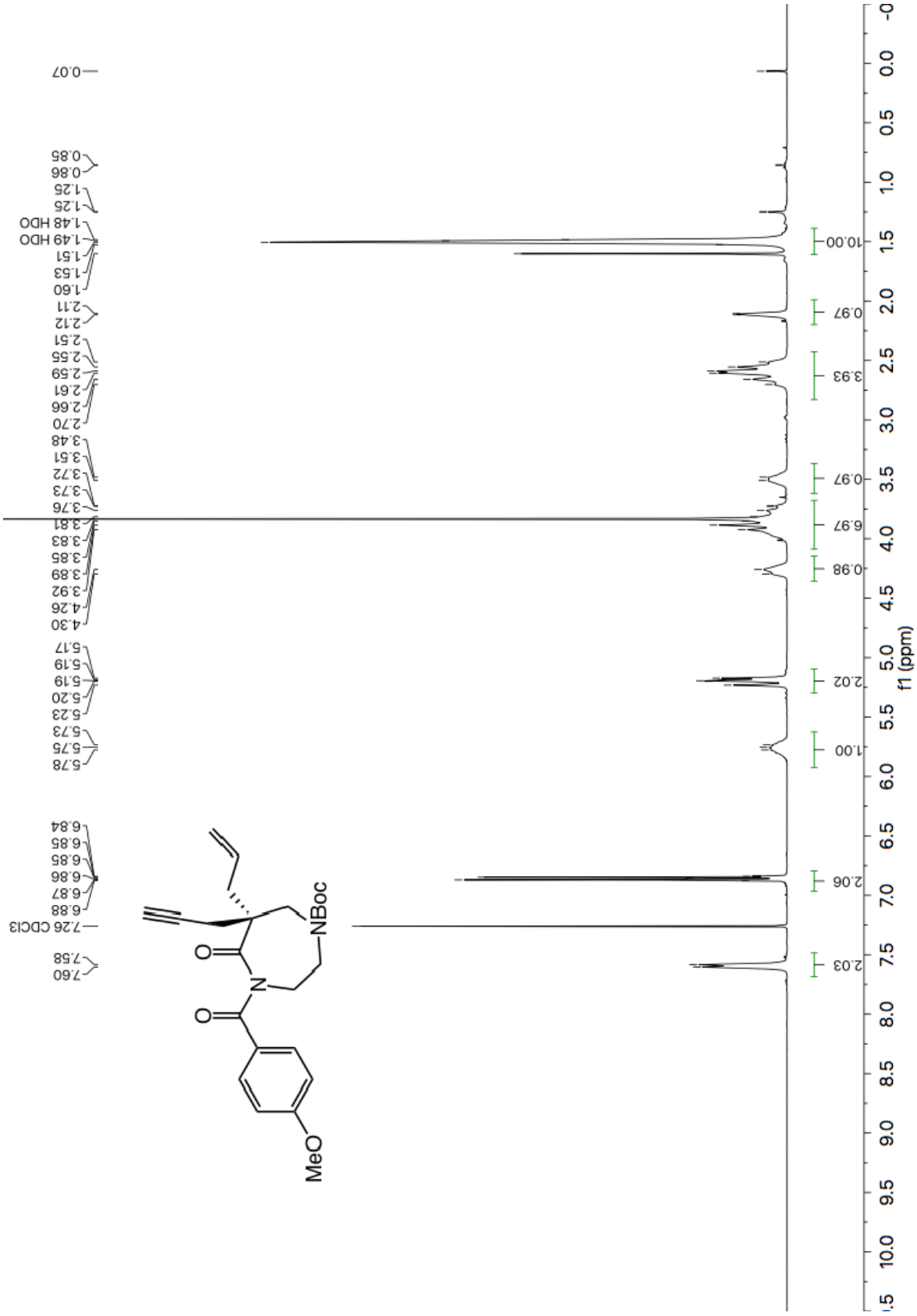

Figure A3.34 ^{1}H NMR (600 MHz, $CDCl_3$) of compound **A2.5h**.

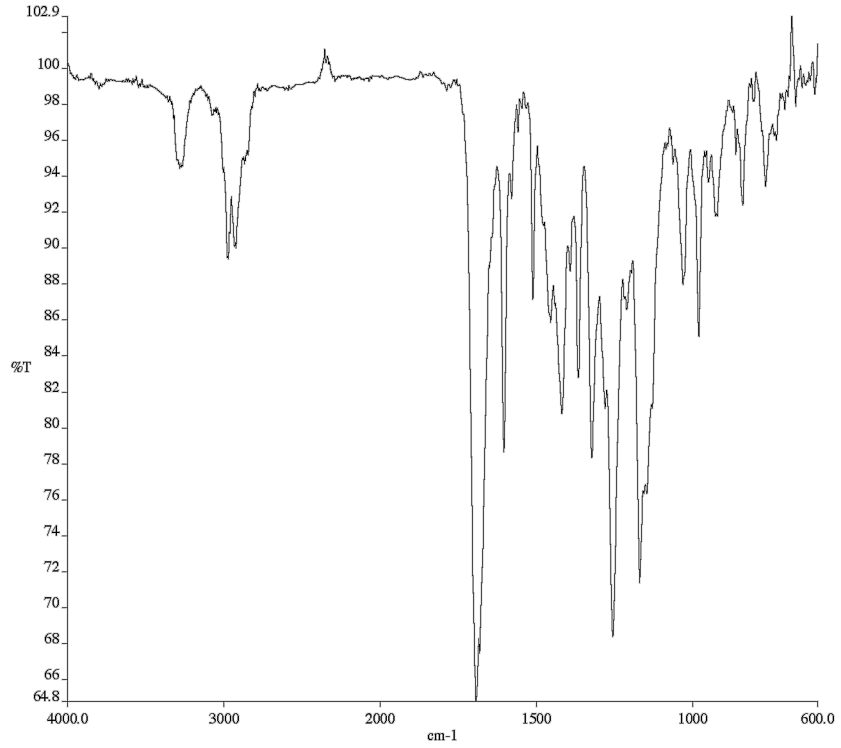

Figure A3.35 Infrared spectrum (Thin Film, NaCl) of compound **A2.5h**.

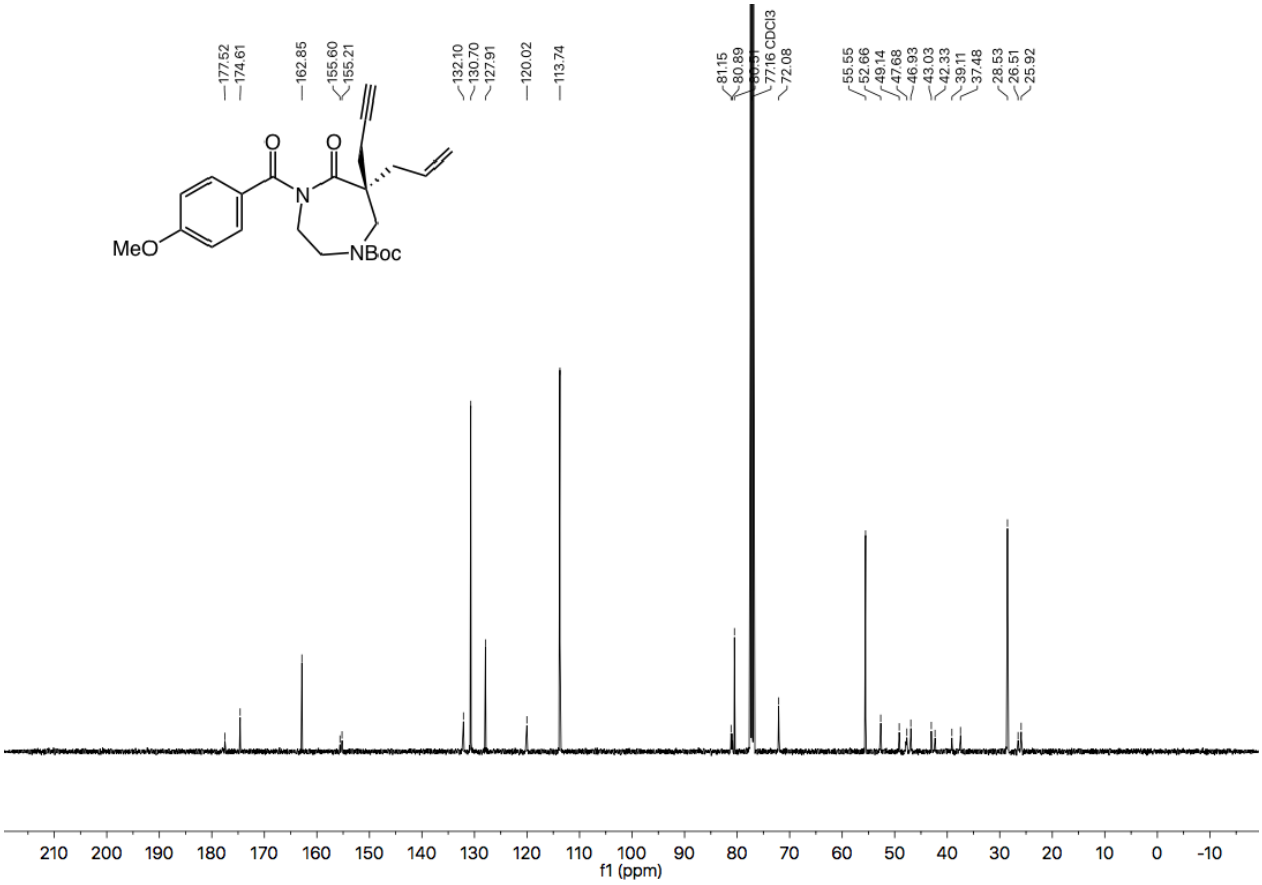

Figure A3.36 ^{13}C NMR (101 MHz, $CDCl_3$) of compound **A2.5h**.

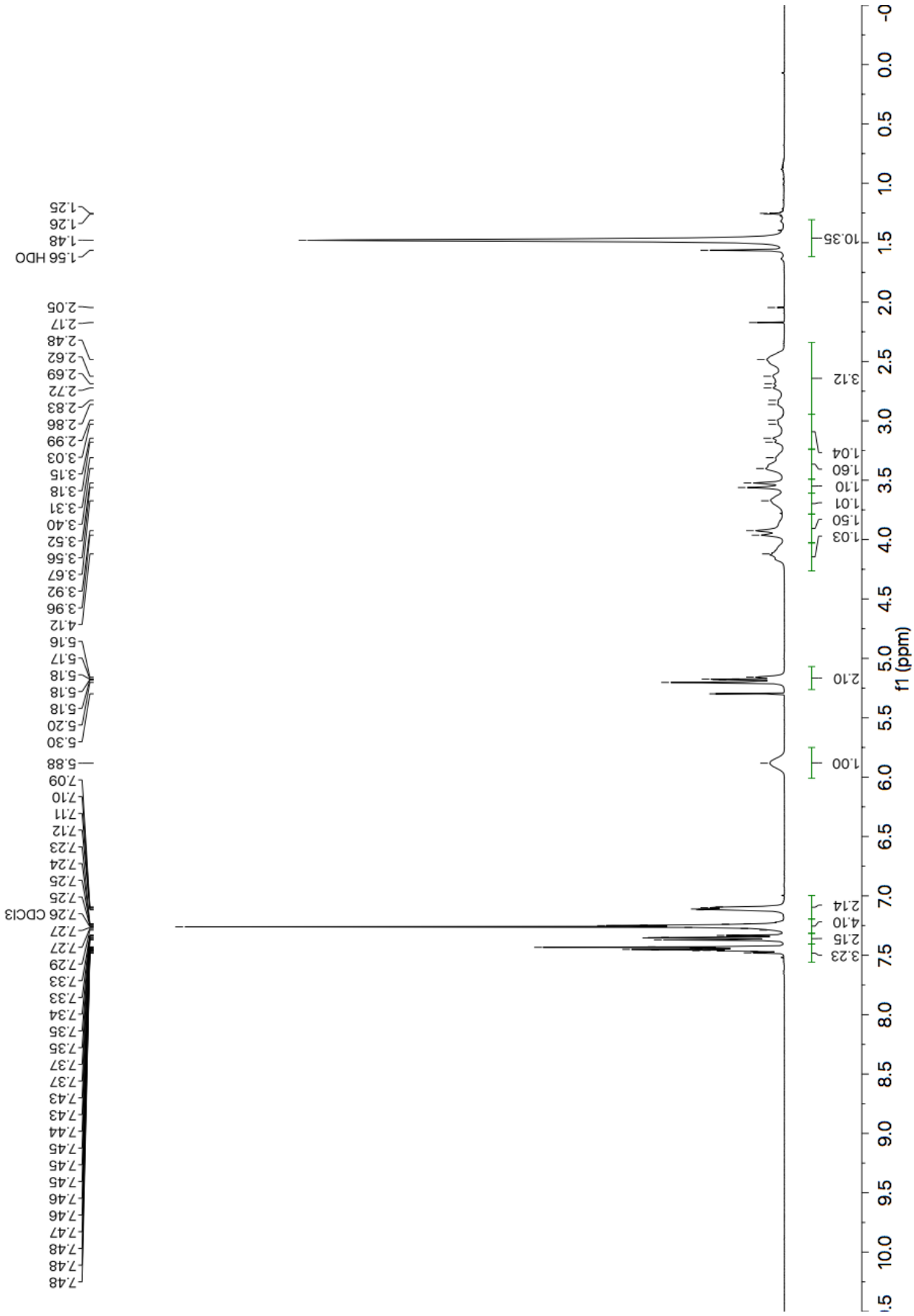

Figure A3.37 ^{1}H NMR (600 MHz, $CDCl_3$) of compound **A2.5l.**

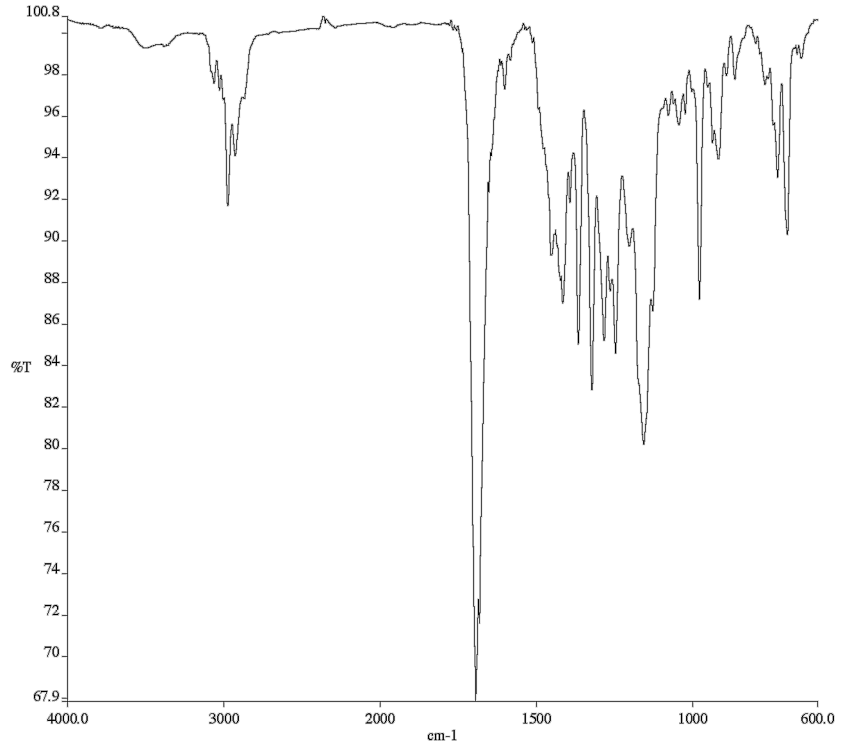

Figure A3.38 Infrared spectrum (Thin Film, NaCl) of compound **A2.5l**.

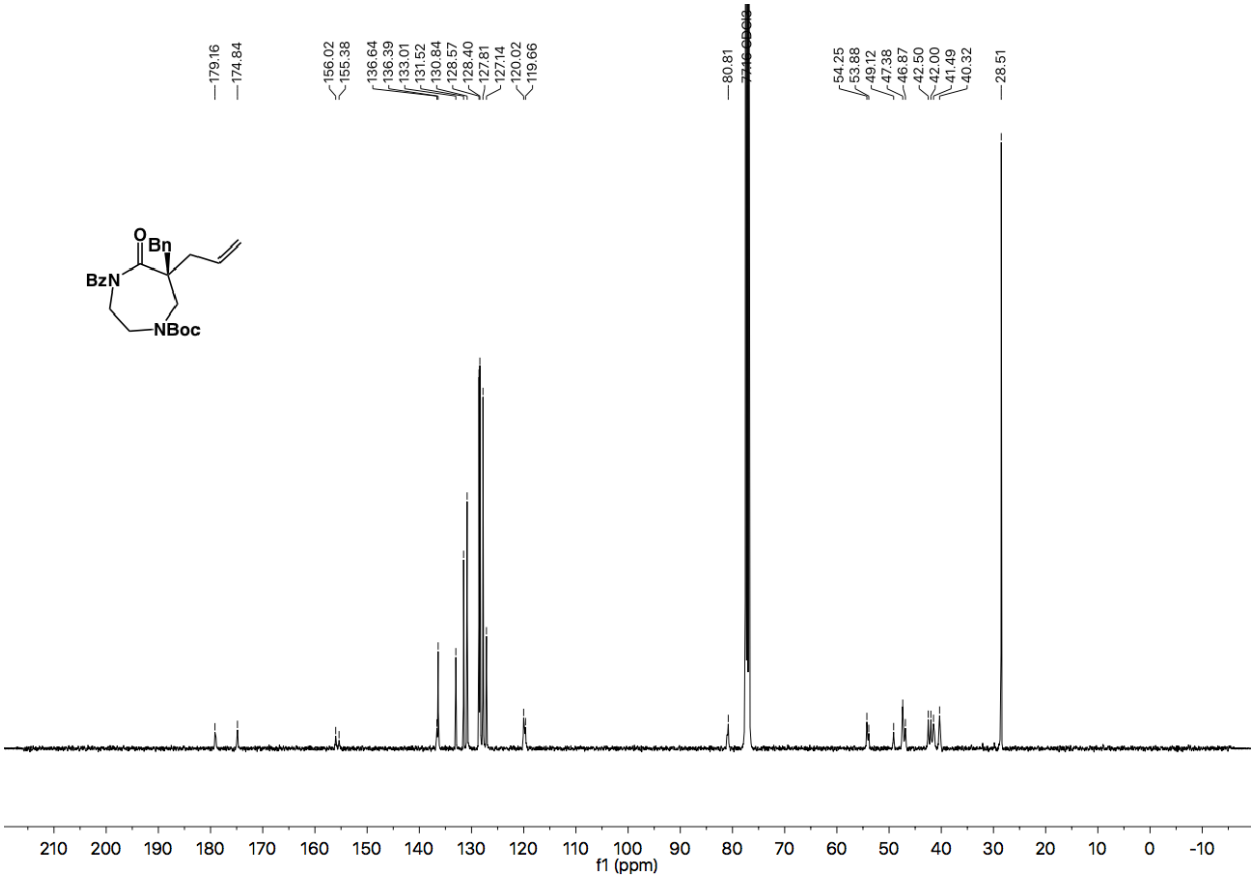

Figure A3.39 ^{13}C NMR (101 MHz, $CDCl_3$) of compound **A2.5l**.

APPENDIX 4

Stereoselective Synthesis of α,α-Disubstituted Amino Acids via Decarboxylative Alkylation of Imidazolinones

A4.1 INTRODUCTION AND BACKGROUND

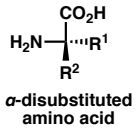

α-disubstituted amino acid

Unnatural amino acids exhibit tremendous biological and chemical utility. They function as chemical intermediates and building blocks for peptide therapeutics, are heavily featured in biological studies of unnatural peptides and proteins, and are found in natural products[1] (Figure A4.1). For example, alpha-disubstituted amino acids can alter peptide conformation and protein structure due increased conformational rigidity, thus serving as useful tools to probe the biological effects of protein structure.[2,3] Because of their conformational effects and their enhanced resistance to chemical and enzymatic degradation, alpha-disubstituted amino acids are featured in a number of experimental peptide therapeutics.[4–6]

Figure A4.1 *Biological important of disubstituted amino acids*

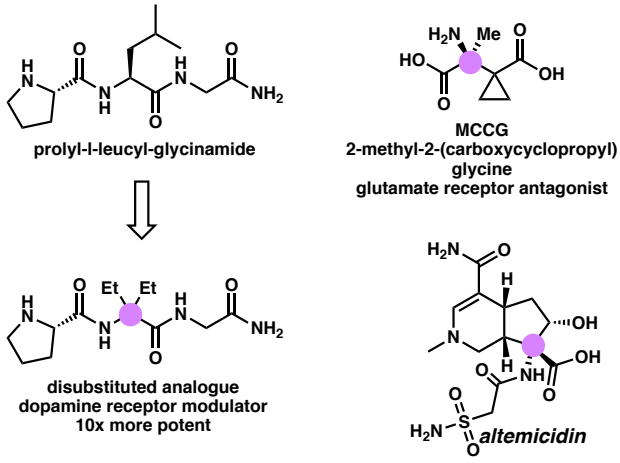

Given the biological utility of disubstituted amino acids, researchers have developed myriad methods to synthesize chiral alpha-disubstituted amino acids. Here we cover just a few of the most prevalent strategies (Scheme A4.1); the interested reader is directed to a number of more comprehensive reviews.[1,7–9] Classical approaches include enzymatic resolution of racemic mixtures, and installation of chiral auxiliaries. Seebach has pioneered the diastereoselective alkylation of cyclic oxazoline scaffolds, which are formed upon cyclization of an amino acid with a chiral aldehyde (Scheme A4.1A).[10,11] The rigid cyclic structure enables highly diastereoselective alkylations; however, the substrate scope is limited by the availability of substituted amino acid precursors as well as the relatively harsh basic reaction conditions. In a modern twist on Seebach's diastereoselective functionalization method Clayden recently developed an innovative N-to-C aryl migration strategy to generate alpha-arylated amino acids (Scheme A4.1B).[12] Other popular chiral auxiliary strategies involve appending a removable chiral scaffold to either the carboxylic acid or the amine of an acyclic amino acid substrate, in the latter case forming a chiral Schiff base (Scheme A4.1C).[13]

In the realm of asymmetric catalysis, modern approaches include enantioselective Mannich reactions, Strecker reactions (Scheme A4.1D),[14] phase transfer conditions (Scheme A4.1E)[15,16] and allylic alkylation reactions (Scheme A4.2).

Scheme A4.1 *Synthetic methods for disubstituted amino acids*

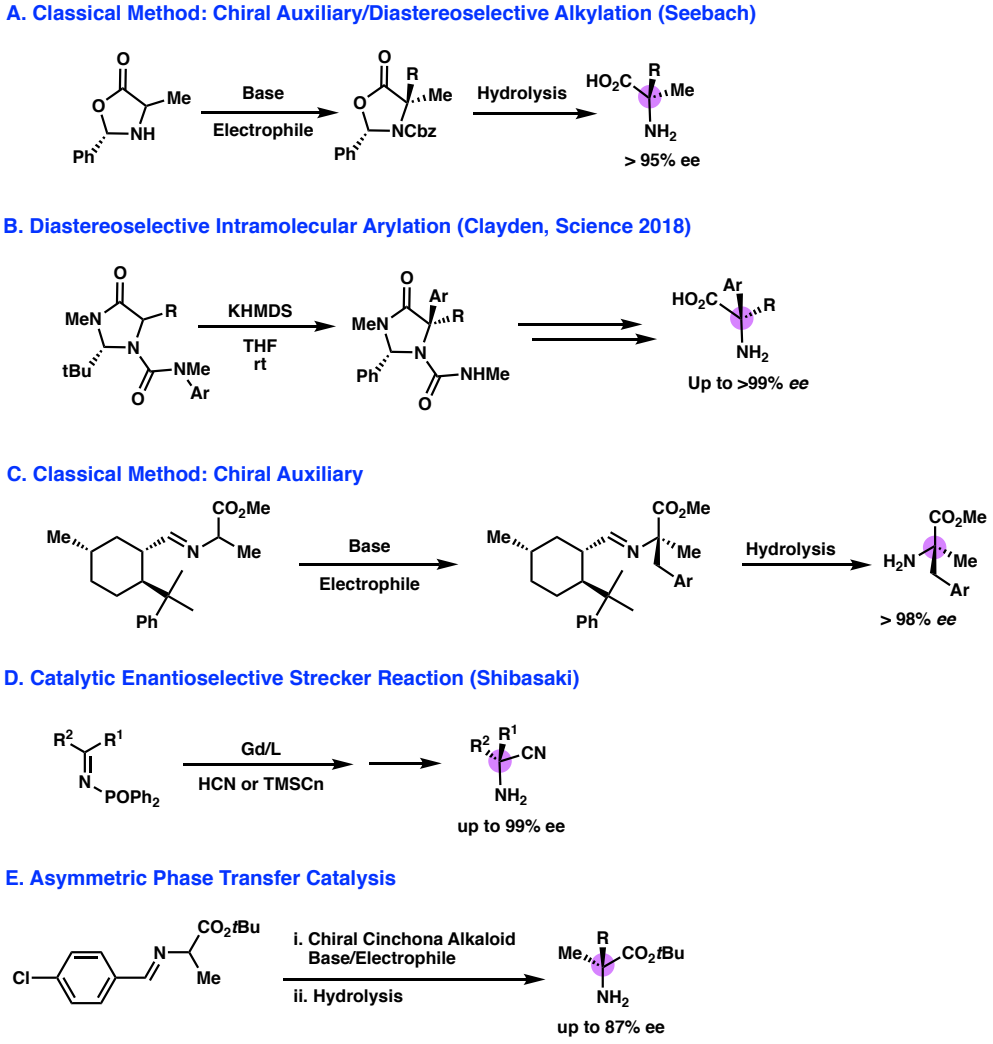

The cyclic azlactone scaffold (Scheme A4.2A) is commonly used in asymmetric catalysis to generate functionalized precursors that can be hydrolyzed to provide chiral alpha-disubstituted amino acids.[17,18] Transition metal catalyzed allylic alkylation approaches, pioneered by Trost and others, allow access to unique alpha-disubstituted amino acids containing a synthetically versatile allyl handle (Scheme A4.2A).[19–21]

However, these methods display limited substrate variation as the cyclic substrates are synthesized from existing amino acids. In a series of significant advances, mild allylic alkylation conditions using acyclic Schiff base scaffolds were recently developed Scheme A4.2B &C).[22–24] Compared to previous acyclic strategies,[25] these new developments feature broader substrate scope; however, their substrate variation is still limited by beginning from synthetically and commercially available amino acids.

Scheme A4.2 *Transition metal catalyzed asymmetric allylic alkylation methods*

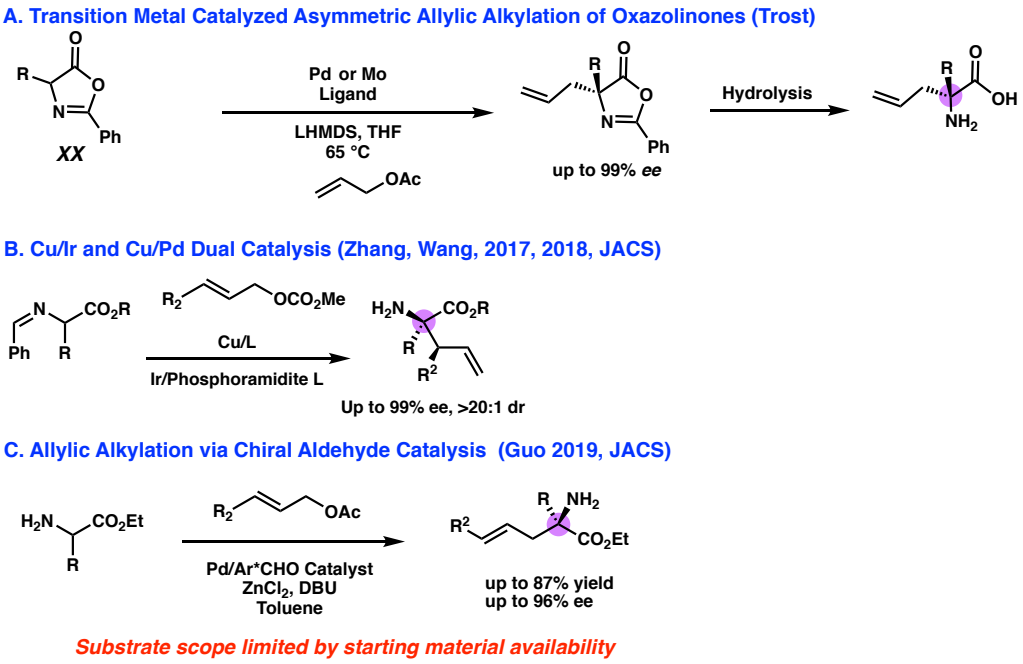

In the Stoltz laboratories, we previously attempted to optimize the DAAA of various oxazole and oxazolidine substrates (Scheme S4.3), which could theoretically be directly hydrolyzed to afford chiral amino acids.[26] However, a series of conditions using Trost and PHOX ligands with various solvents resulted in low enantioselectivity. These poor results were consistent with our previous experience performing decarboxylative alkylation on lactone substrates. Furthermore, we believe the stabilized aromatic character of the prochiral decarboxylated intermediate contributes to the poor

enantioselectivity. Overcoming initial disappointments, we eventually identified a successful DAAA scaffold that when hydrolyzed, would result in a disubstituted amino acid. In the following section, we detail these efforts to significantly expand upon the substrate scope of chiral disubstituted amino acid synthesis via decarboxylative asymmetric allylic alkylation.

Scheme A4.3 *Previous attempts toward the decarboxylative alkylation of cyclic amino acid scaffolds*

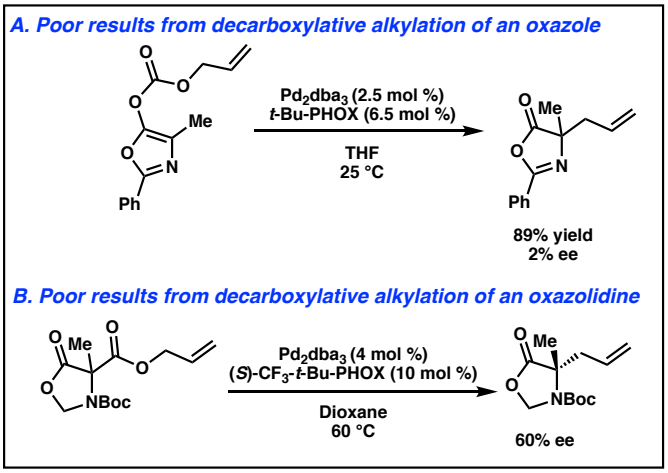

A4.2 SYNTHESIS OF CYCLIC AMINO ACID SCAFFOLDS

Scheme S4.4 *Routes toward a cyclic amino acid imidazolinone scaffold*

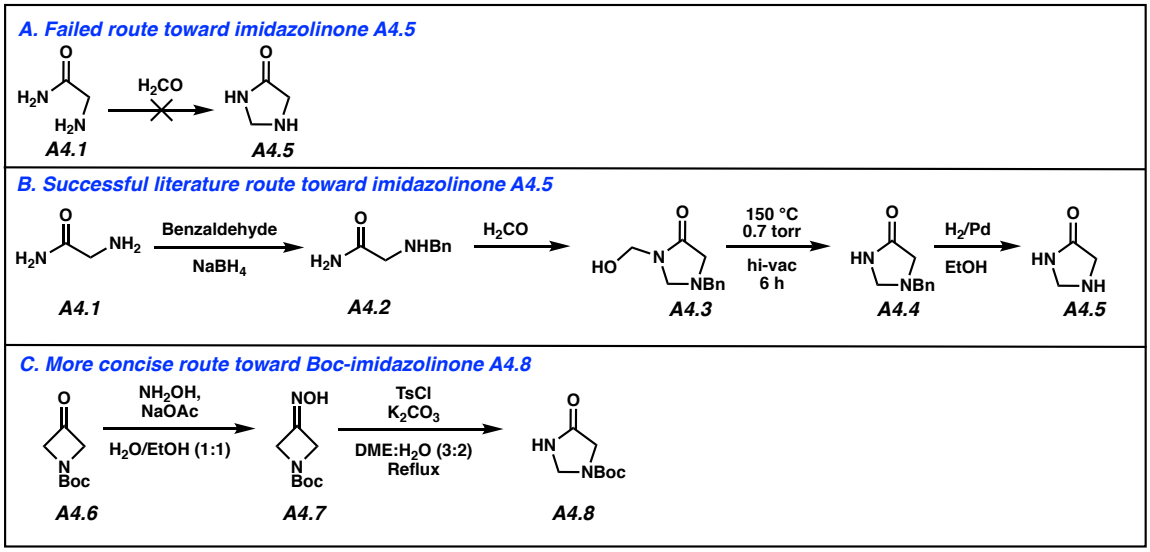

In light of our unsuccessful DAAA attempts with oxazole type scaffolds, we sought an alternative cyclic core; the imidazolinone core **A4.5** (Scheme A4.4) is logically the next simplest scaffold on which to perform DAAA explorations, with hydrolysis ultimately yielding a chiral disubstituted amino acid. We thus sought to synthesize a model substrate based on the imidazolinone core. Initial attempts to cyclize glycinamide with formaldehyde (Scheme A4.4A) were unsuccessful. Looking to the literature, we found a multi-step patent route starting from glycinamide.[27] Benzylation, followed by cyclization with formaldehyde affords hydroxyimidazolinone **A4.3**. Formaldehyde is then eliminated by heating under vacuum to yield benzyl-protected **A4.4**, with hydrogenolysis finally leading to imidazolinone **A4.5**. While this patent route proved reliable, we nevertheless sought a more concise route; Boc-azetidinone **A4.6** is commercially available at <$1.25/gram, and Beckmann rearrangement would directly afford Boc-imidazolinone **A4.8**. After screening a variety of conditions, we eventually found that Beckmann rearrangement of the oxime sulfonate under reflux provided the product **A4.8** in rather low yields of around 20%. We are currently exploring other Beckmann rearrangement conditions to improve the yield.

With Boc-imidazolinone **A4.8** in hand, we next sought to synthesize the dicarbonyl compound **A4.10**, which would serve as a divergent point of entry to a variety of novel DAAA substrates. Benzoylation to give **A4.9** was facile. However, acylation with allyl cyanoformate proved more difficult. At -78 °C, enolate formation by slowly adding a solution of **A4.9** into a solution of LHMDS led to significant amounts of self-cleavage of the benzoyl protecting group, significantly lowering the yield of dicarbonyl

A4.10. Fortunately, performing the deprotonation at -114 °C, at which point the THF reaction solvent began to solidify, avoided degradation and afforded **A4.10** in 90% yield.

Scheme A4.5 *Synthesis of the imidazolinone DAAA substrate*

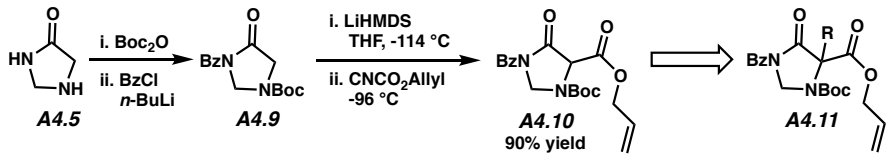

Divergent intermediate S4.10 significantly expands substrate scope

A4.3 DECARBOXYLATIVE ASYMMETRIC ALLYLIC ALKYLATION OF IMIDAZOLINONES

With dicarbonyl **A4.10** in hand, we next synthesized a range of DAAA substrates. Using methyl and aminomethyl substrate **A4.11a** and **A4.11b** for initial optimization attempts, we found that in line with previous results on six and seven-membered diazaheterocycles, a nonpolar solvent mixture of 2:1 hexanes/toluene or 2:1 methylcyclohexane/toluene provided high enantioselectivity (Table A4.1, entries 2 & 3). In contrast, pure toluene resulted in lower ee (entry 1). To our delight, we achieved a 91% ee in our first screening attempt.

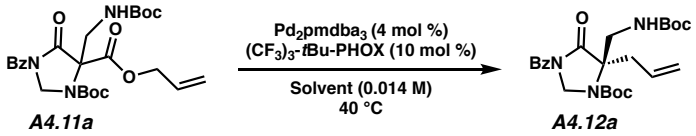

Entry	Solvent	*ee*
1	Toluene	80
2	2:1 MeCy/Toluene	91
3	2:1 Hexanes/Toluene	91

Reactions performed on 10 mg scale

With the methyl model substrate **A4.11b**, we found that (*S*)-$(CF_3)_3$-*t*Bu-PHOX was the optimal ligand (Table A4.2, entry 3). ANDEN-Ph-Trost ligand in dioxane (entry 2) resulted in lowered enantioselectivity and longer reaction times; however, the entry should be repeated using 2:1 toluene/hexanes to provide a direct comparison to the other entries. While conducting the reaction at 40 °C resulted in higher enantioselectivity, the reaction was incomplete even after 72 hours, with significant amounts of starting material remaining.

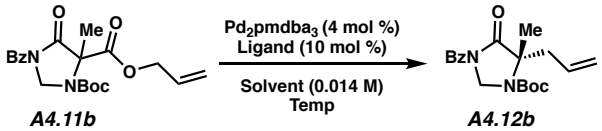

A4.11b ***A4.12b***

Entry	Ligand	Solvent	Temp °C	*ee*
1	(*S*)-$(CF_3)_3$-*t*Bu-PHOX	2:1 Hexanes/Toluene	40	96[a]
2	(S,S)-ANDEN-Ph-Trost	Dioxane	60	70[a,b]
2	(*S*)-$(CF_3)_3$-*t*Bu-PHOX	2:1 Hexanes/Toluene	60	94

[a] Incomplete conversion after 72 h. [b] 0.5 M concentration. *Reactions performed on 10 mg scale*

With these initial results in hand, we examined the DAAA of additional substrates (Table A4.3). The benzyl, benzyloxymethyl, and propargyl substrates **A4.11c-d** provided uniformly excellent *ee*. Yields will be determined in future larger scale reactions.

Table A4.3 *Initial Substrate Scope*

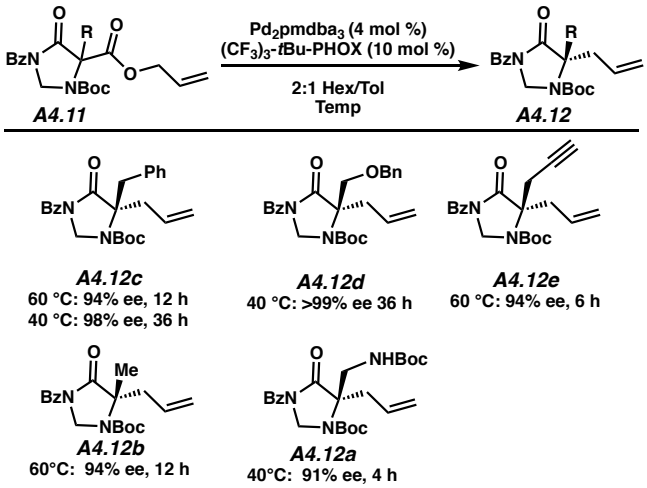

Reactions performed on 10 mg scale

A4.4 CONCLUSIONS

In summary, we report the enantioselective synthesis of unprecedented *gem*-disubstituted imidazolinones using the venerable Pd-catalyzed decarboxylative asymmetric allylic alkylation. The versatile (*S*)-$(CF_3)_3$-*t*-Bu-PHOX ligand performs well, yielding products in *ee*'s up to >99%. Future directions include further exploration of the substrate scope of this reaction and product transformations. These novel chiral imidazolinones are anticipated to find utility in the design of novel alpha-disubstituted amino acids.

A4.5 EXPERIMENTAL SECTION

A4.5.1 MATERIALS AND METHODS

Unless otherwise stated, reactions were performed in flame-dried glassware under an argon or nitrogen atmosphere using dry, deoxygenated solvents. Solvents were dried

by passage through an activated alumina column under argon. Boc-azetidinone **S4.6** was obtained from Combi-Blocks. Commercially obtained reagents were used as received. Chemicals were purchased from Sigma Aldrich/Strem/Alfa Aesar/Combi-Blocks and used as received.

Reaction temperatures were controlled by an IKAmag temperature modulator. Glove box manipulations were performed under a nitrogen atmosphere. Thin-layer chromatography (TLC) was performed using E. Merck silica gel 60 F254 precoated plates (0.25 mm) and visualized by UV fluorescence quenching, iodine on silica, ninhydrin, or $KMnO_4$ staining. Silia*Flash* P60 Academic Silica gel (particle size 0.040–0.063 mm) was used for flash chromatography.

Analytical SFC was performed with a Mettler SFC supercritical CO_2 analytical chromatography system utilizing a Chiralpak IC column (4.6 mm x 25 cm) obtained from Daicel Chemical Industries, Ltd. with visualization at 254 nm. Reverse Phase Preparatory HPLC was performed with a Teledyne ISCO ACCQPrep HP125 preparative liquid chromatography system equipped with a RediSep Prep C18 5 µm column (20 x 250 mm).

^{1}H NMR spectra were recorded on a Varian Inova 600 MHz or 500 MHz spectrometer or a Bruker Avance HD 400 MHz spectrometer and are reported relative to residual $CHCl_3$ (δ 7.26 ppm) or CH_3OH (δ 3.31 ppm). ^{13}C NMR spectra were recorded on a Varian Inova 500 MHz spectrometer or a Bruker Avance HD 400 MHz spectrometer and are reported relative to residual $CDCl_3$ (δ 77.16 ppm) or CD_3OD (δ 49.00 ppm). Data for ^{1}H NMR are reported as follows: s = singlet, d = doublet, t = triplet, q = quartet, p = pentet, sept = septuplet, m = multiplet, br s = broad singlet. Data for ^{13}C NMR are reported in terms of chemical shifts (δ ppm). Some reported spectra include minor

solvent impurities of water (δ 1.56 or 4.87 ppm), ethyl acetate (δ 4.12, 2.05, 1.26 ppm), methylene chloride (δ 5.30 ppm), acetone (δ 2.17 ppm), grease (δ 1.26, 0.86 ppm), and/or silicon grease (δ 0.07 ppm), which do not impact product assignments.

IR spectra were obtained using a Perkin Elmer Paragon 1000 spectrometer using thin films deposited on NaCl plates and reported in frequency of absorption (cm^{-1}). High resolution mass spectra (HRMS) were obtained from an Agilent 6200 Series TOF with an Agilent G1978A Multimode source in electrospray ionization (ESI+), atmospheric pressure chemical ionization (APCI+), or mixed ionization mode (MM: ESI-APCI+). Optical rotations were measured with a Jasco P-2000 polarimeter operating on the sodium D-line (589 nm), using a 100 mm pathlength cell and are reported as: $[\alpha]_D^T$ (concentration in g/100 mL, solvent). Stereochemistry is assigned by analogy to previous results. [28–33]

A4.5.2 EXPERIMENTAL PROCEDURES AND SPECTROSCOPIC DATA

A4.5.2.1 Procedures for the Synthesis of Imidazolinone Allylic Alkylation Substrates

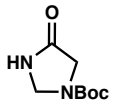

***tert*-butyl 4-oxoimidazolidine-1-carboxylate (S4.8)**. Can be prepared by two separate procedures. **Procedure A**: To a solution of imidazolinone **S4.5**[27] (1.47 g, 1 equiv) in THF (170 mL, 0.1 M) was added NEt_3 (2.38 mL, 1 equiv) followed by Boc_2O (3.72 g, 1 equiv) portionwise. The solution was stirred for 4 h at rt and then concentrated. The crude residue was purified by automated silica gel flash chromatography (Teledyne ISCO, 0 → 20% MeOH/CH_2Cl_2) to provide **S4.8** as a clear oil (2.5g, 79% yield). **Procedure B**: To a solution of Boc-azetidinone **S4.6** (5 g, 1 equiv) in EtOH (60 mL, 0.25 M total

concentration) was added a solution of NaOAc (6.72 g, 2 equiv) and NH_2OH-HCl (4.06 g, 2 equiv) in H_2O (60 mL, 0.25 M total concentration). The solution was stirred at 50 °C for 2 h, and then extracted with CH_2Cl_2 (3x). The combined organic layers were backwashed with $NaHCO_3$ (1x) dried over Na_2SO_4, concentrated, and then placed under high vacuum to remove AcOH. The crude oxime was then dissolved in 260 mL of 3:2 DME/H_2O. K_2CO_3 (8.92 g, 2.5 equiv) and TsCl (5.9 g, 1.5 equiv) were added. The reaction was refluxed for 3 h until complete consumption of starting material was observed by TLC (5% MeOH/CH_2Cl_2). DME was concentrated off. The aqueous layer was extracted with EtOAc (6x). The combined organic layers were dried over Na_2SO_4 and concentrated. The crude imidazolinone was purified by automated silica gel flash chromatography (0 → 30% MeOH/CH_2Cl_2) to provide the Boc-imidazolinone **S4.8**. **^{1}H NMR (400 MHz, Chloroform-*d*)** δ 7.66 (d, *J* = 52.9 Hz, 1H), 4.76 (d, *J* = 11.0 Hz, 2H), 3.87 (d, *J* = 15.1 Hz, 2H), 1.47 (s, 9H). **^{13}C NMR (101 MHz, $CDCl_3$)** δ 172.1, 153.1, 152.7, 81.2, (59.0, 58.8 two peaks due to hindered rotation), (47.5, 47.0 two peaks due to hindered rotation), 28.4.

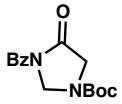

***tert*-butyl 3-benzoyl-4-oxoimidazolidine-1-carboxylate (S4.9)**. **S4.8** (1.4 g, 1 equiv) in THF (75 mL), 0.1 M at −78 °C was added dropwise *n*BuLi (3.61 mL, 2.5 M solution in hexane, 1.2 equiv). The resulting yellow solution was stirred for 5 min at −78 °C. Benzoyl chloride (1.14 mL, 1.3 equiv) was then added dropwise at −78 °C, giving a deep

yellow solution. The reaction was stirred for 10 min at −78 °C, quenched by addition of saturated aqueous NH_4Cl, and diluted with ethyl acetate. The layers were separated and the aqueous layer was extracted with ethyl acetate (3 × 100 mL). The combined organic layers were dried over anhydrous Na_2SO_4, decanted, and concentrated under reduced pressure. The crude product was purified by automated silica gel flash column chromatography (0 → 80% EtOAc/hexanes) to give protected imidazolinone as a white solid. **^{1}H NMR (400 MHz, Chloroform-*d*)** δ 7.68 – 7.61 (m, 2H), 7.61 – 7.51 (m, 1H), 7.48 – 7.39 (m, 2H), 5.29 (s, 2H), 4.17 (s, 2H), 1.51 (s, 9H). **^{13}C NMR (101 MHz, $CDCl_3$)** δ 168.6, 167.5, 152.6, 133.0, 132.7, 129.1, 128.0, 81.8, 61.8, 49.3, 28.4. **IR (Neat Film, NaCl)** 2979, 1763, 1708, 1476, 1448, 1410,1367, 1305, 1212, 1163, 1127, 894, 858, 767, 727, 704, 661 cm^{-1}; **HRMS (MM: ESI-APCI):** *m/z* calc'd for $C_{15}H_{22}N_3O_4$ $[M+NH_4]^+$: 308.1605, found 308.1600.

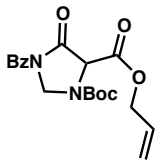

5-allyl 1-(*tert*-butyl) 3-benzoyl-4-oxoimidazolidine-1,5-dicarboxylate (A4.10). To a solution of LHMDS (1.52 g, 1.1 equiv) in THF (15 mL 0.1 M total concentration) was slowly added **A4.9** (2.4 g, 1.0 equiv) in THF (68 mL, 0.1 M total concentration) at −114 °C. The resulting light orange reaction mixture (slurry/frozen) was stirred for 5 min at −114 °C. Then, allyl cyanoformate (368 μL, 1.2 equiv) was added dropwise at −114 °C, giving a light yellow solution. After stirring for 20 min at −96 °C, the reaction was quenched with 1 M HCl (10 mL) and diluted with ethyl acetate (20 mL). The aqueous phase was extracted with ethyl acetate (3 x 30 mL). The combined organic layers were

dried over anhydrous Na_2SO_4 and solid $NaHCO_3$, decanted, and concentrated under reduced pressure The crude product was purified by automated silica gel flash chromatography (Teledyne ISCO, 0% → 80% EtOAc/hexanes) to give dicarbonyl **A4.10** as a clear oil; **^{1}H NMR (400 MHz, Chloroform-*d*)** δ 7.65 – 7.57 (m, 2H), 7.57 – 7.51 (m, 1H), 7.42 (t, *J* = 7.8 Hz, 2H), 5.98 – 5.82 (m, 1H), 5.41 – 5.31 (m, 3H), 5.26 (dd, *J* = 15.2, 10.4 Hz, 1H), 4.80 – 4.63 (m, 2H), 1.52 (s, 4H), 1.46 (s, 4H); **^{13}C NMR (101 MHz, $CDCl_3$)** δ (168.42, 168.20 two peaks due to hindered rotation), (165.70, 165.55 two peaks due to hindered rotation), (163.49, 163.24 two peaks due to hindered rotation), (152.14, 151.89 two peaks due to hindered rotation), 132.99, 132.63, (131.00, 130.94 two peaks due to hindered rotation), 129.18, 128.14, (119.79, 119.18 two peaks due to hindered rotation), (82.75, 82.61 two peaks due to hindered rotation), 67.16, 63.46, (63.01, 61.50 two peaks due to hindered rotation), (28.34, 28.23 two peaks due to hindered rotation). **IR (Neat Film, NaCl)** 2977, 1747, 1715, 1449, 1405, 1369,1302, 1250, 1167, 1135, 986, 938, 769, 725, 696, 668 cm^{-1}; **HRMS (MM: ESI-APCI):** *m/z* calc'd for $C_{19}H_{26}N_3O_6$ $[M+NH_4]^+$: 392.1816, found 392.1822.

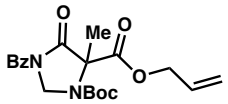

5-allyl 1-(tert-butyl) 3-benzoyl-5-methyl-4-oxoimidazolidine-1,5-dicarboxylate (A4.11b). Sodium hydride (60% in mineral oil, 32 mg, 1.2 equiv) was added to a solution of dicarbonyl **A4.10** (250 mg, 1.0 equiv) in THF (6.7 mL, 0.1 M) at rt. After stirring for 30 min at rt, MeI (208 μL, 5 equiv) was added. The reaction mixture was stirred for 2 h. The reaction was quenched with aqueous NH_4Cl (10 mL) and extracted with EtOAc (3 x 5 mL). The combined organic phases were dried over anhydrous Na_2SO_4, decanted, and concentrated under reduced pressure. The crude product was purified by automated silica

gel flash chromatography (Teledyne ISCO, 0 → 50% acetone/hexanes) to give methyl allyl ester **A4.11b** as a clear oil; **^{1}H NMR (400 MHz, Chloroform-*d*)** δ 7.71 – 7.50 (m, 3H), 7.42 (t, *J* = 7.6 Hz, 2H), 5.89 (dtt, *J* = 15.9, 10.3, 5.7 Hz, 1H), 5.46 – 5.15 (m, 4H), 4.80 – 4.50 (m, 2H), 1.81 (d, *J* = 21.1 Hz, 3H), 1.50 (s, 9H). **^{13}C NMR (101 MHz, $CDCl_3$)** δ (168.6, 168.3 two peaks due to hindered rotation), 167.4, 167.2, (152.3, 152.2 two peaks due to hindered rotation), 132.9, 132.7, (131.2, 130.9 two peaks due to hindered rotation), 129.1, 128.1, (119.6, 119.0 two peaks due to hindered rotation), (82.6, 82.4 two peaks due to hindered rotation), (68.4, 68.2 two peaks due to hindered rotation), 67.1, (61.1, 61.0 two peaks due to hindered rotation), (28.3, 28.2 two peaks due to hindered rotation), (20.4, 19.8 two peaks due to hindered rotation); **IR (Neat Film, NaCl)** 2978, 1772, 1740, 1713, 1601, 1476, 1449, 1385,1369, 1304, 1244, 1161, 1123, 1066, 912, 858, 769, 732, 702, 667 cm^{-1}; **HRMS (MM: ESI-APCI):** *m/z* calc'd for $C_{20}H_{28}N_3O_6$ $[M+NH_4]^+$: 406.1973, found 406.1975.

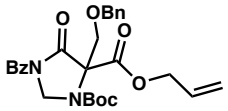

5-allyl 1-(tert-butyl) 3-benzoyl-5-((benzyloxy)methyl)-4-oxoimidazolidine-1,5-dicarboxylate (A4.11d). Sodium hydride (60% in mineral oil, 32 mg, 1.2 equiv) was added to a solution of dicarbonyl **A4.10** (250 mg, 1.0 equiv) in THF (6.7 mL, 0.1 M) at rt. After stirring for 30 min at rt, BOMCl (185 μL, 2 equiv) was added. The reaction mixture was stirred for 2 h. The reaction was quenched with aqueous NH_4Cl (10 mL) and extracted with EtOAc (3 x 5 mL). The combined organic phases were dried over anhydrous Na_2SO_4, decanted, and concentrated under reduced pressure. The crude

product was purified by automated silica gel flash chromatography (Teledyne ISCO, 0 → 40% acetone/hexanes) to give benzyloxymethyl allyl ester **A4.11d** as a clear oil; **^{1}H NMR (400 MHz, Chloroform-*d*)** δ 7.69 – 7.48 (m, 3H), 7.47 – 7.17 (m, 7H), 5.87 (dddt, *J* = 17.3, 10.4, 8.8, 5.8 Hz, 1H), 5.51 – 5.12 (m, 4H), 4.84 – 4.44 (m, 4H), 4.42 – 4.03 (m, 2H), 1.52 (s, 5H), 1.38 (s, 5H); **^{13}C NMR (101 MHz, $CDCl_3$)** δ (168.5, 168.3 two peaks due to hinded rotation), (166.0, 165.7 two peaks due to hinded rotation), (165.3, 165.21 two peaks due to hinded rotation), (151.9, 151.5 two peaks due to hinded rotation), (137.7, 137.3 two peaks due to hindered rotation), 132.9, 132.7, (131.1, 130.8 two peaks due to hindered rotation), 129.2, (128.68, 128.5 two peaks due to hindered rotation), 128.1, 128.0, 127.9, (127.6 127.4 two peaks due to hindered rotation), (119.8, 119.2 two peaks due to hindered rotation), (82.5, 82.4 two peaks due to hindered rotation), 73.7, (72.0, 71.8 two peaks due to hindered rotation), (69.5, 69.0 two peaks due to hindered rotation), 67.0, 61.6, (28.4, 28.2 two peaks due to hindered rotation). **IR (Neat Film, NaCl)** 2975, 1771,1744, 1713, 1450, 1389, 1369,1308, 1236, 1158, 1068, 858, 795, 744, 696, 668 cm^{-1}; **HRMS (MM: ESI-APCI):** *m/z* calc'd for $C_{27}H_{34}N_3O_7$ $[M+NH_4]^+$: 512.2398, found 512.2395.

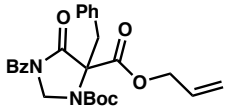

5-allyl 1-(tert-butyl) 3-benzoyl-5-benzyl-4-oxoimidazolidine-1,5-dicarboxylate (A4.11c). Sodium hydride (60% in mineral oil, 32 mg, 1.2 equiv) was added to a solution of dicarbonyl **A4.10** (250 mg, 1.0 equiv) in THF (6.7 mL, 0.1 M) at rt. After stirring for 30 min at rt, BnBr (169 μL, 2 equiv) was added. The reaction mixture was stirred for 5 h, turning cloudy in minutes. The reaction was quenched with aqueous $NaHCO_3$ (10 mL)

and extracted with EtOAc (3 x 5 mL). The combined organic phases were dried over anhydrous Na_2SO_4, decanted, and concentrated under reduced pressure. The crude product was purified by automated silica gel flash chromatography (Teledyne ISCO, 10 → 30% acetone/hexanes) to give benzyl allyl ester **A4.11c** as a clear oil; **^{1}H NMR (400 MHz, Chloroform-*d*)** δ 7.62 – 7.47 (m, 1H), 7.47 – 7.27 (m, 7H), 7.18 (ddd, *J* = 7.1, 5.3, 1.8 Hz, 2H), 5.92 (dddt, *J* = 17.2, 10.4, 7.9, 5.8 Hz, 1H), 5.44 – 5.19 (m, 3H), 5.16 (d, *J* = 7.0 Hz, 1H), 4.79 (ddt, *J* = 13.1, 5.7, 1.4 Hz, 1H), 4.74 – 4.59 (m, 2H), 4.40 (d, *J* = 7.0 Hz, 1H), 3.82 (d, *J* = 13.9 Hz, 1H), 3.67 – 3.49 (m, 1H), 1.56 (d, *J* = 2.8 Hz, 10H). **^{13}C NMR (101 MHz, $CDCl_3$)** δ 168.3, 168.0, 166.7, 166.6, 166.26, 166.1, 152.1, 151.8, 134.8, 134.2, 132.8, 132.7, 131.3, 130.9, 130.3, 129.0, 128.8, 128.67, 128.0, 128.0, 127.9, 127.7, 119.7, 119.1, 82.9, 82.4, 72.9, 67.2, 61.3, 38.0, 37.2, 28.4, 28.4. **IR (Neat Film, NaCl)** 2977, 1770, 1712, 1602, 1449, 1393, 1294, 1230, 1147, 1074, 1009, 768, 701 cm^{-1}; **HRMS (MM: ESI-APCI):** *m/z* calc'd for $C_{26}H_{32}N_3O_6$ $[M+NH_4]^+$: 482.2286, found 482.2284.

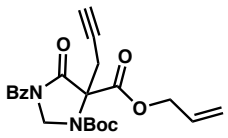

5-allyl 1-(tert-butyl) 3-benzoyl-4-oxo-5-(prop-2-yn-1-yl)imidazolidine-1,5-dicarboxylate (A4.11e). Sodium hydride (60% in mineral oil, 32 mg, 1.2 equiv) was added to a solution of dicarbonyl **A4.10** (250 mg, 1.0 equiv) in THF (6.7 mL, 0.1 M) at rt. After stirring for 15 min at rt, propargyl bromide (80% wt/wt in toluene, 252 μL, 4 equiv) was added. The reaction mixture was stirred for 1 h, turning light orange and cloudy in minutes. The reaction was quenched with aqueous $NaHCO_3$ (10 mL) and extracted with EtOAc (3 x 5 mL). The combined organic phases were dried over anhydrous Na_2SO_4,

decanted, and concentrated under reduced pressure. The crude product was purified by automated silica gel flash chromatography (Teledyne ISCO, 0 → 30% acetone/hexanes) to give propargyl allyl ester **A4.11e** as a clear oil; **^{1}H NMR (400 MHz, Chloroform-*d*)** δ 7.67 (dt, *J* = 8.5, 1.5 Hz, 2H), 7.61 – 7.51 (m, 1H), 7.51 – 7.34 (m, 2H), 5.86 (dtt, *J* = 17.3, 10.4, 5.8 Hz, 1H), 5.42 (dd, *J* = 18.4, 7.0 Hz, 1H), 5.37 – 5.18 (m, 3H), 4.82 – 4.48 (m, 2H), 3.46 (dd, *J* = 17.2, 2.7 Hz, 1H), 3.38 – 3.09 (m, 2H), 2.12 (dt, *J* = 5.4, 2.6 Hz, 1H), 1.49 (d, *J* = 20.7 Hz, 9H). **^{13}C NMR (101 MHz, $CDCl_3$) δ** 168.42, 168.17, 165.88, 165.83, 165.68, 165.59, 151.97, 151.53, 133.06, 132.52, 131.00, 130.69, 129.22, 128.13, 119.93, 119.35, 82.98, 82.76, 78.24, 77.57, 77.16, 72.37, 71.80, 71.13, 70.88, 67.36, 67.33, 62.01, 28.31, 28.20, 24.20, 23.29. **IR (Neat Film, NaCl)** 3280, 2977, 1771, 1746, 1713, 1601, 1449, 1391, 1370, 1295, 1228, 1151, 1058, 1018, 858, 790, 769, 739, 701, 665 cm^{-1}; **HRMS (MM: ESI-APCI):** *m/z* calc'd for $C_{22}H_{28}N_3O_6$ $[M+NH_4]^+$: 430.1973, found 430.1969.

A4.5.2.2 General Procedure for Allylic Alkylation Optimization Screen

In a nitrogen-filled glovebox, an oven-dried 1 dram vial was charged with $Pd_2(pmdba)_3$ (4 mol %), ligand (10 mol %), solvent (1 mL), and a magnetic stir bar. The vial was stirred at ambient glovebox temperature (27 °C) for 30 min and then substrate (10 mg, 1.0 equiv) was added as a solution in solvent (total concentration 0.014 M). The vial was sealed with a teflon cap and heated to 40 or 60 °C. When complete consumption of the starting material was observed by thin layer chromatography, the reaction mixture was removed from the glovebox and concentrated under reduced pressure. The residue was purified by silica gel flash chromatography to afford the imidazolinone.

A4.5.2.3 General Procedure for Pd-Catalyzed Decarboxylative Allylic Alkylation Reactions

Please note The absolute configuration for all other products has been inferred by analogy.[28–33] For respective SFC conditions, please refer to the section **Determination of Enantiomeric Excess**.

In a nitrogen-filled glovebox, an oven-dried 1 dram vial or 20 mL scintillation vial was charged with $Pd_2(pmdba)_3$ or $Pd_2(dba)_3$ (4 mol %), (*S*)-$(CF_3)_3$-*t*Bu-PHOX (10 mol %), 2:1 hexanes/toluene, and a magnetic stir bar. The vial was stirred at ambient glovebox temperature (27 °C) for 30 min and then the substrate (10 mg, 1.0 equiv) was added as a solution in 2:1 hexanes/toluene (total concentration 0.014 M). The vial was sealed with a teflon cap and heated to 40 or 60 °C. When complete consumption of the starting material was observed by thin layer chromatography, the reaction mixture was removed from the glovebox and concentrated under reduced pressure. The residue was purified by silica gel flash chromatography to afford the desired imidazolinone.

A4.5.2.4 Experimental Procedures and Spectroscopic data for the Pd-Catalyzed Decarboxylative Asymmetric Allylic Alkylation of Imidazolinone Substrates

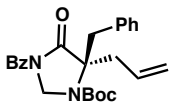

tert-butyl (*R*)-5-allyl-3-benzoyl-5-benzyl-4-oxoimidazolidine-1-carboxylate (A4.12c). IR (Neat Film, NaCl) 2927, 1757, 1707,1389, 1367, 1295, 1167, 701, 660 cm^{-1}; **HRMS (MM: ESI-APCI):** *m/z* calc'd for $C_{25}H_{29}N_2O_4$ $[M+H]^+$: 421.2122, found 421.2108.

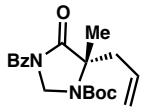

tert-butyl (*S*)-5-allyl-3-benzoyl-5-methyl-4-oxoimidazolidine-1-carboxylate (A4.12b). Following the general procedure, allyl ester **A4.11b** (46 mg, 1.0 equiv) in 2:1 Hex/Tol (7.5 mL) was added to a solution of $Pd_2(pmdba)_3$ (5.2 mg, 4 mol %) and (*S*)-$(CF_3)_3$-*t*Bu-PHOX (7 mg, 10 mol %) in 2:1 Hex/Tol (1.0 mL). Reaction performed at 60 °C. Purification by automated silica gel flash chromatography (Teledyne ISCO, 0 → 20% acetone/hexanes) gave methyl imidazolinone **A4.12b** as a clear oil (94% ee); **^{1}H NMR (400 MHz, Chloroform-*d*)** δ 7.68 – 7.50 (m, 3H), 7.43 (t, *J* = 7.6 Hz, 2H), 5.70 (ddt, *J* = 17.3, 9.9, 7.5 Hz, 1H), 5.31 – 5.13 (m, 3H), 5.07 (dd, *J* = 13.8, 7.7 Hz, 1H), 3.16 (dd, *J* = 13.7, 7.8 Hz, 1H), 2.48 (ddd, *J* = 20.5, 13.6, 7.4 Hz, 1H), 1.76 – 1.40 (m, 13H); **^{13}C NMR (101 MHz, $CDCl_3$)** δ 172.6, 168.7, 168.5, 152.7, 151.7, 133.2, 132.7, 132.1, 131.8, 129.0, 128.0, 120.4, 81.8, 81.3, 77.4, 66.1, 65.7, 60.8, 60.7, 41.3, 40.0, 28.5, 28.5, 23.6, 22.6; **IR (Neat Film, NaCl)** 3076, 2977, 2931, 1759, 1702, 1602,1477, 1449, 1388,1368, 1296, 1262,1227, 1168,1124, 1059, 997, 964, 928, 906, 879, 859, 823.08 95.51 792, 773, 732, 703, 661, 614 cm^{-1}; **HRMS (MM: ESI-APCI):** *m/z* calc'd for $C_{19}H_{25}N_2O_3$ $[M+H]^+$: 345.1809, found 345.1805.

A4.6 REFERENCES AND NOTES

(1) Ohfune, Y.; Shinada, T. Enantio- and Diastereoselective Construction of α,α-Disubstituted α-Amino Acids for the Synthesis of Biologically Active Compounds. *Eur. J. Org. Chem.* **2005**, *2005* (24), 5127–5143.

(2) Toniolo, C.; Crisma, M.; Formaggio, F.; Peggion, C. Control of Peptide Conformation by the Thorpe-Ingold Effect (Cα-Tetrasubstitution). *Peptide Science* **2001**, *60* (6), 396–419. (2001)60:6<396::AID-BIP10184>3.0.CO;2-7.

(3) Dehner, A.; Planker, E.; Gemmecker, G.; Broxterman, Q. B.; Bisson, W.; Formaggio, F.; Crisma, M.; Toniolo, C.; Kessler, H. Solution Structure, Dimerization, and Dynamics of a Lipophilic α/310-Helical, Cα-Methylated Peptide. Implications for Folding of Membrane Proteins. *J. Am. Chem. Soc.* **2001**, *123* (27), 6678–6686.

(4) Evans, M. C.; Pradhan, A.; Venkatraman, S.; Ojala, W. H.; Gleason, W. B.; Mishra, R. K.; Johnson, R. L. Synthesis and Dopamine Receptor Modulating Activity of Novel Peptidomimetics of L-Prolyl-l-Leucyl-Glycinamide Featuring α,α-Disubstituted Amino Acids. *J. Med. Chem.* **1999**, *42* (8), 1441–1447.

(5) Etienne, M. A.; Aucoin, J. P.; Fu, Y.; McCarley, R. L.; Hammer, R. P. Stoichiometric Inhibition of Amyloid β-Protein Aggregation with Peptides Containing Alternating α,α-Disubstituted Amino Acids. *J. Am. Chem. Soc.* **2006**, *128* (11), 3522–3523.

(6) Castro, V. I. B.; Carvalho, C. M.; Fernandes, R. D. V.; Pereira-Lima, S. M. M. A.; Castanheira, E. M. S.; Costa, S. P. G. Peptaibolin Analogues by Incorporation of

α,α-Dialkylglycines: Synthesis and Study of Their Membrane Permeating Ability. *Tetrahedron* **2016**, *72* (7), 1024–1030.

(7) Cativiela, C.; Díaz-de-Villegas, M. D. Recent Progress on the Stereoselective Synthesis of Acyclic Quaternary α-Amino Acids. *Tetrahedron: Asymmetry* **2007**, *18* (5), 569–623.

(8) Bera, K.; Namboothiri, I. N. N. Asymmetric Synthesis of Quaternary α-Amino Acids and Their Phosphonate Analogues. *Asian J. Org. Chem.* **2014**, *3* (12), 1234–1260.

(9) Vogt, H.; Bräse, S. Recent Approaches towards the Asymmetric Synthesis of α,α-Disubstituted α-Amino Acids. *Org. Biomol. Chem.* **2007**, *5* (3), 406–430.

(10) Fitzi, R.; Seebach, D. Resolution and Use in α-Amino Acid Synthesis of Imidazolidinone Glycine Derivatives. *Tetrahedron* **1988**, *44* (17), 5277–5292.

(11) Seebach, D.; Hoffmann, M. Preparation and Use in Amino Acid Synthesis of a New Chiral Glycine Derivative – (R)- and (S)-Tert-Butyl 2-Tert-Butyl-4-Methoxy-2,5-Dihydroimidazole-1-Carboxylate (BDI). *Eur. J. Org. Chem.* **1998**, *1998* (7), 1337–1351.

(12) Leonard, D. J.; Ward, J. W.; Clayden, J. Asymmetric α-Arylation of Amino Acids. *Nature* **2018**, *562* (7725), 105–109.

(13) Meyer, L.; Poirier, J.-M.; Duhamel, P.; Duhamel, L. Chiral Auxiliaries with a Switching Center: New Tools in Asymmetric Synthesis. Application to the Synthesis of Enantiomerically Pure (R)- and (S)-α-Amino Acids. *J. Org. Chem.* **1998**, *63* (23), 8094–8095.

(14) Masumoto, S.; Usuda, H.; Suzuki, M.; Kanai, M.; Shibasaki, M. Catalytic Enantioselective Strecker Reaction of Ketoimines. *J. Am. Chem. Soc.* **2003**, *125* (19), 5634–5635.

(15) Ooi, T.; Takeuchi, M.; Kameda, M.; Maruoka, K. Practical Catalytic Enantioselective Synthesis of α,α-Dialkyl-α-Amino Acids by Chiral Phase-Transfer Catalysis. *J. Am. Chem. Soc.* **2000**, *122* (21), 5228–5229.

(16) Maruoka, K.; Ooi, T. Enantioselective Amino Acid Synthesis by Chiral Phase-Transfer Catalysis. *Chemical Reviews* **2003**, *103* (8), 3013–3028.

(17) de Castro, P. P.; Carpanez, A. G.; Amarante, G. W. Azlactone Reaction Developments. *Chem. Eur. J.* **2016**, *22* (30), 10294–10318.

(18) Serra, M.; Bernardi, E.; Marrubini, G.; Lorenzi, E. D.; Colombo, L. Palladium-Catalyzed Asymmetric Decarboxylative Allylation of Azlactone Enol Carbonates: Fast Access to Enantioenriched α-Allyl Quaternary Amino Acids. *Eur. J. Org. Chem.* **2019**, *2019* (4), 732–741.

(19) Trost, B. M.; Ariza, X. Catalytic Asymmetric Alkylation of Nucleophiles: Asymmetric Synthesis of α-Alkylated Amino Acids. *Angew. Chem. Int. Ed.* **1997**, *36* (23), 2635–2637.

(20) Trost, B. M.; Ariza, X. Enantioselective Allylations of Azlactones with Unsymmetrical Acyclic Allyl Esters. *J. Am. Chem. Soc.* **1999**, *121* (46), 10727–10737.

(21) Trost, B. M.; Dogra, K. Synthesis of Novel Quaternary Amino Acids Using Molybdenum-Catalyzed Asymmetric Allylic Alkylation. *J. Am. Chem. Soc.* **2002**, *124* (25), 7256–7257.

(22) Chen, L.; Luo, M.-J.; Zhu, F.; Wen, W.; Guo, Q.-X. Combining Chiral Aldehyde Catalysis and Transition-Metal Catalysis for Enantioselective α-Allylic Alkylation of Amino Acid Esters. *J. Am. Chem. Soc.* **2019**.

(23) Huo, X.; Zhang, J.; Fu, J.; He, R.; Zhang, W. Ir/Cu Dual Catalysis: Enantio- and Diastereodivergent Access to α,α-Disubstituted α-Amino Acids Bearing Vicinal Stereocenters. *J. Am. Chem. Soc.* **2018**, *140* (6), 2080–2084.

(24) Huo, X.; He, R.; Fu, J.; Zhang, J.; Yang, G.; Zhang, W. Stereoselective and Site-Specific Allylic Alkylation of Amino Acids and Small Peptides via a Pd/Cu Dual Catalysis. *J. Am. Chem. Soc.* **2017**, *139* (29), 9819–9822. https://doi.org/10.1021/jacs.7b05460.

(25) Kanayama, T.; Yoshida, K.; Miyabe, H.; Kimachi, T.; Takemoto, Y. Synthesis of β-Substituted α-Amino Acids with Use of Iridium-Catalyzed Asymmetric Allylic Substitution. *J. Org. Chem.* **2003**, *68* (16), 6197–6201.

(26) Behenna, D. C.; Mohr, J. T.; Sherden, N. H.; Marinescu, S. C.; Harned, A. M.; Tani, K.; Seto, M.; Ma, S.; Novák, Z.; Krout, M. R.; et al. Enantioselective Decarboxylative Alkylation Reactions: Catalyst Development, Substrate Scope, and Mechanistic Studies. *Chem. Eur. J.* **2011**, *17* (50), 14199–14223.

(27) Pfeiffer, U.; Riccaboni, M. T.; Erba, R.; Pinza, M. A Short Synthesis of 4-imidazolidinone. *Liebigs Annalen der Chemie* **1988**, *1988* (10), 993–995.

(28) Behenna, D. C.; Stoltz, B. M. The Enantioselective Tsuji Allylation. *J. Am. Chem. Soc.* **2004**, *126*, 15044–15045.

(29) Mohr, J. T.; Behenna, D. C.; Harned, A. M.; Stoltz, B. M. Deracemization of Quaternary Stereocenters by Pd-Catalyzed Enantioconvergent Decarboxylative Allylation of Racemic β-Ketoesters. *Angew. Chem. Int. Ed.* **2005**, *44*, 6924–6927.

(30) Reeves, C. M.; Eidamshaus, C.; Kim, J.; Stoltz, B. M. Enantioselective Construction of α-Quaternary Cyclobutanones by Catalytic Asymmetric Allylic Alkylation. *Angew. Chem. Int. Ed.* **2013**, *52*, 6718–6721.

(31) Behenna, D. C.; Liu, Y.; Yurino, T.; Kim, J.; White, D. E.; Virgil, S. C.; Stoltz, B. M. Enantioselective Construction of Quaternary *N*-Heterocycles by Palladium-Catalysed Decarboxylative Allylic Alkylation of Lactams. *Nat. Chem.* **2012**, *4*, 130–133.

(32) Seto, M.; Roizen, J. L.; Stoltz, B. M. Catalytic Enantioselective Alkylation of Substituted Dioxanone Enol Ethers: Ready Access to C(α)-Tetrasubstituted Hydroxyketones, Acids, and Esters. *Angew. Chem.* **2008**, *120* (36), 6979–6982.

(33) McDougal, N. T.; Streuff, J.; Mukherjee, H.; Virgil, S. C.; Stoltz, B. M. Rapid Synthesis of an Electron-Deficient t-BuPHOX Ligand: Cross-Coupling of Aryl Bromides with Secondary Phosphine Oxides. *Tetrahedron Lett.* **2010**, *51*, 5550–5554.

APPENDIX 5

Spectra Relevant to Appendix 4:

Stereoselective Synthesis of α,α-Disubstituted Amino Acids via

Decarboxylative Alkylation of Imidazolinones

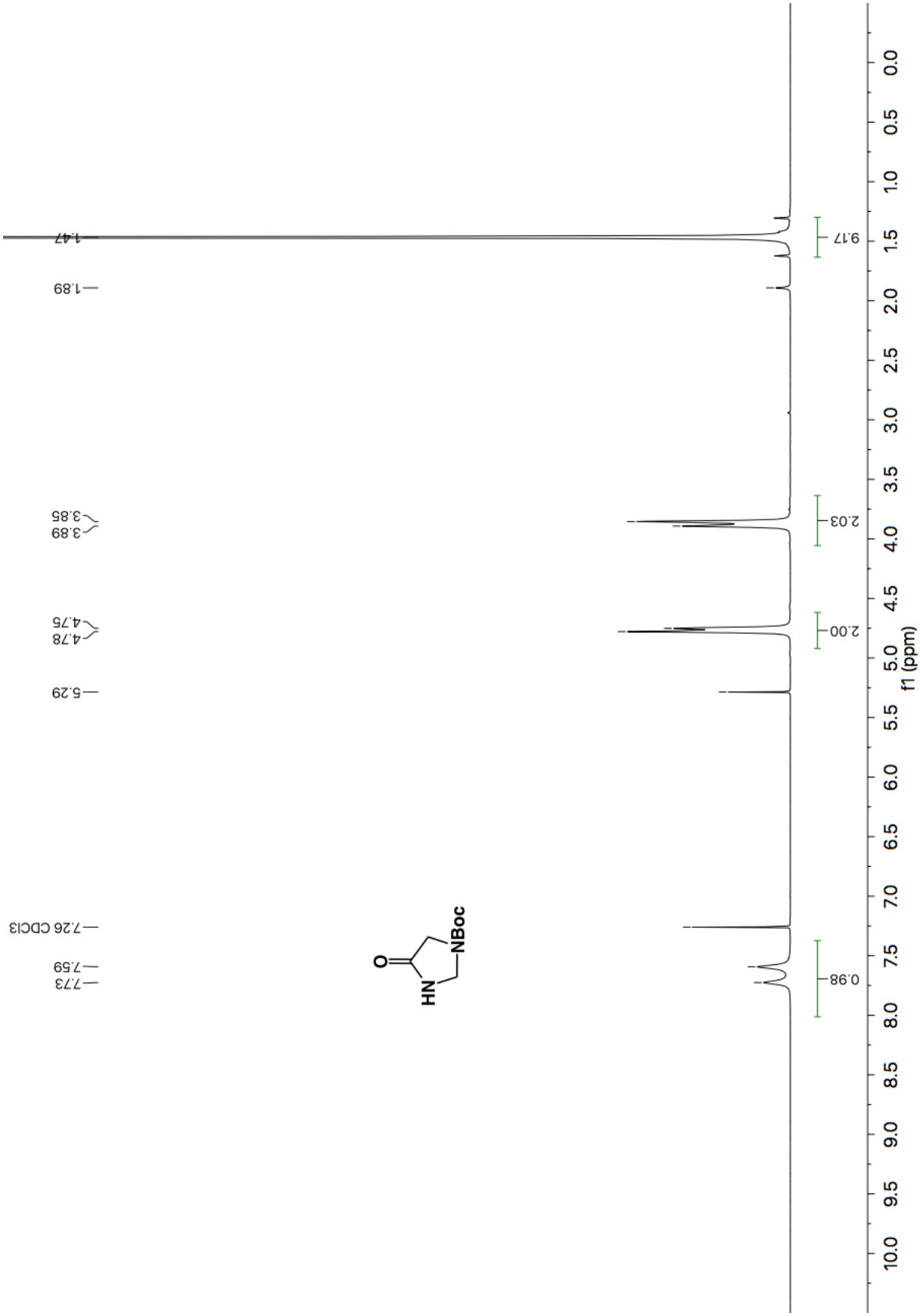

Figure A5.1 ^{1}H NMR (600 MHz, $CDCl_3$) of compound **A4.8**

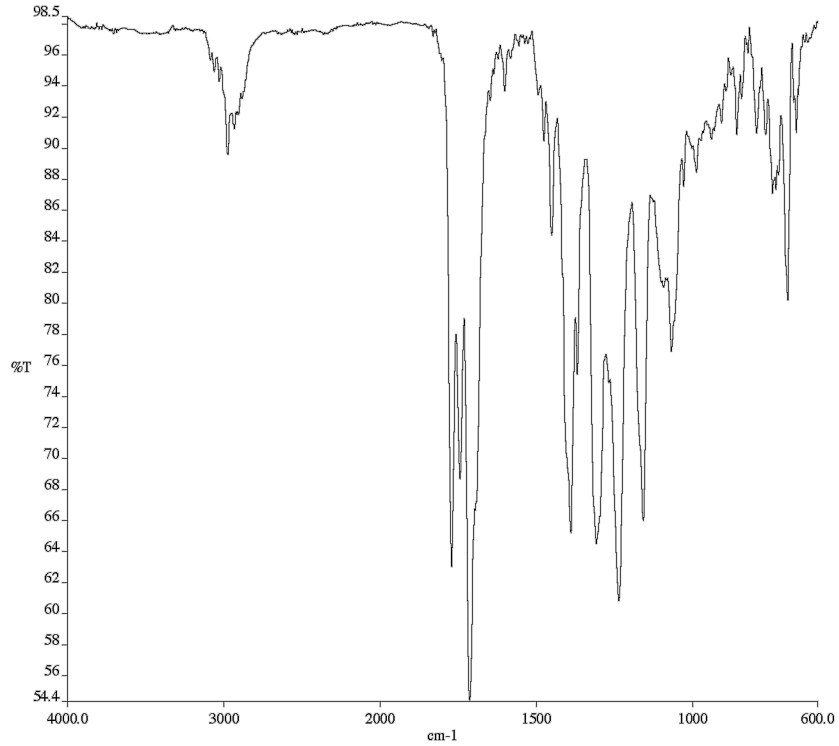

Figure A5.2 Infrared spectrum (Thin Film, NaCl) of compound **A4.8**

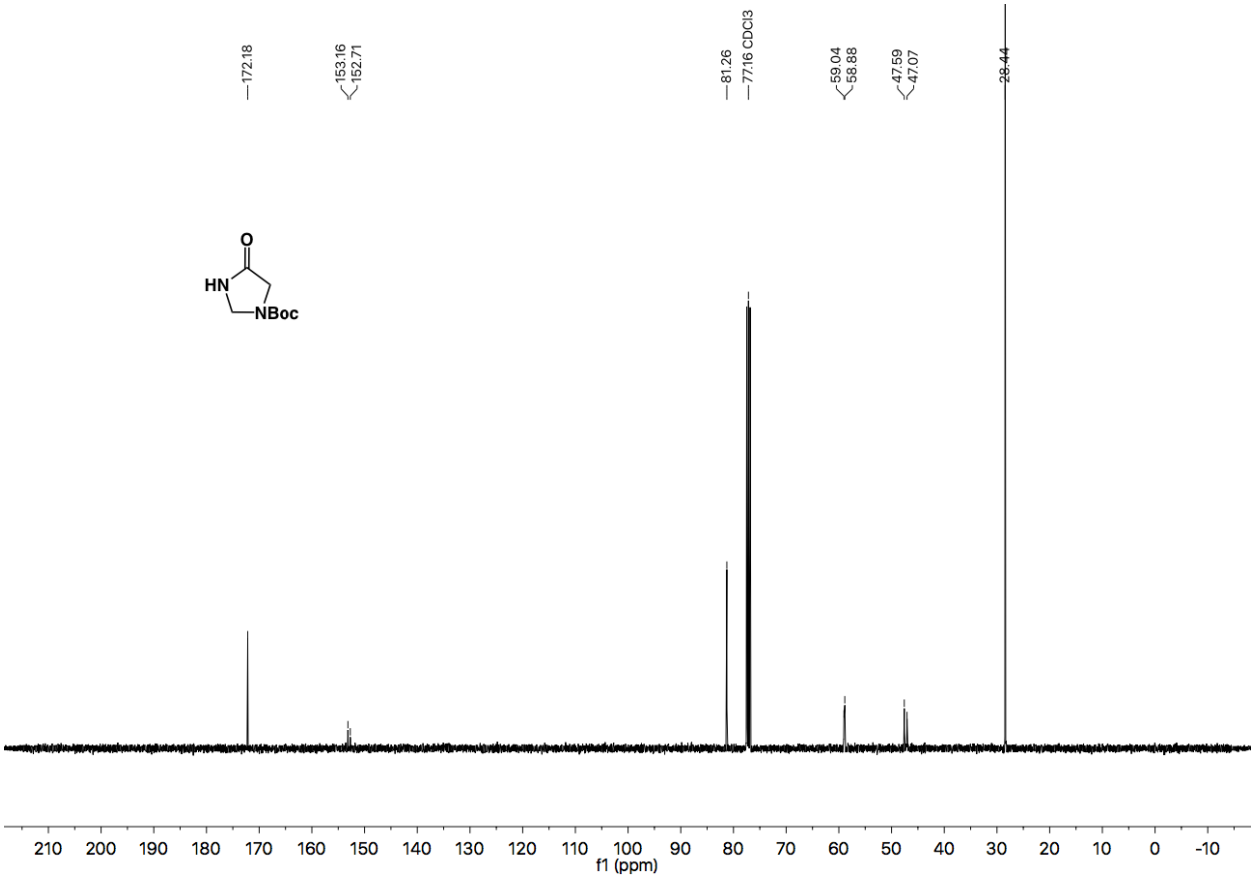

Figure A5.3 ^{13}C NMR (101 MHz, $CDCl_3$) of compound **A4.8**

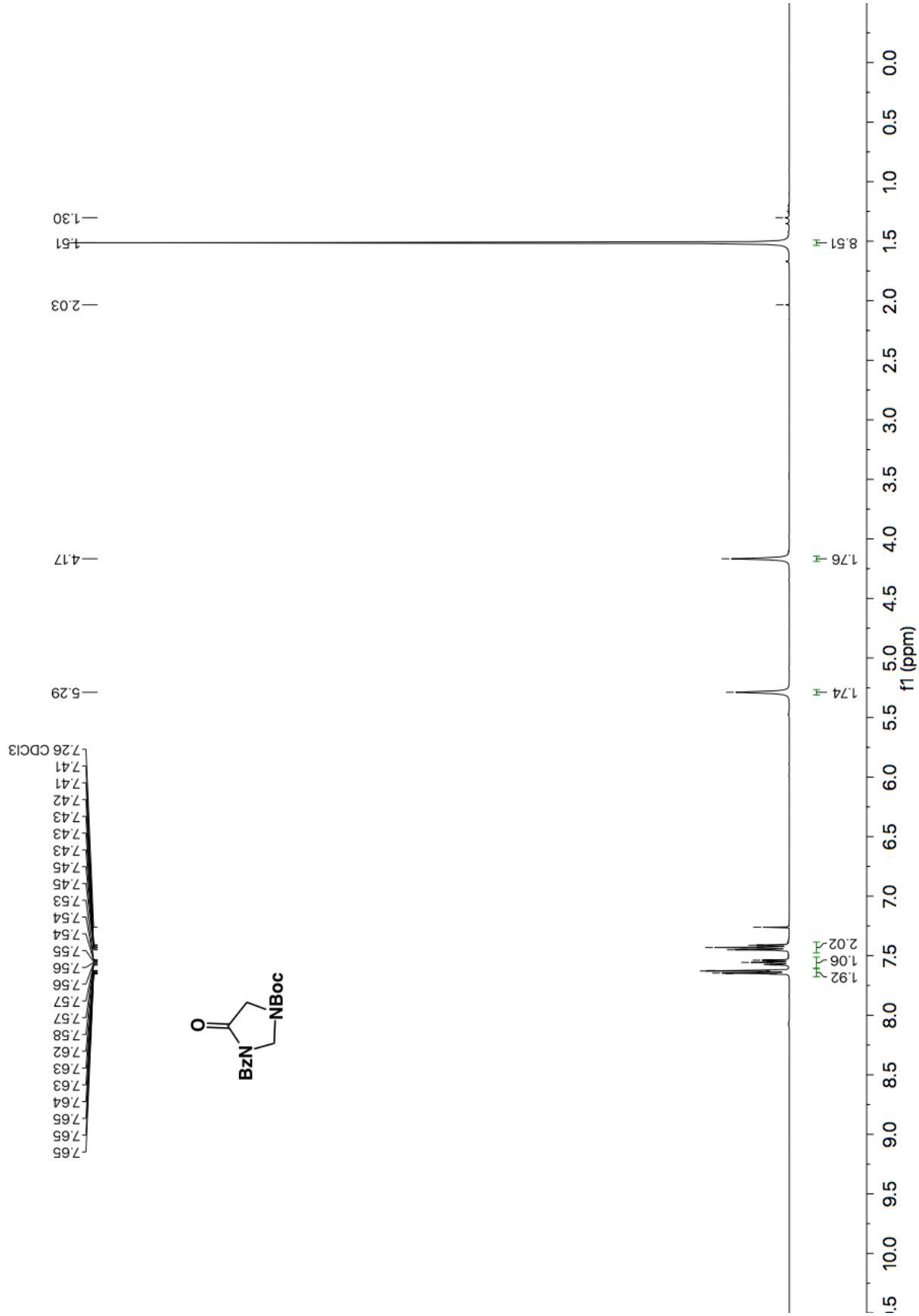

Figure A5.4 ^{1}H NMR (600 MHz, $CDCl_3$) of compound **A4.9.**

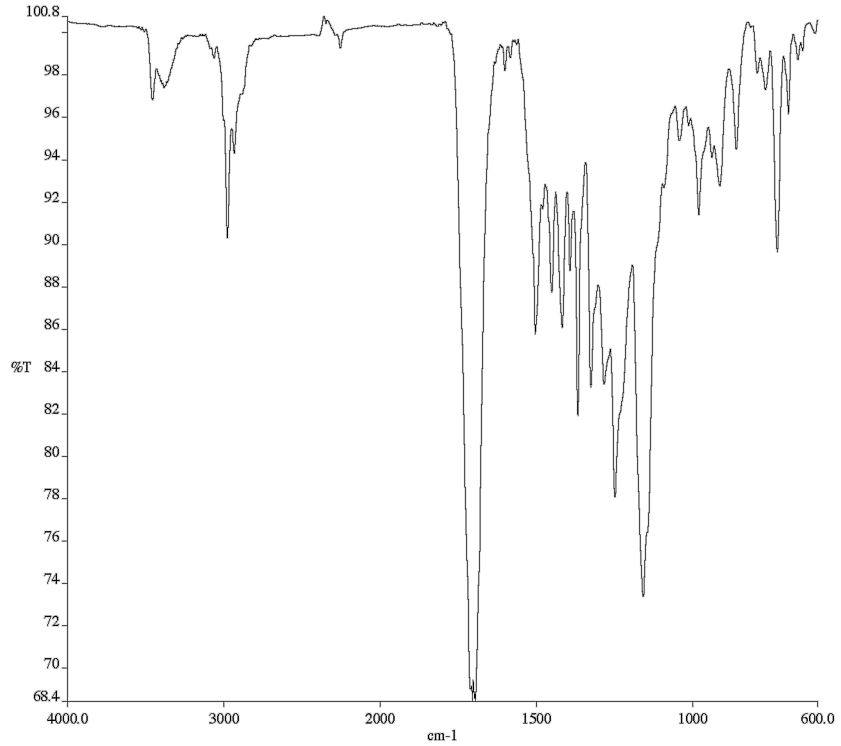

Figure A5.5 Infrared spectrum (Thin Film, NaCl) of compound **A4.9**.

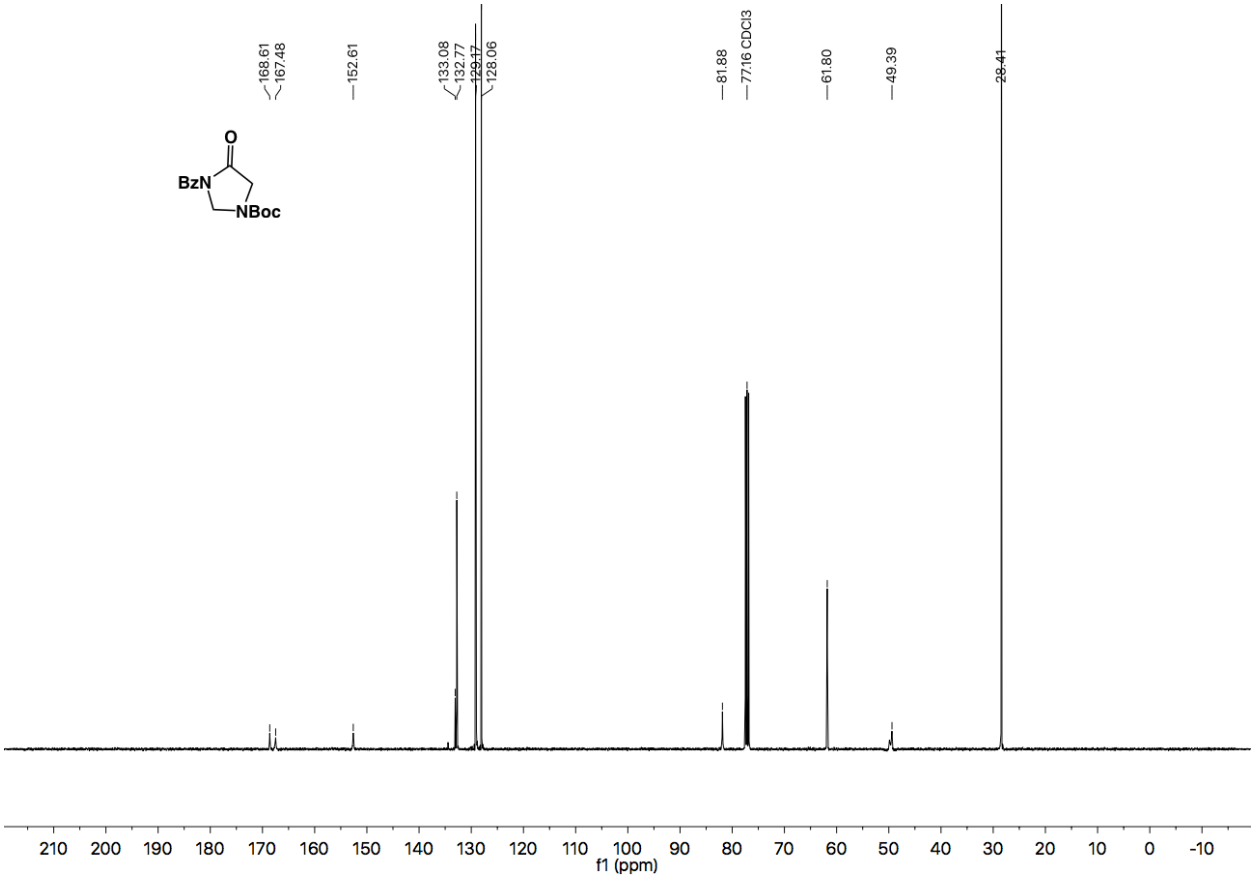

Figure A5.4 ^{13}C NMR (101 MHz, $CDCl_3$) of compound **A4.9**

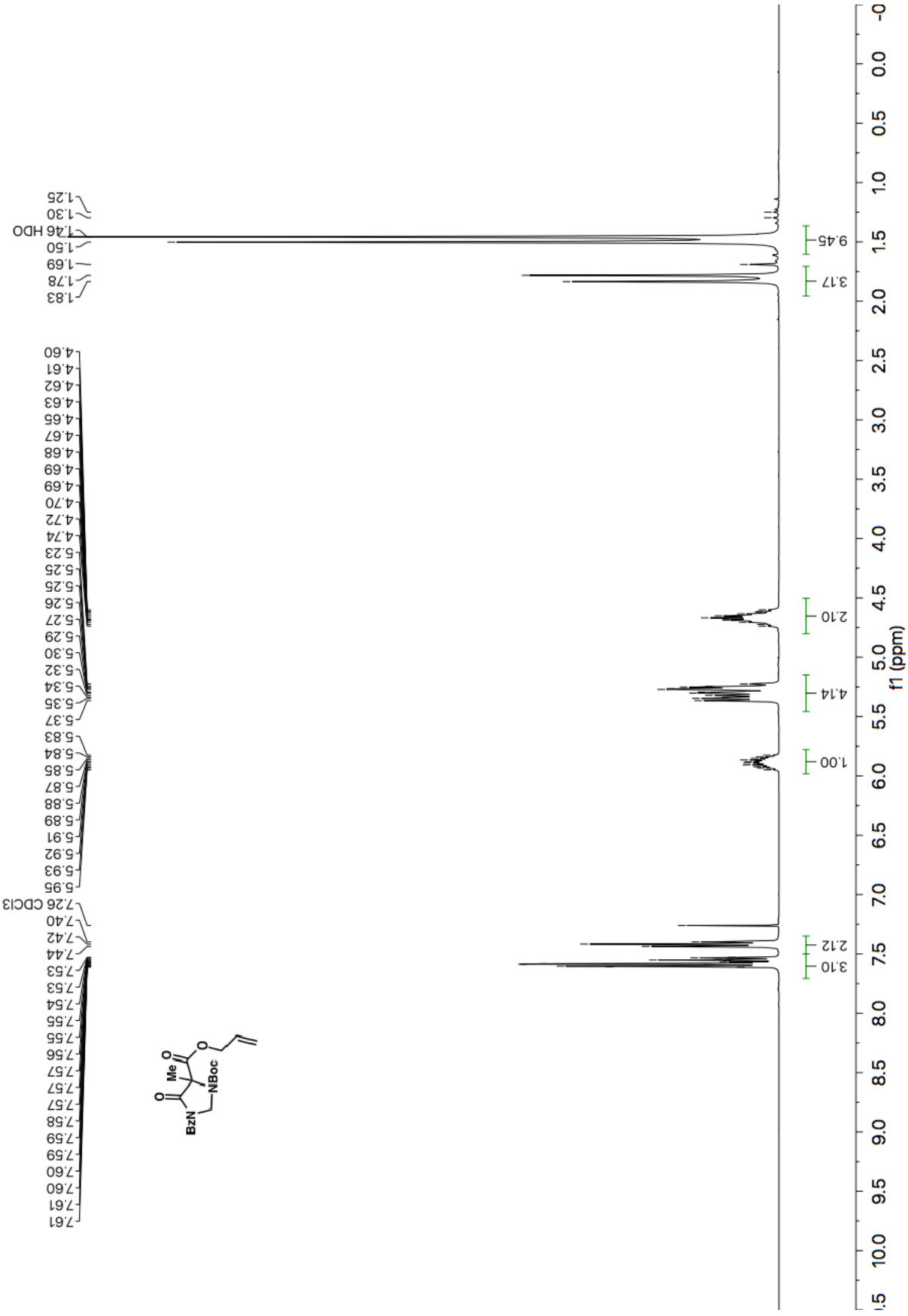

Figure A5.7 ^{1}H NMR (600 MHz, $CDCl_3$) of compound **A4.11b**

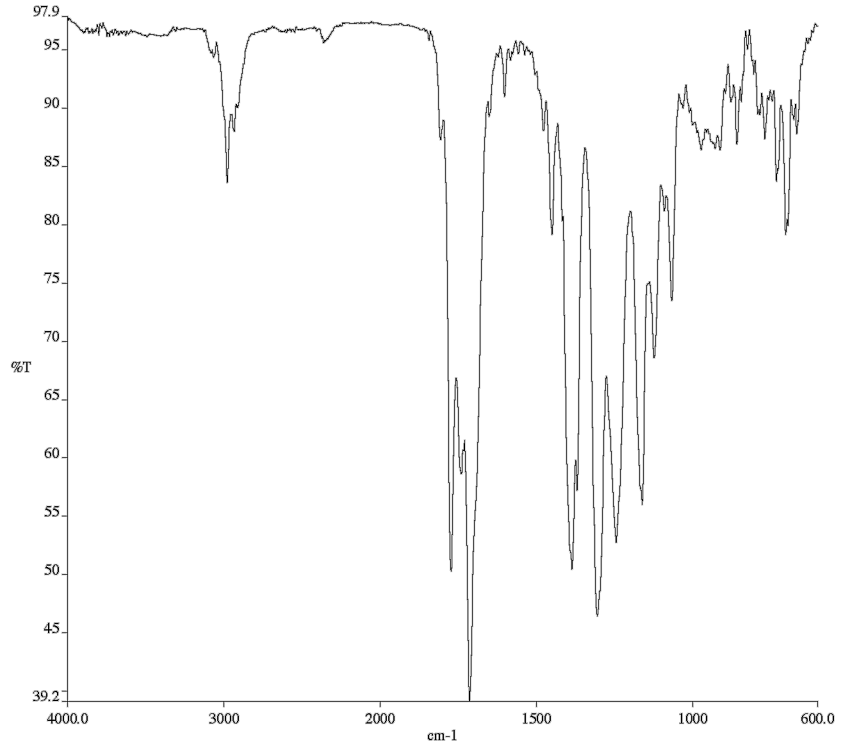

Figure A5.8 Infrared spectrum (Thin Film, NaCl) of compound **A4.11b**

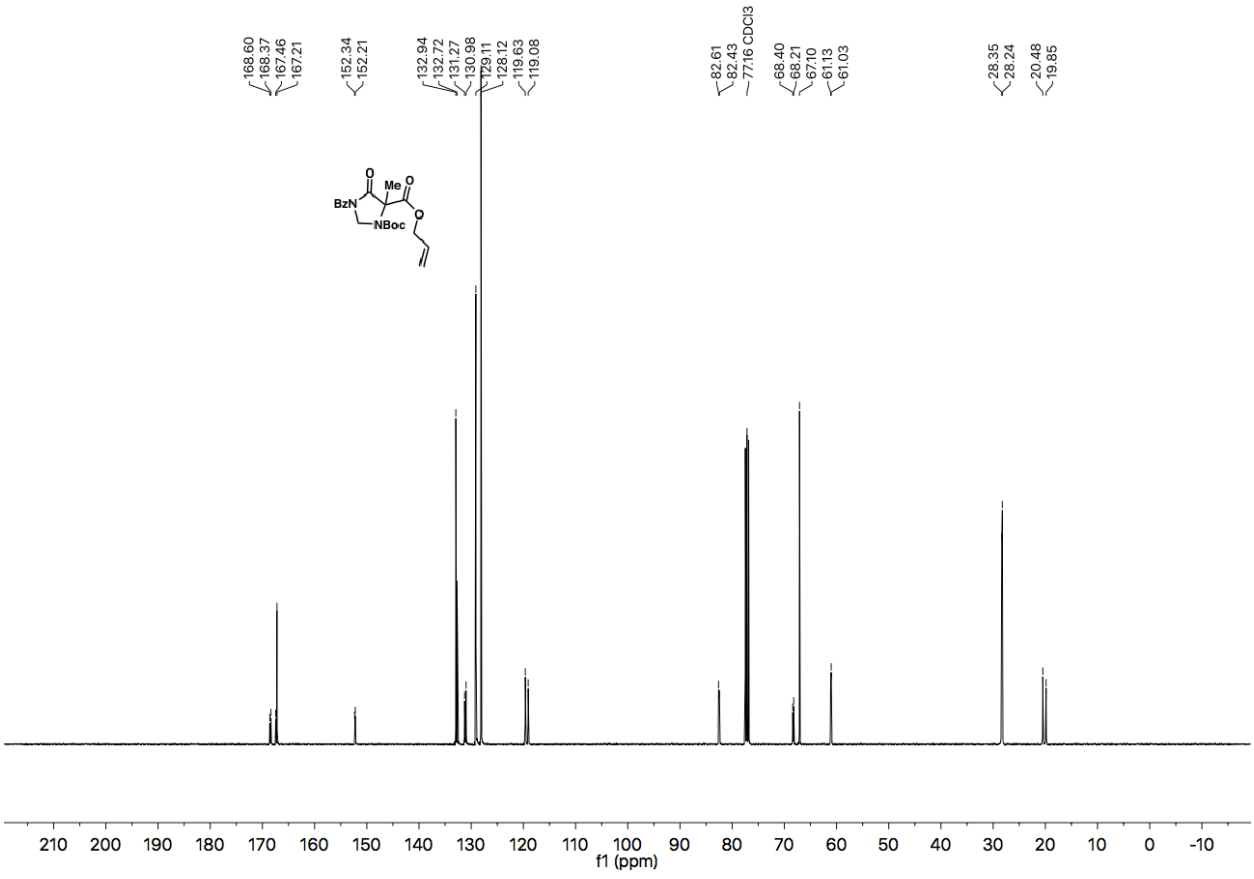

Figure A5.9 ^{13}C NMR (101 MHz, $CDCl_3$) of compound **A4.11b**

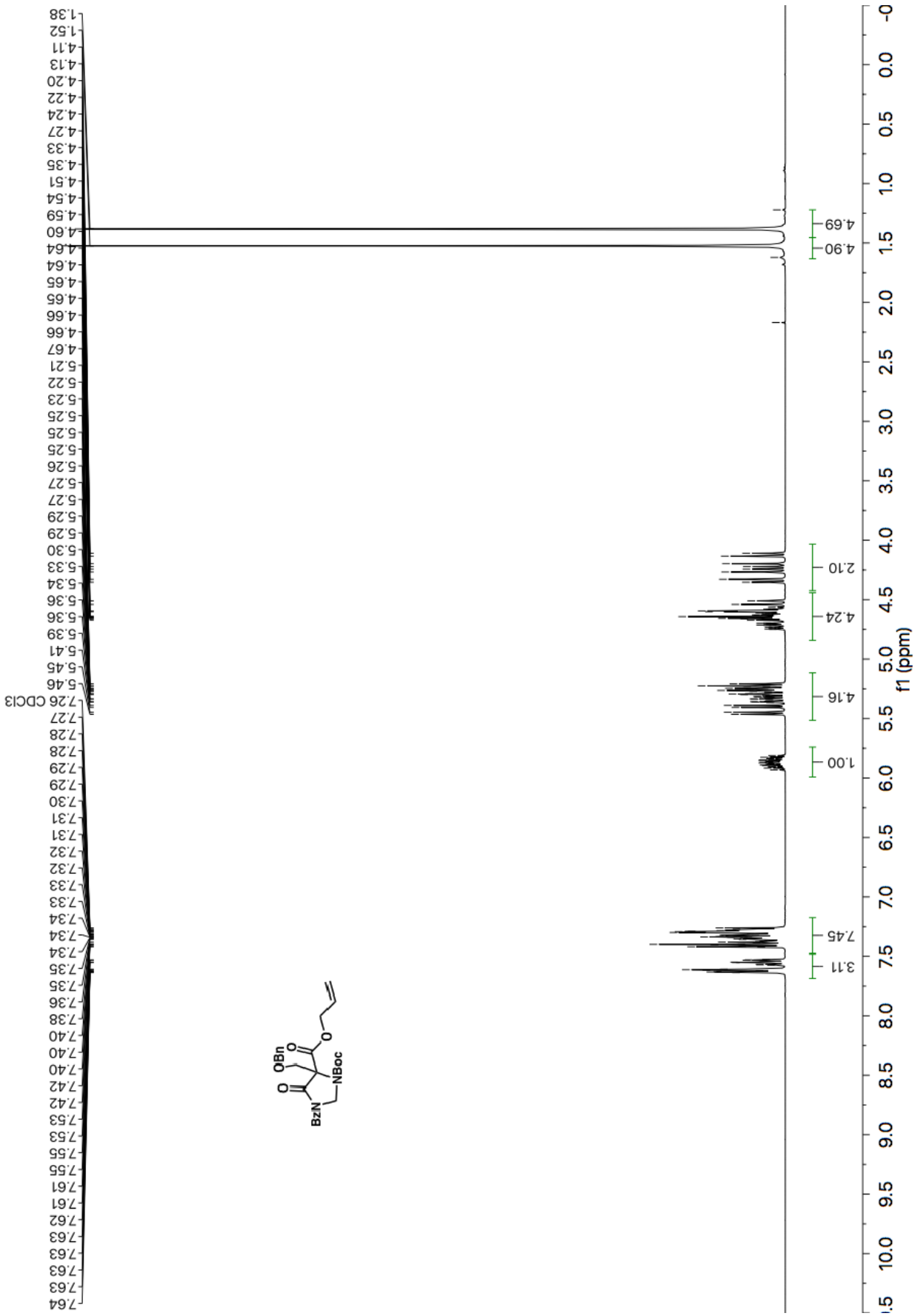

Figure A5.10 ^{1}H NMR (600 MHz, $CDCl_3$) of compound **A4.11d**

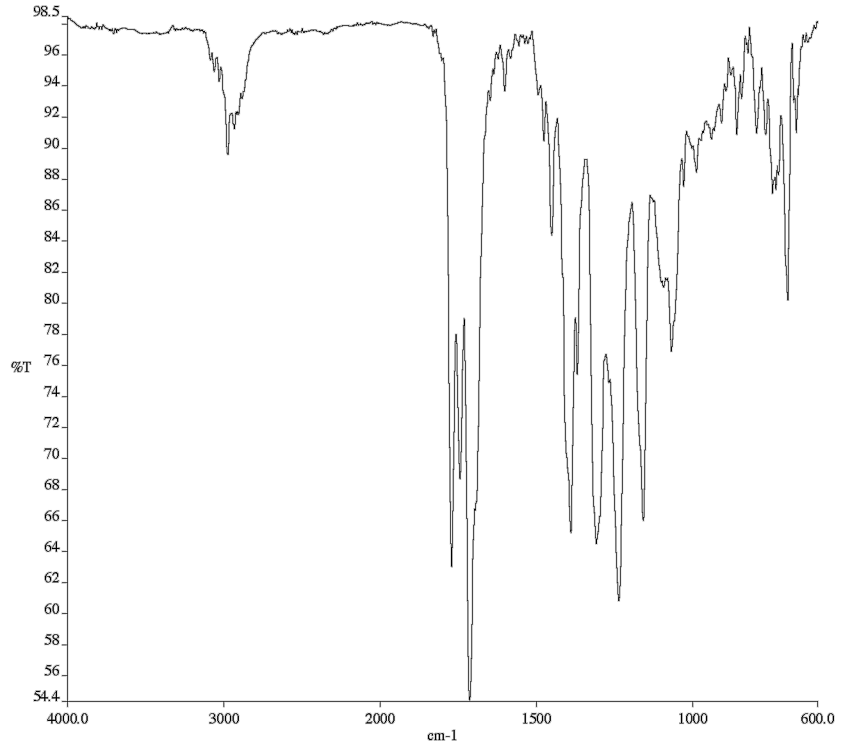

Figure A5.11 Infrared spectrum (Thin Film, NaCl) of compound **A4.11d**

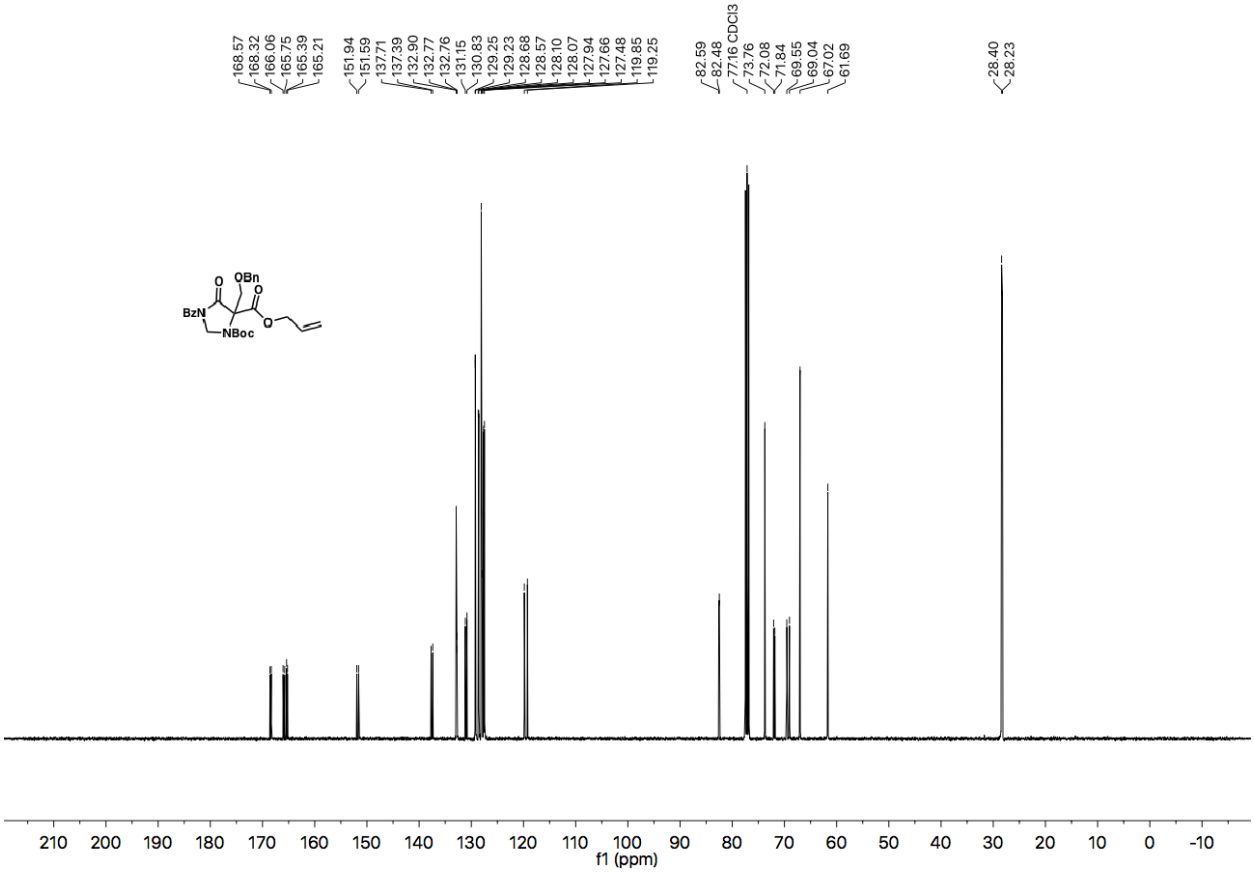

Figure A5.12 ^{13}C NMR (101 MHz, $CDCl_3$) of compound **A4.11d**

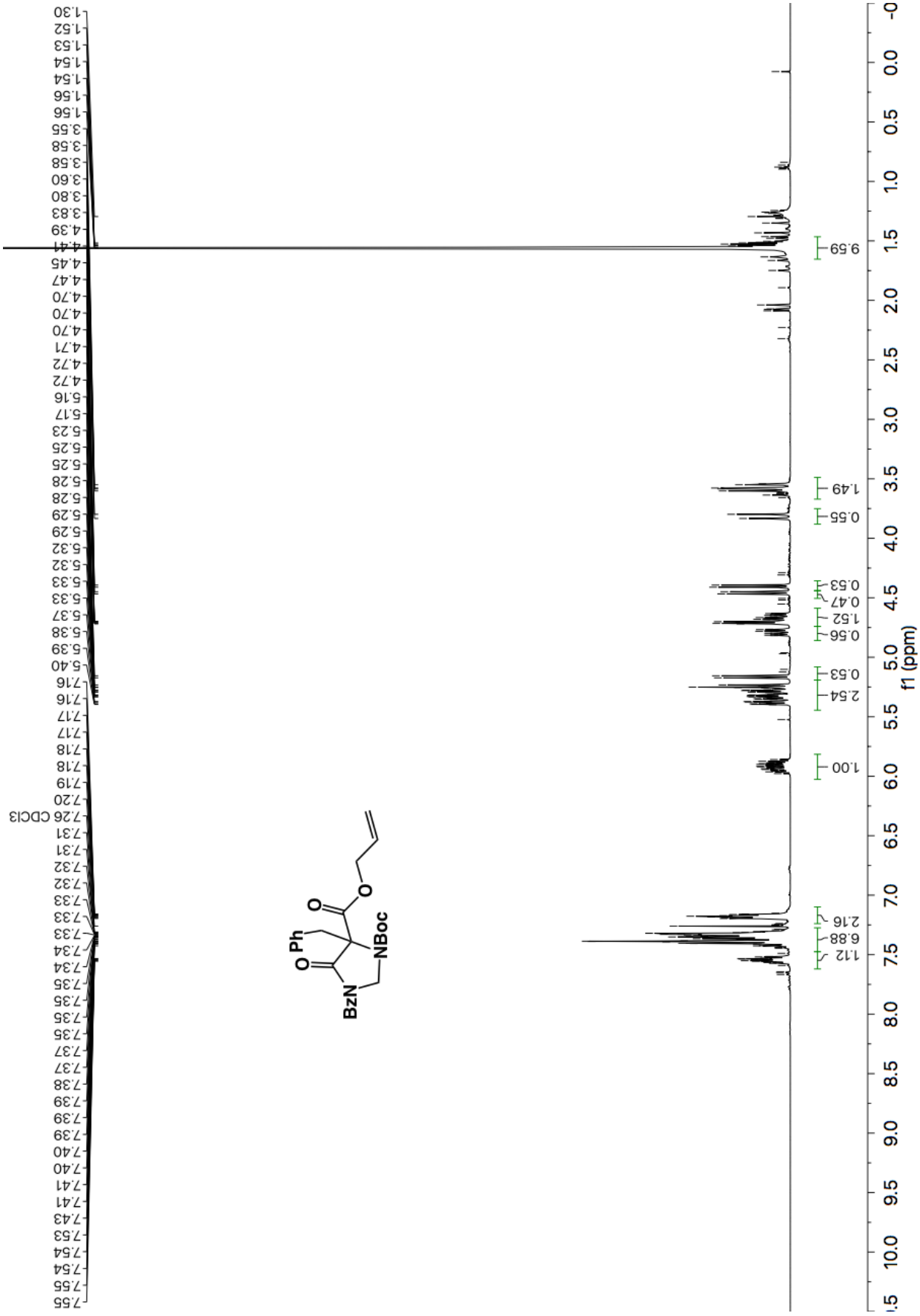

Figure A5.13 ^{1}H NMR (600 MHz, $CDCl_3$) of compound **A4.11c**

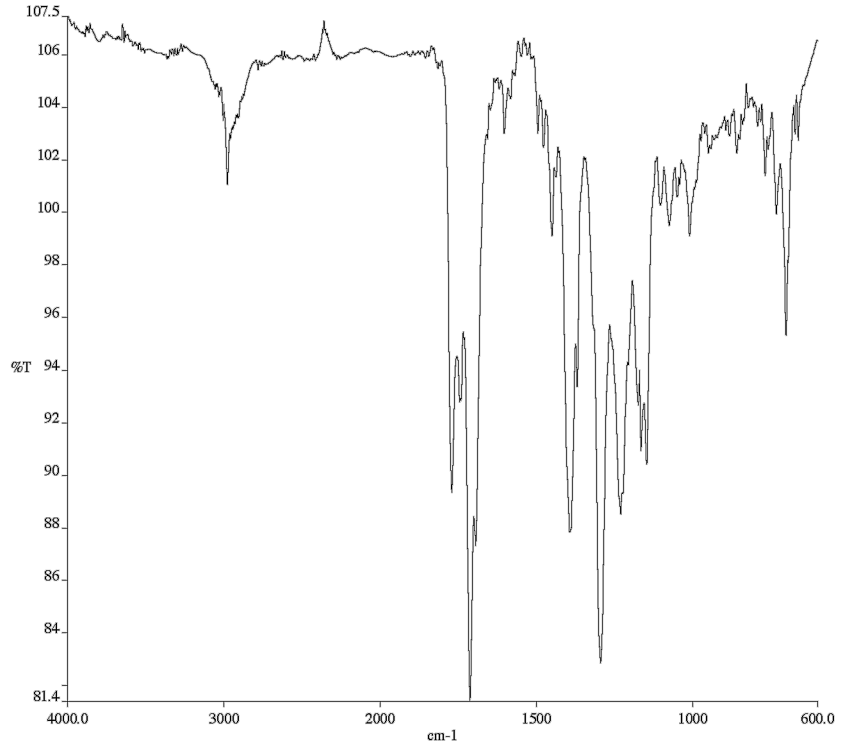

Figure A5.14 Infrared spectrum (Thin Film, NaCl) of compound **A4.11c**

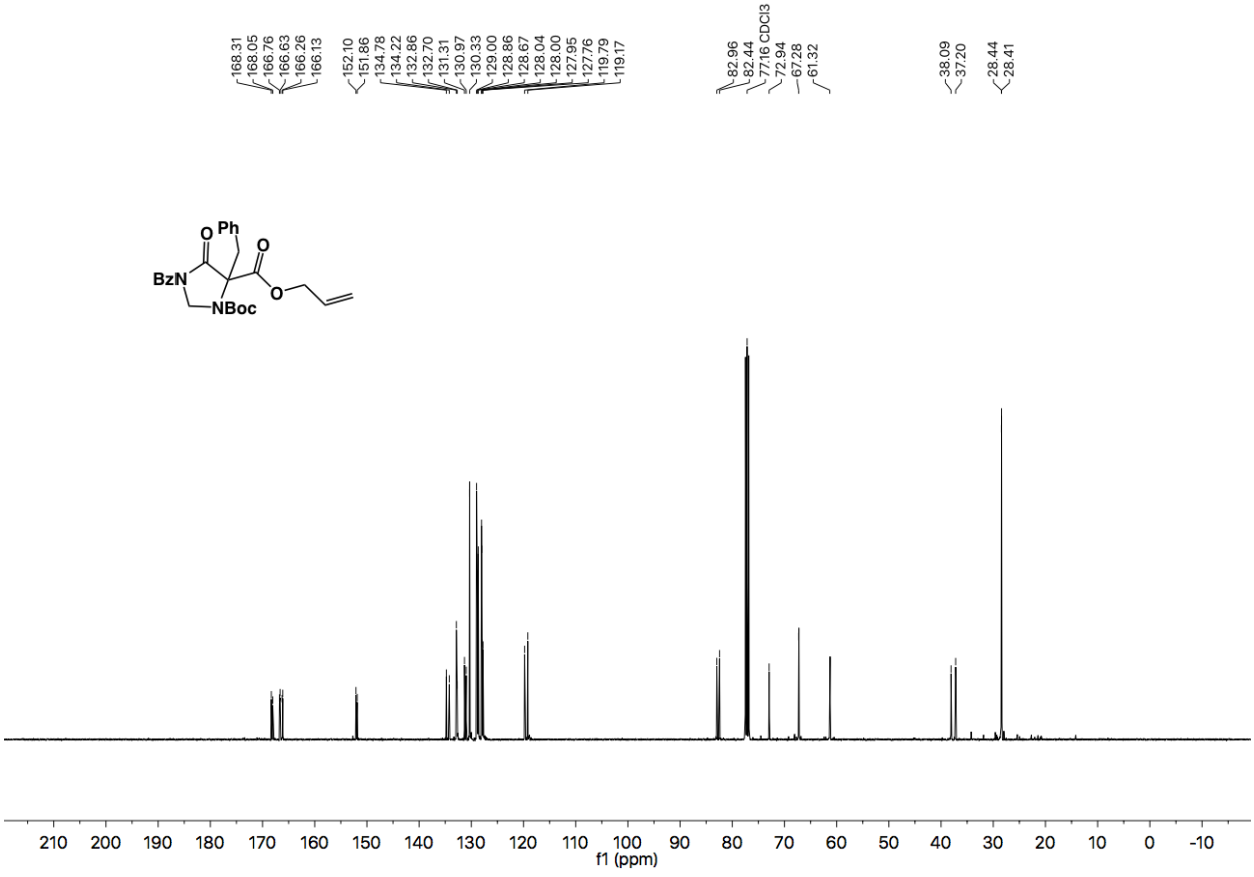

Figure A5.15 ^{13}C NMR (101 MHz, $CDCl_3$) of compound **A4.11c**

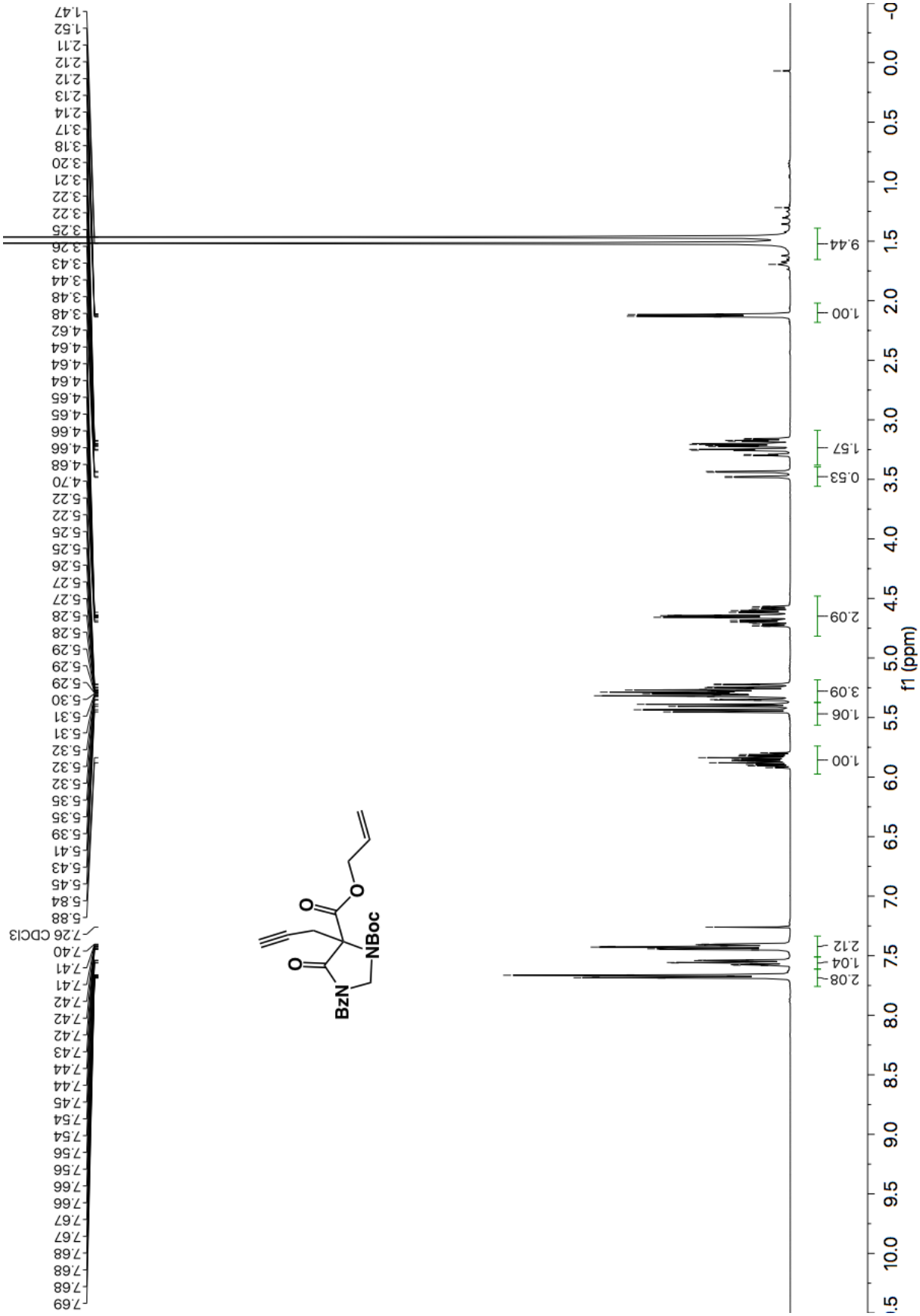

Figure A5.16 ^{1}H NMR (600 MHz, $CDCl_3$) of compound **A4.11e**

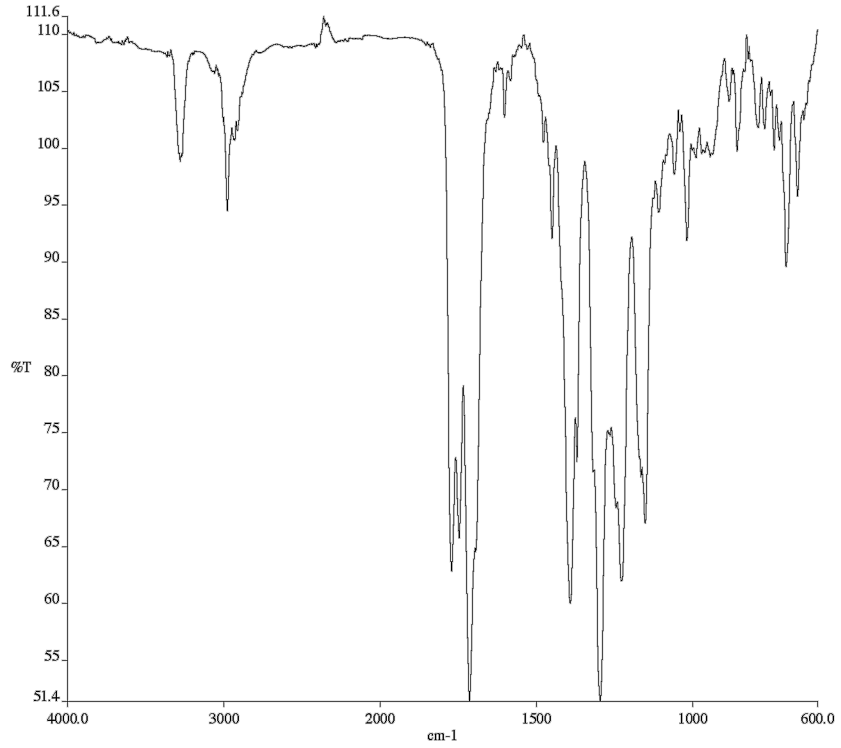

Figure A5.17 Infrared spectrum (Thin Film, NaCl) of compound **A4.11e**

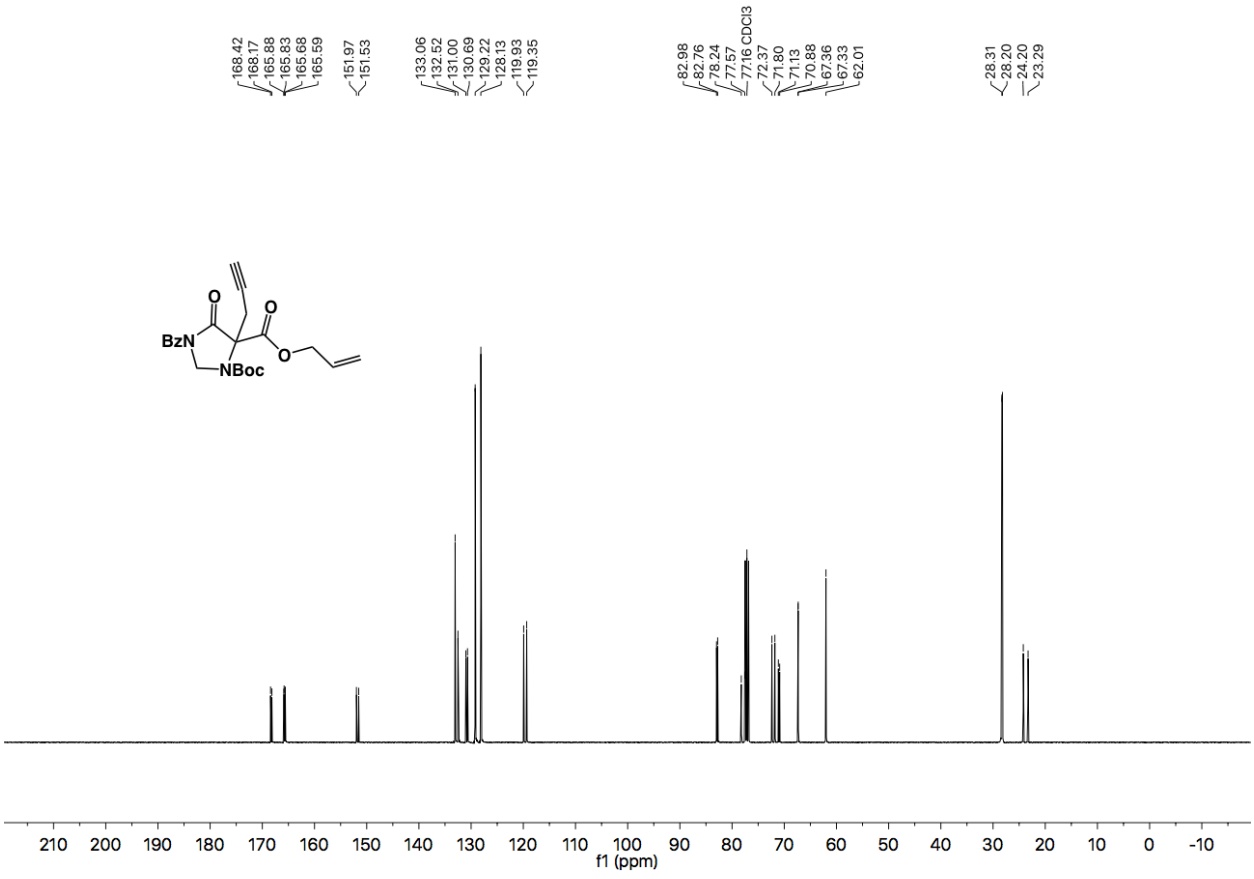

Figure A5.18 ^{13}C NMR (101 MHz, $CDCl_3$) of compound **A4.11e**

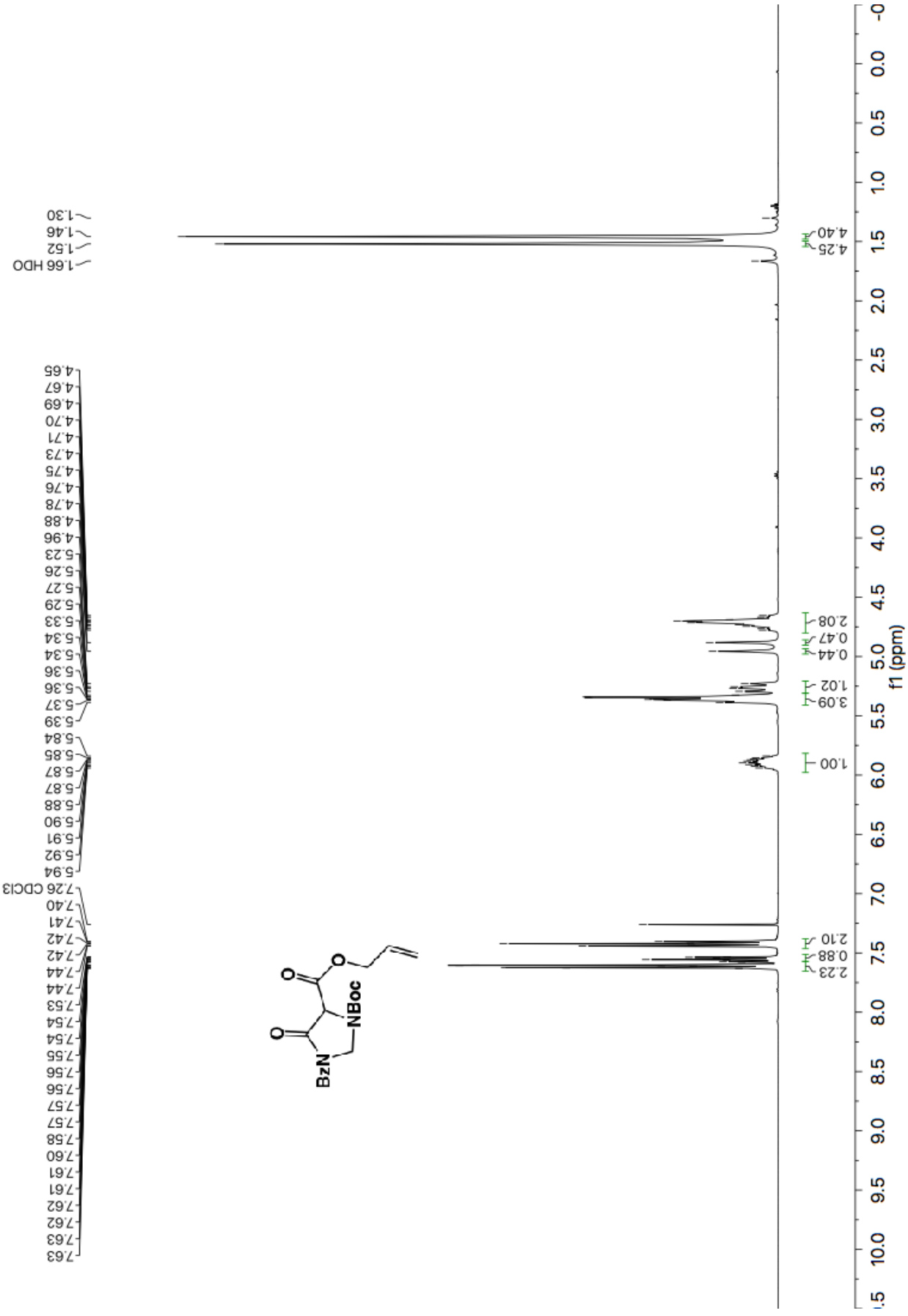

Figure A5.19 ^{1}H NMR (600 MHz, $CDCl_3$) of compound **A4.10**

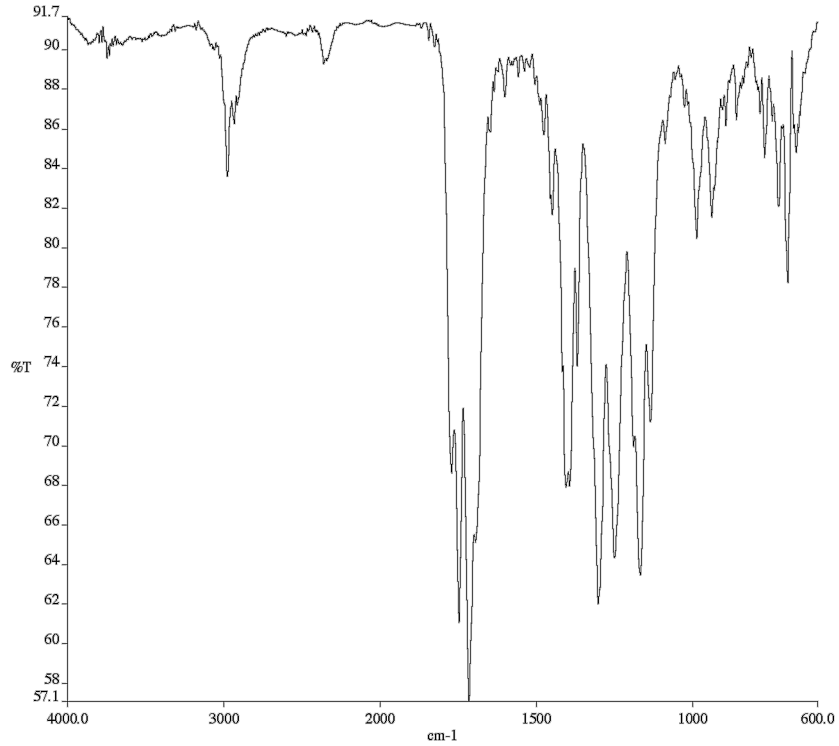

Figure A5.20 Infrared spectrum (Thin Film, NaCl) of compound **A4.10**

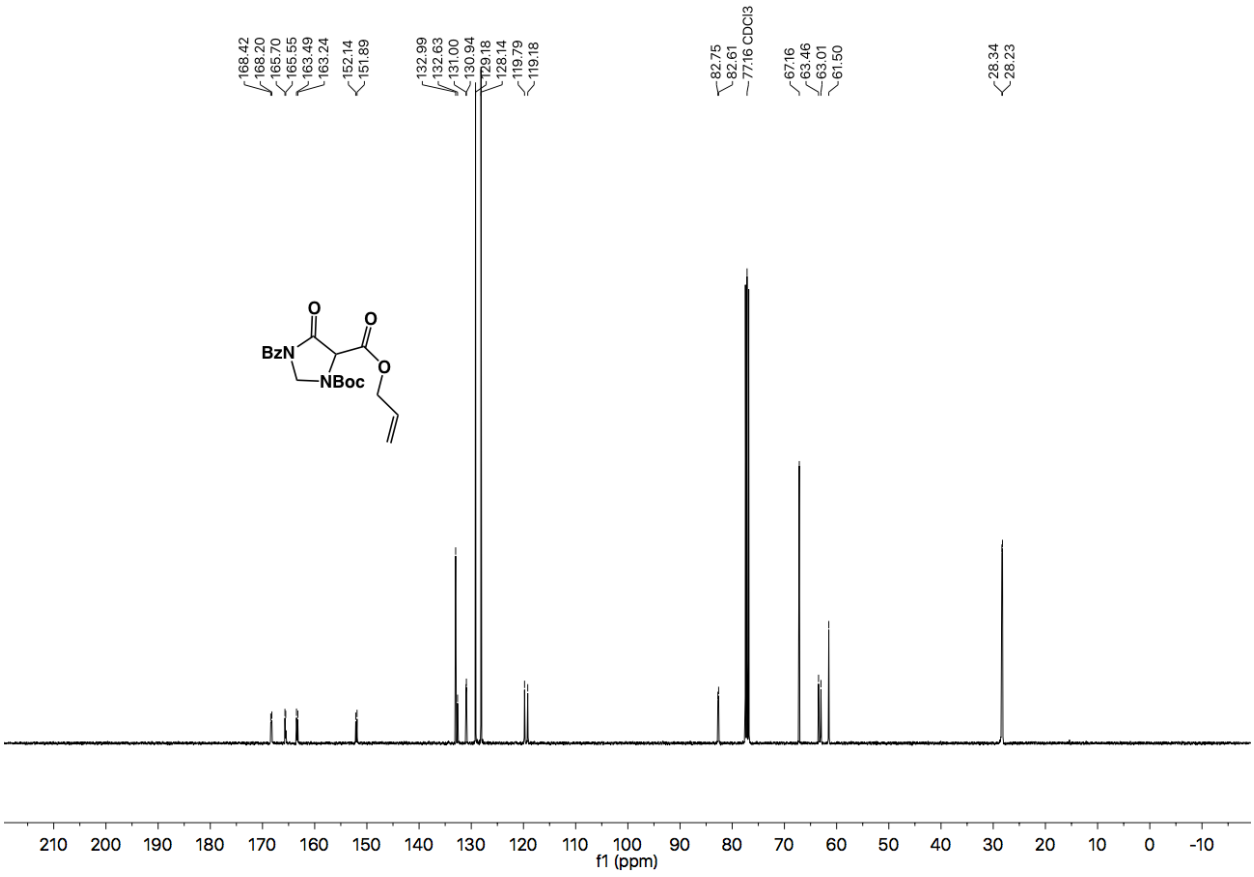

Figure A5.21 ^{13}C NMR (101 MHz, $CDCl_3$) of compound **A4.10**

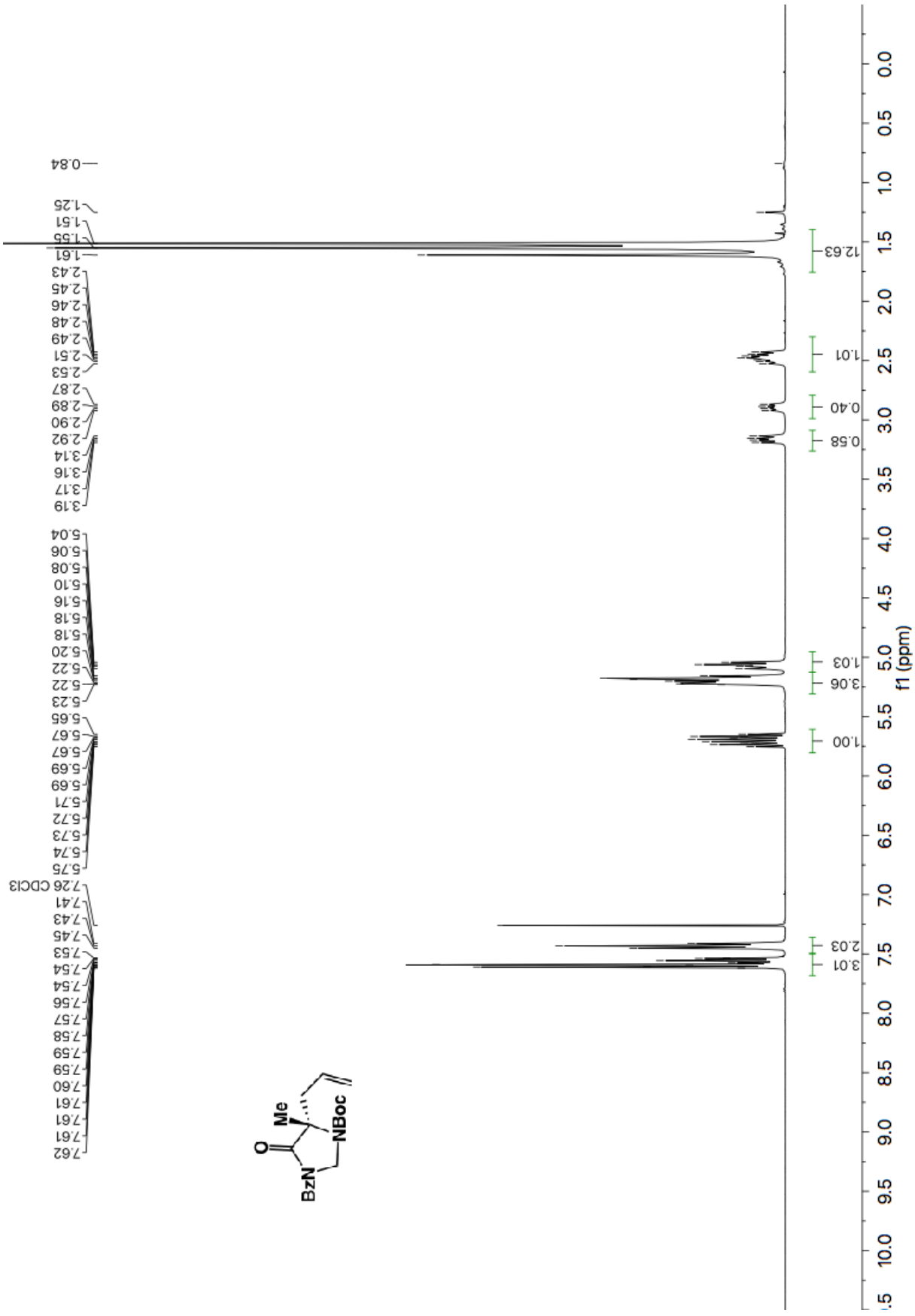

Figure A5.22 ^{1}H NMR (600 MHz, $CDCl_3$) of compound **A4.12b**

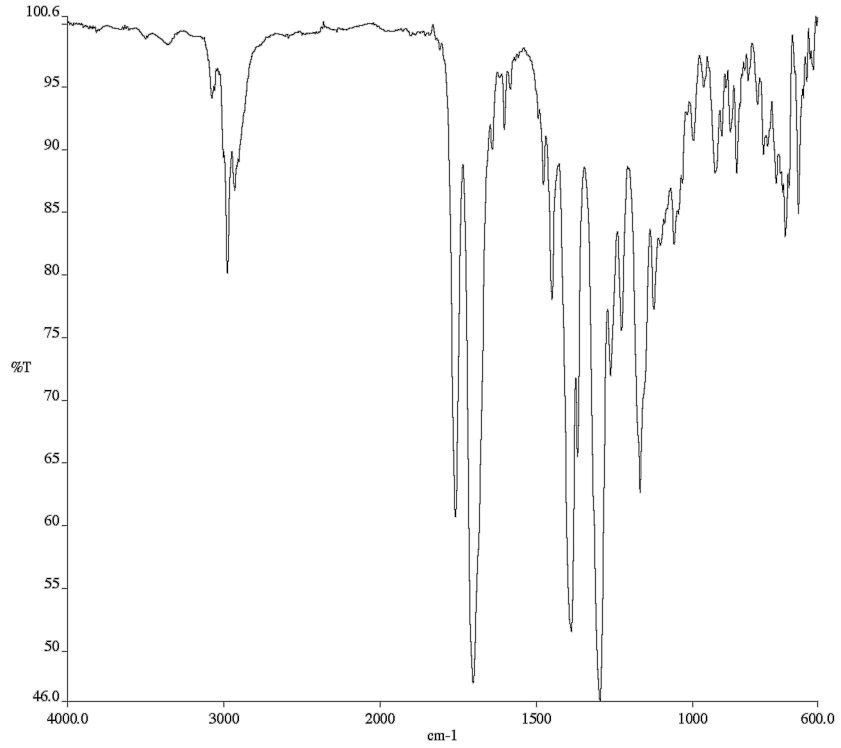

Figure A5.23 Infrared spectrum (Thin Film, NaCl) of compound **A4.12b**

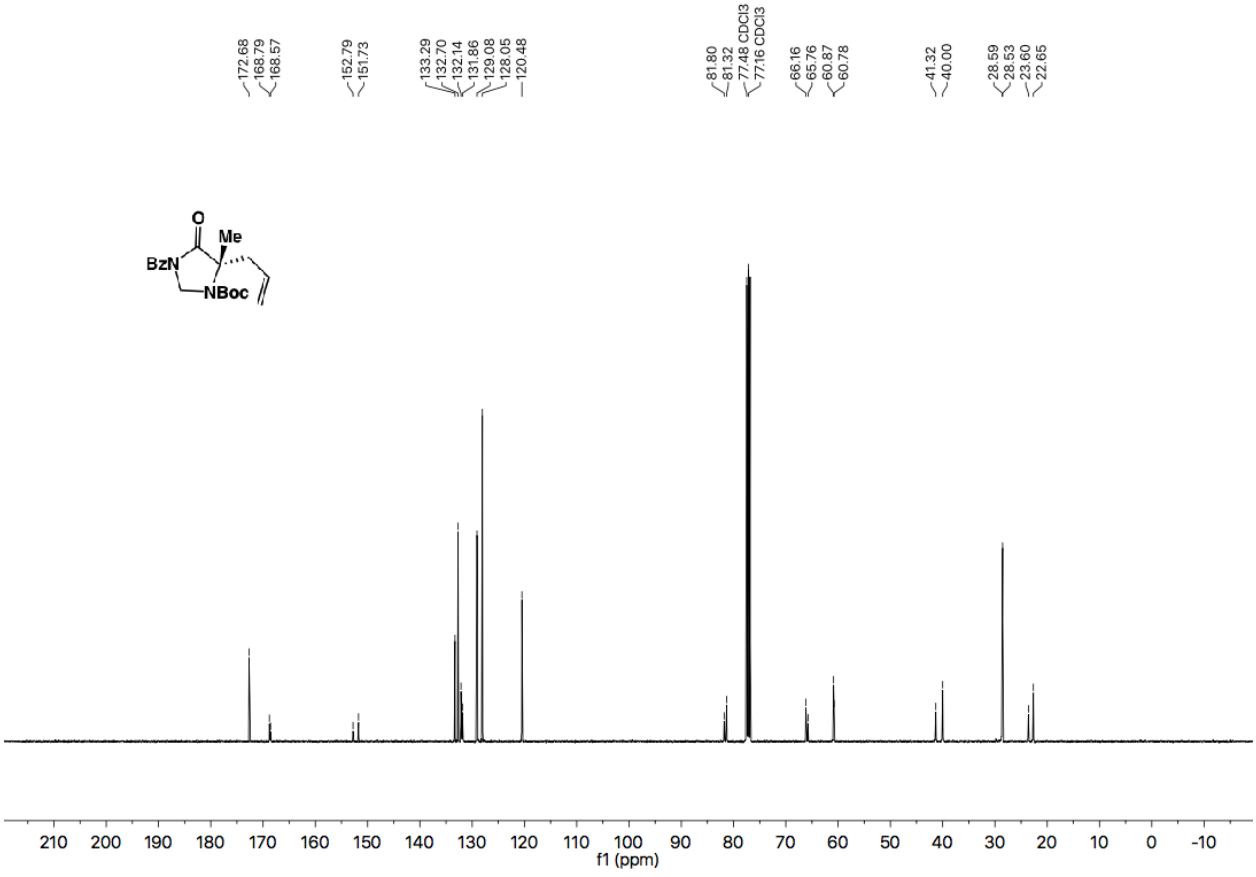

Figure A5.24 ^{13}C NMR (101 MHz, $CDCl_3$) of compound **A4.12b**

CHAPTER 2

gem-Disubstituted Morpholine Analogues of Linezolid

2.1 Introduction

Figure 2.1 *N-Heterocycles are valuable components of small molecule drugs.*

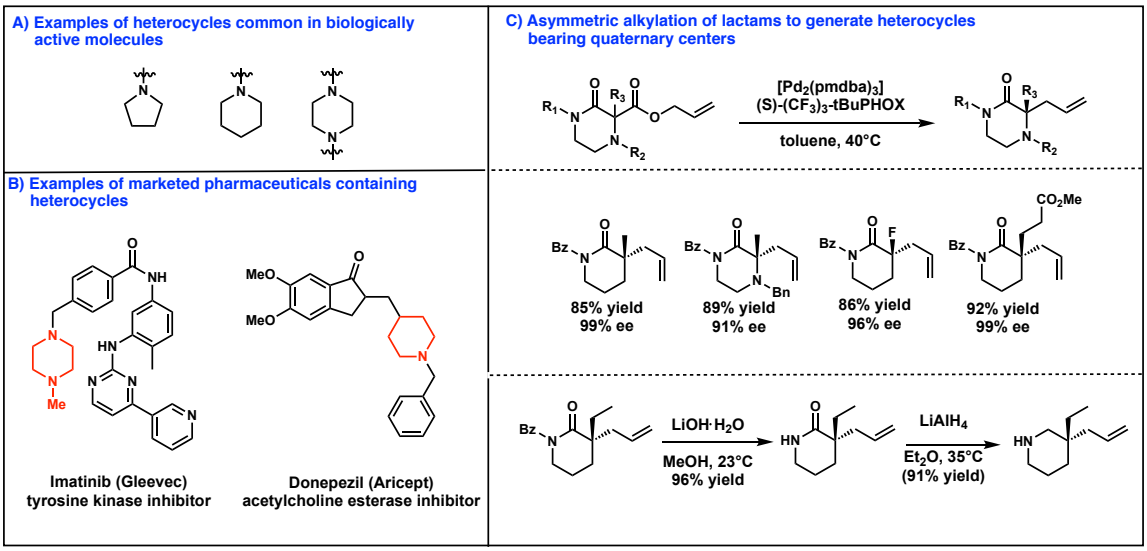

Traditionally, small molecule pharmaceuticals are rich in flat, aromatic motifs; however, studies have shown that increased sp^3 character is associated with improved target specificity.[1,2] One method of enhancing sp^3 character in small molecule drugs involves incorporating saturated nitrogen heterocycles such as piperidine, piperazine,

pyrrolidine, and morpholine, which rank amongst the most common *N*-heterocycles in small molecule drugs (Figure 2.1A).[3]

Figure 2.2 *Substitution patterns of common saturated heterocycles found in small molecule drugs*

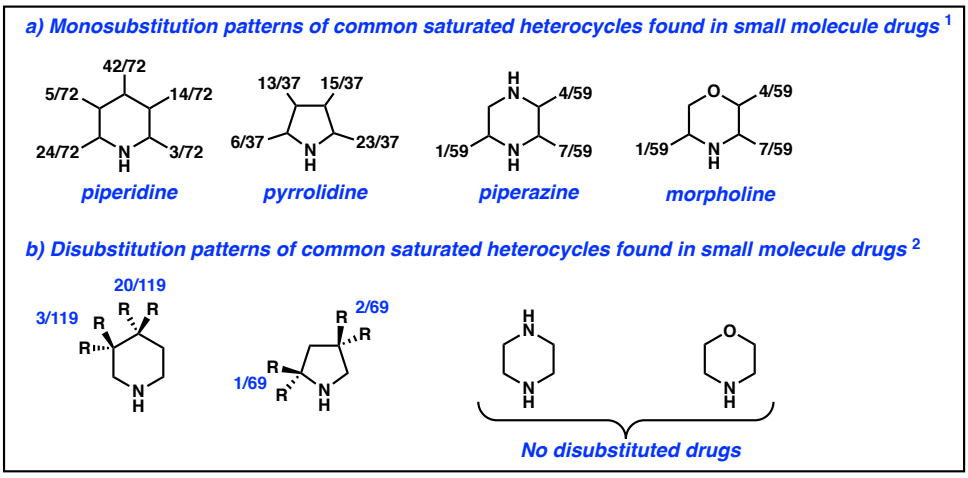

The native sp^3 complexity imparted by these saturated *N*-heterocycles can be further augmented by substituting the carbon atoms of the ring. Functionalizing these ring systems with carbon *gem*-disubstitutions—also termed quaternary centers—would potentially result in a number of improvements in the drug-like properties of such molecules, such as enhanced solubility, permeability, potency, and efficacy (Figure 2.1C). Interestingly however, a 2014 analysis found that a majority of piperidine and pyrrolidine-containing drugs contained one or more *C*-substitutions (Figure 2.2a).[3] In contrast, *gem*-disubstituted heterocyclic drugs are relatively rare (Figure 2.2b). For example, an analysis of the drugbank.ca structural database reveals that of all 139 FDA approved non-natural product derived piperazine and morpholine-containing small molecule drugs, none contain a chiral *gem*-disubstituted piperazine or morpholine.[4] And in 69 pyrrolidine containing drugs, only three chiral *gem*-disubstituted molecules exist. Only in the most common *N*-heterocycle, piperidine, are *gem*-disubstitutions more prevalent; out of 119 FDA approved piperidine-containing drugs, 23 are *gem*-

disubstituted. The dearth of *gem*-disubstituted heterocycles in the pharmacopeia is partially due to the difficulty of preparing such heterocycles in a high yielding, enantioselective manner. In recent years, however, powerful methods have been developed to enantioselectively synthesize *gem*-disubstituted heterocycles. For instance, our laboratory has pioneered the development of Pd-catalyzed decarboxylative asymmetric allylic alkylation methodologies to synthesize a range of *gem*-disubstituted lactams of ring size 5 to 7 (Figure 1c).[5–8] Such lactams can be deprotected and reductively transformed into the corresponding *gem*-disubstituted *N*-heterocycles.

While such *gem*-disubstituted heterocycles are rare in small molecule pharmaceuticals, they hold the potential to further enhance the drug-like properties of small molecules (Figure 2.3).

Figure 2.3 *Biological properties altered by hypothetical gem-disubstitution of the antibiotic linezolid.*

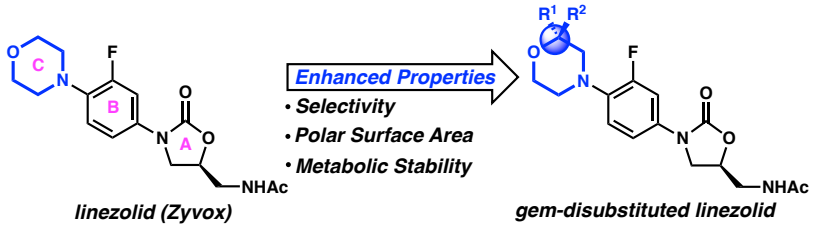

2.2 Results

Given this potential, we sought to investigate the practical utility of *gem*-disubstituted heterocycles in bioactive small molecules. After surveying various *N*-heterocyclic drugs for cases in which physicochemical attributes could be improved upon heterocyclic *gem*-disubstitution, we selected the morpholine-containing oxazolidinone antibiotic Linezolid (Zyvox) (Figure 2.4). Approved by the FDA in 2001, Linezolid

inhibits bacterial ribosome assembly by binding to the 50S subunit of the ribosome.[9] Linezolid and the recently approved oxazolidinone Tedizolid are important last resort antibiotics that are active against drug-resistant pathogens like methicillin-resistant *Staphylococcus aureus* (MRSA),[10] vancomycin-resistant *Enterococcus faecalis* (VRE),[11] and multi-drug resistant *Mycobacterium tuberculosis* (MDR-TB).[12]

Figure 2.4 *Summary of oxazolidinone antibiotics*

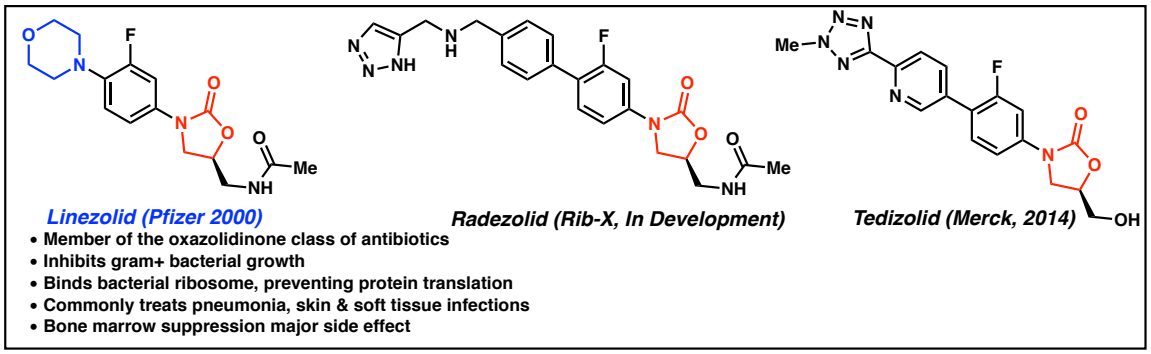

Because the bacterial and human mitochondrial ribosomes are highly homologous, oxazolidinone antibiotics bind a commonly conserved site and thus also inhibit mitochondrial protein synthesis (MPS).[13,14] This off-target binding is thought to be responsible for the more significant side-effects of linezolid, including myelosuppression, hyperlactatemia, and peripheral neuropathy.[15] Similarly, other ribosome-targeting antibiotics such as clindamycin and chloramphenicol also exhibit corresponding myelotoxic side effects.[16,17] If a structure-activity-relationship (SAR) could be determined for linezolid's mitochondrial binding ability, then new oxazolidinones could be designed with reduced MPS inhibition. In fact, reducing myelotoxic side effects while maintaining antibacterial potency is often cited as one of the greatest challenges in new oxazolidinone design.[18]

Fortunately, the modular structure of oxazolidinones enables chemical modification of all three rings, A, B, and C, facilitating SAR studies for mitochondrial ribosome binding (Figure 2.3). Some patterns have already been emerged. In 2006, McKee identified several oxazolidinones that more potently inhibit MPS yet display MIC values comparable to that of linezolid (Table 2.1).[19] In these cases, the morpholine ring was replaced with other heterocycles, suggesting the C-ring may be the greatest determinant of MPS inhibition. In spite of these initial results, there are no known reports of a potent oxazolidinone featuring reduced MPS inhibition.

Table 2.1. *MIC and MPS IC_{50} values for linezolid analogues*

	MIC[a]	IC_{50}[b]
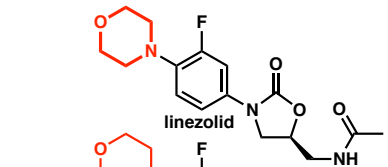 linezolid	2	12.8
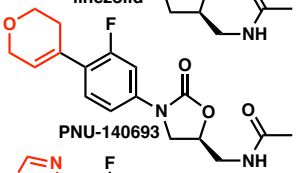 PNU-140693	1	0.95
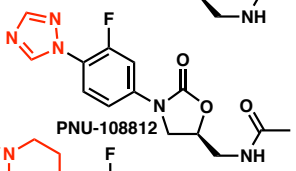 PNU-108812	4	1.7
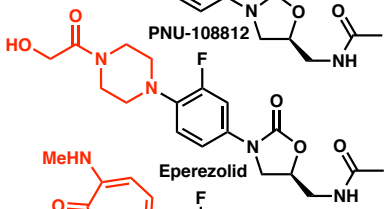 Eperezolid	2	4.2
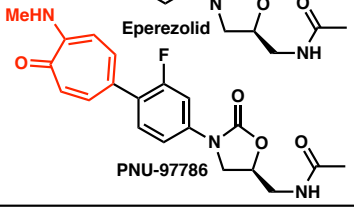 PNU-97786	2	0.83

[a] MIC (μg/mL) for *S. aureus* JC9213. [b] IC_{50} (μg/mL) for mitochondrial protein synthesis

We thus initiated a medicinal chemistry project seeking to modify the morpholine C-ring of linezolid with the goal of reducing MPS inhibition. Importantly, crystal structure studies note that the morpholine ring does not make significant interactions with the binding pocket, suggesting that the ring can be modified without compromising binding.[20] Because increased molecular complexity is associated with reduced ligand promiscuity, we hypothesized that *gem*-disubstitution of the morpholine ring could potentially increase selectivity for the bacterial ribosome and reduce off-target side effects such as MPS inhibition (Figure 2.3). To test this hypothesis, we began by identifying a modular route to enable the synthesis of a library of *gem*-disubstituted linezolid analogs (Scheme 2.1). Cross-coupling of a *gem*-disubstituted morpholine with aryl halide **2.7** was identified as an efficient route. Thus, aryl halide **2.7** was synthesized by adapting a patent procedure.[21] Briefly, (*S*)-epichlorohydrin (**2.2**) was coupled with 4-chlorobenzaldehyde (**2.1**) and ammonia to give imine **3**. To forge the oxazolidinone intermediate **2.5**, imine **2.3** was then subjected to a base-catalyzed coupling reaction with carbamate **2.4**,[22] which itself was made by addition of benzyl chloroformate to 3-fluoroaniline. Finally, imine hydrolysis, *N*-acetylation, and iodination provided the aryl iodide **2.7**. **2.7** was cross-coupled under copper-catalyzed Ullmann conditions[23] with a variety of *gem*-disubstituted morpholines resulting in linezolid analogues **2.12**-**2.19** (Figure 2.5). Notably, this synthetic route will facilitate future efforts to modify the C morpholine ring of linezolid.

Scheme 2.1. *Synthesis of gem-disubstituted linezolid analogues via Cu-catalyzed Ullmann coupling*

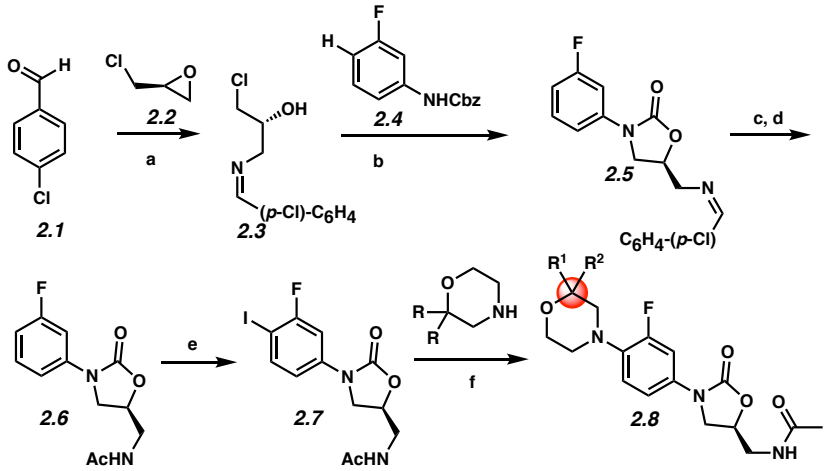

[a] (*S*)-epichlorohydrin, NH_4OH (aq). THF, 40 °C, 12 h, 55% yield; [b] LiO*t*-Bu, CH_2Cl_2, rt to 40 °C, 87% yield; [c] 1N HCl, H_2O/EtOAc; [d] Ac_2O, CH_2Cl_2, 96% yield over 2 steps; [e] NIS, TFA, rt, 92% yield; f. Substituted morpholine **2.11a-p**, CuBr (10 mol %), BINOL (20 mol %), K_3PO_4, DMF, 80 °C.

Scheme 2.2. *Synthesis of gem-disubstituted morpholines by benzoyl cleavage and reduction of morpholinone decarboxylative alkylation products*

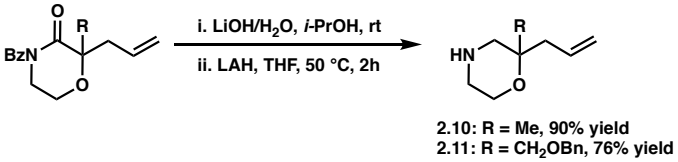

Two analogues **2.13** and **2.14** were prepared using substituted morpholines **2.10** and **2.11**, which were synthesized via a decarboxylative alkylation protocol and subsequent deprotective and reductive transformations (Scheme 2.2).[6] Other analogues including the *gem*-dimethyl compound **2.12** and spiro compounds **2.15-2.19** were prepared from commercially available di-substituted morpholines. We note that all analogs were synthesized as racemates.

***Figure 2.5**. gem-Disubstituted linezolid analogues synthesized via Ullmann coupling*

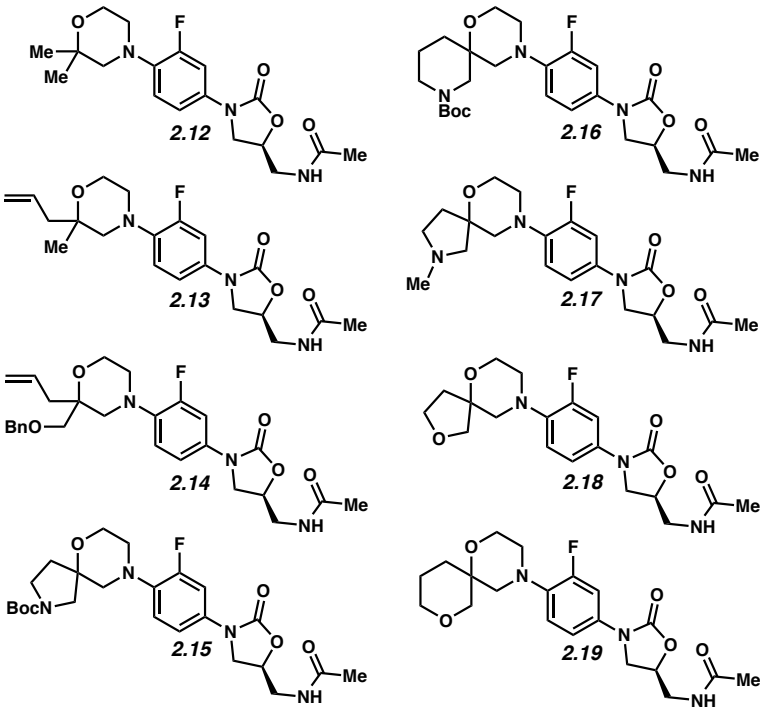

Additionally, analogues synthesized via Ullman coupling could be further derivatized (Scheme 2.3). Taking advantage of the versatile allyl handle of **2.13**, hydroboration-oxidation afforded hydroxyl analogue **2.20**, which could be acetyl-protected to give analogue **2.21**. Additionally, a Lemieux–Johnson oxidation provided the aldehyde intermediate, which was reductively aminated with dimethylamine to provide analogue **2.23**. Catalytic hydrogenation afforded the reduced analogue **2.22**. Similarly, the benzyloxy analogue **2.14** could also be hydrogenated using catalytic $Pd(OH)_2$ on carbon to provide the hydroxyl analogue **2.24**. Finally, Boc-spiro compound **2.16** was deprotected using HCl resulting in spiropiperidine **2.25**; subsequent acetyl protection gave **2.26**. Similarly, acid-catalyzed Boc-cleavage of **2.15** afforded spiropyrrolidine **2.27**.

Scheme 2.3. *Additional analogues synthesized by derivatization*

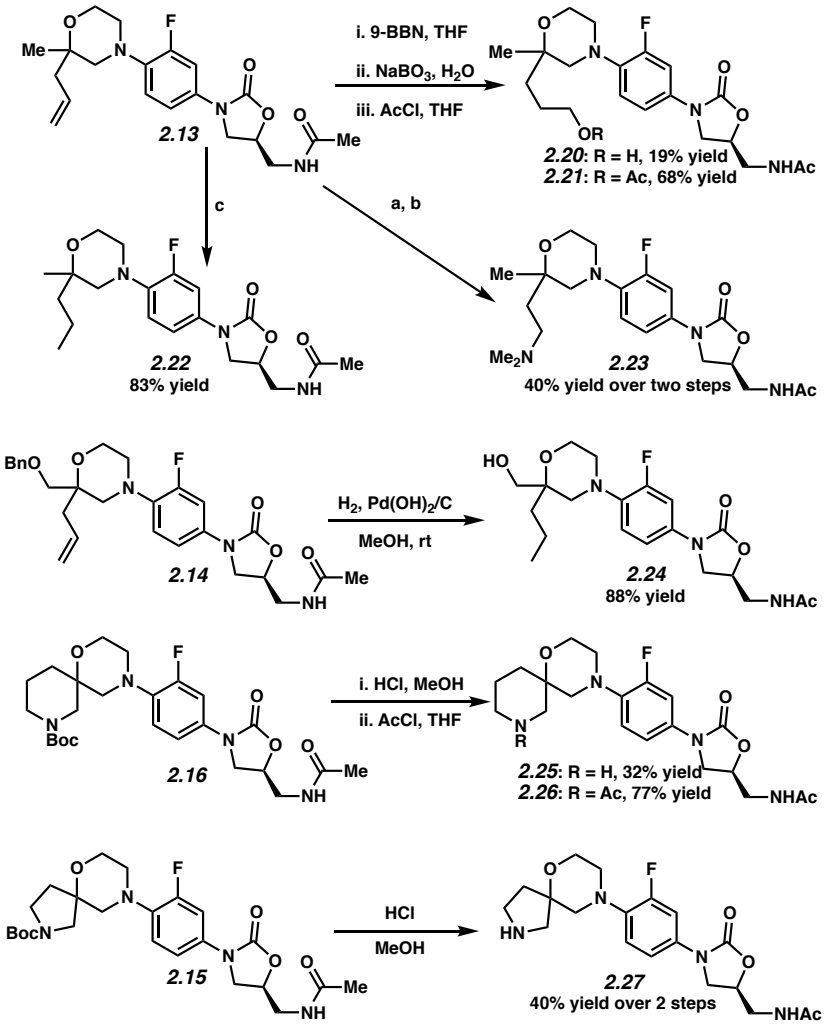

With a diverse set of *gem*-disubstituted linezolid analogues in hand, we proceeded with broth microdilution assays against *S. aureus* to determine minimum inhibitory concentration (MIC) values (Table 2.2). The initial three compounds, **2.12**, **2.13**, **2.24**, were noticeably less potent than linezolid, suggesting that bulky alkyl di-substitution on the morpholino ring reduces activity. Similarly, bulky hydroxyl-substituted analogue **2.20** and protected alcohols **2.21** and **2.14** were also inactive. In contrast, hydroxyl analogue **2.25** retained a moderate amount of activity, displaying 48% growth inhibition at the maximal tested concentration of 16 μM. The amine-bearing derivatives, **2.23**, **2.27**, **2.17**,

and **2.25**, featuring methylamino, dimethyl amino, and spiroamine functionalities, were uniformly inactive up to 64 μM concentrations. Interestingly, when the basic nitrogen of **2.25** was masked as an amide as in **2.27**, an 18% growth inhibition at the maximal tested concentration of 16 μM was achieved, suggesting that positively charged substituted morpholines are not tolerated. Finally, we were excited to observe increased growth inhibition when the spirofuran **2.18** and spirotetrahydropyran **2.19** analogues were tested, with **2.19** displaying the greatest potency of all analogues examined.

***Table 2.2**. MIC values against ATCC 8235-4 (MSSA) or ATCC 43300 (MRSA)*

Compound	MIC (μM)	Compound	MIC (μM)
Linezolid	4[a,b]	**2.23**	> 64[b]
2.12	22[a]	**2.27**	> 64[b]
2.13	32[a]	**2.17**	> 64[b]
2.22	41[a]	**2.25**	> 64[b]
2.20	> 64[a]	**2.26**	16 uM: 18% inhib.[b,d]
2.21	> 64[b]	**2.18**	16 uM: 65% inhib.[b,d]
2.14	> 64[b]	**2.19**	16[b]
2.24	16 uM: 48% inhib.[b,d]	**2.19a**	14[b]
		2.19b	22[b]

[a] MIC: the lowest concentration of molecule preventing visible growth. [b] Tested against ATCC 43300 (MRSA). [c] Tested against ATCC 8235-4 (MSSA). [d] 16 μM was the maximal concentration tested.

Since stereoisomers often exhibit differing biological activity, we used chiral HPLC to obtain both diastereomers of **2.19**, and then assigned their absolute stereochemistry using vibrational circular dichroism (VCD) and optical rotation calculations, both of which were in agreement (Figure 2.6). Notably a eudysmic difference between the two diastereomers **2.19a** and **2.19b** was observed, with the more active diastereomer **2.19a** displaying an MIC of 14 μM, roughly threefold less potent than linezolid (Table 2.2).

Figure 2.6. Diastereomers of analogue **2.19**. Absolute configuration of the spirocyclic stereocenter determined by both VCD and optical rotations (See Appendix 6 for details).

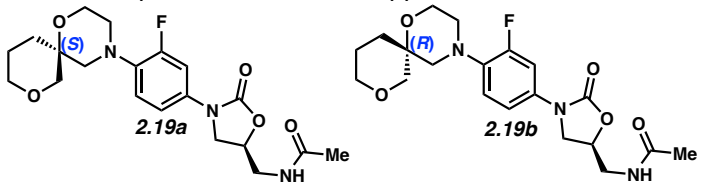

We further investigated the bioactivity of **2.19a** against other strains of *S. aureus*, determining the MIC values to be consistent against a range of MSSA and MRSA strains (Table 2.3).

Table 2.3. *MIC values of lead analogue **2.19a** against various S. aureus strains*

Strain	Linezolid MIC (uM)	2.19a MIC (μM)
ATCC 8235-4 (MSSA)	4	12
43300 (MSSA)	4	12
29213 (MRSA)	4	12
25923 (MSSA)	4	12

We next examined the pharmacokinetic properties of **2.19a** and **2.19b**, determining most properties were slightly lower but comparable to that of linezolid (Table 2.4). For instance, **2.19a** and **2.19b** demonstrated slightly lower aqueous solubility and stability at low pH. Microsomal stability for was also lower than that of linezolid, perhaps due to the metabolic susceptibility of the tetrahydropyran ring. Initial safety data including cytotoxicity and cytochrome P450 isoform inhibition were satisfactory. One interesting difference was MPS inhibition, in which linezolid displayed a relatively potent 8 μM IC_{50}. In contrast, **2.19a** displayed an IC_{50} value of 30 μM. This finding correlates with the relative MIC values of linezolid and **2.19a**; in this case, MPS inhibition is also roughly three-fold less potent, suggesting that the spirotetrahydropyran ring of **2.19a** maintains moderate binding affinity to the bacterial ribosome while reducing inhibition of the mitochondrial ribosome.

***Table 4**. Pharmacokinetic properties, inhibitory activity, and physicochemical properties*

	Linezolid	2.19a	2.19b
Aq. solubility (μg/mL)	**>67.47**	**>52.15**	**>48.89**
Stability at gastric pH (% remaining 24h)	**98%**	**94%**	**89%**
$t_{1/2}$ microsomes (min)[a]	**>216.8**	**170.0**	**128.3**
Cytotoxicity EC_{50} (μM)[b]	**>30**	**> 30**	**> 30**
CYP Inhibition (μM)[c]	**>100**	**>100**	**>100**
MT Protein synthesis inhibition IC_{50} (μM)[d]	**8.19**	**30**	**> 30**

[a] Metabolic stability performed with mouse liver microsomes
[b] Cytotoxicity against HepG2 cells using CellTiter Glo
[c] Measured against CYP1A2, 2C9, 2C19, 2D6, 3A4
[d] MitoBiogenesis In-Cell ELISA assay for COXI and SDH-A mitochondrial proteins

2.3 CONCLUSIONS

In conclusion, we identified a *gem*-disubstituted morpholine analogue of linezolid bearing a spirotetrahydropyran substitution, **2.19a,** that displays slightly reduced potency compared to linezolid against various *S. aureus* strains while also having reduced mitochondrial inhibition. These results contribute to the existing SAR of MPS inhibition (Table 2.1). Although the mitochondrial and bacterial ribosomes share homology, they have structural differences that may be exploited to design molecules with reduced selectivity for the mitochondrial ribosome.[13] Our research further contributes to the body of data suggesting that the morpholine ring is a key structural component whose modification can reduce mitochondrial inhibition while maintaining bacterial ribosome inhibition. Continued efforts are needed to identify a molecule as potent as linezolid but with reduced MPS inhibition. This ability of *gem*-disubstituted heterocycles to alter selectivity for a target such as the bacterial ribosome highlights one of the many useful properties of heterocyclic substitution. Efforts such as those underway in our laboratory

to incorporate *gem*-disubstituted heterocycles into other small molecule scaffolds will undoubtedly shed light on the broader medicinal utility of *gem*-disubstituted heterocycles.

2.4 EXPERIMENTAL SECTION

2.4.1 MATERIALS AND METHODS

Unless otherwise stated, reactions were performed in flame-dried glassware under an argon or nitrogen atmosphere using dry, deoxygenated solvents. Solvents were dried by passage through an activated alumina column under argon. Commercially obtained reagents were used as received. Chemicals were purchased from Sigma Aldrich/Strem/Alfa Aesar/Combi-Blocks/Enamine/PharmaBlock and used as received. From Combi-Blocks: (S)-epichlorohydrin, 2,2-dimethylmorpholine. From Enamine: 1,8-dioxa-4-azaspiro[5.5]undecane, *tert*-butyl 1-oxa-4,8-diazaspiro[5.5]undecane-8-carboxylate, 6-oxa-2,9-diazaspiro[4.5]decane, 2,6-dioxa-9-azaspiro[4.5]decane. From PharmaBlock: *tert*-butyl 8-oxo-6-oxa-2,9-diazaspiro[4.5]decane-2-carboxylate.

Reaction temperatures were controlled by an IKAmag temperature modulator. Glove box manipulations were performed under a nitrogen atmosphere. Thin-layer chromatography (TLC) and preparatory TLC was performed using E. Merck silica gel 60 F254 precoated plates (0.25 mm) and visualized by UV fluorescence quenching or $KMnO_4$ staining. Silia*Flash* P60 Academic Silica gel (particle size 0.040–0.063 mm) was used for flash chromatography.

Analytical SFC was performed with a Mettler SFC supercritical CO_2 analytical chromatography system utilizing a Chiralpak IC column (4.6 mm x 25 cm) obtained from Daicel Chemical Industries, Ltd. with visualization at 254 nm. Reverse Phase Preparatory

HPLC was performed with a Teledyne ISCO ACCQPrep HP125 preparative liquid chromatography system equipped with a RediSep Prep C18 5 µm column (20 x 250 mm).

^{1}H NMR spectra were recorded on a Varian Inova 600 MHz or 500 MHz spectrometer or a Bruker Avance HD 400 MHz spectrometer and are reported relative to residual $CHCl_3$ (δ 7.26 ppm) or CH_3OH (δ 3.31 ppm). ^{13}C NMR spectra were recorded on a Varian Inova 500 MHz spectrometer or a Bruker Avance HD 400 MHz spectrometer and are reported relative to residual $CDCl_3$ (δ 77.16 ppm) or CD_3OD (δ 49.00 ppm). Data for ^{1}H NMR are reported as follows: s = singlet, d = doublet, t = triplet, q = quartet, p = pentet, sept = septuplet, m = multiplet, br s = broad singlet. Data for ^{13}C NMR are reported in terms of chemical shifts (δ ppm). Some reported spectra include minor solvent impurities of water (δ 1.56 or 4.87 ppm), ethyl acetate (δ 4.12, 2.05, 1.26 ppm), methylene chloride (δ 5.30 ppm), acetone (δ 2.17 ppm), grease (δ 1.26, 0.86 ppm), and/or silicon grease (δ 0.07 ppm), which do not impact product assignments.

^{1}H NMR spectra were recorded on a Varian Inova 600 MHz or 500 MHz spectrometer or a Bruker Avance HD 400 MHz spectrometer and are reported relative to residual $CHCl_3$ (δ 7.26 ppm) or CH_3OH (δ 3.31 ppm). ^{13}C NMR spectra were recorded on a Varian Inova 500 MHz spectrometer or a Bruker Avance HD 400 MHz spectrometer and are reported relative to residual $CDCl_3$ (δ 77.16 ppm) or CD_3OD (δ 49.00 ppm). Data for ^{1}H NMR are reported as follows: s = singlet, d = doublet, t = triplet, q = quartet, p = pentet, sept = septuplet, m = multiplet, br s = broad singlet. Data for ^{13}C NMR are reported in terms of chemical shifts (δ ppm). Some reported spectra include minor solvent impurities of water (δ 1.56 or 4.87 ppm), ethyl acetate (δ 4.12, 2.05, 1.26 ppm),

methylene chloride (δ 5.30 ppm), acetone (δ 2.17 ppm), grease (δ 1.26, 0.86 ppm), and/or silicon grease (δ 0.07 ppm), which do not impact product assignments.

IR spectra were obtained using a Perkin Elmer Paragon 1000 spectrometer using thin films deposited on NaCl plates and reported in frequency of absorption (cm^{-1}). High resolution mass spectra (HRMS) were obtained from an Agilent 6200 Series TOF with an Agilent G1978A Multimode source in electrospray ionization (ESI+), atmospheric pressure chemical ionization (APCI+), or mixed ionization mode (MM: ESI-APCI+). Optical rotations were measured with a Jasco P-2000 polarimeter operating on the sodium D-line (589 nm), using a 100 mm pathlength cell and are reported as: $[\alpha]_D^T$ (concentration in g/100 mL, solvent).

MIC values were obtained in collaboration with UCLA (P.L.B. and J.F.M.) and the CO-ADD. Pharmacokinetic data was obtained with WuXi AppTec, a contract research organization.

2.4.2 EXPERIMENTAL PROCEDURES AND SPECTROSCOPIC DATA

2.4.2.1 Determination of Absolute Configuration of 2.19a and 2.19b.

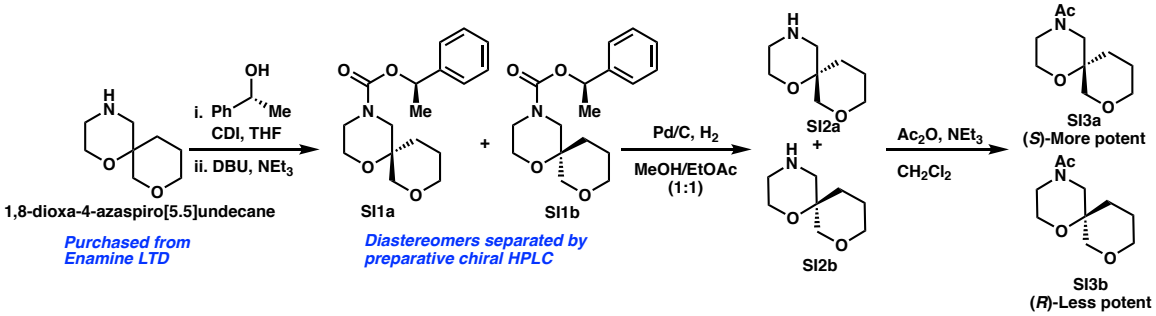

Diastereomers SI1a and SI1b: To a solution of (*S*)-(−)-1-Phenylethanol (599 uL, 1.1 equiv) in THF (4.5 mL, 1M), was added CDI (794 mg, 1.1 equiv). The solution was stirred for 1 h at room temperature. Then NEt_3 (686 uL, 1.1 equiv) and DBU (732 uL, 1.1

equiv) were added and the solution was stirred for 5 min. Then 1,8-dioxa-4-azaspiro[5.5]undecane was added and the solution was stirred for 16 h before quenching with NH_4Cl. Following extraction with EtOAc (3x10 mL) and backwashing with $NaHCO_3$ (5 mL), the combined organic layers were dried over Na_2SO_4 and concentrated. The crude product was purified by silica gel flash chromatography (33% EtOAc:Hexanes). The diastereomers were then separated by chiral preparative HPLC (CHIRALPAK IC Column 20 x 150 mm), 30% *i*PrOH:Hexanes. The diastereomer **SI1a** which results in the more potent analogue **2.19a** elutes first from the chiral column.

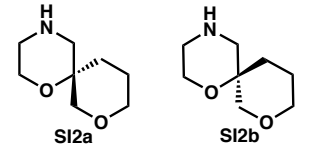

***(R)* and *(S)*-1,8-dioxa-4-azaspiro[5.5]undecane, enantiopure SI2a and SI2b:** To a solution of carbamate **SI1a** or **SI1b** (460 mg, 1 equiv) in 1:1 EtOAc/MeOH (16 mL, 0.1 M) under nitrogen was added Pd/C (10%, 80 mg, 0.05 equiv). The reaction vessel was evacuated and filled with hydrogen three times and then left to stir for 12 h at room temperature. Following completion as determined by TLC, the reaction was filtered through celite, rinsed with EtOAc, and then concentrated to afford the enantiopure amines **SI2a** or **SI2b**, which were used in subsequent reactions without further purification.

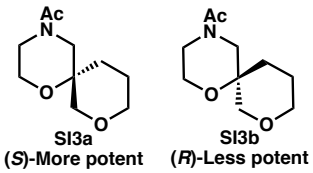

(*R*) and **(*S*)-1-(1,8-dioxa-4-azaspiro[5.5]undecan-4-yl)ethan-1-one** (Acylated enantiomers **SI3a** and **SI3b**): To a solution of **SI2a** or **SI2b** in CH_2Cl_2 (5 mL, 0.1 M) was

added NEt_3 (106 uL, 1.5 equiv) and Ac_2O (53 uL, 1.1 equiv). The reaction was stirred at rt for 1 h and then purified by automated silica gel flash chromatography (Teledyne ISCO): MeOH/CH_2Cl_2 (0 → 30%) to afford the acylated amine **SI3a** or **SI3b** as a clear oil (65 mg, 65% yield); **^{1}H NMR (400 MHz, Chloroform-*d*)** δ 3.84 – 3.21 (m, 10H), 2.09 (d, *J* = 5.2 Hz, 3H), 1.88 – 1.48 (m, 4H); **^{13}C NMR (101 MHz, $CDCl_3$)** δ (169.6 & 169.4 appear as two peaks due to hindered rotation), (71.1 & 70.9 appear as two peaks due to hindered rotation), (70.2 & 69.4 appear as two peaks due to hindered rotation), (68.5 & 68.4 appear as two peaks due to hindered rotation), (60.4 & 60.1 appear as two peaks due to hindered rotation), (51.1 & 41.7 appear as two peaks due to hindered rotation) (46.8 & 46.6 appear as two peaks due to hindered rotation), (30.9 & 29.8 appear as two peaks due to hindered rotation), (22.8 & 22.0 appear as two peaks due to hindered rotation), (21.2 & 21.11 appear as two peaks due to hindered rotation). **IR:** See VCD section; **HRMS (MM: ESI-APCI)** *m/z* calc'd for $C_{10}H_{21}N_2O_3$ $[M+NH_4]^+$: 217.1547, found 217.1552. **$[\alpha]_D^{22.7}$** –22.00 (c 1.0, $CHCl_3$) for (*S*) ent. **$[\alpha]_D^{22.4}$** +17.38 (c 21.0, $CHCl_3$) for (*R*) ent.

Note: We elected to acylate these amines to facilitate absolute stereochemistry determination by both VCD and optical rotations.

Method 1 – Vibrational Circular Dichroism (VCD)

Experimental Protocol. Solutions of **SI3a** and **SI3b** (65 mg/mL) were prepared in $CDCl_3$ and loaded into a front-loading SL-4 cell (International Crystal Laboratories) possessing BaF_2 windows and 100 μm path length. Infrared (IR) and VCD spectra were acquired on a BioTools ChiralIR-2X VCD spectrometer as a one-hour block of 3120 scans for each enantiomer. A 15-minute acquisition of neat (+)-α-pinene control

(separate 75 μm BaF_2 cell) yielded a VCD spectrum in agreement with literature spectra. IR and VCD spectra were background-corrected using a 5-minute block acquisition of the empty instrument chamber under gentle N_2 purge. The resultant VCD spectra of **SI3a** and **SI3b** were enantiomer subtracted (half-difference).

Computational Protocol. The arbitrarily chosen (*R*) enantiomer of compound **SI3b** was subjected to an exhaustive initial molecular mechanics-based conformational search (MMFF94 force field, 0.08 Å geometric RMSD cutoff, and 30 kcal/mol energy window) as implemented in MOE 2018.1 (Chemical Computing Group, Montreal, CA). All conformers retained the (*R*) configuration. All MMFF94 conformers were then subjected to geometry optimization, harmonic frequency calculation, and VCD rotational strength evaluation using density functional theory. All quantum mechanical calculations utilized the B3PW91 functional, cc-pVTZ basis, and implicit IEFPCM chloroform solvation model as implemented in the *Gaussian 16* program system (Rev. B.01; Frisch *et al*., Gaussian, Inc., Wallingford, CT). Resultant harmonic frequencies were scaled by 0.98. All structurally unique conformers were Boltzmann weighted by relative free energy at 298.15 K. The predicted IR and VCD frequencies and intensities were convolved using Lorentzian line shapes (γ = 4 cm^{-1}) and summed using the respective Boltzmann weights to yield the final predicted IR and VCD spectra of the (*R*) enantiomer of **SI3b**. The predicted VCD of the corresponding (*S*) enantiomer was generated by inversion of sign. From the agreement between the predicted and measured IR and VCD spectra in the useful range (1150-1325 cm^{-1}; see below) the absolute configuration of the *N*-acylated derivative of the desired, more active spirocyclic amine tail group was established as (*S*).

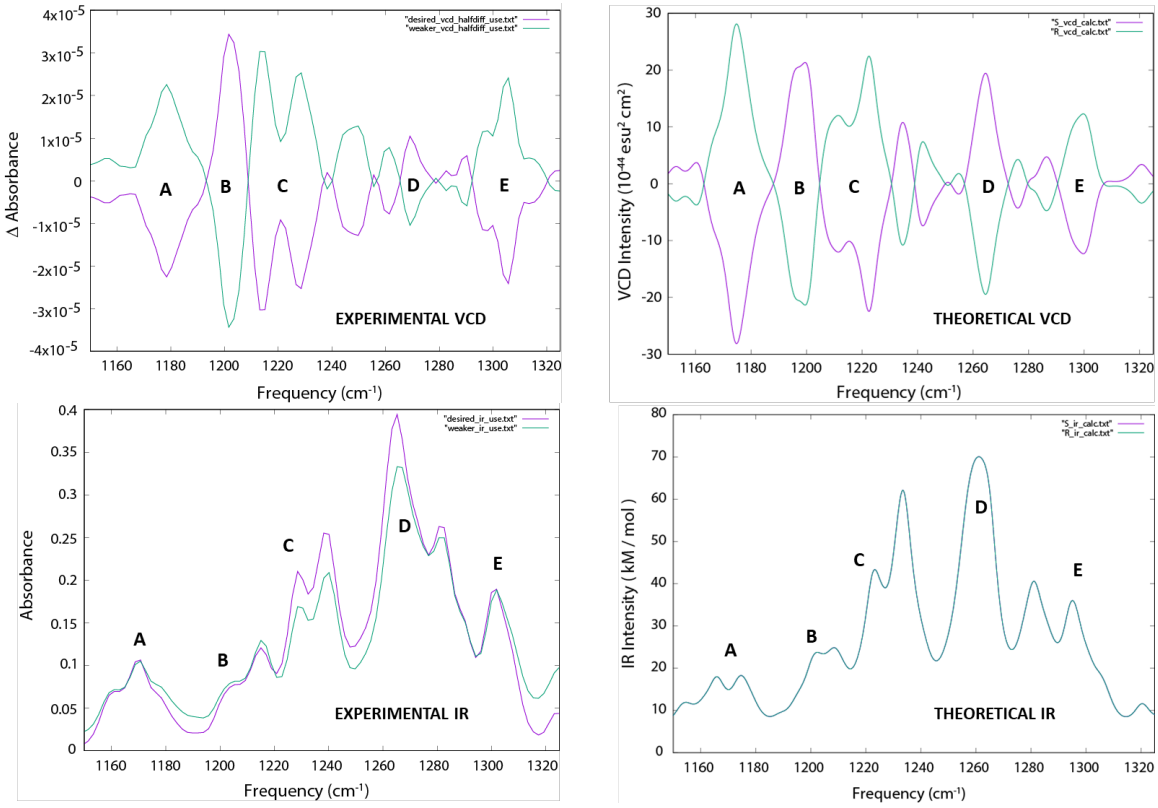

Experimental (left) and computed (right) IR and VCD spectra for **SI3a** and **SI3b.**

Method 2 – Optical Rotation (OR)

Computational Protocol. The ensemble of unique B3PW91/cc-PVTZ conformers of the (R) enantiomer of **SI3b** generated in Method 1 above were subjected to optical rotation calculation at 589.0 nm using the B3LYP hybrid density functional, the large and diffuse 6-311++G(2df,2pd) basis set, and the IEFPCM implicit chloroform solvent model. From the computed B3PW91/cc-pVTZ free energies at 298.15 K and IEFPCM-B3LYP/6-31++G(2df,2pd) optical rotations, a Boltzmann-weighted OR value of +33.6° was determined for the *(R)*-configuration of the above *N*-acylated derivative. (Thus -33.6° for the (*S*) configuration). As the measured specific rotations ($CHCl_3$ solvent, 22.7 °C, c = 1.0, 100 mm path length) were found to be +17.4° (less potent enantiomer) and -20.0° (more potent enantiomer) the OR-based assignment is therefore in accord with the VCD-

based assignment above (more active = *(S)*, less active = *(R)*. Individual free energies and optical rotational signatures are provided in the accompanying Microsoft Excel file.

2.4.2.2 Experimental Procedures for Biological Assays

Broth microdilution method A (Performed by the CO-ADD)

Samples were provided by the collaborator and stored frozen at -20 °C. Samples were prepared in DMSO and water to a final testing concentration of 32 μg/mL or 20 μM (unless otherwise indicated in the data sheet) and serially diluted 1:2 fold 8 times. Each sample concentration was prepared in 384-well plates, non-binding surface plate (NBS; Corning 3640) for each bacterial/fungal strain or Tissue-culture treated (TC-treated; Corning 3712/3764) black for mammalian cell types, all in duplicate (n=2), and keeping the final DMSO concentration to a maximum of 0.5% DMSO. All sample preparation was done using liquid handling robots.

Whole cell growth inhibition assays against S. aureus ATCC 43300 MRSA were conducted as an 8-point dose response to determine the Minimum Inhibitory Concentration (MIC), in duplicate (n=2). All bacteria were cultured in Cation-adjusted Mueller Hinton broth (CAMHB) at 37 °C overnight. A sample of each culture was then diluted 40-fold in fresh broth and incubated at 37 °C for 1.5-3 h. The resultant mid-log phase cultures were diluted (CFU/mL measured by OD_{600}), then added to each well of the compound containing plates, giving a cell density of 5Å~10^5 CFU/mL and a total volume of 50 μL. All the plates were covered and incubated at 37 °C for 18 h without shaking. Inhibition of bacterial growth was determined measuring absorbance at 600 nm (OD_{600}), using a Tecan M1000 Pro monochromator plate reader. The percentage of growth inhibition was calculated for each well, using the negative control (media only) and

positive control (bacteria without inhibitors) on the same plate as references. The percentage of growth inhibition was calculated for each well, using the negative control (media only) and positive control (bacteria without inhibitors) on the same plate. The MIC was determined as the lowest concentration at which the growth was fully inhibited, defined by an inhibition ≥ 80%. In addition, the maximal percentage of growth inhibition is reported as D_{Max} , indicating any compounds with partial activity.

Broth microdilution method B (Performed by UCLA, P.L.B and J.F.M.)

A broth microdilution method was used to estimate the MIC of synthesized compounds against Staphylococcus aureus ATCC 8235-4 (MSSA), 43300 (MSSA), 29213 (MRSA), and 25293 (MSSA). Compounds were diluted in Luria-Bertani (LB) broth to concentrations ranging from 4 μM to 22 μM (in 2 μM steps) in 96 well plates (100 μl per well). DMSO-treated wells (carrier-only) were used as negative controls, and linezolid-treated wells were used as positive controls. Wells at the edge of the plate were not used to avoid broth evaporation during incubation. Overnight cultures of S. aureus 8235-4 were diluted 1:200 in experimental plates, and plates were sealed with a plastic cover and tape. Inoculated plates were gently shaken (150 RPM) at 37 °C for 16hrs, at which point the optical density at 600nm (OD_{600}) for each well was determined using an Epoch microplate spectrophotometer (BioTek Instruments). MIC was defined as the concentration at which at least 90% of S. aureus growth was inhibited, relative to DMSO-treated controls.

2.4.2.3 Procedures and Spectroscopic Data for the Synthesis of Linezolid Analogues

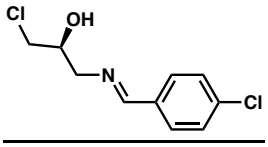

(*S*)-1-chloro-3-((4-chlorobenzylidene)amino)propan-2-ol (2.3). To a solution of benzaldehyde (25 g, 1 equiv) in THF (180 mL, 1M) was added aqueous ammonia (28 wt %, 18 mL, 1.5 equiv). The mixture was stirred at rt for 20 min. Then, (*S*)-epichlorohydrin (13.9 mL, 1.0 equiv) was added. The reaction was stirred at 30 °C for 4 h, then at 40 °C for 12 h. with a reflux condenser attached. Then, another 18 mL aq. NH_3 was added and stirring was continued at 40 °C for another 12 h. The solvent was concentrated under reduced pressure. 50 mL PhMe was added and then removed under reduced pressure to azeotrope remaining volatiles. The aqueous solution was then extracted with EtOAc (3x50 mL). The combined organic layers were dried over Na_2SO_4 and concentrated under reduced pressure. The crude product was recrystallized using hot hexanes, rinsed with hexanes, and isolated as white needles (22.7 g, 55% yield). Product identity matched previously reported characterization data.[24]

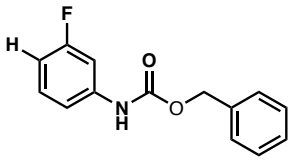

benzyl (3-fluorophenyl)carbamate (2.4). To a solution of 3-fluoroaniline (5 g, 1 equiv) and K_2CO_3 (7.46 g, 1.2 equiv) in THF at rt was added CbzCl (7 mL, 1.1 equiv). The

solution was stirred at rt for 5 h and then quenched with 200 mL sat. Na_2CO_3. The layers were separated and the organic layer was washed with Na_2CO_3 (2x). The combined aqueous layers were extracted with CH_2Cl_2 (4x). The combined organic layers were dried over Na_2SO_4 and concentrated under reduced pressure. The crude mixture was triturated with hexanes at rt: after cooling at -20 °C, the white precipitate was isolated by filtration and used in the next step. Product identity matched previously reported characterization data.[25]

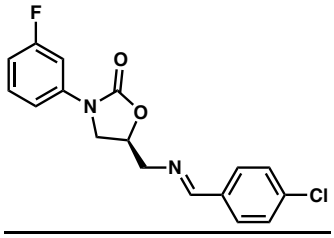

(*S*)-5-(((4-chlorobenzylidene)amino)methyl)-3-(3-fluorophenyl)oxazolidin-2-one (2.5). To a solution of carbamate **2.4** (4 g, 1 equiv) and LiOtBu (3.27 g, 2.5 equiv) in CH_2Cl_2 (22 mL, 0.75 M) was added a solution of imine **2.3** in CH_2Cl_2 (11 mL, 2.27 M). The reaction was refluxed for 16 h, and then allowed to cool to rt before being quenched with half saturated brine. The solution was extracted with CH_2Cl_2 (4x30 mL). Addition H_2O and CH_2Cl_2 were added to clear emulsions formed in the separatory funnel. The combined organic layers were dried over Na_2SO_4, filtered over celite to remove suspended particles, and then concentrated under reduced pressure. The crude product was triturated by adding hot Et_2O, which solvated the byproduct, but left the product unsolvated. The hot Et_2O was allowed to cool to rt and then the product was isolated by filtration and rinsed with cold Et_2O to provide the imine **2.5** as a white fluffy solid (4.73 g, 87% yield); **^{1}H NMR (400 MHz, Chloroform-*d*)** δ 8.35 (s, 1H), 7.62 (d, *J* = 8.3 Hz,

2H), 7.54 – 7.14 (m, 5H), 6.84 (td, J = 8.2, 2.5 Hz, 1H), 4.97 (dq, J = 8.9, 5.2 Hz, 1H), 4.29 – 4.04 (m, 2H), 4.04 – 3.79 (m, 2H); **^{13}C NMR (101 MHz, $CDCl_3$)** δ 163.21 (d, J_{CF} = 245.0 Hz), 163.68, 154.45, 139.94 (d, J_{CF} = 10.7 Hz), 137.44, 134.09, 130.35 (d, J_{CF} = 9.4 Hz), 129.66, 129.10, 113.43 (d, J_{CF} = 3.0 Hz), 110.85 (d, J_{CF} = 21.2 Hz), 105.90 (d, J_{CF} = 26.9 Hz), 71.90, 63.28, 48.27; **IR (Neat Film, NaCl)** 3746, 2360, 1748, 1646, 1614, 1495, 1456, 1405, 1224, 1195, 1168, 1087, 837 cm^{-1}; **HRMS (MM: ESI-APCI)** *m/z* calc'd for $C_{17}H_{15}FN_2O_2$ $[M+H]^+$: 333.0801, found 333.0803. **$[\alpha]_D^{22.7}$** –99.9 (c 2.0, $CHCl_3$).

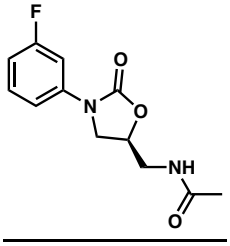

(*S*)-*N*-((3-(3-fluorophenyl)-2-oxooxazolidin-5-yl)methyl)acetamide (2.6). To a solution of imine **2.5** in a 1:1 mixture of EtOAc/H_2O (80 mL, 0.17 M) was added concentrated HCl (2.26 mL, 2 equiv). The reaction was stirred at rt for 5 h and then slowly quenched with $NaHCO_3$(aq). Then, KOH was added until pH = 14. The solution was extracted with EtOAc (4x40 mL) and CH_2Cl_2 (4x40 mL). The combined organic layers were dried over Na_2SO_4 and concentrated under reduced pressure. The crude product was triturated with Et_2O to afford crude amine, which was used in the next step without purification.

To a solution of crude amine in CH_2Cl_2 (45 mL, 0.3 M) was added NEt_3 (3.78 mL, 2 equiv) followed by Ac_2O (2.55 mL, 2 equiv). The reaction was stirred for 2 h at rt and then quenched with H_2O. Following extraction with EtOAc (3x20 mL) and drying with Na_2SO_4, the combined organic layers were concentrated under reduced pressure. The

crude product was dissolved in a minimal amount of hot CH_2Cl_2 and then Et_2O was added. The solution was left overnight at -20 °C, resulting in crystallization of pure **2.6**. The solid product (3.28 g, was isolated by filtration and rinsed with Et_2O. Product identity matched previously reported characterization data.

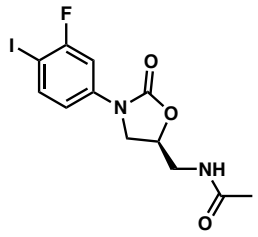

(S)-N-((3-(3-fluoro-4-iodophenyl)-2-oxooxazolidin-5-yl)methyl)acetamide (2.7). To a solution of **(*S*)-*N*-((3-(3-fluorophenyl)-2-oxooxazolidin-5-yl)methyl)acetamide (2.6)** (2.9 g, 1 equiv) in TFA (12 mL, 1M) was added NIS (2.72 g, 1.05 equiv) portion-wise. The reaction was stirred for 1 h at rt. While stirring, the exothermic reaction turned pinked. Next, the TFA was concentrated off under reduced pressure. The crude mixture was diluted with $Na_2S_2O_3$ (10%), and then KOH was added until pH = 14. Next the solution was diluted to ~700 mL volume with H_2O. Extraction with CH_2Cl_2 (4x50 mL) and EtOAc (4x50 mL) was followed by drying with Na_2SO_4 and concentration of the combined organic layers under reduced pressure. The crude product was then purified by silica gel flash chromatography (5 → 10% MeOH/CH_2Cl_2) to afford the desired iodinated compound **2.7** (4 g, 92% yield). Product identity matched previously reported characterization data.[27]

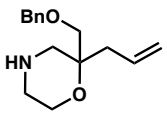

2-allyl-2-((benzyloxy)methyl)morpholine (2.11). Prepared according to literature procedure.[6] Product identity matched previously reported characterization data.[6]

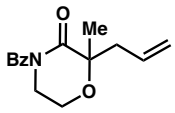

2-allyl-4-benzoyl-2-methylmorpholin-3-one.[6] Prepared according to an adapted procedure from our publications:[6,28] In the glove box, in a 100 mL Schlenck bomb, Pd(OAc) (2.7 mg, 0.005 equiv), GlyPHOX[29,30] (16 mg, 0.02 equiv), and MTBE (5 mL) were added. The solution was stirred at rt for 30 min. Then, allyl 4-benzoyl-2-methyl-3-oxomorpholine-2-carboxylate[6] dissolved in 10 mL toluene was added. The reaction was heated to 60 °C for 5 h, at which time TLC analysis showed complete consumption of starting material. The solution was loaded onto a silica gel flash column and purified (10 → 20% EtOAc/Hexanes) to afford racemic **2-allyl-4-benzoyl-2-methylmorpholin-3-one** as a white solid (620 mg, 98% yield). Product identity matched previously reported characterization data.[6]

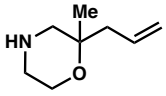

2-allyl-2-methylmorpholine (10). To a solution of **2-allyl-4-benzoyl-2-methylmorpholin-3-one** (620 mg, 1 equiv) in iPrOH (60 mL, 0.04 M) was added LiOH-H_2O (150 mg, 1.5 equiv) dissolved in H_2O (16 mL, 0.15 M). The reaction was stirred at room temperature for 2 h and then concentrated into SiO_2. The dry-loaded crude product was purified by silica gel flash chromatography (2.5 → 5% MeOH/CH_2Cl_2) to afford the deprotected lactam, which was carried onto the next step:

To a solution of deprotected lactam (370 mg, 1 equiv) in THF (24 mL, 0.1 M) was added LAH (271 mg, 3 equiv) portionwise at 0 °C. The reaction was then heated to 50 °C for 2 h. A Fieser workup was performed: the reaction was diluted with Et_2O (12 mL) at 0 °C, then the following were slowly and sequentially added at 0 °C: 270 uL H_2O, 270 uL 15% aq. NaOH, and lastly 800 uL H_2O. The suspension was stirred at 0 °C for 15 min and then $MgSO_4$ was added. The mixture was allowed to warm to rt and then filtered over celite, rinsing with EtOAc. The solvent was concentrated under reduced pressure. The crude product was purified by silica gel flash chromatography (5 → 10% MeOH/CH_2Cl_2) to yield racemic **2.10** as a clear oil (305 mg, 90% yield over two steps); **^{1}H NMR (600 MHz, Chloroform-*d*)** δ 5.80 (dddd, *J* = 14.6, 12.9, 6.1, 3.8 Hz, 1H), 5.14 – 5.02 (m, 2H), 3.67 (dq, *J* = 5.7, 3.3, 2.7 Hz, 2H), 2.79 (q, *J* = 4.4, 4.0 Hz, 2H), 2.74 – 2.57 (m, 2H), 2.48 (dt, *J* = 12.1, 5.5 Hz, 1H), 2.21 (dt, *J* = 12.7, 5.9 Hz, 1H), 2.06 (d, *J* = 7.5 Hz, 1H), 1.26 – 1.10 (m, 3H); **^{13}C NMR (101 MHz, $CDCl_3$)** δ 133.6, 117.9, 72.1, 61.6, 54.3, 46.0, 41.7, 22.0; **IR (Neat Film, NaCl)** 3335, 3074,2973, 2938, 2868, 2818, 2741,2360, 1639, 1455, 1375, 1324, 1259, 1200, 1177, 1130, 1084, 997, 914, 852, 797, 750, 669 cm^{-1}; **HRMS (MM: ESI-APCI)** *m/z* calc'd for $C_8H_{16}NO$ $[M+H]^+$: 142.1226, found 142.1229.

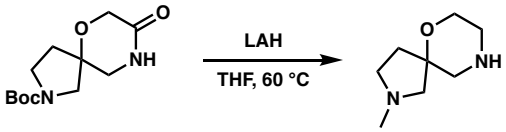

2-methyl-6-oxa-2,9-diazaspiro[4.5]decane (SI5). To a solution of *tert*-butyl 8-oxo-6-oxa-2,9-diazaspiro[4.5]decane-2-carboxylate (100 mg, 1 equiv) in THF (3.9 mL, 0.1 M) at 0 °C was slowly added LAH (59 mg, 4 equiv). The reaction was stirred at 60 °C for 6 h and then allowed to cool to ambient temperature. A Fieser workup was performed: the

reaction was diluted two-fold with Et_2O at 0 °C, then the following were slowly and sequentially added at 0 °C: 60 uL H_2O, 60 uL 15% aq. NaOH, and lastly 180 uL H_2O. The suspension was stirred at 0 °C for 15 min and then $MgSO_4$ was added. The mixture was allowed to warm to rt and then filtered over celite, rinsing with EtOAc. The solvent was concentrated under reduced pressure. The crude product was used without further purification.

2.4.2.4 Preparation of linezolid analogues via Cu-Catalyzed Ullman Coupling

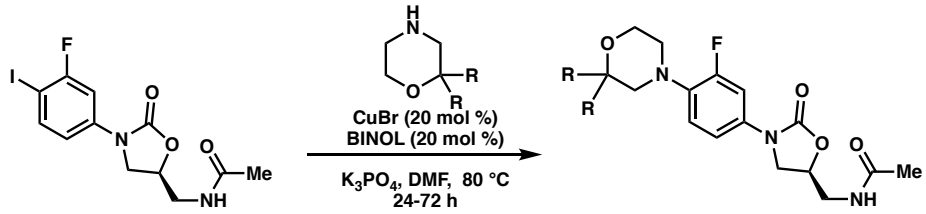

To a flame-dried one-dram vial equipped with a Teflon screw cap and a stir bar was added CuBr (0.1 - 0.3 equiv), BINOL (0.1 - 0.3 equiv), aryl iodide **2.7** (1 equiv), and K_3PO_4 (2 equiv). The vial was cycled into a glovebox and then DMF (0.2 M final concentration) was added to the vial, followed by the amine (2 equiv). The reaction was stirred at 80 °C for 24-72 hours until complete consumption of starting material was noted by LC-MS analysis. In some cases, conversion of the starting material stopped, at which point 0.2 equiv of CuBr and 0.2 equiv of BINOL was added to the reaction, which then proceeded to completion. The reaction was diluted with EtOAc and filtered through a plug of silica, rinsing with 10% MeOH/EtOAc. The solution was concentrated in vacuo until all DMF solvent was removed. The crude material was purified by by silica gel flash chromatography or reverse phase prep HPLC to afford the desired linezolid analog.

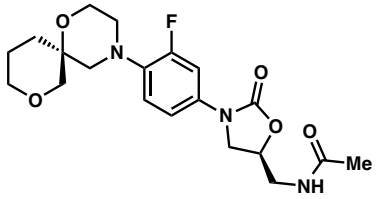

N-(((*S*)-3-(3-fluoro-4-((*S*)-1,8-dioxa-4-azaspiro[5.5]undecan-4-yl)phenyl)-2-oxooxazolidin-5-yl)methyl)acetamide (**2.19a**). Prepared according to the general procedure using: CuBr (2.3 mg, 0.016 mmol, 0.2 equiv), BINOL (4.5 mg, 0.016 mmol, 0.2 equiv), aryl iodide **2.7** (30 mg, 0.079 mmol, 1 equiv), K_3PO_4 (34 mg, 0.16 mmol, 2 equiv), enantiopure **(*S*)-1,8-dioxa-4-azaspiro[5.5]undecane (SI2a)** (18 mg, 0.16 mmol, 2 equiv), and 400 uL DMF. The crude residue was purified by silica gel flash chromatography (2 → 3 → 5% MeOH/CH_2Cl_2) to yield spirotetrahydropyran analogue **2.19a** (8 mg, 28% yield) as a clear oil: **^{1}H NMR (400 MHz, $CDCl_3$)** δ 7.40 (dd, *J* = 14.1, 2.6 Hz, 1H), 7.04 (ddd, *J* = 8.8, 2.6, 1.1 Hz, 1H), 6.88 (t, *J* = 9.1 Hz, 1H), 6.39 (t, *J* = 6.2 Hz, 1H), 4.76 (dddd, *J* = 8.8, 6.7, 5.5, 3.3 Hz, 1H), 4.00 (t, *J* = 9.0 Hz, 1H), 3.91 (t, *J* = 4.9 Hz, 2H), 3.85 – 3.77 (m, 1H), 3.74 (dd, *J* = 9.2, 6.7 Hz, 1H), 3.71 – 3.54 (m, 5H), 3.09 – 2.94 (m, 2H), 2.92 (s, 2H), 2.01 (s, 3H), 1.95 – 1.78 (m, 3H), 1.58 (dddd, *J* = 14.3, 11.4, 6.8, 2.4 Hz, 1H); **^{13}C NMR (101 MHz, $CDCl_3$)** δ 171.3, 155.6 (d, J_{CF} = 246.5 Hz), 154.5, 136.9 (d, J_{CF} = 9.0 Hz), 133.0 (d, J_{CF} = 10.3 Hz), 119.2 (d, J_{CF} = 4.0 Hz), 114.0 (d, *J* = 3.4 Hz), 107.6 (d, *J* = 26.1 Hz), 72.1, 71.7, 70.0, 68.7, 61.0, 56.9, 50.8, 47.8, 42.0, 31.0, 23.2, 22.4; **IR (Neat Film, NaCl)** 3312, 3073, 2953, 2846, 2244, 1748, 1660, 1517, 1486, 1446, 1416, 1374, 1324, 1279, 1225, 1196, 1097, 1044, 985, 910, 871, 809, 732, 674, 646 cm^{-1}; **HRMS (MM: ESI-APCI)** *m/z* calc'd for $C_{20}H_{27}FN_3O_5$ $[M+H]^+$: 408.1929, found 408.1909 **$[\alpha]_D^{22.7}$** –20.8 (c 1.5, $CHCl_3$).

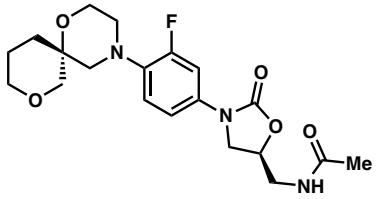

***N*-(((*S*)-3-(3-fluoro-4-((*R*)-1,8-dioxa-4-azaspiro[5.5]undecan-4-yl)phenyl)-2-oxooxazolidin-5-yl)methyl)acetamide (2.19b)**. Prepared according to the general procedure using: CuBr (2.3 mg, 0.016 mmol, 0.2 equiv), BINOL (4.5 mg, 0.016 mmol, 0.2 equiv), aryl iodide **2.7** (30 mg, 0.079 mmol, 1 equiv), K_3PO_4 (34 mg, 0.16 mmol, 2 equiv), enantiopure ***(R)*-1,8-dioxa-4-azaspiro[5.5]undecane (SI2b)** (18 mg, 0.16 mmol, 2 equiv), and 400 uL DMF. The crude residue was purified by silica gel flash chromatography (2 → 3 → 5% MeOH/CH_2Cl_2) to yield spirotetrahydropyran analogue **2.19b** (10 mg, 32% yield) as a clear oil: **^{1}H NMR (400 MHz, Chloroform-*d*)** δ 7.43 (dd, *J* = 14.1, 2.6 Hz, 1H), 7.06 (ddd, *J* = 8.8, 2.7, 1.1 Hz, 1H), 6.91 (t, *J* = 9.1 Hz, 1H), 6.06 (t, *J* = 6.2 Hz, 1H), 4.76 (dddd, *J* = 8.9, 6.7, 5.8, 3.2 Hz, 1H), 4.02 (t, *J* = 9.0 Hz, 1H), 3.93 (t, *J* = 4.9 Hz, 2H), 3.81 (d, *J* = 11.7 Hz, 1H), 3.78 – 3.55 (m, 6H), 3.08 – 2.96 (m, 2H), 2.94 (s, 2H), 2.02 (s, 3H), 1.96 – 1.77 (m, 3H), 1.59 (dddd, *J* = 15.1, 12.8, 6.9, 2.4 Hz, 2H); **^{13}C NMR (101 MHz, $CDCl_3$)** δ 171.1, 155.6 (d, *J* = 246.6 Hz), 154.3, 136.81 (d, *J* = 8.9 Hz), 133.06 (d, *J* = 10.4 Hz), 119.27 (d, *J* = 4.0 Hz), 113.99 (d, *J* = 3.5 Hz), 107.62 (d, *J* = 26.2 Hz), 71.9, 71.7, 70.0, 68.7, 60.9, 56.9, 50.8, 47.7, 42.1, 31.0, 23.3, 22.5; **IR (Neat Film, NaCl)** 3318, 3067, 2927, 2850, 1748, 1667, 1516, 1486, 1416, 1374, 1326, 1277, 1225, 1097, 939, 870, 815, 733 cm^{-1}; **HRMS (MM: ESI-APCI)** *m/z* calc'd for $C_{20}H_{27}FN_3O_5$ $[M+H]^+$: 408.1929, found 408.1932. **$[\alpha]_D^{22.7}$** +1.7 (c 1.0, $CHCl_3$).

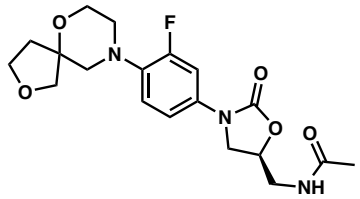

***N*-(((5*S*)-3-(3-fluoro-4-(2,6-dioxa-9-azaspiro[4.5]decan-9-yl)phenyl)-2-oxooxazolidin-5-yl)methyl)acetamide (2.18).** Prepared according to the general procedure using: CuBr (7.5 mg, 0.052 mmol, 0.3 equiv), BINOL (15.0 mg, 0.052 mmol, 0.3 equiv), aryl iodide **2.7** (66 mg, 0.17 mmol, 1 equiv), K_3PO_4 (74 mg, 0.35 mmol, 2 equiv), **2,6-dioxa-9-azaspiro[4.5]decane (**50 mg, 0.35 mmol, 2 equiv), and 873 uL DMF. The crude residue was purified by reverse phase preparatory HPLC (0 → 100% MeCN/H_2O gradient over 10 minutes, 30x250 mm C_{18} column, 60 mL/min flow rate) to yield spirotetrahydrofuran analogue **2.18** (35 mg, 51% yield) as a clear oil. Note: HPLC H_2O solvent contained 0.25% TFA: **^{1}H NMR (400 MHz, Chloroform-*d*)** δ (Note TFA appears in the ^{1}H and ^{13}C NMR) 7.41 (dd, *J* = 14.0, 2.6 Hz, 1H), 7.05 (ddd, *J* = 8.8, 2.6, 1.1 Hz, 1H), 6.92 (t, *J* = 9.0 Hz, 1H), 4.82 (dddd, *J* = 8.8, 6.4, 5.1, 3.6 Hz, 1H), 4.14 – 3.83 (m, 7H), 3.79 (dd, *J* = 9.3, 6.4 Hz, 1H), 3.75 – 3.65 (m, 2H), 3.03 (d, *J* = 5.2 Hz, 4H), 2.24 – 2.13 (m, 2H), 2.13 – 2.00 (m, 4H); **^{13}C NMR (101 MHz, $CDCl_3$)** δ 171.4, 155.6 (d, *J* = 246.6 Hz), 154.5, 136.4 (d, *J* = 9.0 Hz), 133.3 (d, *J* = 10.4 Hz), 119.1 (d, *J* = 4.0 Hz), 114.0 (d, *J* = 3.3 Hz), 107.6 (d, *J* = 26.1 Hz), 82.6, 75.5, 72.1, 67.6, 63.1, 57.9, 50.1, 47.7, 42.0, 36.4, 23.2; **IR (Neat Film, NaCl)** 3304, 3070, 2955, 2870, 1751, 1662, 1517, 1446, 1415, 1374, 1326, 1278, 1227, 1195, 1083, 1060, 992, 919, 731 cm^{-1}; **HRMS (MM: ESI-APCI)** *m/z* calc'd for $C_{19}H_{25}FN_3O_5$ $[M+H]^+$: 394.1773 found 394.1779. **$[\alpha]_D^{2.8}$** –5.54 (c 1.0, $CHCl_3$).

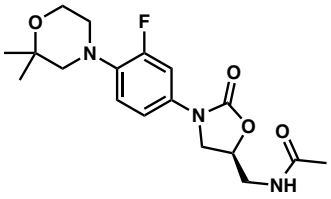

(S)-N-((3-(4-(2,2-dimethylmorpholino)-3-fluorophenyl)-2-oxooxazolidin-5-yl)methyl)acetamide (2.12). Prepared according to the general procedure using: CuBr (2.3 mg, 0.016 mmol, 0.2 equiv), BINOL (4.5 mg, 0.016 mmol, 0.2 equiv), aryl iodide **2.7** (30 mg, 0.079 mmol, 1 equiv), K_3PO_4 (34 mg, 0.16 mmol, 2 equiv), dimethyl morpholine (18 mg, 0.16 mmol, 2 equiv), and 400 uL DMF. The crude residue was purified by silica gel flash chromatography (2 → 3 → 5% MeOH/CH_2Cl_2) to yield dimethyl analogue **2.12** (8 mg, 28% yield) as a clear oil: **^{1}H NMR (400 MHz, $CDCl_3$)** δ 7.42 (dd, *J* = 14.2, 2.6 Hz, 1H), 7.05 (ddd, *J* = 8.8, 2.6, 1.1 Hz, 1H), 6.88 (t, *J* = 9.1 Hz, 1H), 6.16 (t, *J* = 6.2 Hz, 1H), 4.76 (dddd, *J* = 8.9, 6.7, 5.7, 3.3 Hz, 1H), 4.01 (t, *J* = 9.0 Hz, 1H), 3.92 – 3.85 (m, 2H), 3.80 – 3.65 (m, 2H), 3.61 (dt, *J* = 14.7, 6.1 Hz, 1H), 3.01 – 2.93 (m, 2H), 2.81 (s, 2H), 2.02 (s, 3H), 1.34 (s, 6H); **^{13}C NMR (101 MHz, $CDCl_3$)** δ 171.2, 155.6 (d, J_{CF} = 247.5 Hz), 154.45, 137.1 (d, J_{CF} = 9.1 Hz), 132.71 (d, J_{CF} = 10.1 Hz), 119.02 (d, J_{CF} = 4.0 Hz), 114.03 (d, J_{CF} = 4.0 Hz), 107.7 (d, J_{CF} = 133.3 Hz), 72.0, 71.6, 61.4, 60.89, 60.86, 50.5, 47.8, 42.1, 24.8, 23.3; δ **IR (Neat Film, NaCl)** 3300, 2971, 1748, 1659, 1517, 1415, 1366, 1325, 1272, 1224, 1194, 1100, 987, 862, 752 cm^{-1}; **HRMS (MM: ESI-APCI)** *m/z* calc'd for $C_{18}H_{25}FN_3O_4$ $[M+H]^+$: 366.1824, found 366.1827 **$[\alpha]_D^{22.8}$** –5.60 (c 0.5, $CHCl_3$).

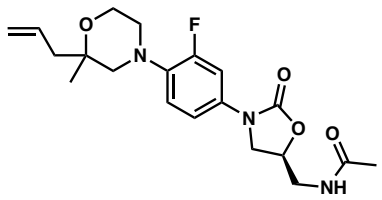

***N*-(((5*S*)-3-(4-(2-allyl-2-methylmorpholino)-3-fluorophenyl)-2-oxooxazolidin-5-yl)methyl)acetamide (2.13).** Prepared according to the general procedure using: CuBr (9.1 mg, 0.064 mmol, 0.3 equiv), BINOL (18 mg, 0.064 mmol, 0.3 equiv), aryl iodide **2.7** (80 mg, 0.21 mmol, 1 equiv), K_3PO_4 (90 mg, 0.42 mmol, 2 equiv), methallyl morpholine **2.10** (60 mg, 0.42 mmol, 2 equiv), and 1.1 mL DMF. The crude residue was purified by reverse phase preparatory HPLC (50 → 70% MeCN/H_2O gradient over 7 minutes, 30x250 mm C_{18} column, 60 mL/min flow rate) to yield methallyl analogue **2.13** (45 mg, 54% yield) as a light brown oil; **^{1}H NMR (400 MHz, $CDCl_3$)** δ 7.40 (dd, *J* = 14.1, 2.6 Hz, 1H), 7.04 (dd, *J* = 8.8, 2.6 Hz, 1H), 6.90 (t, *J* = 9.1 Hz, 1H), 6.74 (t, *J* = 6.2 Hz, 1H), 5.93 – 5.78 (m, 1H), 5.17 – 5.07 (m, 2H), 4.85 – 4.75 (m, 1H), 4.05 (t, *J* = 9.0 Hz, 1H), 3.91 (td, *J* = 4.6, 2.8 Hz, 2H), 3.81 – 3.59 (m, 3H), 3.05 – 2.95 (m, 2H), 2.90 (dd, *J* = 11.6, 1.1 Hz, 1H), 2.79 (dd, *J* = 11.6, 1.0 Hz, 1H), 2.66 (dd, *J* = 14.1, 7.1 Hz, 1H), 2.34 (ddt, *J* = 14.1, 7.5, 1.2 Hz, 1H), 2.07 (s, 3H), 1.29 (s, 3H): **^{13}C NMR (101 MHz, $CDCl_3$)** δ 172.9 (C=O), 155.6 (d, J_{CF} = 247.5 Hz), 154.9 (C=O), 137.1 (d, J_{CF} = 8.1 Hz), 133.4, 132.5 (d, J_{CF} = 10.1 Hz), 119.2 (d, J_{CF} = 4.0 Hz), 118.3, 114.3 (d, J_{CF} = 4.0 Hz), 107.9 (d, J_{CF} = 26.3 Hz), 73.5, 72.0, 61.1, 59.7, 50.4, 47.9, 42.3, 41.5, 22.9, 22.4; δ **IR (Neat Film, NaCl)** 3300, 3077, 2976, 2822, 1752, 1662, 1546, 1517, 1486, 1445, 1415, 1377, 1326, 1269, 1222, 1196, 1172, 1086, 995, 918, 867, 817, 750, 703 cm^{-1}; **HRMS (MM: ESI-APCI)** *m/z* calc'd for $C_{20}H_{27}FN_3O_4$ $[M+H]^+$: 392.1980, found 392.1976 **$[\alpha]_D^{23.0}$** –4.55 (c 1.0, $CHCl_3$).

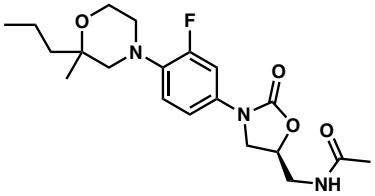

N-(((5*S*)-3-(3-fluoro-4-(2-methyl-2-propylmorpholino)phenyl)-2-oxooxazolidin-5-yl)methyl)acetamide (2.22). To a solution of methallyl analogue **2.13** (12 mg, 0.031 mmol, 1 equiv) in MeOH (300 uL, 0.1 M) was added Pd/C (10% wt/wt, 3.3 mg, 0.1 equiv). The reaction vial was evacuated and backfilled with H_2 three times, and then sparged with H_2 for 5 min. The reaction was stirred for 7 h and then the Pd/C was filtered off through a plug of celite, rinsing with EtOAc. The solution was concentrated under reduced pressure and purified by silica gel flash chromatography (2 → 5% MeOH/CH_2Cl_2) to yield the methyl-propyl analogue **2.22** as a clear oil (10 mg, 83% yield); **^{1}H NMR (400 MHz, Chloroform-*d*)** δ 7.41 (ddd, *J* = 14.2, 2.5, 0.9 Hz, 1H), 7.04 (ddq, *J* = 8.8, 2.6, 1.0 Hz, 1H), 6.89 (t, *J* = 9.1 Hz, 1H), 6.52 – 6.28 (m, 1H), 4.78 (dddd, *J* = 8.9, 6.6, 5.8, 3.2 Hz, 1H), 4.03 (t, *J* = 9.0 Hz, 1H), 3.86 (tdd, *J* = 11.6, 5.7, 4.3 Hz, 2H), 3.79 – 3.67 (m, 2H), 3.63 (dt, *J* = 14.7, 6.1 Hz, 1H), 3.05 – 2.92 (m, 2H), 2.83 (q, *J* = 11.5 Hz, 2H), 2.06 (s, 3H), 1.84 (ddd, *J* = 12.9, 10.3, 6.0 Hz, 1H), 1.55 – 1.31 (m, 3H), 1.29 (s, 3H), 0.95 (t, *J* = 7.2 Hz, 3H); **^{13}C NMR (101 MHz, $CDCl_3$)** δ 172.2, 155.6 (d, J_{CF} = 246.7 Hz), 154.6, 137.2 (d, J_{CF} = 8.8 Hz), 132.5 (d, J_{CF} = 10.3 Hz), 119.1 (d, J_{CF} = 4.2 Hz), 114.1 (d, J_{CF} = 3.3 Hz), 107.8 (d, J_{CF} = 26.3 Hz), 73.6, 71.9, 61.0, 60.1, 60.1, 50.4, 50.4, 47.8, 42.2, 39.6, 23.0, 22.0, 16.4, 14.8. **IR (Neat Film, NaCl)** 3297, 3074, 2957, 2872, 1753, 1659, 1517, 1485, 1448, 1414, 1377, 1326, 1278, 1226, 1195,

1101,1087, 994, 919, 867, 750 cm^{-1}; **HRMS (MM: ESI-APCI)** *m/z* calc'd for $C_{20}H_{29}FN_3O_4$ $[M+H]^+$: 394.2137, found 394.2147 $\mathbf{[\alpha]_D^{22.0}}$ –8.45 (c 0.7, $CHCl_3$).

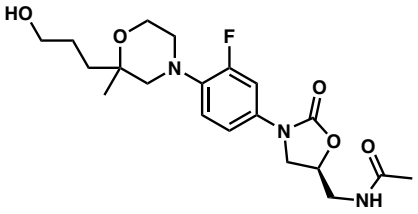

N-(((5S)-3-(3-fluoro-4-(2-(3-hydroxypropyl)-2-methylmorpholino)phenyl)-2-oxooxazolidin-5-yl)methyl)acetamide (2.20). In a glovebox, to a solution of methallyl analogue **2.13** (20 mg, 0.051 mmol, 1 equiv) in THF (500 uL, 0.1 M), was added 9-BBN dimer (25 mg, 0.10 mmol, 2 equiv). The reaction was stirred for 3 h at ambient temperature amd then taken out of the glovebox. Then, a solution of $NaBO_3 \cdot 4H_2O$ in H_2O (500 uL) was added and the mixture was stirred for 2 h before being concentrated down. The crude residue was purified by reverse phase preparatory HPLC (0 → 100% MeCN/H_2O gradient over 10 minutes, 30x250 mm C_{18} column, 60 mL/min flow rate) to yield hydroxyl analogue **2.20** (4 mg, 19% yield) as a clear oil; **^{13}C NMR (101 MHz, $CDCl_3$)** δ 172.0, 155.6 (d, *J* = 246.7 Hz), 154.6, 137.0 (d, *J* = 8.9 Hz), 132.7 (d, *J* = 10.4 Hz), 119.1 (dd, *J* = 4.1, 1.9 Hz), 114.1 (d, *J* = 3.3 Hz), 107.7 (d, *J* = 26.1 Hz), 73.6, 72.9, 71.9, 68.6, 63.4, 61.2, 61.1, 60.3, 60.3, 60.1, 60.1, 50.3, 50.2, 50.3, 47.8, 42.2, 34.8, 32.6, 26.3, 23.1, 22.2, 22.1, 21.4. **IR (Neat Film, NaCl)** 3314, 2937, 1783, 1747, 1666, 1517, 1486, 1416, 1379, 1223, 1168, 1100, 866, 820, 745, 667 cm^{-1}; **HRMS (MM: ESI-APCI)** *m/z* calc'd for $C_{20}H_{29}FN_3O_4$ $[M+H]^+$: 410.2086, found 410.2084 $\mathbf{[\alpha]_D^{24.3}}$ –6.35 (c 0.33, $CHCl_3$).

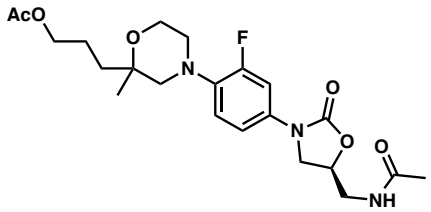

3-(4-(4-((*S*)-5-(acetamidomethyl)-2-oxooxazolidin-3-yl)-2-fluorophenyl)-2-methylmorpholin-2-yl)propyl acetate (**2.21**). To a solution of hydroxyl analogue **2.20** (4 mg, 1 equiv) in CH_2Cl_2 (200 uL, 0.05 M) was added NEt_3 (4 uL, 3 equiv) and AcCl (1 uL, 2 equiv). The solution was stirred at rt for 4 h, then concentrated, and purified by silica gel flash chromatography (3 → 5% MeOH/CH_2Cl_2) to give acetylated analogue **2.21** as a clear oil (3 mg, 68% yield). **1H NMR (400 MHz, Chloroform-*d*)** δ 7.42 (ddd, *J* = 14.2, 2.5, 0.9 Hz, 1H), 7.06 (dddt, *J* = 8.7, 2.7, 1.9, 1.0 Hz, 1H), 6.88 (t, *J* = 9.1 Hz, 1H), 6.11 (t, *J* = 6.3 Hz, 1H), 4.76 (dddd, *J* = 8.9, 6.6, 5.7, 3.2 Hz, 1H), 4.47 – 4.32 (m, 1H), 4.10 (td, *J* = 6.6, 5.2 Hz, 1H), 4.02 (t, *J* = 9.0 Hz, 1H), 3.88 – 3.80 (m, 2H), 3.76 – 3.66 (m, 2H), 3.65 – 3.58 (m, 1H), 2.97 (t, *J* = 4.9 Hz, 2H), 2.86 (d, *J* = 11.6 Hz, 1H), 2.80 (dd, *J* = 11.5, 1.6 Hz, 1H), 2.04 (d, *J* = 11.9 Hz, 6H), 1.86 (d, *J* = 6.7 Hz, 2H), 1.75 – 1.70 (m, 1H), 1.57 – 1.51 (m, 1H), 1.30 (d, *J* = 2.6 Hz, 3H); **^{13}C NMR (101 MHz, $CDCl_3$)** δ 171.0, 171.2, 156.8, 154.4, 136.9 (dd, J_{CF} = 12.6, 9.0 Hz), 132.8 (t, J_{CF} = 10.5 Hz), 119.1 (t, J_{CF} = 3.5 Hz), 114.0 (d, J_{CF} = 3.3 Hz), 107.6 (d, J_{CF} = 26.2 Hz), 73.0, 71.9, 68.7, 65.0, 61.1, 60.1, 50.3, 47.8, 42.1, 23.2, 22.6, 22.1, 21.1. **IR (Neat Film, NaCl)** 3311, 3063, 2962, 1747, 1667, 1516, 1415, 1371, 1222,1169, 1087, 1036, 919, 867, 803, 737, 703 cm^{-1}; **HRMS (MM: ESI-APCI)** *m/z* calc'd for $C_{22}H_{31}FN_3O_6$ $[M+H]^+$: 452.2191, found 452.2185 **$[\alpha]_D^{24.0}$** +3.67 (c .33, $CHCl_3$).

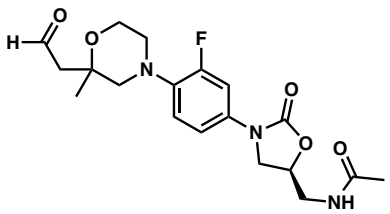

***N*-(((5*S*)-3-(3-fluoro-4-(2-methyl-2-(2-oxoethyl)morpholino)phenyl)-2-oxooxazolidin-5-yl)methyl)acetamide** (**SI4**). To a solution of methallyl analogue **2.13** (54 mg, 1 equiv) in 2:1 THF/H_2O (14 mL, 0.01 M) was added a solution of OsO_4 in PhMe (87 uL, 0.079 M, 0.05 equiv) followed by NaIO4 (89 mg, 3 equiv) The reaction was stirred for 16 h at ambient temperature, and was then quenched with $Na_2S_2O_3$. The mixture was extracted with EtOAc (5x) and the combined organic layers were dried over Na_2SO_4. The residue was purified by silica gel chromatography (10 → 20% → 30% MeOH/CH_2Cl_2) to yield dimethylamino analogue **SI4** (15 mg, 94% yield) as a yellow oil. **^{1}H NMR (400 MHz, Chloroform-*d*)** δ 9.89 (t, *J* = 2.9 Hz, 1H), 7.42 (dd, *J* = 14.1, 2.6 Hz, 1H), 7.06 (ddd, *J* = 8.8, 2.6, 1.2 Hz, 1H), 6.89 (t, *J* = 9.1 Hz, 1H), 6.21 (t, *J* = 6.2 Hz, 1H), 4.76 (dddd, *J* = 8.9, 6.7, 5.7, 3.3 Hz, 1H), 4.07 – 3.78 (m, 3H), 3.78 – 3.56 (m, 3H), 3.10 – 3.02 (m, 2H), 3.02 – 2.89 (m, 2H), 2.82 (d, *J* = 11.7 Hz, 1H), 2.63 (dd, *J* = 15.4, 2.9 Hz, 1H), 2.02 (s, 3H), 1.44 (s, 3H); **^{13}C NMR (101 MHz, $CDCl_3$)** δ 201.9, 171.2, 155.7 (d, *J* = 246.5 Hz), 154.4, 136.4 (d, *J* = 9.1 Hz), 133.2 (d, *J* = 10.4 Hz), 119.3 (d, *J* = 3.9 Hz), 114.0 (d, *J* = 3.3 Hz), 107.6 (d, *J* = 26.1 Hz), 72.7, 72.0, 61.4, 60.0, 50.3, 49.5, 47.7, 42.0, 23.7, 23.2; **IR (Neat Film, NaCl)** 3316, 2937, 1748, 1659, 1517, 1415,1379,1279, 1225,1085, 868, 751 cm^{-1}; **HRMS (MM: ESI-APCI)** *m/z* calc'd for $C_{19}H_{25}FN_3O_5$ $[M+H]^+$: 394.1773, found 394.1770 **$[\alpha]_D^{25.3}$** +3.97 (c .47, $CHCl_3$).

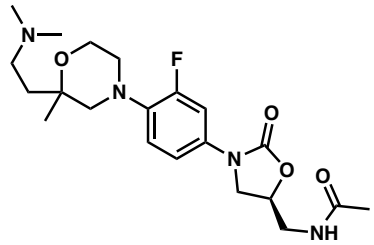

N-(((5S)-3-(4-(2-(2-(dimethylamino)ethyl)-2-methylmorpholino)-3-fluorophenyl)-2-oxooxazolidin-5-yl)methyl)acetamide (2.23). To a solution of aldehyde **SI4** (15 mg, 0.038 mmol, 1 equiv) in THF (400 uL, 0.1 M) was added dimethylamine (95 uL, 0.19 mmol, 5 equiv) and AcOH (2 uL, 0.038 mmol, 1 equiv). The solution was stirred for 5 min, and then $NaBH(OAc)_3$ (16 mg, 0.076 mmol, 2 equiv) was added. The reaction was stirred for 3 h at ambient temperature, and was then concentrated onto SiO_2. The silica loaded crude residue was purified by silica gel chromatography (10 → 20% → 30% MeOH/CH_2Cl_2) to yield dimethylamino analogue **2.23** (15 mg, 94% yield) as a clear oil; **^{1}H NMR (600 MHz, $CDCl_3$)** δ 7.41 (dt, *J* = 14.1, 2.8 Hz, 1H), 7.05 (dt, *J* = 9.0, 2.7 Hz, 1H), 6.86 (t, *J* = 9.1 Hz, 1H), 6.43 (t, *J* = 6.2 Hz, 1H), 4.76 (dtd, *J* = 9.3, 6.2, 3.4 Hz, 1H), 4.00 (t, *J* = 8.9 Hz, 1H), 3.84 (h, *J* = 6.8 Hz, 2H), 3.75 (dd, *J* = 9.1, 6.6 Hz, 1H), 3.68 (ddd, *J* = 14.6, 6.2, 3.4 Hz, 1H), 3.60 (dt, *J* = 14.6, 6.1 Hz, 1H), 3.02 – 2.92 (m, 4H), 2.86 (d, *J* = 11.6 Hz, 1H), 2.80 (d, *J* = 11.6 Hz, 1H), 2.66 (s, 6H), 2.46 – 2.38 (m, 1H), 2.01 (d, *J* = 8.8 Hz, 3H), 1.91 – 1.82 (m, 1H), 1.32 (s, 3H); **^{13}C NMR (101 MHz, $CDCl_3$)** δ 171.38, 155.62 (d, *J* = 246.1 Hz), 154.49, 136.54 (d, *J* = 9.1 Hz), 133.13 (d, *J* = 10.5 Hz), 119.19 (d, *J* = 4.0 Hz), 114.05 (d, *J* = 3.2 Hz), 107.60 (d, *J* = 26.3 Hz), 72.2, 72.0, 61.3, 60.1, 53.0, 50.25, 47.8, 43.2, 42.1, 31.3, 23.2, 22.3. **IR (Neat Film, NaCl)** 3250, 2924, 2270, 1750, 1669, 1554, 1517, 1484, 1413, 1381, 1325, 1278, 1226,1195, 1097, 993,

867,749, 674 cm^{-1}; **HRMS (MM: ESI-APCI)** *m/z* calc'd for $C_{21}H_{32}FN_4O_4$ $[M+H]^+$: 423.2402, found 423.2393 $\mathbf{[\alpha]_D^{24.0}}$ –3.59 (c 1.0, $CHCl_3$).

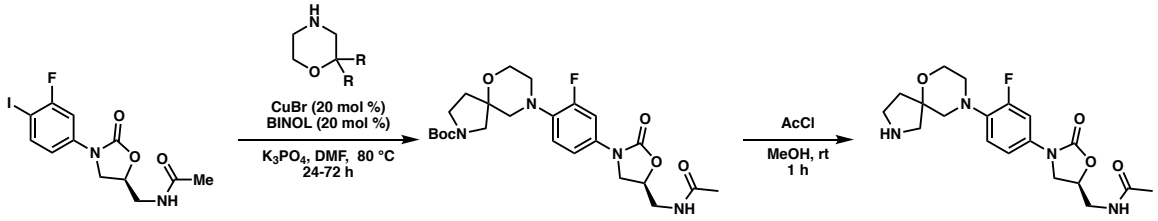

N-(((5S)-3-(3-fluoro-4-(6-oxa-2,9-diazaspiro[4.5]decan-9-yl)phenyl)-2-oxooxazolidin-5-yl)methyl)acetamide (**2.27**). Prepared according to the general procedure using: CuBr (2.3 mg, 0.016 mmol, 0.2 equiv), BINOL (4.5 mg, 0.016 mmol, 0.2 equiv), aryl iodide **2.7** (30 mg, 0.079 mmol, 1 equiv), K_3PO_4 (34 mg, 0.16 mmol, 2 equiv), 6-oxa-2,9-diazaspiro[4.5]decane (38 mg, 0.16 mmol, 2 equiv), and 400 uL DMF. The crude residue was filtered through a silica column (2 → 3 → 5 → 10% MeOH/CH_2Cl_2) to yield a mixture of Boc-protected spirocyclic analogue **2.15** and starting material aryl iodide **2.7**, which was carried forward to the next step: To 2.3 mL MeOH at 0 °C was added AcCl (230 uL), generating HCl *in situ*. This HCl solution was stirred for 5 min at 0°C and then transferred by syringe into a 20 mL scintillation vial containing Boc analogue **2.15**. The reaction was stirred for 1 h at ambient temperature and then the solvent was concentrated under reduced pressure onto SiO_2. The silica-loaded residue was purified by silica gel flash chromatography (5 → 10 → 20% MeOH/CH_2Cl_2) to yield spiropyrrolidine analogue **2.27** as a light yellow oil (12 mg, 40% yield over 2 steps). **^{1}H NMR (400 MHz, CD_3OD)** δ 7.53 (dd, *J* = 14.5, 2.5 Hz, 1H), 7.19 (ddd, *J* = 8.8, 2.6, 1.0 Hz, 1H), 7.08 (t, *J* = 9.2 Hz, 1H), 4.83 – 4.73 (m, 1H), 4.12 (t, *J* = 9.0 Hz, 1H), 3.94 (dd, *J* = 5.4, 4.3 Hz, 2H), 3.80 (dd, *J* = 9.2, 6.3 Hz, 1H), 3.72 (dd, *J* = 12.6, 1.6 Hz, 1H), 3.56 (d, *J* = 5.0 Hz, 2H), 3.50 – 3.40 (m, 2H), 3.26 (d, *J* = 12.6 Hz, 1H), 3.17 (d, *J* = 11.8 Hz, 1H), 3.13 –

2.97 (m, 3H), 2.42 – 2.29 (m, 1H), 2.17 – 2.00 (m, 2H), 1.96 (s, 3H); **^{13}C NMR (101 MHz, CD_3OD)** δ 174.1, 156.9 (d, *J* = 244.3 Hz), 156.6, 137.2 (d, *J* = 10.1 Hz), 135.5 (d, *J* = 10.6 Hz), 120.7 (d, *J* = 4.0 Hz), 115.5 (d, *J* = 3.0 Hz), 108.4 (d, *J* = 26.3 Hz), 82.2, 73.5, 63.5, 57.5, 52.6, 51.5, 49.2, 45.3, 43.1, 34.5, 22.4 (Note: A ^{1}H-^{13}C HSQC experiment revealed the chemical shift of a methylene carbon to be at 49.2 ppm, obscured by MeOD resonance); **IR (Neat Film, NaCl)** 3287, 2924, 2282, 1754, 1667, 1548, 1516, 1415, 1377, 1325, 1278, 1226, 1083, 989, 869, 751 cm^{-1}; **HRMS (MM: ESI-APCI)** *m/z* calc'd for $C_{19}H_{26}FN_4O_4$ $[M+H]^+$: 393.1933, found 393.1937 **$[\alpha]_D^{24.2}$** –3.78 (c 0.5, MeOH).

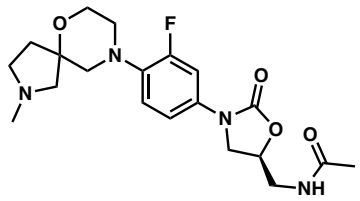

***N*-(((5*S*)-3-(3-fluoro-4-(2-methyl-6-oxa-2,9-diazaspiro[4.5]decan-9-yl)phenyl)-2-oxooxazolidin-5-yl)methyl)acetamide (2.17)**. Prepared according to the general procedure using: CuBr (2.3 mg, 0.2 equiv), BINOL (4.6 mg, 0.2 equiv), aryl iodide **2.7** (30 mg, 1 equiv), K_3PO_4 (34 mg, 2 equiv), **2-methyl-6-oxa-2,9-diazaspiro[4.5]decane (SI5)** (25 mg, 2 equiv), and 400 uL DMF. The crude residue was purified by silica gel flash chromatography (5 → 10 → 20 MeOH/CH_2Cl_2) to yield *N*-methyl spiropyrrolidine analogue **2.17** (15 mg, 47% yield) as a light yellow oil; **^{1}H NMR (400 MHz, $CDCl_3$)** δ 7.45 (dd, *J* = 14.1, 2.6 Hz, 1H), 7.08 (ddd, *J* = 8.8, 2.6, 1.1 Hz, 1H), 6.90 (t, *J* = 9.0 Hz, 1H), 6.05 (t, *J* = 6.2 Hz, 1H), 4.77 (dddd, *J* = 8.9, 6.7, 5.9, 3.3 Hz, 1H), 4.02 (td, *J* = 9.0, 0.8 Hz, 1H), 3.95 – 3.81 (m, 2H), 3.79 – 3.66 (m, 2H), 3.60 (dt, *J* = 14.7, 6.1 Hz, 1H),

3.25 (s, 1H), 3.11 (d, J = 11.6 Hz, 2H), 3.01 (t, J = 10.5 Hz, 5H), 2.66 (s, 3H), 2.20 (m, 2H), 2.02 (s, 3H); **^{13}C NMR (101 MHz, $CDCl_3$)** δ 171.1, 155.8 (d, J = 246.5 Hz), 154.4, 136.0 (d, J = 9.1 Hz), 133.6 (d, J = 10.4 Hz), 119.4 (d, J = 3.7 Hz), 114.0 (d, J = 3.4 Hz), 107.6 (d, J = 26.2 Hz), 81.7, 72.0, 63.4, 62.8, 57.84, 55.0, 50.4, 47.8, 42.4, 42.1, 35.4, 23.3; **IR (Neat Film, NaCl)** 3264, 2925, 2283, 1747, 1666, 1516, 1444, 1377, 1325, 1225, 1082, 869, 752 cm^{-1}; **HRMS (MM: ESI-APCI)** *m/z* calc'd for $C_{20}H_{28}FN_4O_4$ $[M+H]^+$: 407.2089, found 407.2095; **$[\alpha]_D^{24.8}$** –6.65 (c 1.0, MeOH).

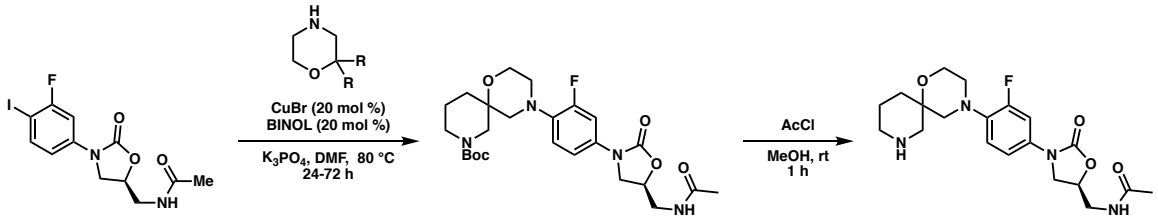

N-(((5S)-3-(3-fluoro-4-(1-oxa-4,8-diazaspiro[5.5]undecan-4-yl)phenyl)-2-oxooxazolidin-5-yl)methyl)acetamide (2.25). Prepared according to the general procedure using: CuBr (2.1 mg, 0.015 mmol, 0.2 equiv), BINOL (4.2 mg, 0.015 mmol, 0.2 equiv), aryl iodide **2.7** (28 mg, 0.074 mmol, 1 equiv), K_3PO_4 (31 mg, 0.15 mmol, 2 equiv), *tert*-butyl 1-oxa-4,8-diazaspiro[5.5]undecane-8-carboxylate (38 mg, 0.15 mmol, 2 equiv), and 370 uL DMF. The crude residue was filtered through a silica column (40% $MeCN/CH_2Cl_2$) to yield a mixture of Boc-protected spirocyclic analogue **2.16** and starting material aryl iodide **2.7**, which was carried forward to the next step: To 2.2 mL MeOH at 0 °C was added AcCl (220 uL), generating HCl *in situ*. This HCl solution was stirred for 5 min at 0°C and then transferred by syringe into a 20 mL scintillation vial containing Boc analogue **2.16**. The reaction was stirred for 1 h at ambient temperature and then the solvent was concentrated under reduced pressure onto SiO_2. The silica-

loaded residue was purified by silica gel flash chromatography (1 → 2 → 5 → 10 → 100% MeOH/CH_2Cl_2 with 1% NH_4OH) to yield spiropiperidine analogue **2.25** as a light yellow oil (12 mg, 32% yield over two steps): **^{1}H NMR (600 MHz, CD_3OD)** δ 7.51 (dd, *J* = 14.4, 2.5 Hz, 1H), 7.18 (ddd, *J* = 8.8, 2.6, 1.0 Hz, 1H), 7.06 (t, *J* = 9.2 Hz, 1H), 4.83 – 4.77 (m, 1H), 4.14 (t, *J* = 9.0 Hz, 1H), 3.98 (ddd, *J* = 11.4, 8.0, 3.2 Hz, 1H), 3.91 (ddd, *J* = 11.9, 5.0, 3.4 Hz, 1H), 3.88 – 3.80 (m, 2H), 3.56 (d, *J* = 5.1 Hz, 2H), 3.38 – 3.32 (m, 2H), 3.13 – 3.06 (m, 1H), 3.06 – 2.97 (m, 4H), 2.86 (d, *J* = 12.0 Hz, 1H), 2.20 – 2.14 (m, 1H), 2.14 – 2.01 (m, 1H), 1.97 (s, 3H), 1.81 – 1.76 (m, 1H), 1.63 (td, *J* = 13.7, 4.3 Hz, 1H); **^{13}C NMR (101 MHz, $CDCl_3$)** δ 171.3, 155.6 (d, *J* = 246.3 Hz), 154.6, 136.8 (d, *J* = 9.0 Hz), 133.0 (d, *J* = 10.4 Hz), 119.2 (d, *J* = 5.6 Hz), 114.0 (t, *J* = 3.8 Hz), 107.6 (d, *J* = 26.1 Hz), 72.1, 69.8, 60.9, 58.5, 50.7, 47.8, 46.13, 42.1, 31.6, 29.8, 23.3, 21.3; **IR (Neat Film, NaCl)** 3275, 2931, 2359, 1748, 1668, 1540, 1517, 1417, 1374, 1286, 1224, 1195, 1084, 867, 732 cm^{-1}; **HRMS (MM: ESI-APCI)** *m/z* calc'd for $C_{20}H_{28}FN_4O_4$ $[M+H]^+$: 407.2089, found 407.2080 **$[\alpha]_D^{25.2}$** –5.83 (c 0.8, $CHCl_3$).

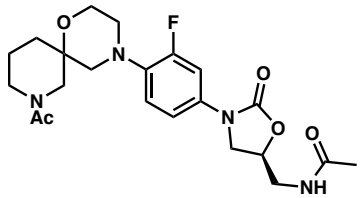

***N*-(((5*S*)-3-(4-(8-acetyl-1-oxa-4,8-diazaspiro[5.5]undecan-4-yl)-3-fluorophenyl)-2-oxooxazolidin-5-yl)methyl)acetamide (2.26)**. To a solution of spiropiperidine **2.25** (12 mg, 1 equiv) in MeCN was added NEt_3 (12 uL, 3 equiv) followed by DMAP (0.4 mg, 0.1 equiv), and then Ac_2O (4 uL, 1.5 equiv). The reaction was stirred at rt for 2 h, concentrated, and then purified by silica gel flash chromatography (2 → 5 → 10%

MeOH/CH_2Cl_2) to afford acetylated analogue **2.26** as a clear oil (10 mg, 77% yield). **^{1}H NMR (400 MHz, Chloroform-*d*)** δ 7.42 (dddd, *J* = 20.9, 14.2, 2.6, 1.6 Hz, 1H), 7.05 (ttd, *J* = 8.8, 2.6, 1.1 Hz, 1H), 6.94 – 6.82 (m, 1H), 6.34 – 6.17 (m, 1H), 4.86 (dd, *J* = 14.0, 6.1 Hz, 1H), 4.81 – 4.70 (m, 1H), 4.11 (ddd, *J* = 12.0, 8.9, 3.0 Hz, 1H), 4.05 – 3.82 (m, 2H), 3.82 – 3.43 (m, 6H), 3.23 – 2.64 (m, 5H), 2.15 – 2.05 (m, 3H), 2.02 (s, 3H), 1.89 – 1.83 (m, 1H), 1.74 – 1.66 (m, 2H), 1.60 – 1.50 (m, 1H); **^{13}C NMR (101 MHz, $CDCl_3$)** δ (Note: multiple peaks observed due to the presence of rotamers) 171.2, 171.2, 169.9, 169.3, 156.9, 156.8, 154.5, 154.4, 136.8, 136.7, 136.7, 136.6, 136.4, 136.3, 133.5, 133.4, 132.9, 132.8, 119.4, 119.4, 119.2, 114.0, 114.0, 113.9, 107.7, 107.6, 107.5, 107.4, 107.3, 72.0, 71.9, 71.2, 70.8, 61.6, 61.3, 58.3, 56.5, 51.4, 51.1, 51.1, 50.3, 47.7, 47.3, 45.9, 45.8, 42.3, 42.1, 42.1, 42.1, 33.1, 33.0, 23.2, 21.7, 21.4, 20.9; **IR (Neat Film, NaCl)** cm^{-1}; **HRMS (MM: ESI-APCI)** *m/z* calc'd for $C_{22}H_{30}FN_4O_5$ $[M+H]^+$: 449.2195, found 449.2193 **$[\alpha]_D^{24.4}$** –11.08 (c 0.7, $CHCl_3$).

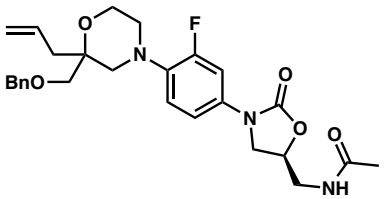

N-(((5*S*)-3-(4-(2-allyl-2-((benzyloxy)methyl)morpholino)-3-fluorophenyl)-2-oxooxazolidin-5-yl)methyl)acetamide (2.14). Prepared according to the general procedure using: CuBr (2.3 mg, 0.016 mmol, 0.2 equiv), BINOL (4.5 mg, 0.016 mmol, 0.2 equiv), aryl iodide **2.7** (30 mg, 0.079 mmol, 1 equiv), K_3PO_4 (34 mg, 0.16 mmol, 2 equiv), benzyloxy morpholine[6] (18 mg, 0.16 mmol, 2 equiv), and 400 uL DMF. The crude residue was purified by silica gel flash chromatography (2 → 3 → 5% MeOH/CH_2Cl_2) to yield benzyloxy analogue **2.14** (8 mg, 28% yield) as a clear oil: **^{1}H**

NMR (400 MHz, $CDCl_3$) δ 7.46 – 7.34 (m, 1H), 7.33 (d, *J* = 4.4 Hz, 3H), 7.33 – 7.23 (m, 1H), 7.04 (dd, *J* = 8.8, 1.8 Hz, 1H), 6.88 (t, *J* = 9.1 Hz, 1H), 6.29 (t, *J* = 6.1 Hz, 1H), 5.82 (ddt, *J* = 17.5, 10.3, 7.3 Hz, 1H), 5.15 – 5.04 (m, 2H), 4.76 (qd, *J* = 7.8, 6.6, 5.0 Hz, 1H), 4.56 (s, 2H), 4.05 – 3.49 (m, 7H), 3.06 – 2.87 (m, 4H), 2.77 (dt, *J* = 15.0, 7.5 Hz, 1H), 2.46 (dd, *J* = 14.3, 7.6 Hz, 1H), 2.01 (m, 3H); **^{13}C NMR (101 MHz, $CDCl_3$)** δ 171.4, 155.7 (d, *J* = 246.7 Hz), 154.5, 138.4, 137.0 (d, *J* = 9.0 Hz), 133.3, 132.9 (d, *J* = 10.3 Hz), 128.5, 127.8, 127.7, 119.3 (d, *J* = 4.0 Hz), 118.3, 114.0 (d, *J* = 3.3 Hz), 107.6 (d, *J* = 26.1 Hz), 74.9, 73.7, 72.0, 71.0, 61.4, 56.1, 50.5, 47.8, 42.1, 37.2, 23.2; **IR (Neat Film, NaCl)** 3288, 2921, 2364, 1749, 1654, 1516, 1416, 1373, 1324, 1274, 1224, 1103, 747 cm^{-1}; **HRMS (MM: ESI-APCI)** *m/z* calc'd for $C_{27}H_{33}FN_3O_5$ $[M+H]^+$: 498.2399, found 498.2393 **$[\alpha]_D^{22.6}$** –3.54 (c 1.0, $CHCl_3$).

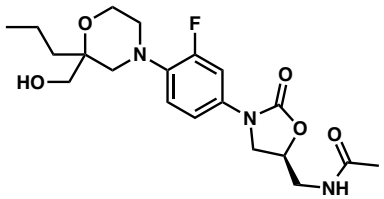

***N*-(((5*S*)-3-(4-(2-allyl-2-((benzyloxy)methyl)morpholino)-3-fluorophenyl)-2-oxooxazolidin-5-yl)methyl)acetamide** (**2.24**). In a 1 dram vial open to the air, benzyloxy analogue **2.14** (20 mg, 0.04 mmol, 1 equiv) was dissolved in MeOH (400 uL, 0.1M). $Pd(OH)_2/C$ (20 wt. %, 4.2 mg, 0.006 mmol, 0.15 equiv) was then added. The vial was then sealed with a septum cap and evacuated and filled using a balloon containing H_2 three times. The solvent was then sparged with H_2 for 5 min and stirred for 16 h until TLC analysis showed the starting material had been consumed. The $Pd(OH)_2/C$ was filtered off using a Celite plug and rinsed with EtOAc. The solvent was concentrated

under reduced pressure onto SiO_2. The silica-loaded residue was purified by silica gel flash chromatography (2 → 3 → 10% MeOH/CH_2Cl_2) to yield hydroxyl analogue **2.24** (14 mg, 88% yield) as a clear oil: **^{1}H NMR (400 MHz, $CDCl_3$)** δ 7.42 (dt, *J* = 14.1, 2.4 Hz, 1H), 7.05 (dtd, *J* = 8.9, 2.4, 1.1 Hz, 1H), 6.90 (t, *J* = 9.1 Hz, 1H), 6.27 (t, *J* = 6.3 Hz, 1H), 4.77 (dddd, *J* = 8.9, 6.7, 5.6, 3.3 Hz, 1H), 4.01 (t, *J* = 9.0 Hz, 1H), 3.92 (t, *J* = 4.9 Hz, 2H), 3.79 – 3.70 (m, 2H), 3.74 – 3.63 (m, 2H), 3.61 (dt, *J* = 14.7, 6.0 Hz, 1H), 3.07 – 2.97 (m, 2H), 2.99 – 2.85 (m, 2H), 2.02 (s, 3H), 1.83 (ddd, *J* = 14.0, 11.6, 5.6 Hz, 1H), 1.60 (ddd, *J* = 14.0, 11.1, 5.8 Hz, 1H), 1.44 – 1.21 (m, 2H), 0.94 (t, *J* = 7.3 Hz, 3H); **^{13}C NMR (101 MHz, $CDCl_3$)** δ 171.3, 155.7 (d, *J* = 246.4 Hz), 154.5, 136.9 (d, *J* = 9.1 Hz), 133.1 (d, *J* = 10.4 Hz), 119.3 (d, *J* = 4.0 Hz), 114.0 (d, *J* = 2.5 Hz), 107.6 (d, *J* = 26.2 Hz), 75.3, 72.0, 64.8, 61.42, 55.4, 50.4, 47.8, 42.1, 35.3, 23.3, 16.4, 14.9; **IR (Neat Film, NaCl)** 3316, 2957, 1747,1659, 1547, 1516, 1416, 1375, 1268, 1229, 1090, 743 cm^{-1}; **HRMS (MM: ESI-APCI)** *m/z* calc'd for $C_{20}H_{29}FN_3O_5$ $[M+H]^+$: 410.2086, found 410.2086 **$[\alpha]_D^{22.3}$** –11.50 (c 1.0, $CHCl_3$).

2.5 REFERENCES AND NOTES

(1) Lovering, F.; Bikker, J.; Humblet, C. Escape from Flatland: Increasing Saturation as an Approach to Improving Clinical Success. *J. Med. Chem.* **2009**, *52* (21), 6752–6756.

(2) Lovering, F. Escape from Flatland 2: Complexity and Promiscuity. *Med. Chem. Commun.* **2013**, *4* (3), 515–519.

(3) Vitaku, E.; Smith, D. T.; Njardarson, J. T. Analysis of the Structural Diversity, Substitution Patterns, and Frequency of Nitrogen Heterocycles among U.S. FDA Approved Pharmaceuticals. *J. Med. Chem.* **2014**, *57* (24), 10257–10274.

(4) Wishart, D. S.; Feunang, Y. D.; Guo, A. C.; Lo, E. J.; Marcu, A.; Grant, J. R.; Sajed, T.; Johnson, D.; Li, C.; Sayeeda, Z.; et al. DrugBank 5.0: A Major Update to the DrugBank Database for 2018. *Nucleic Acids Res.* **2018**, *46* (D1), D1074–D1082.

(5) Behenna, D. C.; Liu, Y.; Yurino, T.; Kim, J.; White, D. E.; Virgil, S. C.; Stoltz, B. M. Enantioselective Construction of Quaternary *N*-Heterocycles by Palladium-Catalysed Decarboxylative Allylic Alkylation of Lactams. *Nature Chemistry* **2012**, *4* (2), 130–133.

(6) Numajiri, Y.; Jiménez-Osés, G.; Wang, B.; Houk, K. N.; Stoltz, B. M. Enantioselective Synthesis of Dialkylated *N* -Heterocycles by Palladium-Catalyzed Allylic Alkylation. *Org. Lett.* **2015**, *17* (5), 1082–1085.

(7) Korch, K. M.; Eidamshaus, C.; Behenna, D. C.; Nam, S.; Horne, D.; Stoltz, B. M. Enantioselective Synthesis of α-Secondary and α-Tertiary Piperazin-2-Ones and Piperazines by Catalytic Asymmetric Allylic Alkylation. *Angew. Chem. Int. Ed.* *54* (1), 179–183.

(8) Sun, A. W.; Hess, S. N.; Stoltz, B. M. Enantioselective Synthesis of Gem-Disubstituted N-Boc Diazaheterocycles via Decarboxylative Asymmetric Allylic Alkylation. *Chem. Sci.* **2019**, *10*, 788–792.

(9) Swaney, S. M.; Aoki, H.; Ganoza, M. C.; Shinabarger, D. L. The Oxazolidinone Linezolid Inhibits Initiation of Protein Synthesis in Bacteria. *Antimicrobial Agents and Chemotherapy* **1998**, *42* (12), 3251–3255.

(10) Ender, M.; McCallum, N.; Adhikari, R.; Berger-Bächi, B. Fitness Cost of SCCmec and Methicillin Resistance Levels in Staphylococcus Aureus. *Antimicrob. Agents Chemother.* **2004**, *48*, 2295–2297.

(11) Gonzales, R. D.; Schreckenberger, P. C.; Graham, M. B.; Kelkar, S.; DenBesten, K.; Quinn, J. P. Infections Due to Vancomycin-Resistant Enterococcus Faecium Resistant to Linezolid. *The Lancet* **2001**, *357* (9263), 1179.

(12) Schecter, G. F.; Scott, C.; True, L.; Raftery, A.; Flood, J.; Mase, S. Linezolid in the Treatment of Multidrug-Resistant Tuberculosis. *Clin Infect Dis* **2010**, *50* (1), 49–55.

(13) Leach, K. L.; Swaney, S. M.; Colca, J. R.; McDonald, W. G.; Blinn, J. R.; Thomasco, L. M.; Gadwood, R. C.; Shinabarger, D.; Xiong, L.; Mankin, A. S. The Site of Action of Oxazolidinone Antibiotics in Living Bacteria and in Human Mitochondria. *Molecular Cell* **2007**, *26* (3), 393–402.

(14) Sharma, M. R.; Koc, E. C.; Datta, P. P.; Booth, T. M.; Spremulli, L. L.; Agrawal, R. K. Structure of the Mammalian Mitochondrial Ribosome Reveals an Expanded Functional Role for Its Component Proteins. *Cell* **2003**, *115* (1), 97–108.

(15) Narita, M.; Tsuji, B. T.; Yu, V. L. Linezolid-Associated Peripheral and Optic Neuropathy, Lactic Acidosis, and Serotonin Syndrome. *Pharmacotherapy* **2007**, *27*, 1189–1197.

(16) Duewelhenke, N.; Krut, O.; Eysel, P. Influence on Mitochondria and Cytotoxicity of Different Antibiotics Administered in High Concentrations on Primary Human Osteoblasts and Cell Lines. *Antimicrob. Agents Chemother.* **2007**, *51*, 54–63.

(17) Li, C.-H.; Cheng, Y.-W.; Liao, P.-L.; Yang, Y.-T.; Kang, J.-J. Chloramphenicol Causes Mitochondrial Stress, Decreases ATP Biosynthesis, Induces Matrix Metalloproteinase-13 Expression, and Solid-Tumor Cell Invasion. *Toxicol Sci* **2010**, *116* (1), 140–150.

(18) Shaw, K. J.; Barbachyn, M. R. The Oxazolidinones: Past, Present, and Future. *Ann. N. Y. Acad. Sci.* **2011**, *1241*, 48–70.

(19) McKee, E. E.; Ferguson, M.; Bentley, A. T.; Marks, T. A. Inhibition of Mammalian Mitochondrial Protein Synthesis by Oxazolidinones. *Antimicrob. Agents Chemother.* **2006**, *50* (6), 2042–2049.

(20) Ippolito, J. A.; Kanyo, Z. F.; Wang, D.; Franceschi, F. J.; Moore, P. B.; Steitz, T. A.; Duffy, E. M. Crystal Structure of the Oxazolidinone Antibiotic Linezolid Bound to the 50S Ribosomal Subunit. *J. Med. Chem.* **2008**, *51* (12), 3353–3356.

(21) Imbordino, R.; Perrault, W.; Reeder, M. Process for Preparing Linezolid. WO/2007/116284, October 19, 2007.

(22) Yang, B.; Shi, L.; Wu, J.; Fang, X.; Yang, X.; Wu, F. Microwave-Assisted Expeditious Synthesis of 5-Fluoroalkyl-3-(Aryl/Alkyl)-Oxazolidin-2-Ones. *Tetrahedron* **2013**, *69* (15), 3331–3337.

(23) Mahy, W.; Leitch, J. A.; Frost, C. G. Copper Catalyzed Assembly of N-Aryloxazolidinones: Synthesis of Linezolid, Tedizolid, and Rivaroxaban. *Eur. J. Org. Chem. 2016* (7), 1305–1313.

(24) McCarthy, J. R. A Convenient Synthesis of the Antibacterial Agent Linezolid. *Tetrahedron Lett.* **2015**, *56* (49), 6846–6847.

(25) Im, W. B.; Choi, S. H.; Park, J.-Y.; Choi, S. H.; Finn, J.; Yoon, S.-H. Discovery of Torezolid as a Novel 5-Hydroxymethyl-Oxazolidinone Antibacterial Agent. *Eur. J. Med. Chem.* **2011**, *46* (4), 1027–1039.

(26) Perrault, W. R.; Pearlman, B. A.; Godrej, D. B.; Jeganathan, A.; Yamagata, K.; Chen, J. J.; Lu, C. V.; Herrinton, P. M.; Gadwood, R. C.; Chan, L.; et al. The Synthesis of N-Aryl-5(S)-Aminomethyl-2-Oxazolidinone Antibacterials and Derivatives in One Step from Aryl Carbamates. *Org. Process Res. Dev.* **2003**, *7* (4), 533–546.

(27) Spaulding, A.; Takrouri, K.; Mahalingam, P.; Cleary, D. C.; Cooper, H. D.; Zucchi, P.; Tear, W.; Koleva, B.; Beuning, P. J.; Hirsch, E. B.; et al. Compound Design Guidelines for Evading the Efflux and Permeation Barriers of Escherichia Coli with the Oxazolidinone Class of Antibacterials: Test Case for a General Approach to Improving Whole Cell Gram-Negative Activity. *Bioorg. Med. Chem. Lett.* **2017**, *27*, 5310–5321.

(28) Marziale, A. N.; Duquette, D. C.; Craig, R. A.; Kim, K. E.; Liniger, M.; Numajiri, Y.; Stoltz, B. M. An Efficient Protocol for the Palladium-Catalyzed Asymmetric Decarboxylative Allylic Alkylation Using Low Palladium Concentrations and a Palladium(II) Precatalyst. *Adv. Synth. Cat.* **2015**, *357*, 2238–2245.

(29) Behenna, D. C.; Stoltz, B. M. The Enantioselective Tsuji Allylation. *J. Am. Chem. Soc.* **2004**, *126* , 15044–15045.

(30) Tani, K.; Behenna, D. C.; McFadden, R. M.; Stoltz, B. M. A Facile and Modular Synthesis of Phosphinooxazoline Ligands. *Org. Lett.* **2007**, *9*, 2529–2531.

APPENDIX 6

Spectra Relevant to Chapter 2:

gem-Disubstituted Morpholine Analogues of Linezolid

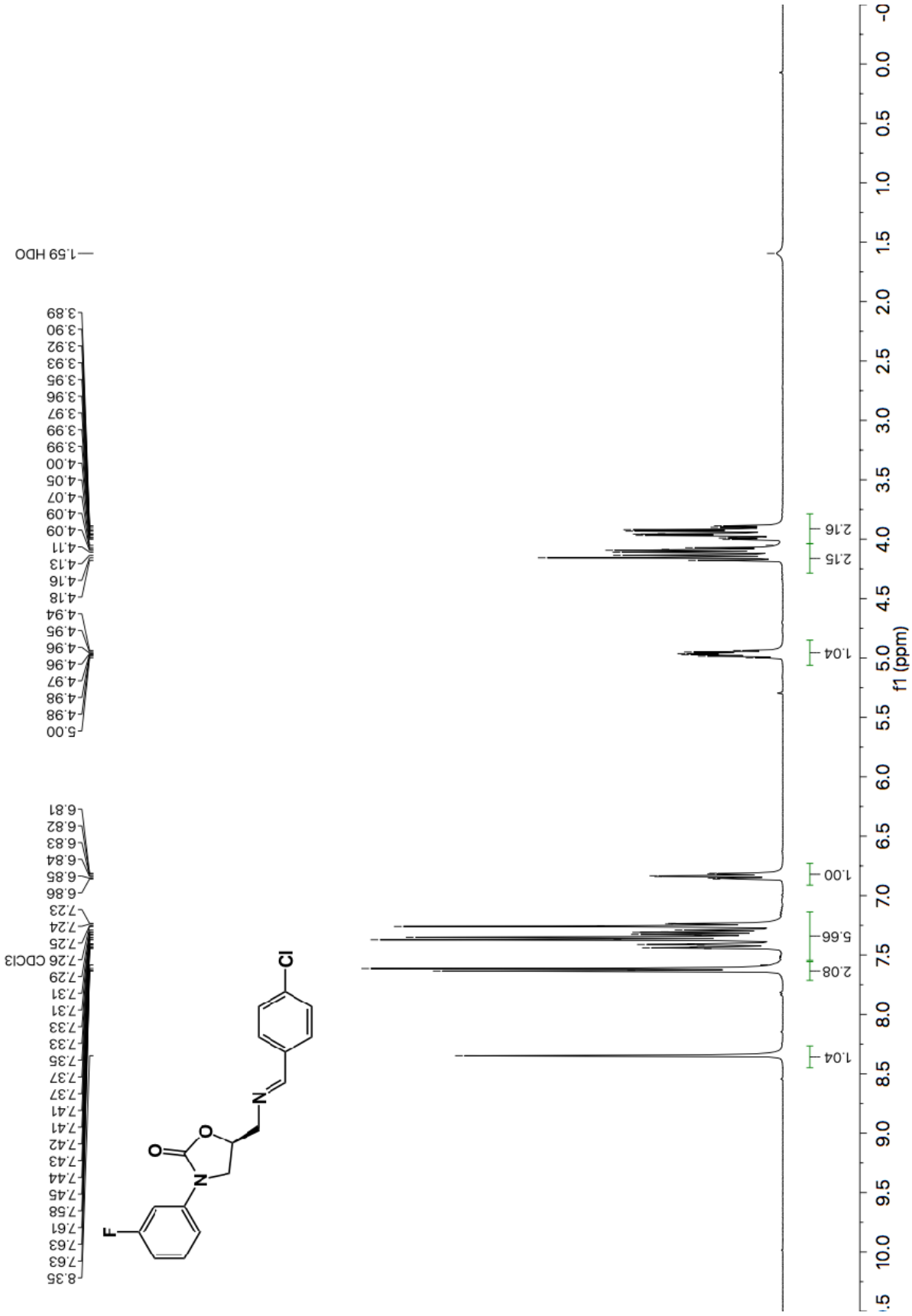

Figure A6.1 *^1H NMR (400 MHz, $CDCl_3$) of compound* ***2.5***

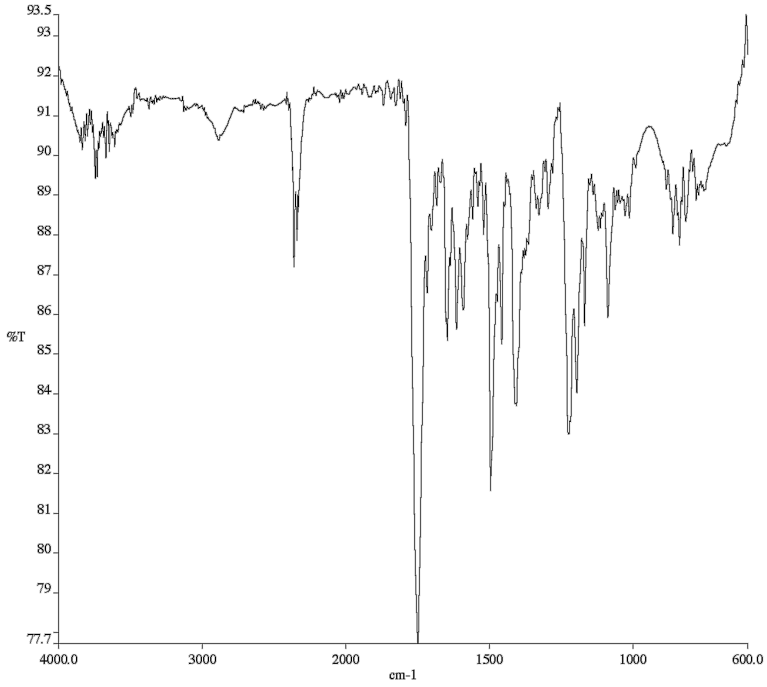

Figure A6.2 *Infrared spectrum (Thin Film, NaCl) of compound* ***2.5***

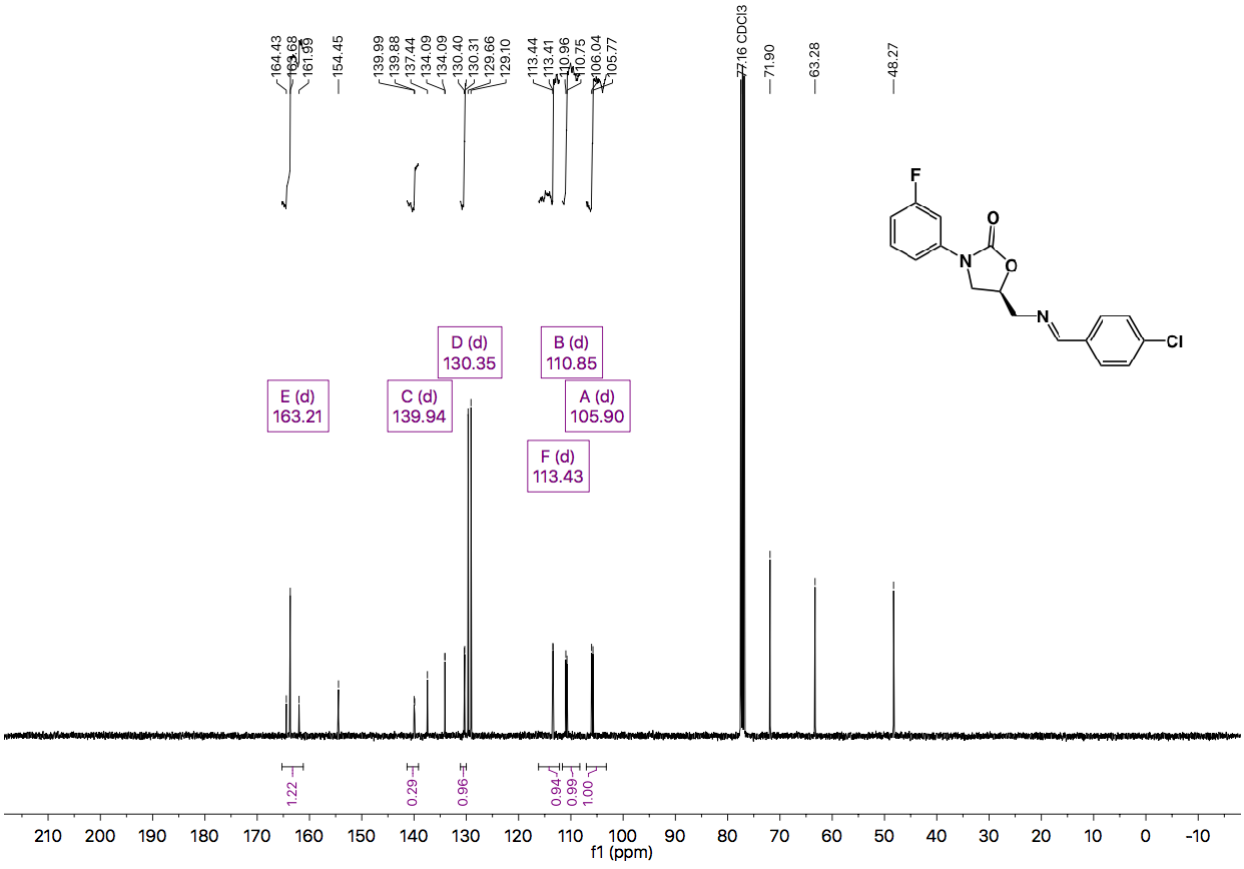

Figure A6.3 *^{13}C NMR (101 MHz, $CDCl_3$) of compound* ***2.5***

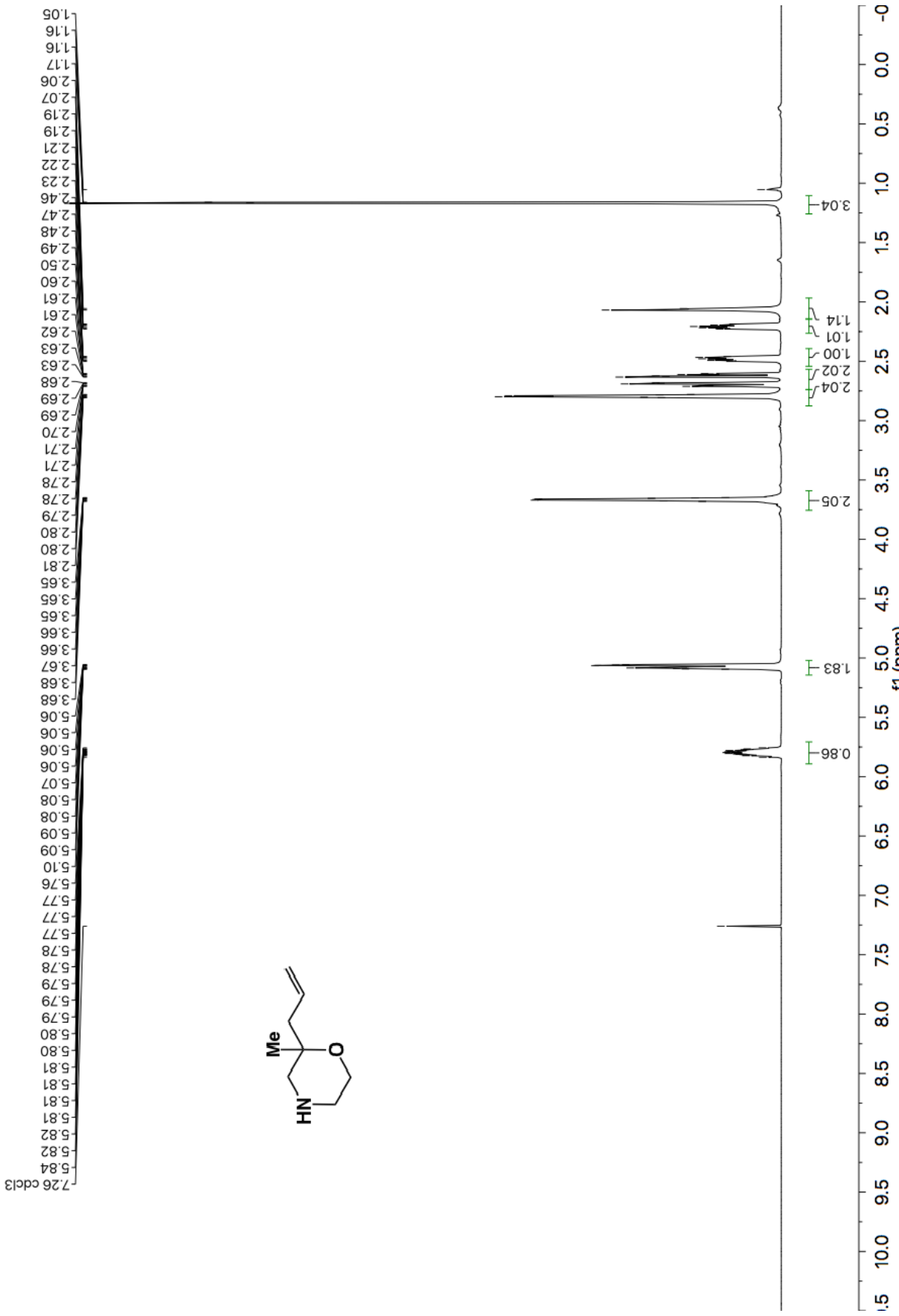

Figure A6.4 *^{1}H NMR (600 MHz, $CDCl_3$) of compound **2.10**.*

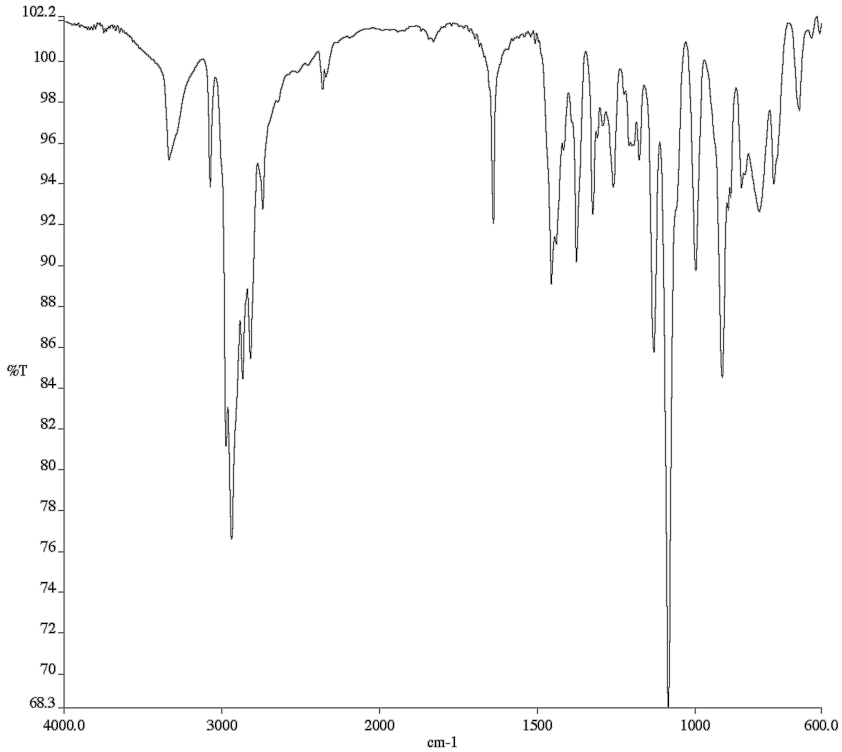

Figure A6.5 *Infrared spectrum (Thin Film, NaCl) of compound* ***2.10.***

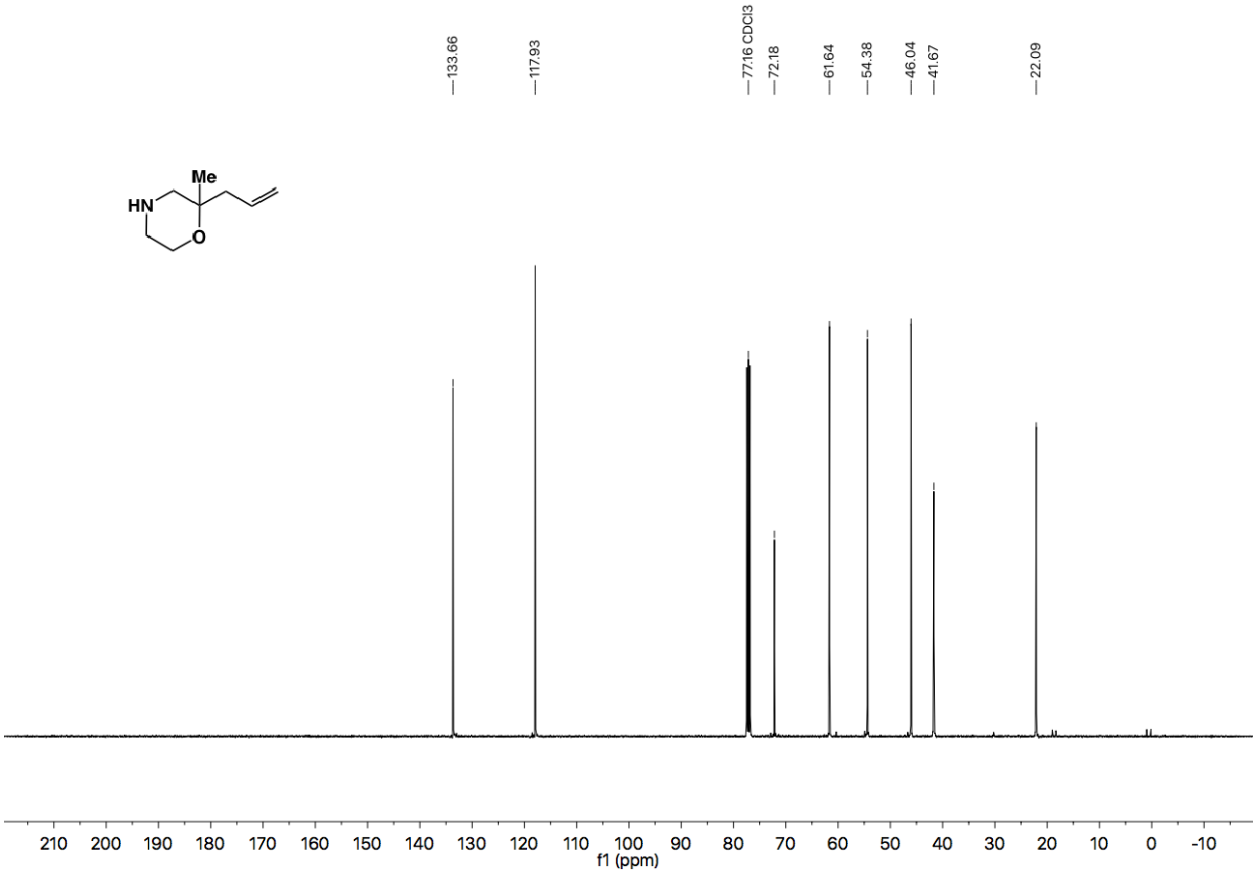

Figure A6.6 *^{13}C NMR (101 MHz, $CDCl_3$) of compound* ***2.10****.*

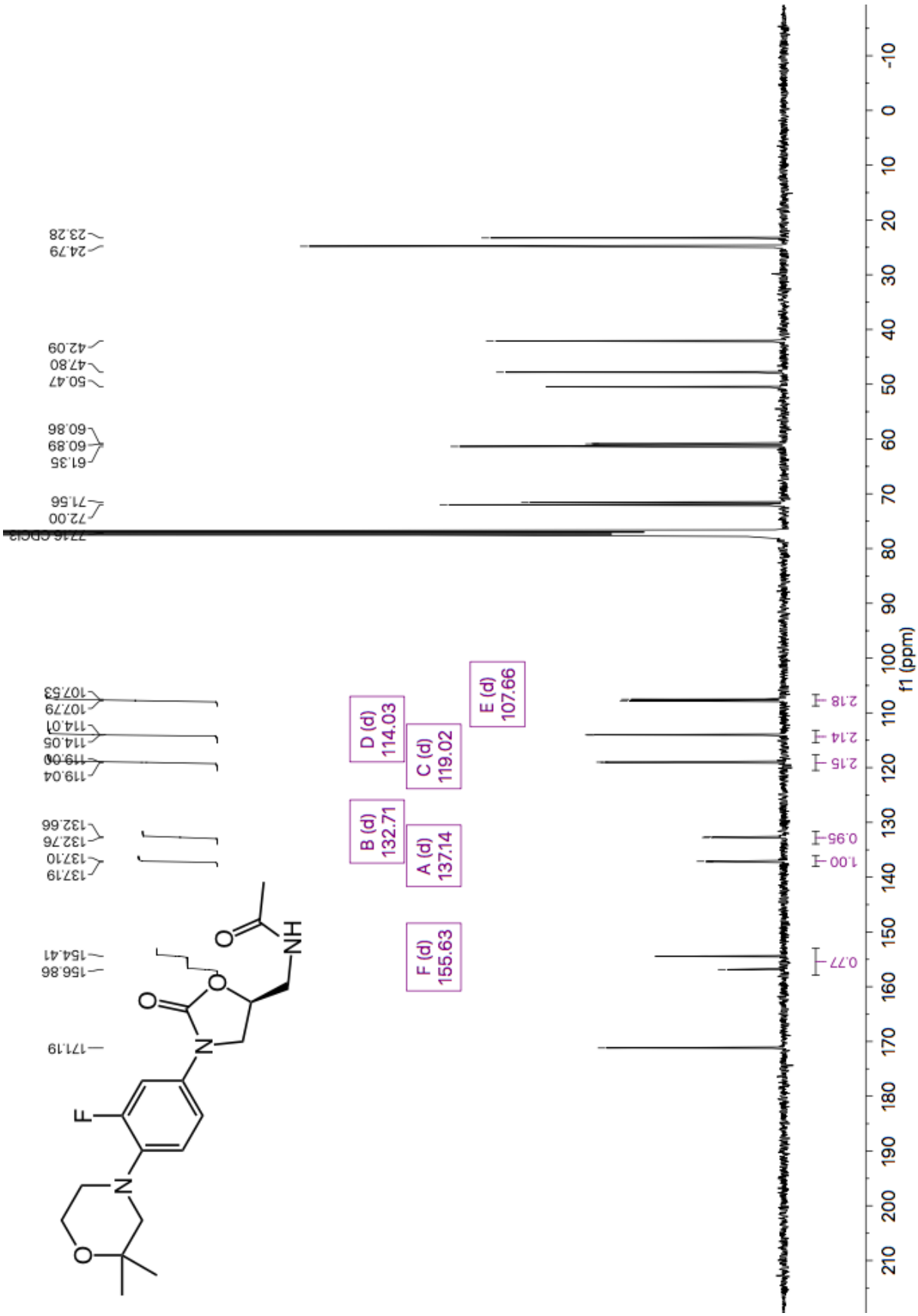

Figure A6.7 *^{1}H NMR (400 MHz, $CDCl_3$) of compound* ***2.12***

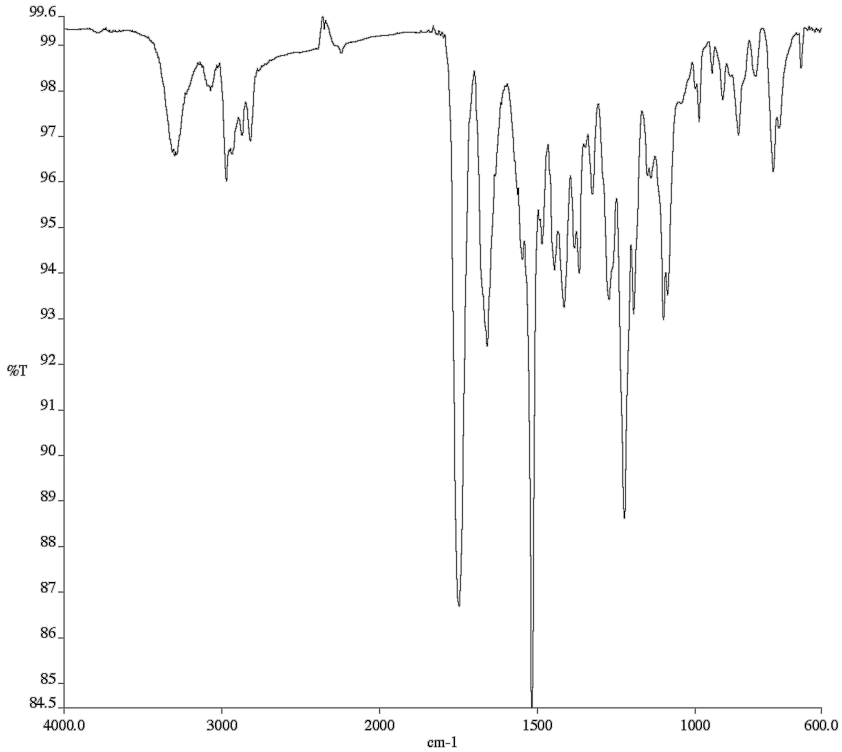

Figure A6.8 *Infrared spectrum (Thin Film, NaCl) of compound* ***2.12.***

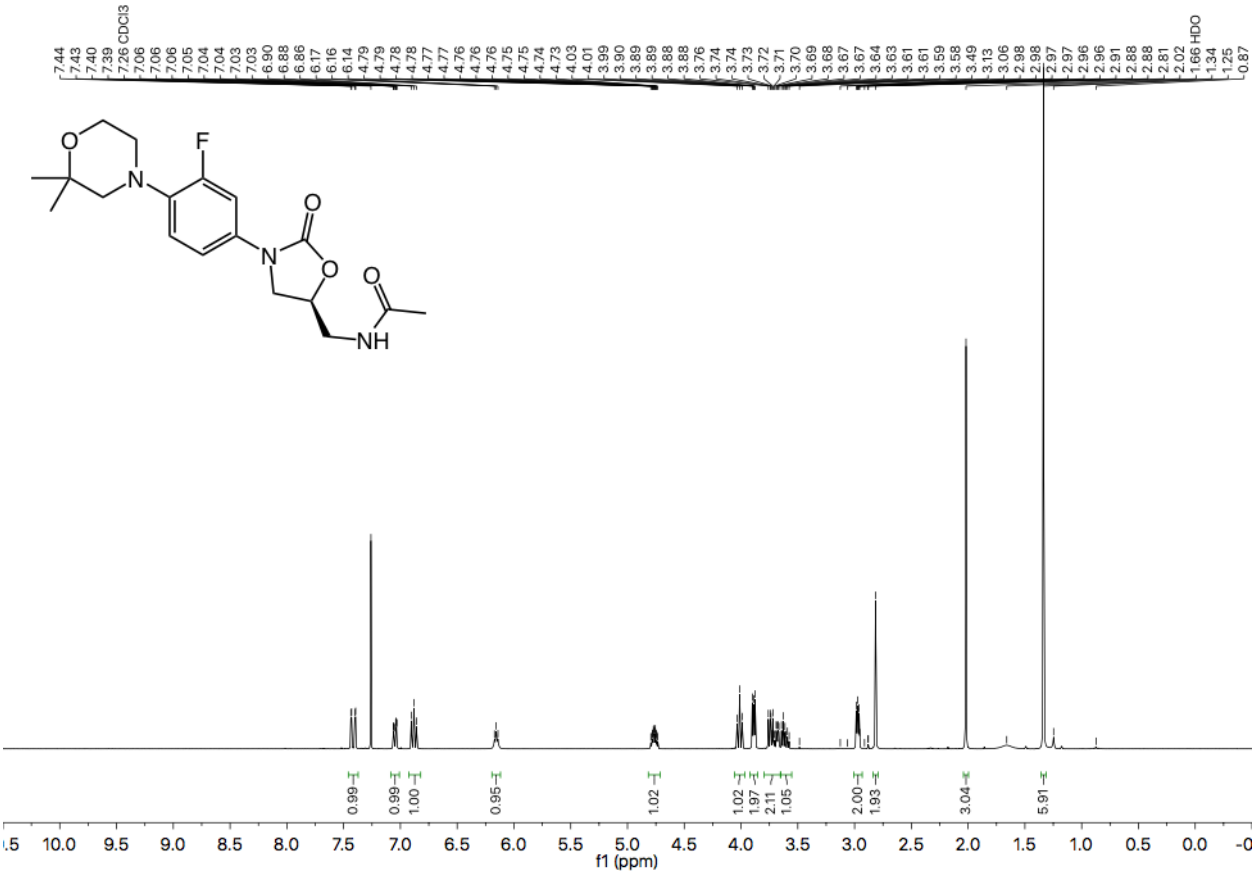

Figure A6.9 *^{13}C NMR (101 MHz, $CDCl_3$) of compound* ***2.12****.*

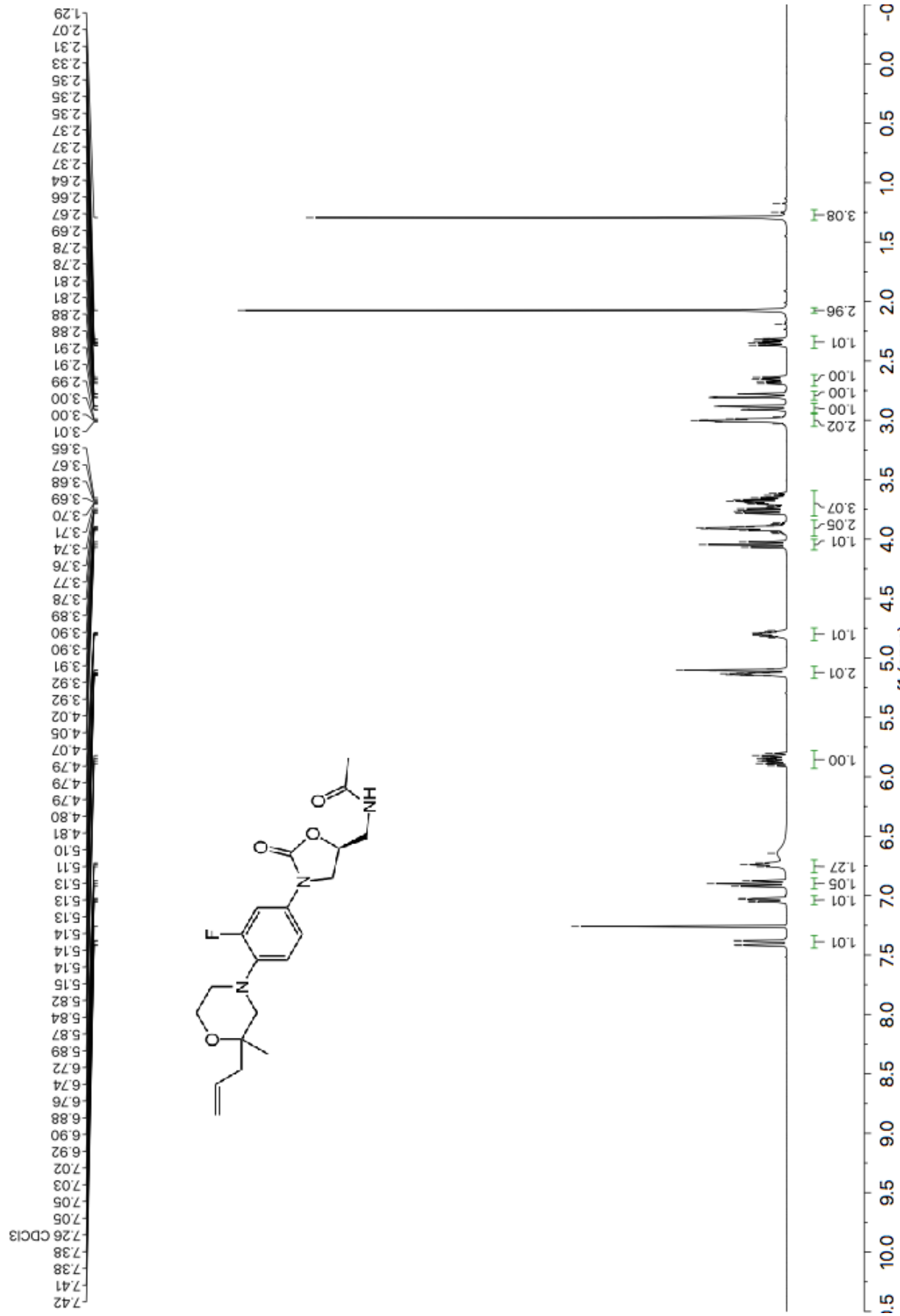

Figure A6.10 *^1H NMR (400 MHz, $CDCl_3$) of compound* ***2.13.***

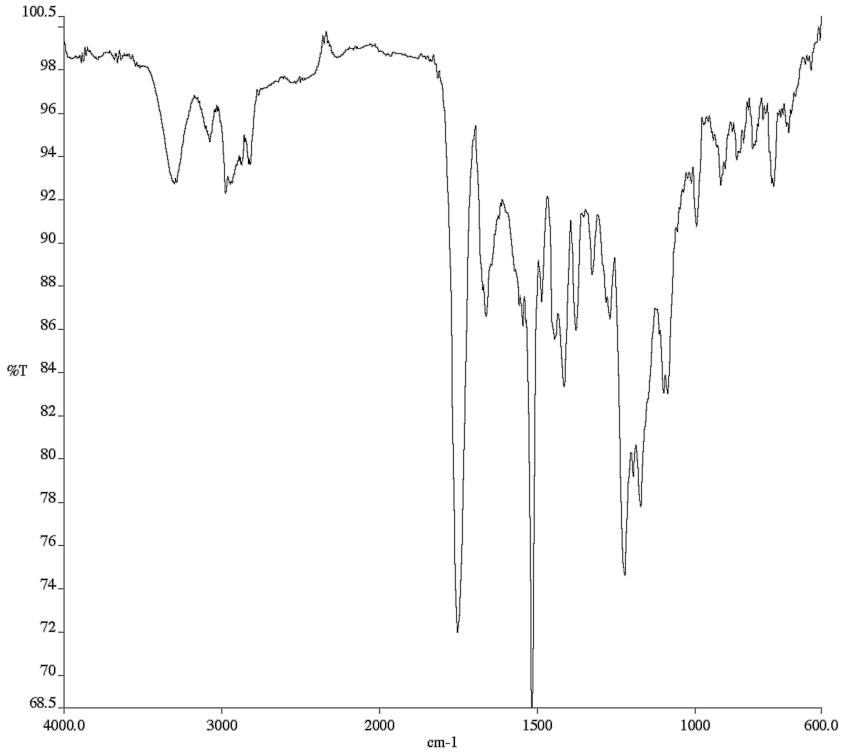

Figure A6.11 *Infrared spectrum (Thin Film, NaCl) of compound* ***2.13****.*

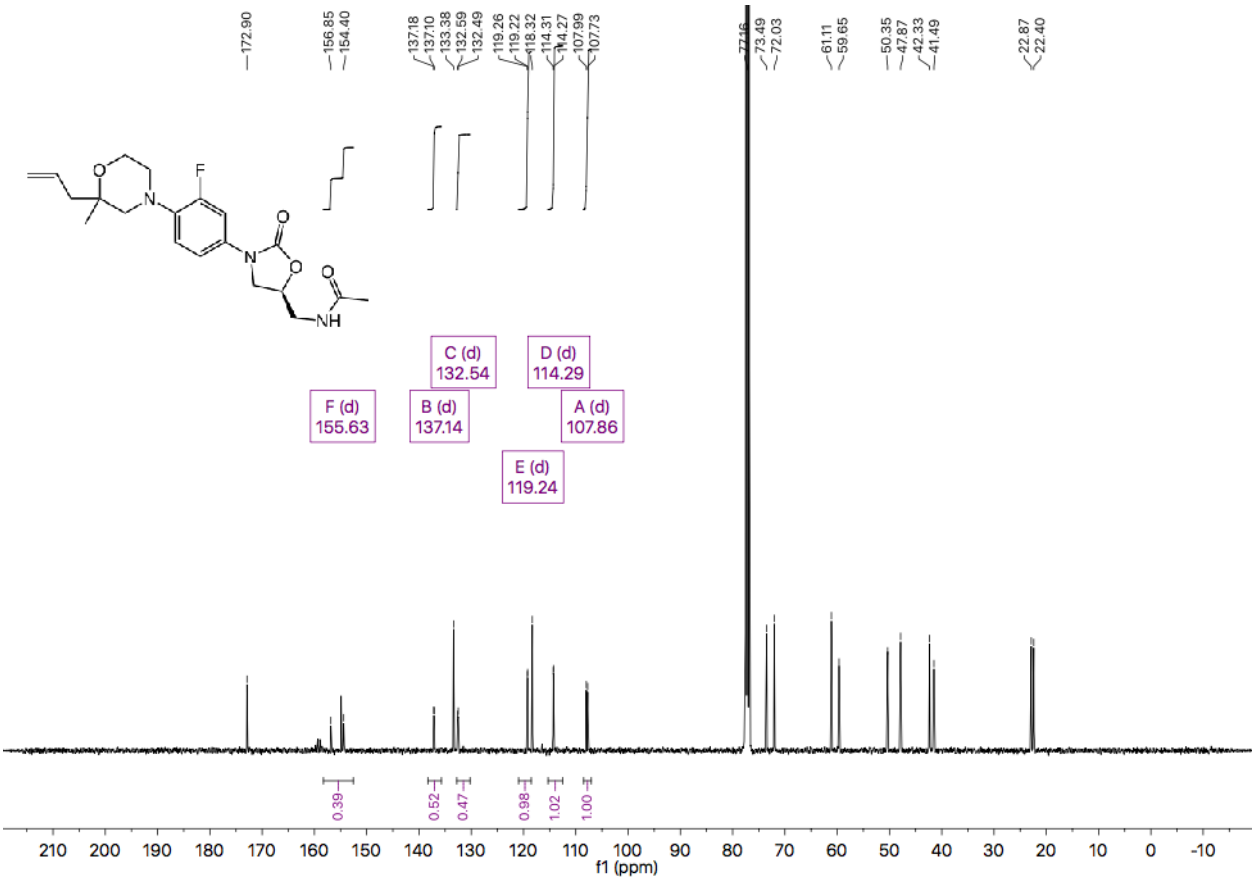

Figure A6.12 *^{13}C NMR (101 MHz, $CDCl_3$) of compound* ***2.13****.*

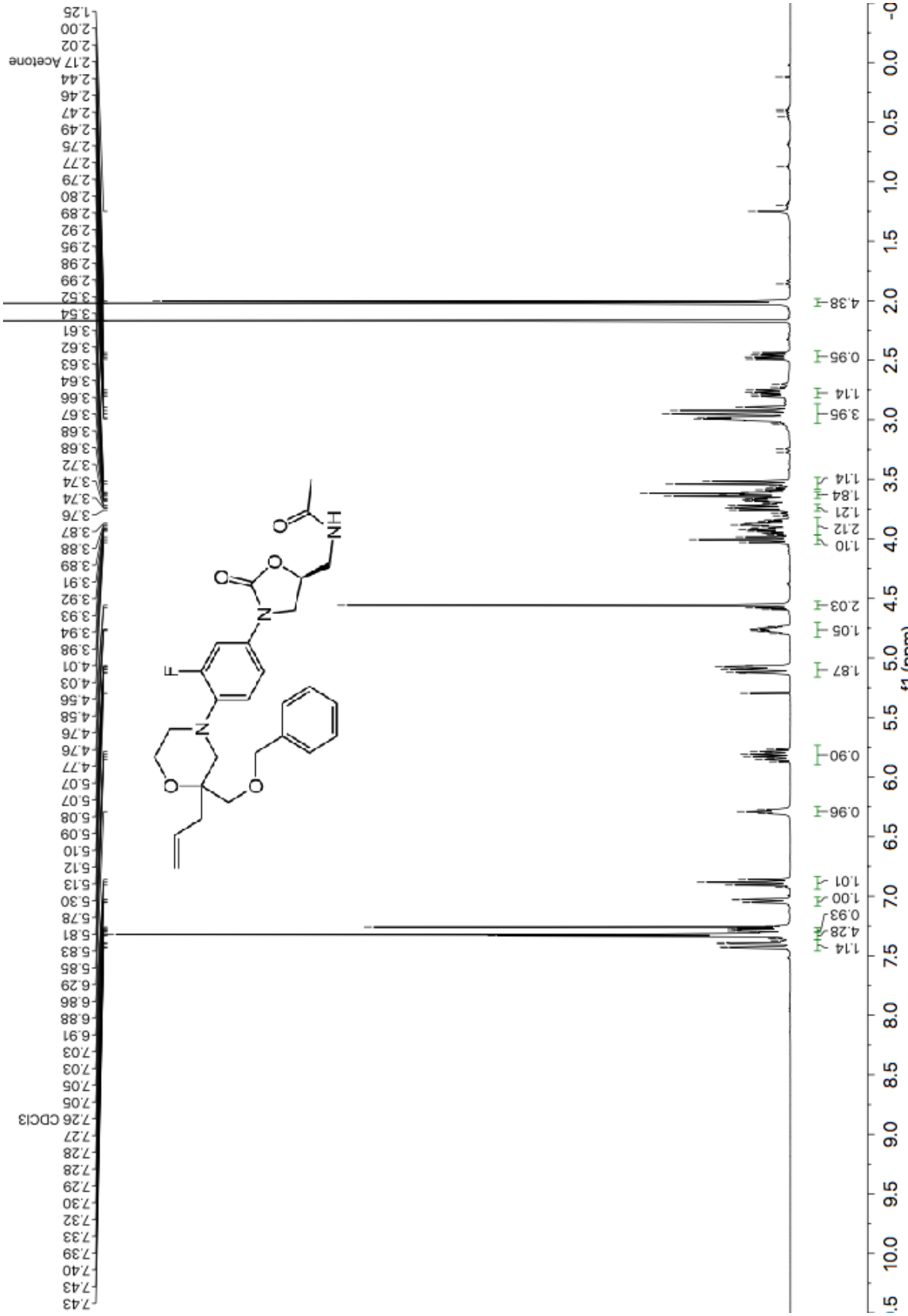

Figure A6.13 *^{1}H NMR (400 MHz, $CDCl_3$) of compound* ***2.14.***

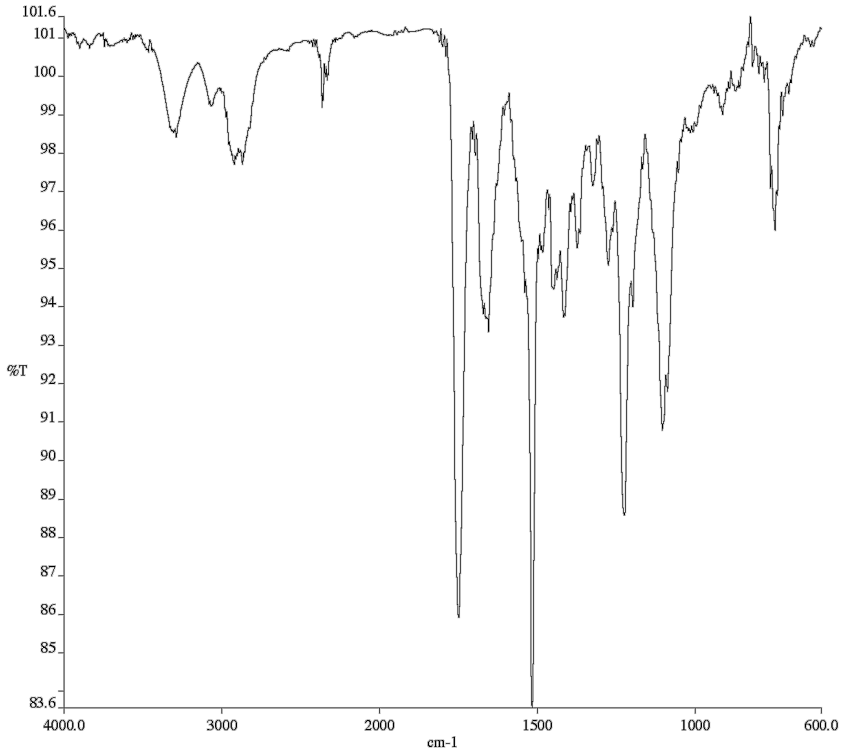

Figure A6.14 Infrared spectrum (Thin Film, NaCl) of compound **2.14**.

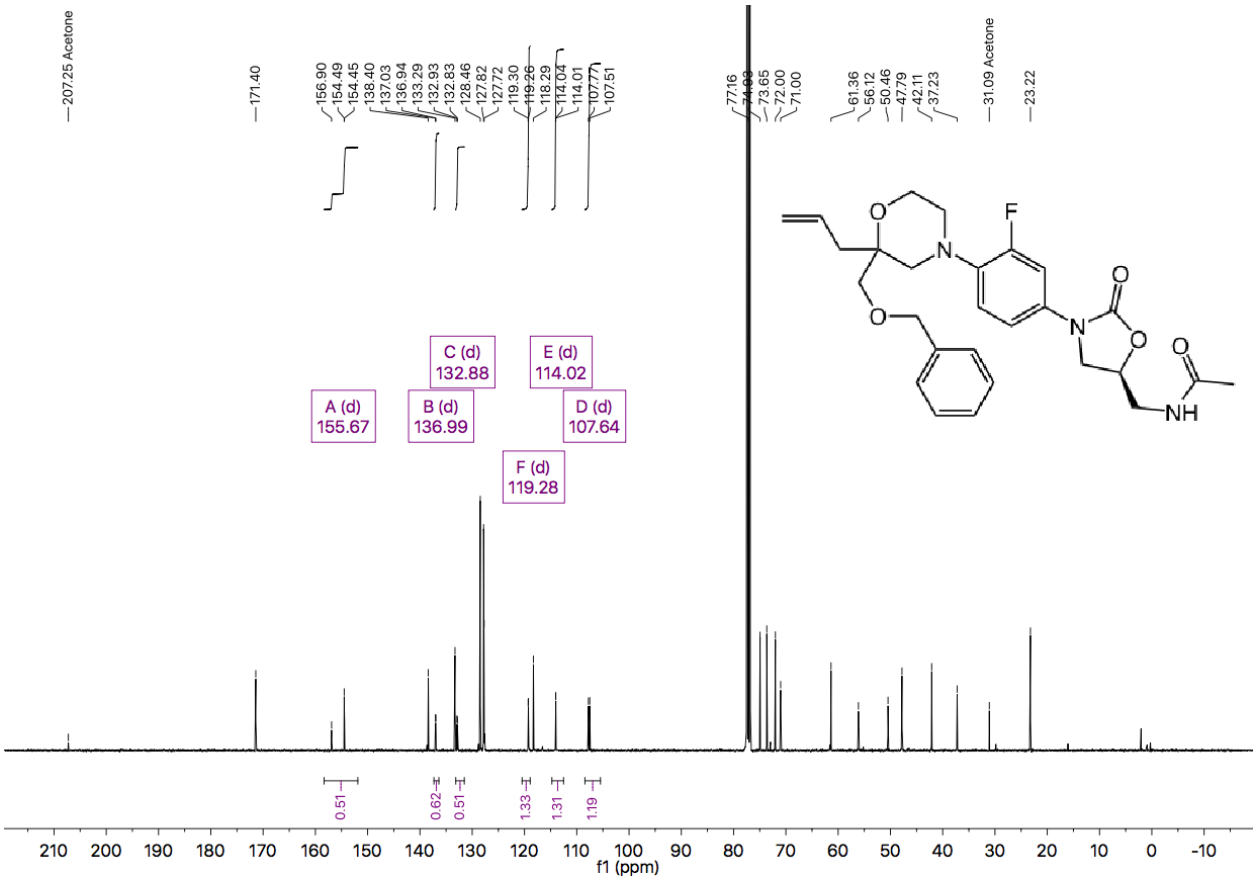

Figure A6.15 *^{13}C NMR (101 MHz, $CDCl_3$) of compound **2.14**.*

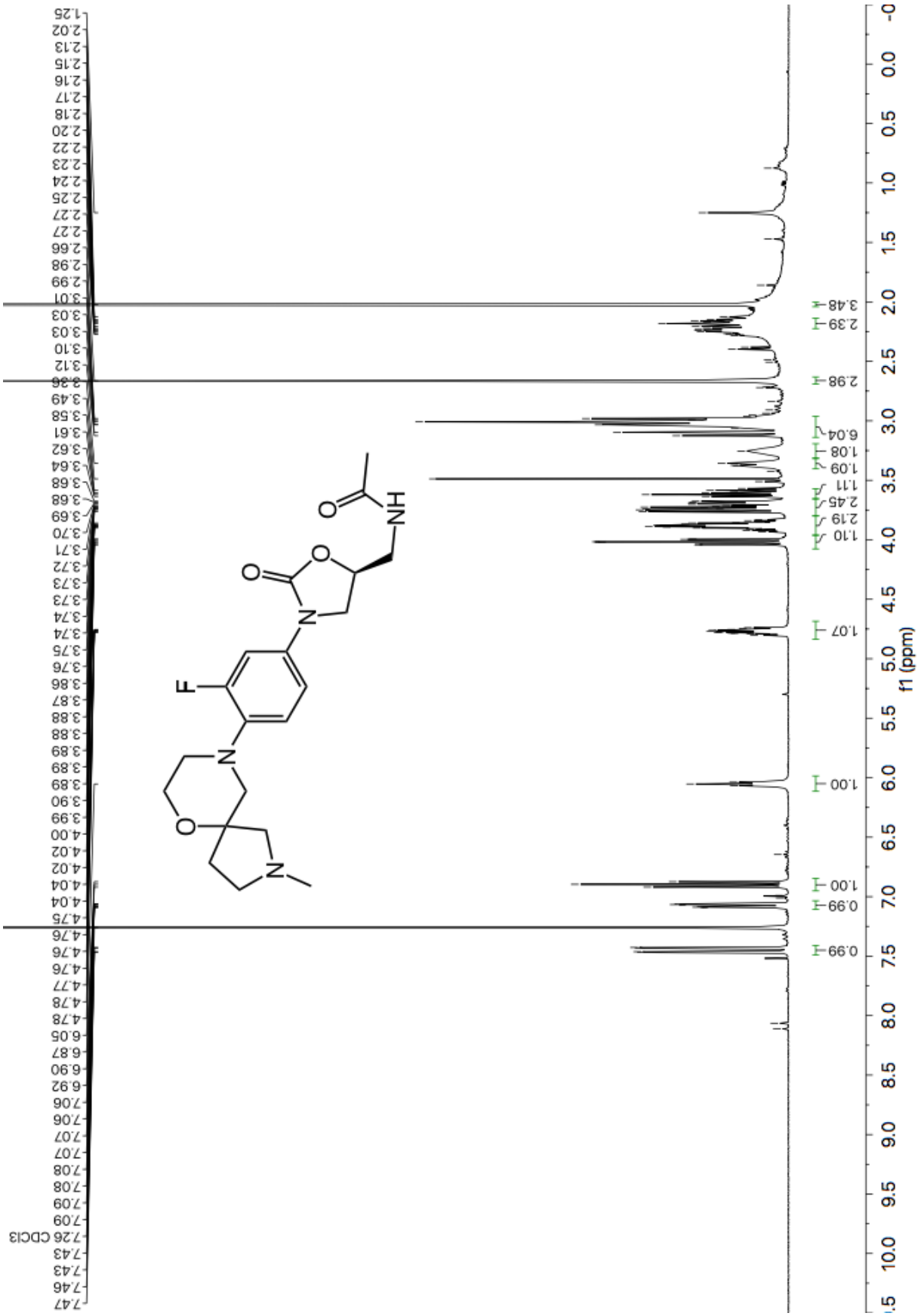

Figure A6.16 *^{1}H NMR (400 MHz, $CDCl_3$) of compound* ***2.17.***

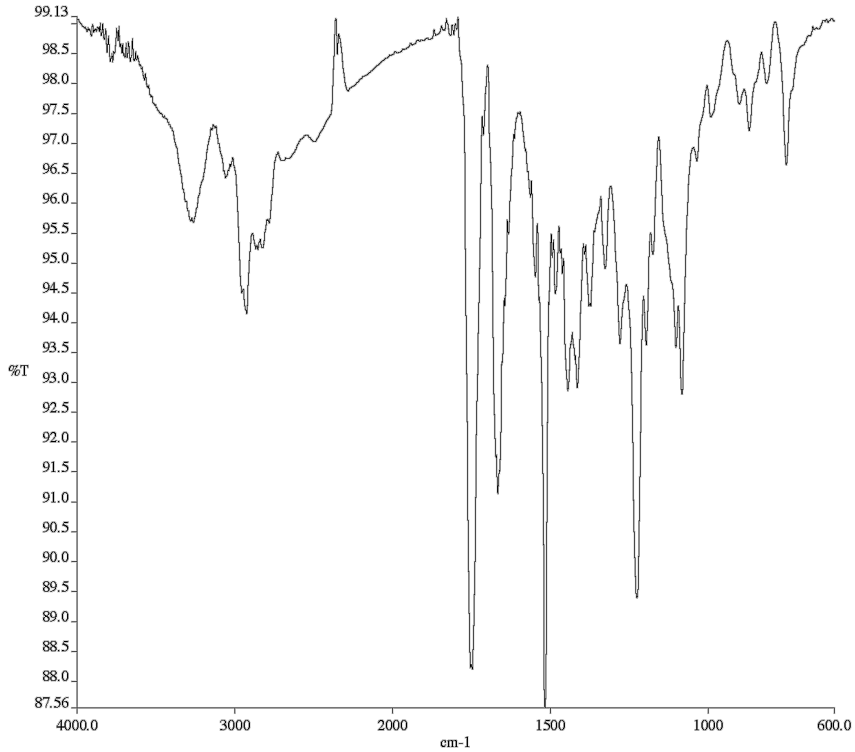

Figure A6.17 *Infrared spectrum (Thin Film, NaCl) of compound* ***2.17***

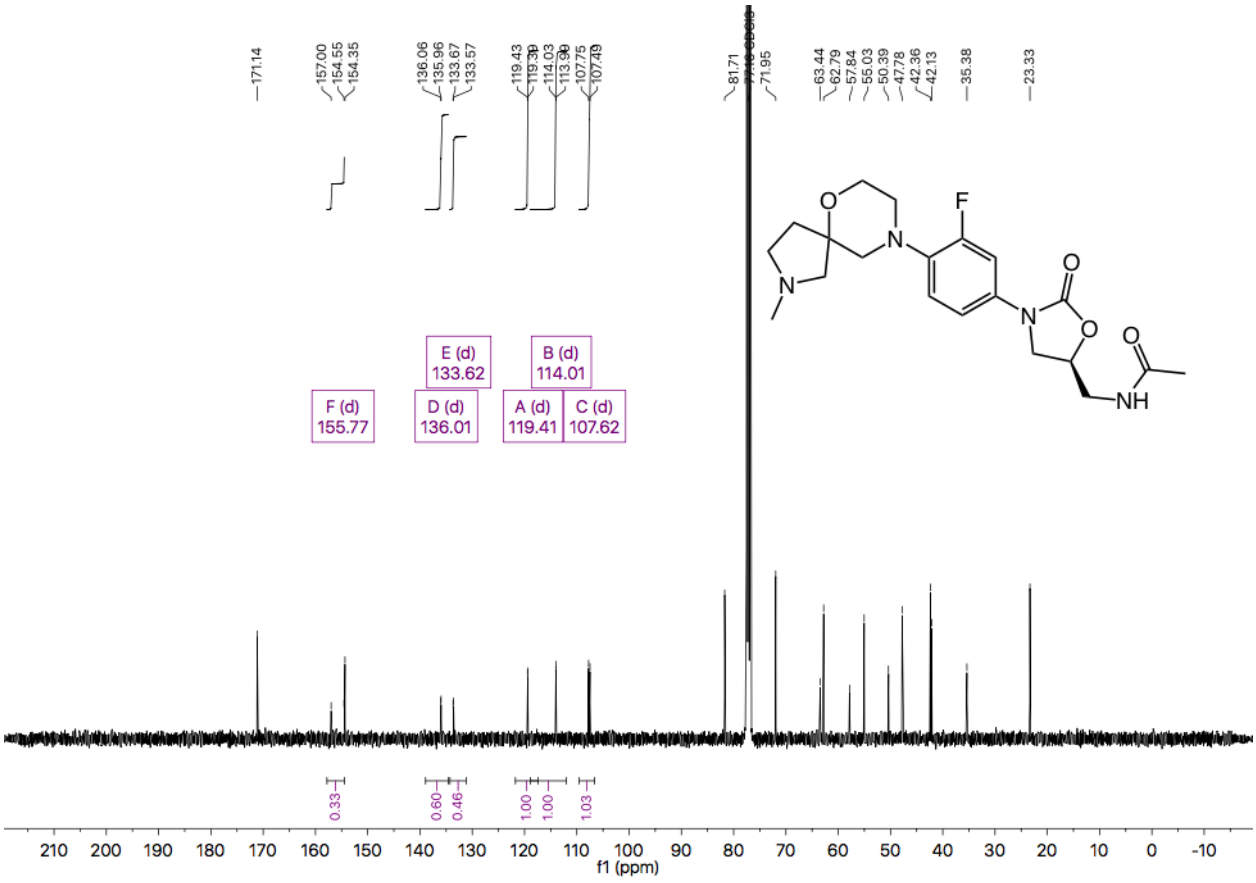

Figure A6.18 *^{13}C NMR (101 MHz, $CDCl_3$) of compound* ***2.17***

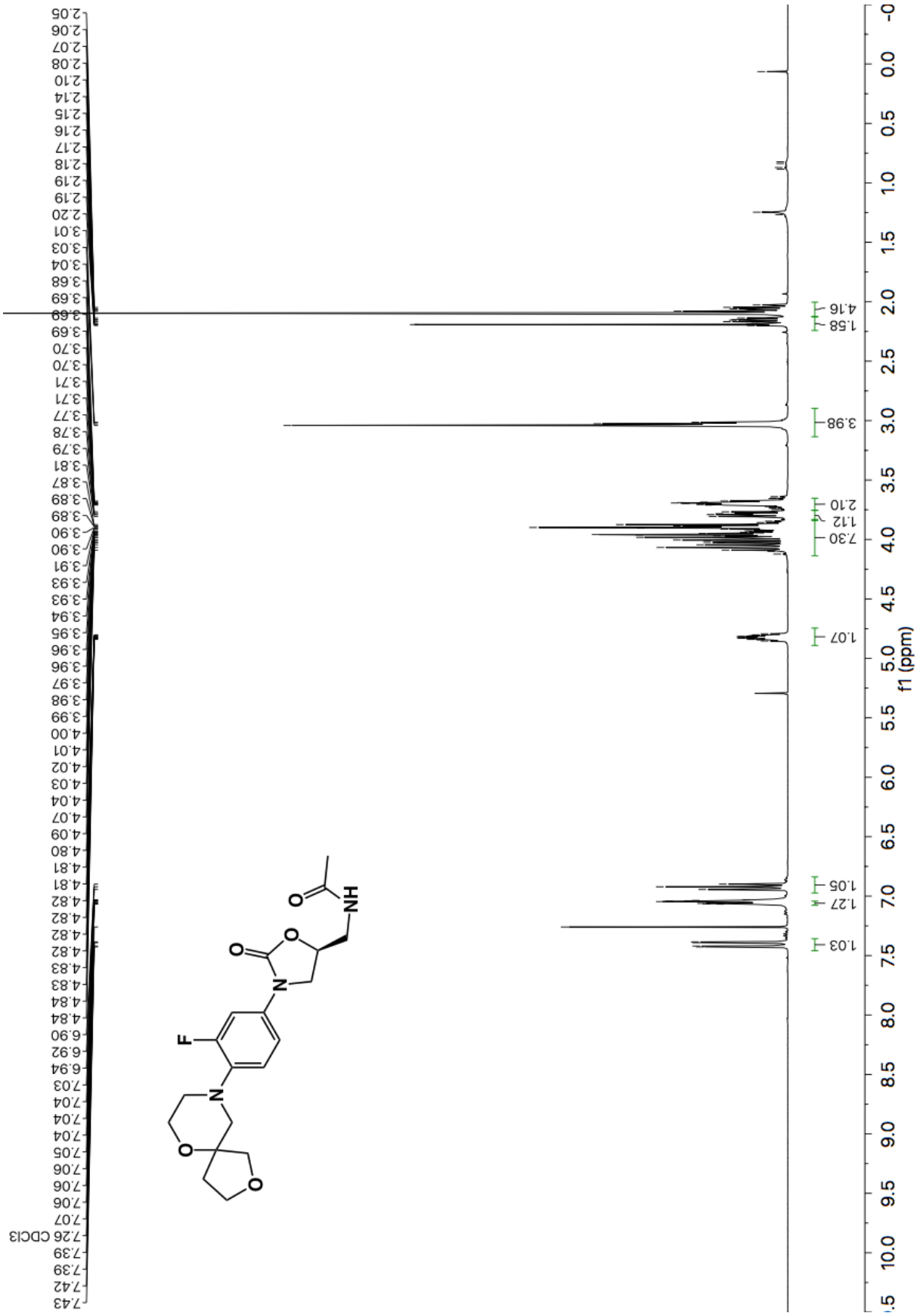

Figure A6.19 *^1H NMR (400 MHz, $CDCl_3$) of compound* ***2.18.***

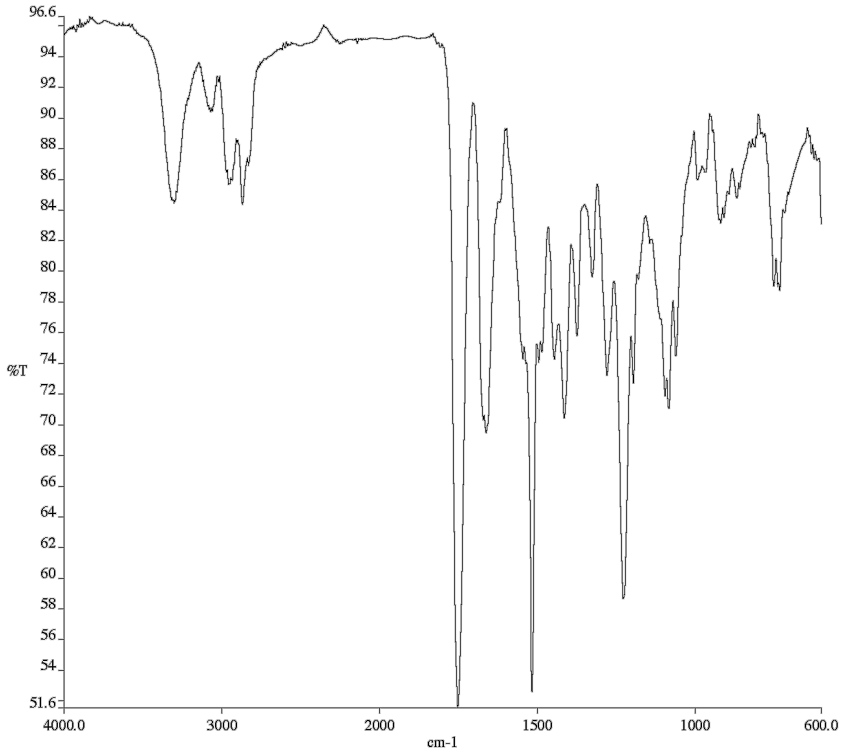

Figure A6.20 *Infrared spectrum (Thin Film, NaCl) of compound* ***2.18***

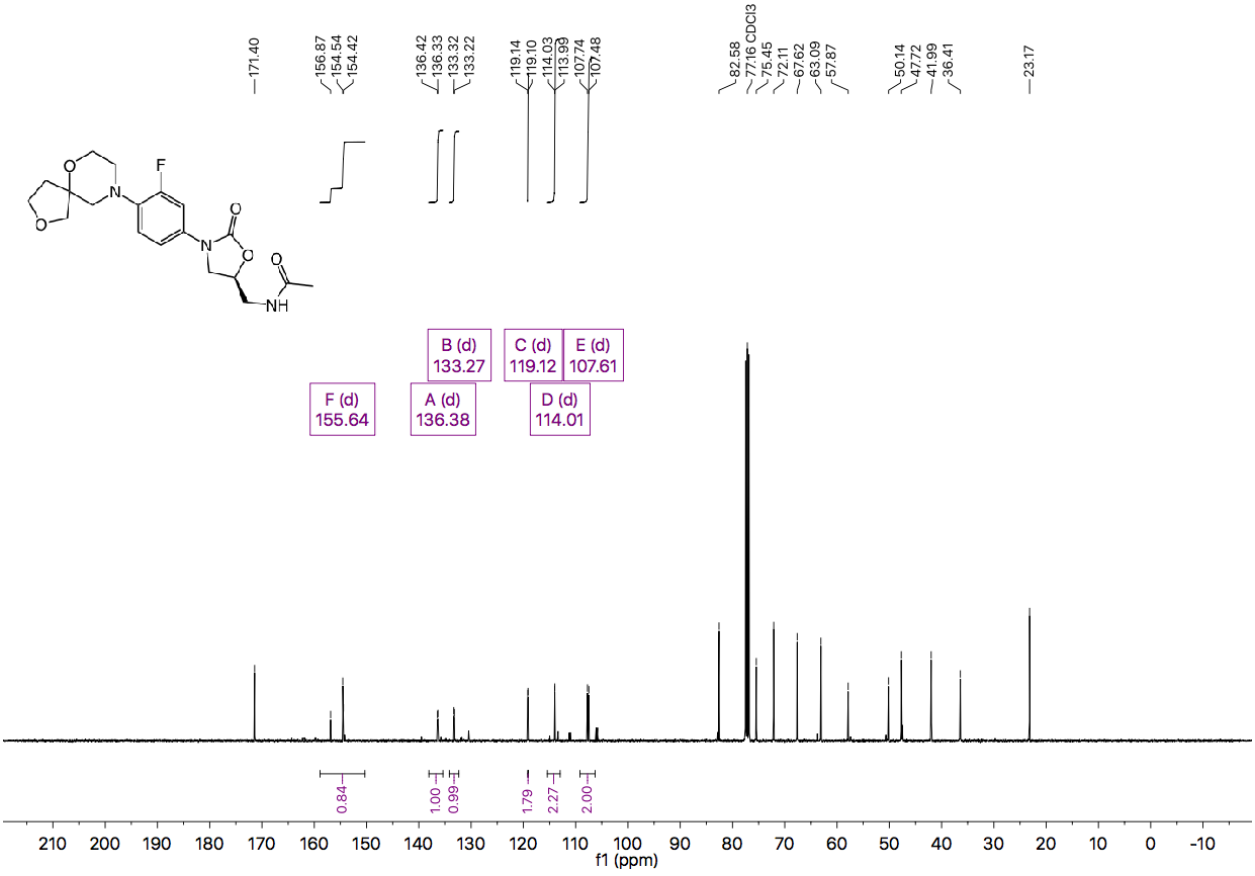

Figure A6.21 *^{13}C NMR (101 MHz, $CDCl_3$) of compound* ***2.18****.*

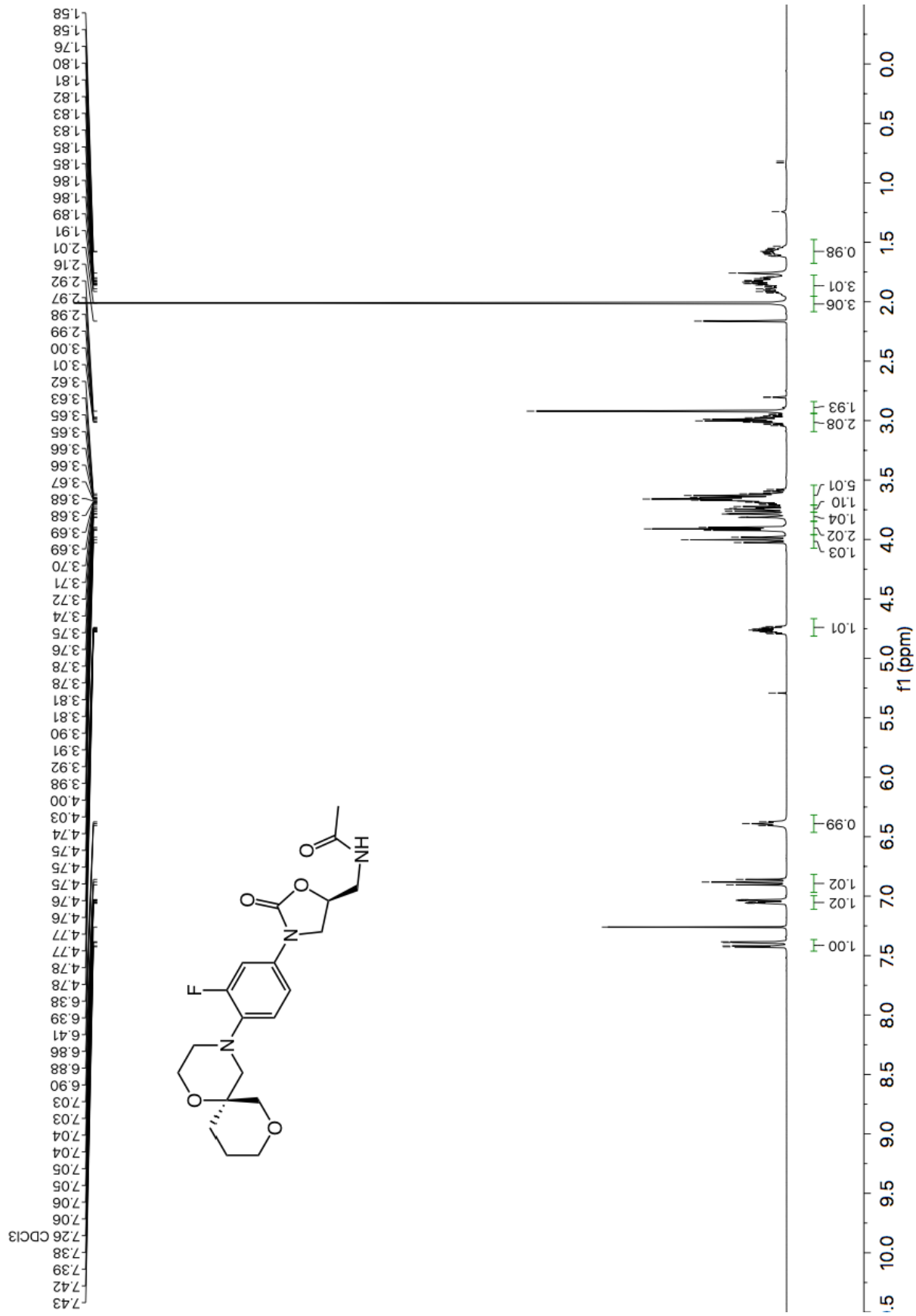

Figure A6.22 *^1H NMR (400 MHz, $CDCl_3$) of compound* ***2.19a.***

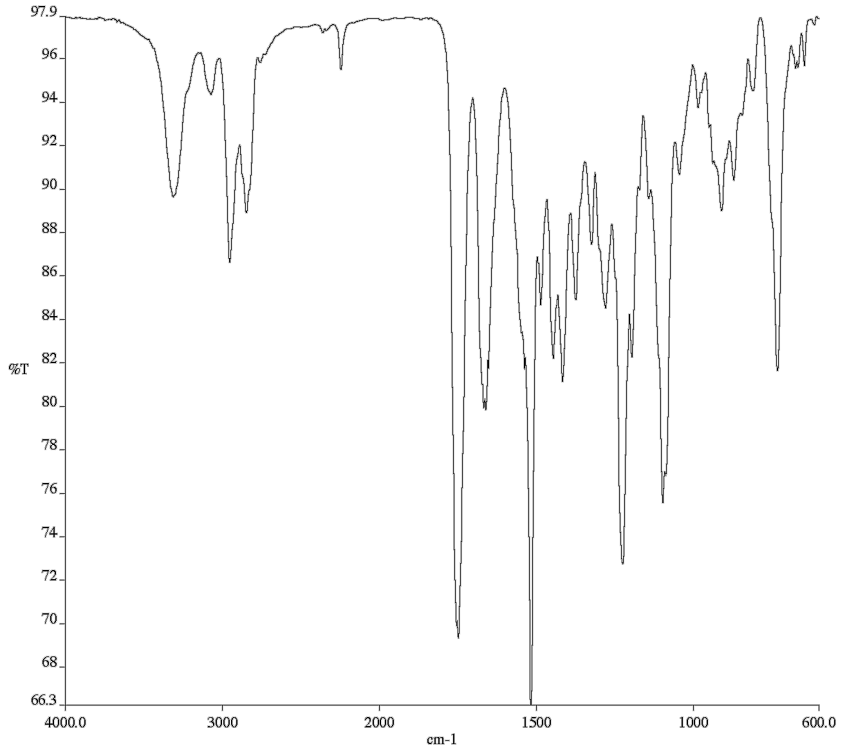

Figure A6.23 *Infrared spectrum (Thin Film, NaCl) of compound* ***2.19a****.*

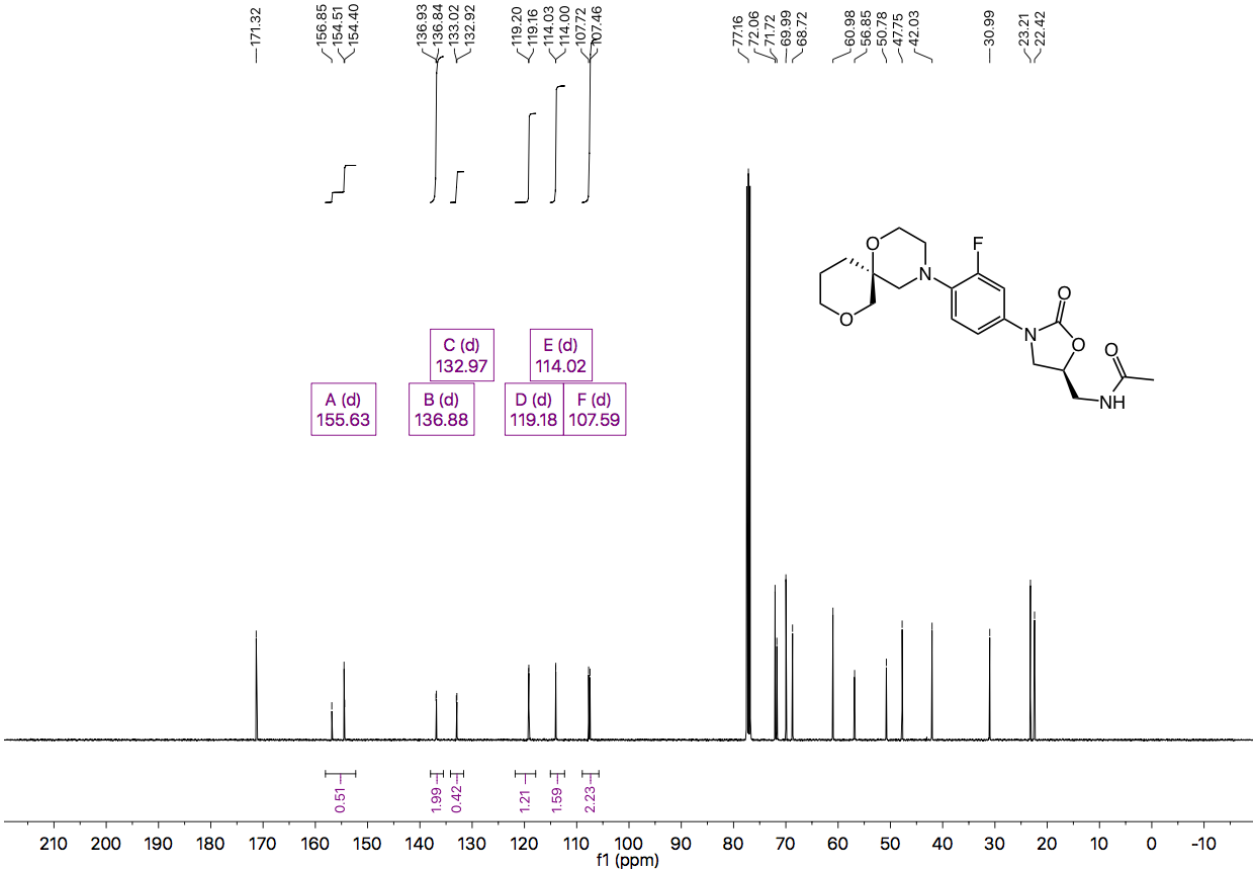

Figure A6.21 *^{13}C NMR (101 MHz, $CDCl_3$) of compound* ***2.19a****.*

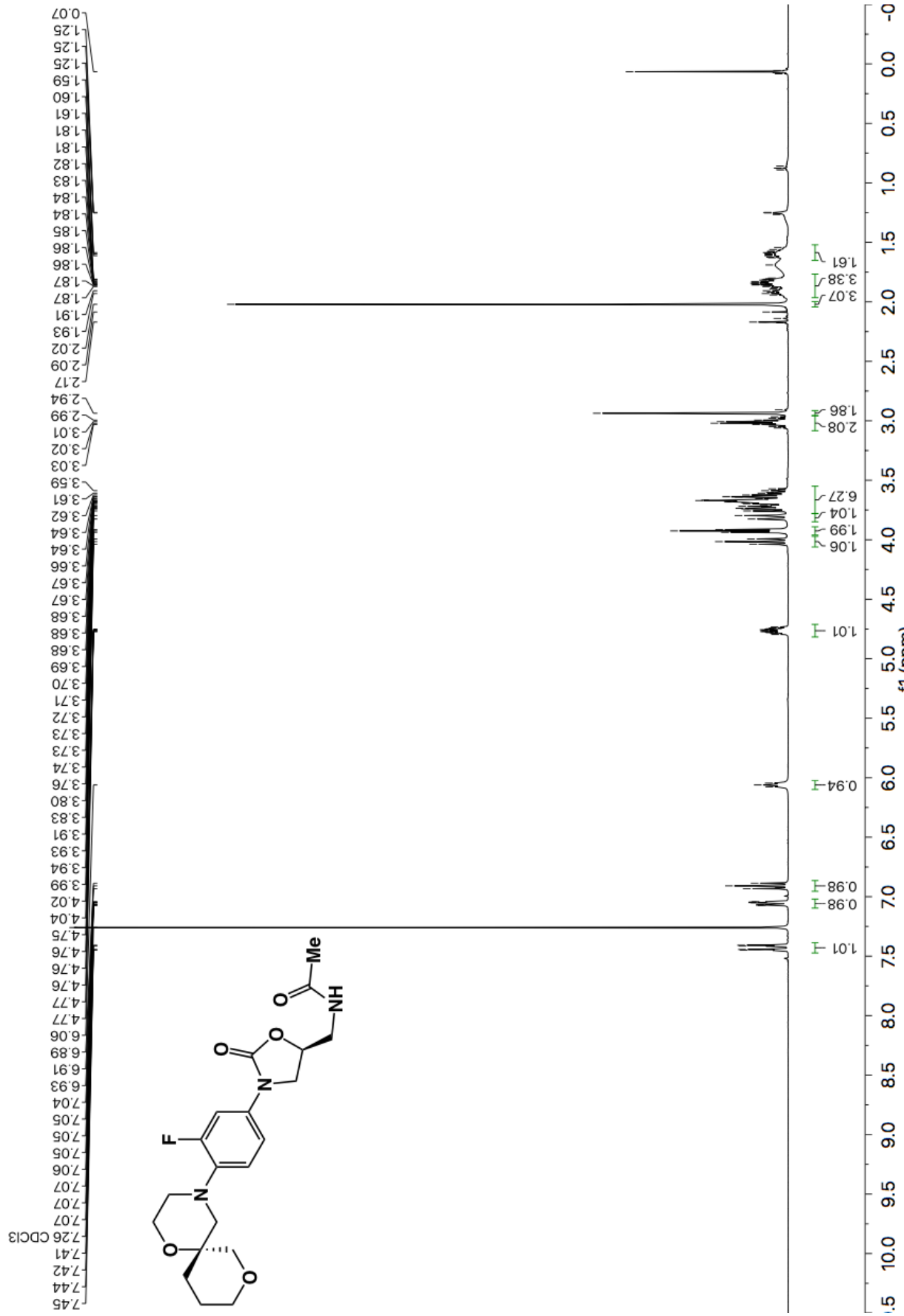

Figure A6.25 ^{1}H NMR (400 MHz, $CDCl_3$) of compound **2.19b.**

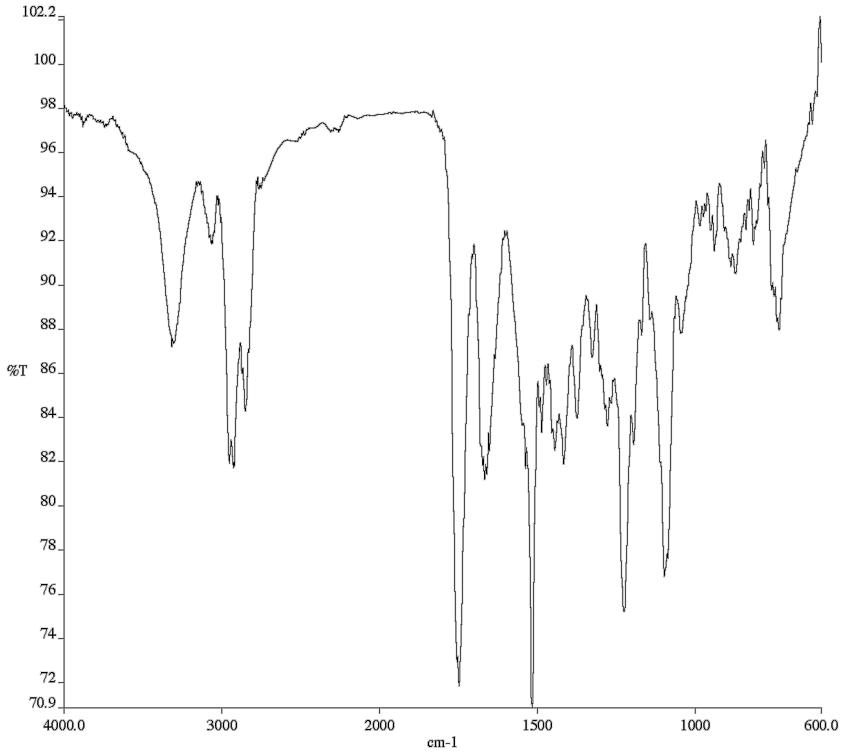

Figure A6.26 Infrared spectrum (Thin Film, NaCl) of compound **2.19b**.

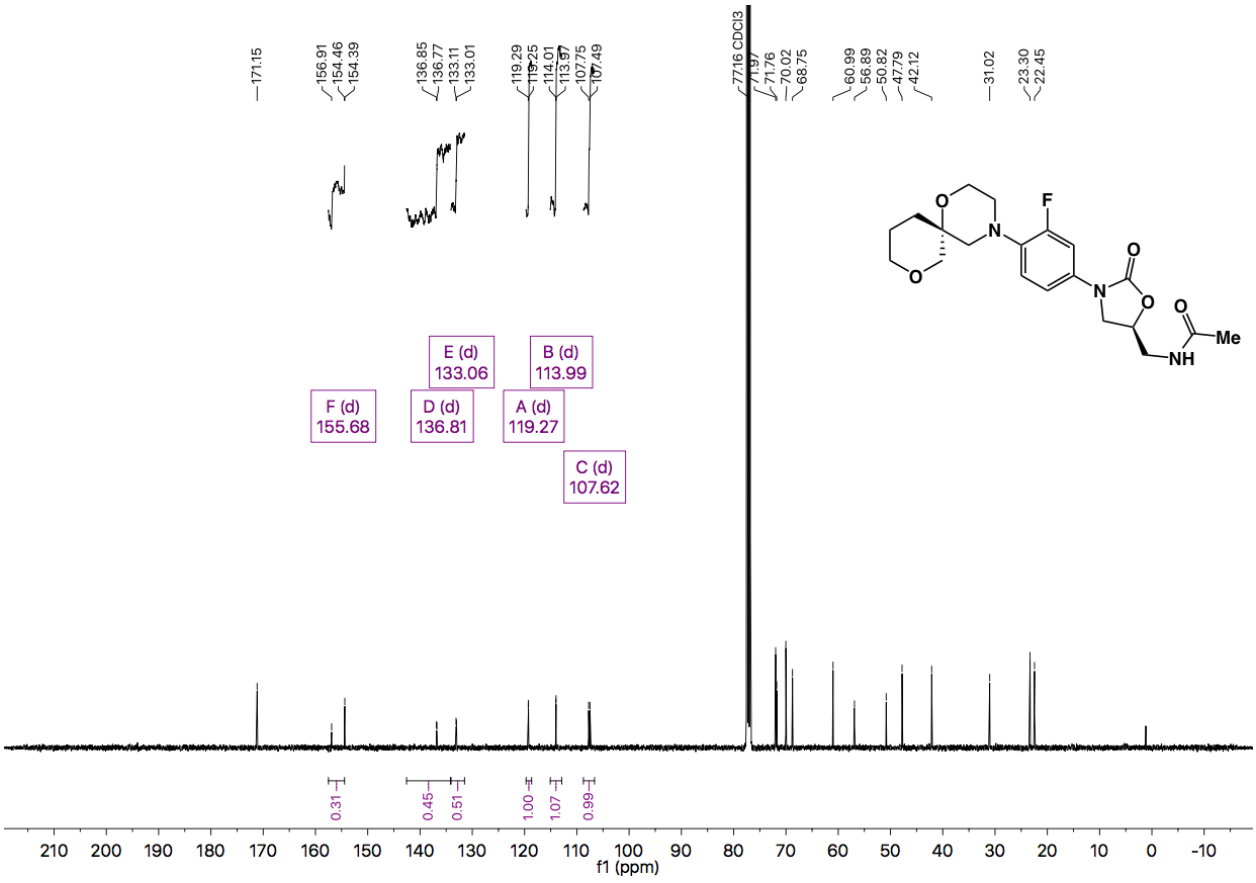

Figure A6.27 ^{13}C NMR (101 MHz, $CDCl_3$) of compound **2.19b**.

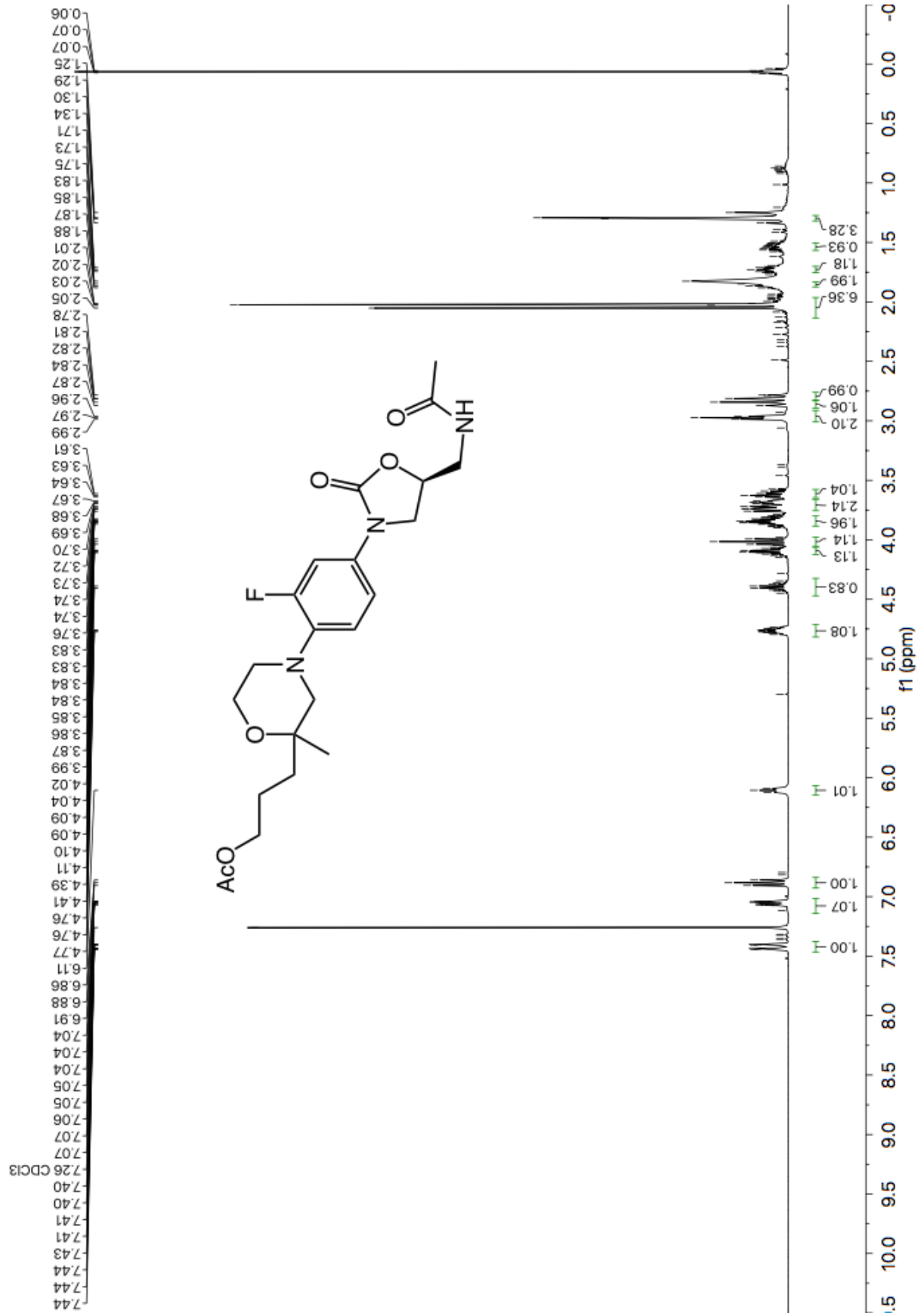

Figure A6.28 ^{1}H NMR (400 MHz, $CDCl_3$) of compound **2.21.**

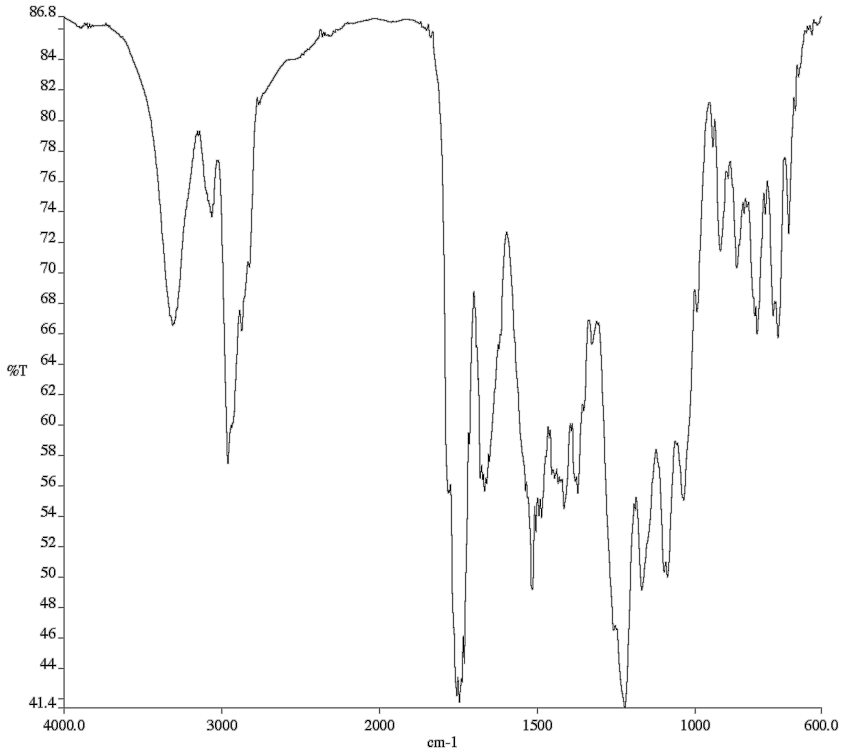

Figure A6.29 Infrared spectrum (Thin Film, NaCl) of compound **2.21.**

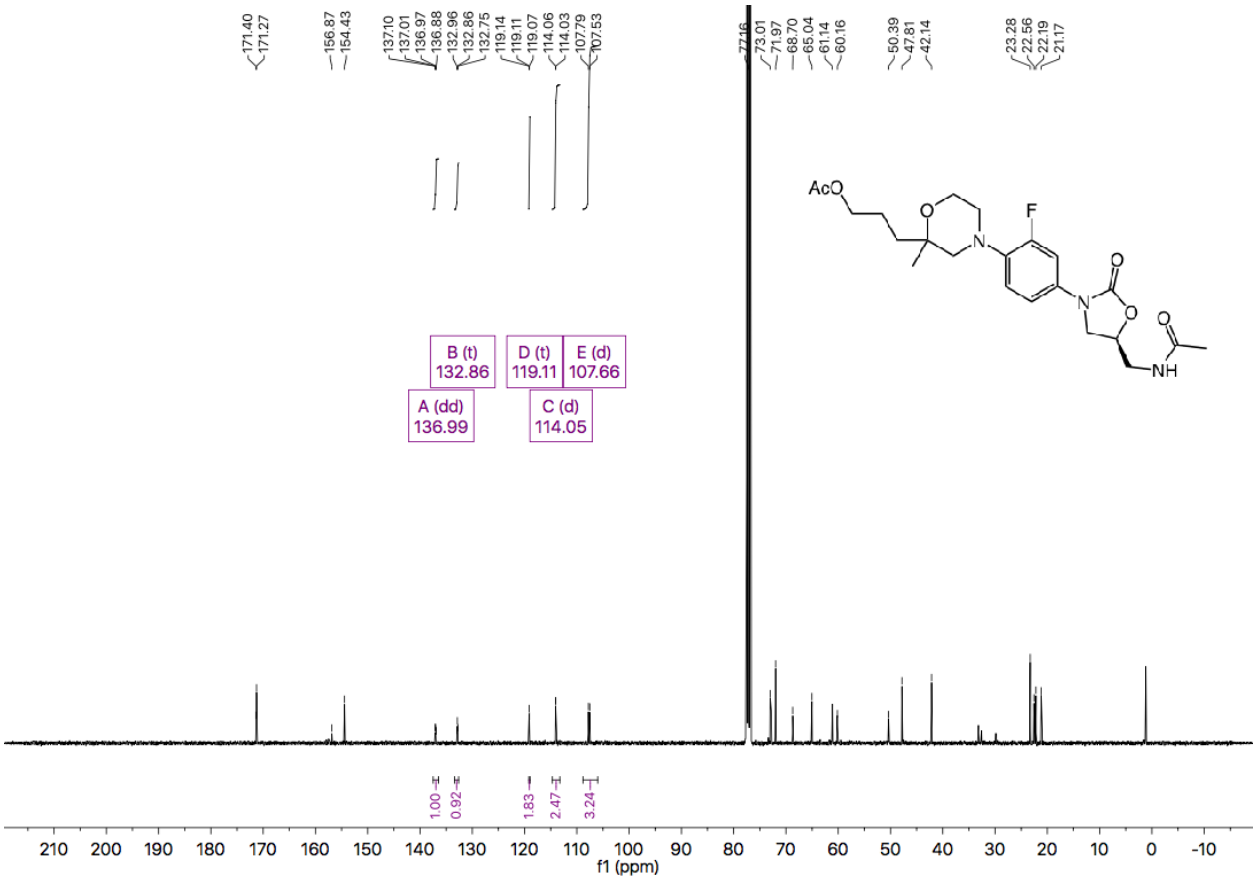

Figure A6.30 ^{13}C NMR (101 MHz, $CDCl_3$) of compound **2.21**.

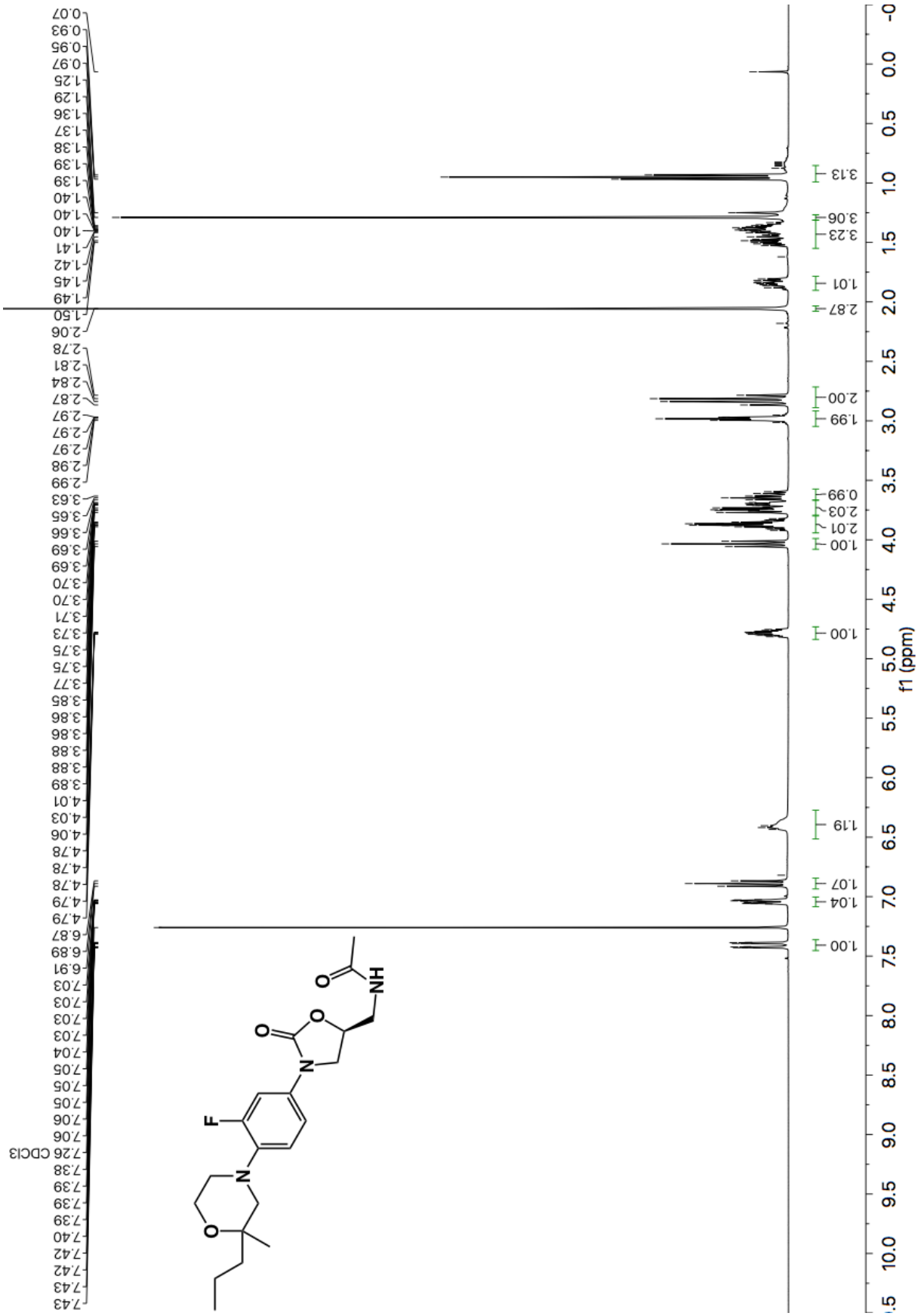

Figure A6.31 ^{1}H NMR (400 MHz, $CDCl_3$) of compound **2.22.**

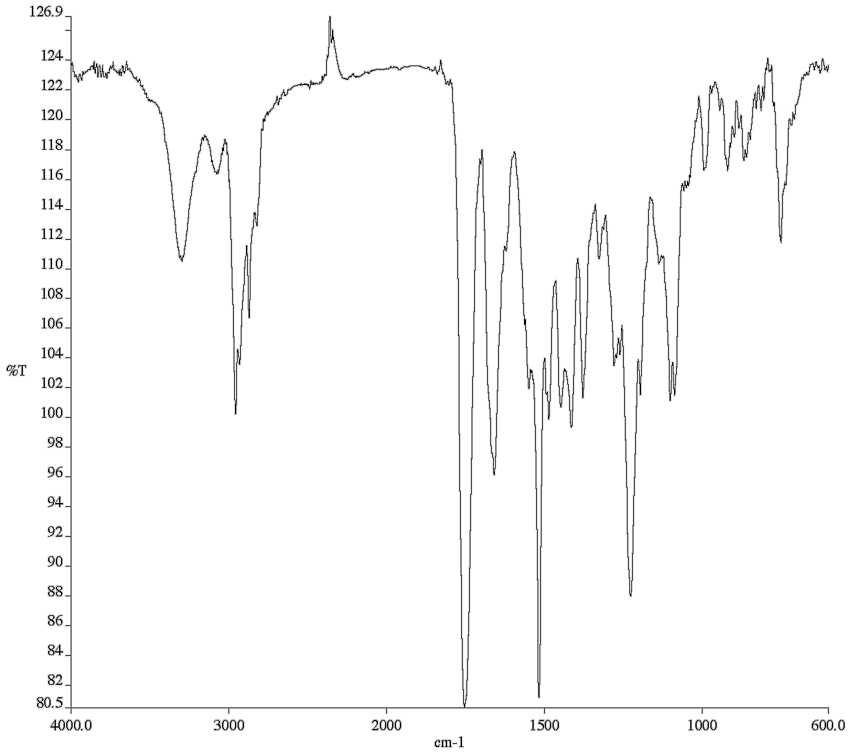

Figure A6.32 Infrared spectrum (Thin Film, NaCl) of compound **2.22**.

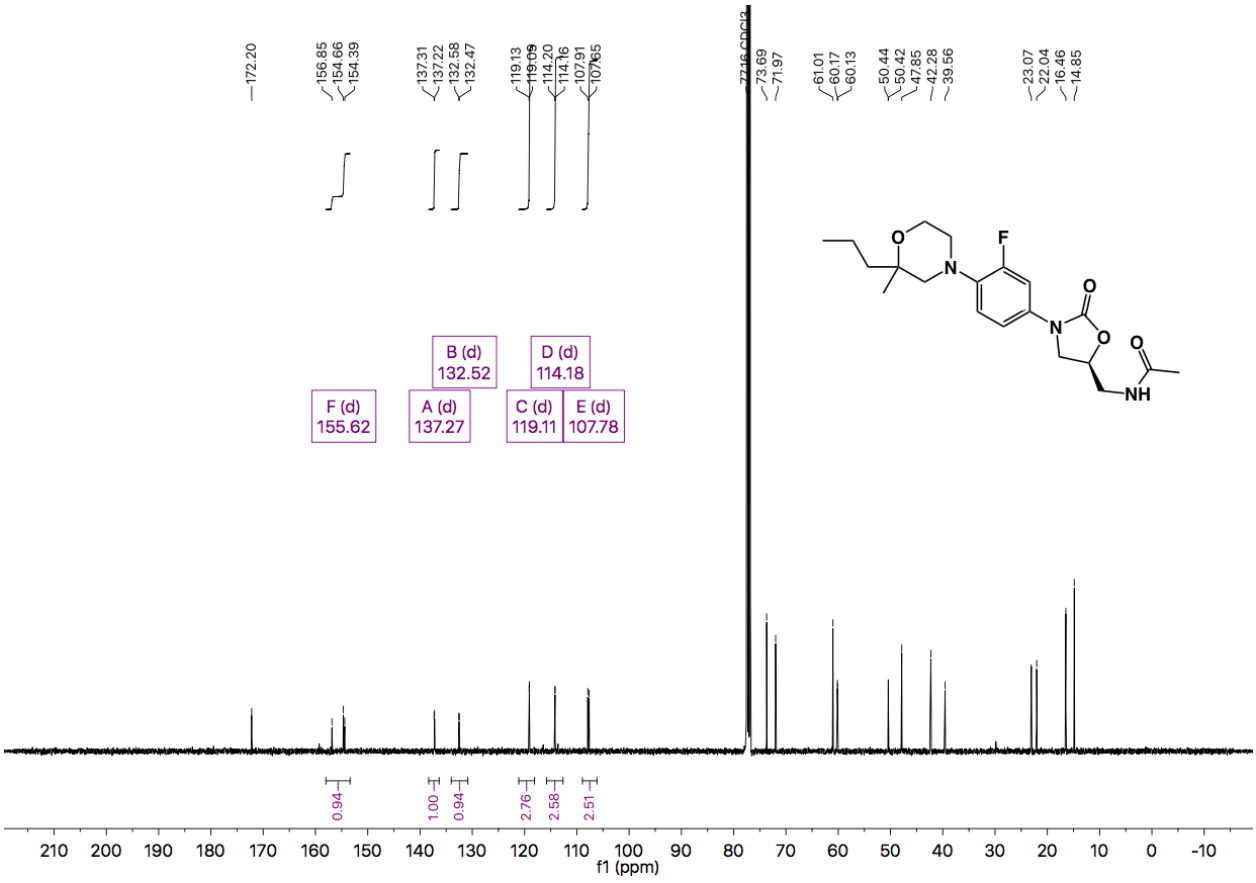

Figure A6.33 ^{13}C NMR (101 MHz, $CDCl_3$) of compound **2.22**.

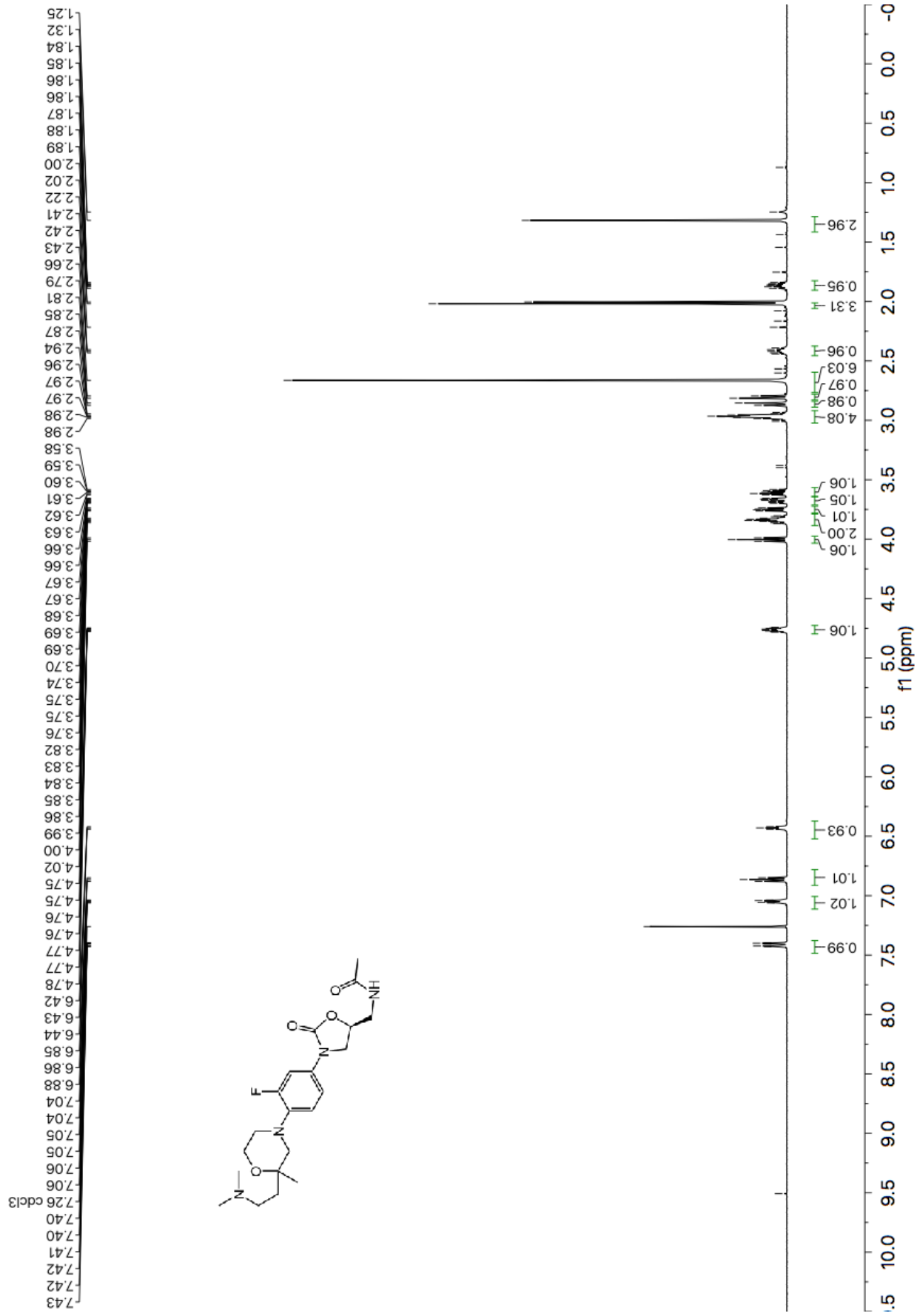

Figure A6.34 ^{1}H NMR (600 MHz, $CDCl_3$) of compound **2.23**.

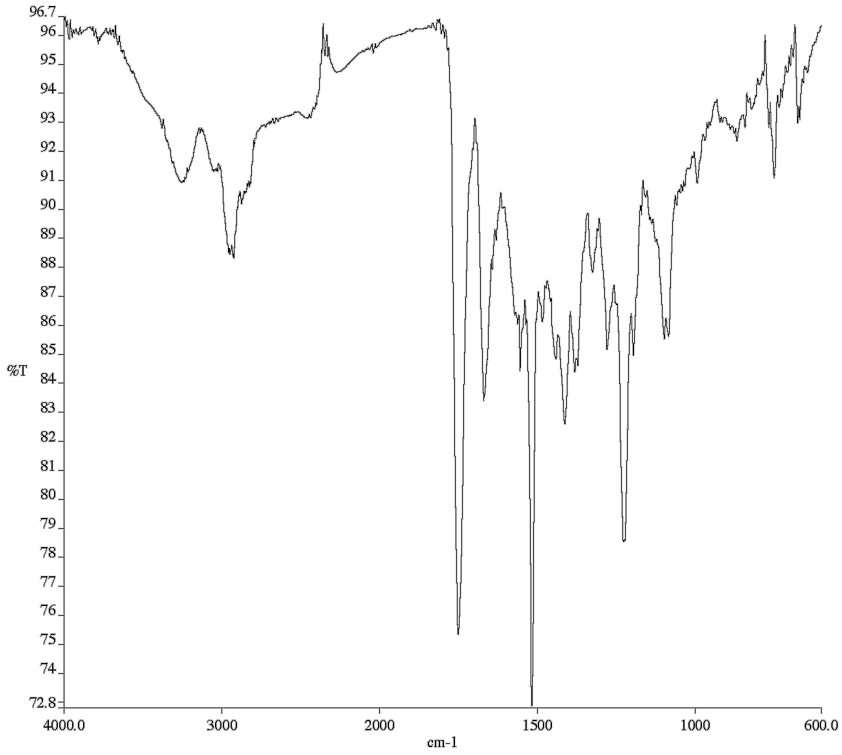

Figure A6.35 Infrared spectrum (Thin Film, NaCl) of compound **2.23**.

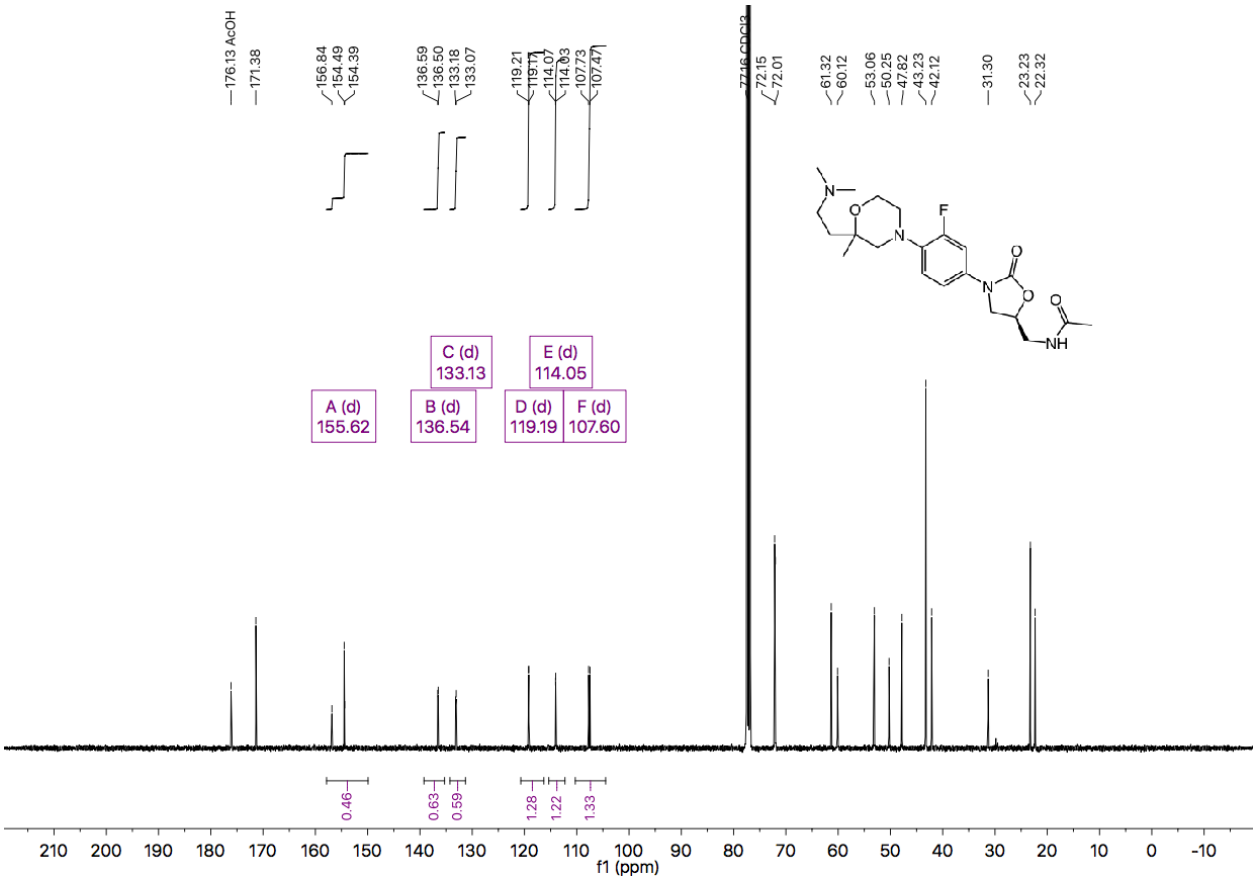

Figure A6.36 ^{13}C NMR (101 MHz, $CDCl_3$) of compound **2.23**.

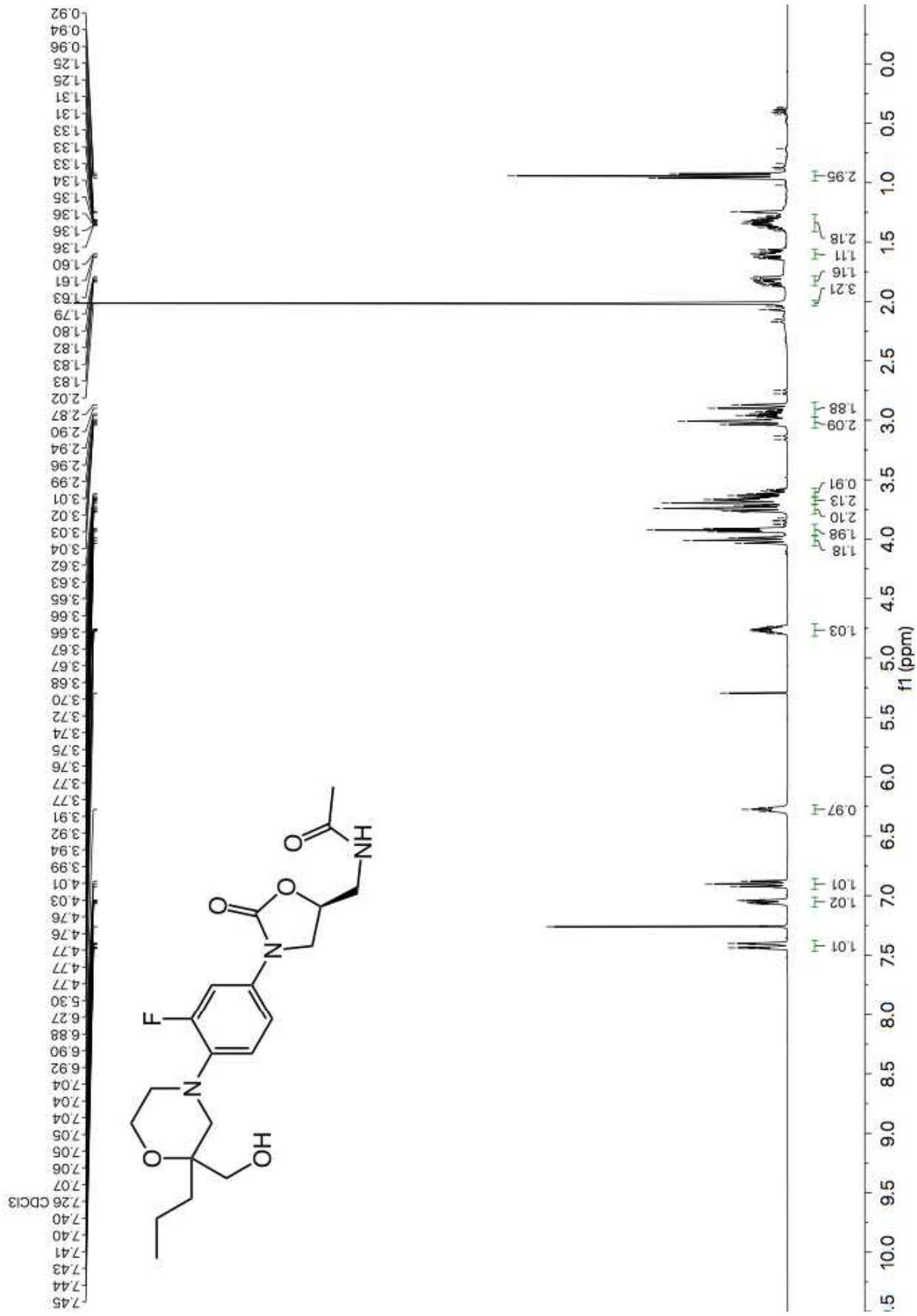

Figure A6.37 ^{1}H NMR (400 MHz, $CDCl_3$) of compound **2.24.**

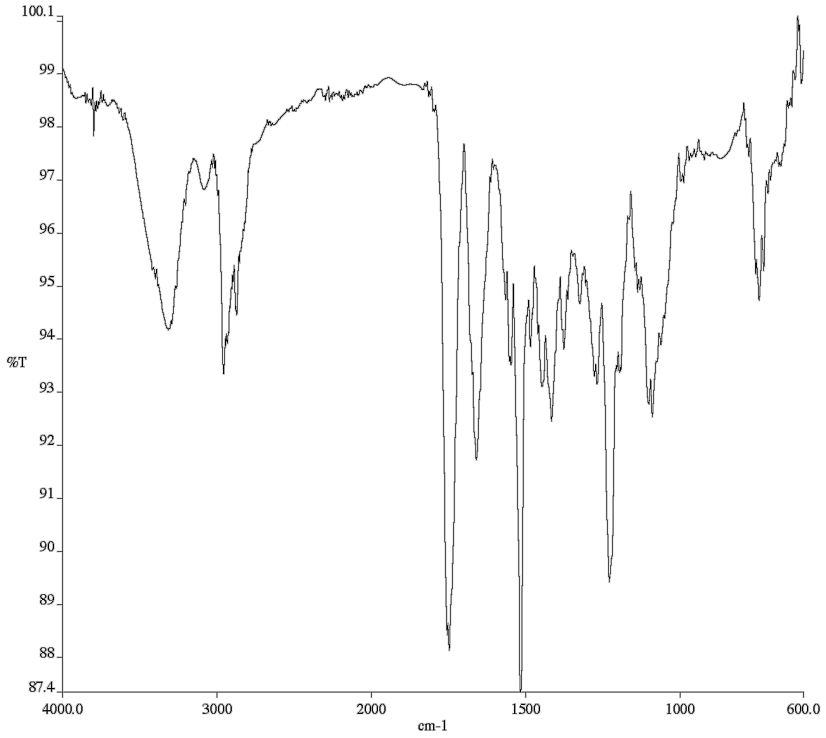

Figure A6.38 Infrared spectrum (Thin Film, NaCl) of compound **2.24**.

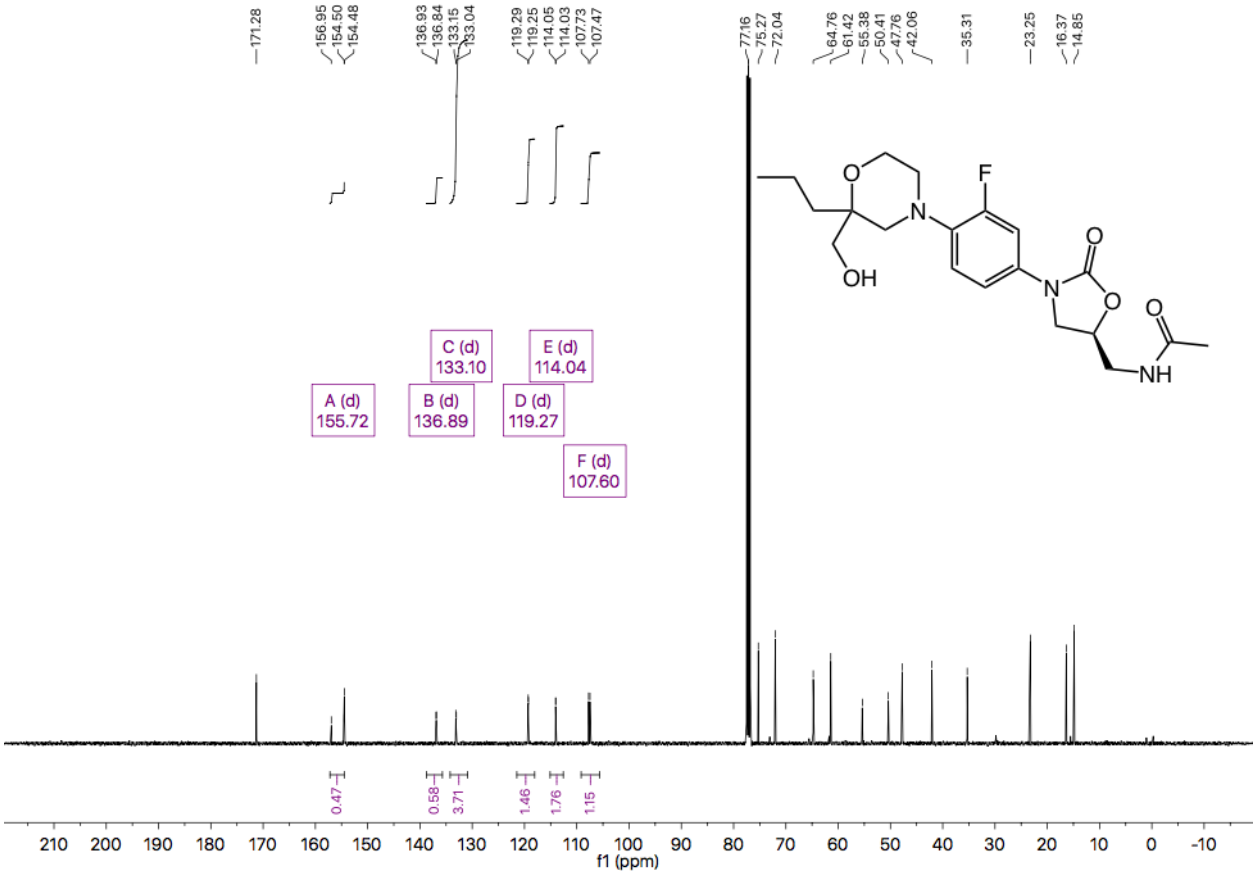

Figure A6.39 ^{13}C NMR (101 MHz, $CDCl_3$) of compound **2.24**.

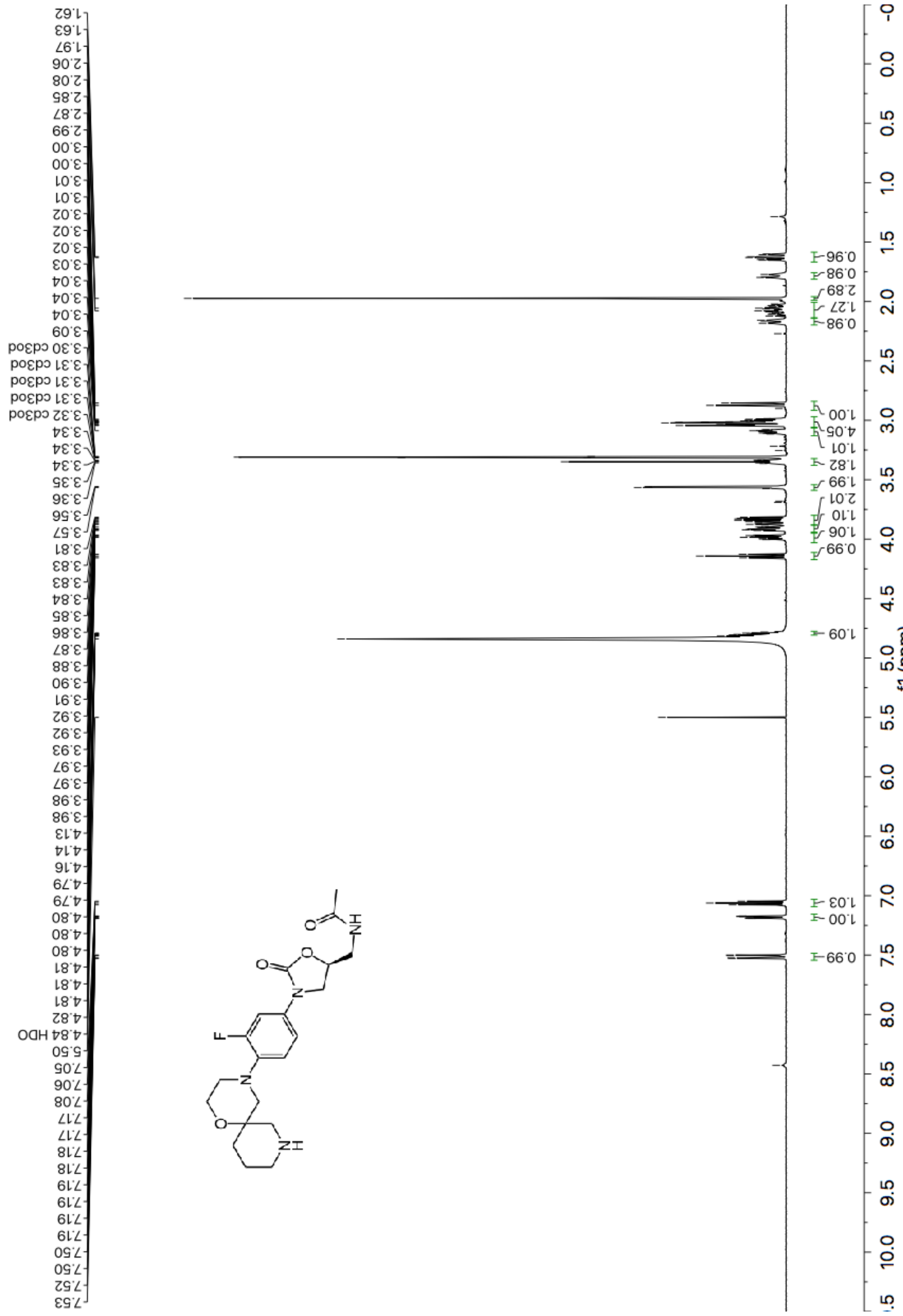

Figure A6.40 ^{1}H NMR (600 MHz, CD_3OD) of compound **2.25.**

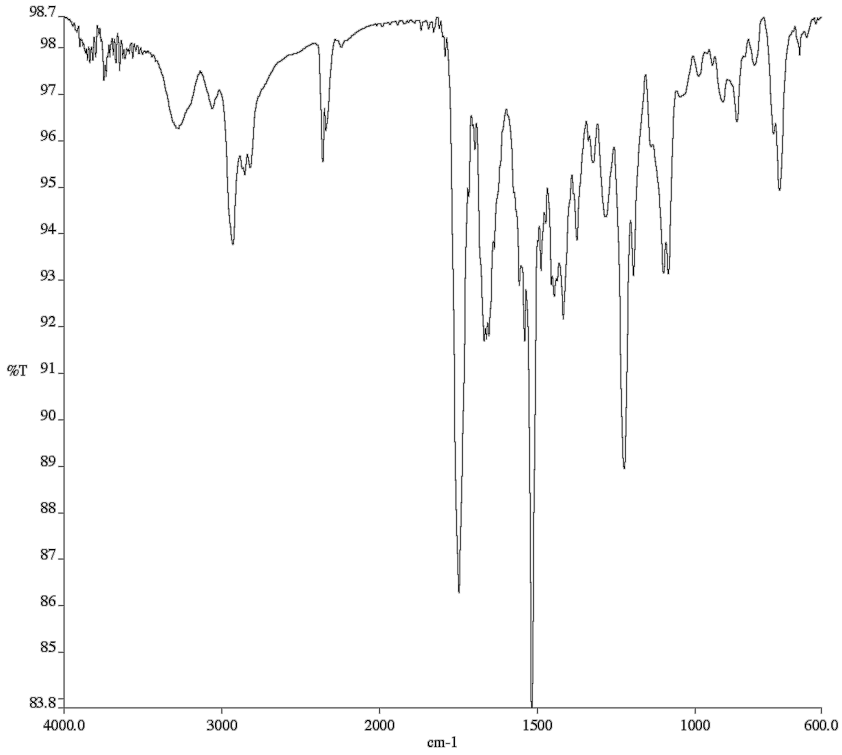

Figure A6.41 Infrared spectrum (Thin Film, NaCl) of compound **2.25**.

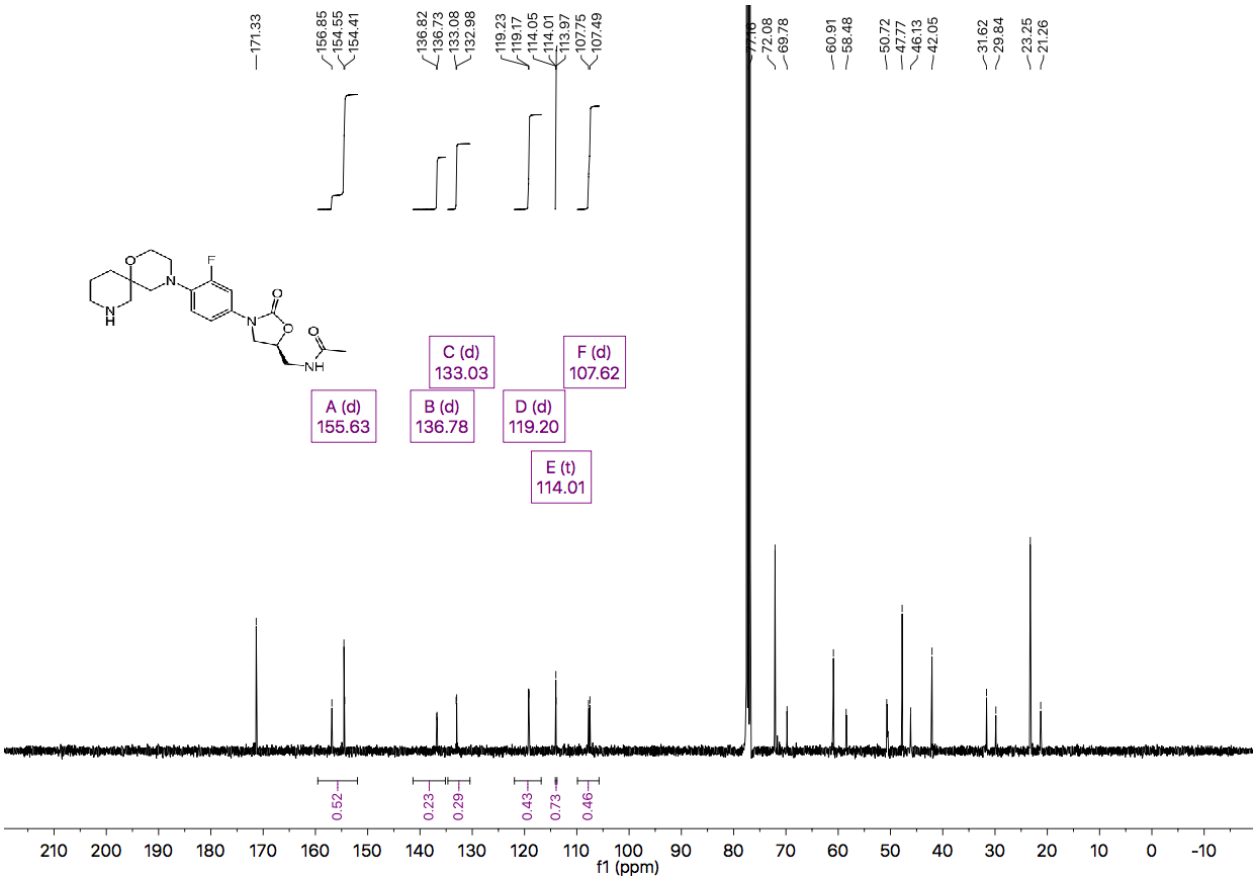

Figure A6.42 ^{13}C NMR (101 MHz, $CDCl_3$) of compound **2.25**.

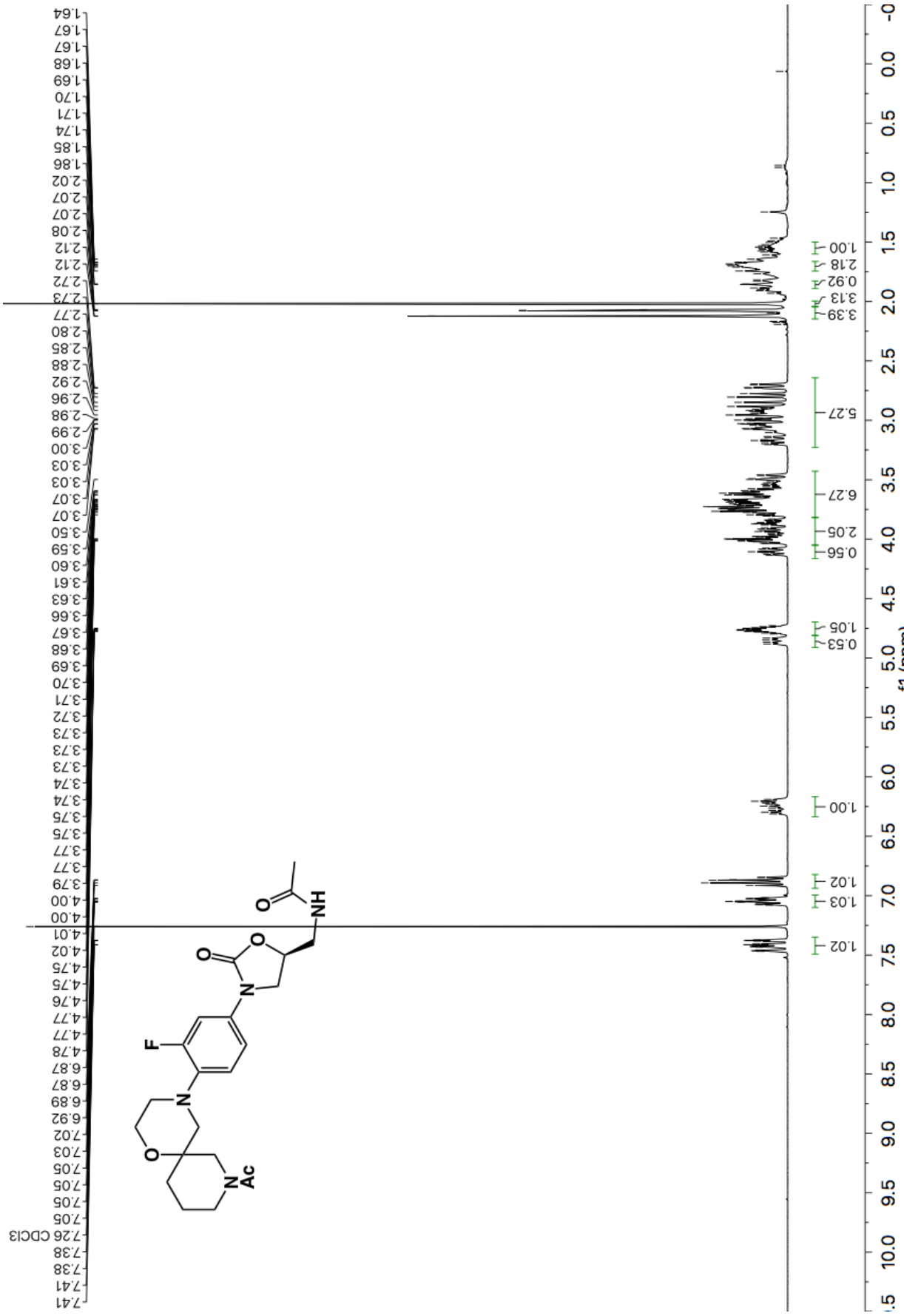

Figure A6.43 ^{1}H NMR (400 MHz, $CDCl_3$) of compound **2.26.**

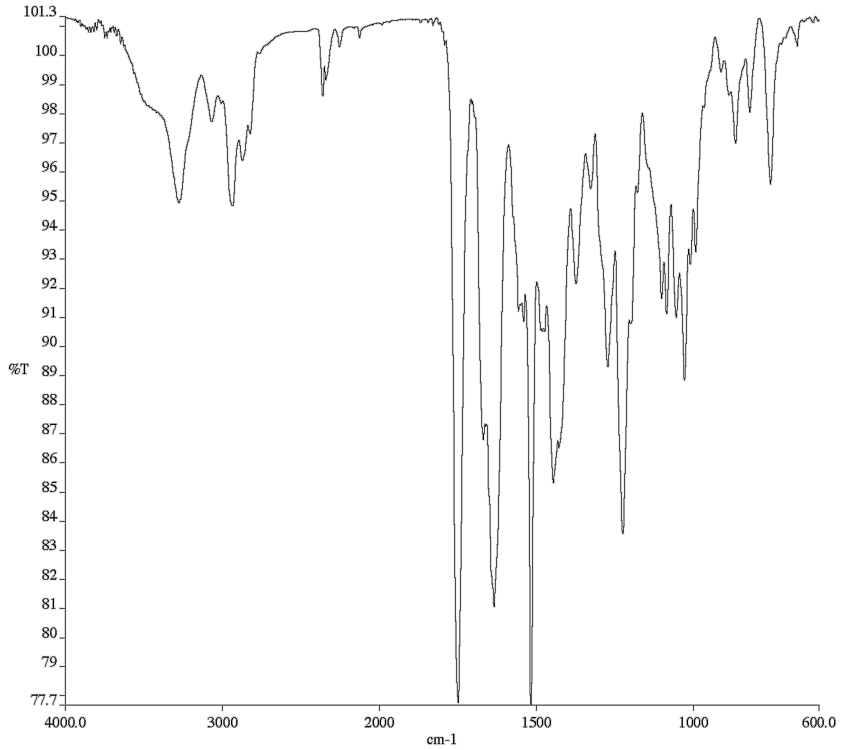

Figure A6.44 Infrared spectrum (Thin Film, NaCl) of compound **2.26**.

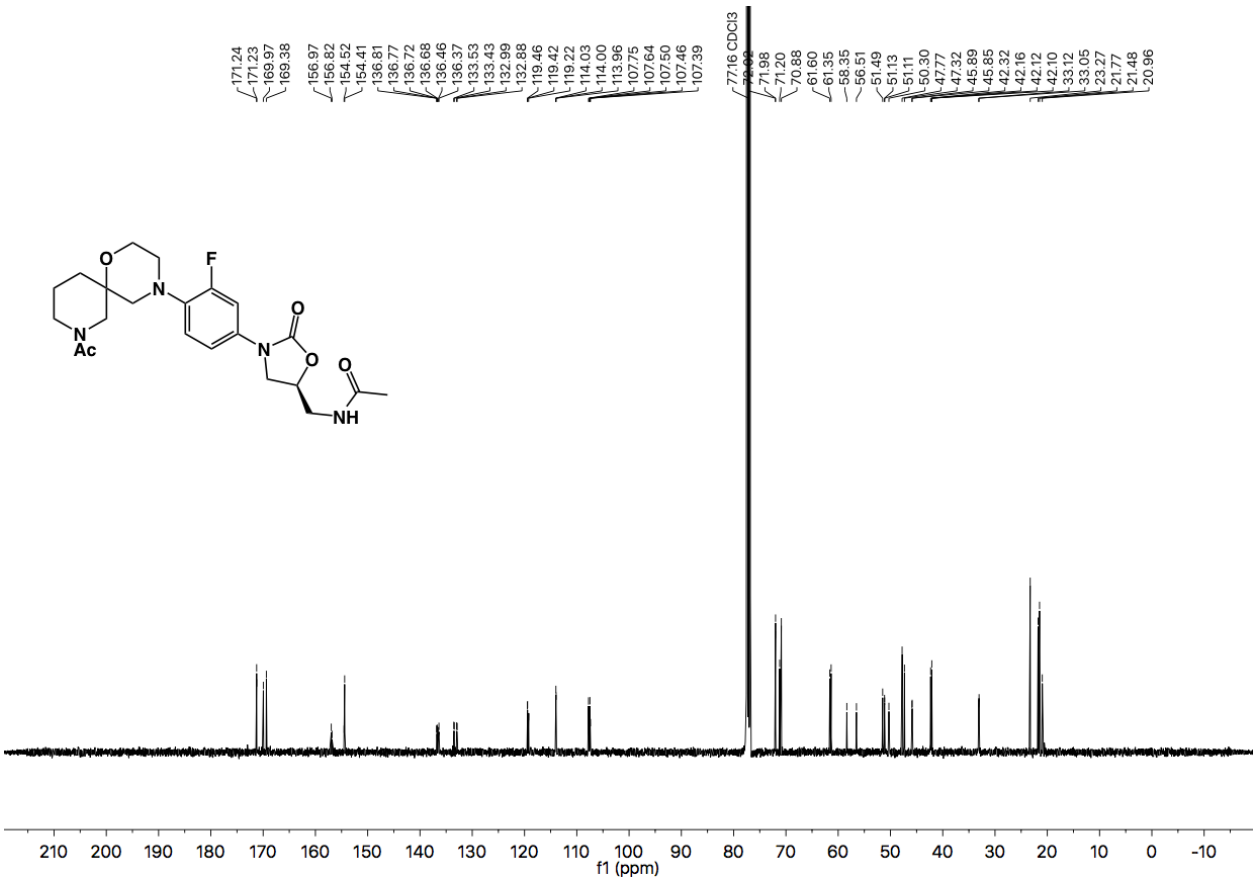

Figure A6.45 ^{13}C NMR (101 MHz, $CDCl_3$) of compound **2.26**.

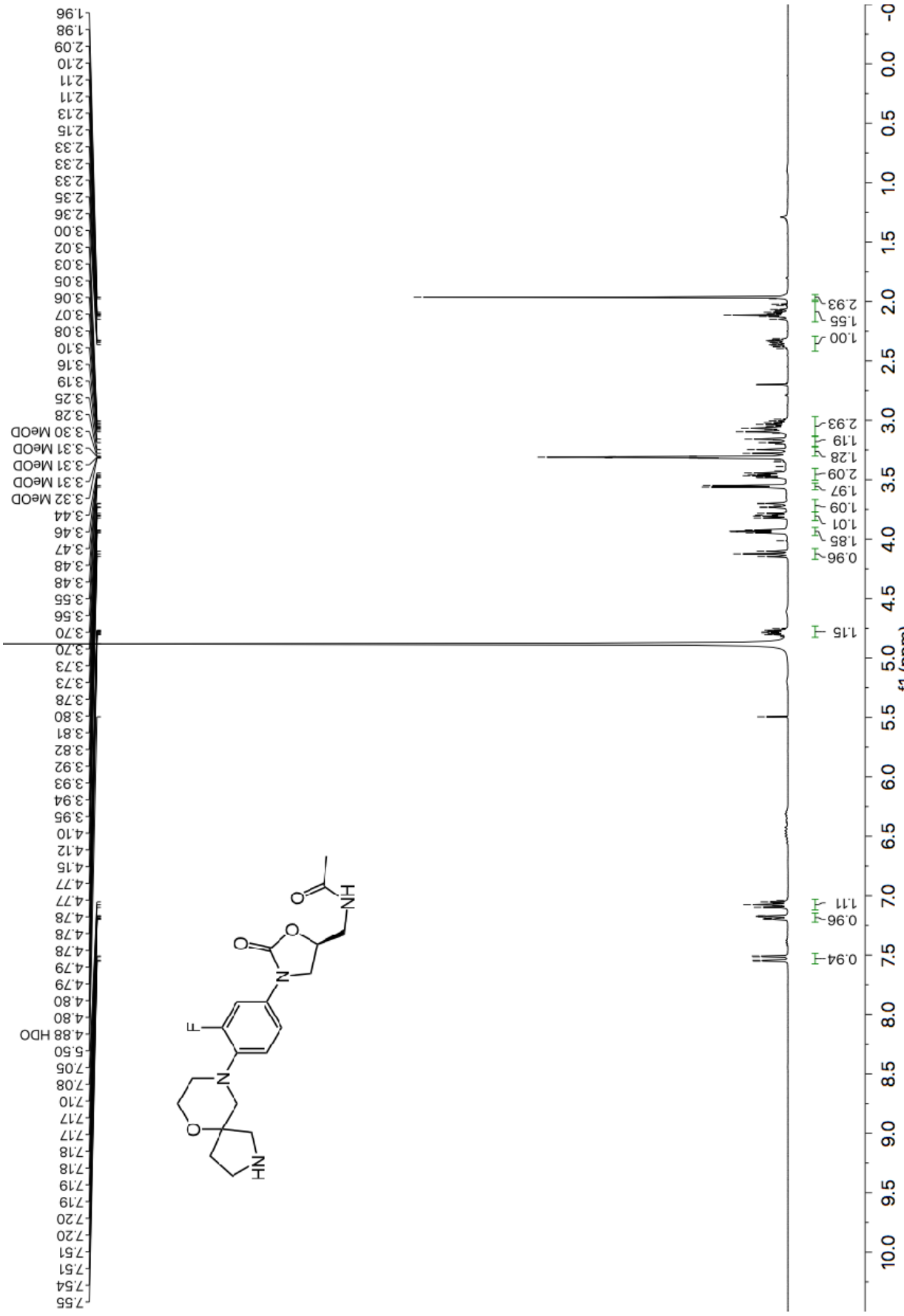

Figure A6.46 ^{1}H NMR (400 MHz, CD_3OD) of compound **2.27.**

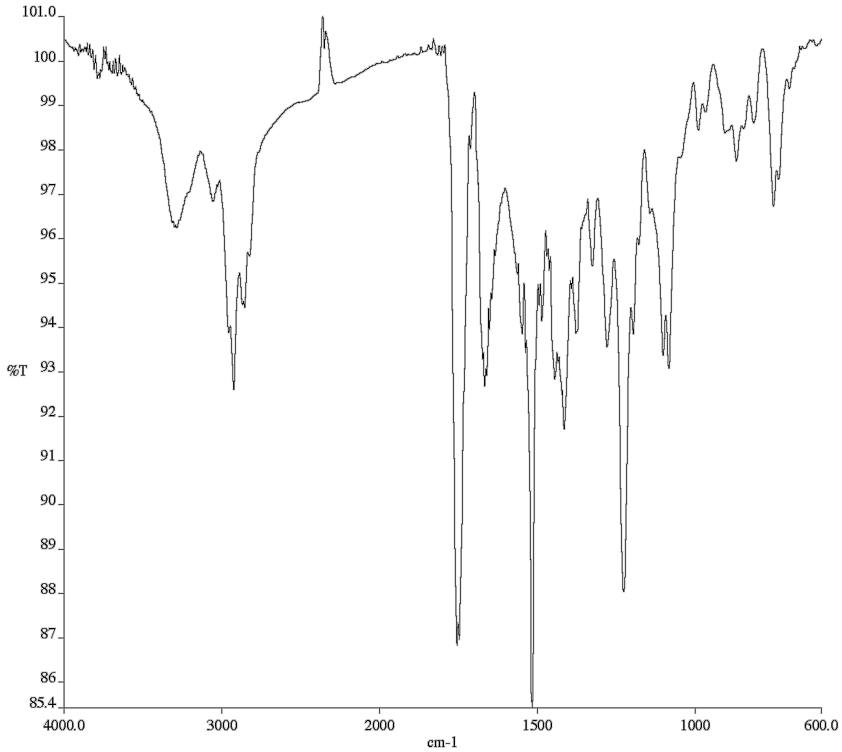

Figure A6.47 Infrared spectrum (Thin Film, NaCl) of compound **2.27**.

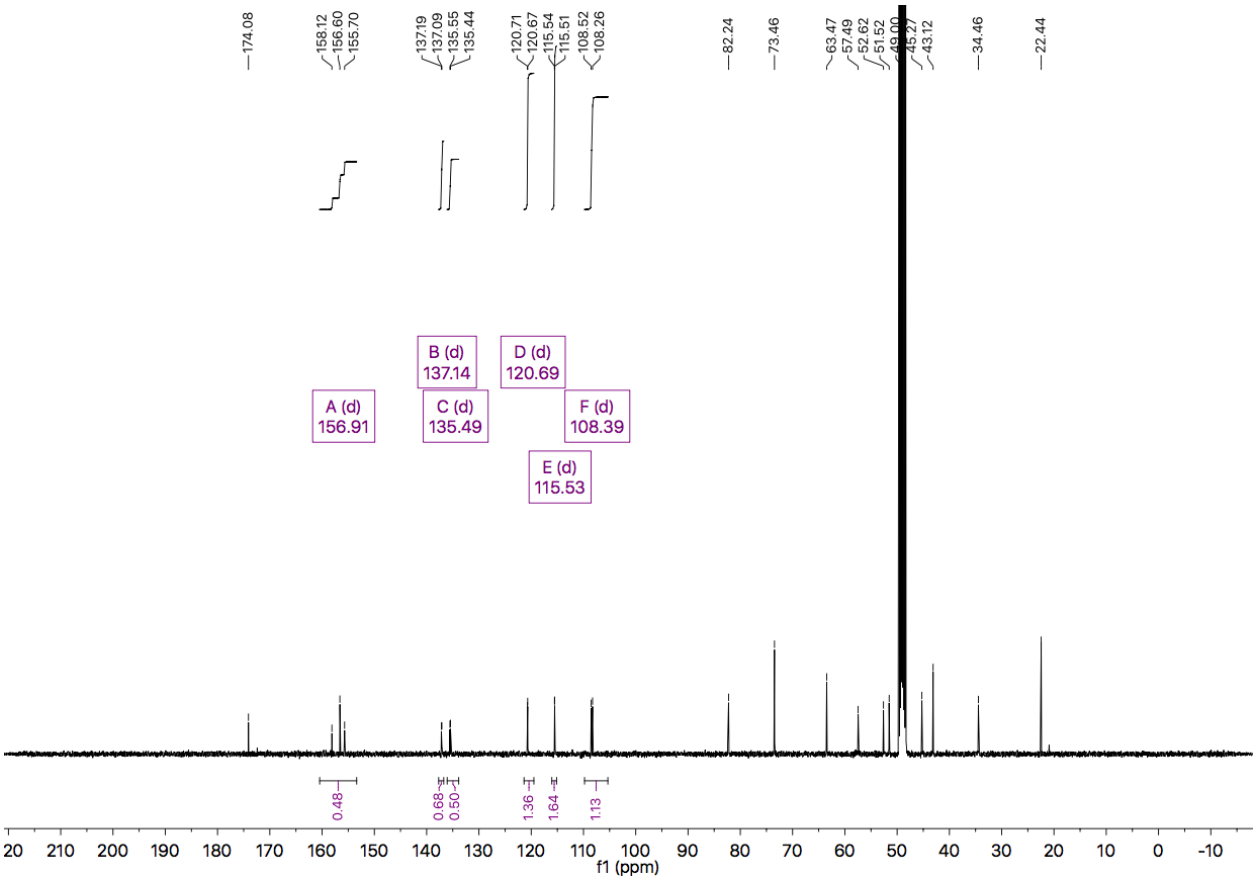

Figure A6.48 ^{13}C NMR (101 MHz, CD_3OD) of compound **2.27**.

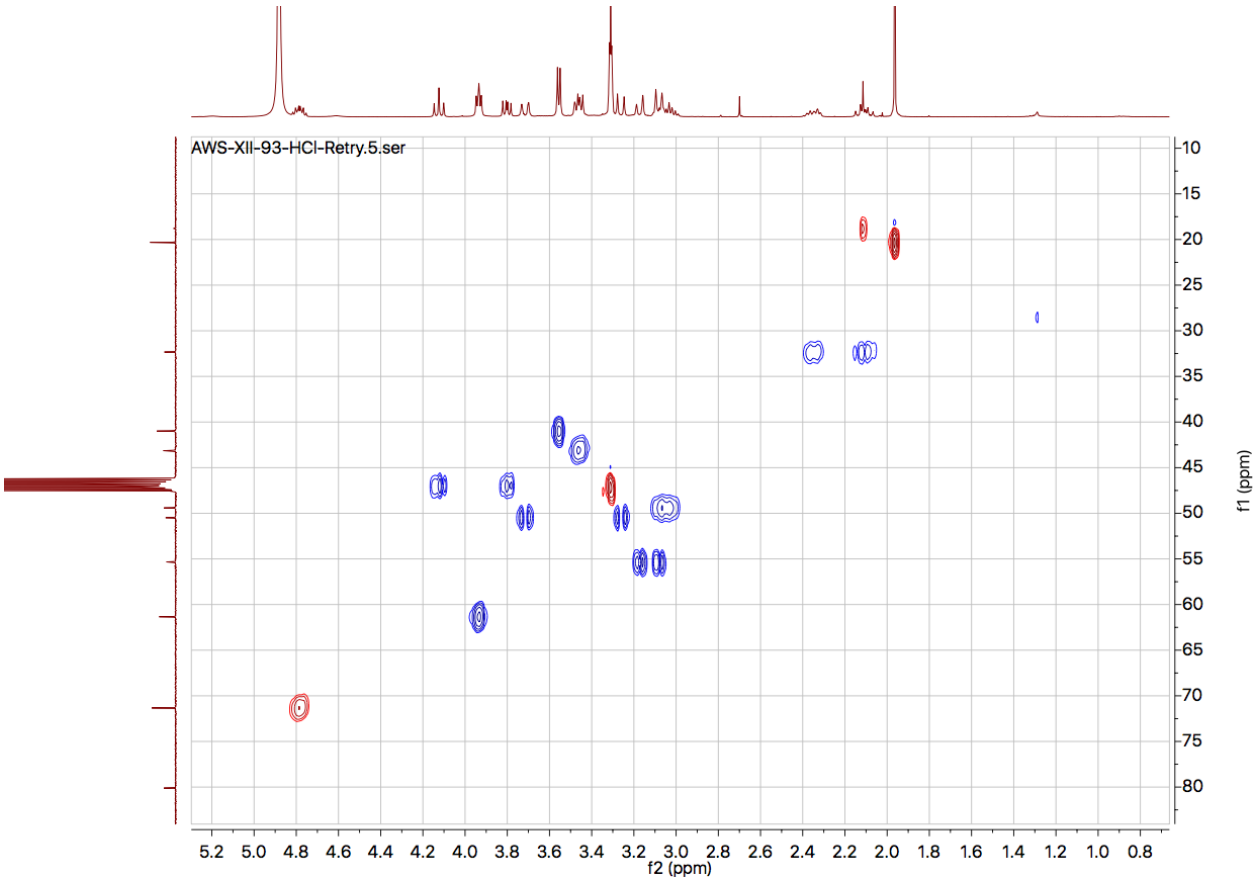

Figure A6.49 HSQC of compound **2.27** revealing one peak obscured by CD_3OD.

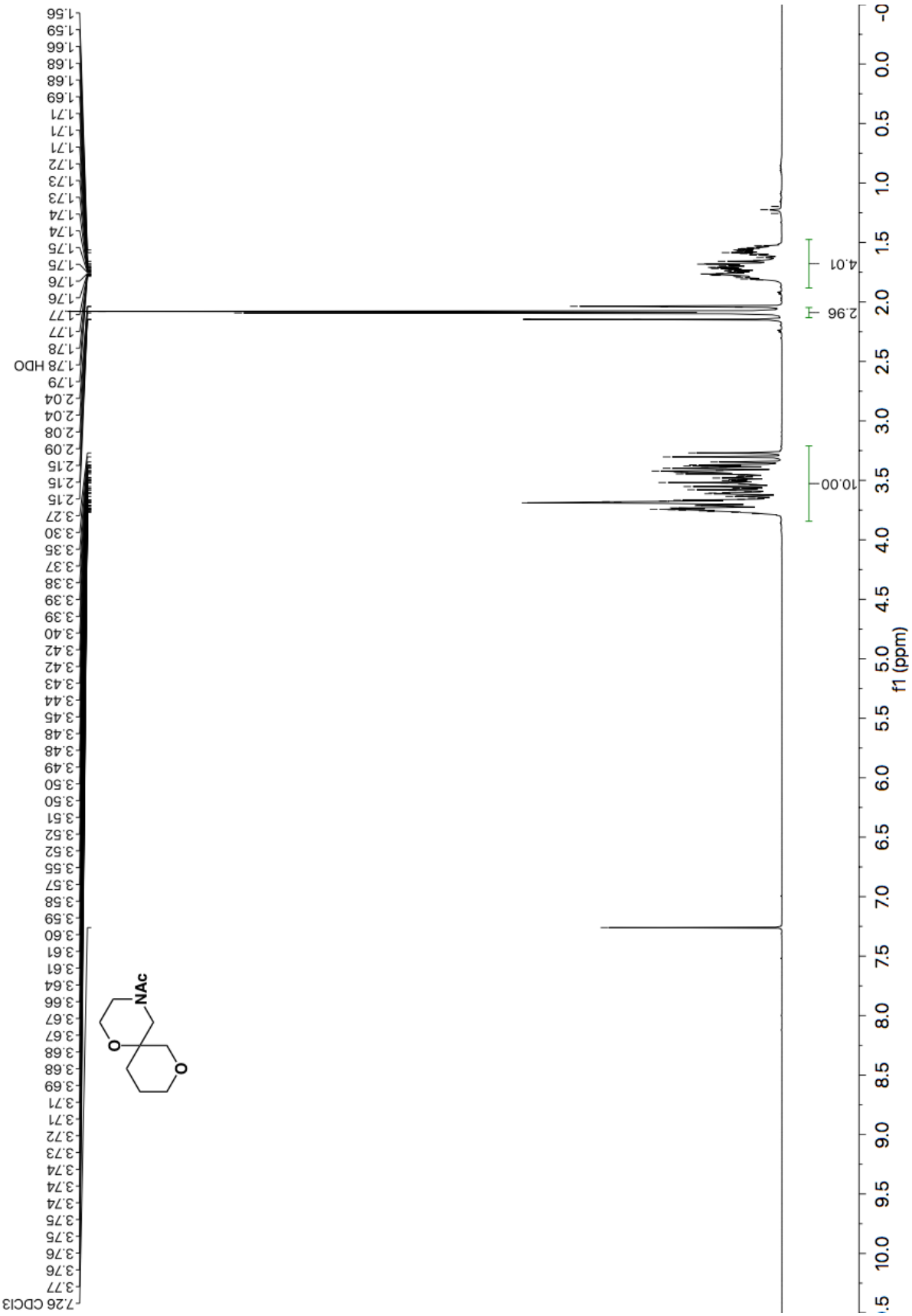

Figure A6.50 ^{1}H NMR (400 MHz, $CDCl_3$) of compound **SI3a.**

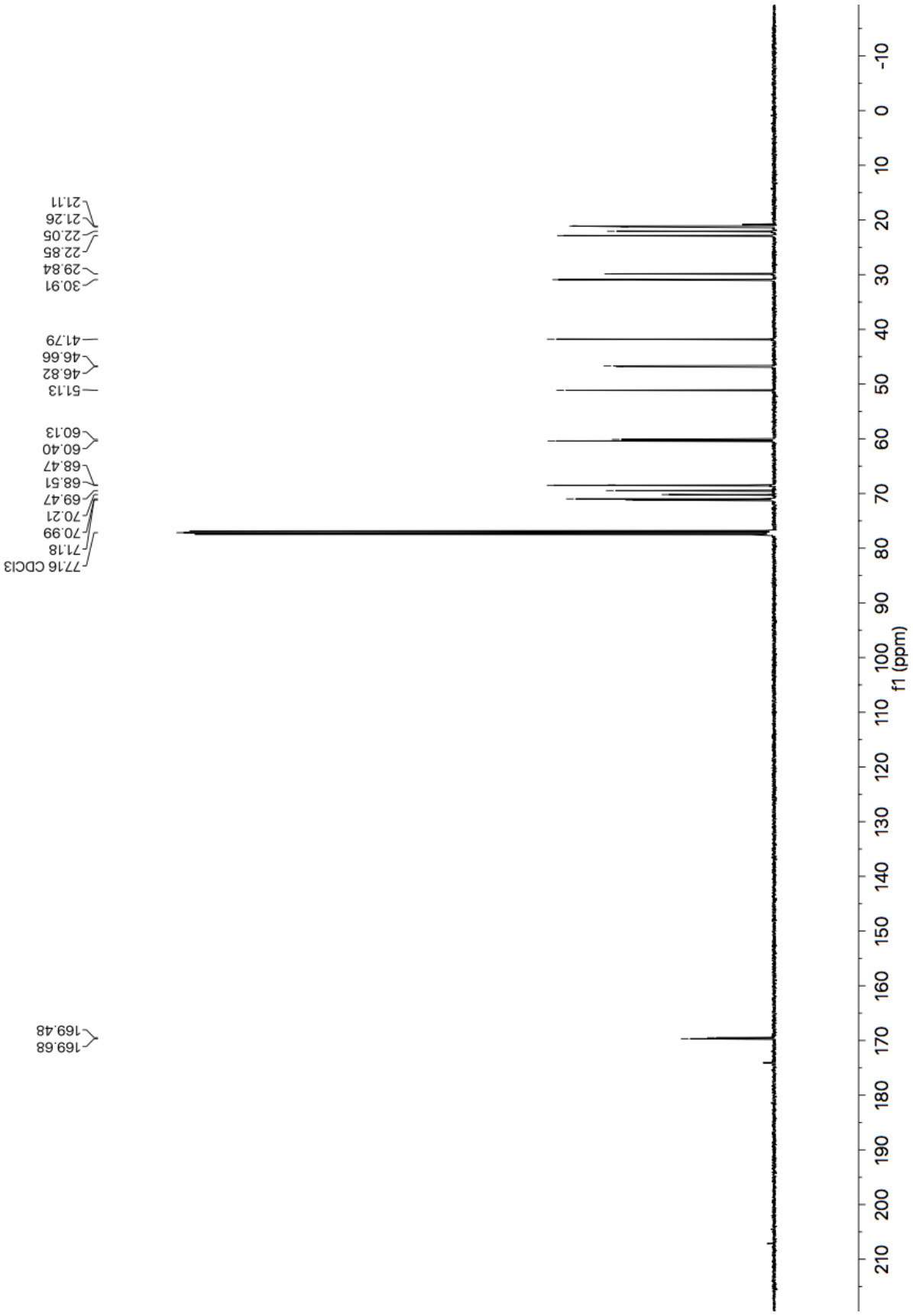

Figure A6.51 ^{13}C NMR (101 MHz, $CDCl_3$) of

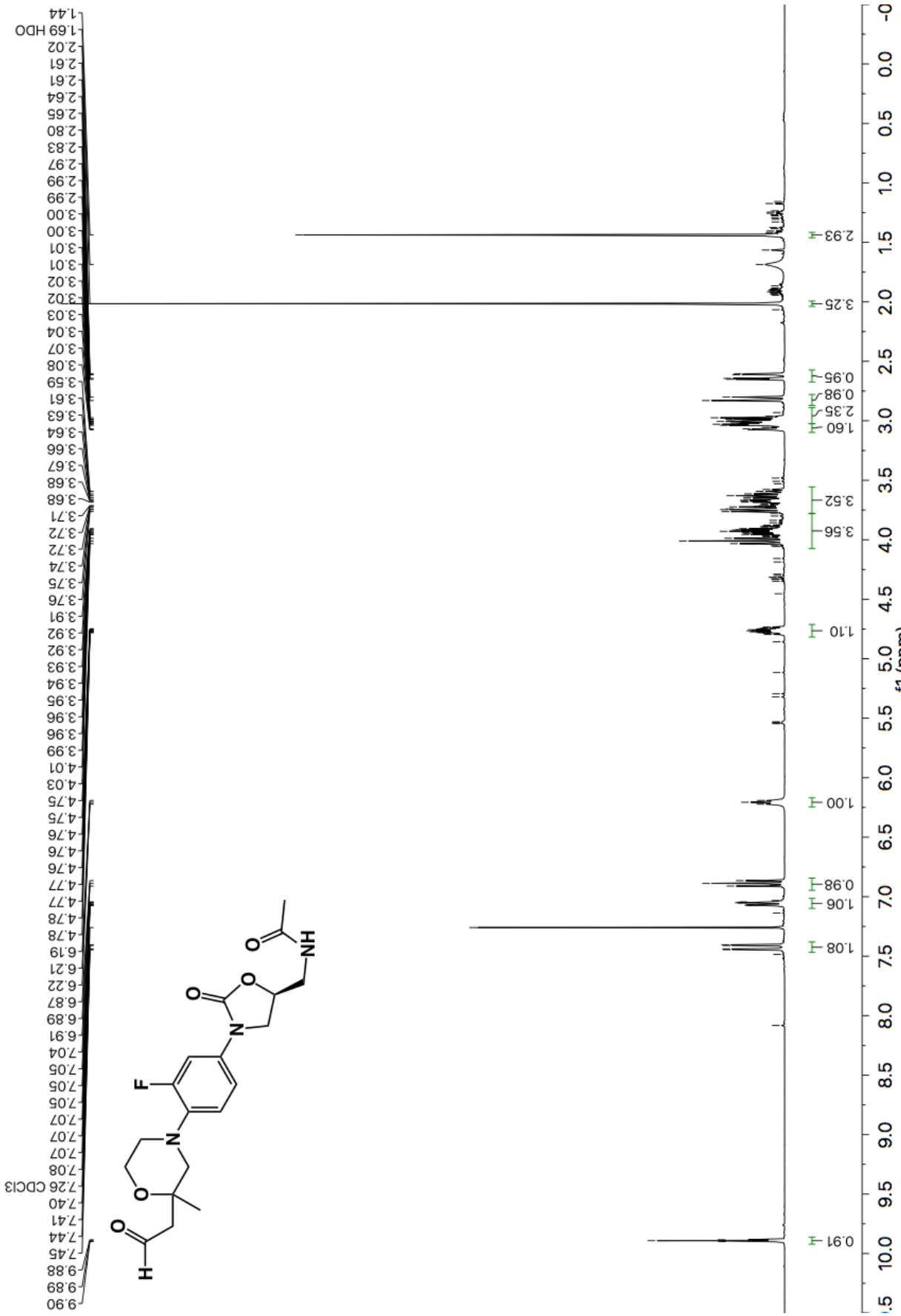

Figure A6.52 ^{1}H NMR (400 MHz, $CDCl_3$) of compound **SI4.**

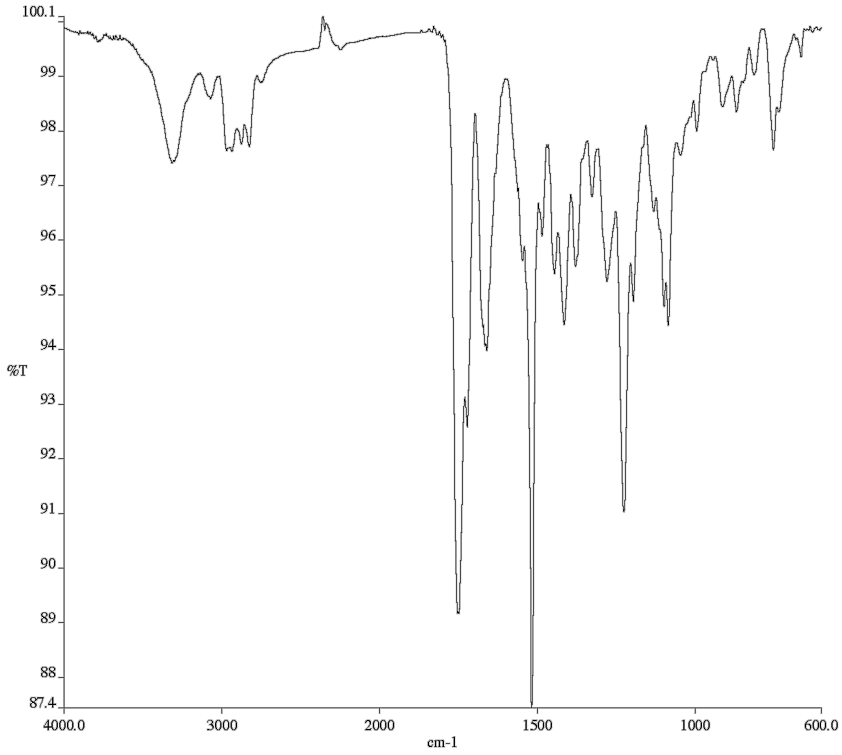

Figure A6.53 Infrared spectrum (Thin Film, NaCl) of compound **SI4**.

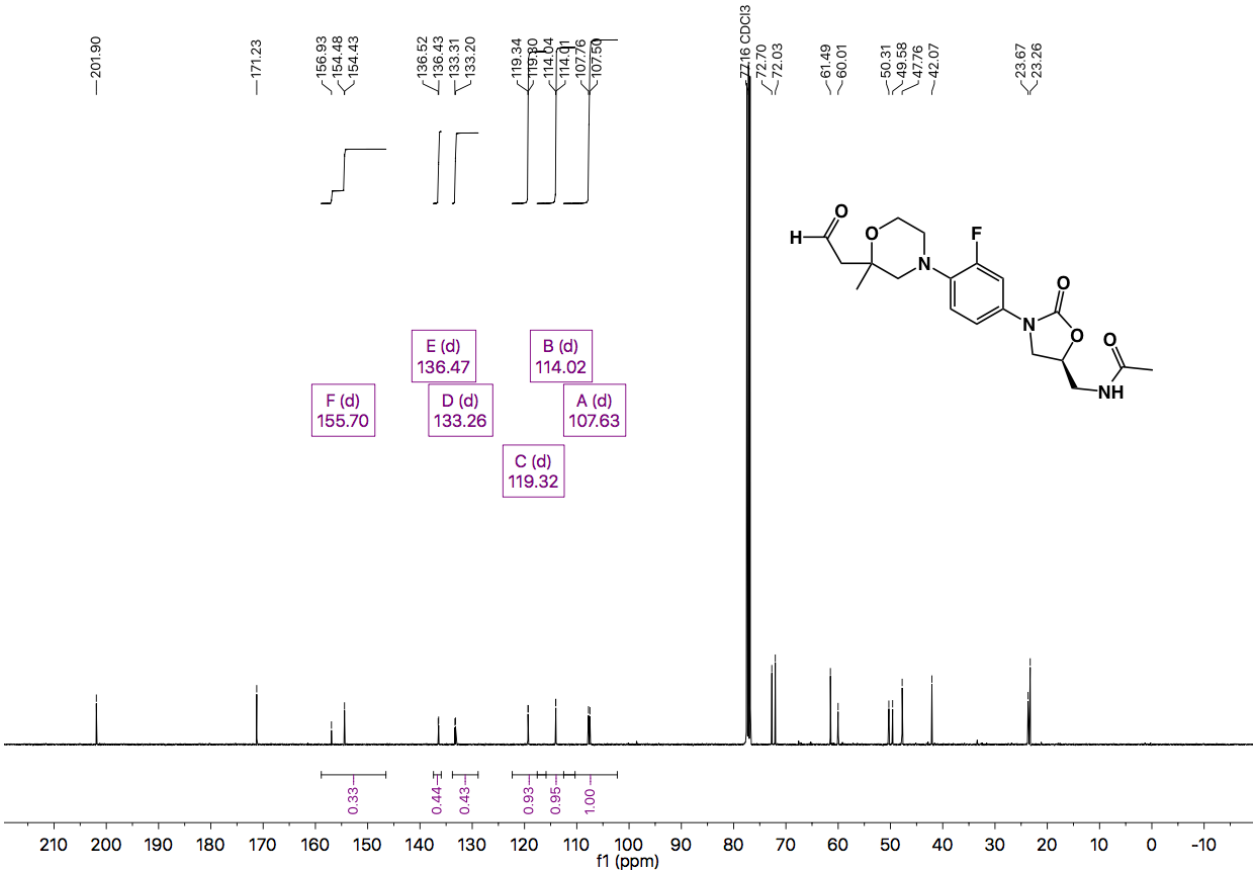

Figure A6.54 ^{13}C NMR (101 MHz, $CDCl_3$) of compound **SI4**.

APPENDIX 7

Decarboxylative Asymmetric Allylic Alkylation of Tertiary Alcohols

A7.1 INTRODUCTION AND BACKGROUND

Enantioenriched tertiary alcohols are valuable motifs found in myriad bioactive natural products and pharmaceuticals, such as the alkaloid chemotherapeutic (−)-vinblastine[1] and the neurotrophic sesquiterpene (+)-jiadifenin[2] (Figure A7.1). Due to the molecular prevalence of chiral tertiary alcohols, diverse methods[3] have been developed to enable the stereoselective α-hydroxylation of a wide range of carbonyl compounds, including acyclic compounds,[4,5,6] oxindoles,[7,8] pyrazolones,[9] and cycloalkanones[10] (Scheme A7.1). Aside from chiral oxidants such as oxaziridines introduced during Davis's pivotal 1981 studies,[11] α-hydroxylation methods can be broadly categorized under either transition metal catalysis or organic catalysis. In the realm of organic catalysis, a number of terminal oxidants have been coupled with structurally diverse chiral organic catalysts such BINOL-derived phosphoric acids,[12] guanidine-bisureas,[13,14,15] cinchona alkaloids,[6,9] aminobenzamides,[5] and photocatalysts composed of a bisoxazoline-diarylketone photosensitizer conjugate[16] (Scheme A7.1a). Similarly,

numerous chiral transition metal complexes also facilitate -hydroxylation,[3] including systems such as Cu-phenanthroline,[17] Zr-Salen,[10] and Ti-TADDOLato.[18]

Contrasting with these traditional enantioselective hydroxylation methods, in which the hydroxyl group is introduced in the enantiodetermining step, is a conceptually unique approach involving allylic alkylation of α-hydroxy compounds. In this case, alkylation of a prochiral hydroxyenolate would engender stereoselectivity. Of particular interest to our group were initial reports by Trost[19,20] utilizing a Pd-catalyzed decarboxylative allylic alkylation protocol to synthesize protected tertiary α-hydroxy ketones and aldehydes (Scheme A7.1b). Trost found that depending on the choice of bisphosphine ligand, isomeric products **A7.3** or **A7.4** could be almost exclusively attained. Later, Trost[21] again reported a decarboxylative alkylation approach toward the synthesis of MOM-protected tetralones (Scheme A7.1c). However, no examples of unprotected alcohols were shown. In a more recent 2017 advance, Zhang[22] demonstrated that a dual catalyst system involving Trost's Zn/ProPhenol system and an Ir catalyst could effect the C-alkylation of unprotected alcohols (Scheme A7.1d). It was hypothesized that the bidentate/ η^2 binding mode of the Zn catalyst reduced the nucleophilicity of the hydroxyl group, precluding O-allylation pathways. Most recently, Zhang[8] utilized a single iridium-phosphoramidite catalyst in the asymmetric allylic alkylation of oxindoles, showing the Zn/ProPhenol partner was not needed. We wondered if subjecting similar tertiary alcohols to decarboxylative allylic alkylation conditions using a simple single catalyst system consisting of Pd-PHOX could likewise enable effective C-alkylation (Scheme A7.1e).

Scheme A7.1 *Approaches toward tertiary α-hydroxy carbonyl compounds*

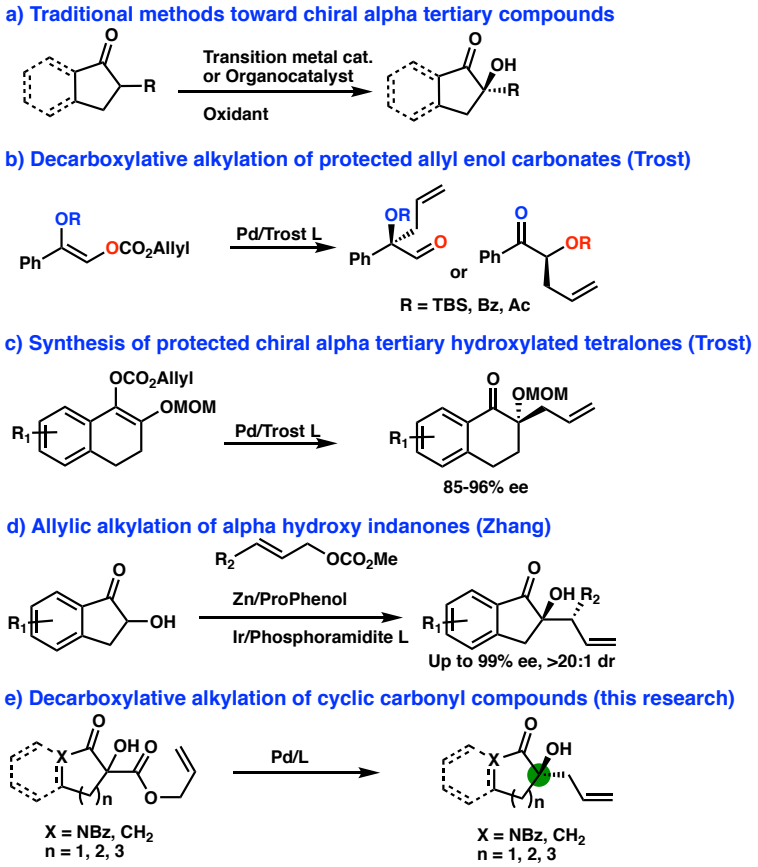

Our investigations were stimulated by an unexpected result[23] during the course of our studies on the decarboxylative allylic alkylation of *N*4-Boc piperazinones, in which we were pleased to obtain α-fluorinated substrate **A7.1** via electrophilic fluorination of the 1,3 dicarbonyl precursor (Scheme A7.2). However, upon subjecting **A7.1** to the optimized Pd-catalyzed alkylation conditions, the α-tertiary hydroxypiperazinone **A7.2** was instead obtained in a moderate 50% yield and 77% ee. The presence of adventitious water could produce this unexpected result; if fluoride anion is eliminated during the course of the reaction, water could attack the resulting iminium species before allylation occurs.

To extend upon this finding, we began by exploring the decarboxylative alkylation of tetralone **A7.3** (Table A7.1). Upon subjecting **A7.3** to standard Pd-catalyzed decarboxylative alkylation conditions using electron-deficient PHOX ligand **L1**, a 5/1 mixture of the desired product **A7.4a** and the isomer **A7.4b** were obtained, both with low *ee*. In contrast, the more electron-rich PHOX ligand **L2** increased the proportion of isomer **A7.4b** (1/3.6), with an improved *ee* of 68% for **A7.4a**. The bisphosphine ligands **L3** and **L4** provided even more of the isomer **A7.4b**, with ratios of 1/25 and 1/24, respectively. Interestingly, **A7.4b** was attained with an *ee* of 98% using **L3**.

Scheme A7.2 *Unexpected formation of a tertiary alcohol*

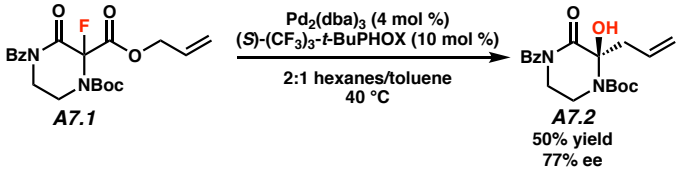

Table A7.1 *Attempts to optimize reaction conditions for model substrate* ***A7.3***

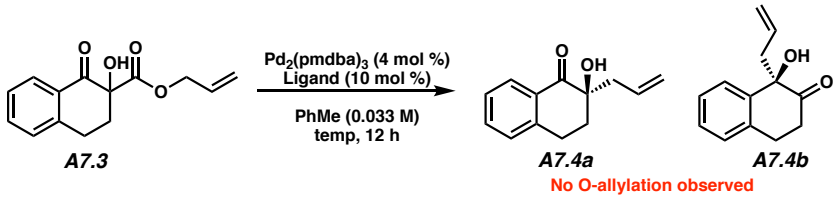

Entry	Ligand	Ratio A7.*4a*/*4b* (Yield %)[a,b]	*ee* A7.4a (%)[c]	*ee* A7.4b (%)[c]
1	**L1**	5/1 (50)	40	10
2	**L2**	1/3.6 (61)	68	10
3	**L3**	**1/25 (76)**	**1**	**98**
4	**L4**	1/24 (75)	4	20

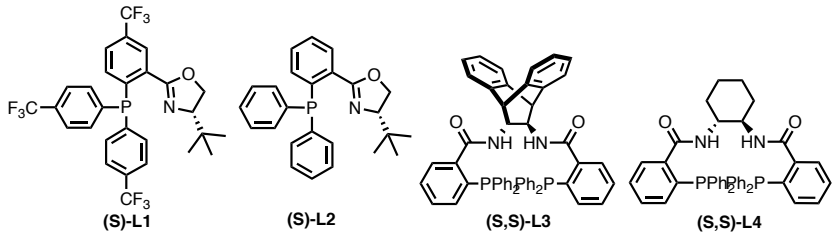

[a] Ratio determined by 400 MHz ^{1}H NMR spectroscopy of the purified mixture. [b] Isolated yield for the mixture of ***A7.4a*** and ***A7.4b***. [c] The ee values were determined by chiral SFC analysis. pmdba = bis(4-methoxybenzylidene)acetone

We then subjected the isomeric tetralone substrate **A7.5** to allylic alkylation conditions with ligands **L1** and **L3**, achieving product ratios of 1.4/1 and <1/25, respectively (Table A7.2). Together, these results suggest there is an equilibration of Pd-bound enolates leading to the observed ratios of products.

Table A7.2 *Investigation into reaction outcomes for isomeric tetralone* ***A7.5***

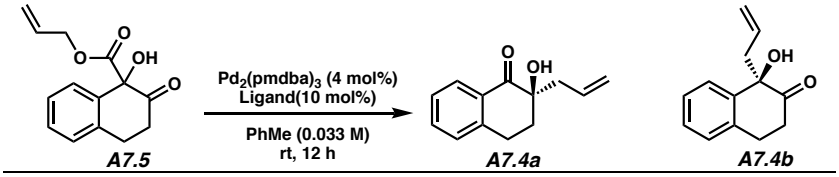

Entry	Ligand	Ratio *A7.4a/4b* (Yield %)[a,b]	*ee A7.4a* (%)[c]	*ee A7.4b* (%)[c]
1	**L1**	1.4/1 (70)	86	1
2	**L3**	<1/25 (65)	–	10

[a] Ratio determined by 400 MHz ^{1}H NMR spectroscopy of the purified mixture. [b] Isolated yield for the mixture of ***4a*** and ***4b***. [c] The *ee* values were determined by chiral SFC analysis.

We can rationalize these results with a relative rate argument considering the rate of alkylation versus equilibration of Pd-bound hydroxyenolates **I** and **II** (Scheme A7.3): If equilibration is faster than alkylation, as may be the case with electron rich ligands **L3** and **L4**, then more of the isomer **A7.4b** should be formed as intermediate **II** is more stable both electronically and sterically. In contrast, if alkylation is faster than equilibration, as may be the case for the electron deficient PHOX ligand **L1**, then **A7.3** should lead to proportionally more desired isomer **A7.4a**, and **A7.5** should lead to more **A7.4b**.

Scheme A7.3 *Mechanistic rationale for formation of isomeric tetralone products*

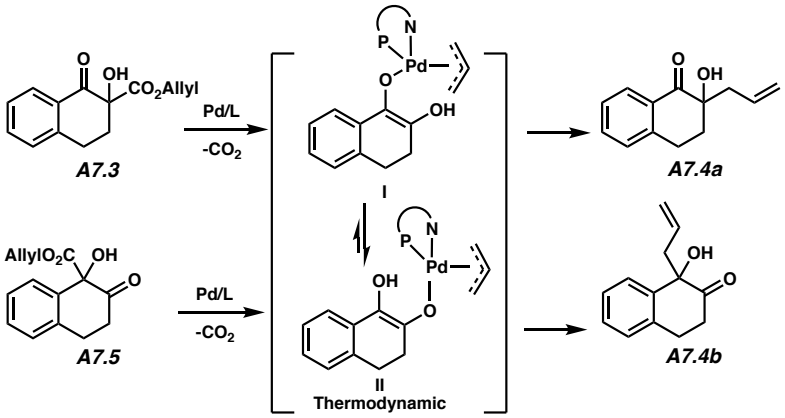

As mixtures of isomeric products may be uniquely obtained in unsaturated α-hydroxy systems such as tetralones, we elected to examine simpler carbocyclic substrates, beginning with cyclohexanone **A7.6a** (Table A7.3). Of the previously utilized ligands, the electron deficient **L1** provided the best results, affording tertiary alcohol **A7.7a** in a moderate 70% *ee*. Similarly, a methallyl variant **A7.7b** and cycloheptanone **A7.7c** were also attained in modest *ee*. The cyclopentanone **A7.7d** was obtained in a disappointing 30% *ee*, suggesting significant influence of conformation on stereoselectivity. In contrast, we were excited to obtain the novel tertiary α-hydroxypiperidinone **A7.7e** in 92% ee. Hydroxylactam **A7.7e** represents an oxidized derivative of the medicinally prevalent 3-hydroxypiperidine, which is found in pharmaceuticals like the chemotherapeutic vinblastine and the antihypertensive agent Benidipine.[24] Unfortunately, a variety of other heterocyclic substrates including piperazinones, caprolactams, and pyrrolidines, were unreactive under these Pd-catalyzed conditions.

Table A7.3 *Decarboxylative alkylation of α-hydroxyl dicarbonyl compounds*[a]

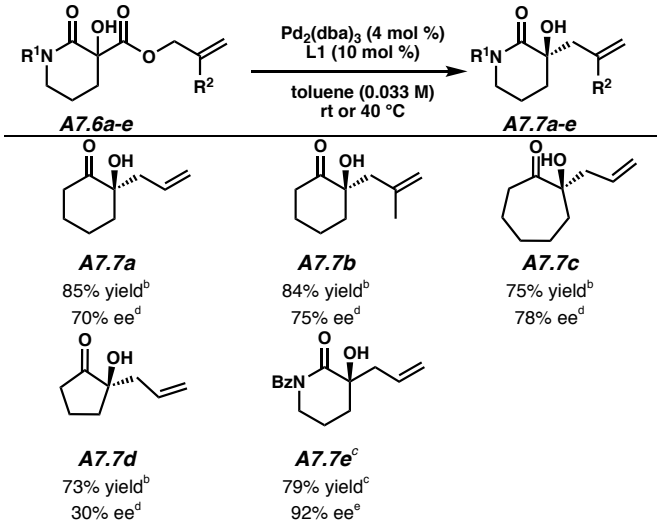

[a] Reported yields are for the isolated products. [b] Reaction performed at rt. [c] Reaction performed at 40 °C. [d] *ee* value determined by chiral GC analysis. [e] *ee* value determined by chiral SFC analysis. dba = dibenzylideneacetone.

Encouraged by these results, we next explored whether a primary hydroxyl group could be tolerated in the Pd-catalyzed decarboxylative alkylation conditions (Scheme A7.4). Our initial test substrate **A7.8** was amenable using **L3** to provide the desired primary hydroxyl product **A7.9** in moderate yield and an *ee* of 93%. Unfortunately, a variety of other primary alcohol substrates including lactams, and carbocyclic motifs were either unreactive, or provided a low-yielding mixture of *β*-elimination and protonation products.

Scheme A7.4 *Decarboxylative alkylation of a primary alcohol.*[a,b]

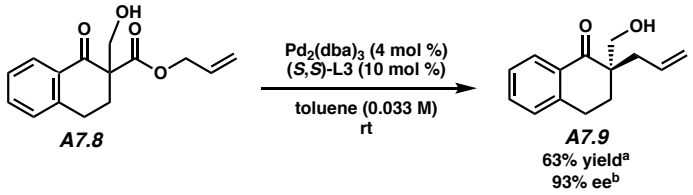

[a] Reported yield is for the isolated product. [b] *ee* value determined by chiral SFC analysis.

A7.2 CONCLUSIONS

In summary, we report initial results using the decarboxylative allylic alkylation reaction to synthesize chiral tertiary α-hydroxy compounds. While a novel tertiary hydroxypiperidinone was obtained in high *ee*, other carbocyclic compounds still require optimization with an appropriate catalyst-ligand combination. Nevertheless, this research provides proof of concept that Pd-catalysts are effective in the decarboxylative *C*-alkylation of unprotected alcohol-containing substrates and can lead to high yield and high enantioselectivities in certain limited cases.

A7.3 EXPERIMENTAL SECTION

A7.3.1 MATERIALS AND METHODS

Unless otherwise stated, reactions were performed in flame-dried glassware under an argon or nitrogen atmosphere using dry, deoxygenated solvents. Solvents were dried by passage through an activated alumina column under argon. Commercially obtained reagents were used as received. Chemicals were purchased from Sigma Aldrich/Strem/Alfa Aesar/Combi-Blocks and used as received.

Reaction temperatures were controlled by an IKAmag temperature modulator. Glove box manipulations were performed under a nitrogen atmosphere. Thin-layer

chromatography (TLC) was performed using E. Merck silica gel 60 F254 precoated plates (0.25 mm) and visualized by UV fluorescence quenching, iodine on silica, or $KMnO_4$ staining. Silia*Flash* P60 Academic Silica gel (particle size 0.040–0.063 mm) was used for flash chromatography.

Analytical SFC was performed with a Mettler SFC supercritical CO_2 analytical chromatography system utilizing a Chiralpak IC column (4.6 mm x 25 cm) obtained from Daicel Chemical Industries, Ltd. with visualization at 254 nm. Automated silica gel flash chromatography was performed with a Teledyne ISCO CombiFlash EZ Prep system.

^{1}H NMR spectra were recorded on a Varian Inova 600 MHz or 500 MHz spectrometer or a Bruker Avance HD 400 MHz spectrometer and are reported relative to residual $CHCl_3$ (δ 7.26 ppm). ^{13}C NMR spectra were recorded on a Varian Inova 500 MHz spectrometer or a Bruker Avance HD 400 MHz spectrometer and are reported relative to residual $CDCl_3$ (δ 77.16 ppm). Data for ^{1}H NMR are reported as follows: s = singlet, d = doublet, t = triplet, q = quartet, p = pentet, sept = septuplet, m = multiplet, br s = broad singlet. Data for ^{13}C NMR are reported in terms of chemical shifts (δ ppm). Some reported spectra include minor solvent impurities of water (δ 1.56 or 4.87 ppm), ethyl acetate (δ 4.12, 2.05, 1.26 ppm), methylene chloride (δ 5.30 ppm), acetone (δ 2.17 ppm), grease (δ 1.26, 0.86 ppm), and/or silicon grease (δ 0.07 ppm), which do not impact product assignments.

IR spectra were obtained using a Perkin Elmer Paragon 1000 spectrometer using thin films deposited on NaCl plates and reported in frequency of absorption (cm^{-1}). High resolution mass spectra (HRMS) were obtained from an Agilent 6200 Series TOF with an Agilent G1978A Multimode source in electrospray ionization (ESI+), atmospheric

pressure chemical ionization (APCI+), or mixed ionization mode (MM: ESI-APCI+). Optical rotations were measured with a Jasco P-2000 polarimeter operating on the sodium D-line (589 nm), using a 100 mm pathlength cell and are reported as: $[\alpha]_D^T$ (concentration in g/100 mL, solvent). Stereochemistry is assigned by analogy to previous results.[1]

A7.3.2 EXPERIMENTAL PROCEDURES AND SPECTROSCOPIC DATA

A7.3.2.1 Experimental Procedures and Spectroscopic Data for the Synthesis of Tertiary Alcohol Allylic Alkylation Substrates and Corresponding Decarboxylative Alkylation Products

A) General Procedure for synthesis of allylic alkylation substrates using CeCl3-7H$_2$O

A solution of the *β*-ketoester (1 equiv) and $CeCl_3$-$7H_2O$ (0.05 equiv) in *i*PrOH (0.1 M) was evacuated and filled with O_2 three times. The solution was stirred at room temperature, changing color from light yellow to dark yellow/dark green over the course of the reaction. When TLC analysis showed the starting material had been completely consumed, the solvent was removed under reduced pressure and the crude product was purified by silica gel flash chromatography to afford the desired alcohol.

B) General Procedure for synthesis of allylic alkylation substrates using samarium(III) trifluoromethanesulfonate

To an orange solution of iodine (0.02 equiv) and samarium (III) triflate (0.05 equiv) in a 1:5 mixture of H_2O/THF (0.1 M) was added the *β*-ketoester substrate (1 equiv). The

solution was evacuated and filled with O_2 three times, sparged with O_2 for 5 minutes, and then allowed to stir until TLC analysis showed the starting material had been completely consumed. If the orange color faded to yellow, then another bolus of iodine was added iodine (0.02 equiv) as needed to restore the orange color. The reaction was then quenched with sodium thiosulfate and extracted with EtOAc (3x). NaCl was added to clear the emulsion formed during extraction. The combined organic layers were dried over Na_2SO_4, concentrated under reduced pressure onto silica gel, and purified by silica gel flash chromatography to afford the desired alcohol.

C) General Procedure for Pd-Catalyzed Decarboxylative Allylic Alkylation Reactions

Please note Racemic products were synthesized according to the general procedure, using achiral GlyPHOX ligand instead of a chiral ligand.[3] The absolute configuration for all other products has been inferred by analogy.[1] SFC and chiral GC conditions are listed at the end of the experimental procedure for each compound.

In a nitrogen-filled glovebox, an oven-dried 1 dram vial or 20 mL scintillation vial was charged with $Pd_2(pmdba)_3$ or $Pd_2(dba)_3$ (4 mol %), ligand (10 mol %), toluene, and a magnetic stir bar. The vial was stirred at ambient glovebox temperature (27 °C) for 30 min and then the substrate (1.0 equiv) was added as a solution in toluene (total concentration 0.033 M). The vial was sealed with a teflon cap stirred at ambient temperature or at 40 °C. When complete consumption of the starting material was observed by thin layer chromatography, the reaction mixture was removed from the glovebox and concentrated under reduced pressure. The residue was purified by silica gel flash chromatography to afford the desired tertiary hydroxyl product.

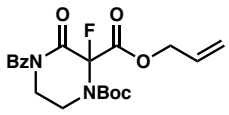

2-allyl 1-(tert-butyl) 4-benzoyl-2-fluoro-3-oxopiperazine-1,2-dicarboxylate (A7.1). Sodium hydride (60% in mineral oil, 11 mg, 0.28 mmol, 1.1 equiv) was added to a solution of 2-allyl 1-(tert-butyl) 4-benzoyl-3-oxopiperazine-1,2-dicarboxylate[4Ref] (100 mg, 0.26 mmol, 1.0 equiv) in THF (0.1 M) at 0 °C. After stirring for 30 min at 0 °C, Selectfluor (109 mg, 0.31 mmol, 1.2 equiv) was added. The reaction mixture was allowed to warm to room temperature and stirred for 16 h. The reaction was quenched with aqueous NH_4Cl (10 mL) and extracted with EtOAc (3 x 5 mL). The combined organic phases were dried over anhydrous Na_2SO_4, decanted, and concentrated under reduced pressure onto silica gel. After purification by silica gel flash chromatography (Et_2O/toluene 3% → 5%), the fluorinated ester **A7.2** was isolated as a colorless oil (70 mg, 67% yield): **^{1}H NMR (400 MHz, $CDCl_3$)** δ 7.67 – 7.48 (m, 3H), 7.48 – 7.29 (m, 2H), 5.93 (ddt, *J* = 17.3, 10.4, 5.9 Hz, 1H), 5.46 – 5.21 (m, 2H), 4.84 – 4.63 (m, 2H), 4.21 (m, 1H), 4.15 – 3.92 (m, 2H), 3.83 (m, 1H), 1.49 (s, 9H); **^{13}C NMR (101 MHz, $CDCl_3$)** δ 171.7, 163.3 (d, J_{CF} = 36 Hz), 162.5 (d, J_{CF} = 29 Hz), 152.5, 133.8, 132.9, 130.9, 128.5, 128.2, 119.9, 95.4 (d, J_{CF} = 227 Hz), 84.7, 67.7, 42.9, 41.2, 28.1; **IR (Neat Film, NaCl)** 3426, 3064, 2982, 2936, 1787, 1724, 1704, 1651, 1600, 1584, 1451, 1382, 1368, 1359, 1322, 1274, 1233, 1157, 1082, 1045, 1012, 993, 942, 849, 800, 774, 756, 725, 696, 624 cm^{-1}; **HRMS (MM: ESI-APCI)** *m/z* calculated for [C20H27FN3O6] ($[M+NH_4]^+$): 424.1878, found 424.1865.

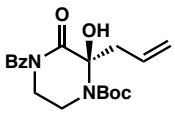

***tert*-butyl (*R*)-2-allyl-4-benzoyl-2-hydroxy-3-oxopiperazine-1-carboxylate (A7.2).** Following general procedure B, fluorinated allyl ester **A7.1** (10 mg, 0.025 mmol, 1.0 equiv) in hexanes/toluene (2:1, 1.3 mL) was added to a solution of $Pd_2(dba)_3$ (0.9 mg, 0.0098 mmol, 4 mol %) and (*S*)-$(CF_3)_3$-*t*Bu-PHOX (1.5 mg, 0.0025 mmol, 10 mol %) in hexanes/toluene (2:1, 0.5 mL). The reaction was stirred at 40 °C for 16 h. Purification by flash chromatography (10 → 15% EtOAc/hexanes) gave hydroxypiperazinone **A7.2** as a yellow oil (5 mg, 50% yield, 77% ee): **^{1}H NMR (400 MHz, $CDCl_3$)** δ 7.70 – 7.58 (m, 2H), 7.58 – 7.48 (m, 1H), 7.41 (dd, *J* = 8.3, 6.9 Hz, 2H), 5.74 (ddt, *J* = 17.5, 10.2, 7.4 Hz, 1H), 5.28 – 5.08 (m, 3H), 4.00 (t, *J* = 4.0 Hz, 2H), 3.86 (ddt, *J* = 11.0, 7.8, 3.9 Hz, 1H), 3.62 (dt, *J* = 13.9, 5.6 Hz, 1H), 3.2 (dd, *J* = 13.7, 7.2 Hz, 1H), 3.06 (dd, *J* = 13.7 fHz, 7.5 Hz, 1H), 1.54 (s, 9H); **^{13}C NMR (101 MHz, $CDCl_3$)** δ 172.3, 169.8, 154.5, 134.8, 132.2, 131.6, 128.4, 128.2, 120.4, 88.1, 82.6, 43.8, 42.4, 42.1, 28.5; **IR (Neat Film, NaCl)** 3375, 2978, 1714, 1600, 1513, 1394, 1368, 1253, 1172, 1028, 987, 833, 735 cm^{-1}; **HRMS (MM: ESI-APCI):** *m/z* calc'd for C19H25N2O5 $[M+H]^+$: 361.1758, found 361.1751; **$[\alpha]_D^{23.4}$** +5.2 (c 0.33, $CHCl_3$); **SFC conditions**: 20% IPA, 2.5 mL/min, Chiralpak AD-H column, λ = 210 nm, t_R (min): major = 5.069, minor = 4.221.

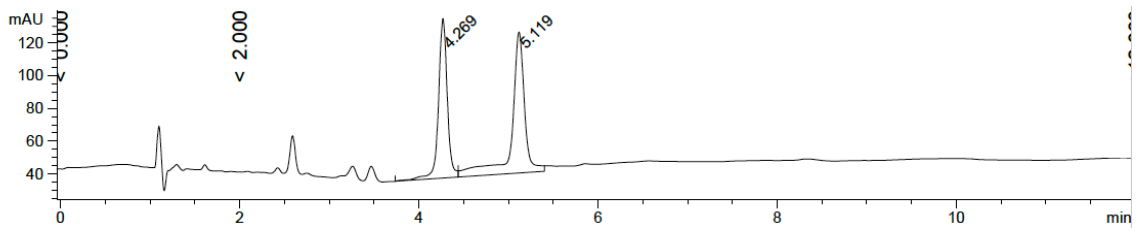

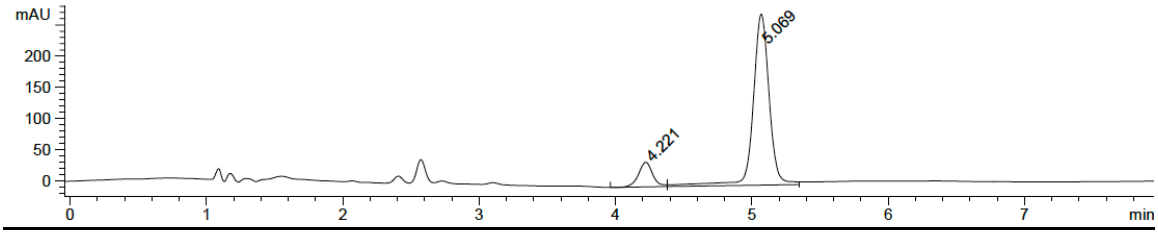

Signal 1: DAD1 A, Sig=210,8 Ref=360,100

Peak #	RetTime [min]	Type	Width [min]	Area [mAU*s]	Height [mAU]	Area %
1	4.221	VV	0.1088	286.42197	39.42324	11.2571
2	5.069	VB	0.1244	2257.93555	273.14166	88.7429
Totals :				2544.35751	312.56491	

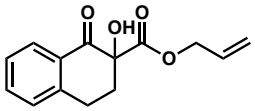

allyl 2-hydroxy-1-oxo-1,2,3,4-tetrahydronaphthalene-2-carboxylate (A7.3). Following general procedure B: to a solution of iodine (11 mg, 0.04 mmol, 0.02 equiv) and samarium (III) triflate (65 mg, 0.11 mmol, 0.05 equiv) in a 1:5 mixture of H_2O/THF (24 mL) was added allyl 1-oxo-1,2,3,4-tetrahydronaphthalene-2-carboxylate (500 mg, 2.17 mmol, 1 equiv). The reaction was stirred for 72 h. Purification by silica gel flash chromatography (20 → 30% EtOAc/hexanes) afforded alcohol **A7.3** as a clear oil (450 mg, 84% yield): **^{1}H NMR (400 MHz, $CDCl_3$)** δ 8.03 (dd, *J* = 7.8, 1.6 Hz, 1H), 7.51 (ddd, *J* = 9.1, 6.6, 1.6 Hz, 1H), 7.32 (td, *J* = 7.2, 6.6, 1.6 Hz, 1H), 7.24 (d, *J* = 7.8 Hz, 1H), 5.80 (ddtd, *J* = 16.6, 11.0, 5.6, 1.5 Hz, 1H), 5.23 – 5.08 (m, 2H), 4.62 (d, *J* = 5.4 Hz, 2H), 4.39 (s, 1H), 3.10 (d, *J* = 5.6 Hz, 2H), 2.71 (ddd, *J* = 13.7, 6.0, 4.3 Hz, 1H), 2.24 (ddd, *J* = 13.6, 8.5, 6.7 Hz, 1H); **^{13}C NMR (101 MHz, $CDCl_3$)** δ 194.5, 170.4, 144.0, 134.5, 131.1,

130.3, 129.0, 128.2, 127.2, 127.0, 118.7, 77.8, 66.4, 32.7, 30.2, 25.6; **IR (Neat Film, NaCl)** 3466, 3073, 3026, 2939, 1745 1689, 1649, 1602,1485, 1456, 1377, 1333, 1292, 1239, 1191, 1159, 1139, 1109, 1035, 996, 970, 944, 919, 806, 744, 690, 661 cm^{-1}; **HRMS (MM: ESI-APCI):** *m/z* calc'd for $[C_{14}H_{15}O_4]$ ($[M+H]^+$): 247.0965, found 247.0965.

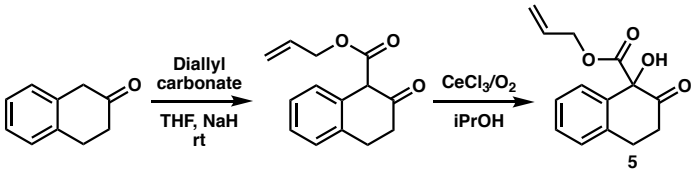

allyl 1-hydroxy-2-oxo-1,2,3,4-tetrahydronaphthalene-1-carboxylate (A7.5). To a suspension of NaH (60% in mineral oil, 684 mg, 17.1 mmol, 2.5 equiv) in THF (20 mL) at 0 °C was added 2-tetralone (1g, 6.84 mmol, 1 equiv) dropwise, producing a yellow-green solution. The solution was stirred for 30 min at 0 °C before adding diallyl carbonate (1.47 mL, 10.3 mmol, 1.5 equiv) dropwise. The reaction was heated to reflux for 16 h, resulting in a dark orange-gold color. The reaction was quenched with aq. NH_4Cl (20 mL) and then extracted with EtOAc (3x15 mL). The combined organic layers were dried with Na_2SO_4 and then concentrated under reduced pressure. Purification of the crude reaction mixture with silica gel flash chromatography (0 → 2.5 → 4% EtOAc/hexanes) afforded the intermediate allyl *β*-ketoester, which was then used in the following hydroxylation reaction following general procedure A: a solution of the *β*-ketoester (400 mg, 1.74 mmol, 1 equiv) and $CeCl_3$-$7H_2O$ (32 mg, 0.087 mmol, 0.05 equiv) in *i*PrOH (17 mL, 0.1 M) was evacuated and filled with O_2 three times. The solution was stirred for 6 h at room temperature, changing color from light yellow to dark

yellow over the course of the reaction. The solvent was removed under reduced pressure and the crude product was purified by silica gel Teledyne ISCO automated flash chromatography (0 → 50% Et_2O/hexanes) to afford alcohol **A7.5** as a clear oil (200 mg, 47% yield): **^{1}H NMR (400 MHz, $CDCl_3$)** δ 7.70 – 7.60 (m, 1H), 7.38 – 7.27 (m, 2H), 7.27 – 7.17 (m, 1H), 5.80 (ddt, *J* = 17.0, 10.6, 5.6 Hz, 1H), 5.23 – 5.16 (m, 1H), 5.15 (dq, *J* = 12.9, 1.6 Hz, 1H), 4.61 (t, *J* = 1.4 Hz, 1H), 4.60 – 4.57 (m, 2H), 3.40 – 3.27 (m, 1H), 3.14 – 2.99 (m, 2H), 2.74 – 2.59 (m, 1H); **^{13}C NMR (101 MHz, $CDCl_3$)** δ 206.9, 169.1, 136.0, 134.6, 130.9, 129.0, 128.0, 127.5, 126.5, 119.1, 79.8, 66.8, 34.6, 27.5; **IR (Neat Film, NaCl)** 3455, 3071, 3026, 2946, 1748, 1727, 1651, 1484, 1455, 1360, 1245, 1209, 1160, 1122, 1070, 1025, 990, 944, 749, 651 cm^{-1}; **HRMS (MM: ESI-APCI):** *m/z* calc'd for $[C_{14}H_{18}NO_4]$ ($[M+NH_4]^+$): 264.1230, found 264.1228.

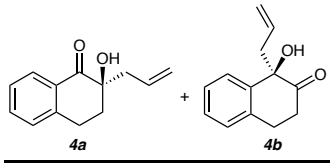

Following general procedure B, tetralone **A7.3** or **A7.5** (20 mg, 0.081 mmol, 1 equiv) in toluene (2.0 mL) was added to a solution of $Pd_2(pmdba)_3$ (3.6 mg, 0.0032 mmol, 4 mol %) and ANDEN (*S*,*S*)-**L3** (6.6 mg, 0.008 mmol, 10 mol %) or (*S*)-**L1** (4.8 mg, 0.008 mmol, 10 mol %) in toluene (0.5 mL). Purification by silica gel flash chromatography (15% EtOAc/hexanes) gave *α*-tertiary tetralones **A7.4a** and **A7.4b** as a mixture, the ratio of which was determined by ^{1}H NMR. Product identities of **A7.4a** and **A7.4b** were confirmed by comparison to previously reported characterization data. **SFC conditions**: 7% IPA, 2.5 mL/min, Chiralpak AD-H column, λ = 210 nm, t_R (min): For 4b: major = 3.664, minor not detected.

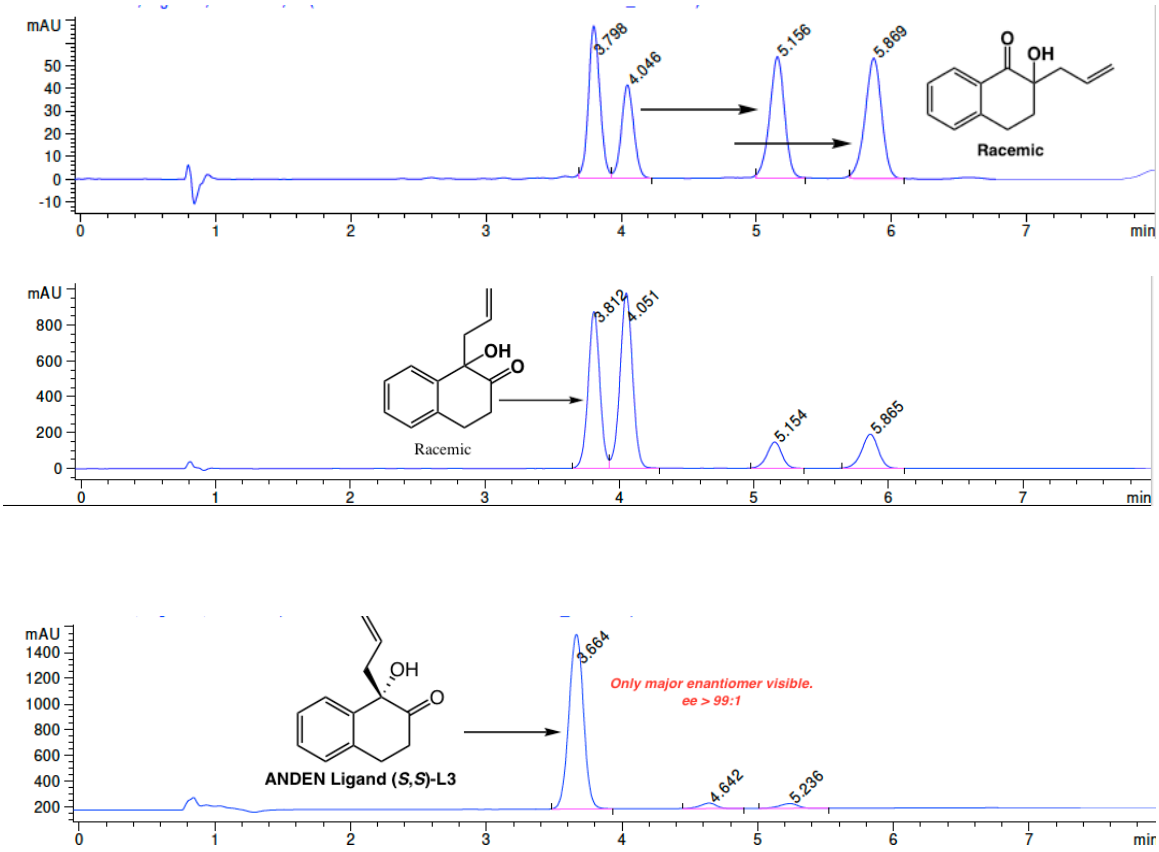

Note: Based on relative retention times, ANDEN (*S*,*S*)-**L3** gives the opposite enantiomer of the product **4b** compared to (*S*)-**L1** and (*S*)-**L2**, [(*S*)-*t*-BuPHOX/(*S*)-CF_3-*t*-BuPHOX].

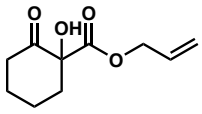

allyl 1-hydroxy-2-oxocyclohexane-1-carboxylate A7.6a. A solution of allyl 2-oxocyclohexane-1-carboxylate (1.7 g, 9.33 mmol, 1 equiv) and $CeCl_3$-$7H_2O$ (173 mg, 0.47 mmol, 0.05 equiv) in *i*-PrOH (93 mL) was evacuated and filled with O_2 three times. The solution was stirred for 1 hour at room temperature, changing color from clear to light pink over the course of the reaction. The solvent was removed under reduced pressure and the crude product was purified by silica gel flash chromatography (10 →

20% EtOAc/hexanes) to afford alcohol **6a** as a clear oil (1.11 g, 60% yield): **^{1}H NMR (400 MHz, $CDCl_3$)** δ 5.89 (ddt, *J* = 17.2, 10.4, 5.8 Hz, 1H), 5.38 – 5.19 (m, 2H), 4.66 (dt, *J* = 5.8, 1.4 Hz, 2H), 4.35 (s, 1H), 2.71 – 2.59 (m, 2H), 2.55 (ddd, *J* = 14.1, 11.8, 6.1 Hz, 1H), 2.13 – 1.96 (m, 1H), 1.96 – 1.77 (m, 2H), 1.77 – 1.58 (m, 2H); **^{13}C NMR (101 MHz, $CDCl_3$)** δ 207.3, 169.8, 131.2, 119.4, 80.8, 66.5, 39.0, 37.8, 27.2, 22.1; **IR (Neat Film, NaCl)** 3780, 3458, 3087, 2947, 2869, 2668, 2403, 1727, 1649, 1452, 1425, 1374, 1337, 1311, 1247, 1207, 1132, 1116, 1094, 1054, 984, 937, 853, 817, 792, 714, 689, 618 cm^{-1}; **HRMS (MM: ESI-APCI)** *m/z* calculated for [C10H18NO4] ($[M+NH_4]^+$): 216.1230, found 216.1232.

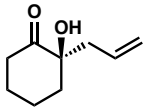

(R)-2-allyl-2-hydroxycyclohexan-1-one (A7.7a). Following general procedure B, ketoester **A7.6a** (15 mg, 0.076 mmol, 1.0 equiv) in toluene (1.8 mL) was added to a solution of $Pd_2(pmdba)_3$ (3.3 mg, 0.003 mmol, 4 mol %) and (*S*)-$(CF_3)_3$-*t*Bu-PHOX (4.5 mg, 0.0076 mmol, 10 mol %) in toluene (0.5 mL). The reaction was stirred at ambient temperature for 16 h. Purification by flash chromatography (15% EtOAc/hexanes) gave α-hydroxycyclohexanone **A7.7a** as a yellow oil (10 mg, 85% yield, 70% ee): **^{1}H NMR (400 MHz, $CDCl_3$)** δ 5.72 (ddt, *J* = 16.6, 10.6, 7.2 Hz, 1H), 5.16 – 5.06 (m, 2H), 3.95 (s, 1H), 2.59 (ddt, *J* = 14.0, 7.4, 1.1 Hz, 1H), 2.55 – 2.43 (m, 2H), 2.48 – 2.38 (m, 1H), 2.22 (dq, *J* = 13.0, 3.0 Hz, 1H), 2.16 – 2.05 (m, 1H), 1.89 – 1.56 (m, 4H); **^{13}C NMR (101 MHz, $CDCl_3$)** δ 213.7, 131.8, 118.9, 78.9, 41.9, 40.5, 38.4, 27.9, 22.7. **IR (Neat Film, NaCl)** 3475, 3073, 2939, 2864, 1711, 1639, 1441, 1379, 1309, 1242, 1156, 1128, 1078, 1047, 1000, 916, 681, 624 cm^{-1}; **HRMS (MM: ESI-APCI):** *m/z* calc'd for C9H17NO2

$[M+NH_4]^+$: 172.1332, found 172.1328; $[\alpha]_D^{23.0}$ –10.2 (c 1.0, $CHCl_3$); **Chiral GC conditions**: Astec® CHIRALDEX G-TA column, 100 °C isotherm, t_R (min): major = 29.288, minor = 36.310.

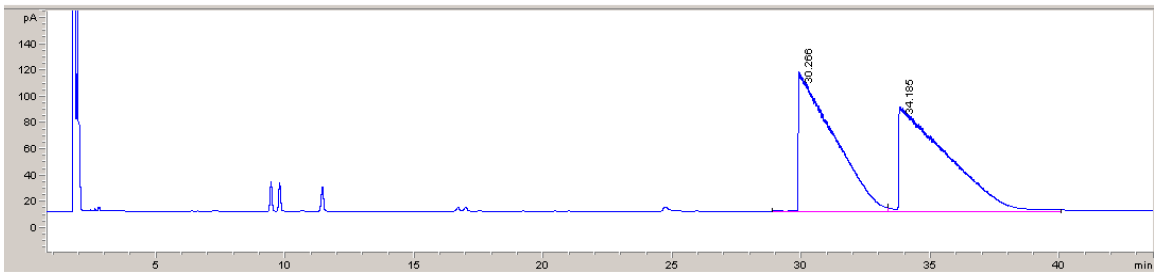

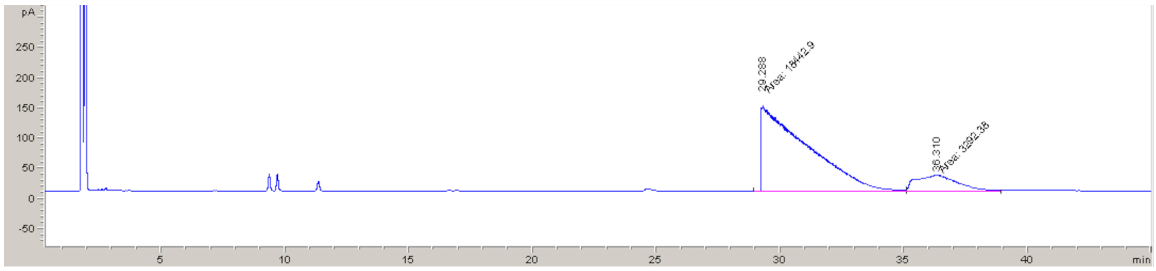

Peak #	RetTime [min]	Type	Width [min]	Area [pA*s]	Height [pA]	Area %
1	29.288	MM	1.9171	1.84429e4	160.33733	84.85236
2	36.310	MM	1.9411	3292.37720	28.26843	15.14764
Totals :				2.17352e4	188.60576	

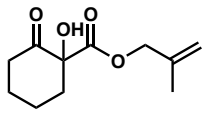

2-methylallyl 1-hydroxy-2-oxocyclohexane-1-carboxylate (A7.6b). Note: While general procedure A using catalytic $CeCl_3$-$7H_2O$ was successful, it led to a mixture that was more difficult to purify. Thus, we used general procedure B: to a solution of iodine (10 mg, 0.04 mmol, 0.02 equiv) and samarium (III) triflate (60 mg, 0.10 mmol, 0.05 equiv) in a 1:5 mixture of H_2O/THF (24 mL) was added 2-methylallyl 2-oxocyclohexane-

1-carboxylate[Ref] (400 mg, 2.0 mmol, 1 equiv). The reaction was stirred for 72 h. Purification by silica gel flash chromatography (1 → 2% Et_2O/CH_2Cl_2) afforded alcohol **A7.6b** as a clear oil (240 mg, 55% yield): **^{1}H NMR (400 MHz, $CDCl_3$)** δ 5.01 – 4.91 (m, 2H), 4.65 – 4.54 (m, 2H), 4.36 (s, 1H), 2.74 – 2.60 (m, 2H), 2.55 (ddd, *J* = 14.0, 11.7, 6.0 Hz, 1H), 2.04 (ddtd, *J* = 14.4, 6.4, 4.2, 3.8, 1.9 Hz, 1H), 1.94 – 1.76 (m, 2H), 1.74 (t, *J* = 1.2 Hz, 3H), 1.73 – 1.62 (m, 2H); **^{13}C NMR (101 MHz, $CDCl_3$)** δ 207.3, 169.9, 139.1, 114.0, 80.9, 69.2, 39.0, 37.7, 27.2, 22.1, 19.6; **IR (Neat Film, NaCl)** 3457, 3084, 2947, 2869, 1722, 1660, 1451, 1378, 1247, 1205, 1116, 1093, 1055, 991, 960, 907, 852, 814, 785, 686, 619 cm^{-1}; **HRMS (MM: ESI-APCI)** *m/z* calculated for [C11H20NO4] ($[M+NH_4]^+$): 230.1387, found 230.1382.

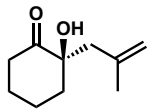

(*R*)-2-hydroxy-2-(2-methylallyl)cyclohexan-1-one (A7.7b). Following general procedure C, alcohol **A7.6b** (15 mg, 0.071 mmol, 1.0 equiv) in toluene (1.6 mL) was added to a solution of $[Pd_2(pmdba)_3]$ (3.1 mg, 0.0028 mmol, 4 mol %) and (*S*)-$(CF_3)_3$-*t*-BuPHOX (4.2 mg, 0.0071 mmol, 10 mol %) in toluene (0.5 mL). Purification by flash chromatography (10% EtOAc/hexanes) gave alcohol **A7.7b** as a clear oil (10 mg, 84% yield, 75% ee): **^{1}H NMR (400 MHz, $CDCl_3$)** δ 4.86 (dd, *J* = 2.1, 1.4 Hz, 1H), 4.73 (dd, *J* = 2.0, 1.0 Hz, 1H), 3.94 (s, 1H), 2.65 – 2.47 (m, 3H), 2.43 (dd, *J* = 13.8, 1.0 Hz, 1H), 2.24 (dq, *J* = 13.2, 3.1 Hz, 1H), 2.19 – 2.06 (m, 1H), 1.86 – 1.72 (m, 5H), 1.72 – 1.56 (m, 2H); **^{13}C NMR (101 MHz, $CDCl_3$)** δ 214.1, 141.0, 115.2, 79.5, 45.3, 41.4, 38.7, 28.2, 24.2, 23.0; **IR (Neat Film, NaCl)** 3482, 3073, 2941, 2865, 2358, 1709, 1644, 1452, 1376, 1308, 1250, 1197, 1154, 1130, 1103, 1069, 1015, 953, 893, 855, 654 cm^{-1}; **HRMS**

(MM: ESI-APCI): *m/z* calc'd for [C10H20NO2] ([M+NH_4]$^+$): 186.1489, found 186.1482; **[α]$_D^{23.3}$** –28.2 (c 0.33, $CHCl_3$); **Chiral GC conditions**: Astec® CHIRALDEX G-TA column, 120 °C isotherm, t_R (min): major = 11.639, minor = 13.805.

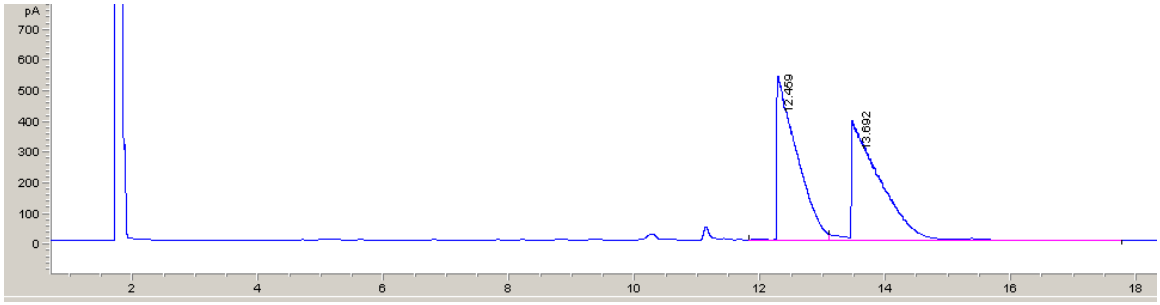

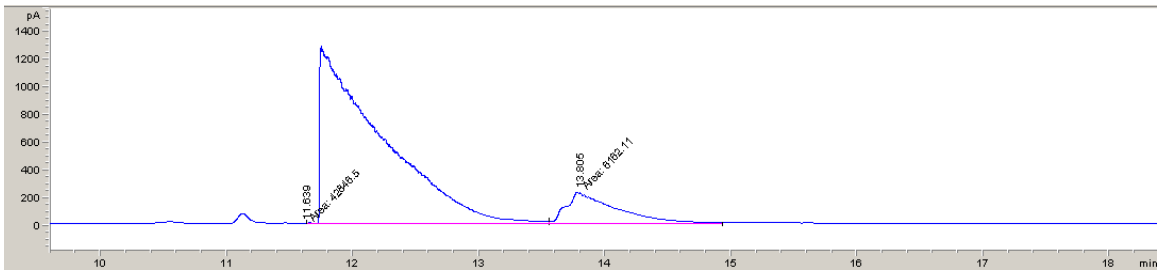

Peak #	RetTime [min]	Type	Width [min]	Area [pA*s]	Height [pA]	Area %
1	11.639	MM N	0.0000	4.28465e4	5.30921e-1	87.42648
2	13.805	MM	0.4419	6162.11133	232.38901	12.57352
Totals :				4.90086e4	232.91993	

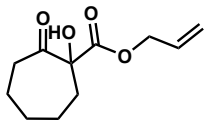

allyl 1-hydroxy-2-oxocycloheptane-1-carboxylate A7.6c. Following general procedure A: A solution of allyl 2-oxocycloheptane-1-carboxylate (500 mg, 2.55 mmol, 1 equiv) and $CeCl_3$-$7H_2O$ (47 mg, 0.13 mmol, 0.05 equiv) in *i*-PrOH (25 mL) was stirred for 1 hour at room temperature, changing color from clear to yellow/golden-green over the course of the reaction. The crude product was purified by silica gel flash chromatography

(20% Et_2O/hexanes) to afford alcohol **A7.6c** as a clear oil (340 mg, 63% yield): **^{1}H NMR (500 MHz, $CDCl_3$)** δ 5.86 (ddt, *J* = 17.3, 10.4, 5.7 Hz, 1H), 5.37 – 5.14 (m, 2H), 4.61 (d, *J* = 5.8 Hz, 2H), 4.30 (d, *J* = 1.6 Hz, 1H), 2.93 (td, *J* = 12.0, 2.9 Hz, 1H), 2.56 (ddd, *J* = 11.7, 7.2, 2.2 Hz, 1H), 2.34 – 2.18 (m, 1H), 2.18 – 2.02 (m, 1H), 1.95 (tq, *J* = 6.3, 1.7 Hz, 1H), 1.88 – 1.72 (m, 2H), 1.46 (qdd, *J* = 8.1, 3.9, 2.3 Hz, 2H), 1.37 – 1.22 (m, 1H); **^{13}C NMR (126 MHz, $CDCl_3$)** δ 209.5, 170.3, 131.2, 119.2, 83.6, 66.5, 40.0, 34.5, 30.2, 27.2, 23.7; **IR (Neat Film, NaCl)** 3790, 3471, 2928, 2857, 2350, 1746, 1722, 1712, 1681, 1453, 1370, 1319, 1268, 1224, 1196, 1167, 1110, 1082, 1038, 992, 938 cm^{-1}; **HRMS (MM: ESI-APCI)** *m/z* calculated for [C11H16O4] $[M+H]^+$: 213.1121, found 213.1119.

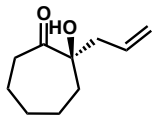

(*R*)-2-allyl-2-hydroxycycloheptan-1-one (A7.7c). Following general procedure C, alcohol **A7.6c** (20 mg, 0.094 mmol, 1.0 equiv) in toluene (2.3 mL) was added to a solution of $[Pd_2(pmdba)_3]$ (4.1 mg, 0.0038 mmol, 4 mol %) and (*S)*-$(CF_3)_3$-*t*-BuPHOX (5.6 mg, 0.0094 mmol, 10 mol %) in toluene (0.5 mL). Purification by flash chromatography (10% EtOAc/hexanes) gave alcohol **A7.7c** as a clear oil (12 mg, 75% yield, 78% ee): **^{1}H NMR (400 MHz, $CDCl_3$)** δ 5.73 (ddt, *J* = 17.0, 10.3, 7.3 Hz, 1H), 5.19 – 4.95 (m, 2H), 3.83 (d, *J* = 1.5 Hz, 1H), 2.74 – 2.63 (m, 1H), 2.50 – 2.29 (m, 3H), 2.07 – 1.93 (m, 2H), 1.91 – 1.81 (m, 1H), 1.81 – 1.71 (m, 1H), 1.67 (ddt, *J* = 14.9, 10.8, 1.3 Hz, 1H), 1.51 – 1.31 (m, 2H), 1.31 – 1.17 (m, 1H); **^{13}C NMR (101 MHz, $CDCl_3$)** δ 215.6, 132.2, 118.9, 81.4, 44.7, 39.0, 36.8, 30.6, 27.4, 23.6; **IR (Neat Film, NaCl)** 3481, 3076, 2928, 2858, 2357, 1703, 1639, 1506, 1453, 1379, 1341, 1320, 1232, 1174, 1141,

1103, 1076, 1062,1043, 996, 947, 918, 839, 789, 671, 633 cm^{-1}; **HRMS (MM: ESI-APCI):** *m/z* calc'd for [C10H17O2] $[M+H]^+$: 169.1223, found 169.1224; **$[\alpha]_D^{23.8}$** –53.3 (c 1.0, $CHCl_3$); **Chiral GC conditions**: Astec® CHIRALDEX G-TA column, 100 °C isotherm, t_R (min): major = 38.348, minor = 37.356.

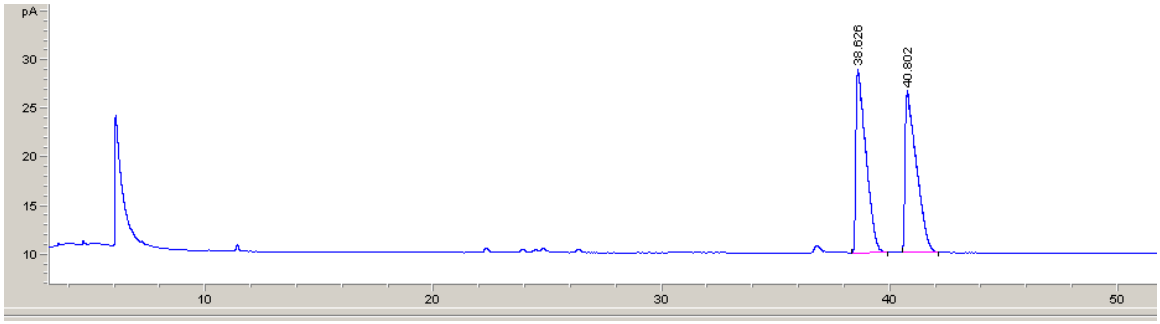

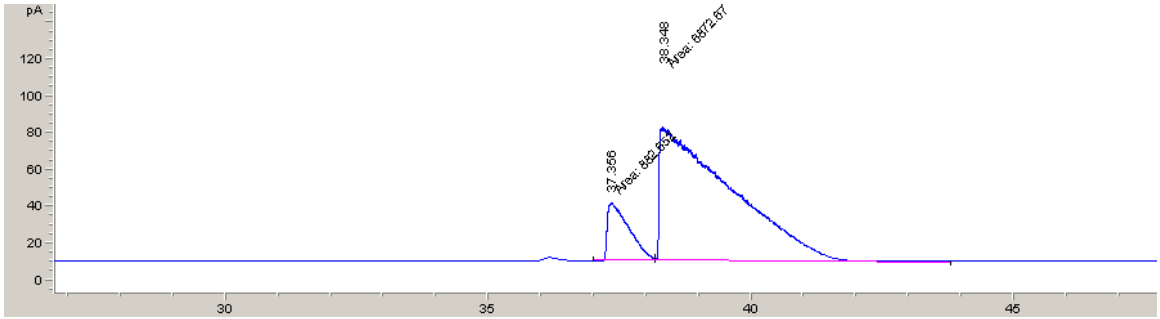

Peak #	RetTime [min]	Type	Width [min]	Area [pA*s]	Height [pA]	Area %
1	37.356	MM	0.4250	882.65198	34.61182	11.38124
2	38.348	MM	1.0946	6872.67139	104.64165	88.61876
Totals :				7755.32336	139.25347	

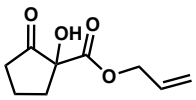

allyl 1-hydroxy-2-oxocyclopentane-1-carboxylate A7.6d. Following general procedure B, to a solution of iodine (15 mg, 0.06 mmol, 0.02 equiv) and samarium (III) triflate (89 mg, 0.15 mmol, 0.05 equiv) in a 1:5 mixture of H_2O/THF (30 mL) was added allyl 2-

oxocyclopentane-1-carboxylate (500 mg, 2.97 mmol, 1 equiv). The reaction was stirred for 72 h. Purification by silica gel flash chromatography (20% EtOAc/hexanes) afforded alcohol **A7.6d** as a clear oil (200 mg, 36% yield): **^{1}H NMR (400 MHz, $CDCl_3$)** δ 5.86 (ddt, *J* = 17.2, 10.4, 5.7 Hz, 1H), 5.34 – 5.21 (m, 2H), 4.66 (ddt, *J* = 5.6, 2.7, 1.4 Hz, 2H), 3.74 (s, 1H), 2.56 – 2.35 (m, 3H), 2.09 (m, 3H); **^{13}C NMR (101 MHz, $CDCl_3$)** δ 213.3, 171.4, 131.1, 119.3, 79.9, 66.9, 35.9, 34.9, 18.5; **IR (Neat Film, NaCl)** 3473, 3088, 2965, 2893, 1758, 1737, 1649, 1447, 1403, 1363,1258, 1169, 1097, 1051, 982, 939,850, 817, 788, 649, 618 cm^{-1}; **HRMS (MM: ESI-APCI)** *m/z* calculated for [C9H16NO4] $[M+NH_4]^+$: 202.1074, found 202.1069.

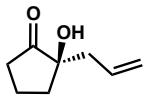

(*R*)-2-allyl-2-hydroxycyclopentan-1-one (A7.7d). Following general procedure C, alcohol **A7.6d** (40 mg, 0.22 mmol, 1.0 equiv) in toluene (4.5 mL) was added to a solution of $[Pd_2(dba)_3]$ (7.7 mg, 0.0087 mmol, 4 mol %) and (*S*)-$(CF_3)_3$-*t*-BuPHOX (12.8 mg, 0.022 mmol, 10 mol %) in toluene (2.1 mL). Purification by flash chromatography (15 → 20% EtOAc/hexanes) gave alcohol **A7.7d** as a yellow oil (22 mg, 73% yield, 30% ee): **^{1}H NMR (400 MHz, $CDCl_3$)** δ 5.79 (dddd, *J* = 16.9, 10.2, 8.1, 6.6 Hz, 1H), 5.31 – 5.08 (m, 2H), 2.46 (s, 1H), 2.41 – 2.17 (m, 4H), 2.17 – 2.06 (m, 1H), 2.06 – 1.75 (m, 3H); **^{13}C NMR (101 MHz, $CDCl_3$)** δ 219.4, 131.7, 120.1, 78.6, 40.4, 34.8, 34.6, 17.2; **IR (Neat Film, NaCl)** 3448, 3077, 2968, 2923, 2361, 1745, 1639, 1434, 1403, 1323, 1245, 1167, 1132, 1064, 1036, 998, 919, 839, 819, 752, 705, 630 cm^{-1}; **HRMS (MM: ESI-APCI):** *m/z* calc'd for [C8H16NO2] $[M+NH_4]^+$: 158.1176, found 158.1169; **$[\alpha]_D^{22.6}$** –19.8 (c 1.1,

$CHCl_3$); **Chiral GC conditions**: Astec® CHIRALDEX G-TA column, 100 °C isotherm, t_R (min): major = 18.666, minor = 23.348.

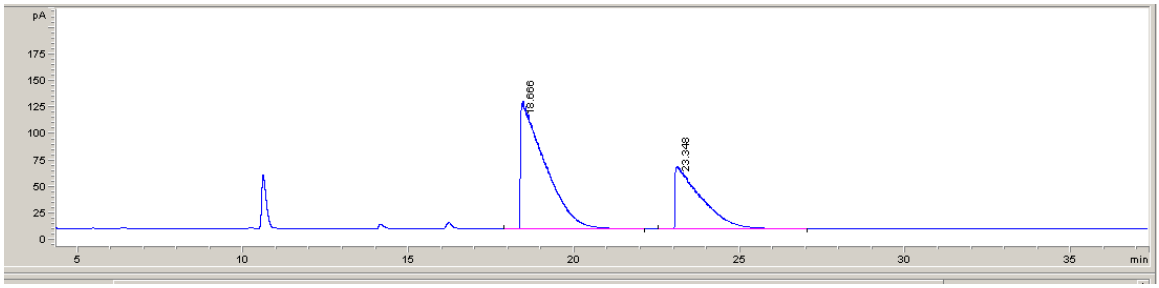

Peak #	RetTime [min]	Type	Width [min]	Area [pA*s]	Height [pA]	Area %
1	18.666	BB	0.8396	6075.01270	104.29378	65.42886
2	23.348	BB	0.8689	3209.90063	50.54222	34.57114
Totals :				9284.91333	154.83600	

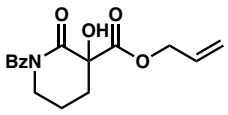

allyl 1-benzoyl-3-hydroxy-2-oxopiperidine-3-carboxylate (A7.6e). Following general procedure B: to a solution of iodine (6.7 mg, 0.026 mmol, 0.02 equiv) and samarium (III) triflate (40 mg, 0.066 mmol, 0.05 equiv) in a 1:5 mixture of H_2O/THF (15 mL) was added allyl 1-benzoyl-2-oxopiperidine-3-carboxylate (380 mg, 1.32 mmol, 1.0 equiv). The reaction was stirred for 6 days. Purification with silica gel flash chromatography (3:1 hexanes/EtOAc) afforded **A7.6e** as an off-white solid (243 mg, 61% yield); **^{1}H NMR (400 MHz, $CDCl_3$)** δ 7.72 – 7.65 (m, 2H), 7.53 – 7.46 (m, 1H), 7.42 – 7.35 (m, 2H), 5.96 (ddt, *J* = 17.3, 10.4, 6.0 Hz, 1H), 5.39 (dq, *J* = 17.1, 1.4 Hz, 1H), 5.33 (dq, *J* = 10.3, 1.2 Hz, 1H), 4.75 (dt, *J* = 5.9, 1.3 Hz, 2H), 4.18 (s, 1H), 4.00 – 3.89 (m, 1H), 3.84 – 3.73 (m,

1H), 2.61 – 2.47 (m, 1H), 2.22 – 2.01 (m, 3H); **^{13}C NMR (101 MHz, $CDCl_3$)** δ 174.0, 172.1, 170.7, 134.9, 132.2, 130.9, 128.3, 128.2, 119.9, 76.9, 67.3, 46.7, 32.4, 19.3; **IR (Neat Film, NaCl)** 3459, 2954, 1747, 1682, 1600, 1478, 1450, 1393, 1270, 1178, 1141, 992, 947, 796, 727, 694, 662 cm^{-1}; **HRMS (MM: ESI-APCI):** *m/z* calc'd for C16H18NO5 $[M+H]^+$: 304.1179, found 304.1182;

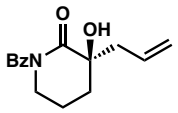

(*R*)-3-allyl-1-benzoyl-3-hydroxypiperidin-2-one (7e). Following general procedure C, *α*-hydroxylated allyl ester **A7.6e** (10 mg, 0.033 mmol, 1.0 equiv) in toluene (0.5 mL) was added to a solution of $[Pd_2(dba)_3]$ (1.2 mg, 1.3 μmol, 0.040 equiv) and (*S*)-$(CF_3)_3$-*t*-Bu-PHOX (2.0 mg, 3.3 μmol, 0.10 equiv) in toluene (0.5 mL). The reaction was stirred at 40 °C for 16 h. Purification by flash chromatography (15% EtOAc/hexanes) gave *α*-hydroxy piperidinone **A7.7e** as a colorless oil (6.8 mg, 79% yield, 92% ee): **^{1}H NMR (400 MHz, $CDCl_3$)** δ 7.59 – 7.54 (m, 2H), 7.52 – 7.48 (m, 1H), 7.40 (t, *J* = 7.5 Hz, 2H), 5.87 (ddt, *J* = 17.4, 10.4, 7.1 Hz, 1H), 5.31 – 5.20 (m, 2H), 3.88 (dtd, *J* = 12.8, 4.7, 1.6 Hz, 1H), 3.84 – 3.74 (m, 1H), 3.31 (s, 1H), 2.66 (d, *J* = 7.2 Hz, 2H), 2.27 – 2.17 (m, 1H), 2.10 – 1.98 (m, 2H), 2.01 – 1.89 (m, 1H); **^{13}C NMR (101 MHz, $CDCl_3$)** δ 178.9, 174.6, 135.6, 132.1, 131.4, 128.5, 127.9, 120.3, 74.2, 47.4, 44.1, 33.1, 20.0; **IR (Neat Film, NaCl)** 3478, 2953, 1682, 1450, 1391, 1286, 1149, 1072, 998, 928, 795, 726, 694, 662 cm^{-1}; **HRMS (MM: ESI-APCI):** *m/z* calc'd for C15H18NO3 $[M+H]^+$: 260.1281, found 260.1278; **$[\alpha]_D^{23.1}$** +9.7 (c 0.64, $CHCl_3$); **SFC conditions**: 20% IPA, 2.5 mL/min, Chiralpak OD-H column, λ = 210 nm, t_R (min): major = 3.548, minor = 2.875.

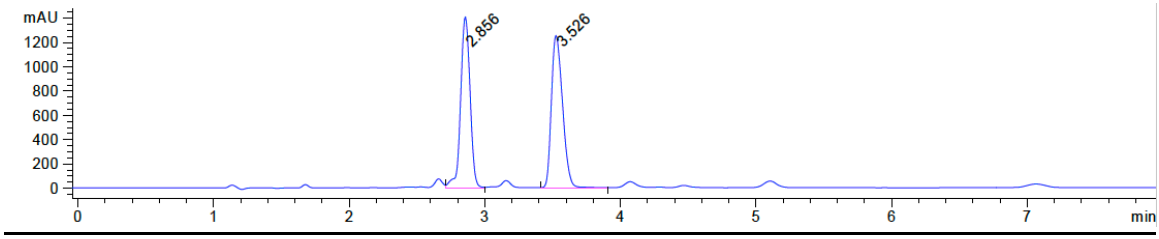

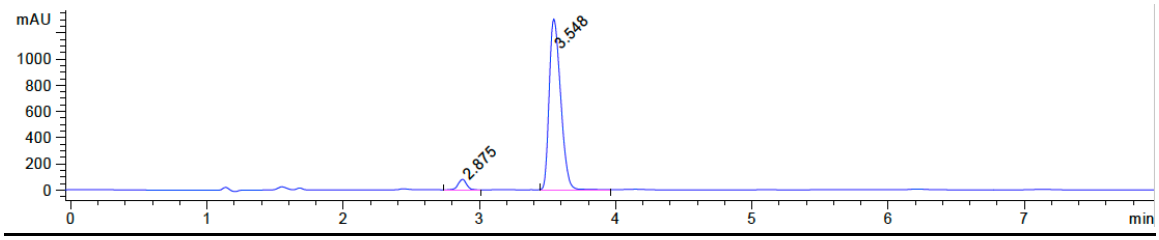

Signal 1: DAD1 A, Sig=210,8 Ref=360,100

Peak #	RetTime [min]	Type	Width [min]	Area [mAU*s]	Height [mAU]	Area %
1	2.875	VV	0.0674	352.26489	79.89040	4.3887
2	3.548	BB	0.0930	7674.29346	1297.33850	95.6113
Totals :				8026.55835	1377.22890	

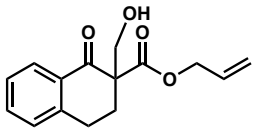

Allyl 2-(hydroxymethyl)-1-oxo-1,2,3,4-tetrahydronaphthalene-2-carboxylate (A7.8). To a solution of allyl 1-oxo-1,2,3,4-tetrahydronaphthalene-2-carboxylate (200 mg, 0.87 mmol, 1.0 equiv) in THF (1.6 mL) at 0 °C was added potassium bicarbonate (261 mg, 2.61 mmol, 3.0 equiv) and aqueous 37% formaldehyde (420 uL, 5.65 mmol, 6.5 equiv). The mixture was allowed to warm to room temperature and stirred for 3 h. Water (2 mL) was added and the mixture was extracted with CH_2Cl_2 (4 x 2 mL). The combined organic layers were dried over Na_2SO_4, decanted, and concentrated under reduced pressure. The

residue was taken up in THF and 1 drop of 1 M aqueous HCl was added. The solution was stirred for 20 minutes before being concentrated under reduced pressure onto silica gel and then purified by silica gel flash chromatography (20 → 25% EtOAc/hexanes) to give alcohol **A7.8** as a clear oil (195 mg, 86% yield): **^{1}H NMR (400 MHz, $CDCl_3$)** δ 8.06 (dd, *J* = 8.0, 1.6 Hz, 1H), 7.49 (td, *J* = 7.5, 1.4 Hz, 1H), 7.33 (t, *J* = 7.6 Hz, 1H), 7.28 – 7.17 (m, 1H), 5.88 – 5.68 (m, 1H), 5.22 – 5.08 (m, 2H), 4.62 (ddd, *J* = 5.3, 3.5, 1.6 Hz, 2H), 4.11 – 3.98 (m, 1H), 3.91 (dd, *J* = 11.4, 9.9 Hz, 1H), 3.42 – 3.28 (m, 1H), 3.10 – 2.89 (m, 2H), 2.45 (dt, *J* = 13.6, 4.4 Hz, 1H), 2.18 (ddd, *J* = 13.5, 10.9, 5.2 Hz, 1H); **^{13}C NMR (101 MHz, $CDCl_3$)** δ 197.3, 171.0, 143.3, 134.2, 132.0, 131.4, 128.9, 127.9, 127.1, 118.4, 66.4, 66.0, 59.3, 29.2, 26.0; **IR (Neat Film, NaCl)** 3521, 3071, 3024, 2940,2881, 1731, 1681, 1650, 1600, 1455, 1414, 1354, 1315, 1268, 1239, 1185, 1137, 1086, 1048, 942, 805,787, 745, 689, 654 cm^{-1}; **HRMS (MM: ESI-APCI):** *m/z* calc'd for $[C_{15}H_{17}O_4]$ $[M+H]^+$: 261.1121, found 261.1117.

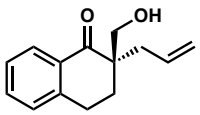

Following general procedure C, alcohol **A7.8** (52 mg, 0.20 mmol, 1.0 equiv) in toluene (4.0 mL) was added to a solution of $[Pd_2(dba)_3]$ (7.3 mg, 0.008 mmol, 4 mol %) and (*S,S*)- ANDEN (**L3**) (16 mg, 0.02 mmol, 10 mol %) in toluene (2.0 mL). The reaction was stirred at ambient temperature for 16 h. Purification by flash chromatography (20 → 25% EtOAc/hexanes) gave primary alcohol **A7.9** as a clear oil (27 mg, 63% yield, 92% ee): **^{1}H NMR (400 MHz, $CDCl_3$)** δ 8.02 (dd, *J* = 8.0, 1.4 Hz, 1H), 7.50 (td, *J* = 7.5, 1.5 Hz, 1H), 7.32 (tdd, *J* = 7.8, 1.6, 0.9 Hz, 1H), 7.26 (m, 1H), 5.89 – 5.73 (m, 1H), 5.21 –

5.09 (m, 2H), 3.77 – 3.63 (m, 2H), 3.20 – 3.07 (m, 1H), 2.92 (dt, *J* = 17.4, 4.6 Hz, 1H), 2.85 (dd, *J* = 8.5, 4.9 Hz, 1H), 2.58 – 2.46 (m, 1H), 2.35 (ddt, *J* = 13.9, 8.1, 1.1 Hz, 1H), 2.05 (ddd, *J* = 13.7, 11.5, 5.1 Hz, 1H), 1.93 (ddd, *J* = 13.8, 5.1, 3.9 Hz, 1H); **^{13}C NMR (101 MHz, $CDCl_3$)** δ 204.0, 143.6, 133.9, 132.9, 131.6, 129.0, 127.9, 127.0, 119.2, 66.5, 49.2, 34.8, 28.0, 24.9. **IR (Neat Film, NaCl)** 3459, 3072, 2928, 1673, 1600, 1454, 1357, 1287, 1229, 1156, 1043, 997, 919, 793, 741 cm^{-1}; **HRMS (MM: ESI-APCI):** *m/z* calc'd for [C14H17O4] $[M+H]^+$: 217.1223, found 217.1214; **$[\alpha]_D^{22.9}$** +39.1 (c 1.00, $CHCl_3$); **SFC conditions**: 3% IPA, 2.5 mL/min, Chiralpak OJ–H column, λ = 210 nm, t_R (min): major = 6.234, minor = 6.752.

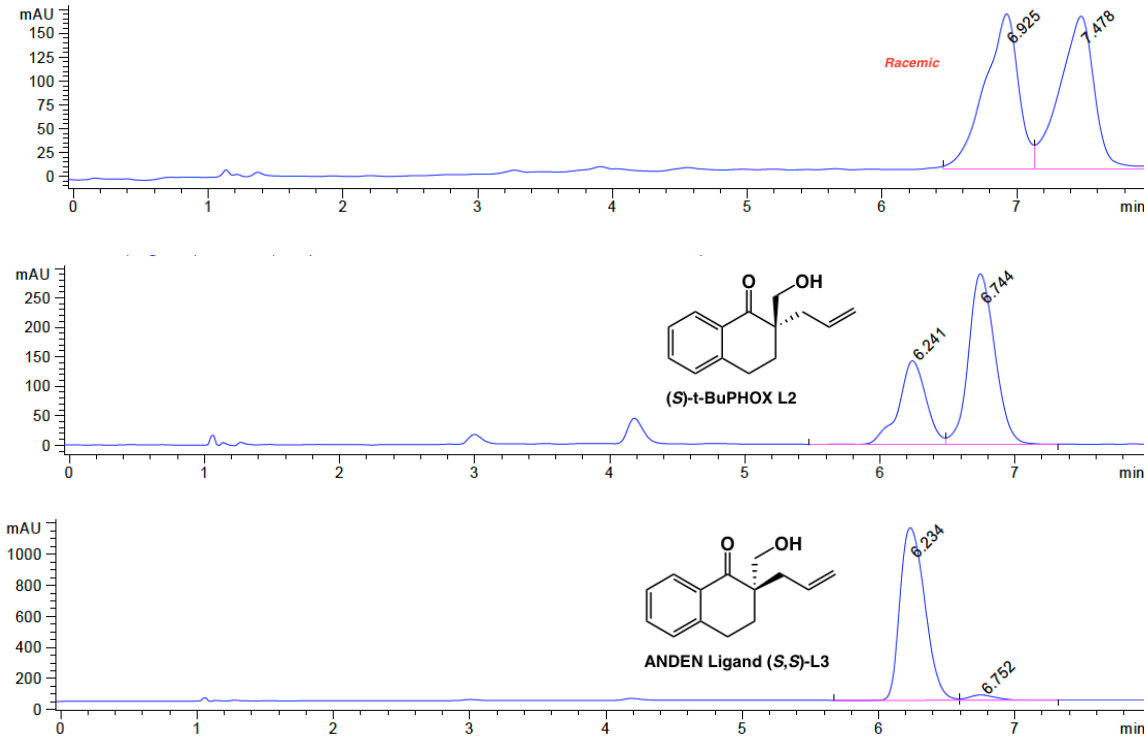


```
Signal 1: DAD1 A, Sig=210,8 Ref=360,100

Peak RetTime Type  Width     Area      Height     Area
  #   [min]        [min]   [mAU*s]     [mAU]       %
----|-------|----|-------|----------|----------|--------|
   1   6.234 VV    0.2048 1.41517e4  1109.75012  96.6666
   2   6.752 VB    0.2154  487.99771   34.84304   3.3334

Totals :                 1.46397e4  1144.59316
```

A7.4 REFERENCES AND NOTES

(1) Kumar, A.; Patil, D.; Rajamohanan, P. R.; Ahmad, A. Isolation, Purification and Characterization of Vinblastine and Vincristine from Endophytic Fungus Fusarium Oxysporum Isolated from Catharanthus Roseus. *PLOS ONE* **2013**, *8* (9), e71805.

(2) Yokoyama, R.; Huang, J.-M.; Yang, C.-S.; Fukuyama, Y. New Seco-Prezizaane-Type Sesquiterpenes, Jiadifenin with Neurotrophic Activity and 1,2-Dehydroneomajucin from Illicium Jiadifengpi. *J. Nat. Prod.* **2002**, *65* (4), 527–531.

(3) Smith, A. M. R.; Hii, K. K. (Mimi). Transition Metal Catalyzed Enantioselective α-Heterofunctionalization of Carbonyl Compounds. *Chem. Rev.* **2011**, *111* (3), 1637–1656.

(4) Reddy, D. S.; Shibata, N.; Nagai, J.; Nakamura, S.; Toru, T. A Dynamic Kinetic Asymmetric Transformation in the α-Hydroxylation of Racemic Malonates and Its Application to Biologically Active Molecules. *Angew. Chem. Int. Ed.* **2009**, *48* (4), 803–806.

(5) Witten, M. R.; Jacobsen, E. N. A Simple Primary Amine Catalyst for Enantioselective α-Hydroxylations and α-Fluorinations of Branched Aldehydes. *Org. Lett.* **2015**, *17* (11), 2772–2775.

(6) Sim, S.-B. D.; Wang, M.; Zhao, Y. Phase-Transfer-Catalyzed Enantioselective α-Hydroxylation of Acyclic and Cyclic Ketones with Oxygen. *ACS Catalysis* **2015**, *5* (6), 3609–3612.

(7) Ishimaru, T.; Shibata, N.; Nagai, J.; Nakamura, S.; Toru, T.; Kanemasa, S. Lewis Acid-Catalyzed Enantioselective Hydroxylation Reactions of Oxindoles and β-Keto Esters Using DBFOX Ligand. *J. Am. Chem. Soc.* **2006**, *128* (51), 16488–16489.

(8) He, R.; Wu, S.; Tang, H.; Huo, X.; Sun, Z.; Zhang, W. Iridium-Catalyzed Enantioselective and Diastereoselective Allylation of Dioxindoles: A One-Step Synthesis of 3-Allyl-3-Hydroxyoxindoles. *Org. Lett.* **2018**, *20* (19), 6183–6187.

(9) Xue, F.; Bao, X.; Zou, L.; Qu, J.; Wang, B. Asymmetric Hydroxylation of 4-Substituted Pyrazolones Catalyzed by Natural Cinchona Alkaloids. *Advanced Synthesis & Catalysis* **2016**, *358* (24), 3971–3976.

(10) Yang, F.; Zhao, J.; Tang, X.; Zhou, G.; Song, W.; Meng, Q. Enantioselective α-Hydroxylation by Modified Salen-Zirconium(IV)-Catalyzed Oxidation of β-Keto Esters. *Org. Lett.* **2017**, *19* (3), 448–451.

(11) Boschelli, D.; Smith, A. B.; Stringer, O. D.; Jenkins, R. H.; Davis, F. A. An Asymmetric Synthesis of (+)-Kjellmanianone. *Tetrahedron Lett.* **1981**, *22* (44), 4385–4388.

(12) Lu, M.; Zhu, D.; Lu, Y.; Zeng, X.; Tan, B.; Xu, Z.; Zhong, G. Chiral Brønsted Acid-Catalyzed Enantioselective α-Hydroxylation of β-Dicarbonyl Compounds. *J. Am. Chem. Soc.* **2009**, *131* (13), 4562–4563.

(13) Novacek, J.; Izzo, J. A.; Vetticatt, M. J.; Waser, M. Bifunctional Ammonium Salt Catalyzed Asymmetric α-Hydroxylation of β-Ketoesters by Simultaneous Resolution of Oxaziridines. *Chem. Eur. J.* **2016**, *22* (48), 17339–17344.

(14) Lin, X.; Ruan, S.; Yao, Q.; Yin, C.; Lin, L.; Feng, X.; Liu, X. Kinetic Resolution of Oxaziridines via Chiral Bifunctional Guanidine-Catalyzed Enantioselective α-Hydroxylation of β-Keto Esters. *Org. Lett.* **2016**, *18* (15), 3602–3605.

(15) Odagi, M.; Furukori, K.; Yamamoto, Y.; Sato, M.; Iida, K.; Yamanaka, M.; Nagasawa, K. Origin of Stereocontrol in Guanidine-Bisurea Bifunctional Organocatalyst That Promotes α-Hydroxylation of Tetralone-Derived β-Ketoesters: Asymmetric Synthesis of β- and γ-Substituted Tetralone Derivatives via Organocatalytic Oxidative Kinetic Resolution. *J. Am. Chem. Soc.* **2015**, *137* (5), 1909–1915.

(16) Ding, W.; Lu, L.-Q.; Zhou, Q.-Q.; Wei, Y.; Chen, J.-R.; Xiao, W.-J. Bifunctional Photocatalysts for Enantioselective Aerobic Oxidation of β-Ketoesters. *J. Am. Chem. Soc.* **2017**, *139* (1), 63–66.

(17) Naganawa, Y.; Aoyama, T.; Kato, K.; Nishiyama, H. Cu(II)-Catalyzed Enantioselective α-Hydroxylation and α-Chlorination of β-Ketoesters with N,N,O-Tridentate Chiral Phenanthroline Ligand. *ChemistrySelect* **2016**, *1* (9), 1938–1942.

(18) Toullec, P. Y.; Bonaccorsi, C.; Mezzetti, A.; Togni, A. Expanding the Scope of Asymmetric Electrophilic Atom-Transfer Reactions: Titanium- and Ruthenium-Catalyzed Hydroxylation of β-Ketoesters. *PNAS* **2004**, *101* (16), 5810–5814.

(19) Trost, B. M.; Xu, J.; Reichle, M. Enantioselective Synthesis of α-Tertiary Hydroxyaldehydes by Palladium-Catalyzed Asymmetric Allylic Alkylation of Enolates. *J. Am. Chem. Soc.* **2007**, *129* (2), 282–283.

(20) Trost, B. M.; Xu, J.; Schmidt, T. Ligand Controlled Highly Regio- and Enantioselective Synthesis of α-Acyloxyketones by Palladium-Catalyzed Allylic Alkylation of 1,2-Enediol Carbonates. *J. Am. Chem. Soc.* **2008**, *130* (36), 11852–11853.

(21) Trost, B. M.; Koller, R.; Schäffner, B. Enantioselective Synthesis of Tertiary α-Hydroxyketones from Unfunctionalized Ketones: Palladium-Catalyzed Asymmetric Allylic Alkylation of Enolates. *Angew. Chem. Int. Ed.* **2012**, *51* (33), 8290–8293.

(22) He, R.; Liu, P.; Huo, X.; Zhang, W. Ir/Zn Dual Catalysis: Enantioselective and Diastereodivergent α-Allylation of Unprotected α-Hydroxy Indanones. *Org. Lett.* **2017**, *19* (20), 5513–5516.

(23) Sun, A. W.; Hess, S. N.; Stoltz, B. M. Enantioselective Synthesis of Gem-Disubstituted N-Boc Diazaheterocycles via Decarboxylative Asymmetric Allylic Alkylation. *Chem. Sci.* **2018**.

(24) Qi, X.; Chen, C.; Hou, C.; Fu, L.; Chen, P.; Liu, G. Enantioselective Pd(II)-Catalyzed Intramolecular Oxidative 6- *Endo* Aminoacetoxylation of Unactivated Alkenes. *J. Am. Chem. Soc.* **2018**, *140* (24), 7415–7419.

APPENDIX 8

Spectra Relevant to Appendix 7:

Decarboxylative Asymmetric Allylic Alkylation of Tertiary Alcohols

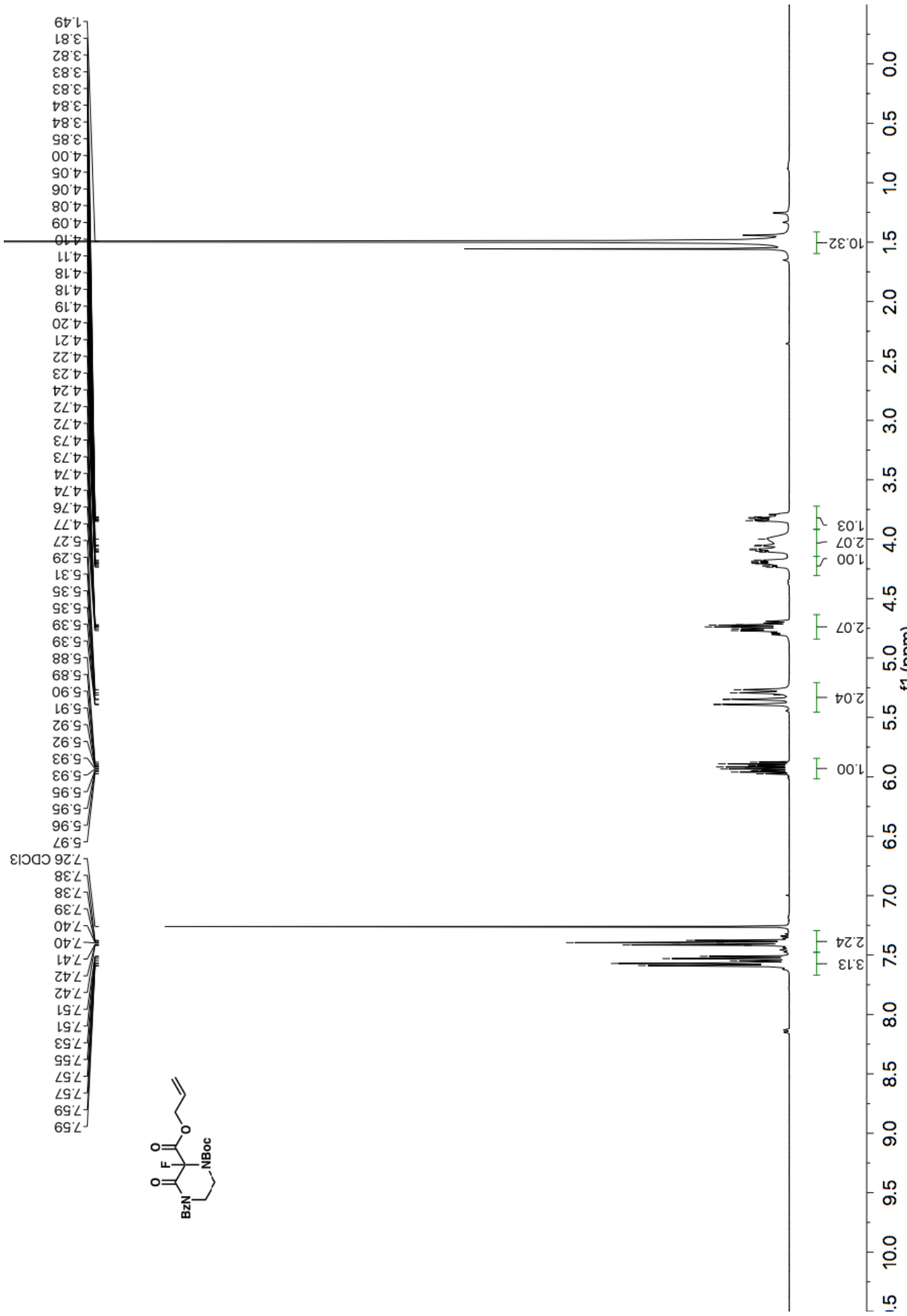

Figure A8.1 ^{1}H NMR (400 MHz, $CDCl_3$) of compound **A7.1.**

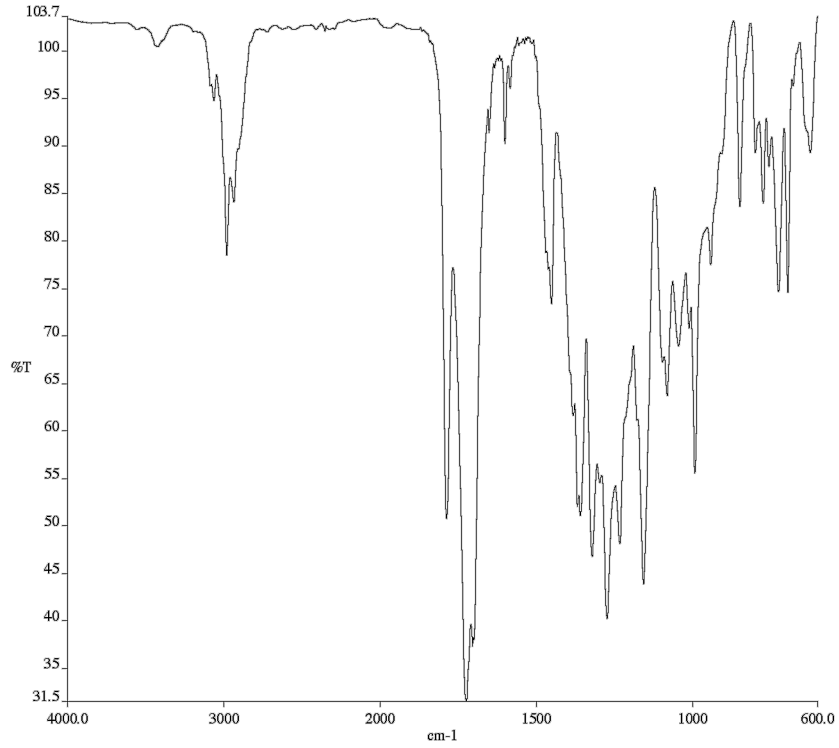

Figure A8.2 Infrared spectrum (Thin Film, NaCl) of compound **A7.1**.

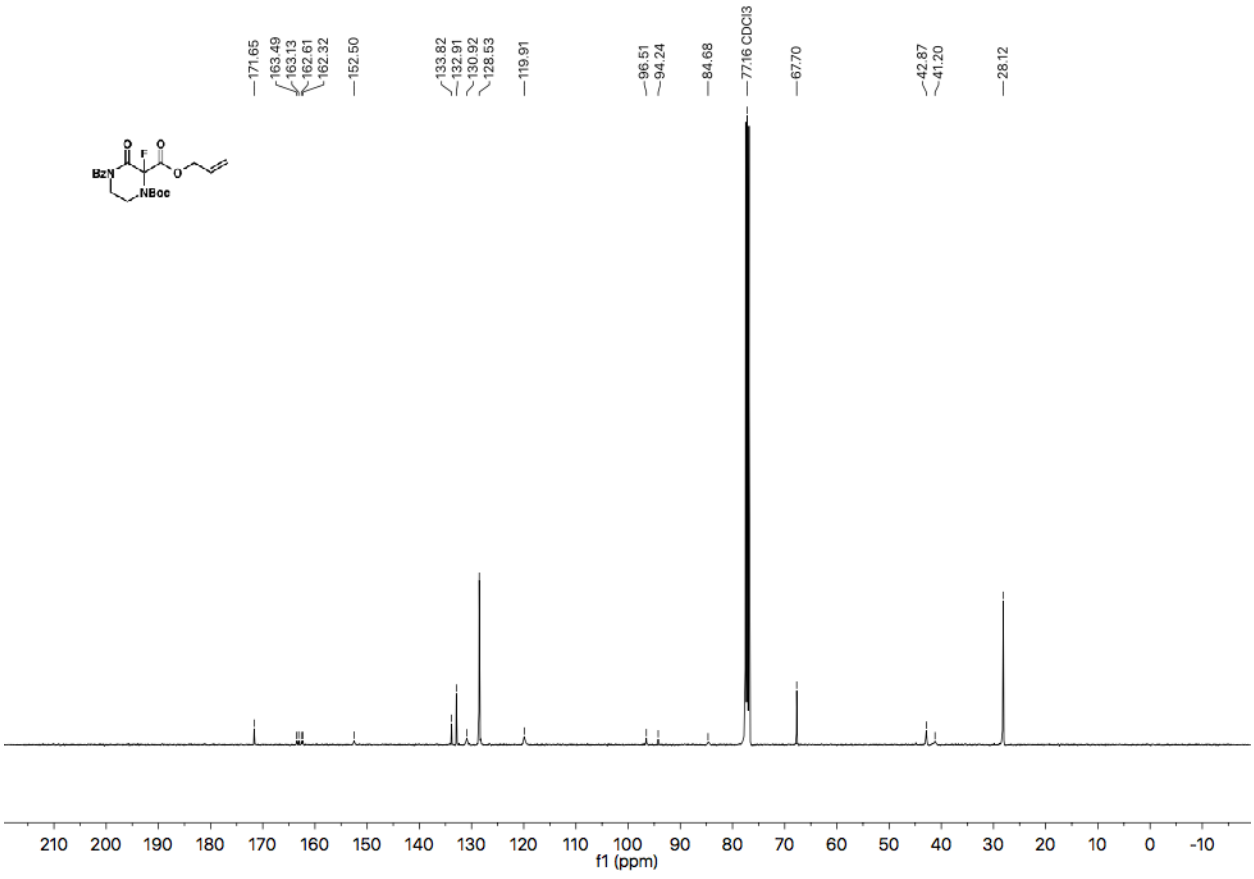

Figure A8.3 ^{13}C NMR (101 MHz, $CDCl_3$) of compound **A7.1**.

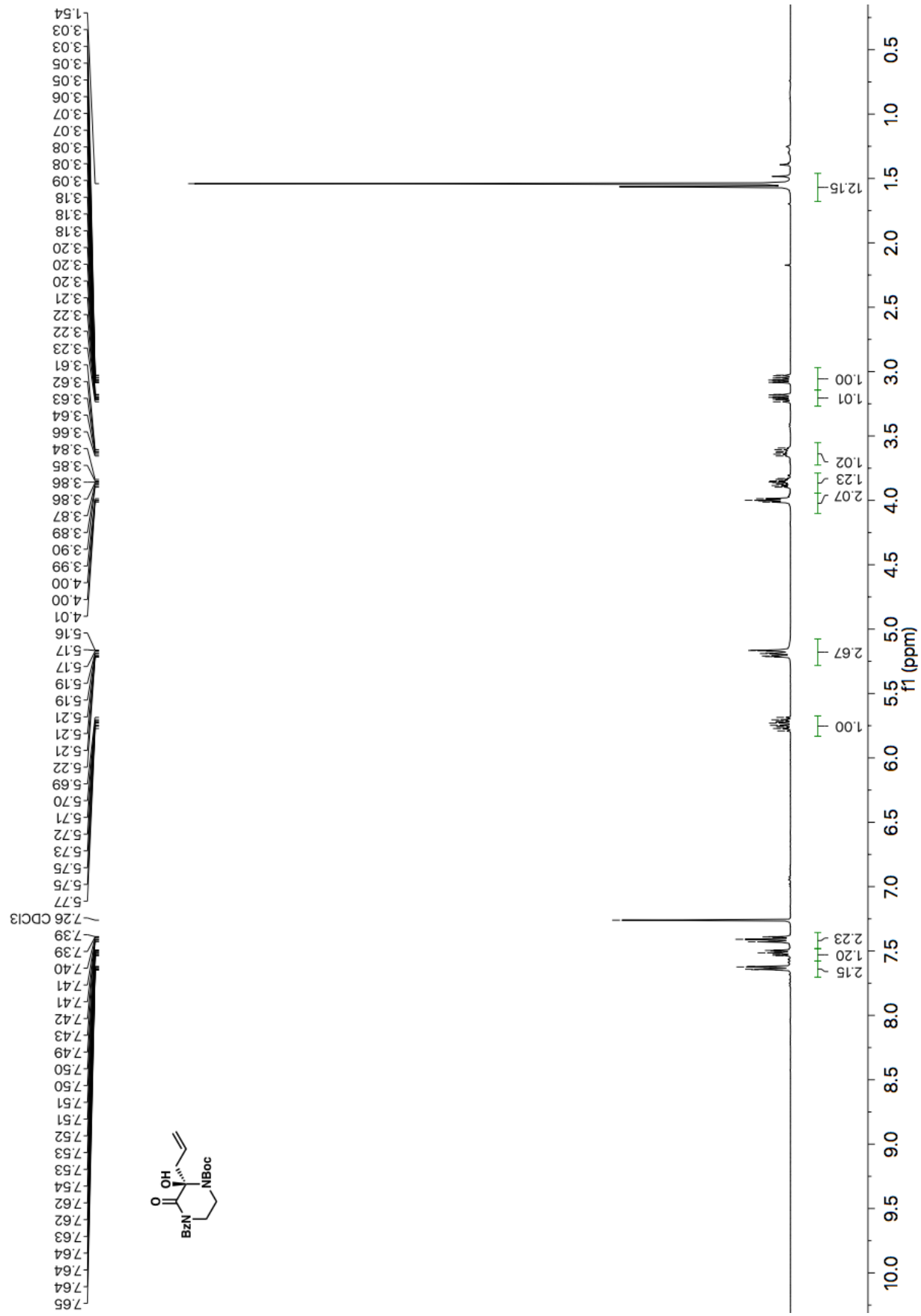

Figure A8.4 ^{1}H NMR (400 MHz, $CDCl_3$) of compound **A7.2.**

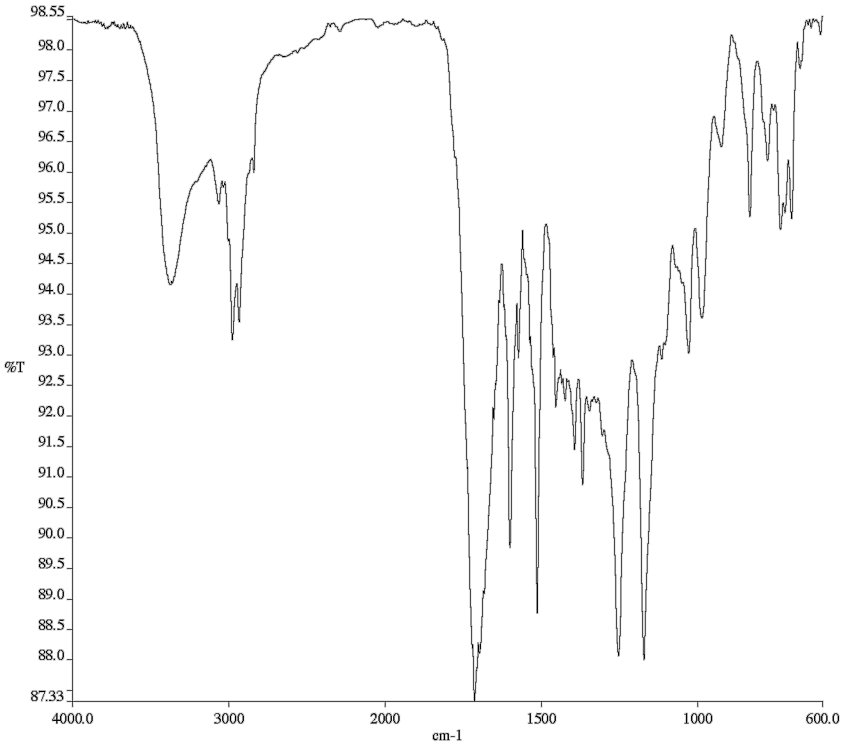

Figure A8.5 Infrared spectrum (Thin Film, NaCl) of compound **A7.2**.

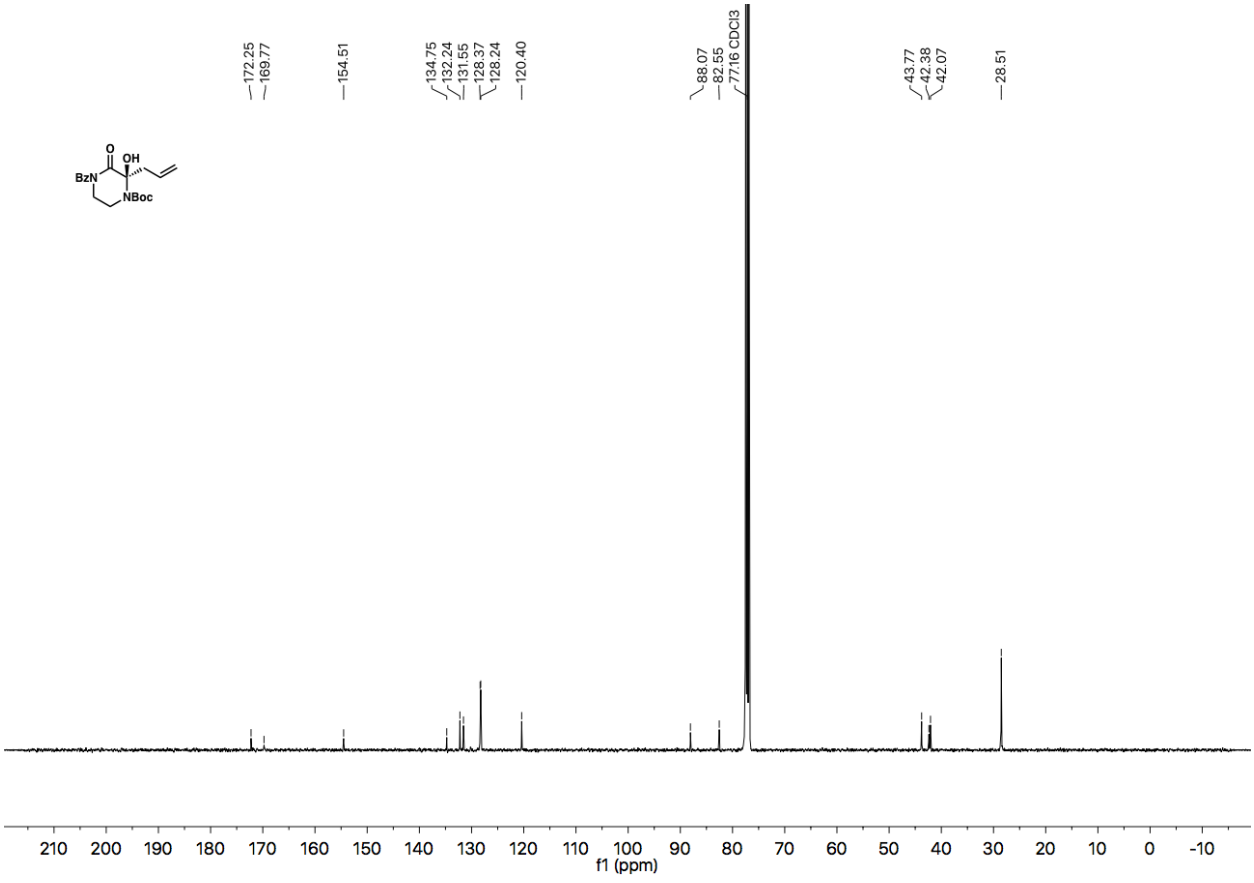

Figure A8.6 ^{13}C NMR (101 MHz, $CDCl_3$) of compound **A7.2**.

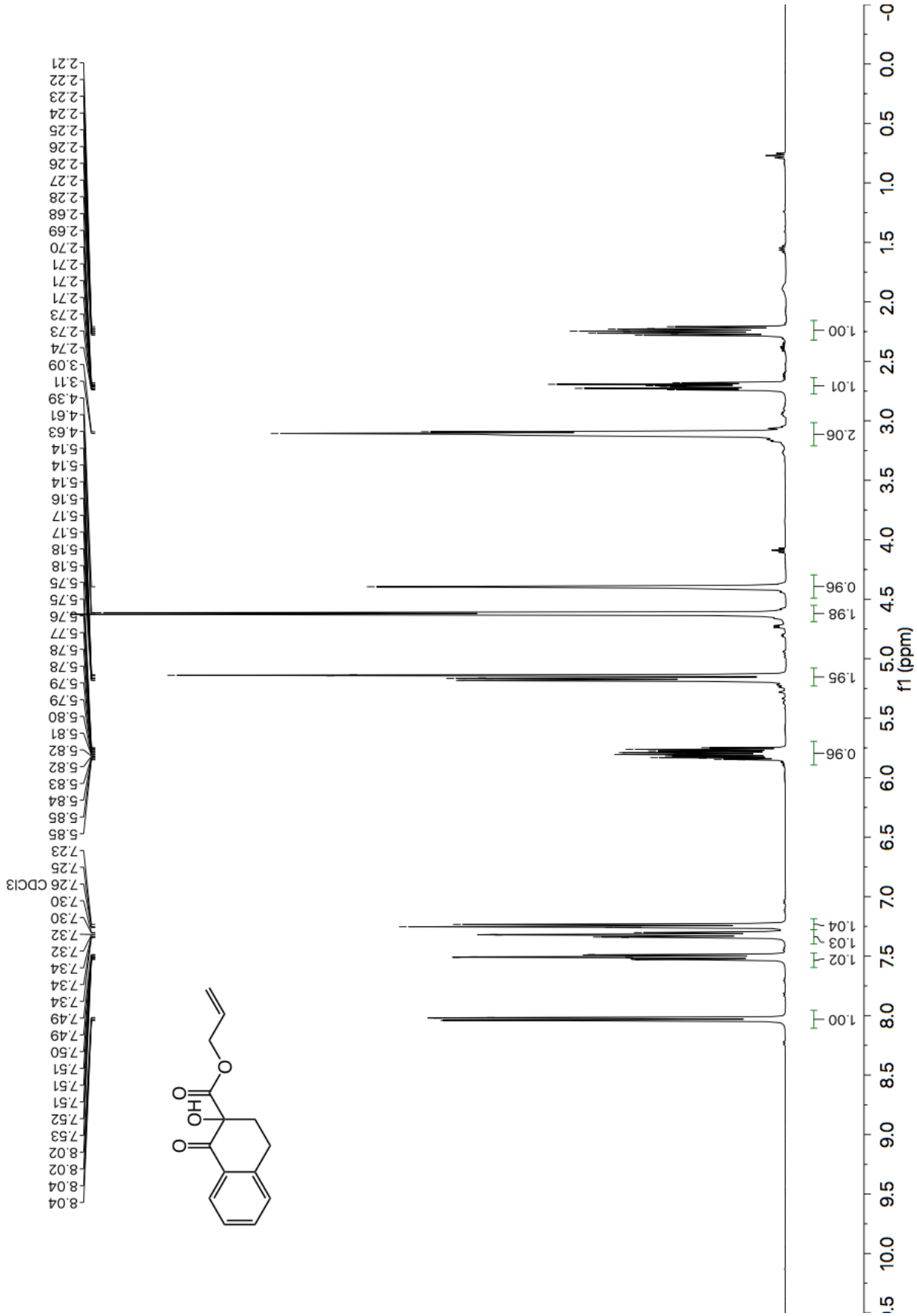

Figure A8.7 ^{1}H NMR (400 MHz, $CDCl_3$) of compound **A7.3.**

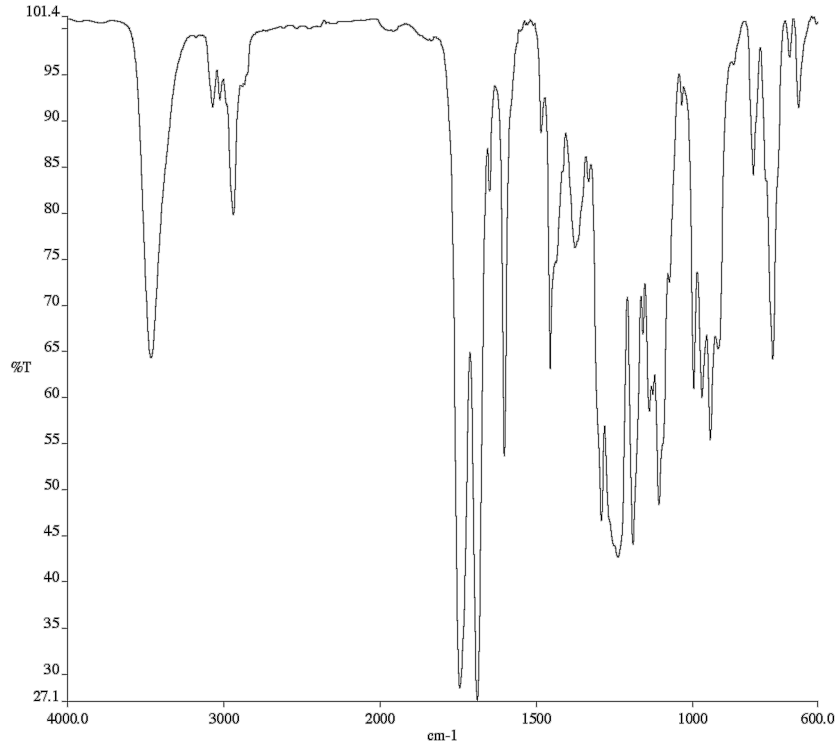

Figure A8.8 Infrared spectrum (Thin Film, NaCl) of compound **A7.3**.

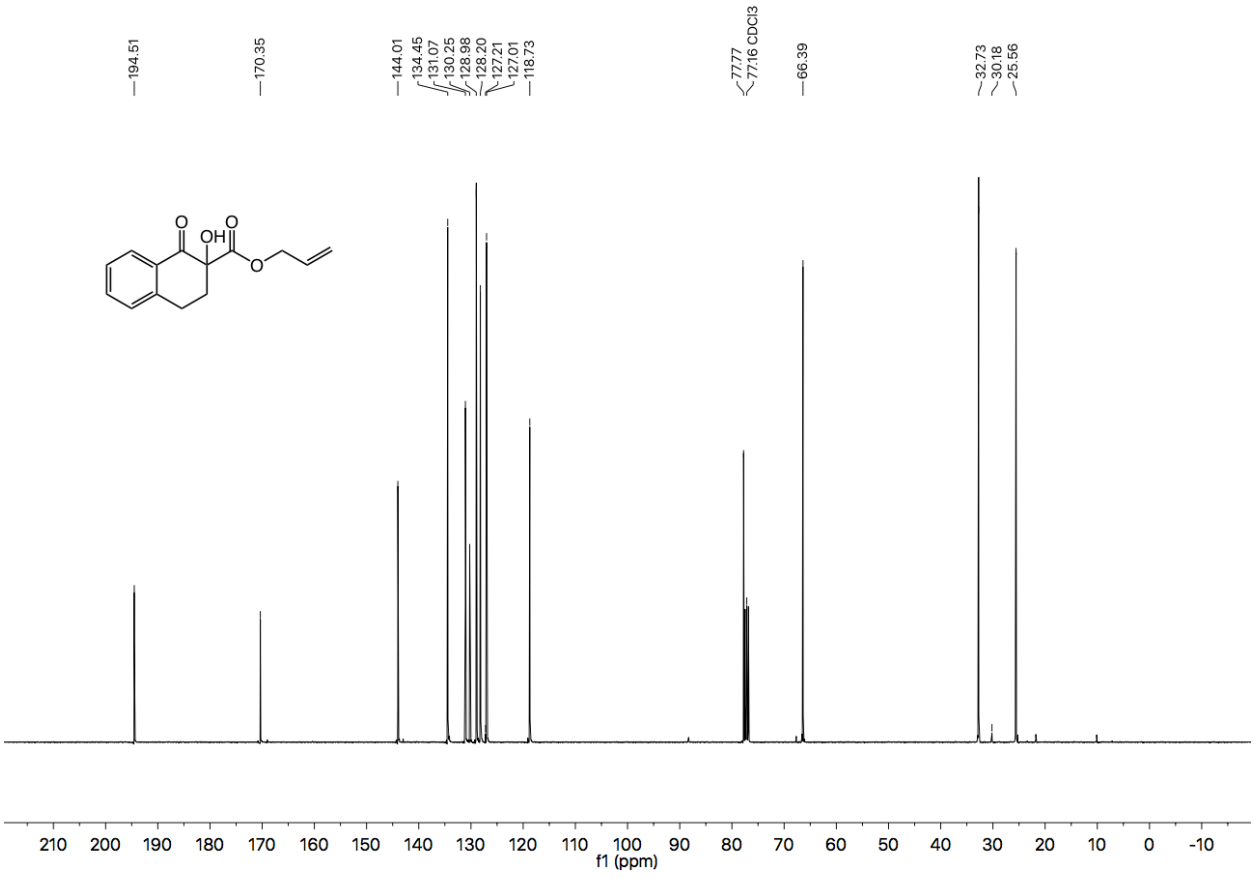

Figure A8.9 ^{13}C NMR (101 MHz, $CDCl_3$) of compound **A7.3**.

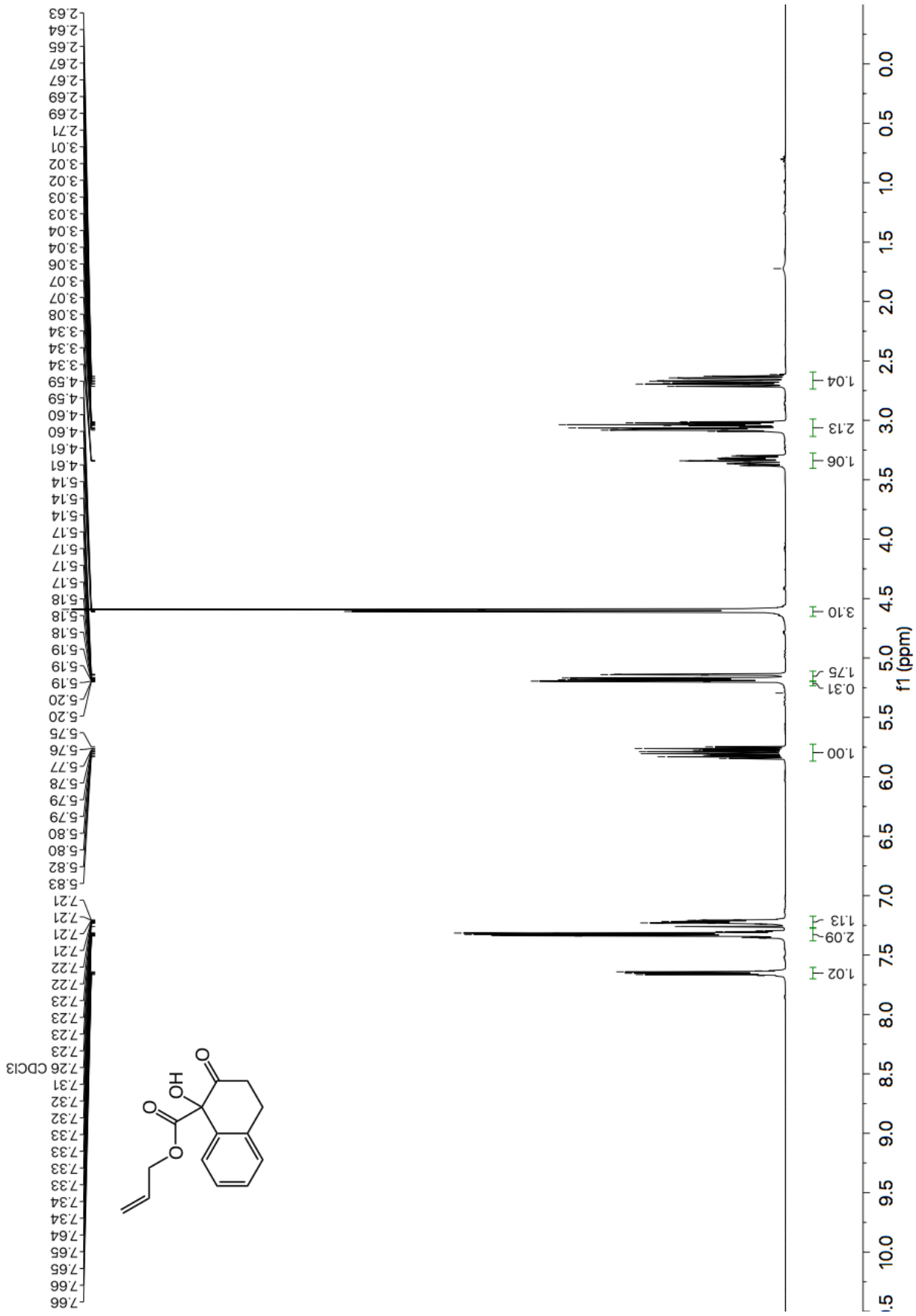

Figure A8.10 ^{1}H NMR (400 MHz, $CDCl_3$) of compound **A7.5.**

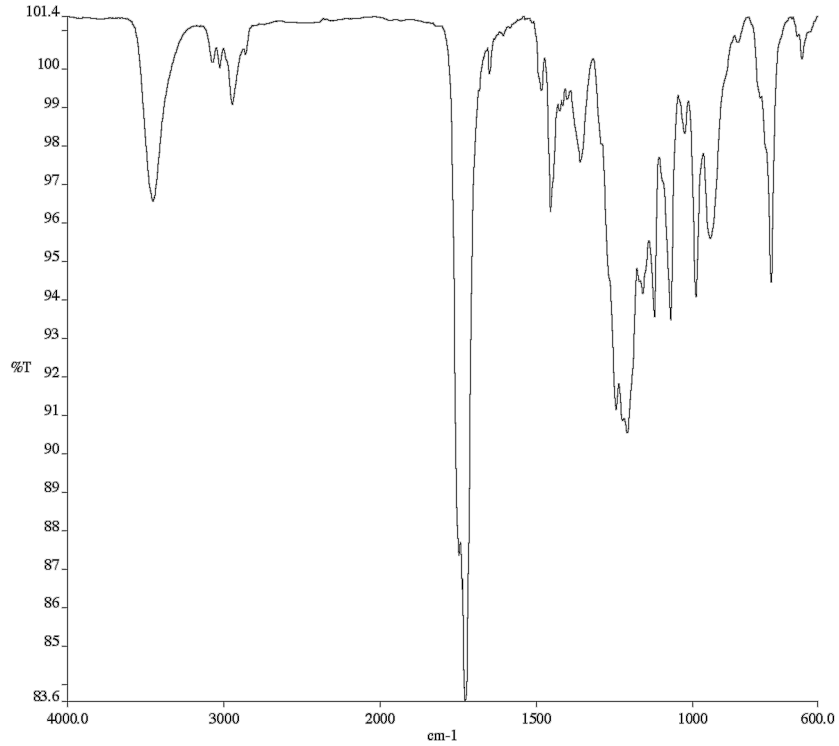

Figure A8.11 Infrared spectrum (Thin Film, NaCl) of compound **A7.5**.

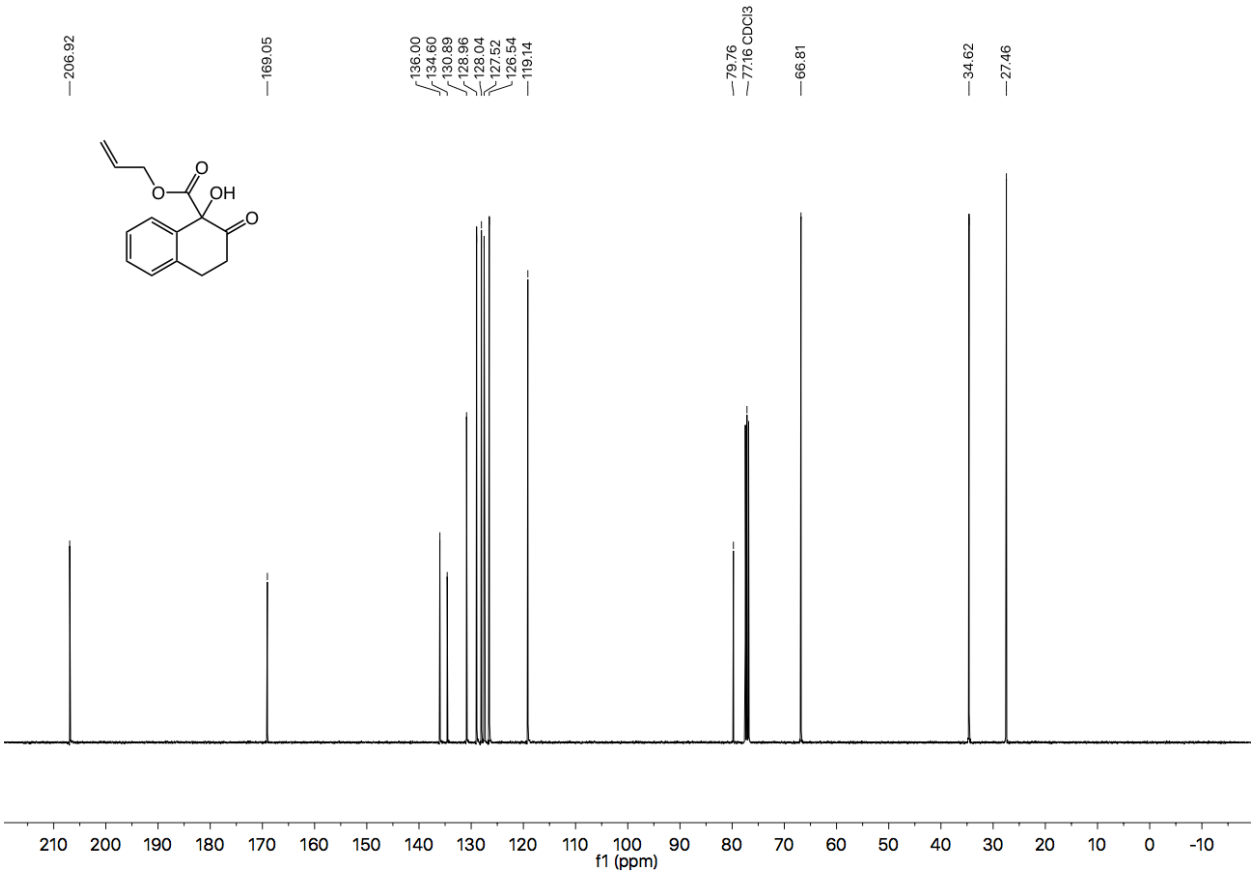

Figure A8.12 ^{13}C NMR (101 MHz, $CDCl_3$) of compound **A7.5**.

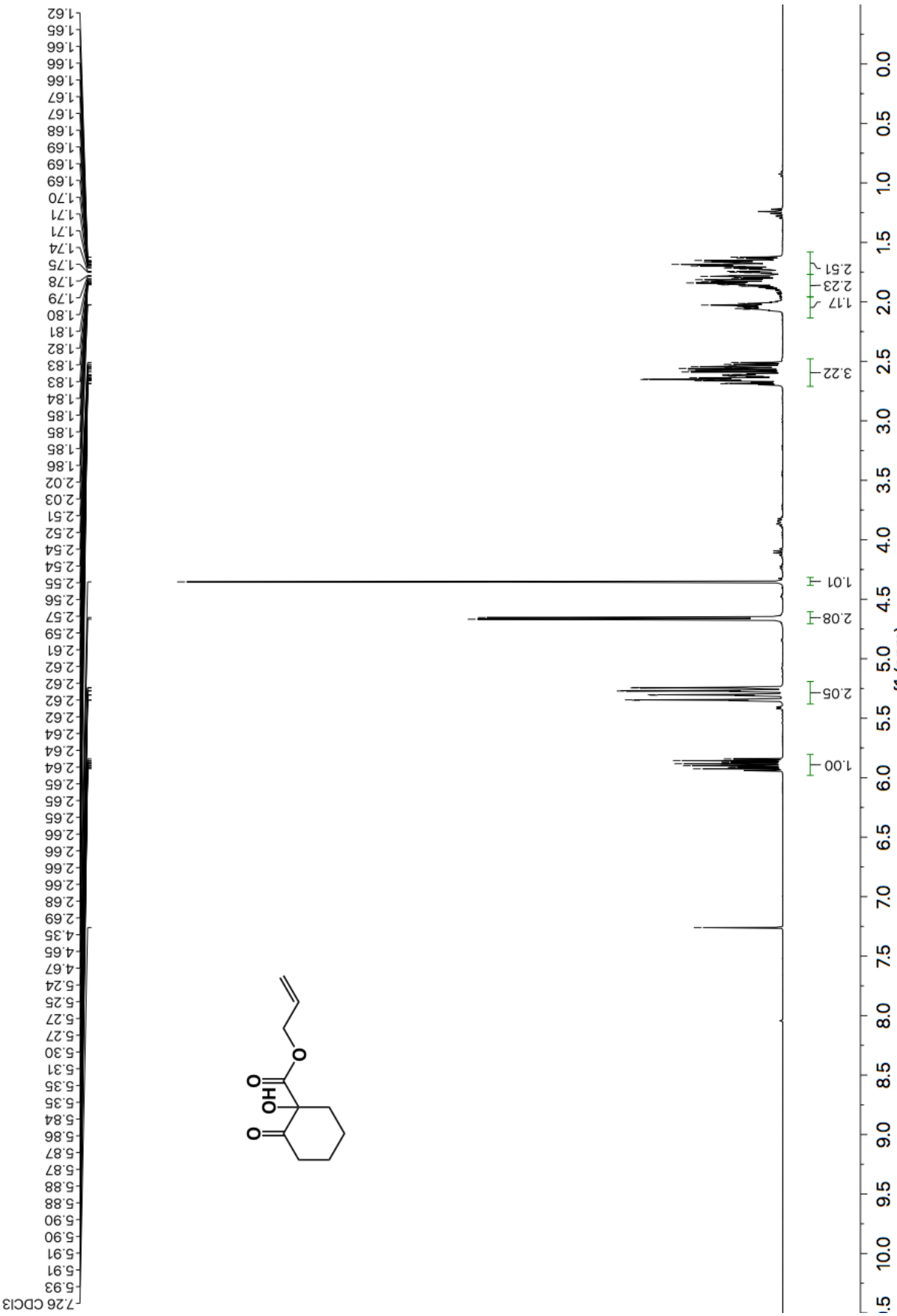

Figure A8.13 ^{1}H NMR (400 MHz, $CDCl_3$) of compound **A7.6a.**

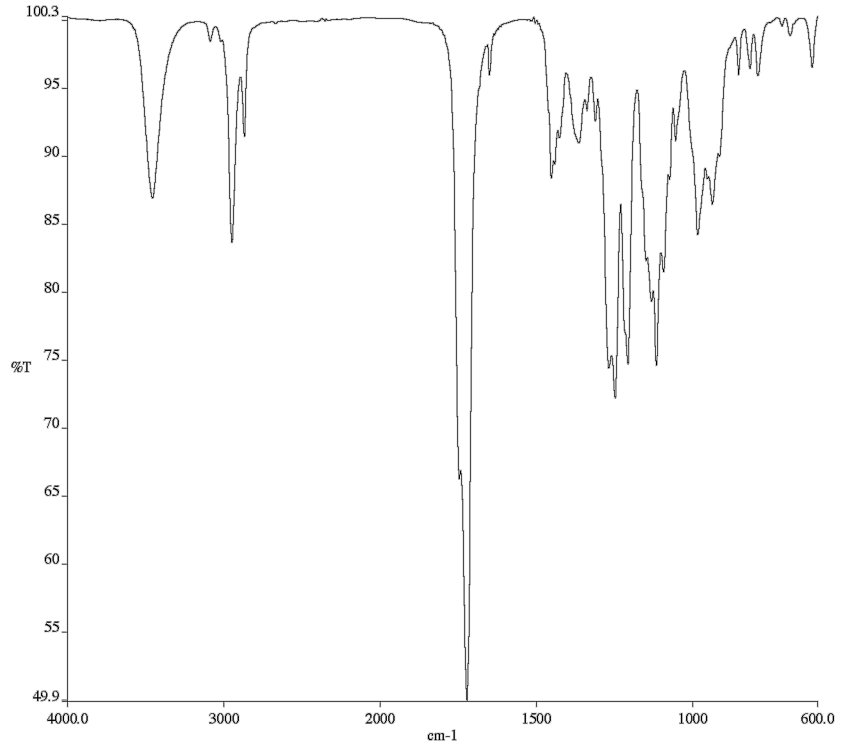

Figure A8.14 Infrared spectrum (Thin Film, NaCl) of compound **A7.6a**.

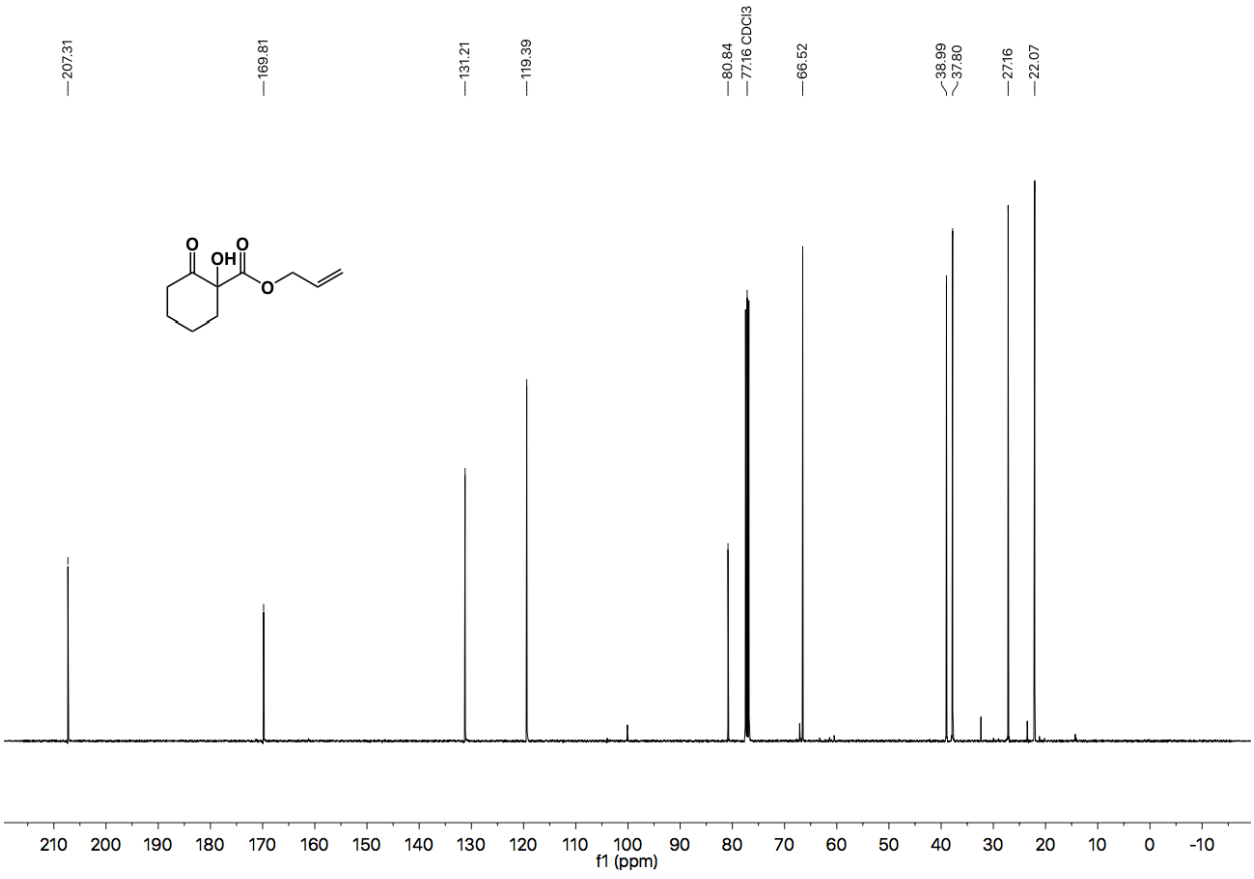

Figure A8.15 ^{13}C NMR (101 MHz, $CDCl_3$) of compound **A7.6a**.

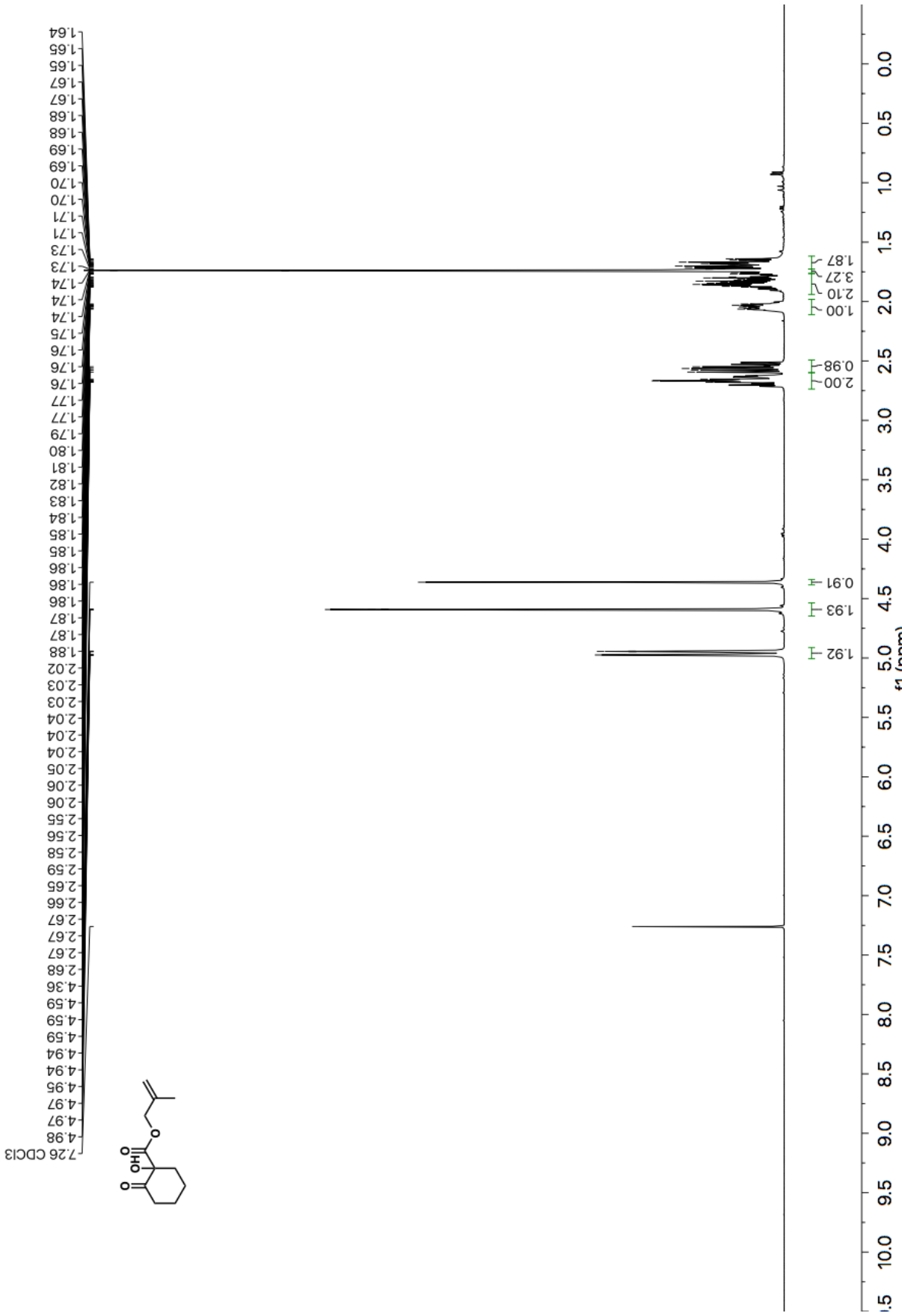

Figure A8.16 ^{1}H NMR (400 MHz, $CDCl_3$) of compound **A7.6b.**

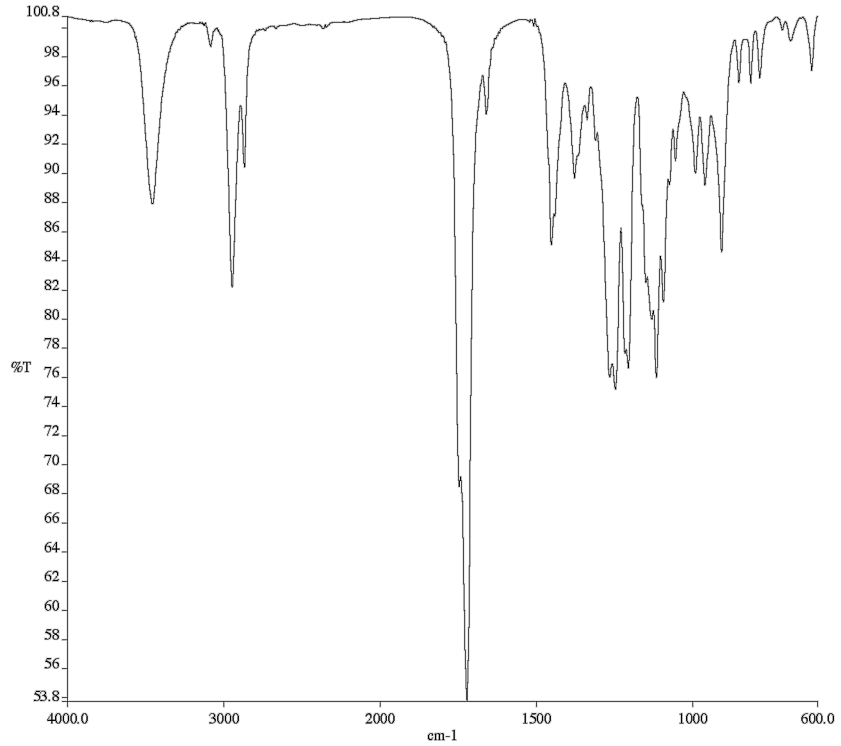

Figure A8.17 Infrared spectrum (Thin Film, NaCl) of compound **A7.6b**.

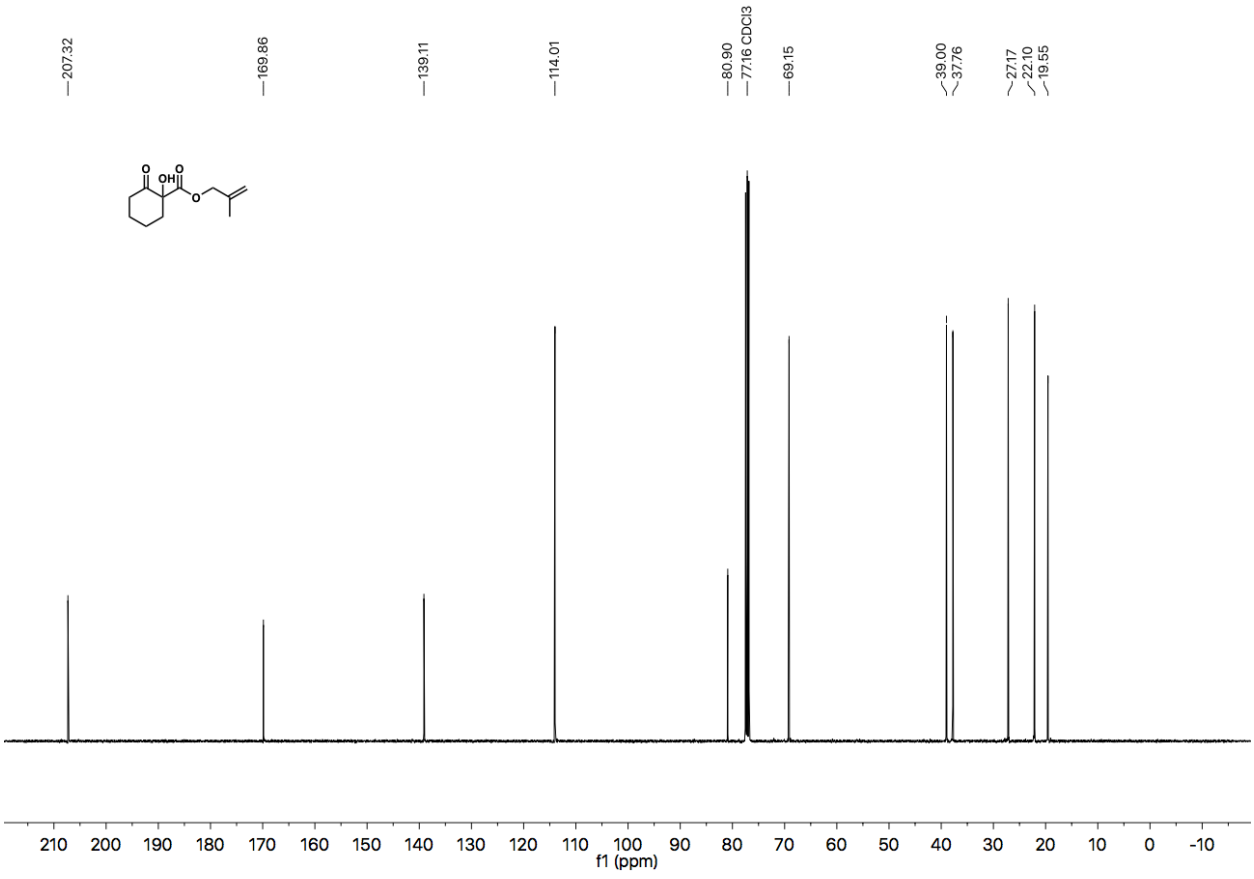

Figure A8.18 ^{13}C NMR (101 MHz, $CDCl_3$) of compound **A7.6b**.

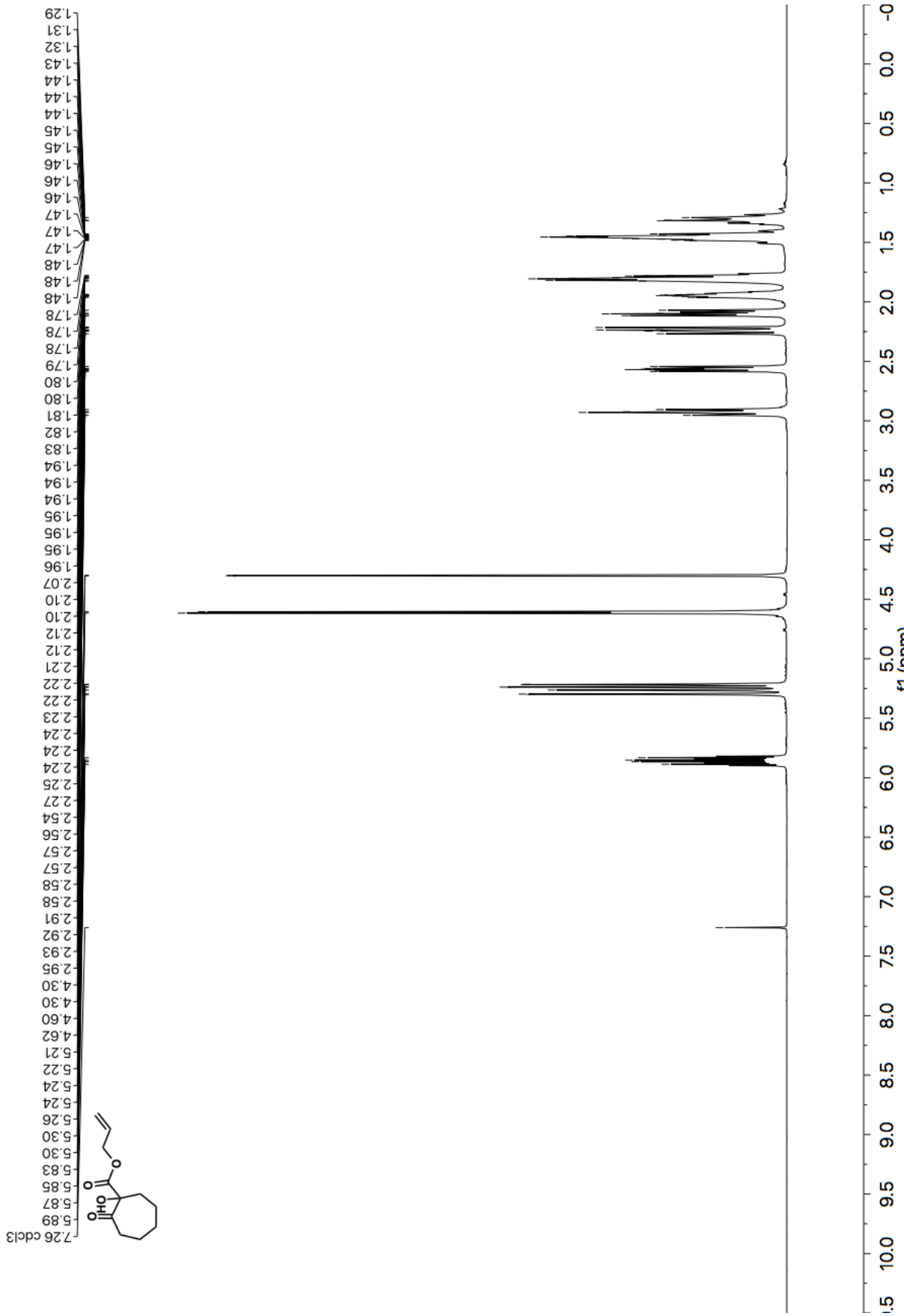

Figure A8.19 ^{1}H NMR (500 MHz, $CDCl_3$) of compound **A7.6c.**

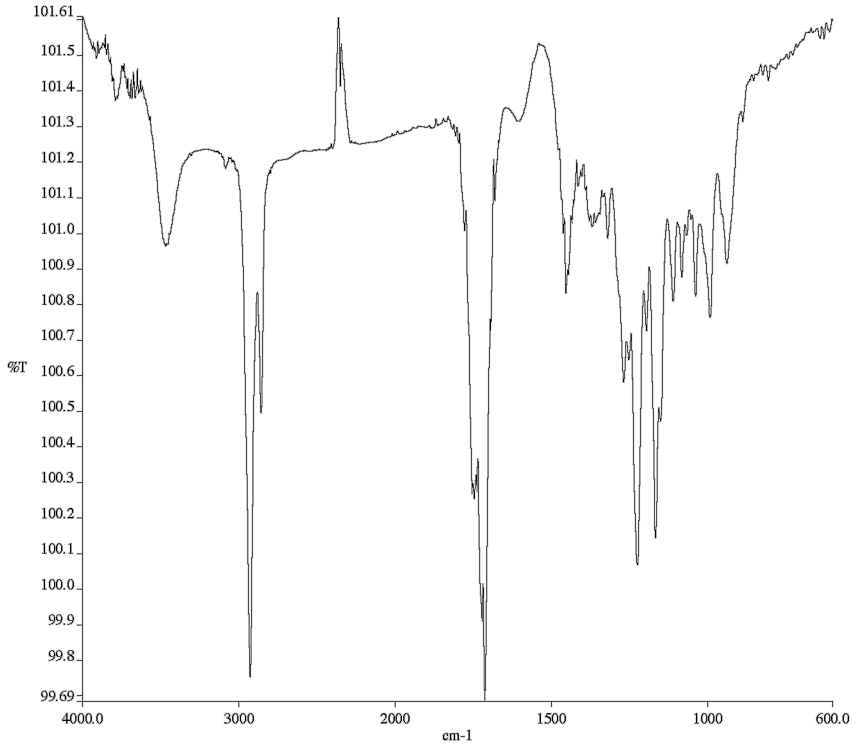

Figure A8.20 Infrared spectrum (Thin Film, NaCl) of compound **A7.6c**.

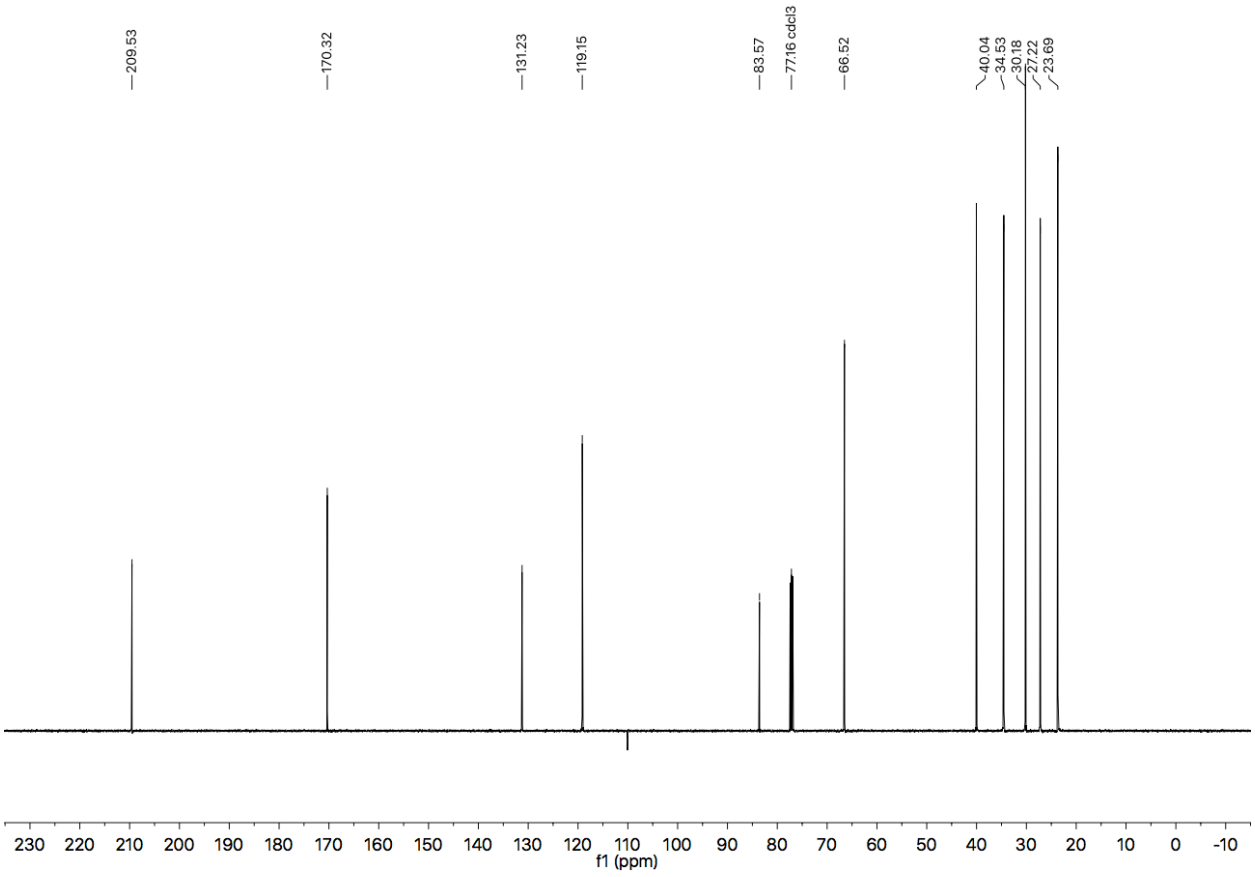

Figure A8.21 ^{13}C NMR (126 MHz, $CDCl_3$) of compound **A7.6c**.

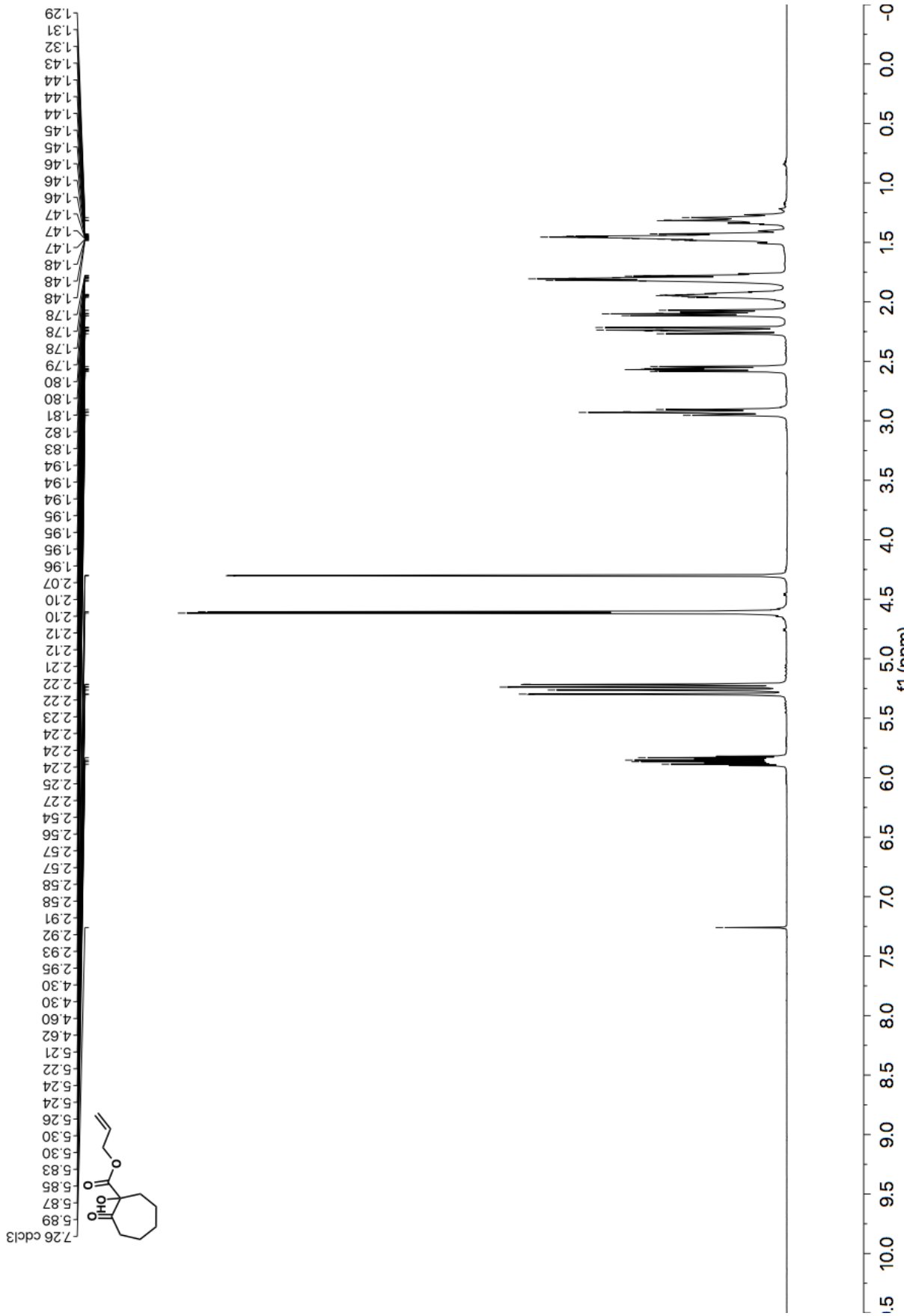

Figure A8.22 ^{1}H NMR (500 MHz, $CDCl_3$) of compound **A7.6d.**

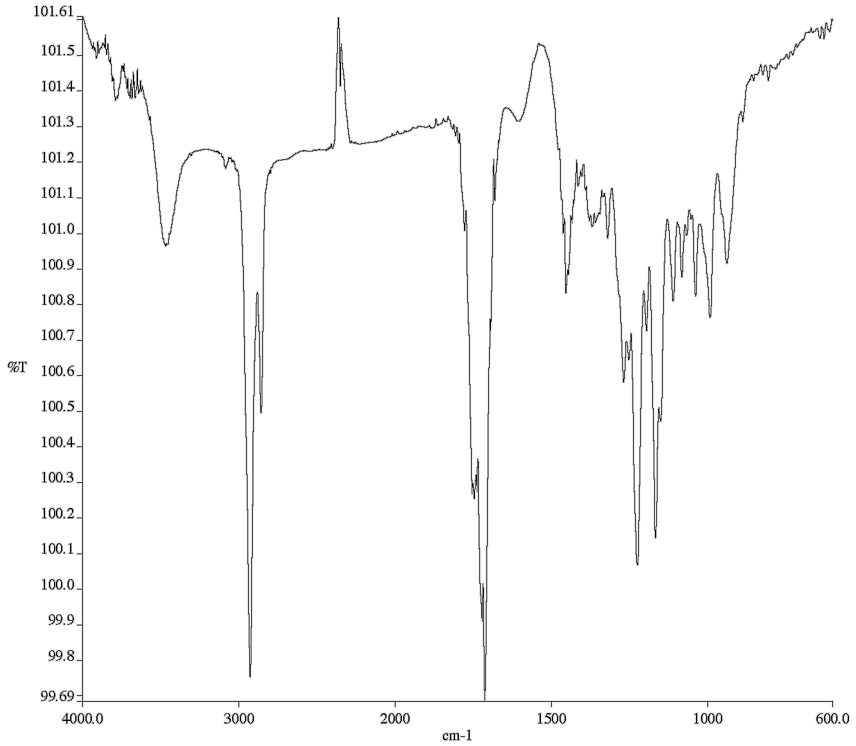

Figure A8.23 Infrared spectrum (Thin Film, NaCl) of compound **A7.6d**.

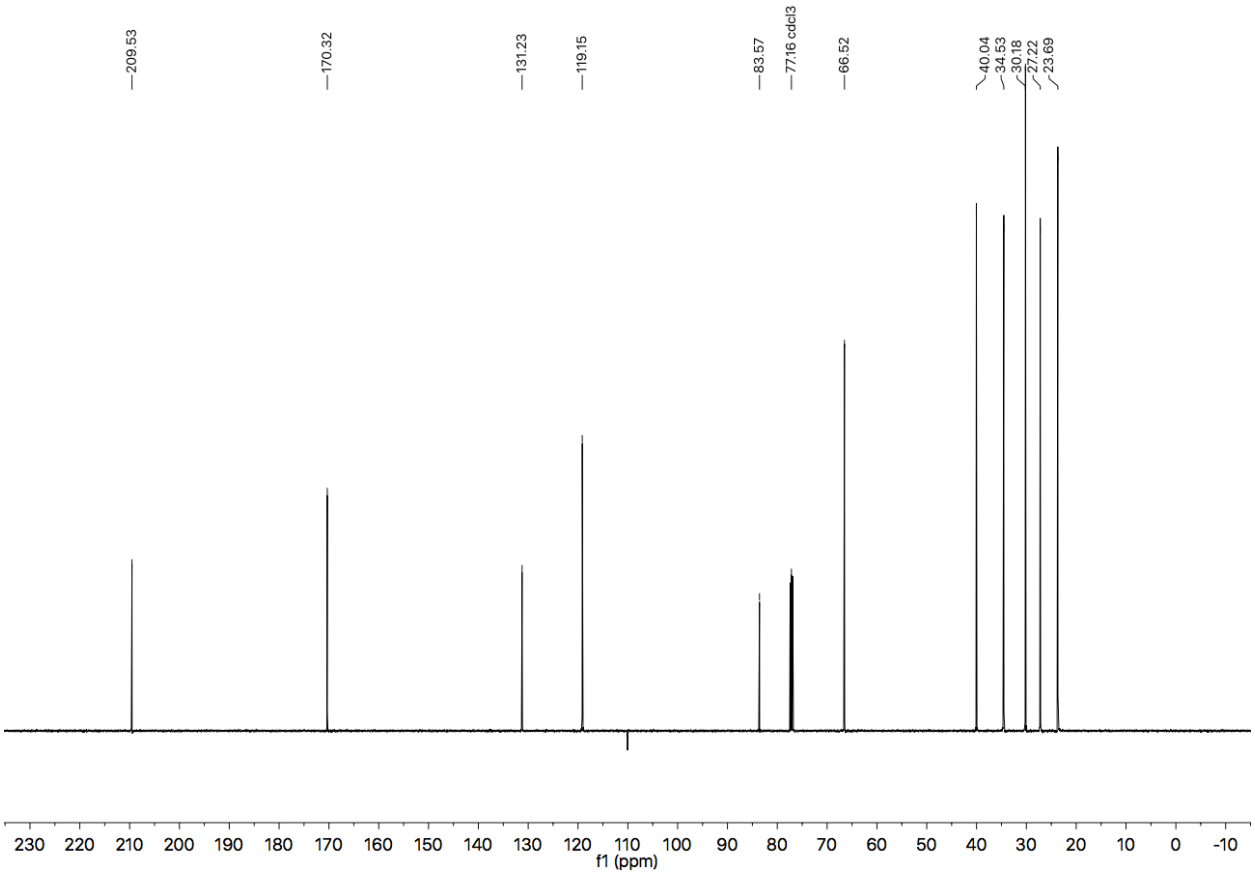

Figure A8.24 ^{13}C NMR (126 MHz, $CDCl_3$) of compound **A7.6d**.

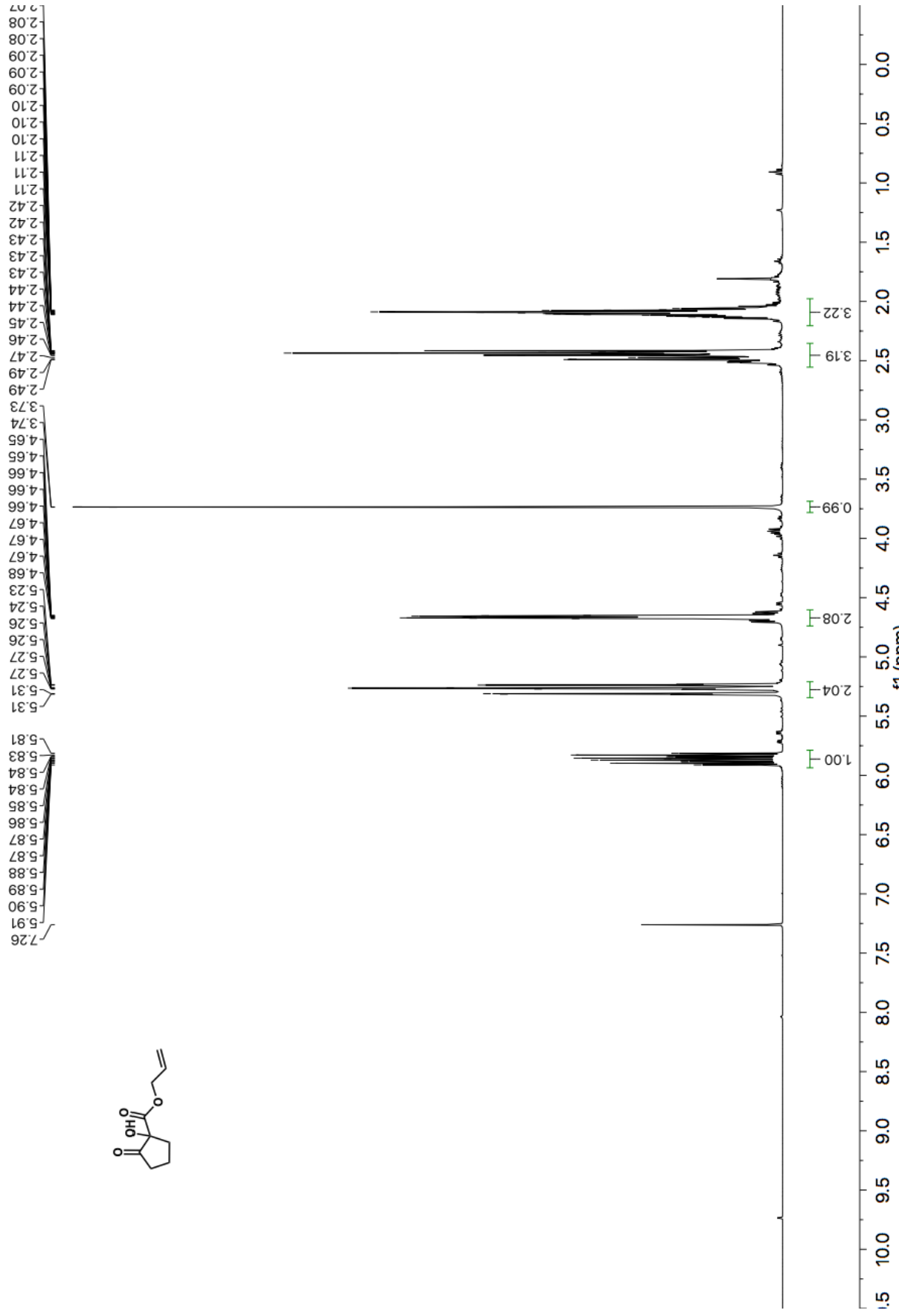

Figure A8.25 ^{1}H NMR (400 MHz, $CDCl_3$) of compound **A7.6d.**

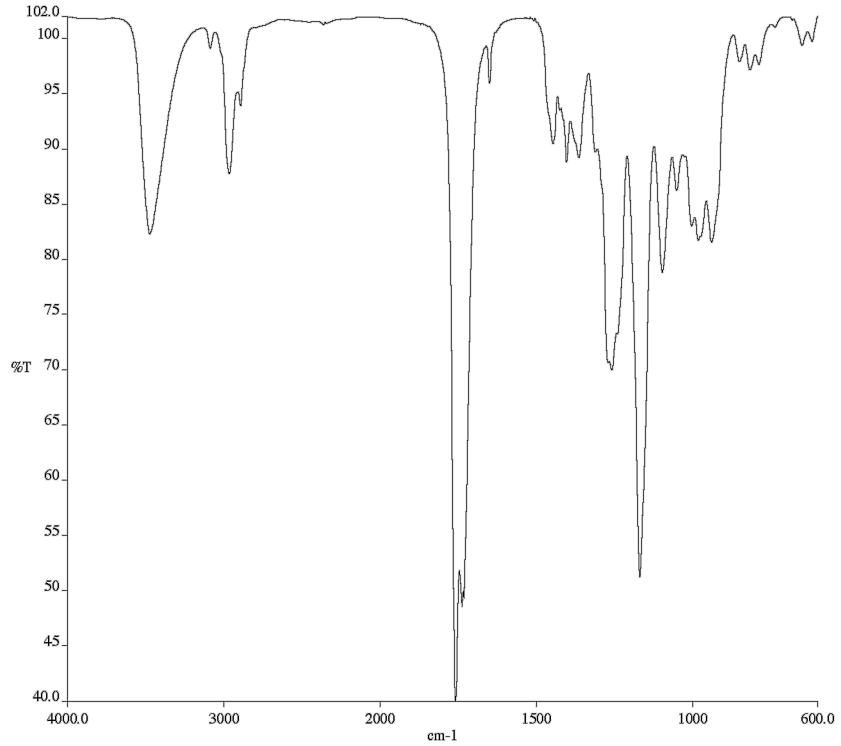

Figure A8.26 Infrared spectrum (Thin Film, NaCl) of compound

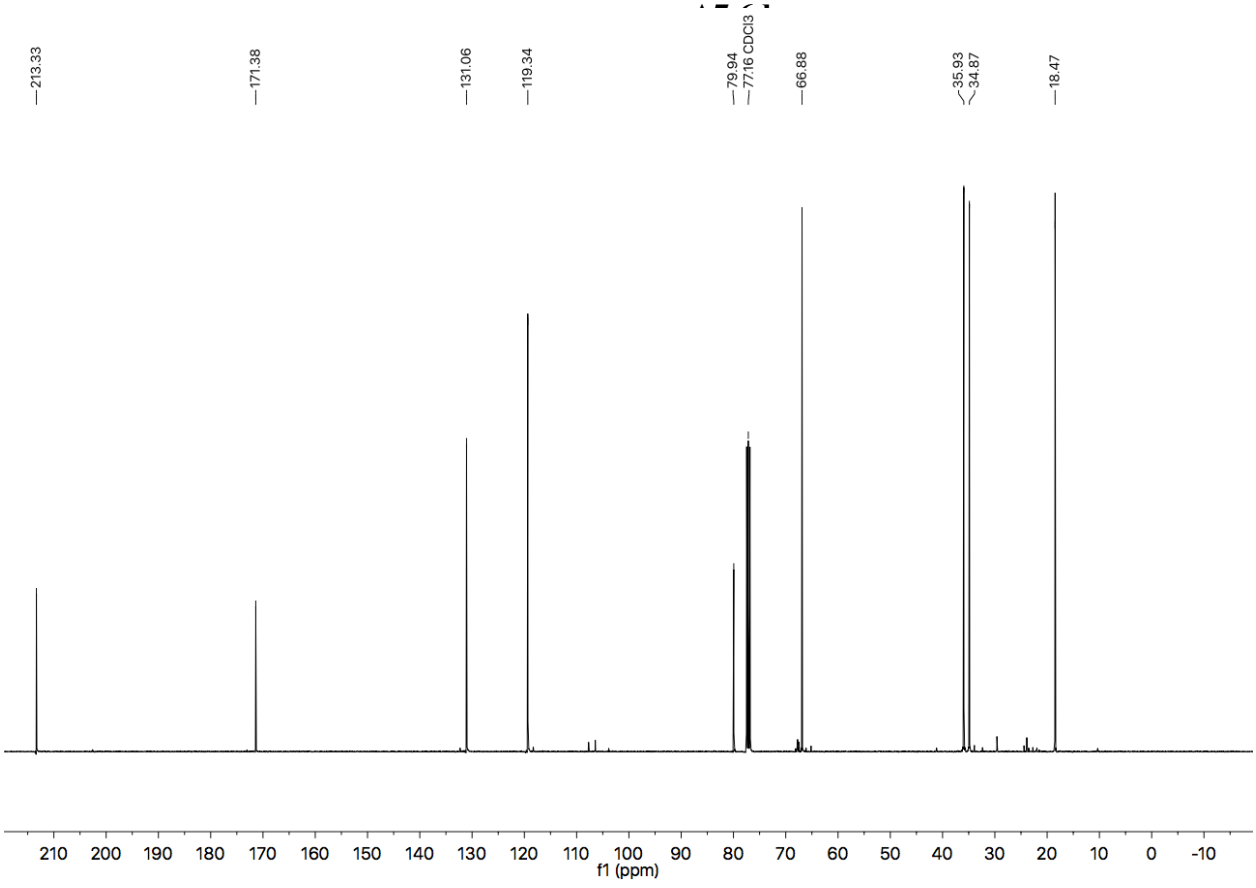

Figure A8.27 ^{13}C NMR (101 MHz, $CDCl_3$) of compound **A7.6d**.

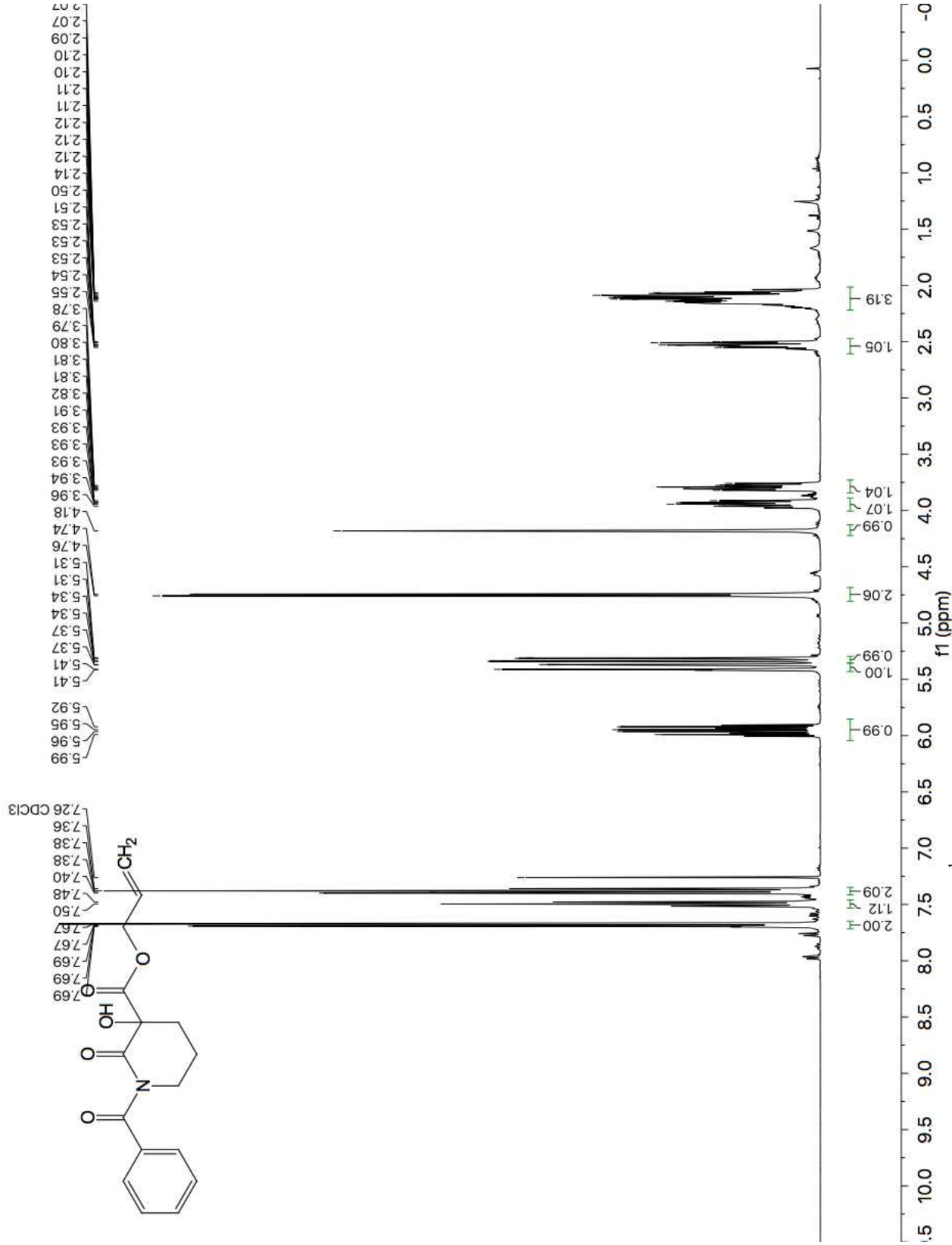

Figure A8.28 ^{1}H NMR (400 MHz, $CDCl_3$) of compound **A7.6e.**

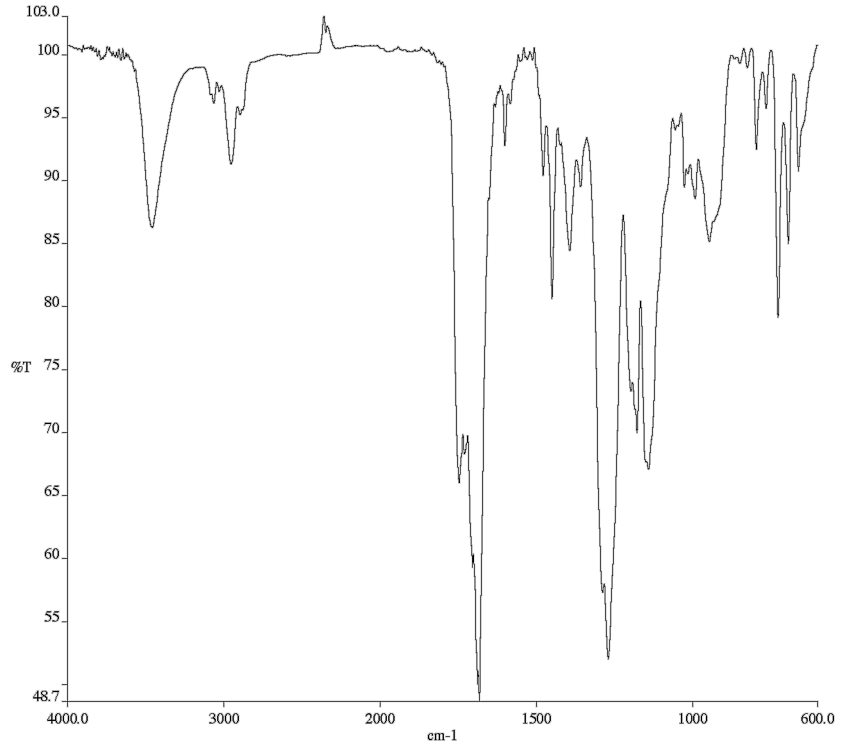

Figure A8.29 Infrared spectrum (Thin Film, NaCl) of compound **A7.6e**.

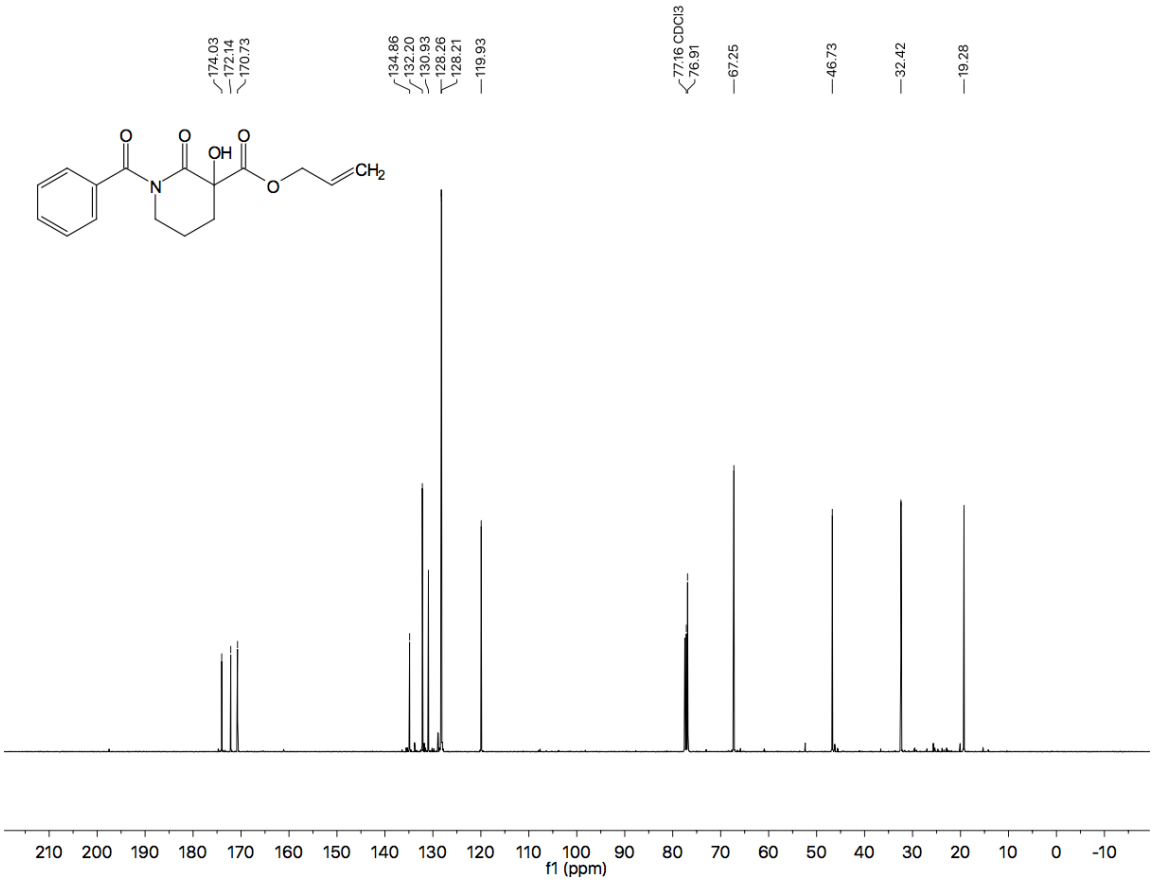

Figure A8.30 ^{13}C NMR (101 MHz, $CDCl_3$) of compound **A7.6e**.

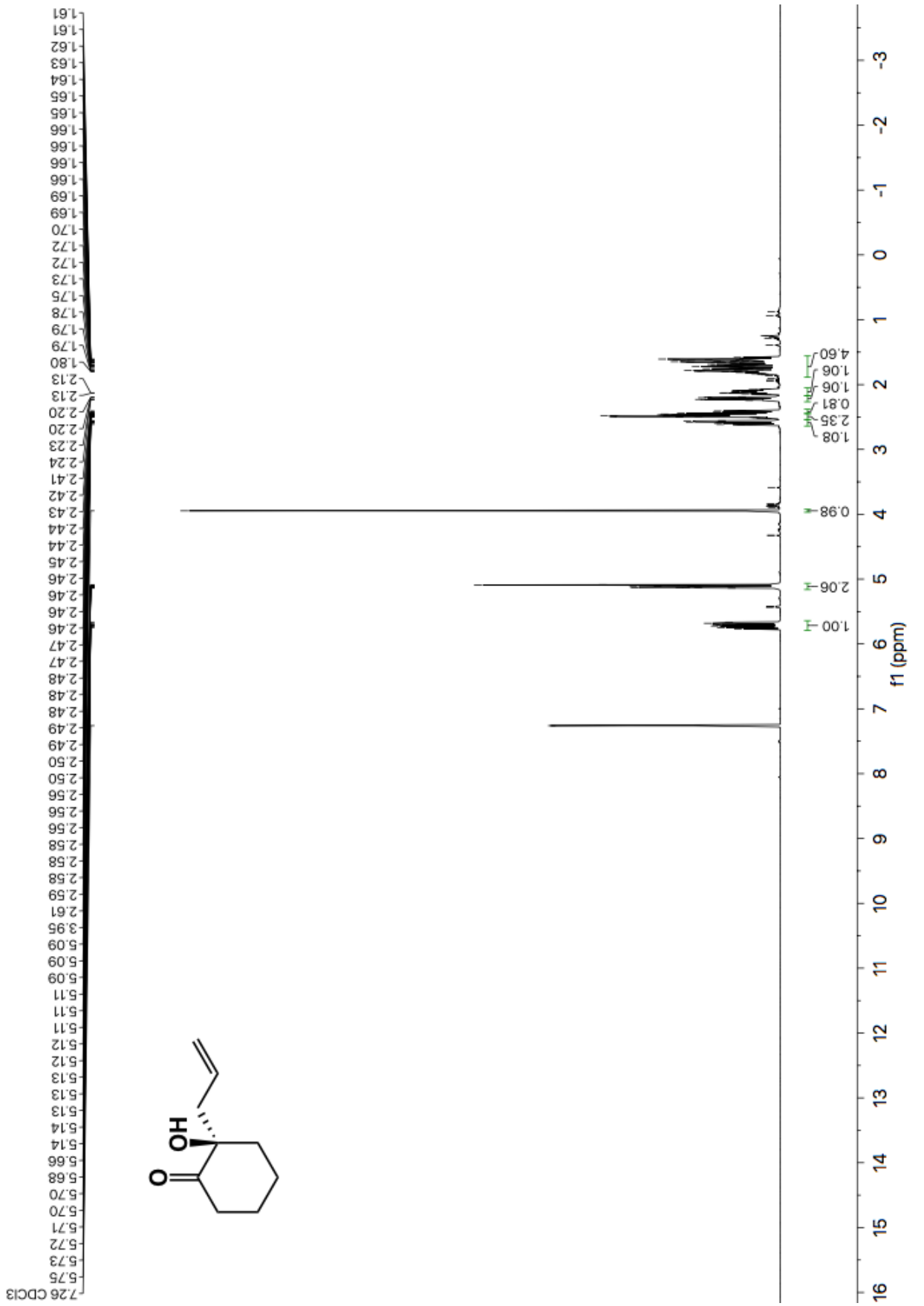

Figure A8.31 ^{1}H NMR (400 MHz, $CDCl_3$) of compound **A7.7a.**

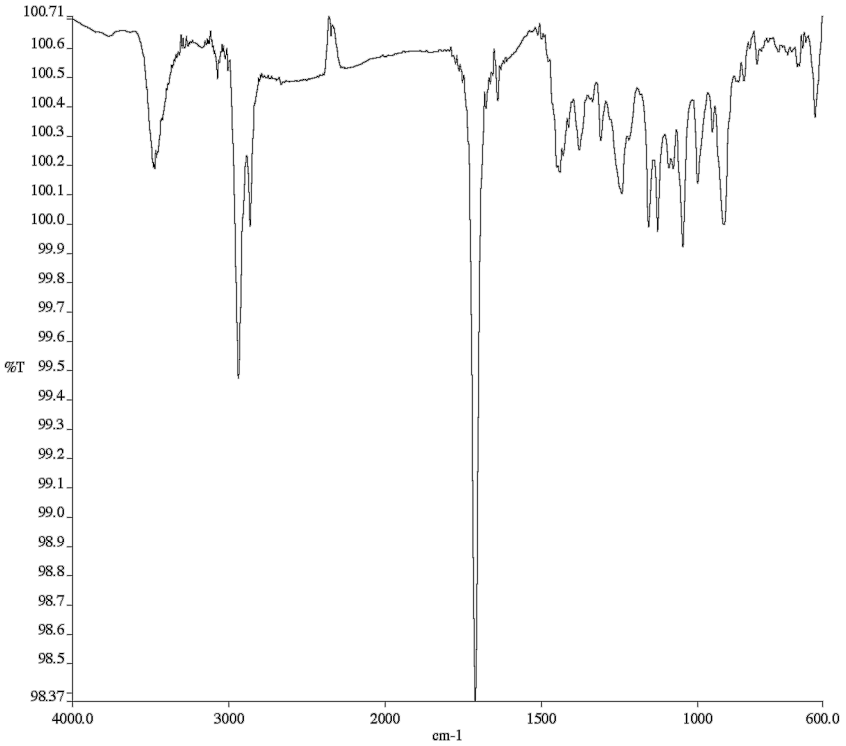

Figure A8.32 Infrared spectrum (Thin Film, NaCl) of compound **A7.7a**.

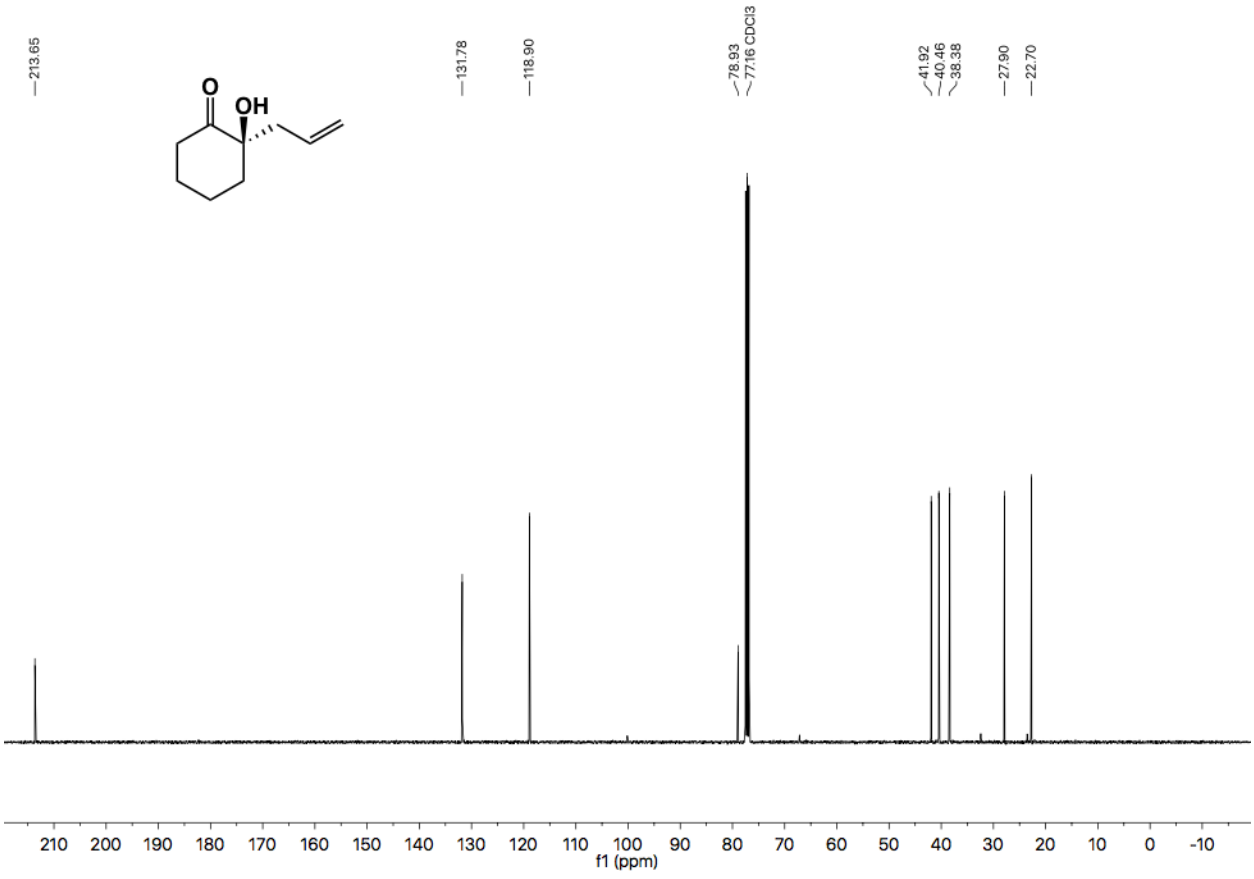

Figure A8.33 ^{13}C NMR (101 MHz, $CDCl_3$) of compound **A7.7a**.

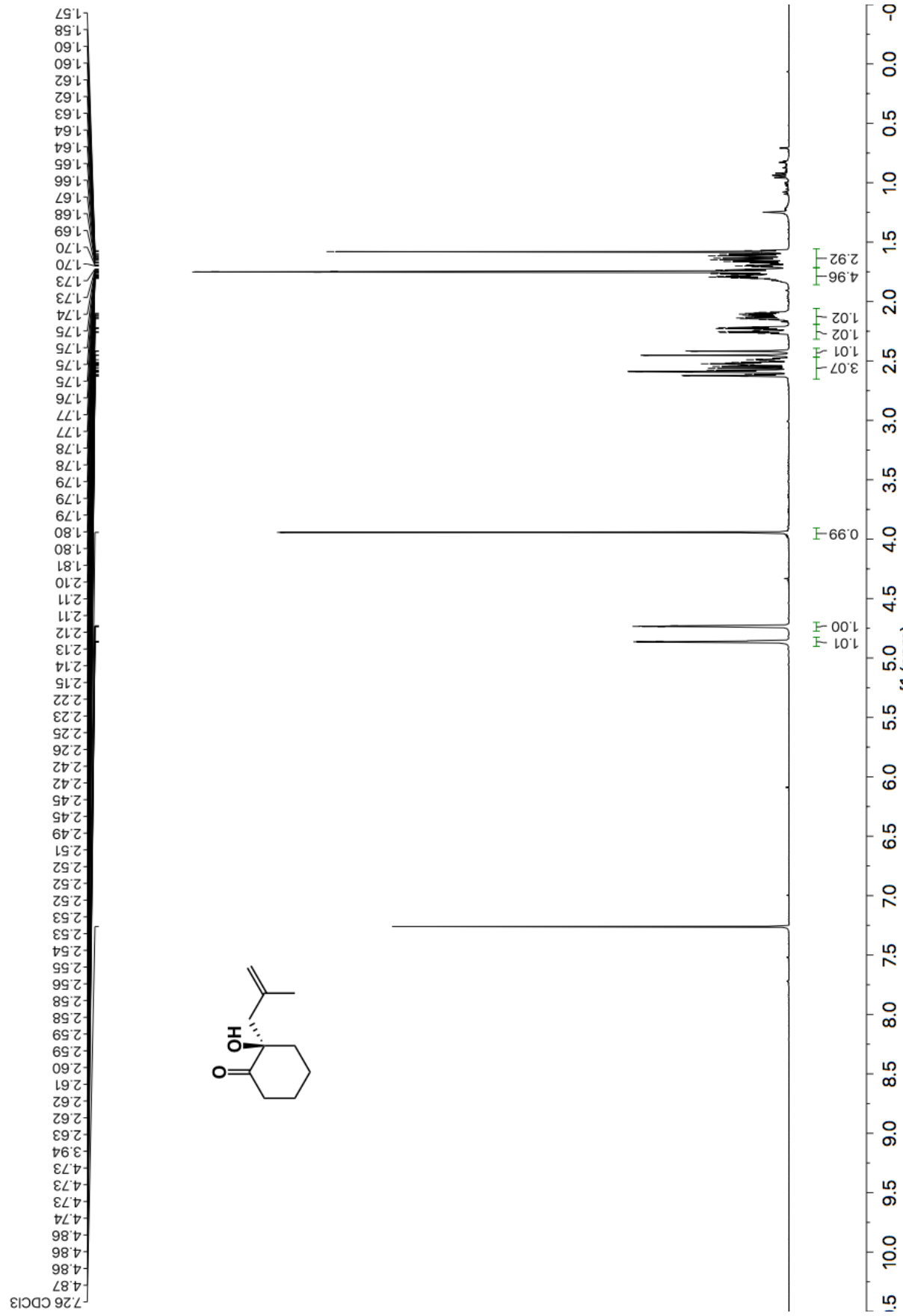

Figure A8.34 ^{1}H NMR (400 MHz, $CDCl_3$) of compound **A7.7b.**

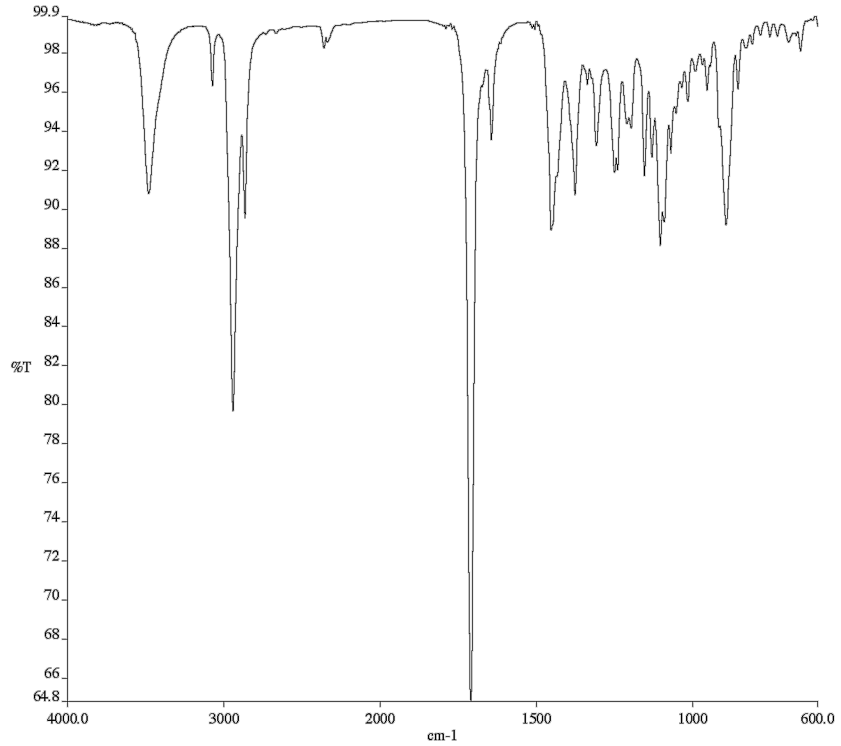

Figure A8.35 Infrared spectrum (Thin Film, NaCl) of compound **A7.7b**.

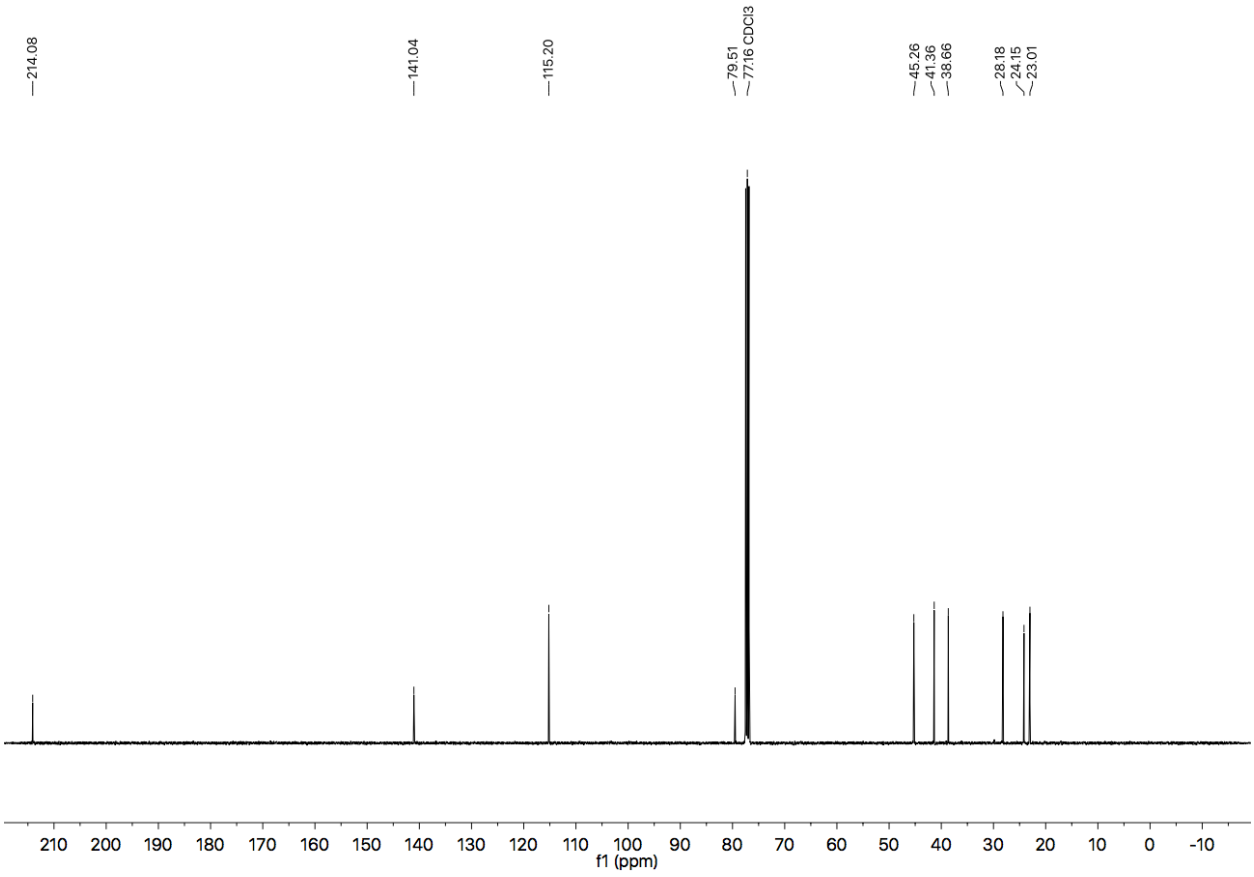

Figure A8.36 ^{13}C NMR (101 MHz, $CDCl_3$) of compound **A7.7a**.

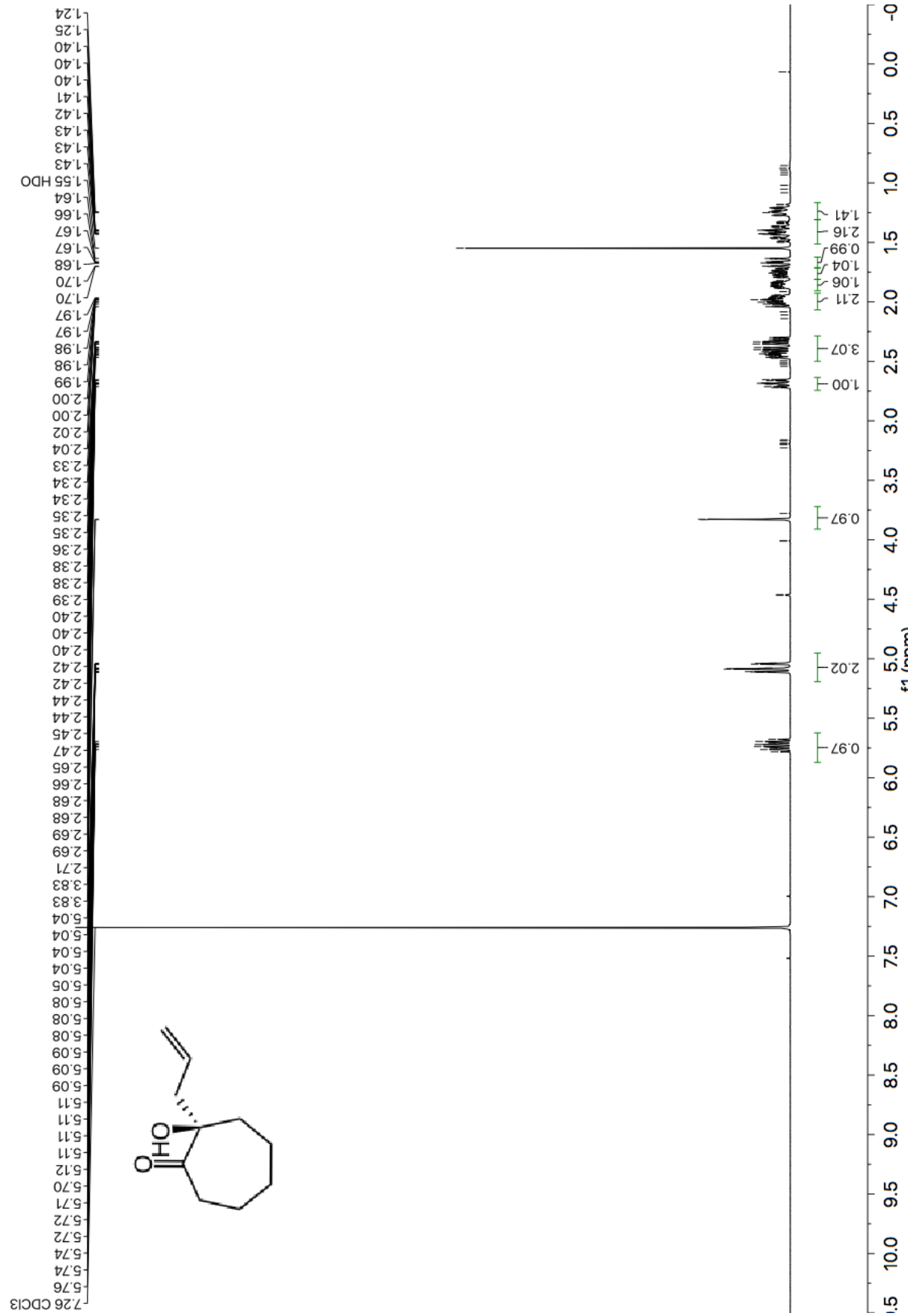

Figure A8.37 ^{1}H NMR (400 MHz, $CDCl_3$) of compound **A7.7c.**

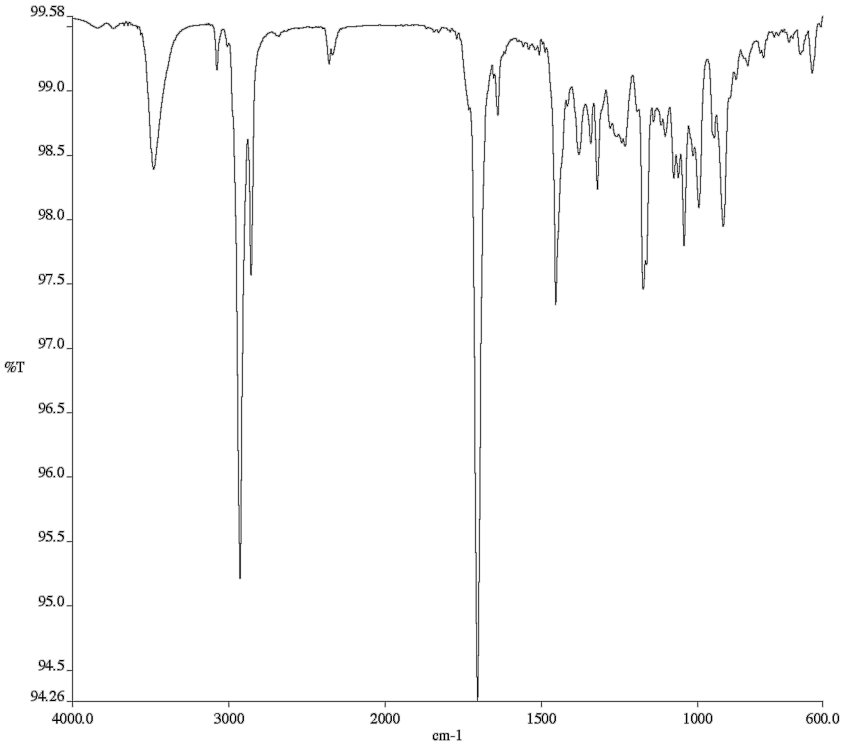

Figure A8.38 Infrared spectrum (Thin Film, NaCl) of compound **A7.7c**.

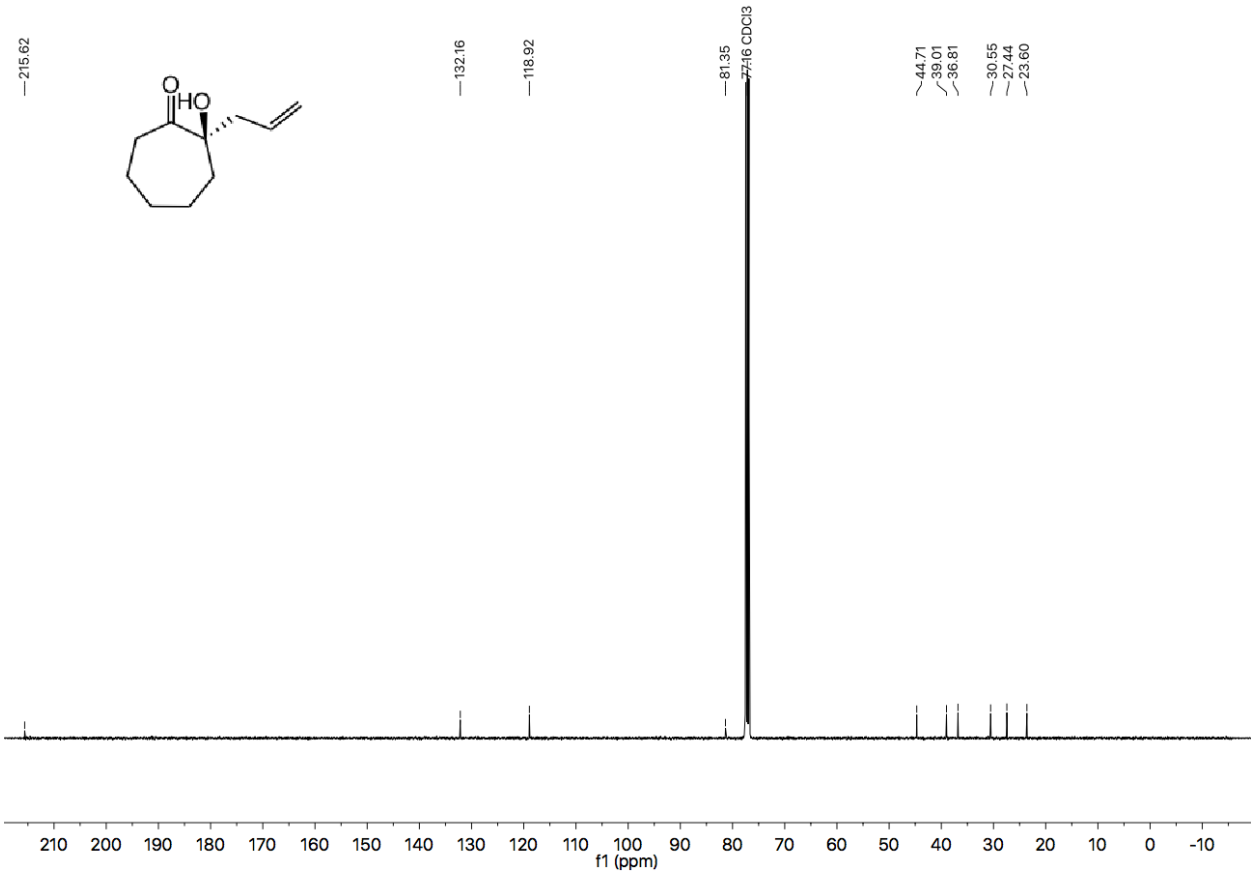

Figure A8.39 ^{13}C NMR (101 MHz, $CDCl_3$) of compound **A7.7c**.

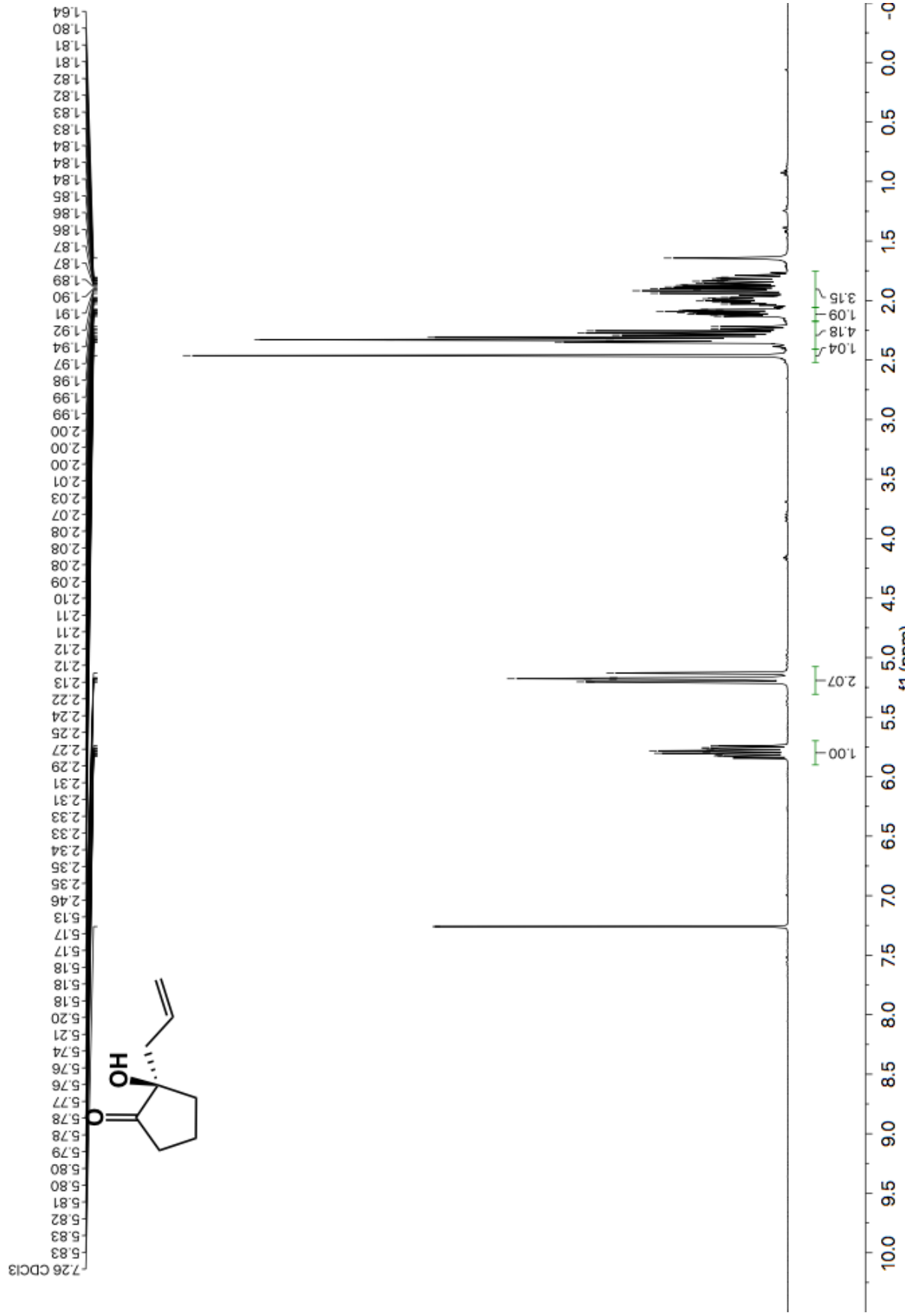

Figure A8.40 ^{1}H NMR (400 MHz, $CDCl_3$) of compound **A7.7d.**

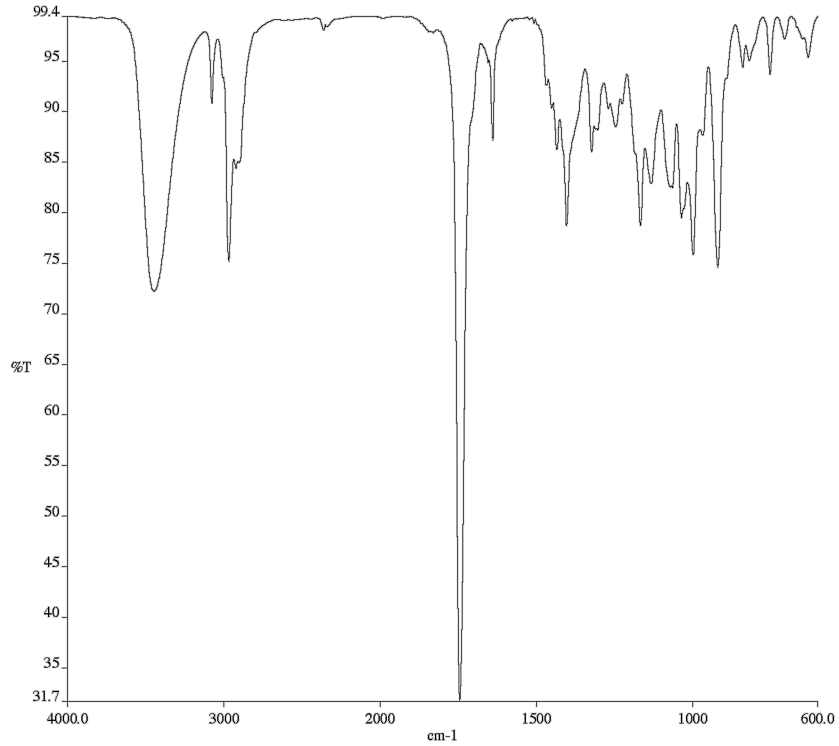

Figure A8.41 Infrared spectrum (Thin Film, NaCl) of compound

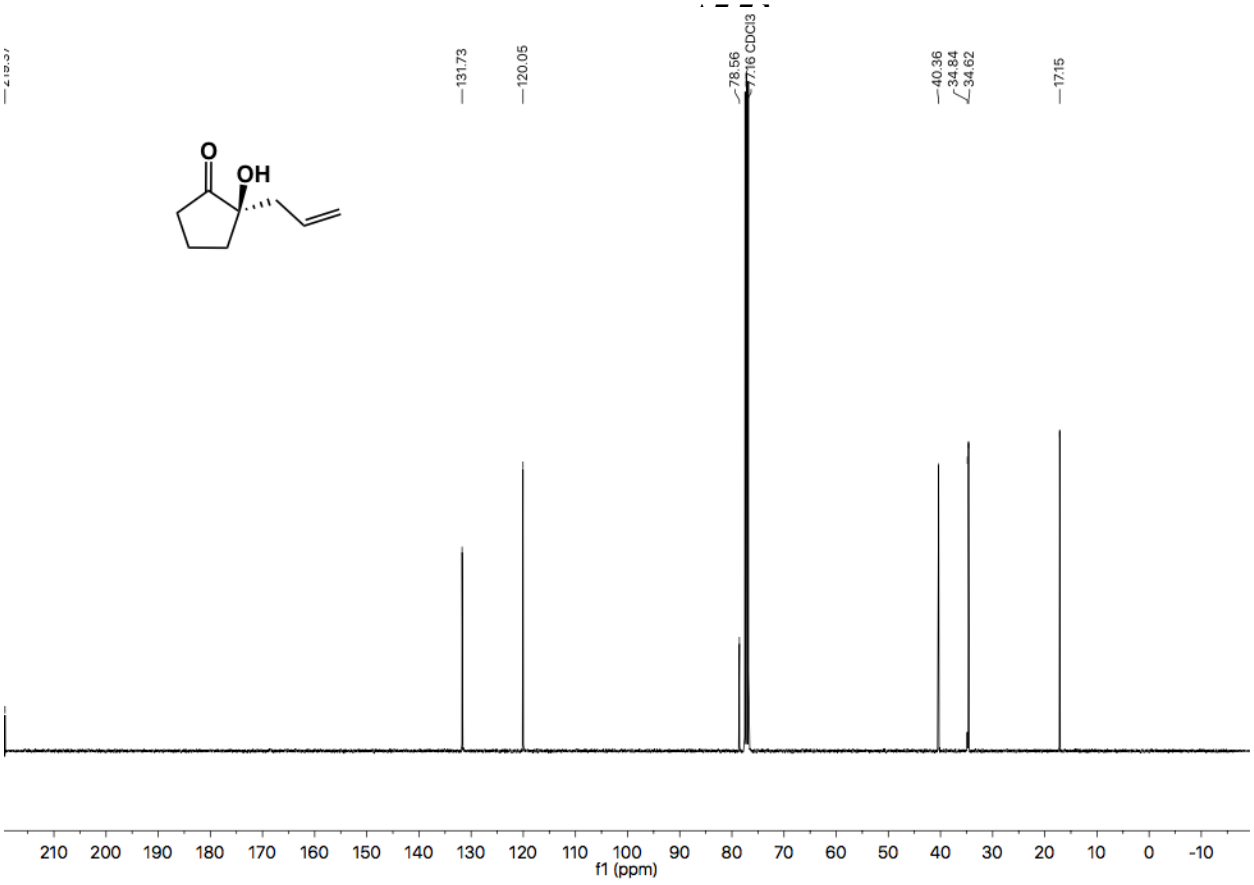

Figure A8.42 ^{13}C NMR (101 MHz, $CDCl_3$) of compound **A7.7d**.

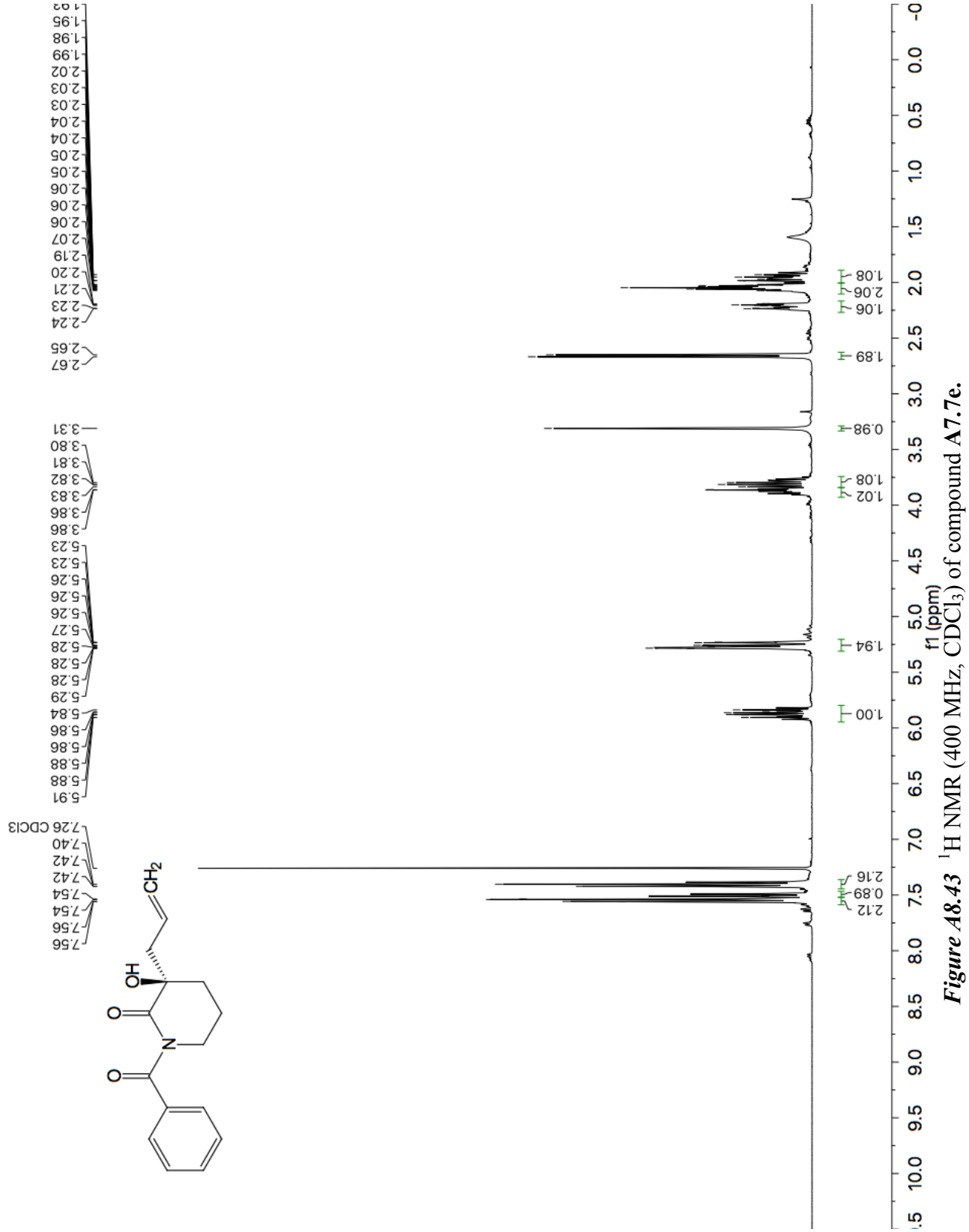

Figure A8.43 ^{1}H NMR (400 MHz, $CDCl_3$) of compound **A7.7e.**

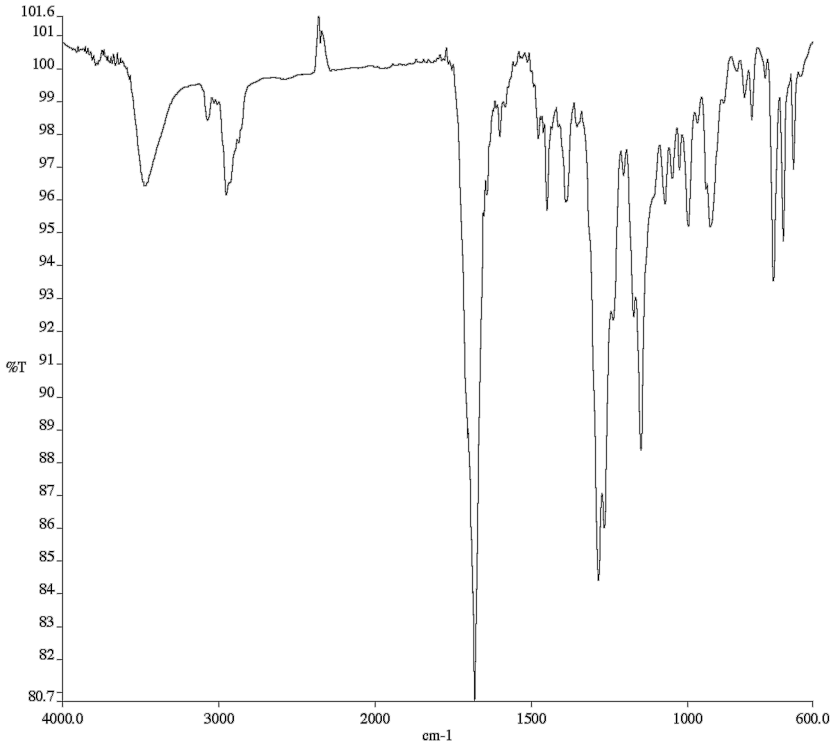

Figure A8.44 Infrared spectrum (Thin Film, NaCl) of compound

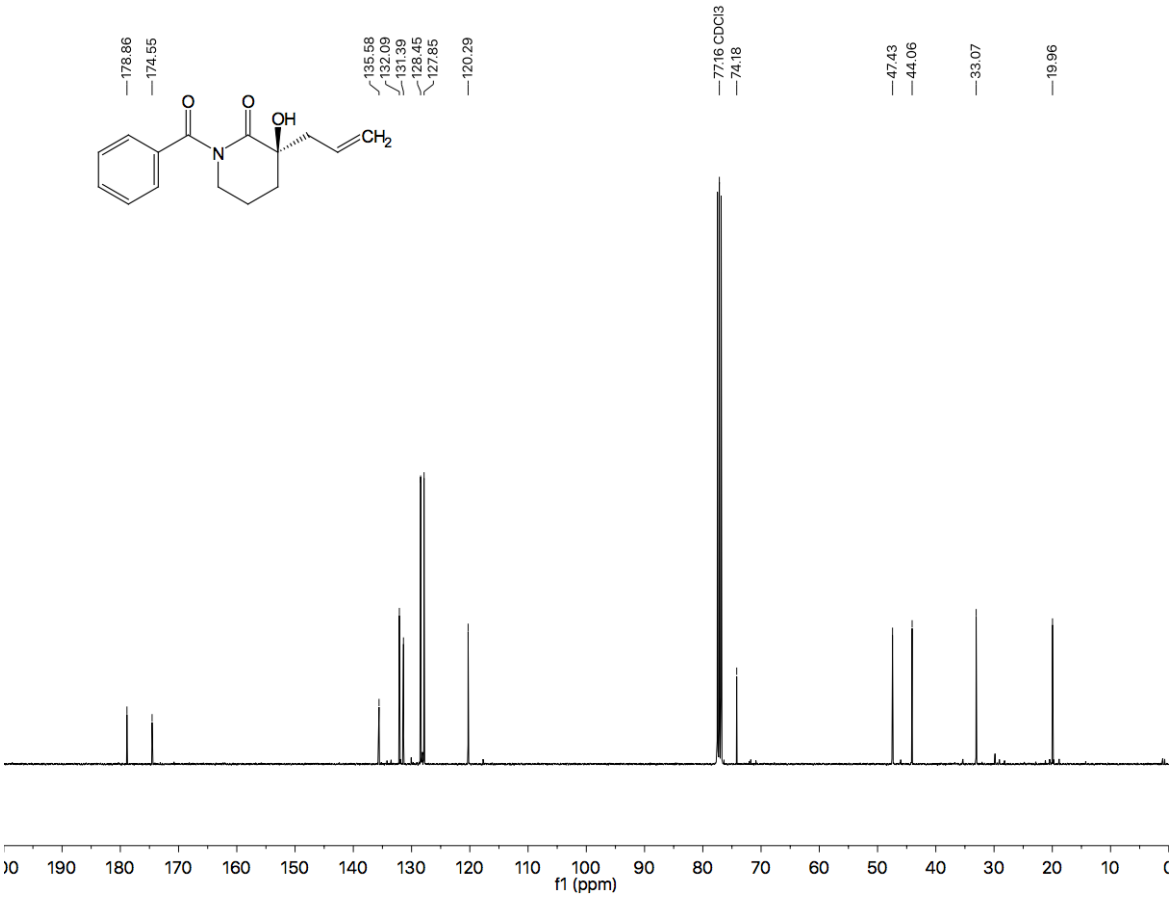

Figure A8.45 ^{13}C NMR (101 MHz, $CDCl_3$) of compound **A7.7e**.

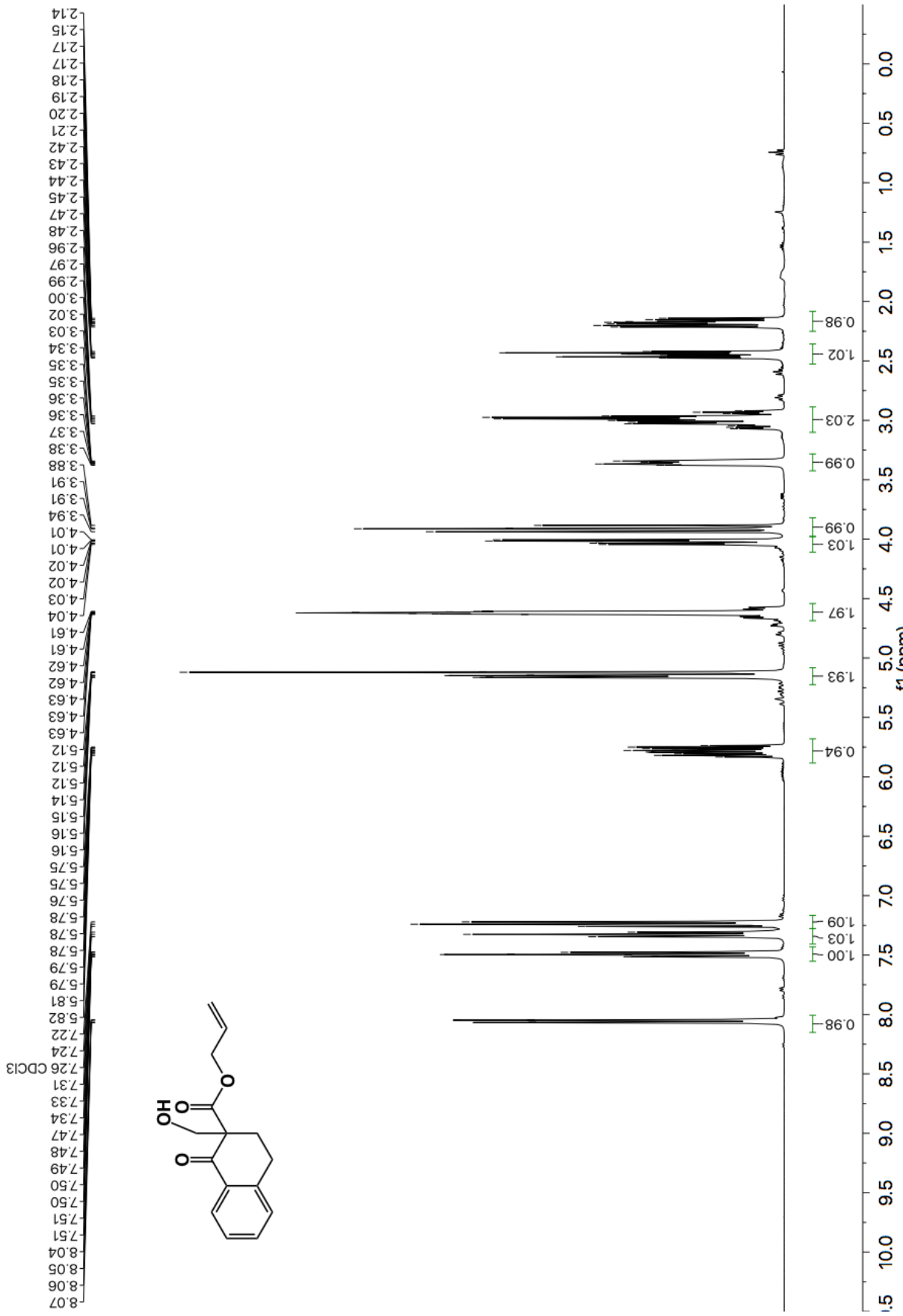

Figure A8.46 ^{1}H NMR (400 MHz, $CDCl_3$) of compound **A7.8.**

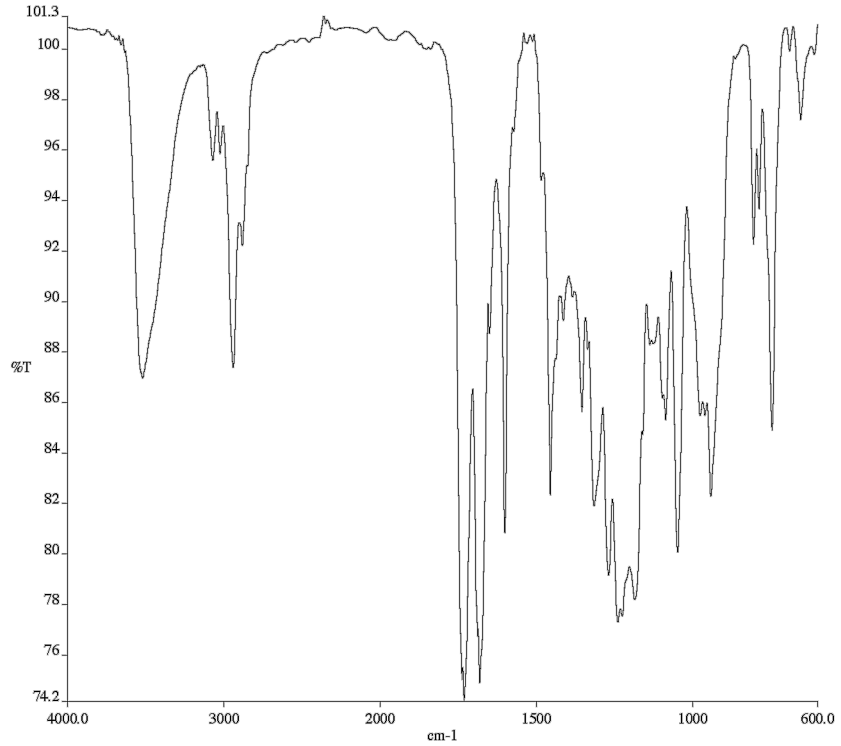

Figure A8.47 Infrared spectrum (Thin Film, NaCl) of compound **A7.8**.

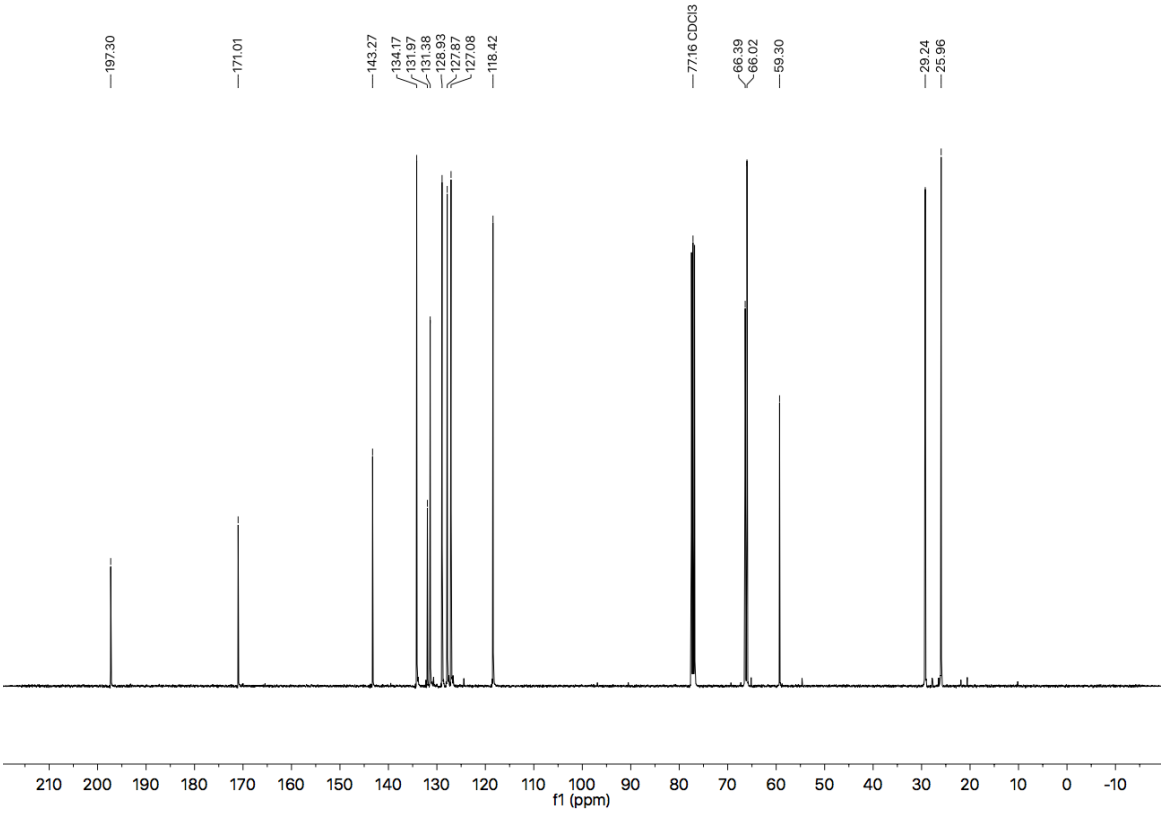

Figure A8.48 ^{13}C NMR (101 MHz, $CDCl_3$) of compound **A7.8.**

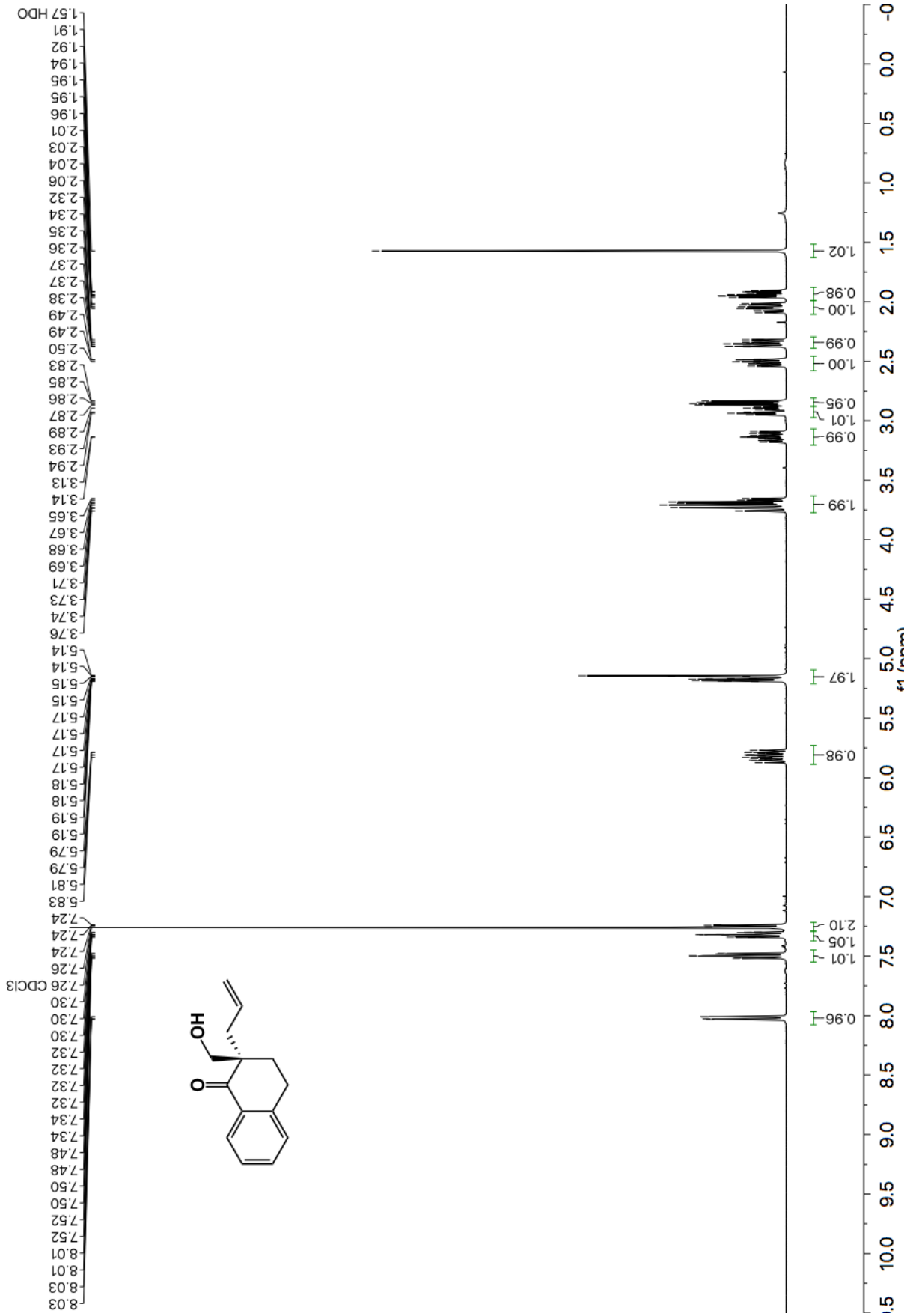

Figure A8.49 ^{1}H NMR (400 MHz, $CDCl_3$) of compound **A7.9.**

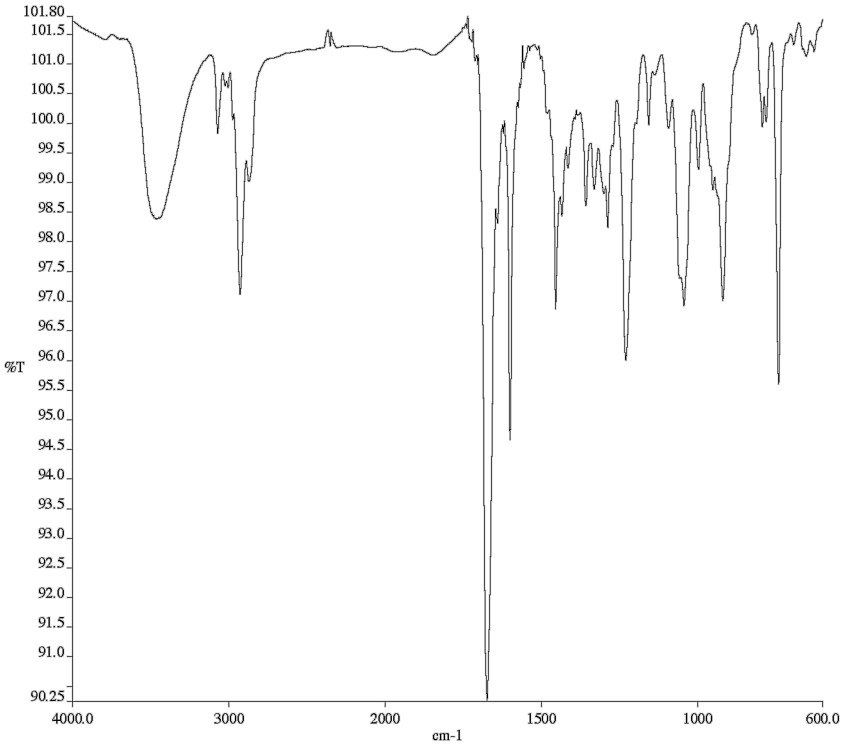

Figure A8.50 Infrared spectrum (Thin Film, NaCl) of compound **A7.9**.

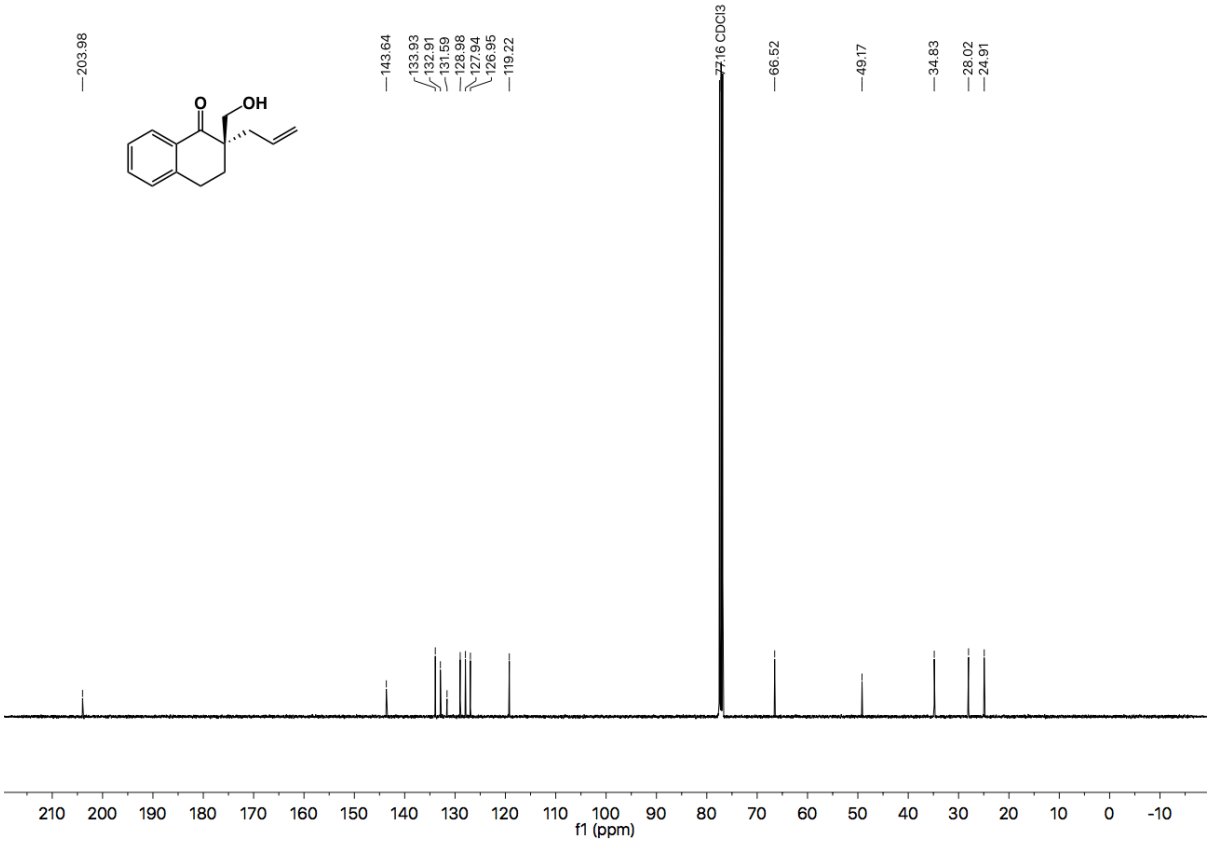

Figure A8.51 ^{13}C NMR (101 MHz, $CDCl_3$) of compound **A7.9**.

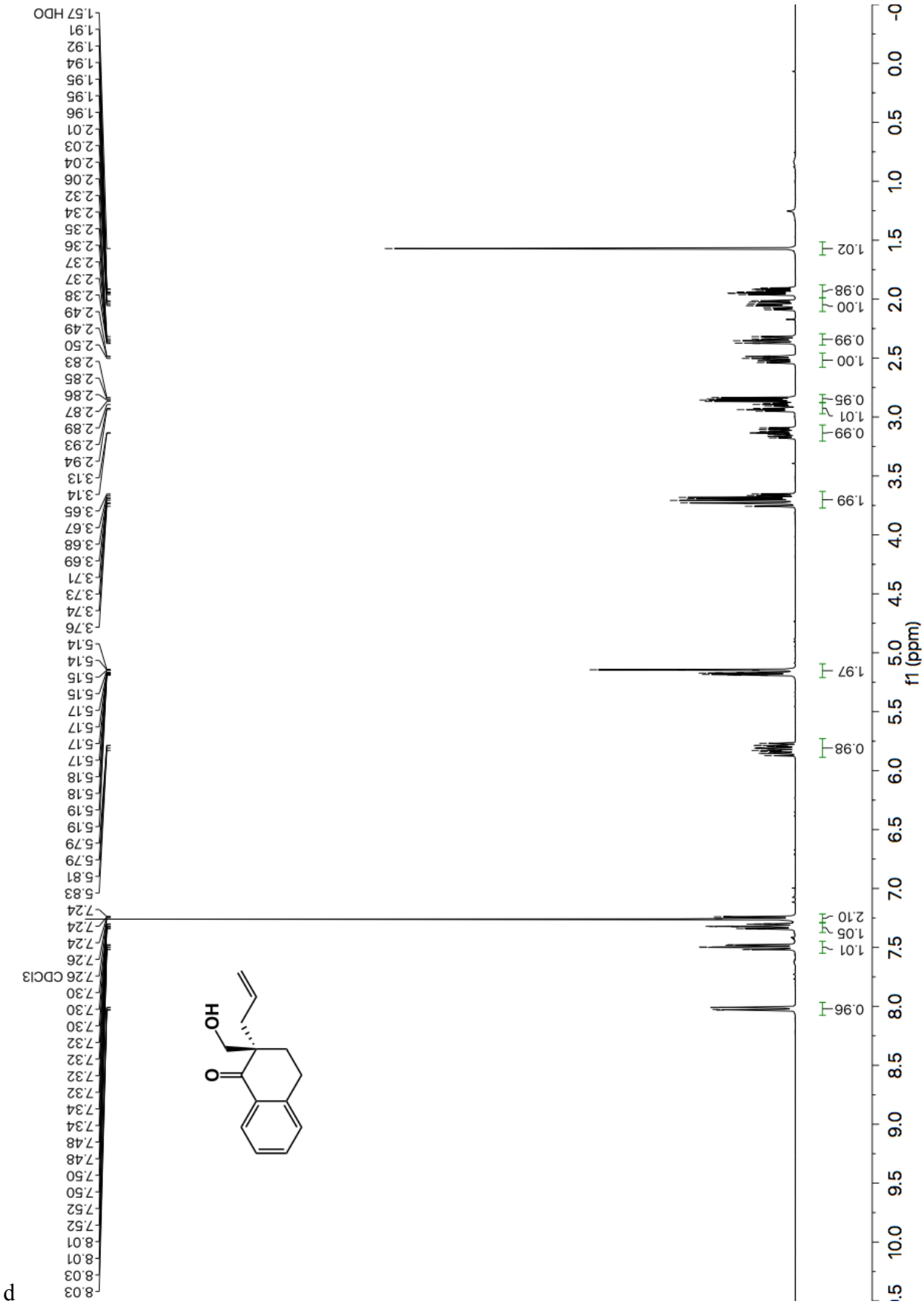

Figure A8.52 ^{1}H NMR (400 MHz, $CDCl_3$) of compound **A7.11.**

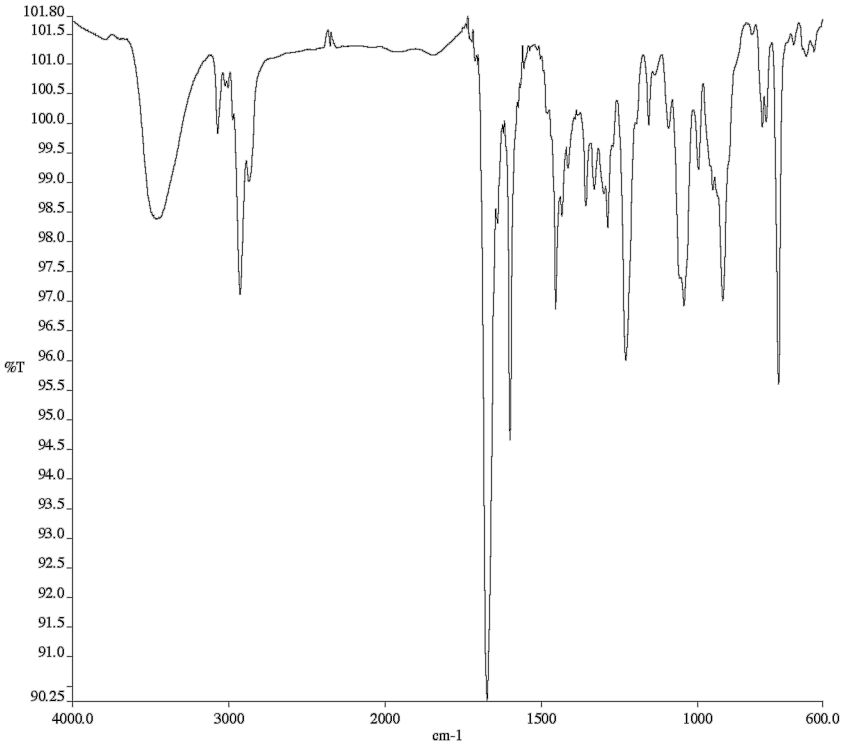

Figure A8.53 Infrared spectrum (Thin Film, NaCl) of compound **A7.11**.

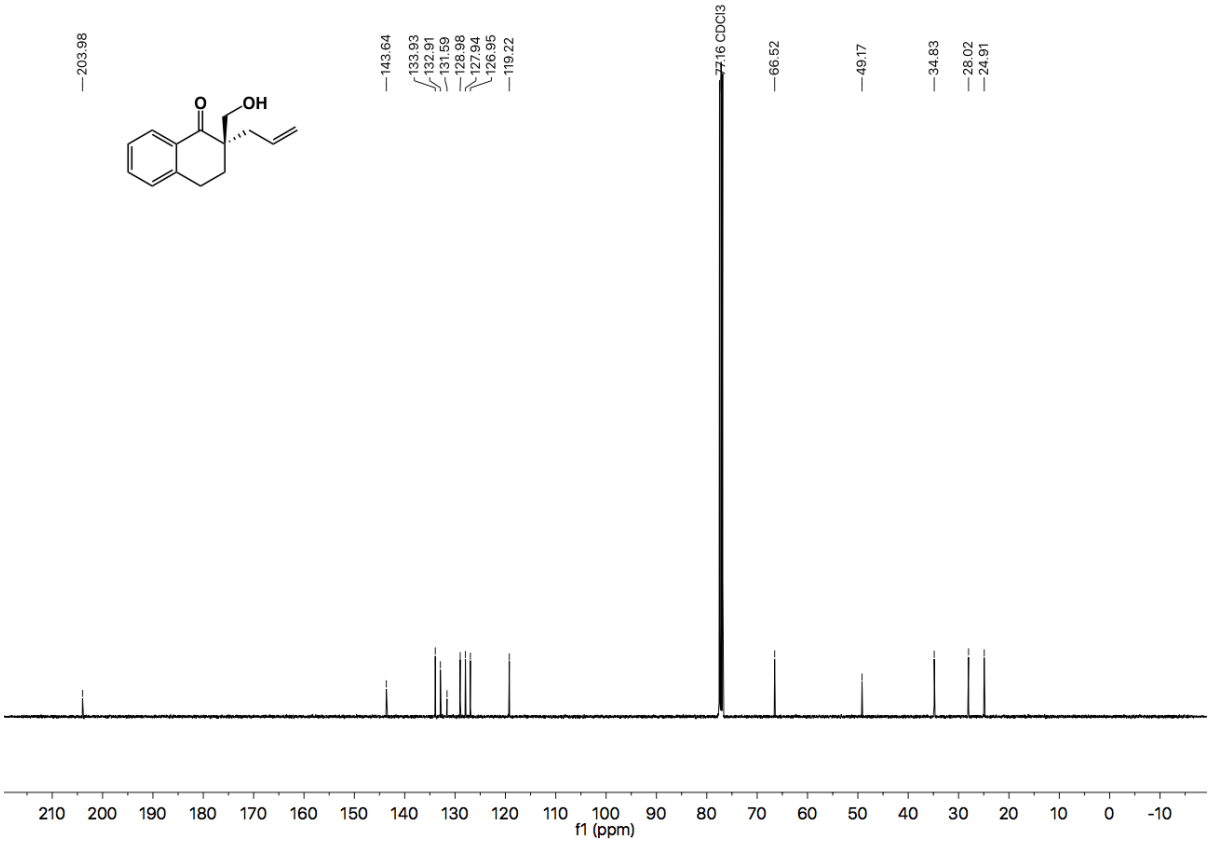

Figure A8.54 ^{13}C NMR (101 MHz, $CDCl_3$) of compound **A7.11**.

COMPREHENSIVE BIBLIOGRAPHY

Alexy, E. J.; Virgil, S. C.; Bartberger, M. D.; Stoltz, B. M. Enantioselective Pd-Catalyzed Decarboxylative Allylic Alkylation of Thiopyranones. Access to Acyclic, Stereogenic α-Quaternary Ketones. *Org. Lett.* **2017**, *19*, 5007–5009.

Alexy, E. J.; Zhang, H.; Stoltz, B. M. Catalytic Enantioselective Synthesis of Acyclic Quaternary Centers: Palladium-Catalyzed Decarboxylative Allylic Alkylation of Fully Substituted Acyclic Enol Carbonates. *J. Am. Chem. Soc.* **2018**, *140*, 10109–10112.

Behenna, D. C.; Liu, Y.; Yurino, T.; Kim, J.; White, D. E.; Virgil, S. C.; Stoltz, B. M. Enantioselective Construction of Quaternary *N*-Heterocycles by Palladium-Catalysed Decarboxylative Allylic Alkylation of Lactams. *Nat. Chem.* **2012**, *4*, 130–133.

Behenna, D. C.; Mohr, J. T.; Sherden, N. H.; Marinescu, S. C.; Harned, A. M.; Tani, K.; Seto, M.; Ma, S.; Novák, Z.; Krout, M. R.; et al. Enantioselective Decarboxylative Alkylation Reactions: Catalyst Development, Substrate Scope, and Mechanistic Studies. *Chem. Eur. J.* **2011**, *17* (50), 14199–14223.

Behenna, D. C.; Stoltz, B. M. The Enantioselective Tsuji Allylation. *J. Am. Chem. Soc.* **2004**, *126*, 15044–15045.

Bera, K.; Namboothiri, I. N. N. Asymmetric Synthesis of Quaternary α-Amino Acids and Their Phosphonate Analogues. *Asian J. Org. Chem.* **2014**, *3* (12), 1234–1260.

Boschelli, D.; Smith, A. B.; Stringer, O. D.; Jenkins, R. H.; Davis, F. A. An Asymmetric Synthesis of (+)-Kjellmanianone. *Tetrahedron Lett.* **1981**, *22* (44), 4385–4388.

Burger, E. C.; Tunge, J. A. Asymmetric Allylic Alkylation of Ketone Enolates: An Asymmetric Claisen Surrogate. *Org. Lett.* **2004**, *6*, 4113–4115.

Cabrera-Pardo, J. R.; Trowbridge, A.; Nappi, M.; Ozaki, K.; Gaunt, M. J. Selective Palladium(II)-Catalyzed Carbonylation of Methylene β-C−H Bonds in Aliphatic Amines. *Angew. Chem. Int. Ed.* **2017**, *56*, 11958–11962.

Castro, V. I. B.; Carvalho, C. M.; Fernandes, R. D. V.; Pereira-Lima, S. M. M. A.; Castanheira, E. M. S.; Costa, S. P. G. Peptaibolin Analogues by Incorporation of α,α-Dialkylglycines: Synthesis and Study of Their Membrane Permeating Ability. *Tetrahedron* **2016**, *72* (7), 1024–1030.

Cativiela, C.; Díaz-de-Villegas, M. D. Recent Progress on the Stereoselective Synthesis of Acyclic Quaternary α-Amino Acids. *Tetrahedron: Asymmetry* **2007**, *18* (5), 569–623.

Chamakuri, S.; Jain, P.; Reddy Guduru, S. K.; Arney, J. W.; MacKenzie, K. R.; Santini, C.; Young, D. W. Synthesis of Enantiomerically Pure 6-Substituted-Piperazine-2-Acetic Acid Esters as Intermediates for Library Production. *J. Org. Chem.* **2018**.

Chen, L.; Luo, M.-J.; Zhu, F.; Wen, W.; Guo, Q.-X. Combining Chiral Aldehyde Catalysis and Transition-Metal Catalysis for Enantioselective α-Allylic Alkylation of Amino Acid Esters. *J. Am. Chem. Soc.* **2019**.

Childs, M. E.; Weber, W. P. Preparation of Cyanoformates. Crown Ether Phase Transfer Catalysis. *J. Org. Chem.* **1976**, *41*, 3486–3487.

Chollet, A.; Mori, G.; Menendez, C.; Rodriguez, F.; Fabing, I.; Pasca, M. R.; Madacki, J.; Korduláková, J.; Constant, P.; Quémard, A.; et al. Design, Synthesis and Evaluation of New GEQ Derivatives as Inhibitors of InhA Enzyme and Mycobacterium Tuberculosis Growth. *Eur. J. Med. Chem.* **2015**, *101*, 218–235.

Cochran, B. M.; Michael, F. E. Synthesis of 2,6-Disubstituted Piperazines by a Diastereoselective Palladium-Catalyzed Hydroamination Reaction. *Org. Lett.* **2008**, *10*, 329–332.

de Castro, P. P.; Carpanez, A. G.; Amarante, G. W. Azlactone Reaction Developments. *Chem. Eur. J.* **2016**, *22* (30), 10294–10318.

Dehner, A.; Planker, E.; Gemmecker, G.; Broxterman, Q. B.; Bisson, W.; Formaggio, F.; Crisma, M.; Toniolo, C.; Kessler, H. Solution Structure, Dimerization, and Dynamics of a Lipophilic α/310-Helical, Cα-Methylated Peptide. Implications for Folding of Membrane Proteins. *J. Am. Chem. Soc.* **2001**, *123* (27), 6678–6686.

Ding, W.; Lu, L.-Q.; Zhou, Q.-Q.; Wei, Y.; Chen, J.-R.; Xiao, W.-J. Bifunctional Photocatalysts for Enantioselective Aerobic Oxidation of β-Ketoesters. *J. Am. Chem. Soc.* **2017**, *139* (1), 63–66.

Drandarov, K.; Guggisberg, A.; Hesse, M. Asymmetric Syntheses of the Macrocyclic Spermine Alkaloids (−)-(S)-Protoverbine, (−)-(S)-Buchnerine, and Their Naturally Occurring Congenial Alkaloids. *Helvetica Chimica Acta* **2002***, 85,* 979–989.

Duewelhenke, N.; Krut, O.; Eysel, P. Influence on Mitochondria and Cytotoxicity of Different Antibiotics Administered in High Concentrations on Primary Human Osteoblasts and Cell Lines. *Antimicrob. Agents Chemother.* **2007**, *51*, 54–63.

Ender, M.; McCallum, N.; Adhikari, R.; Berger-Bächi, B. Fitness Cost of SCCmec and Methicillin Resistance Levels in Staphylococcus Aureus. *Antimicrob. Agents Chemother.* **2004**, *48*, 2295–2297.

Endo, K.; Grubbs, R. H. Chelated Ruthenium Catalysts for Z-Selective Olefin Metathesis. *J. Am. Chem. Soc.* **2011**, *133*, 8525–8527.

Etienne, M. A.; Aucoin, J. P.; Fu, Y.; McCarley, R. L.; Hammer, R. P. Stoichiometric Inhibition of Amyloid β-Protein Aggregation with Peptides Containing Alternating α,α-Disubstituted Amino Acids. *J. Am. Chem. Soc.* **2006**, *128* (11), 3522–3523.

Evans, M. C.; Pradhan, A.; Venkatraman, S.; Ojala, W. H.; Gleason, W. B.; Mishra, R. K.; Johnson, R. L. Synthesis and Dopamine Receptor Modulating Activity of Novel Peptidomimetics of L-Prolyl-l-Leucyl-Glycinamide Featuring α,α-Disubstituted Amino Acids. *J. Med. Chem.* **1999**, *42* (8), 1441–1447.

Fairlamb, I. J. S.; Kapdi, A. R.; Lee, A. F. H2-Dba Complexes of Pd(0): The Substituent Effect in Suzuki−Miyaura Coupling. *Org. Lett.* **2004**, *6*, 4435–4438.

Ferreira, M. del R. R.; Cecere, G.; Pace, P.; Summa, V. Routes to HIV-Integrase Inhibitors: Efficient Synthesis of Bicyclic Pyrimidones by Ring Expansion or Amination at a Benzylic Position. *Tetrahedron Lett.* **2009**, *50*, 148–151.

Firth, J. D.; O'Brien, P.; Ferris, L. Synthesis of Enantiopure Piperazines via Asymmetric Lithiation–Trapping of N-Boc Piperazines: Unexpected Role of the Electrophile and Distal N-Substituent. *J. Am. Chem. Soc.* **2016**, *138*, 651–659.

Fitzi, R.; Seebach, D. Resolution and Use in α-Amino Acid Synthesis of Imidazolidinone Glycine Derivatives. *Tetrahedron* **1988**, *44* (17), 5277–5292.

Gettys, K. E.; Ye, Z.; Dai, M. Recent Advances in Piperazine Synthesis. *Synthesis* **2017**, *49*, 2589–2604.

Gonzales, R. D.; Schreckenberger, P. C.; Graham, M. B.; Kelkar, S.; DenBesten, K.; Quinn, J. P. Infections Due to Vancomycin-Resistant Enterococcus Faecium Resistant to Linezolid. *The Lancet* **2001**, *357* (9263), 1179.

Grady, M. A.; Gasperoni, T. L.; Kirkpatrick, P. Aripiprazole. *Nature Reviews Drug Discovery* **2003**, *2*, 427.

Guggisberg, A.; Drandarov, K.; Hesse, M. Protoverbine, the Parent Member of a Class of Macrocyclic Spermine Alkaloids. *Helvetica Chimica Acta* **2000***, 83*, 3035–3042.

He, R.; Liu, P.; Huo, X.; Zhang, W. Ir/Zn Dual Catalysis: Enantioselective and Diastereodivergent α-Allylation of Unprotected α-Hydroxy Indanones. *Org. Lett.* **2017**, *19* (20), 5513–5516.

He, R.; Wu, S.; Tang, H.; Huo, X.; Sun, Z.; Zhang, W. Iridium-Catalyzed Enantioselective and Diastereoselective Allylation of Dioxindoles: A One-Step Synthesis of 3-Allyl-3-Hydroxyoxindoles. *Org. Lett.* **2018**, *20* (19), 6183–6187.

Herquline A, produced by Penicillium herquei FKI-7215, exhibits anti-influenza virus properties: Bioscience, Biotechnology, and Biochemistry: Vol 81, No 1

Hirata, K.; Kotoku, M.; Seki, N.; Maeba, T.; Maeda, K.; Hirashima, S.; Sakai, T.; Obika, S.; Hori, A.; Hase, Y.; et al. SAR Exploration Guided by LE and Fsp3: Discovery of a Selective and Orally Efficacious RORγ Inhibitor. *ACS Med. Chem. Lett.* **2016**, *7*, 23–27.

Holl, R.; Schepmann, D.; Wünsch, B. Homologous Piperazine-Alcanols: Chiral Pool Synthesis and Pharmacological Evaluation. *Med. Chem. Commun.* **2012**, *3*, 673–679.

Hong, A. Y.; Krout, M. R.; Jensen, T.; Bennett, N. B.; Harned, A. M.; Stoltz, B. M. Ring-Contraction Strategy for the Practical, Scalable, Catalytic Asymmetric Synthesis of Versatile Γ-Quaternary Acylcyclopentenes. *Angew. Chem. Int. Ed.* **2011**, *50*, 2756–2760.

Huang, W.-X.; Liu, L.-J.; Wu, B.; Feng, G.-S.; Wang, B.; Zhou, Y.-G. Synthesis of Chiral Piperazines via Hydrogenation of Pyrazines Activated by Alkyl Halides. *Org. Lett.* **2016**, *18*, 3082–3085.

Hung, A. W.; Ramek, A.; Wang, Y.; Kaya, T.; Wilson, J. A.; Clemons, P. A.; Young, D. W. Route to Three-Dimensional Fragments Using Diversity-Oriented Synthesis. *Proc. Natl. Acad. Sci.*. **2011**, *108*, 6799–6804.

Huo, X.; He, R.; Fu, J.; Zhang, J.; Yang, G.; Zhang, W. Stereoselective and Site-Specific Allylic Alkylation of Amino Acids and Small Peptides via a Pd/Cu Dual Catalysis. *J. Am. Chem. Soc.* **2017**, *139* (29), 9819–9822.

Huo, X.; Zhang, J.; Fu, J.; He, R.; Zhang, W. Ir/Cu Dual Catalysis: Enantio- and Diastereodivergent Access to α,α-Disubstituted α-Amino Acids Bearing Vicinal Stereocenters. *J. Am. Chem. Soc.* **2018**, *140* (6), 2080–2084.

Im, W. B.; Choi, S. H.; Park, J.-Y.; Choi, S. H.; Finn, J.; Yoon, S.-H. Discovery of Torezolid as a Novel 5-Hydroxymethyl-Oxazolidinone Antibacterial Agent. *Eur. J. Med. Chem.* **2011**, *46* (4), 1027–1039.

Imbordino, R.; Perrault, W.; Reeder, M. Process for Preparing Linezolid. WO/2007/116284, October 19, 2007.

Ippolito, J. A.; Kanyo, Z. F.; Wang, D.; Franceschi, F. J.; Moore, P. B.; Steitz, T. A.; Duffy, E. M. Crystal Structure of the Oxazolidinone Antibiotic Linezolid Bound to the 50S Ribosomal Subunit. *J. Med. Chem.* **2008**, *51* (12), 3353–3356.

Ishimaru, T.; Shibata, N.; Nagai, J.; Nakamura, S.; Toru, T.; Kanemasa, S. Lewis Acid-Catalyzed Enantioselective Hydroxylation Reactions of Oxindoles and β-Keto Esters Using DBFOX Ligand. *J. Am. Chem. Soc.* **2006**, *128* (51), 16488–16489.

James, J.; Jackson, M.; Guiry, P. Pd-Catalyzed Decarboxylative Asymmetric Allylic Alkylation: Development, Mechanistic Understanding and Recent Advances. *Adv. Synth. Cat.* In Press.

Kanayama, T.; Yoshida, K.; Miyabe, H.; Kimachi, T.; Takemoto, Y. Synthesis of β-Substituted α-Amino Acids with Use of Iridium-Catalyzed Asymmetric Allylic Substitution. *J. Org. Chem.* **2003**, *68* (16), 6197–6201.

Kearney, S. E.; Zahoránszky-Kőhalmi, G.; Brimacombe, K. R.; Henderson, M. J.; Lynch, C.; Zhao, T.; Wan, K. K.; Itkin, Z.; Dillon, C.; Shen, M.; et al. Canvass: A Crowd-Sourced, Natural-Product Screening Library for Exploring Biological Space. *ACS Cent. Sci.* **2018**, *4*, 1727–1741.

Klepacz, A.; Zwierzak, A. An Expeditious One-Pot Synthesis of Diethyl N-Boc-1-Aminoalkylphosphonates. *Tetrahedron Lett.* **2002**, *43*, 1079–1080.

Klepacz, A.; Zwierzak, A. An Expeditious One-Pot Synthesis of Diethyl N-Boc-1-Aminoalkylphosphonates. *Tetrahedron Lett.* **2002**, *43*, 1079–1080.

Korch, K. M.; Eidamshaus, C.; Behenna, D. C.; Nam, S.; Horne, D.; Stoltz, B. M. Enantioselective Synthesis of α-Secondary and α-Tertiary Piperazin-2-Ones and Piperazines by Catalytic Asymmetric Allylic Alkylation. *Angew. Chem. Int. Ed. 54*, 179–183.

Korch, K. M.; Eidamshaus, C.; Behenna, D. C.; Nam, S.; Horne, D.; Stoltz, B. M. Enantioselective Synthesis of α-Secondary and α-Tertiary Piperazin-2-Ones and Piperazines by Catalytic Asymmetric Allylic Alkylation. *Angew. Chem. Int. Ed. 54* (1), 179–183.

Kumar, A.; Patil, D.; Rajamohanan, P. R.; Ahmad, A. Isolation, Purification and Characterization of Vinblastine and Vincristine from Endophytic Fungus Fusarium Oxysporum Isolated from Catharanthus Roseus. *PLOS ONE* **2013**, *8* (9), e71805.

Kuwano, R.; Ito, Y. Asymmetric Hydrogenation of 1,4,5,6-Tetrahydropyrazine-2-(N-Tert-Butyl)Carboxamide Catalyzed by Trans-Chelating Chiral Diphosphine−Rhodium Complexes. *J. Org. Chem.* **1999**, *64*, 1232–1237.

Leach, K. L.; Swaney, S. M.; Colca, J. R.; McDonald, W. G.; Blinn, J. R.; Thomasco, L. M.; Gadwood, R. C.; Shinabarger, D.; Xiong, L.; Mankin, A. S. The Site of Action of Oxazolidinone Antibiotics in Living Bacteria and in Human Mitochondria. *Molecular Cell* **2007**, *26* (3), 393–402.

Leonard, D. J.; Ward, J. W.; Clayden, J. Asymmetric α-Arylation of Amino Acids. *Nature* **2018**, *562* (7725), 105–109.

Li, C.-H.; Cheng, Y.-W.; Liao, P.-L.; Yang, Y.-T.; Kang, J.-J. Chloramphenicol Causes Mitochondrial Stress, Decreases ATP Biosynthesis, Induces Matrix

Metalloproteinase-13 Expression, and Solid-Tumor Cell Invasion. *Toxicol Sci* **2010**, *116* (1), 140–150.

Lin, X.; Ruan, S.; Yao, Q.; Yin, C.; Lin, L.; Feng, X.; Liu, X. Kinetic Resolution of Oxaziridines via Chiral Bifunctional Guanidine-Catalyzed Enantioselective α-Hydroxylation of β-Keto Esters. *Org. Lett.* **2016**, *18* (15), 3602–3605.

Lovering, F. Escape from Flatland 2: Complexity and Promiscuity. *Med. Chem. Commun.* **2013**, *4*, 515–519.

Lovering, F.; Bikker, J.; Humblet, C. Escape from Flatland: Increasing Saturation as an Approach to Improving Clinical Success. *J. Med. Chem.* **2009**, *52* (21), 6752–6756.

Lu, M.; Zhu, D.; Lu, Y.; Zeng, X.; Tan, B.; Xu, Z.; Zhong, G. Chiral Brønsted Acid-Catalyzed Enantioselective α-Hydroxylation of β-Dicarbonyl Compounds. *J. Am. Chem. Soc.* **2009**, *131* (13), 4562–4563.

Mahy, W.; Leitch, J. A.; Frost, C. G. Copper Catalyzed Assembly of N-Aryloxazolidinones: Synthesis of Linezolid, Tedizolid, and Rivaroxaban. *Eur. J. Org. Chem. 2016* (7), 1305–1313.

Marson, C. M. Chapter Two - Saturated Heterocycles with Applications in Medicinal Chemistry. In *Advances in Heterocyclic Chemistry*; Scriven, E. F. V., Ramsden, C. A., Eds.; Heterocyclic Chemistry in the 21st Century; Academic Press, 2017; Vol. 121, pp 13–33.

Maruoka, K.; Ooi, T. Enantioselective Amino Acid Synthesis by Chiral Phase-Transfer Catalysis. *Chemical Reviews* **2003**, *103* (8), 3013–3028.

Marziale, A. N.; Duquette, D. C.; Craig, R. A.; Kim, K. E.; Liniger, M.; Numajiri, Y.; Stoltz, B. M. An Efficient Protocol for the Palladium-Catalyzed Asymmetric Decarboxylative Allylic Alkylation Using Low Palladium Concentrations and a Palladium(II) Precatalyst. *Adv. Synth. Cat.* **2015**, *357*, 2238–2245.

Masumoto, S.; Usuda, H.; Suzuki, M.; Kanai, M.; Shibasaki, M. Catalytic Enantioselective Strecker Reaction of Ketoimines. *J. Am. Chem. Soc.* **2003**, *125* (19), 5634–5635.

McCarthy, J. R. A Convenient Synthesis of the Antibacterial Agent Linezolid. *Tetrahedron Lett.* **2015**, *56* (49), 6846–6847.

McDermott, B. P.; Campbell, A. D.; Ertan, A. First Example of S-BuLi/(-)-Sparteine-Mediated Chiral Deprotonation of a Piperazine and Proof of the Sense of Induction. *Synlett* **2008**, *2008*, 875–879.

McDougal, N. T.; Streuff, J.; Mukherjee, H.; Virgil, S. C.; Stoltz, B. M. Rapid Synthesis of an Electron-Deficient t-BuPHOX Ligand: Cross-Coupling of Aryl Bromides with Secondary Phosphine Oxides. *Tetrahedron Lett.* **2010**, *51*, 5550–5554.

McKee, E. E.; Ferguson, M.; Bentley, A. T.; Marks, T. A. Inhibition of Mammalian Mitochondrial Protein Synthesis by Oxazolidinones. *Antimicrob. Agents Chemother.* **2006**, *50* (6), 2042–2049.

Meyer, L.; Poirier, J.-M.; Duhamel, P.; Duhamel, L. Chiral Auxiliaries with a Switching Center: New Tools in Asymmetric Synthesis. Application to the Synthesis of Enantiomerically Pure (R)- and (S)-α-Amino Acids. *J. Org. Chem.* **1998**, *63* (23), 8094–8095.

Meyers, J.; Carter, M.; Mok, N. Y.; Brown, N. On the Origins of Three-Dimensionality in Drug-like Molecules. *Future Medicinal Chemistry* **2016**, *8*, 1753–1767.

Mohr, J. T.; Behenna, D. C.; Harned, A. M.; Stoltz, B. M. Deracemization of Quaternary Stereocenters by Pd-Catalyzed Enantioconvergent Decarboxylative Allylation of Racemic β-Ketoesters. *Angew. Chem. Int. Ed.* **2005**, *44*, 6924–6927.

Monteleone, S.; Fuchs, J. E.; Liedl, K. R. Molecular Connectivity Predefines Polypharmacology: Aliphatic Rings, Chirality, and Sp3 Centers Enhance Target Selectivity. *Frontiers in Pharmacology* **2017**, *8*, 552.

Montgomery, T. D.; Rawal, V. H. Palladium-Catalyzed Modular Synthesis of Substituted Piperazines and Related Nitrogen Heterocycles. *Org. Lett.* **2016**, *18*, 740–743.

Naganawa, Y.; Aoyama, T.; Kato, K.; Nishiyama, H. Cu(II)-Catalyzed Enantioselective α-Hydroxylation and α-Chlorination of β-Ketoesters with N,N,O-Tridentate Chiral Phenanthroline Ligand. *ChemistrySelect* **2016**, *1* (9), 1938–1942.

Nakhla, J. S.; Wolfe, J. P. A Concise Asymmetric Synthesis of Cis-2,6-Disubstituted N-Aryl Piperazines via Pd-Catalyzed Carboamination Reactions. *Org. Lett.* **2007**, *9*, 3279–3282.

Narita, M.; Tsuji, B. T.; Yu, V. L. Linezolid-Associated Peripheral and Optic Neuropathy, Lactic Acidosis, and Serotonin Syndrome. *Pharmacotherapy* **2007**, *27*, 1189–1197.

Nascimento de Oliveira, M.; Arseniyadis, S.; Cossy, J. Palladium-Catalyzed Asymmetric Allylic Alkylation of 4-Substituted Isoxazolidin-5-Ones: A Straightforward Access to B2,2-Amino Acids. *Chem. Eur. J.* **2018**, *24*, 4810–4814.

Novacek, J.; Izzo, J. A.; Vetticatt, M. J.; Waser, M. Bifunctional Ammonium Salt Catalyzed Asymmetric α-Hydroxylation of β-Ketoesters by Simultaneous Resolution of Oxaziridines. *Chem. Eur. J.* **2016**, *22* (48), 17339–17344.

Numajiri, Y.; Jiménez-Osés, G.; Wang, B.; Houk, K. N.; Stoltz, B. M. Enantioselective Synthesis of Dialkylated *N* -Heterocycles by Palladium-Catalyzed Allylic Alkylation. *Org. Lett.* **2015**, *17*, 1082–1085.

Numajiri, Y.; Pritchett, B. P.; Chiyoda, K.; Stoltz, B. M. Enantioselective Synthesis of α-Quaternary Mannich Adducts by Palladium-Catalyzed Allylic Alkylation: Total Synthesis of (+)-Sibirinine. *J. Am. Chem. Soc.* **2015**, *137*, 1040–1043.

Odagi, M.; Furukori, K.; Yamamoto, Y.; Sato, M.; Iida, K.; Yamanaka, M.; Nagasawa, K. Origin of Stereocontrol in Guanidine-Bisurea Bifunctional Organocatalyst That Promotes α-Hydroxylation of Tetralone-Derived β-Ketoesters: Asymmetric Synthesis of β- and γ-Substituted Tetralone Derivatives via Organocatalytic Oxidative Kinetic Resolution. *J. Am. Chem. Soc.* **2015**, *137* (5), 1909–1915.

Ohfune, Y.; Shinada, T. Enantio- and Diastereoselective Construction of α,α-Disubstituted α-Amino Acids for the Synthesis of Biologically Active Compounds. *Eur. J. Org. Chem.* **2005**, *2005* (24), 5127–5143.

Ooi, T.; Takeuchi, M.; Kameda, M.; Maruoka, K. Practical Catalytic Enantioselective Synthesis of α,α-Dialkyl-α-Amino Acids by Chiral Phase-Transfer Catalysis. *J. Am. Chem. Soc.* **2000**, *122* (21), 5228–5229.

Perrault, W. R.; Pearlman, B. A.; Godrej, D. B.; Jeganathan, A.; Yamagata, K.; Chen, J. J.; Lu, C. V.; Herrinton, P. M.; Gadwood, R. C.; Chan, L.; et al. The Synthesis of N-Aryl-5(S)-Aminomethyl-2-Oxazolidinone Antibacterials and Derivatives in One Step from Aryl Carbamates. *Org. Process Res. Dev.* **2003**, *7* (4), 533–546.

Pfeiffer, U.; Riccaboni, M. T.; Erba, R.; Pinza, M. A Short Synthesis of 4-imidazolidinone. *Liebigs Annalen der Chemie* **1988**, *1988* (10), 993–995.

Qi, X.; Chen, C.; Hou, C.; Fu, L.; Chen, P.; Liu, G. Enantioselective Pd(II)-Catalyzed Intramolecular Oxidative 6- *Endo* Aminoacetoxylation of Unactivated Alkenes. *J. Am. Chem. Soc.* **2018**, *140* (24), 7415–7419.

Reddy, D. S.; Shibata, N.; Nagai, J.; Nakamura, S.; Toru, T. A Dynamic Kinetic Asymmetric Transformation in the α-Hydroxylation of Racemic Malonates and Its Application to Biologically Active Molecules. *Angew. Chem. Int. Ed.* **2009**, *48* (4), 803–806.

Reeves, C. M.; Eidamshaus, C.; Kim, J.; Stoltz, B. M. Enantioselective Construction of α-Quaternary Cyclobutanones by Catalytic Asymmetric Allylic Alkylation. *Angew. Chem. Int. Ed.* **2013**, *52*, 6718–6721.

Ruider, S. A.; Müller, S.; Carreira, E. M. Ring Expansion of 3-Oxetanone-Derived Spirocycles: Facile Synthesis of Saturated Nitrogen Heterocycles. *Angew. Chem. Int. Ed. 52*, 11908–11911.

Schecter, G. F.; Scott, C.; True, L.; Raftery, A.; Flood, J.; Mase, S. Linezolid in the Treatment of Multidrug-Resistant Tuberculosis. *Clin Infect Dis* **2010**, *50* (1), 49–55.

Seebach, D.; Beck, A. K.; Bierbaum, D. J. The World of Beta- and Gamma-Peptides Comprised of Homologated Proteinogenic Amino Acids and Other Components. *Chem. Biodivers.* **2004**, *1*, 1111–1239.

Seebach, D.; Hoffmann, M. Preparation and Use in Amino Acid Synthesis of a New Chiral Glycine Derivative – (R)- and (S)-Tert-Butyl 2-Tert-Butyl-4-Methoxy-2,5-Dihydroimidazole-1-Carboxylate (BDI). *Eur. J. Org. Chem.* **1998**, *1998* (7), 1337–1351.

Serra, M.; Bernardi, E.; Marrubini, G.; Lorenzi, E. D.; Colombo, L. Palladium-Catalyzed Asymmetric Decarboxylative Allylation of Azlactone Enol Carbonates: Fast Access to Enantioenriched α-Allyl Quaternary Amino Acids. *Eur. J. Org. Chem.* **2019**, *2019* (4), 732–741.

Seto, M.; Roizen, J. L.; Stoltz, B. M. Catalytic Enantioselective Alkylation of Substituted Dioxanone Enol Ethers: Ready Access to C(α)-Tetrasubstituted Hydroxyketones, Acids, and Esters. *Angew. Chem.* **2008**, *120*, 6979–6982.

Sharma, M. R.; Koc, E. C.; Datta, P. P.; Booth, T. M.; Spremulli, L. L.; Agrawal, R. K. Structure of the Mammalian Mitochondrial Ribosome Reveals an Expanded Functional Role for Its Component Proteins. *Cell* **2003**, *115* (1), 97–108.

Shaw, K. J.; Barbachyn, M. R. The Oxazolidinones: Past, Present, and Future. *Ann. N. Y. Acad. Sci.* **2011**, *1241*, 48–70.

Shimizu, I.; Yamada, T.; Tsuji, J. Palladium-Catalyzed Rearrangement of Allylic Esters of Acetoacetic Acid to Give γ,δ-Unsaturated Methyl Ketones. *Tetrahedron Lett.* **1980**, *21*, 3199–3202.

Sikriwal, D.; Kant, R.; Maulik, P. R.; Dikshit, D. K. A Short Formal Synthesis of Three Epimers of Penmacric Acid. *Tetrahedron* **2010**, *66*, 6167–6173.

Sim, S.-B. D.; Wang, M.; Zhao, Y. Phase-Transfer-Catalyzed Enantioselective α-Hydroxylation of Acyclic and Cyclic Ketones with Oxygen. *ACS Catalysis* **2015**, *5* (6), 3609–3612.

Smith, A. M. R.; Hii, K. K. (Mimi). Transition Metal Catalyzed Enantioselective α-Heterofunctionalization of Carbonyl Compounds. *Chem. Rev.* **2011**, *111* (3), 1637–1656.

Spaulding, A.; Takrouri, K.; Mahalingam, P.; Cleary, D. C.; Cooper, H. D.; Zucchi, P.; Tear, W.; Koleva, B.; Beuning, P. J.; Hirsch, E. B.; et al. Compound Design Guidelines for Evading the Efflux and Permeation Barriers of Escherichia Coli with the Oxazolidinone Class of Antibacterials: Test Case for a General Approach to Improving Whole Cell Gram-Negative Activity. *Bioorg. Med. Chem. Lett.* **2017**, *27*, 5310–5321.

Steer, D. L.; Lew, R. A.; Perlmutter, P.; Smith, A. I.; Aguilar, M.-I. Beta-Amino Acids: Versatile Peptidomimetics. *Curr. Med. Chem.* **2002**, *9*, 811–822.

Sudhakar, G.; Bayya, S.; Reddy, K. J.; Sridhar, B.; Sharma, K.; Bathula, S. R. Synthesis and Cytotoxicity of the Proposed Structure of Piperazirum, Its Stereoisomers and Analogues. *Euro. J. Org. Chem.* **2014**, 1253–1265.

Sun, A. W.; Hess, S. N.; Stoltz, B. M. Enantioselective Synthesis of Gem-Disubstituted N-Boc Diazaheterocycles via Decarboxylative Asymmetric Allylic Alkylation. *Chem. Sci.* **2019**, *10*, 788–792.

Swaney, S. M.; Aoki, H.; Ganoza, M. C.; Shinabarger, D. L. The Oxazolidinone Linezolid Inhibits Initiation of Protein Synthesis in Bacteria. *Antimicrobial Agents and Chemotherapy* **1998**, *42* (12), 3251–3255.

Tani, K.; Behenna, D. C.; McFadden, R. M.; Stoltz, B. M. A Facile and Modular Synthesis of Phosphinooxazoline Ligands. *Org. Lett.* **2007**, *9*, 2529–2531.

Taylor, R. R. R.; Twin, H. C.; Wen, W. W.; Mallot, R. J.; Lough, A. J.; Gray-Owen, S. D.; Batey, R. A. Substituted 2,5-Diazabicyclo[4.1.0]Heptanes and Their Application as General Piperazine Surrogates: Synthesis and Biological Activity of a Ciprofloxacin Analogue. *Tetrahedron* **2010**, *66*, 3370–3377.

Toniolo, C.; Crisma, M.; Formaggio, F.; Peggion, C. Control of Peptide Conformation by the Thorpe-Ingold Effect (Cα-Tetrasubstitution). *Peptide Science* **2001**, *60* (6), 396–419. (2001)60:6<396::AID-BIP10184>3.0.CO;2-7.

Toullec, P. Y.; Bonaccorsi, C.; Mezzetti, A.; Togni, A. Expanding the Scope of Asymmetric Electrophilic Atom-Transfer Reactions: Titanium- and Ruthenium-Catalyzed Hydroxylation of β-Ketoesters. *PNAS* **2004**, *101* (16), 5810–5814.

Trost, B. M. Metal Catalyzed Allylic Alkylation: Its Development in the Trost Laboratories. *Tetrahedron* **2015**, *71*, 5708–5733.

Trost, B. M.; Ariza, X. Catalytic Asymmetric Alkylation of Nucleophiles: Asymmetric Synthesis of α-Alkylated Amino Acids. *Angew. Chem. Int. Ed.* **1997**, *36* (23), 2635–2637.

Trost, B. M.; Ariza, X. Enantioselective Allylations of Azlactones with Unsymmetrical Acyclic Allyl Esters. *J. Am. Chem. Soc.* **1999**, *121* (46), 10727–10737.

Trost, B. M.; Dogra, K. Synthesis of Novel Quaternary Amino Acids Using Molybdenum-Catalyzed Asymmetric Allylic Alkylation. *J. Am. Chem. Soc.* **2002**, *124* (25), 7256–7257.

Trost, B. M.; Koller, R.; Schäffner, B. Enantioselective Synthesis of Tertiary α-Hydroxyketones from Unfunctionalized Ketones: Palladium-Catalyzed Asymmetric Allylic Alkylation of Enolates. *Angew. Chem. Int. Ed.* **2012**, *51* (33), 8290–8293.

Trost, B. M.; Xu, J. Regio- and Enantioselective Pd-Catalyzed Allylic Alkylation of Ketones through Allyl Enol Carbonates. *J. Am. Chem. Soc.* **2005**, *127*, 2846–2847.

Trost, B. M.; Xu, J.; Reichle, M. Enantioselective Synthesis of α-Tertiary Hydroxyaldehydes by Palladium-Catalyzed Asymmetric Allylic Alkylation of Enolates. *J. Am. Chem. Soc.* **2007**, *129* (2), 282–283.

Trost, B. M.; Xu, J.; Schmidt, T. Ligand Controlled Highly Regio- and Enantioselective Synthesis of α-Acyloxyketones by Palladium-Catalyzed Allylic Alkylation of 1,2-Enediol Carbonates. *J. Am. Chem. Soc.* **2008**, *130* (36), 11852–11853.

Trost, Cb.-C.; Jiang, C. Catalytic Enantioselective Construction of All-Carbon Quaternary Stereocenters. *New York* **2006**, No. 3, 28.

Tsuda, T.; Chujo, Y.; Nishi, S.; Tawara, K.; Saegusa, T. Facile Generation of a Reactive Palladium(II) Enolate Intermediate by the Decarboxylation of Palladium(II) .Beta.-Ketocarboxylate and Its Utilization in Allylic Acylation. *J. Am. Chem. Soc.* **1980**, *102*, 6381–6384.

Ukai, T.; Kawazura, H.; Ishii, Y.; Bonnet, J. J.; Ibers, J. A. Chemistry of Dibenzylideneacetone-Palladium(0) Complexes: I. Novel Tris(Dibenzylideneacetone)Dipalladium(Solvent) Complexes and Their Reactions with Quinones. *J. Organomet. Chem.* ***1999****, 65, 253–266.*

Vitaku, E.; Smith, D. T.; Njardarson, J. T. Analysis of the Structural Diversity, Substitution Patterns, and Frequency of Nitrogen Heterocycles among U.S. FDA Approved Pharmaceuticals. *J. Med. Chem.* **2014**, *57*, 10257–10274.

Vo, C.-V. T.; Bode, J. W. Synthesis of Saturated N-Heterocycles. *J. Org. Chem.* **2014**, *79*, 2809–2815.

Vogt, H.; Bräse, S. Recent Approaches towards the Asymmetric Synthesis of α,α-Disubstituted α-Amino Acids. *Org. Biomol. Chem.* **2007**, *5* (3), 406–430.

Wang, H.; Kowalski, M. D.; Lakdawala, A. S.; Vogt, F. G.; Wu, L. An Efficient and Highly Diastereoselective Synthesis of GSK1265744, a Potent HIV Integrase Inhibitor. *Org. Lett.* **2015**, *17*, 564–567.

Weiner, B.; Szymański, W.; Janssen, D. B.; Minnaard, A. J.; Feringa, B. L. Recent Advances in the Catalytic Asymmetric Synthesis of β-Amino Acids. *Chem. Soc. Rev.* **2010**, *39*, 1656–1691.

White, D. E.; Stewart, I. C.; Grubbs, R. H.; Stoltz, B. M. The Catalytic Asymmetric Total Synthesis of Elatol. *J. Am. Chem. Soc.* **2008**, *130*, 810–811.

Wishart, D. S.; Feunang, Y. D.; Guo, A. C.; Lo, E. J.; Marcu, A.; Grant, J. R.; Sajed, T.; Johnson, D.; Li, C.; Sayeeda, Z.; et al. DrugBank 5.0: A Major Update to the DrugBank Database for 2018. *Nucleic Acids Res.* **2018**, *46* (D1), D1074–D1082.

Witten, M. R.; Jacobsen, E. N. A Simple Primary Amine Catalyst for Enantioselective α-Hydroxylations and α-Fluorinations of Branched Aldehydes. *Org. Lett.* **2015**, *17* (11), 2772–2775.

Xue, F.; Bao, X.; Zou, L.; Qu, J.; Wang, B. Asymmetric Hydroxylation of 4-Substituted Pyrazolones Catalyzed by Natural Cinchona Alkaloids. *Advanced Synthesis & Catalysis* **2016**, *358* (24), 3971–3976.

Yang, B.; Shi, L.; Wu, J.; Fang, X.; Yang, X.; Wu, F. Microwave-Assisted Expeditious Synthesis of 5-Fluoroalkyl-3-(Aryl/Alkyl)-Oxazolidin-2-Ones. *Tetrahedron* **2013**, *69* (15), 3331–3337.

Yang, F.; Zhao, J.; Tang, X.; Zhou, G.; Song, W.; Meng, Q. Enantioselective α-Hydroxylation by Modified Salen-Zirconium(IV)-Catalyzed Oxidation of β-Keto Esters. *Org. Lett.* **2017**, *19* (3), 448–451.

Yokoyama, R.; Huang, J.-M.; Yang, C.-S.; Fukuyama, Y. New Seco-Prezizaane-Type Sesquiterpenes, Jiadifenin with Neurotrophic Activity and 1,2-Dehydroneomajucin from Illicium Jiadifengpi. *J. Nat. Prod.* **2002**, *65* (4), 527–531.

Yu, J.-S.; Noda, H.; Shibasaki, M. Quaternary B2,2-Amino Acids: Catalytic Asymmetric Synthesis and Incorporation into Peptides by Fmoc-Based Solid Phase Peptide Synthesis. *Angew. Chem. Int. Ed.* **2018**, *57*, 818–822.

Ziegler, R. E.; Desai, B. K.; Jee, J.-A.; Gupton, B. F.; Roper, T. D.; Jamison, T. F. 7-Step Flow Synthesis of the HIV Integrase Inhibitor Dolutegravir. *Angew. Chem. Int. Ed.* **2018**, *57*, 7181–7185.

ABOUT THE AUTHOR

Alexander W. Sun was born on May 1, 1990. He lived in Eugene, OR for 16 years, devoting most of his free time to swimming and water polo. Later on in high school, Alex became fascinated by organic synthesis, having been inspired both by the synthesis of aspirin during a routine laboratory course and an excellent organic chemistry course taught by Professor Gary O. Spessard. In 2008, Alex went on to attend the University of Oregon for his freshman year, undertaking his first research experience in the inorganic chemistry laboratory of Professor David R. Tyler.

Seeking to explore a new environment, Alex spent his final three years of college at the University of Pennsylvania, majoring in Chemistry, Biochemistry, and Biology, while also submatriculating to obtain an M.Sc. in Chemistry. There, Alex further solidified his interest in organic chemistry by completing his master's thesis on the synthesis of HIV-1 entry inhibitors in the research group of Professor Amos B. Smith, III. At Penn, in the Smith group, and surrounded by excellent mentors such as Professor Ponzy Lu, Alex became interested in the applications of organic chemistry to medicine, and decided to pursue an MD/PhD.

In 2012, Alex joined the UCLA-Caltech MD/PhD program. During the summers, he worked in the groups of Professor Neil Garg and Professor Peter Dervan. Ultimately, Alex began doctoral studies with Professor Brian Stoltz, working on the synthesis and medicinal applications of chiral heterocycles. Following completion of his graduate studies, Alex will return to UCLA to finish the final two years of medical school, aiming to pursue residency with the continued goal of applying chemistry to medicine.